frontiers | Research Topics

Mineral nutrition and plant stress tolerance

Edited by
Md Sazzad Hossain, Pedro Garcia and Karl H. Mühling

Published in
Frontiers in Plant Science

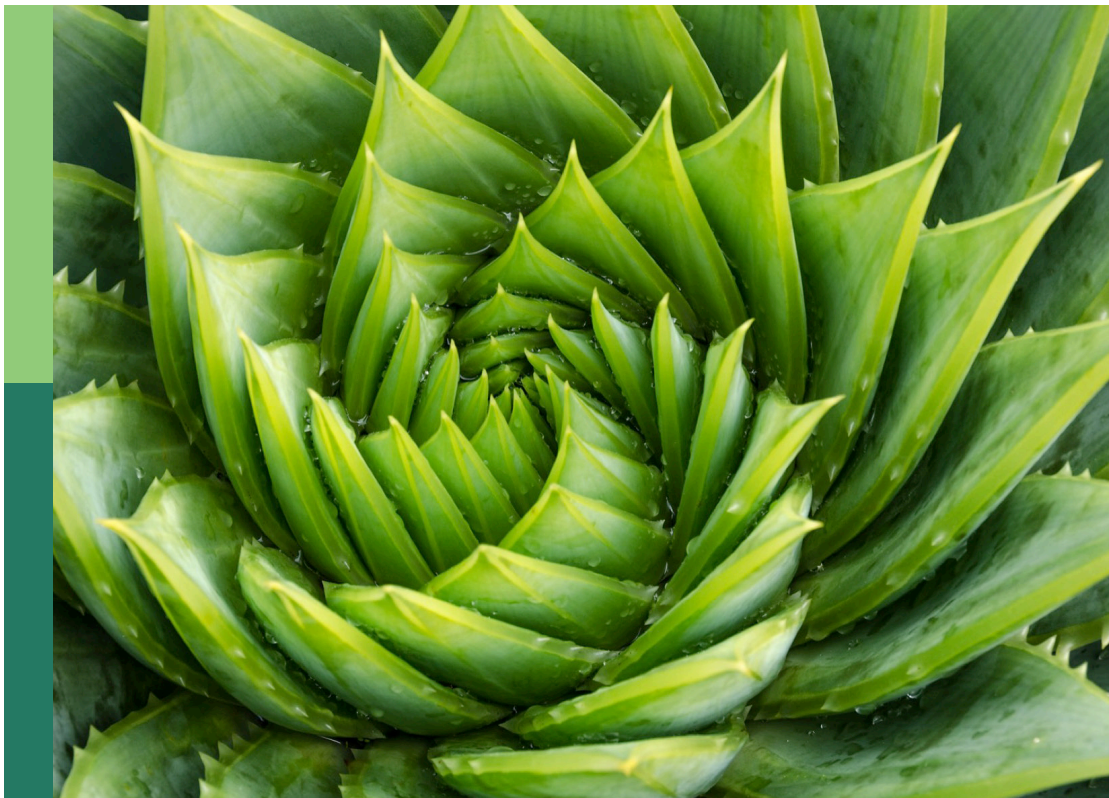

ISSN 1664-8714
ISBN 978-2-8325-5262-9
DOI 10.3389/978-2-8325-5262-9

About Frontiers

Frontiers is more than just an open access publisher of scholarly articles: it is a pioneering approach to the world of academia, radically improving the way scholarly research is managed. The grand vision of Frontiers is a world where all people have an equal opportunity to seek, share and generate knowledge. Frontiers provides immediate and permanent online open access to all its publications, but this alone is not enough to realize our grand goals.

Frontiers journal series

The Frontiers journal series is a multi-tier and interdisciplinary set of open-access, online journals, promising a paradigm shift from the current review, selection and dissemination processes in academic publishing. All Frontiers journals are driven by researchers for researchers; therefore, they constitute a service to the scholarly community. At the same time, the *Frontiers journal series* operates on a revolutionary invention, the tiered publishing system, initially addressing specific communities of scholars, and gradually climbing up to broader public understanding, thus serving the interests of the lay society, too.

Dedication to quality

Each Frontiers article is a landmark of the highest quality, thanks to genuinely collaborative interactions between authors and review editors, who include some of the world's best academicians. Research must be certified by peers before entering a stream of knowledge that may eventually reach the public - and shape society; therefore, Frontiers only applies the most rigorous and unbiased reviews. Frontiers revolutionizes research publishing by freely delivering the most outstanding research, evaluated with no bias from both the academic and social point of view. By applying the most advanced information technologies, Frontiers is catapulting scholarly publishing into a new generation.

What are Frontiers Research Topics?

Frontiers Research Topics are very popular trademarks of the *Frontiers journals series*: they are collections of at least ten articles, all centered on a particular subject. With their unique mix of varied contributions from Original Research to Review Articles, Frontiers Research Topics unify the most influential researchers, the latest key findings and historical advances in a hot research area.

Find out more on how to host your own Frontiers Research Topic or contribute to one as an author by contacting the Frontiers editorial office: frontiersin.org/about/contact

Mineral nutrition and plant stress tolerance

Topic editors
Md Sazzad Hossain — University of Kiel, Germany
Pedro Garcia — University of Almeria, Spain
Karl H. Mühling — University of Kiel, Germany

Citation
Hossain, M. S., Garcia, P., Mühling, K. H., eds. (2024). *Mineral nutrition and plant stress tolerance*. Lausanne: Frontiers Media SA. doi: 10.3389/978-2-8325-5262-9

Table of contents

frontiers | Frontiers in Plant Science

TYPE Editorial
PUBLISHED 25 July 2024
DOI 10.3389/fpls.2024.1461651

OPEN ACCESS

EDITED AND REVIEWED BY
Marta Wilton Vasconcelos,
Catholic University of Portugal, Portugal

*CORRESPONDENCE
Md Sazzad Hossain
sazzadmh.aha@sau.ac.bd
Karl Hermann Mühling
khmuehling@plantnutrition.uni-kiel.de

RECEIVED 08 July 2024
ACCEPTED 12 July 2024
PUBLISHED 25 July 2024

CITATION
Hossain MS, Garcia Caparros P and Mühling KH (2024) Editorial: Mineral nutrition and plant stress tolerance.
Front. Plant Sci. 15:1461651.
doi: 10.3389/fpls.2024.1461651

Editorial: Mineral nutrition and plant stress tolerance

Md Sazzad Hossain[1,2]*, Pedro Garcia Caparros[3] and Karl Hermann Mühling[1]*

[1]Kiel University, Kiel, Germany, [2]Sylhet Agricultural University, Sylhet, Bangladesh, [3]University of Almeria, Almería, Spain

KEYWORDS

plants, mineral elements, abiotic stress, biotic stress, plant physiology and biochemistry, nutrient deficiency and toxicity

Editorial on the Research Topic
Mineral nutrition and plant stress tolerance

The provision of so-called global food safety and security is threatened by global warming, climate change, and the increasing food demand for an ever-growing human population (Berkhout et al., 2019; Sun and Weaver, 2020; Dobermann et al., 2022). Improper plant nutritional management reduces crop production and quality becomes a vital global concern affecting billions of people worldwide (Kumssa et al., 2015; Hofmann et al., 2020; Dobermann et al., 2022). Any stress (biotic or abiotic) can disrupt plant metabolism and lead to reduced growth, fitness, and productivity (Hossain and Dietz, 2016; Ahmed et al., 2020). Understanding crop physiological and biochemical responses to adverse environmental conditions is critical (Bashir et al., 2021). Mineral nutrition is one of the most effective ways to reduce various stresses in crops to increase yield and quality. It plays a crucial role in the response of plants to both biotic and abiotic stresses (Marschner and Cakmak, 1989; Cakmak, 2005; Waraich et al., 2011; Marschner, 2012; Elmer and Datnoff, 2014; Cabot et al., 2019; Sarwar et al., 2019; Kumari et al., 2022). Interactions between mineral elements and biotic and abiotic stress responses are important for developing strategies to improve crop productivity and quality in stressed environments. Proper nutrient management can effectively mitigate the adverse effects of different stresses through diversified mechanisms (Shoukat et al., 2024a, b; Waraich et al., 2011; Mannan et al., 2022; Van Nguyen et al., 2022; Chowdhury et al., 2024).

Although considerable progress has been made in plant nutrition and stress tolerance many aspects of plant nutrition remain unknown. However, more extensive efforts are required to understand better the relationship between mineral elements and plant stress tolerance. Mechanisms underlying the role of mineral nutrition and its interactions with plants are proposed in this Research Topic, comprising diverse research articles, including two reviews and seven original research papers.

Nitrogen metabolism in crops is crucial for various physiological processes and plant growth, especially in staple crops like tea. In this review, Zhang et al. summarized the current information on the underlying mechanisms to identify key regulators in functional phenotypes and improve nitrogen use efficiency. The review highlighted the significance of ammonium as the primary nitrogen source. The biological and molecular mechanisms underlying the GS-GOGAT pathway, including nitrate reductase (NR), nitrite reductase

(NiR), glutamine synthetase (GS), glutamate synthase (GOGAT), and glutamate dehydrogenase (GDH), were also explained in detail.

Phan et al. conducted a genome-wide association study to identify quantitative trait loci (QTLs) linked to nitrogen use efficiency (NUE) in rice under saline conditions. The research involved 2,391 rice accessions grown under two nitrogen conditions and two NaCl concentrations to assess dry weight. A total of 55 QTLs associated with the evaluated traits were identified, with 28 being novel discoveries. These findings offer valuable genetic resources for improving NUE in rice, particularly in saline environments.

Sugar and acid metabolism are pivotal in tomato development and fruit quality, necessitating further investigation into the underlying transcripts, particularly under high temperature and nitrogen fertilizer conditions. Zheng et al. reported that both conditions elevated the levels of soluble sugars and organic acids in young tomato fruits. Additionally, the study identified several genes involved in sucrose metabolism (CWINV2, HK2, SPS, PK) and sucrose transporters (SUT1, SUT4, SWEETs).

Chen et al. experimented to discern the main physiological and molecular mechanisms of *Acacia melanoxylon* stem in response to boron deficiency. Under boron-deficit conditions, stem growth was reduced with shortened internodes. Transcriptomic analysis revealed that genes linked to cell wall metabolism and structural components were downregulated. Furthermore, additional genes linked to hormone signaling showed significant alterations.

Moradi and Siosemardeh investigated the influence of seed priming and foliar application of various chemical fertilizers on rainfed wheat. Their study demonstrated that combining these application methods significantly enhanced the physiological and yield traits of the wheat. This information is crucial for growers seeking to improve plant growth and yield under drought-stressed conditions.

The review by Mukarram et al. focused on the interaction between silicon nanoparticles (SiNPs) and trace elements (TEs) toxicity. The authors emphasize exploring this interaction from an omics perspective, encompassing plant metabolomics, proteomics, and genomics. Furthermore, the review delves into the physiological and biochemical mechanisms underlying this interaction.

Pitann and Mühling examined the waterlogging resistance of oat at various developmental stages as an alternative for crop rotation in regions with temporary submergence. Their findings revealed that while late waterlogging negatively impacted the vegetative phase, it led to improved performance in the generative phase, resulting in increased grain yield. In contrast, early waterlogging severely affected oat performance during vegetative and generative phases.

Delgado et al. assessed the facilitation effects of *Gevuina avellana*, an aluminum hyperaccumulator, on the seedling growth and performance of *Vaccinium corymbosum*, a plant sensitive to aluminum intolerance and phosphorus deficiency, in soils supplemented with varying aluminum doses. The results indicated that co-cultivation with *G. avellana* ameliorated the growth conditions for *V. corymbosum*, highlighting the beneficial influence of *G. avellana*.

Luo et al. investigated the role of SPX-domain-containing proteins (SPXs) in phosphorus homeostasis in maize, with a particular emphasis on ZmSPX1. Their study demonstrated that overexpressed lines exhibited increased root sensitivity to both phosphorus deficiency and high-phosphorus conditions. These findings hold significant implications for enhancing phosphorus efficiency in maize breeding programs.

In conclusion, the articles included in this Research Topic contribute to our understanding of the efficacy of various nutrients in alleviating diverse stresses and plant nutrient relations, while illustrating the need for more such research. A better understanding of different nutrient elements could lead to more rational fertilizing practices, avoiding interactions that could contribute to the unbalanced mineral nutrition of plants for maximizing crop yield. This knowledge is also necessary to obtain more efficient genotypes in the acquisition of different nutrients.

Author contributions

MH: Conceptualization, Writing – original draft, Writing – review & editing. PG: Writing – original draft, Writing – review & editing. KM: Supervision, Writing – original draft, Writing – review & editing.

Acknowledgments

MH greatly acknowledges the support of the Alexander von Humboldt Foundation (AvH), Germany.

Conflict of interest

The authors declare that the research was conducted in the absence of any commercial or financial relationships that could be construed as a potential conflict of interest.

The author(s) declared that they were an editorial board member of Frontiers, at the time of submission. This had no impact on the peer review process and the final decision.

Publisher's note

References

Ahmed, M., Hasanuzzaman, M., Raza, M. A., Malik, A., and Ahmad, S. (2020). Plant nutrients for crop growth, development and stress tolerance. *Sustain. Agric. era Climate Change* 1, 43–92. doi: 10.1007/978-3-030-45669-6_3

Bashir, S. S., Hussain, A., Hussain, S. J., Wani, O. A., Zahid Nabi, S., Dar, N. A., et al. (2021). Plant drought stress tolerance: Understanding its physiological, biochemical and molecular mechanisms. *Biotech. Biotech. Equip.* 35, 1912–1925. doi: 10.1080/13102818.2021.2020161

Berkhout, E. D., Malan, M., and Kram, T. (2019). Better soils for healthier lives? An econometric assessment of the link between soil nutrients and malnutrition in Sub-Saharan Africa. *PLoS One* 14, e0210642. doi: 10.1371/journal.pone.0210642

Cabot, C., Martos, S., Llugany, M., Gallego, B., Tolrà, R., and Poschenrieder, C. (2019). A role for zinc in plant defense against pathogens and herbivores. *Front. Plant Sci.* 10. doi: 10.3389/fpls.2019.01171

Cakmak, I. (2005). The role of potassium in alleviating detrimental effects of abiotic stresses in plants. *J. Plant Nutr. Soil Sci.* 168, 521–530. doi: 10.1002/jpln.200420485

Chowdhury, M. S. N., Sani, M. N. H., Siddique, A. B., Hossain, M. S., and Yong, J. W. H. (2024). Synergistic effects of biochar and potassium co-application on growth, physiological attributes, and antioxidant defense mechanisms of wheat under water deficit conditions. *Plant Stress* 12, 100452. doi: 10.1016/j.stress.2024.100452

Dobermann, A., Bruulsema, T., Cakmak, I., Gerard, B., Majumdar, K., McLaughlin, M., et al. (2022). Responsible plant nutrition: A new paradigm to support food system transformation. *Glob Food Sec.* 33, 100636. doi: 10.1016/j.gfs.2022.100636

Elmer, W. H., and Datnoff, L. E. (2014). Mineral nutrition and suppression of plant disease. *Encyclopedia of Agriculture and Food Systems.* 4, 231–244. doi: 10.1016/B978-0-444-52512-3.00251-5

Hofmann, T., Lowry, G. V., Ghoshal, S., Tufenkji, N., Brambilla, D., Dutcher, J. R., et al. (2020). Technology readiness and overcoming barriers to sustainably implement nanotechnology-enabled plant agriculture. *Nat. Food.* 1, 416–425. doi: 10.1038/s43016-020-0110-1

Hossain, M. S., and Dietz, K. J. (2016). Tuning of redox regulatory mechanisms, reactive oxygen species and redox homeostasis under salinity stress. *Front. Plant Sci.* 7. doi: 10.3389/fpls.2016.00548

Kumari, V. V., Banerjee, P., Verma, V. C., Sukumaran, S., Chandran, M. A. S., Gopinath, K. A., et al. (2022). Plant nutrition: An effective way to alleviate abiotic stress in agricultural crops. *Int. J. Mol. Sci.* 23, 8519. doi: 10.3390/ijms23158519

Kumssa, D. B., Joy, E. J., Ander, E. L., Watts, M. J., Young, S. D., Walker, S., et al. (2015). Dietary calcium and zinc deficiency risks are decreasing but remain prevalent. *Sci. Rep.* 5, 10974. doi: 10.1038/srep10974

Mannan, M. A., Tithi, M. A., Islam, M. R., Al Mamun, M. A., Mia, S., Rahman, M. Z., et al. (2022). Soil and foliar applications of zinc sulfate and iron sulfate alleviate the destructive impacts of drought stress in wheat. *Cer Res. Commun.* 50, 1279–1289. doi: 10.1007/s42976-022-00262-5

Marschner, P. (2012). *Marschner's Mineral Nutrition of Higher Plants. 3rd Edn* (London: Academic Press).

Marschner, H., and Cakmak, I. (1989). High light intensity enhances chlorosis and necrosis in leaves of zinc, potassium, and magnesium deficient bean (Phaseolus vulgaris) plants. *J. Plant Physiol.* 134, 308–315. doi: 10.1016/S0176-1617(89)80248-2

Sarwar, M., Saleem, M. F., Ullah, N., Ali, S., Rizwan, M., Shahid, M. R., et al. (2019). Role of mineral nutrition in alleviation of heat stress in cotton plants grown in glasshouse and field conditions. *Sci. Rep.* 9, 13022. doi: 10.1038/s41598-019-49404-6

Shoukat, A., Pitann, B., Hossain, M. S., Saqib, Z. A., Nawaz, A., and Mühling, K. H. (2024b). Zinc and silicon fertilizers in conventional and nano-forms: Mitigating salinity effects in maize (*Zea mays* L.). *J. Plant Nutri Soil Sci*. 1–12. doi: 10.1002/jpln.202300267

Shoukat, A., Saqib, Z. A., Akhtar, J., Aslam, Z., Pitann, B., Hossain, M. S., et al. (2024a). Zinc and silicon nano-fertilizers influence ionomic and metabolite profiles in maize to overcome salt stress. *Plants* 13, 1224. doi: 10.3390/plants13091224

Sun, H., and Weaver, C. M. (2020). Rise in potassium deficiency in the us population linked to agriculture practices and dietary potassium deficits. *J. Agric. Food Chem.* 68, 11121–11127. doi: 10.1021/acs.jafc.0c05139

Van Nguyen, D., Nguyen, H. M., Le, N. T., Nguyen, K. H., Nguyen, H. T., Le, H. M., et al. (2022). Copper nanoparticle application enhances plant growth and grain yield in maize under drought stress conditions. *J. Plant Growth Regul.* 41, 364–375. doi: 10.1007/s00344-021-10301-w

Waraich, E. A., Ahmad, R., and Ashraf, M. Y. (2011). Role of mineral nutrition in alleviation of drought stress in plants. *Aust. J. Crop Sci.* 5, 764–777. doi: 10.3316/informit.282340708899391

frontiers | Frontiers in Plant Science

TYPE Original Research
PUBLISHED 19 July 2023
DOI 10.3389/fpls.2023.1197553

OPEN ACCESS

EDITED BY
Pedro Garcia,
University of Almeria, Spain

REVIEWED BY
Juan Pablo Martinez,
Agricultural Research Institute, Chile
Yuanyue Shen,
Beijing University of Agriculture, China

*CORRESPONDENCE
Zaiqiang Yang
yzq@nuist.edu.cn

RECEIVED 31 March 2023
ACCEPTED 27 June 2023
PUBLISHED 19 July 2023

CITATION
Zheng Y, Yang Z, Luo J, Zhang Y, Jiang N and Khattak WA (2023) Transcriptome analysis of sugar and acid metabolism in young tomato fruits under high temperature and nitrogen fertilizer influence.
Front. Plant Sci. 14:1197553.
doi: 10.3389/fpls.2023.1197553

Transcriptome analysis of sugar and acid metabolism in young tomato fruits under high temperature and nitrogen fertilizer influence

Yanjiao Zheng[1], Zaiqiang Yang[1*], Jing Luo[1], Yao Zhang[1], Nan Jiang[1] and Wajid Ali Khattak[2]

[1]Jiangsu Key Laboratory of Agricultural Meteorology, School of Applied Meteorology, Nanjing University of Information Science and Technology, Nanjing, Jiangsu, China, [2]School of Environment and Safety Engineering, Jiangsu University, Zhenjiang, Jiangsu, China

Introduction: Environmental temperature and nitrogen (N) fertilizer are two important factors affecting the sugar and organic acid content of tomato fruit. N is an essential nutrient element for plant growth and development, and plays a key role in regulating plant growth, fruit quality and stress response. However, the comparative effect of different N fertilizer levels on the accumulation of soluble sugar and organic acid in tomato young fruit under high temperature stress and its mechanism are still unknown.

Methods: Three N fertilizer levels (N1, N2, N3) combined with two temperatures (28/18°C, CK; 35/25°C, HT) were used to study the effects of N fertilizer, HT and their interaction on the soluble sugar and organic acid components, content, metabolic enzyme activity and the expression level of key genes in tomato young fruit, revealing how N fertilizer affects the sugar and organic acid metabolism of tomato young fruit under HT at physiological and molecular levels.

Results: The content of soluble sugar and organic acid in tomato young fruit under HT exposure was increased by appropriate N fertilizer (N1) treatment, which was due to the accumulation of glucose, fructose, citric acid and malic acid. High N (N3) and HT exposure had a negative impact on soluble sugar and reduce sugar accumulation. Further studies showed that due to the up-regulation of the expression of sucrose metabolizing enzyme genes (*CWINV2, HK2, SPS, PK*) and sucrose transporter (*SUT1, SUT4, SWEETs*) in tomato, N fertilizer increased the accumulation of soluble sugar by improving the sucrose metabolism, absorption intensity and sucrose transport of fruit under HT exposure. Due to the increase of PEPC gene expression, N fertilizer increased the accumulation of citric acid and malic acid by improving the TCA cycle of fruit under HT exposure.

Discussion: Nitrogen fertilizer can improve the heat tolerance of tomato young fruits by improving sugar metabolism under HT exposure. The results can provide theoretical support for the correct application of N fertilizer to improve the quality of tomato fruit under HT exposure.

KEYWORDS

transcriptomics, tomato, sugar, organic acid, high temperature, nitrogenous fertilizer

1 Introduction

Tomato (*Solanum lycopersicum* L.) is one of the most important horticultural crops in the world. The most efficient method for obtaining premium fresh tomatoes for markets is the protective planting of tomato crops (Renau-Morata et al., 2021). China grows protected tomatoes on 810,000 ha cultivated land (Zheng et al., 2022). Since tomato is rich in sugar and organic acid, lycopene, β-carotene, flavonoids, ascorbic acid, phenolic acid, and other nutrients that contributes to the maintenance of human health and people's taste (Wu et al., 2023), people have higher requirements for tomato flavor and quality. However, in late spring and early summer, the heat generated by solar radiation caused the temperature in the greenhouse to rise sharply. In addition, the greenhouse is a tightly sealed and inadequately ventilated environment, resulting in the interior temperature being 20°C to 30°C higher than the outside temperature (Shamshiri, 2017; Zheng et al., 2020; Zheng et al., 2022). Therefore, high temperature is always a common meteorological disaster in greenhouses.

High temperature (HT) is one of the important environmental factors affecting the sensory and nutritional quality of tomato fruits (Ayenan et al., 2021). Exposure to HT reduces the content of sugar, organic acid, lycopene, and other components in the fruit, thus impacting negatively tomato fruit quality (Hernández et al., 2018; Almeida et al., 2021; Hernández et al., 2022; Mesa et al., 2022). Previous studies mainly focused on the ripening stage of tomatoes; however, little is known about the impact of HT exposure on young fruits. The young fruit stage (< 10 days post-anthesis) is the most sensitive and golden period of the entire fruit development process (Quinet et al., 2019; Zheng et al., 2022). This stage is the peak of cell division activity, which determines the number of cells and, subsequently influences the size, weight, and shape of the fruit (Azzi et al., 2015). In addition to these morphological characteristics, the sensory and nutritional quality characteristics of mature tomato fruits are also identified early, including the accumulation of sugars and organic acids (Azzi et al., 2015; Bauchet et al., 2017). Eighty percent of the sugars in tomato fruits originate from the source organs (leaves) and are transported through the phloem and released into the fruit in the form of sucrose (Powell et al., 2012). Sucrose is broken down into monosaccharide and uridine diphosphate glucose (UDPG) under the action of invertase and sucrose synthase (SS), providing energy to the fruit for the synthesis of starch, cellulose, and various other cellular components (Li et al., 2012). The timely unloading and utilization of sucrose in the sink contributes to the formation of a sucrose concentration difference between the source leaves and the fruit, which promotes the continuous transport of sucrose to the fruit and plays a crucial role in regulating the distribution and intensity of photosynthetic compounds sink (Zhang et al., 2021). Moreover, sucrose and its hexose cleavage products can regulate plant development and stress response through carbon partitioning and sugar signaling (Vijayakumar et al., 2021; Zhang et al., 2022). Several molecular and physiological studies have shown that glucose serves as a signal to promote cell division in embryos during early development (Ruan et al., 2010). Research has shown that heat leads to a reduction in the source/sink ratio, which impairs fruit development by shortening cell division time and reducing cell number and size, ultimately leading to accelerated fruit development and reduced fruit quality (Adams et al., 2001; Bertin, 2005). Therefore, examining the effect of HT on sugar and acid metabolism during the young fruit stage is critical for understanding the effect of HT on fruit quality of tomato.

In addition to HT, nitrogen (N) fertilizer application during cultivation can also affect fruit development and quality (Erdinc et al., 2018). Experimental results indicate that sugar and organic acid content in tomato fruits is proportional to N fertilizer at a certain level, which improves fruit quality (Hernández et al., 2020; Ronga et al., 2020). Although N has a positive effect on fruit quality, excess N affects the carbon (C) and N balance, decreasing the amount of soluble sugar in tomato fruit, while increasing the organic acid content, and decreasing fruit flavor quality (Bénard et al., 2009; Gruda et al., 2018; Truffault et al., 2019).

Considering that both HT and N fertilizers are important factors affecting fruit quality, some studies have investigated the comprehensive effects of HT and N. N can reduce the reactive oxygen species toxicity in rice (Wei et al., 2018) and corn (Yan et al., 2017) to resist HT by increasing antioxidant concentration and photosynthetic utilization rate. Xu et al. (2022) found that adequate N fertilization can mitigate the adverse effects of HT during grain filling on milling quality and chalky occurrence to some extent. Previous research has shown that N fertilizer increases the sensitivity of maize (Ordóñez et al., 2015), rice (Tang et al., 2019), and wheat (Elía et al., 2018) to HT, and these studies suggest that excessive N exacerbates yield losses due to temperature increase. These results highlight the complex relationship between N levels and HT, suggesting that each crop species may have the best combination of HT and N levels (Yang et al., 2015). Unfortunately, few studies have shown the possibility of such interactions between HT and N fertilizer rates in tomato young stage.

The development of high-throughput sequencing and genome sequencing data for tomato offers important methods and references for exploring complex regulatory networks and identifying new key genes (Su et al., 2022). With the improved of RNA sequencing (RNA-seq) efficiency, transcriptome analysis has identified many genes involved in tomato response to heat stress. For example, Gul et al. (2021) and Su et al. (2022) discovered key genes associated with heat tolerance in tomato using RNA-seq technology. In addition, the key genes involved in the biochemical pathway and expression characteristics of transport, accumulation,

Abbreviations: AI, acid invertase; NI, neutral invertase; SSc, sucrose synthase-cleavage; SSs, sucrose synthase-synthesis; SPS, sucrose phosphate synthase; HK, hexokinase; G6PD, glucose 6-phosphate dehydrogenase; 6PGD, 6-phosphogluconate dehydrogenase; PFK, phosphofructokinase; PK, pyruvate kinase; SUT, sucrose transporter; SWEET, sugars will eventually be exported transporters; PEPC, phosphoenolpyruvate carboxylase; MDH, malate dehydrogenase; ME, malic enzyme; CS, citrate synthase; cyt-ACO, cytosolic aconitase; mit-ACO, mitochondrion aconitase; IDH, isocitrate dehydrogenase.

and metabolism of sugars and organic acids in tomato fruit were also discovered using RNA-seq technology (Li et al., 2022; Tao et al., 2022; Wu et al., 2023). More importantly, the key genes that respond to N and regulate the metabolism of sugar and organic acids in fruits have been discovered (Wang et al., 2021; Cao et al., 2022). With the advancement of molecular biology technology, more genes involved in plant response to abiotic stress will be discovered and identified in the future.

We hypothesize that there is an interaction between HT and N fertilizer in young tomato fruit, and we also hypothesize that N fertilizer resists heat stress by regulating the activity of sugar and organic acid metabolism enzymes and gene expression. In this paper, three N levels and two temperature treatments were applied to compare the biochemical pathways of sugar and acid metabolism in tomato fruits under different N and temperature treatments. The objective of this study was to determine the interaction between N and HT and to investigate their comprehensive effects on the content, composition, and metabolic enzyme activity of soluble sugars and organic acids in young tomato fruits. RNA Seq analysis was used to identify the key genes involved in sugar and organic acid metabolism in tomato young fruits exposed to N and HT. The research results may provide a theoretical basis for appropriate N application rates under HT conditions to improve heat resistance in young tomato fruits.

2 Materials and methods

2.1 Experimental design

The experiment was conducted at the Agricultural Meteorological Research Station of Nanjing University of Information Science and Technology (32°13′N, 118°43′E; 29 m above mean sea level) in Nanjing, Jiangsu Province, China. "Powder crown" was used as test material, and once it formed 4-5 true leaves, it was planted in a flower pot with dimensions of 28 cm (height) × 34 cm (upper caliber) × 28 cm (bottom diameter), dated February 27, 2022. Soils contained fertilizers, including organic carbon (12.93 g kg^{-1}), organic matter (22.29 g kg^{-1}), available phosphorus (69.36 mg kg^{-1}), available potassium (13.8 mg L^{-1}), and total nitrogen (0.13%). Before transplanting, phosphate and potassium fertilizer were applied to the planting soil all at once as base fertilizer, with the amount of phosphate fertilizer (monocalcium phosphate) being 200 kg ha^{-1} (5.67 g $plant^{-1}$) and the amount of potassium fertilizer (potassium sulphate) being 300 kg ha^{-1} (8.51 g $plant^{-1}$). N fertilizer was applied in three levels: 188 kg ha^{-1} (N1), 250 kg ha^{-1} (N2), and 313 kg ha^{-1} (N3). The N application rate of 250 kg ha^{-1} is the rate currently used by the local farmers. N fertilizer (urea) was used as a topdressing (hole fertilization). Based on the planting density of tomatoes, we calculated that the N application for each tomato plant during the entire growth period was N1 (5.33 g $plant^{-1}$), N2 (7.10 g $plant^{-1}$), and N3 (8.88 g $plant^{-1}$), respectively. We applied N in a ratio of 3:3:2:2 during the seedling, flowering, second, and fourth ear fruit expansion stages of tomato plants. Since our research focused on tomato young fruits, we didn't consider topdressing after flowering. The specific N application was shown in Table 1. Each N level treatment was repeated 20 times (i.e. 20 pots), with one tomato seedling per pot, resulting in a total of 60 pots of tomatoes. After 10 days of transplanting (March 9, 2022), tomato seedlings with consistent growth were randomly selected for the first fertilization as topdressing during the seedling stage. Transplanted tomato potted plants grew in a Velon glass greenhouse. The greenhouse structure has an area of 30 m in length × 9.6 m in width, and 4.5 m in height with north-south orientation. The distance between pots was 35 × 40 cm, and watered every 2 days according to the needs of plant growth to maintain appropriate growth conditions. Until the first order of tomato flowers fully bloomed, N was applied again to the corresponding N level pots as topdressing (April 4, 2022). After 5 days, we conducted a heat stress test, during which the fruits that successfully set were marked and the date of set was recorded. To evaluate the interaction between temperature and nitrogen fertilizer application, we randomly divided pot plants with the same N level into two groups and simultaneously treated them at two different temperatures for 5 days (April 9, 2022)Two artificial climate chambers (Convion BDW40, Canada) were used, one designed for suitable temperature (CK) and the other designed for heat stress (HT). The temperature range of CK treatment was 18-28°C (with an error of ± 0.5°C), and the daily average temperature was 22.7°C; the temperature range of HT treatment was 25-35°C (with an error of ± 0.5°C), the daily average temperature was 29.6°C. The daily variation of temperature was similar to the daily variation of temperature in the natural atmosphere of Nanjing. The minimum and maximum temperatures occurred at 5:00 and 14:00 respectively, as shown in Figure S1. The tomato plants in the artificial climate chamber were arranged in three rows, one row (10 pots) at each N level. Plants at the same N level were randomized. The two artificial climate chambers had the same climate conditions except for temperature treatment. Photosynthetically active radiation (PAR) of the artificial climate

TABLE 1 Application period and amount of N fertilizer (urea) (g $plant^{-1}$).

Growth stage	First application of N fertilizer	Second application of N fertilizer
	Seedling stage (10 days after transplanting, March 9, 2022)	Flowering period (the first order flower is in full bloom, April 4, 2022)
N1	1.60	1.60
N2	2.13	2.13
N3	2.66	2.66

room was set as follows: 6:00-10:00 (800 μmol m^{-2} s^{-1}), 11:00-14:00 (1000 μmol m^{-2} s^{-1}), 15:00-18:00 (800 μmol m^{-2} s^{-1}), and the remaining period was 0 μmol m^{-2} s^{-1}. The humidity was set to 60% at 6:00-18:00 in the daytime, 80% at night, and the CO_2 concentration was set to 400 μmol mol^{-1}. During heat stress, plants were watered once a day to ensure the necessary water for normal plant growth. Six treatments were set: N1 application in the CK environment (CKN1); N2 application in the CK environment (CKN2); N3 application in the CK environment (CKN3); N1 application in the HT environment (HTN1); N2 application in the HT environment (HTN2); N3 application in the HT environment (HTN3). After the heat stress test, three tomato young fruit samples that set on the same day were taken from each treatment, the skin and seeds were removed, the flesh was cut into silk and placed in a zipper bag. Then, it was quickly frozen in liquid nitrogen and stored at -80°C until subsequent analysis.

2.2 Measurements and methods

2.2.1 Determination of soluble sugars

Fructose, glucose, and sucrose contents were measured following the procedure given by Ma et al. (2019) with slight modifications. The soluble sugars in the fruit were determined using the colorimetric method. The samples of tomato (5 g) were finely grounded using mortar and pestle with the addition of 10 ml of 80% ethanol, stirred evenly and keep it in a water bath at 80-85°C for 40 min. After cooling, added 0.2 g activated carbon for decolorization for 20 minutes, then centrifuged at 4000 r min^{-1} for 30 minutes. Take the supernatant into a 25 mL volumetric flask. This extraction procedure was repeated three times and the supernatants were combined and finally dilute to 25 mL with distilled water. The solution was then used for the sugar analysis.

2.2.2 Determination of organic acids

The contents of organic acids were measured by high performance liquid chromatography (HPLC) using the method reported by Zheng et al. (2022) with some modifications. The samples of tomato (1 g) were finely grounded using mortar and pestle with the addition of 3 mL of distilled water. The solution was transferred into a centrifuge tube and added distilled water to make a constant volume of 5 mL, and then centrifuged at 4000 r min^{-1} for 10 minutes at 4°C. For each sample, 20 μL of the supernatant was filtered through a 0.45 μm membrane and then injected into the HPLC system for analysis. 0.01 mol L^{-1} KH_2PO_4 (pH 2.55): methanol (97/3) (v/v) was used as the mobile phase with a flow rate of 0.5 mL min^{-1}. The column was 0.5 μm C18 column (250 mm×4.6 mm, Agilent, USA) at 30°C. Organic acids were detected at a wavelength of 210 nm.

2.2.3 Extraction and determination of sucrose and organic acids metabolism-related enzymes

Enzymes involved in sucrose metabolism were extracted following the procedure proposed by Wu et al. (2020) with slight modifications. All procedures were conducted at 4°C. Tomato samples (1 g) were homogenized with 10 mL of 100 mmol L^{-1} phosphate buffer (pH 7.5) containing 10 mmol L^{-1} $MgCl_2$, 1 mmol L^{-1} EDTA, 0.1% (v/v) tritonX-100, 0.2% 2-Hydroxy-1-ethanethiol, and 2% polyvinyl pyrrolidone (PVP). The homogenate was centrifuged at 4000 r min^{-1} for 15 min. The supernatant (crude enzyme extract) was used to determine the activity of enzymes involved in sucrose metabolism (acid invertase (AI), neutral invertase (NI), sucrose synthase-cleavage (SSc), sucrose synthase-synthesis (SSs), sucrose phosphate synthase (SPS)) following the procedure given by Zheng et al. (2022) with slight modifications.

Enzymes involved in organic acids metabolism were extracted following the procedure proposed by (Wu et al., 2020) with slight modifications. Tomato samples (10 g) were homogenized with 10 mL of 200 mmol L^{-1} Tris-HCl buffer solution (pH 8.2) containing 600 mmol L^{-1} sucrose and 10 mmol L^{-1} isoascorbic acid. The homogenate was centrifuged at 4000 r min^{-1} for 20 min, and then taken the supernatant and made up to the final volume (10 mL) with ice-cold extract buffer as crude enzyme solution. The solution was used to determine the activity of enzymes involved in organic acids metabolism, which included phosphoenolpyruvate carboxylase (PEPC), malate dehydrogenase (MDH), malic enzyme (ME), citrate synthase (CS), cytosolic aconitase (cyt-ACO), mitochondrion aconitase (mit-ACO) and isocitrate dehydrogenase (IDH).

2.2.4 Transcriptome sequencing analysis

The transcriptome analysis of tomato pulp grown under two temperatures and three N levels was carried out. There were 3 biological replicates per sample, a total of eighteen samples. Total RNA was extracted from the tissue using the TrizolLysis Reagent reagent (Qiagen, Germany) according to the manufacturer's instructions. garose gel electrophoresis Biowest Agarose (Biowest, Spain) was used to detect whether RNA was degraded, and Nanodrop 2000 (Thermo Fisher Scientific, USA) was used to detect the concentration and purity of the extracted RNA. Then RNA quality was determined by 5300 Bioanalyser (Agilent, USA) and quantified using the ND-2000 (NanoDrop Technologies, USA). Approximately, 1μg of RNA per sample was used for cDNA library construction by Illumina NovaSeq Reagent Kit for Illumina (New England BioLabs, USA) following the manufacturer's recommendations. The NovaSeq 6000 sequencing platform was used for high-throughput sequencing, and 150 bp double ended data was obtained. The sequencing process was completed by Shanghai Majorbio. To ensure the accuracy of subsequent biological information analysis, the original sequencing data was filtered through fastp (Renau-Morata et al., 2021) software to obtain high-quality clean data. The original data after quality control was compared with the reference genome (ftp://ftp.solgenomics.net/genomes/Solanum_lycopersicum/Heinz1706/assembly/build_4.00/) through HiSat2 software to obtain mapped data (reads), and the quality of the transcriptome sequencing comparison results was evaluated. RSEM was used to quantify gene abundances. Essentially, differential expression analysis was performed using the DESeq2 (Liao et al., 2022). DEGs with |

log2FC| > 2 and FDR ≤ 0.05 (DESeq2) were considered significantly different expressed genes. In addition, functional-enrichment analysis including GO and KEGG was performed to identify which DEGs were significantly enriched in GO terms and metabolic pathways at BH-corrected P-adjust ≤ 0.5 compared with the whole-transcriptome background (Li et al., 2021).

2.3 Statistical analysis

Data were analyzed and graphed (bar graphs and heat maps) using Origin 2023 (Electronic Arts Inc, USA). The data significance was tested using the LSD method in one-way ANOVA with a significance level of $P < 0.05$. Values were presented as the means standard error (SE) in at least biological triplicate for each measurement.

3 Results

3.1 Effect of nitrogen-temperature treatments on sucrose metabolism

Under different temperatures (CK and HT), the main sugars (i.e. sucrose, fructose, and glucose) involved in sucrose metabolism in tomato young fruits showed varying degrees of response to N levels (Figure 1). The results showed that temperature, N levels, and their interactions had a significant impact on sucrose, glucose, and fructose content ($P < 0.001$). Under the same N level, HT exposure significantly reduced sucrose content. In addition, under the same temperature environment (CK and HT), the sucrose content was ranked as N3>N2>N1 (Figure 1A). Contrary to sucrose, HT exposure significantly increased glucose content at the same N level. In the CK environment, the glucose content increased with the increase of N application, while in the HT environment, N3 was significantly lower than N2 (10.045%) (Figure 1B). For fructose content, at the N1 and N3 levels, compared to CK, HT exposure significantly increased fructose content by 65.646% and 13.049%, respectively (Figure 1C). The highest soluble sugar content was observed under HTN1 treatment (Figure 1D).

Figure 2 shows the effect of N fertilizer on the key enzyme activity of sucrose metabolism (i.e. AI, NI, SSs, SSc, and SPS) in tomato young fruits under different temperature environments. The results showed that temperature, N levels, and their interactions had a significant impact on AI, NI, SSs, SSc, and SPS enzyme activities ($P < 0.001$). Fertilizing to N2 and N3, HT exposure increased AI activity by 193.647% and 95.716%, respectively (Figure 2A), and increased SSc activity by 25.177% and 23.416%, respectively (Figure 2B). At three N levels, HT exposure significantly increased the activity of NI and SPS (Figures 2C, D); on the contrary, HT exposure at the N1 and N2 reduced SSs activity by 52.673% and 26.223%, respectively. In addition, under the same temperature, the activity of SSs was negatively correlated with N application (Figure 2E).

3.2 Effect of nitrogen-temperature treatments on organic acid metabolism

Figure 3 shows the effect of N fertilizer on organic acid composition (i.e. citric acid, malic acid, tartaric acid, α-ketoglutaric acid, and succinic acid) at different temperatures. The variance results showed that temperature, N levels, and their interactions had a significant impact on the organic acid compositions ($P < 0.001$). Under N1 and N2 treatments, compared to CK, HT exposure increased the citric acid content by 21.975% and 14.284%, respectively, while under N3 treatment, HT exposure reduced the citric acid content by 11.462% (Figure 3B). Fertilizing to N2 and N3, HT exposure increased the malic acid content by 47.743% and 121.448%, respectively (Figure 3C). On the contrary, at the same N level, HT exposure significantly reduced the content of tartaric acid, α-ketoglutaric acid, and succinic acid, compared to CK (Figures 3D–F). Overall, the organic acid content was highest at CKN1, and fertilizing to N2 and N3, HT exposure increased the organic acid content by 6.253% and 13.894%, respectively. In addition, CKN2 and CKN3, HTN1 and HTN3 treatments had no significant effect on organic acid content (Figure 3A).

Figure 4 shows the effect of N fertilizer on the key enzyme activity of organic acid metabolism (i.e. PEPC, ME, MDH, CS, cyt-ACO, mit-ACO, and IDH) in tomato young fruits under different temperature environments. The results showed that temperature, N levels, and their interactions had a significant impact on the key enzyme activities ($P < 0.001$). At the same N level, compared to CK, HT exposure significantly reduced the enzyme activities of PEPC, MDH, cyt-ACO, mit-ACO, and IDH (Figures 4A, C, E–G). At HT environment, PEPC enzyme activity decreased with the increase of N application, while MDH enzyme activity increased with the increase of N application, and IDH enzyme activity had no significant effect on N application. At the N3 level, HT exposure significantly reduced CS enzyme activity by 31.078%, while at the N1 and N2 levels, CK and HT temperature treatments had no significant effect on CS enzyme activity (Figure 4D).

3.3 Quality assessment of transcriptome sequencing results

To further explore the molecular events of sugar and organic acid metabolism as affected by N and temperature, RNA sequence analysis was performed on 18 tomato young fruit samples from 6 treatments and 3 biological replicates. The quality assessment of transcriptome sequencing was shown in Table 2. At least 46719846 raw reads were obtained in all samples, after screening and filtering, 138,086,648 clean reads and 44977486 clean bases were obtained. The proportion of clean reads in each sample was greater than 96%, Q20 was more than 98%, Q30 was more than 94%, and the GC content was higher than 43%. These results indicated that the sequencing quality was favorable for subsequent analyses.

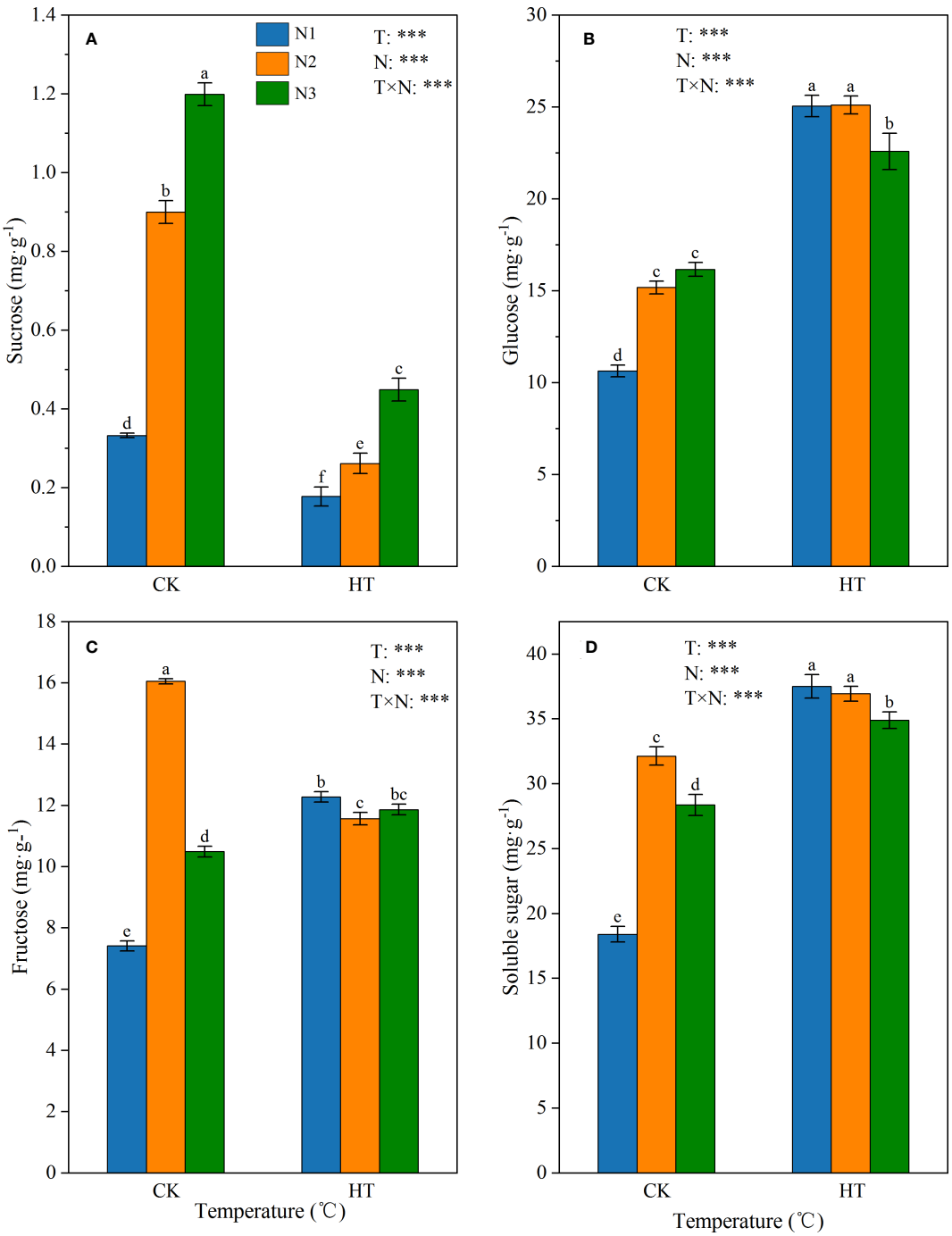

FIGURE 1
The contents of sucrose **(A)**, glucose **(B)**, fructose **(C)**, and soluble sugar **(D)** in tomato young fruits under different nitrogen (N1, N2, and N3) and temperature (CK, control; HT, high temperature) treatments. Different alphabets (a, b, and c) indicate significant differences between means at $P < 0.05$ using the LSD method. Error bars indicate standard errors (n=3); T, N, and T × N represent temperature treatment, N fertilizer treatment, and their interaction, respectively; *** represents the significant level at $P < 0.001$.

3.4 Screening results of DEGs

To study the transcription of tomato fruit under HT at the same N level, we compared and analyzed the transcriptome data of HTN1 vs CKN1, HTN2 vs CKN2, HTN3 vs CKN3. According to the volcano map Figure 5, a total of 5217 DEGs were screened from HTN1 vs CKN1. Among them, 2161 genes were up-regulated and 3056 genes were down-regulated in the HTN1group compared with the CKN1 group, respectively (Figure 5A). In HTN2 vs CKN2 group, a total of 1624 DEGs were screened, including 549 up-regulated genes and 1075 down-regulated genes, respectively (Figure 5B). A total of 1337 DEGs were screened out in HTN3 vs CKN3 group, of which 726 genes were up-regulated and 611 genes were down-regulated, respectively (Figure 5C). The group of HTN1 vs CKN1 had the

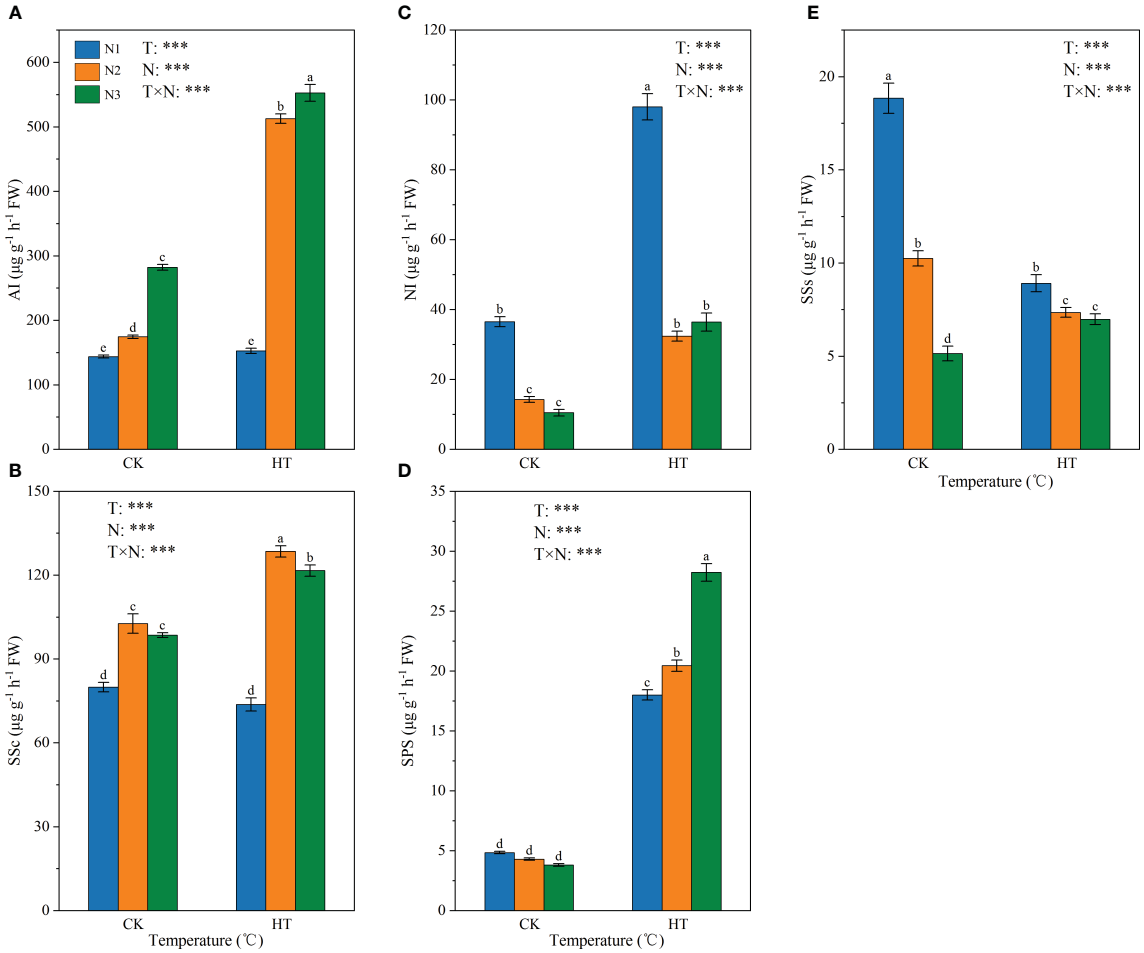

FIGURE 2
The activity of AI **(A)**, SSc **(B)**, NI **(C)**, SPS **(D)**, and SSs **(E)** in tomato young fruits under different nitrogen (N1, N2, and N3) and temperature (CK, control; HT, high temperature) treatments. AI, acid invertase; NI, neutral invertase; SSc, sucrose synthase-cleavage; SSs, sucrose synthase-synthesis; SPS, sucrose phosphate synthase. Different alphabets (a, b, and c) indicate significant differences between means at $P < 0.05$ using the LSD method. Error bars indicate standard errors (n=3); T, N, and T × N represent temperature treatment, N fertilizer treatment, and their interaction, respectively; *** represents the significant level at $P < 0.001$.

largest value of DEGs, and the number of DEGs in the HTN2 vs CKN2 groups was greater than that in HTN3 vs CKN3 groups (Figure 5D and Table S1), indicating that some genes are differentially expressed in the various treatments of nitrogen-temperature and that the number of differentially expressed genes decreases with the increase of N fertilizer application.

3.5 GO functional categorization of DEGs

To further characterize nitrogen-temperature treatment-responsive DEGs, GO analysis was performed. The top-20 GO enrichment histograms of the DEGs was presented in Figure 6 and Table S2. According to GO functional analysis, DEGs were mainly divided into three functional categories: molecular function (MF), cellular component (CC), and biological process (BP). The three groups (HTN1 vs CKN1, HTN2 vs CKN2, and HTN3 vs CKN3) of generated DEGs showed certain similarity in GO enrichment analysis. There were eight items enriched in BP, among which GO: 0009987 (cellular process), GO: 0008152 (metabolic process), and GO: 0065007 (biological regulation) were enriched in more DEGs. There were seven entries enriched in CC, among which GO: 0044464 (cell part), GO: 0044425 (membrane part), and GO: 0043226 (organelle) were enriched in more DEGs. There were five entries enriched in MF, among which GO: 0003824 (catalytic activity) and GO: 0005488 (binding) were enriched in more DEGs. The functional classification results of DEGs in metabolic process, cell part and catalytic activity showed that the metabolism and enzyme catalytic function of tomato young fruits would change with the variation of temperature and N fertilizer application.

3.6 KEGG enrichment analysis of DEGs

To further investigate the possible molecular functions of DEGs in HTN1 vs CKN1, HTN2 vs CKN2, and HTN3 vs CKN3, KEGG enrichment analysis was performed, and 20 pathways with the most significant enrichment were selected for representation a bubble chart (Figure 7 and Table S3). The three groups were enriched with 1704, 549, and 461 DEGs, respectively, in which the categories of

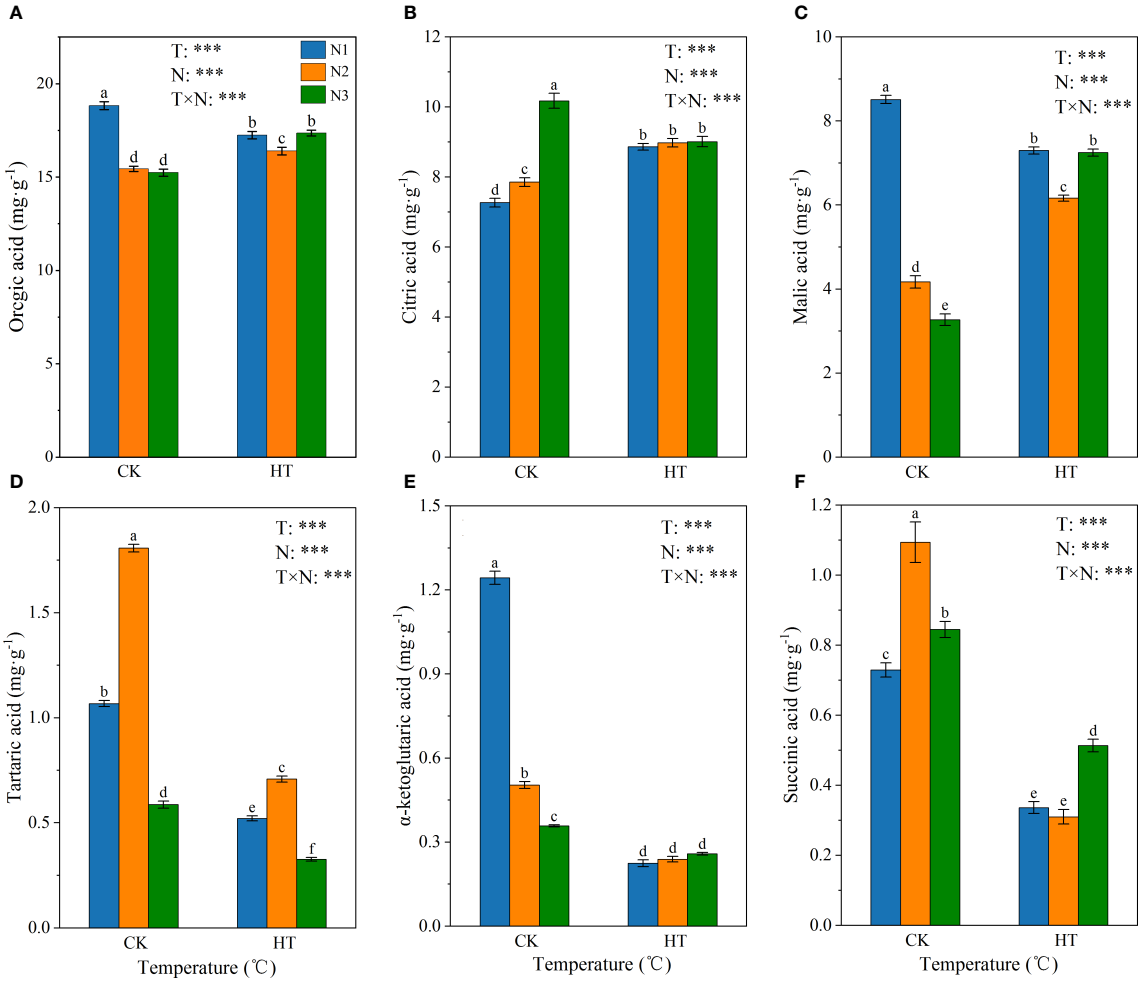

FIGURE 3
The content of organic acid **(A)**, citric acid **(B)**, malic acid **(C)**, tartaric acid **(D)**, α-ketoglutaric acid **(E)** and succinic acid **(F)** in tomato young fruits under different nitrogen (N1, N2, and N3) and temperature (CK, control; HT, high temperature) treatments. Different alphabets (a, b, and c) indicate significant differences between means at $P < 0.05$ using the LSD method. Error bars indicate standard errors (n=3); T, N, and T × N represent temperature treatment, N fertilizer treatment, and their interaction, respectively; *** represents the significant level at $P < 0.001$.

biosynthesis, signal transduction, and metabolism were the most enriched pathways. Notably, in the metabolism category, the most enriched pathway was carbohydrate metabolism, amino acid metabolism, and lipid metabolism. KEGG analysis showed that many DEGs were involved in starch and sucrose metabolism, purine metabolism, glycolysis/gluconeogenesis, glyoxylate and dicarboxylate metabolism, fructose and mannose metabolism, amino sugar and nucleotide sugar metabolism, and glycosaminoglycan degradation. These pathways were related to sugar and acid metabolism in tomato young fruits, indicating that nitrogen-temperature treatments during this period may have a significant regulatory effect on sugar and organic acid metabolism.

3.7 Screening and differential expression of sucrose and organic acid-related genes

To further analyze the DEGs encoding enzymes related to sucrose and organic acid metabolism in HTN1 vs CKN1, HTN2 vs CKN2, and HTN3 vs CKN3, 115 DEGs related to sucrose and organic acid metabolism were screened from RNA-seqdata. Among them, 74 DEGs related to sucrose metabolism were compared in three groups, including 31 down-regulated genes and 26 up-regulated genes in every group. There were 41 organic acid-related DEGs in the three groups, including 21 down-regulated genes and 20 up-regulated genes in HTN1 vs CKN1 group, and 19 down-regulated genes and 22 up-regulated genes in HTN2 vs CKN2 and HTN3 vs CKN3 groups. In the three groups, the genes related to sucrose and organic acid metabolism were differentially expressed in different N-temperature treatments.

In the process of sugar metabolism, the DEGs were mainly annotated in the metabolisms of sucrose, fructose, and glucose (Figure 8A). Sucrose produced by photosynthesis is mainly converted into hexose by invertase. After HT exposure, the expression of *Invertase* was changed with the log2FC ranging from -4.483 to 3.545 (Figure 8B). HTN1 and HTN2 decreased the expression level of invertase and inhibited the conversion of sucrose into fructose and glucose. Additionally, six genes related to *SS* were found in 57 sucrose-related genes, of which HTN1 vs CKN1 and HTN3 vs CKN3 were down-regulated and HTN2 vs CKN2 were up-

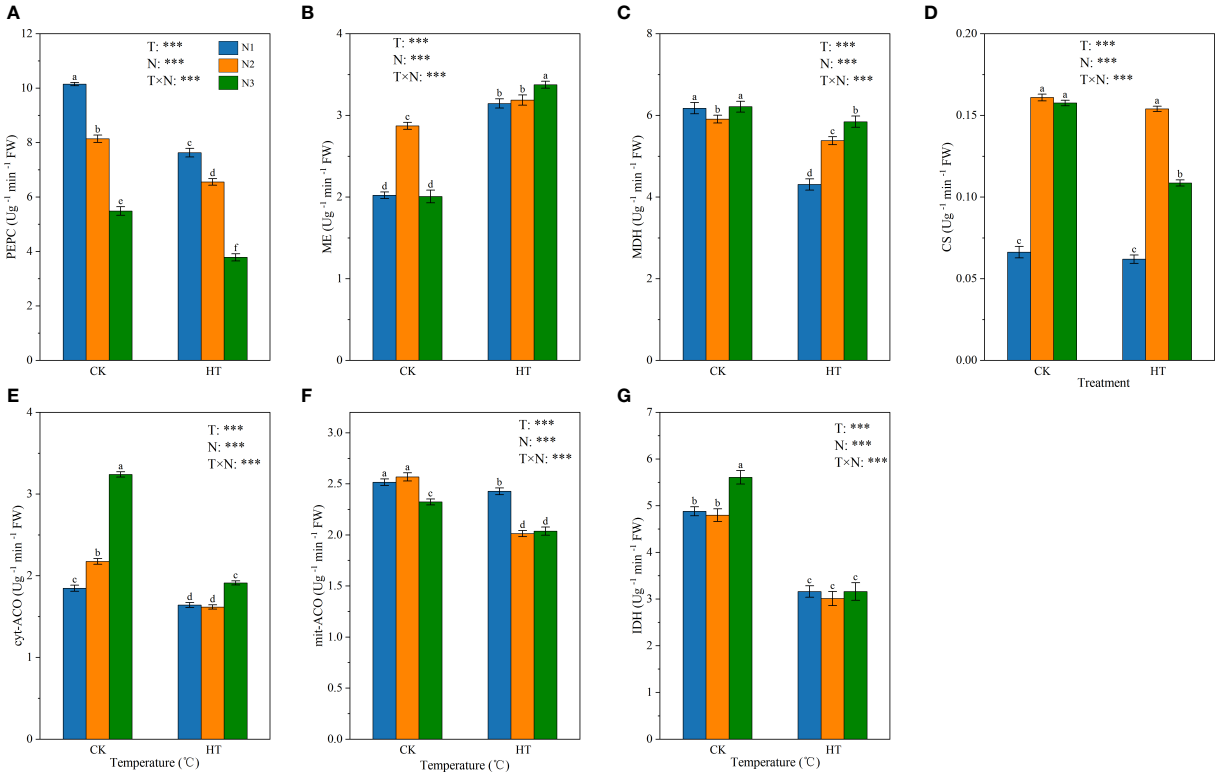

FIGURE 4
The activity of three malate metabolism-related enzymes (PEPC **(A)**, ME **(B)**, and MDH **(C)**) and four citric acid metabolism-related enzymes (CS **(D)**, cyt-ACO **(E)**, mit-ACO **(F)**, and IDH **(G)**) in tomato young fruits under different nitrogen (N1, N2, and N3) and temperature (CK, control; HT, high temperature) treatments. PEPC, phosphoenolpyruvate carboxylase; MDH, malate dehydrogenase; ME, malic enzyme; CS, citrate synthase; cyt-ACO, cytosolic aconitase; mit-ACO, mitochondrion aconitase; IDH, isocitrate dehydrogenase. Different alphabets (a, b, and c) indicate significant differences between means at $P < 0.05$ using the LSD method. Error bars indicate standard errors (n=3); T, N, and T × N represent temperature treatment, N fertilizer treatment, and their interaction, respectively; *** represents the significant level at P < 0.001.

TABLE 2 Statistical results of transcriptome sequencing of young tomato fruit.

Sample	Raw reads	Clean reads	Clean bases	Q20 (%)	Q30 (%)	GC content (%)
CKN3-1	59711860	57773462	8389310670	98.09	94.41	43.56
CKN3-2	55895760	54011280	7945575293	98.14	94.50	43.45
CKN3-3	50871570	49138204	7212091624	98.12	94.52	43.18
CKN2-1	48281446	46532680	6894668437	98.12	94.47	43.59
CKN2-2	54235798	52550584	7745223564	98.10	94.44	43.50
CKN2-3	58843248	56702642	8324739785	98.16	94.60	43.72
CKN1-1	46859574	44977486	6626960613	98.00	94.15	43.18
CKN1-2	46719846	45752190	6726803489	98.44	95.11	43.38
CKN1-3	56527124	54751366	8076012865	98.22	94.74	43.30
HTN3-1	60819686	58929074	8628629685	98.19	94.67	43.43
HTN3-2	53312832	51365932	7550787419	98.07	94.38	43.39
HTN3-3	52782316	50938414	7415134572	98.19	94.74	43.49
HTN2-1	58130288	56421662	8110418149	98.12	94.49	43.59
HTN2-2	49348802	47686502	6967694734	98.21	94.72	43.62

(Continued)

TABLE 2 Continued

Sample	Raw reads	Clean reads	Clean bases	Q20 (%)	Q30 (%)	GC content (%)
HTN2-3	55090132	53376982	7762799158	98.17	94.65	43.61
HTN1-1	50823150	49075548	7247235508	98.16	94.64	43.52
HTN1-2	51939976	50196488	7375184416	98.07	94.35	43.49
HTN1-3	52178858	50151088	7411129052	98.05	94.34	43.44
mean	53465125.89	51685088				
total	962372266	930331584				

Q20: The percentage of the number of bases with a Qphred value not less than 20 in the total number of bases. Q30: The percentage of the number of bases with a Qphred value not less than 30 in the total number of bases. GC Content: The percentage of the sum of the quantities of G and C in the total number of bases in high-quality reads.

regulated. *SPS* had five DEGs, of which most were up-regulated at HT exposure. The expression of *hexokinase* (*HK*) increased at HTN1 vs CKN1, while it decreased at HTN2 vs CKN2 and HTN3 vs CKN3. *Glucose 6-phosphate dehydrogenase* (*G6PD*) had three DEGs, two of which were down-regulated. *6-phosphogluconate dehydrogenase* (*6PGD*) and *phosphofructokinase* (*PFK*) had four and eight DEGs, respectively, of which most were down-regulated at HT exposure; while the expression levels of *pyruvate kinase* (*PK*) increased at HT exposure. These genes regulated the conversion between hexoses, further promoting the accumulation of sugars. In addition, sucrose transporters (sucrose transporter (SUT) and sugars will eventually be exported transporters (SWEET)) changed significantly under different nitrogen-temperature treatments. The expression of *SUT* decreased at HTN1 vs CKN1, while it increased at HTN2 vs CKN2 and HTN3 vs CKN3; conversely, the expression of *SWEET* increased at HTN1 vs CKN1, while it decreased at HTN2 vs CKN2 and HTN3 vs CKN3, which ensured sugar transportation.

The organic acid metabolism of tomato is mainly the tricarboxylic acid cycle (TCA cycle), mainly involving citric acid metabolism and malic acid metabolism. The expression of *PEPC* increased under HTN1 vs CKN1 and HTN2 vs CKN2, while it decreased at HTN3 vs CKN3. In the comparison of the three groups, the expression of *CS* was down-regulated, while the expression of *IDH* was up-regulated, and the increase of HTN2 vs CKN2 and HTN3 vs CKN3 groups was higher than that of HTN1 vs CKN1. The expression of *cyt-ACO* was up-regulated in HTN2 vs CKN2, it was down-regulated in HTN1 vs CKN1 and HTN3 vs CKN3. The differential expression of these genes regulates the synthesis and degradation of citric acid. The expression of *PEPC* under HTN1 and HTN2 was increased, thus promoting the synthesis of malic acid. The down-regulation of *ME* expression inhibited the oxidative decarboxylation of malic acid to pyruvate. The expression levels of *MDH1* decreased at HT exposure. The expression of *MDH2* was up-regulated in HTN1 vs CKN1 and HTN3 vs CKN3, it was down-regulated in HTN2 vs CKN2. The differential expression of these genes regulates the synthesis and degradation of malic acid.

4 Discussion

Global warming is causing temperature changes on a scale unprecedented in the last 500 thousand years (Tiwari et al., 2020), and the frequency and intensity of global heat stress are steadily increasing (IPCC, 2021), with significant negative impacts on agricultural production. As an important agricultural country, China must face the challenges posed by global warming. Against this background, this study aims to simulate heat stress events through pot control experiments and determine the response of sugar and organic acid metabolism in tomato young fruits to heat stress. These results will help to develop reasonable and effective cultivation strategies for greenhouse tomatoes.

4.1 Appropriate N application improved the sucrose metabolism and transport under HT exposure

Soluble sugars, especially sucrose, fructose, and glucose, play a central role in metabolite signaling and response to external stresses in fruit structure and metabolism (Vijayakumar et al., 2021; Zhang et al., 2022). Studies have shown that HT can promote the accumulation of sugar content in fruits (Lokesha et al., 2019), thereby increasing the cell osmotic potential, reducing the cell water potential, and protecting the cell components from pressure-induced damage (Alsamir et al., 2021). In this study, the order of soluble sugar content among the six treatments was HTN1>HTN2>HTN3>CKN2>CKN3>CKN1 (Figure 1D). This result confirms that HT exposure significantly increases soluble sugar content in fruits, which is consistent with previous reports (Mesa et al., 2022). We also found that the soluble sugar content in tomato fruit was more sensitive to heat stress, indicating that HT environment was the main reason for the increase in soluble sugar content compared to N fertilization. Soluble sugar components responded differently to N levels under HT exposure. At the same N level, HT exposure significantly reduced sucrose content, whereas the sucrose content of HTN3 was significantly higher than that of CKN1 (Figure 1A), indicating that excessive nitrogen application under HT exposure may offset the negative effect of HT on sucrose. Under HT exposure, N1 had the highest glucose and fructose content, and with the increase of N application, the hexose content decreased (Figures 1B, C), suggesting that excessive N application under HT exposure may reduce the positive effect of HT on hexose. The highest soluble sugar content was observed under HTN1 treatment (Figure 1D), indicating that N1 was the

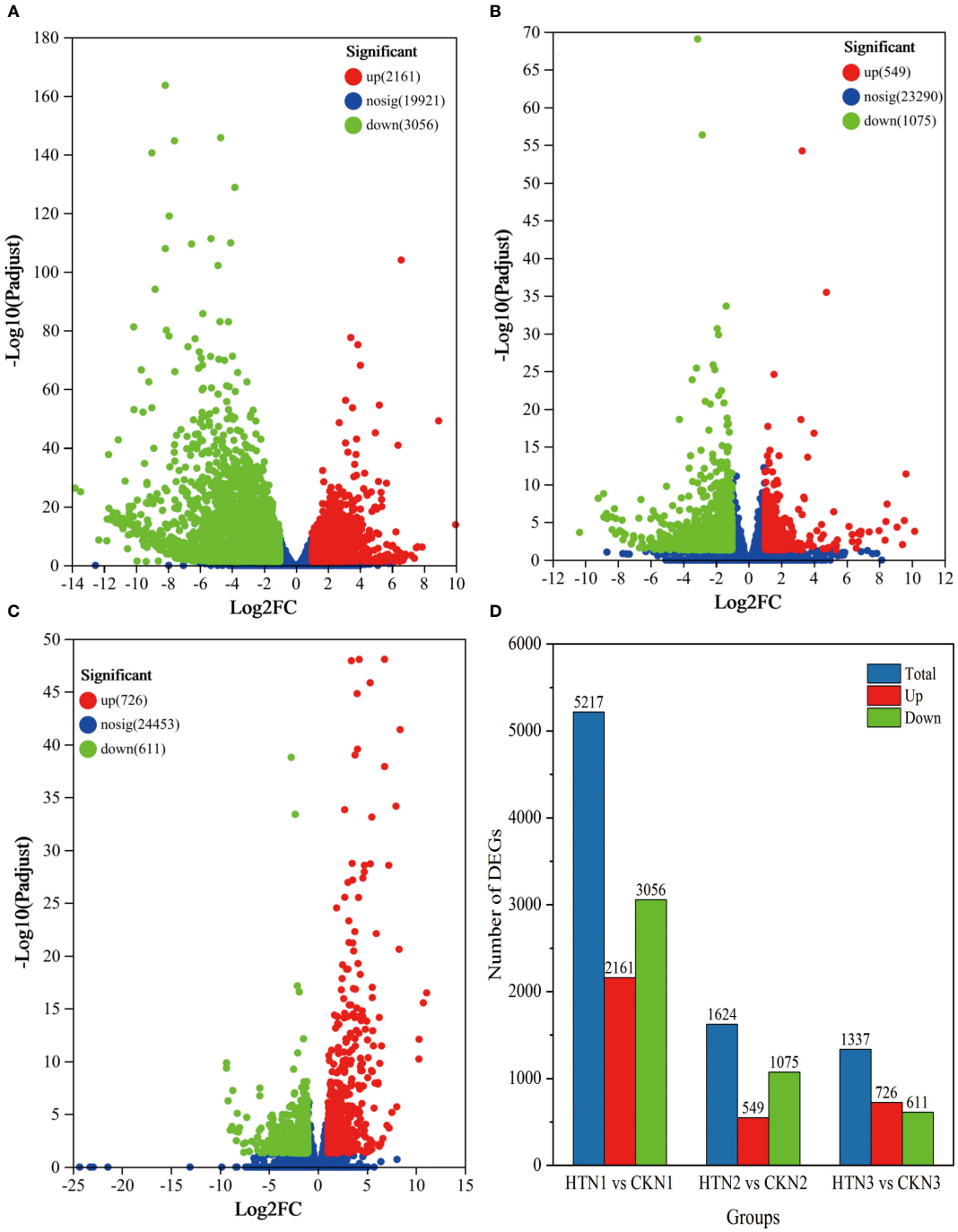

FIGURE 5
The volcano plot of DEGs. DEGs were selected by |log 2 FC| > 2 and padj < 0.05. The x-axis shows the fold change in gene expression, and the y-axis shows the statistical significance of the differences. **(A–C)** represent the GO functions of DEGs at HTN1 vs CKN1, HTN2 vs CKN2, and HTN3 vs CKN3. **(D)** The bar plot of DEG number generated by comparison of HTN1 vs CKN1, HTN2 vs CKN2, and HTN3 vs CKN3.

optimal N application for tomato young fruits under HT exposure. In conclusion, under the interaction of HT and nitrogen fertilizer, the decrease in sucrose and the concomitant increase in glucose and fructose indicate that sucrose degradation dominates its synthesis as a strategy for tomato resistance to heat stress.

The content of soluble sugars and their components in fruits are strongly regulated by metabolism and transport. Invertases (AI and NI) irreversibly catalyze the hydrolysis of sucrose to glucose and fructose, which is crucial for the normal fruit development and response to biotic and abiotic stresses (Qin et al., 2016; Chen et al., 2021). In this study, AI activity of HTN2 and HTN3 was significantly increased, and NI activity was significantly increased at three N levels (Figures 2A, C). We also found a significant negative correlation between sucrose content and NI, while glucose content was significantly positively correlated with AI and NI (Figure S2), indicating that the increase in invertase activity

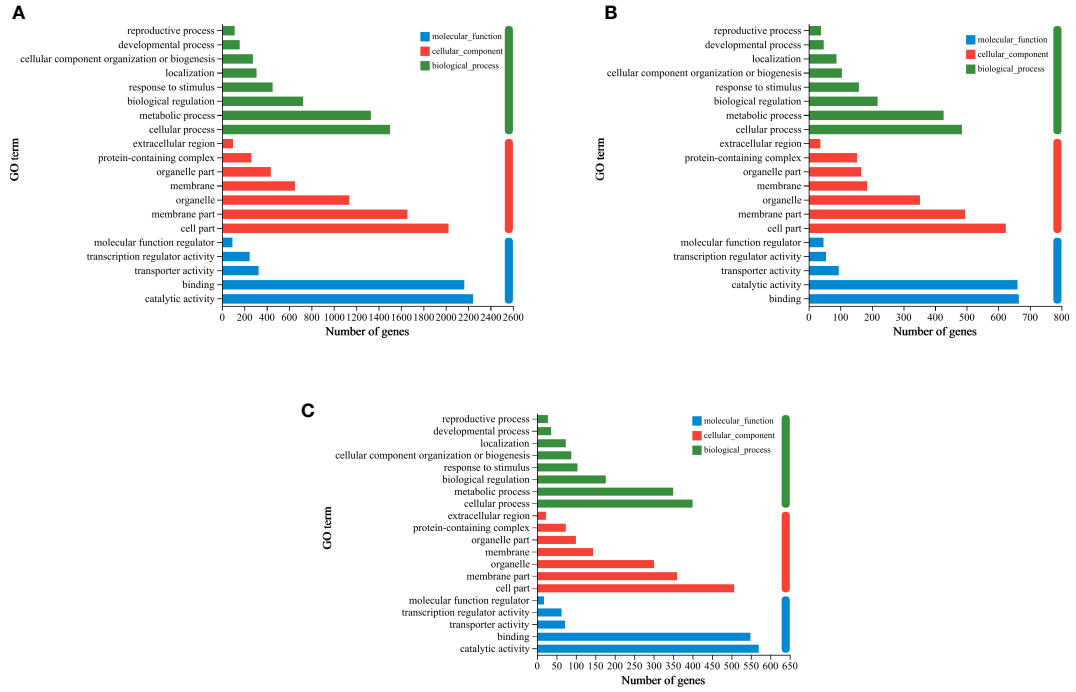

FIGURE 6
GO enrichment column plot. Differentially expressed genes generated by a comparison of **(A)** HTN1 vs CKN1, **(B)** HTN2 vs CKN2, **(C)** HTN3 vs CKN3 are grouped into different GO terms of three ontologies: biological process, cellular component and molecular function.

regulated by N fertilizer under HT exposure was the reason for sucrose degradation. In addition, N2 and N3 treatments under HT exposure resulted in up-regulation of invertase genes, particularly the cell wall invertase *CWINV2* (*Solyc10g085650.2* and *Solyc10g085640.1*) (Figure 8), indicating that N fertilizer has a positive regulatory effect on *CWIN* expression under HT exposure. Up-regulation of *CWIN* expression accelerates sucrose degradation while reducing sucrose concentration in the fruit, promoting phloem unloading and generating sugar signals to regulate cell division, ultimately providing more energy and carbon scaffold for fruit development (Palmer et al., 2015; Li et al., 2016). In the early stages of fruit development, tomato fruits are a strong carbohydrate pool, and previous studies have suggested that SSc plays an important role in the formation of the pool because it can control the ability of tomato young fruits to unload sucrose (Alsamir et al., 2021). However, in this study, the results obtained have large variations. The SSc activity in response to HT was significantly increased at N2 and N3 levels but still significantly lower than AI (Figures 2A, B), and we could not find any significant correlation between it and sucrose content (Figure S2). Therefore, we speculated that N fertilizer regulates sucrose unloading ability of tomato young fruits by affecting AI activity and gene expression under HT stress, rather than SSc. SPS is a key enzyme that promotes sucrose biosynthesis in the cytoplasm and supports sugar exchange between the cytoplasm and vacuoles (Quinet et al., 2019). In this study, SPS activity and gene expression were up-regulated under HT exposure at three N levels (Figures 2D, 8), suggesting that N fertilizer has a positive regulatory effect on SPS under HT exposure. We found a significant positive correlation among SPS activity, AI, and SSc, indicating that SPS can promote sucrose metabolism and contribute to increased sucrose unloading in fruits (Gao et al., 2022). N fertilizer regulates the interaction between sucrose and hexose in fruits by regulating the activity and gene expression of AI, NI, SS, and SPS under HT exposure, thereby controlling sugar content and composition.

Sucrose degrades to fructose and glucose, which are phosphorylated by *HK* and then enter glycolysis and the TCA cycle, providing energy for plant growth and development (Fernie et al., 2004; Zhu et al., 2013). *HK* activity is negatively correlated with hexose content (D'Aoust et al., 1999). In this study, *HK* expression was down-regulated under HT exposure at N2 and N3 (Figure 8), which may lead to a decrease in HK activity, limiting hexose metabolism and ultimately leading to hexose accumulation (Figures 1B, C). In particular, *HK2* (*Solyc06g066440.3*) was most down-regulated and played an important role in hexose accumulation at high temperatures. *PFK* expression was significantly downregulated in HTN1 and HTN3, suggesting that HTN1 inhibits the entry of glucose into glycolysis more strongly, leading to glucose accumulation (Figure 1B). These results clarify that N fertilizer increases the heat resistance of tomato fruit by regulating hexose content and hexose sensor activity.

In addition to structural enzymes involved in sucrose metabolism, sugar transporters (*SUTs* and *SWETs*) also play a key role in the soluble sugar profile (Schroeder et al., 2013). In this study, *SUT1* (Solyc11g017010.2) was up-regulated in HTN2 vs CKN2 (Figure 8), indicating that N2 treatment under HT could increase the concentration of sucrose in phloem sap. *SUT4* was significantly up-regulated under HT exposure, indicating that it

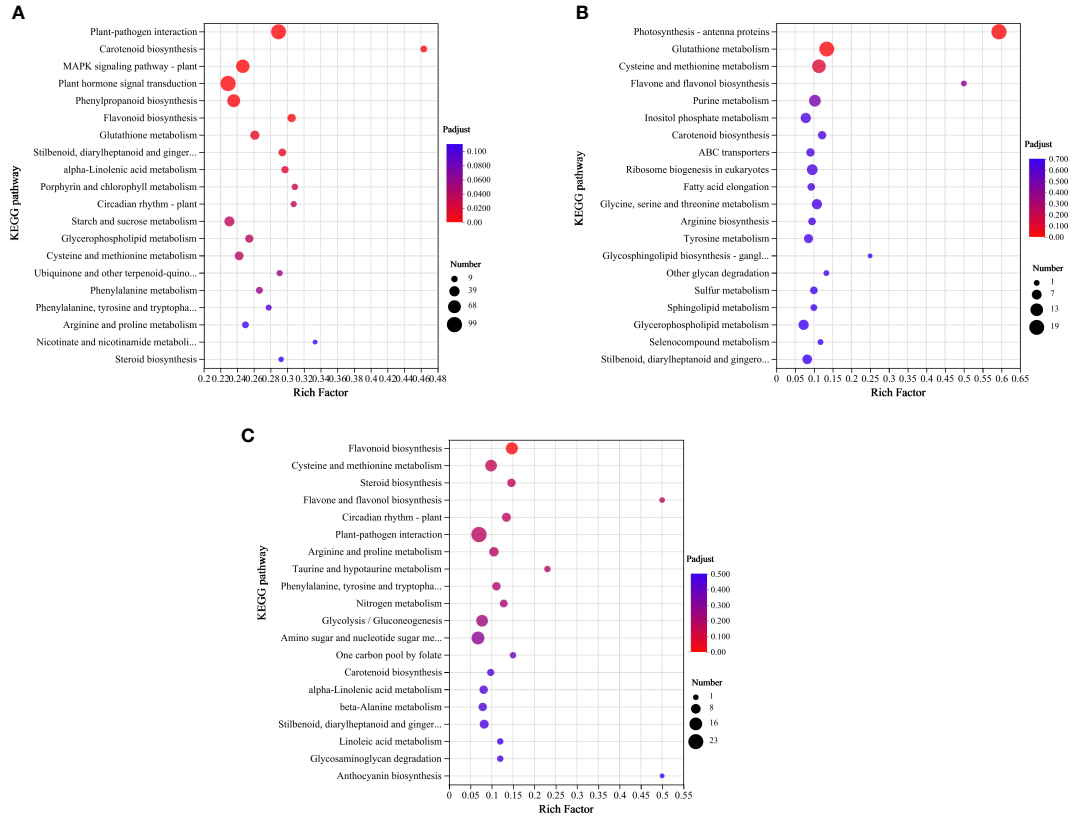

FIGURE 7
KEGG enrichment bubble plot. Differentially expressed genes generated by a comparison of **(A)** HTN1 vs CKN1, **(B)** HTN2 vs CKN2, **(C)** HTN3 vs CKN3. Rich factor represents the ratio of the number of DEGs enriched by the pathway to the number of annotated genes. The color bar represents the significance test p value adjusted for multiple hypothesis testing. The number represents the number of DEGs enriched in the pathway.

played an important role in sugar accumulation of tomato fruit under HT exposure. The above results indicated that N fertilizer had different regulatory effects on *SUTs* under HT exposure. Most *SWEETs* were up-regulated under HT exposure (Figure 8), which promoted the sugar flux between intercellular spaces or between pulp cells and phloem, while *SWEET2* (*Solyc07g062120.4*) and *SWEET1* (*Solyc04g064610.3*) were down-regulated, indicating that these genes may act as exporters to extract sugar from the vacuolar membrane and reduce its concentration, similar to that reported previously (Yue et al., 2015). In summary, the changes in soluble sugar content and components in fruits were not regulated by a few/single genes, but rather by the joint efforts of multiple metabolic pathways.

4.2 Nitrogen application improved CA synthesis and TCA cycle, which contribute to organic acid accumulations in tomato young fruit

Sugar and organic acid metabolism are closely linked through the TCA cycle. Organic acids are the material basis of the TCA cycle and glycolysis and play an important role in fruit development (Li et al., 2021). In this study, under HT exposure, citric acid content significantly increased at N1 and N2 (Figure 3B), malic acid content increased at N1 (Figure 3C), while succinic acid, α-ketoglutaric acid, and tartaric acid content significantly decreased at the three N levels (Figures 3D–F). Therefore, HT at the N1 level significantly decreased while the N2 and N3 levels significantly increased the total acid content (Figure 3A).

The synthesis and conversion of citric acid are affected by the activities of CS, ACO, and IDH (Liao et al., 2022). Chen et al. (2012) found that citric acid content was positively correlated with CS and negatively correlated with ACO and IDH. However, Liao et al. (2019) found that the citric acid accumulation was regulated by ACO and not CS. In this study, we found a significant negative correlation between citric acid content and mit-ACO, whereas there was no significant correlation with CS activity (Figure S2). Because HT exposure significantly decreased CS activity at N3, we speculated that N fertilizer-induced changes in organic acids are normally triggered under excessive N conditions (Parisi et al., 2004). Consistent with the changes in enzymes, *CS* gene expression was downregulated under HT exposure. At the same N level, HT exposure significantly reduced the activities of mit-ACO and IDH, inhibiting citric acid degradation. This suggests that the accumulation of citric acid content in response to HT under N regulation is due to the weakened degradation of citric acid. IDH is the major rate-limiting enzyme in the TCA cycle (Wu et al., 2023). And it's also the key enzyme of C-N metabolism involved in N metabolism, glyoxylate cycle, and other biochemical metabolic

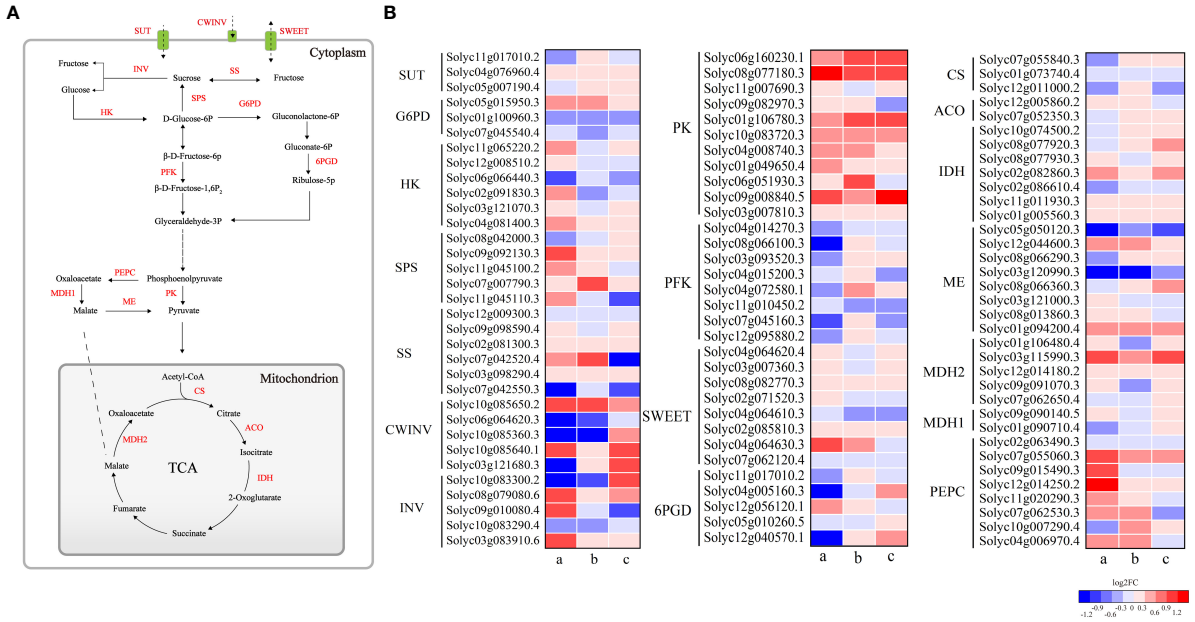

FIGURE 8
(A, B) represent sugar and organic acid metabolic pathways and heatmaps of gene expression for related enzymes, respectively. Small letters a, b and c represent HTN1 vs CKN1, HTN2 vs CKN2 and HTN3 vs CKN3, respectively. SUT, sucrose transporter; SWEET, sugars will eventually be exported transporters; INV, invertase; CWINV, cell wall invertase; SS, sucrose synthase; SPS, sucrose phosphate synthase; HK, hexokinase; G6PD, glucose 6-phosphate dehydrogenase; 6PGD, 6-phosphogluconate dehydrogenase; PFK, phosphofructokinase; PK, pyruvate kinase; PEPC, phosphoenolpyruvate carboxylase; MDH, malate dehydrogenase; ME, malic enzyme; CS, citrate synthase; ACO, aconitase; IDH, isocitrate dehydrogenase.

pathways in plants (Anderson et al., 2000). Interestingly, although the activity of IDH decreased during HT exposure, the expression of *IDH* (*Solyc01g005560.3*, *Solyc11g011930.3*, *Solyc02g082860.3*) was significantly upregulated (Figure 8), which may be due the fact that tomato is forced to produce free oxygen under HT stress, which increases the content of free ammonium in cells involved in the glutamine synthase/glutamate synthase (GS/GOGAT) metabolic pathway. Up-regulation of *IDH* expression provided the necessary α-ketoglutarate for this metabolic pathway, which may reduce the toxicity of free ammonium to plants.

N application can affect the nitrogen metabolism of fruits. This study mainly investigated the regulation of nitrogen application on sugar and organic acid metabolism in tomato young fruits under HT exposure, with little involvement in its impact on fruit nitrogen metabolism. Therefore, the results of this study are similar to those of previous studies, but there are some differences, which may be related to this. The next research work will focus on the effect of nitrogen-temperature treatment on the nitrogen metabolism of tomato fruit.

5 Conclusions

Nitrogen fertilizer, HT, and their interactions had significant impact on the soluble sugar and organic acid content, composition, and metabolic enzyme activity of tomato young fruits. N fertilizer improved sugar metabolism under HT exposure by increasing the activity of AI, NI, SSc, and SPS, upregulating the expression of *CWINV2*, *HK2*, *SPS*, and *PK*, and increasing sucrose transport by upregulating *SUT1*, *SUT4*, and *SWEETs*, thereby improving the heat tolerance of tomato fruits. In addition, N fertilizer upregulated the gene expression of *PEPC* under HT exposure and downregulated the expression of *ACO*, *MDH*, and *ME*, thereby reducing the degradation of citric acid and malic acid, leading to the accumulation of citric acid and malic acid. The soluble sugar content and organic acid content were the highest under HTN1 treatment, while the soluble sugar content was the lowest under HTN3 treatment. Therefore, we concluded that N fertilizer increased the heat resistance of tomato young fruits and improved fruit quality mainly due to the upregulation of sucrose metabolism enzyme gene expression, and N1 was the optimal nitrogen application under HT exposure. These results will help to further develop reasonable and effective tomato fertilization strategies in the context of global warming.

Data availability statement

The datasets presented in this study can be found in online repositories. The names of the repository/repositories and accession number(s) can be found below: NCBI Bioproject accession number: PRJNA948909.

Author contributions

The YZhe and ZY designed the experiments, analyzed the data and wrote the manuscript. JL, YZha, and NJ performed the

laboratory measurements. YZhe and ZY discussed the results and provide critical idea in greenhouse experiment. WK revised manuscript. All authors contributed to the article and approved the submitted version.

Funding

This work was supported by National Natural Science Foundation of China (41975142).

Acknowledgments

The authors would like to thank Yanchen Li and Fengyin Zhang for their help in measuring physiological indicators.

Conflict of interest

The authors declare that the research was conducted in the absence of any commercial or financial relationships that could be construed as a potential conflict of interest.

Publisher's note

Supplementary material

The Supplementary Material for this article can be found online at: https://www.frontiersin.org/articles/10.3389/fpls.2023.1197553/full#supplementary-material

SUPPLEMENTARY TABLE 1
Detailed table of expression differences between different control groups.

SUPPLEMENTARY TABLE 2
Statistical table of GO classification between different control groups.

SUPPLEMENTARY TABLE 3
Statistical table for KEGG enrichment analysis between different control groups.

References

Adams, S. R., Cockshull, K. E., and Cave, C. R. J. (2001). Effect of temperature on the growth and development of tomato fruits. *Ann. Bot.* 88, 869–877. doi: 10.1006/anbo.2001.1524

Almeida, J., Perez-Fons, L., and Fraser, P. D. (2021). A transcriptomic, metabolomic and cellular approach to the physiological adaptation of tomato fruit to high temperature. *Plant Cell Environ.* 44, 2211–2229. doi: 10.1111/pce.13854

Alsamir, M., Mahmood, T., Trethowan, R., and Ahmad, N. (2021). An overview of heat stress in tomato (*Solanum lycopersicum* l.). *Saudi J. Biol. Sci.* 28, 1654–1663. doi: 10.1016/j.sjbs.2020.11.088

Anderson, S. L., Minard, K. I., and McAlister-Henn, L. (2000). Allosteric inhibition of NAD^+-specific isocitrate dehydrogenase by a mitochondrial mRNA. *Biochemistry* 39, 5623–5629. doi: 10.1021/bi000272e

Ayenan, M. A. T., Danquah, A., Agre, P. A., Hanson, P., Asante, I. K., and Danquah, E. Y. (2021). Genomic and phenotypic diversity of cultivated and wild tomatoes with varying levels of heat tolerance. *Genes* 12, 503. doi: 10.3390/genes12040503

Azzi, L., Deluche, C., Gevaudant, F., Frangne, N., Delmas, F., Hernould, M., et al. (2015). Fruit growth-related genes in tomato. *J. Exp. Bot.* 66, 1075–1086. doi: 10.1093/jxb/eru527

Bauchet, G., Grenier, S., Samson, N., Segura, V., Kende, A., Beekwilder, J., et al. (2017). Identification of major loci and genomic regions controlling acid and volatile content in tomato fruit: implications for flavor improvement. *New Phytol.* 215, 624–641. doi: 10.1111/nph.14615

Bénard, C., Gautier, H., Bourgaud, F., Grasselly, D., Navez, B., Caris-Veyrat, C., et al. (2009). Effects of low nitrogen supply on tomato (*Solanum lycopersicum*) fruit yield and quality with special emphasis on sugars, acids, ascorbate, carotenoids, and phenolic compounds. *J. Agric. Food Chem.* 57, 4112–4123. doi: 10.1021/jf8036374

Bertin, N. (2005). Analysis of the tomato fruit growth response to temperature and plant fruit load in relation to cell division, cell expansion and DNA endoreduplication. *Ann. Bot.* 95, 439–447. doi: 10.1093/aob/mci042

Cao, X. J., Li, W. F., Wang, P., Ma, Z. H., Mao, J., and Chen, B. H. (2022). New insights into *MdSPS4*-mediated sucrose accumulation under different nitrogen levels revealed by physiological and transcriptomic analysis. *Int. J. Mol. Sci.* 23, 16073. doi: 10.3390/ijms232416073

Chen, M., Jiang, Q., Yin, X. R., Lin, Q., Chen, J. Y., Allan, A. C., et al. (2012). Effect of hot air treatment on organic acid- and sugar-metabolism in ponkan (*Citrus reticulata*) fruit. *Sci. Hortic.* 147, 118–125. doi: 10.1016/j.scienta.2012.09.011

Chen, T., Zhang, Z., Li, B. Q., Qin, G. Z., and Tian, S. P. (2021). Molecular basis for optimizing sugar metabolism and transport during fruit development. *aBIOTECH.* 2, 330–340. doi: 10.1007/S42994-021-00061-2

D'Aoust, M. A., Yelle, S., and Nguyen-Quoc, B. (1999). Antisense inhibition of tomato fruit sucrose synthase decreases fruit setting and the sucrose unloading capacity of young fruit. *Plant Cell* 11, 2407–2418. doi: 10.1105/tpc.11.12.2407

Elía, M., Slafer, G. A., and Savin, R. (2018). Yield and grain weight responses to post-anthesis increases in maximum temperature under field grown wheat as modified by nitrogen supply. *Field Crops Res.* 221, 228–237. doi: 10.1016/j.fcr.2018.02.030

Erdinc, C., Ekincialp, A., Gundogdu, M., Eser, F., and Sensoy, S. (2018). Bioactive components and antioxidant capacities of different miniature tomato cultivars grown by altered fertilizer applications. *J. Food Meas. Charact.* 12, 1519–1529. doi: 10.1007/s11694-018-9767-7

Fernie, A. R., Carrari, F., and Sweetlove, L. J. (2004). Respiratory metabolism: glycolysis, the TCA cycle and mitochondrial electron transport. *Curr. Opin. Plant Biol.* 7, 254–261. doi: 10.1016/j.pbi.2004.03.007

Gao, L. J., Wang, W. X., Xu, C. Q., Han, X. T., Li, Y. N., Liu, Y. L., et al. (2022). Physiological and transcriptomic analyses reveal the effects of elevated root-zone CO_2 on the metabolism of sugars and starch in the roots of oriental melon seedlings. *Int. J. Mol. Sci.* 23, 12537. doi: 10.3390/ijms232012537

Gruda, N., Savvas, D., Colla, G., and Rouphael, Y. (2018). Impacts of genetic material and current technologies on product quality of selected greenhouse vegetables-a review. *Eur. J. Hortic. Sci.* 83, 319–328. doi: 10.17660/eJHS.2018/83.5.5

Gul, S., Shah, K. N., Rana, R. M., Khan, M. A., El-Shehawi, A. M., and Elseehy, M. M. (2021). Phylogenetic and expression dynamics of tomato *ClpB/Hsp100* gene under heat stress. *PloS One* 16, e0255847. doi: 10.1371/journal.pone.0255847

Hernández, V., Hellín, P., Botella, M., Vicente, E., Fenoll, J., and Flores, P. (2022). Oligosaccharins alleviate heat stress in greenhouse-grown tomatoes during the spring-summer season in a semi-arid climate. *Agronomy* 12, 802. doi: 10.3390/agronomy12040802

Hernández, V., Hellín, P., Fenoll, J., Cava, J., Garrido, I., Molina, M. V., et al. (2018). The use of biostimulants can mitigate the effect of high temperature on productivity and quality of tomato. *Acta Hortic.* 1194, 85–90. doi: 10.17660/actahortic.2018.1194.14

Hernández, V., Hellín, P., Fenoll, J., and Flores, P. (2020). Impact of nitrogen supply limitation on tomato fruit composition. *Sci. Hortic.* 264, 109173. doi: 10.1016/j.scienta.2020.109173

IPCC. (2021). "Summary for policymakers," in *Climate change 2021: the physical science basis. contribution of working group I to the sixth assessment report of the intergovernmental panel on climate change*. Eds. V. Masson-Delmotte, P. Zhai, A. Pirani, S. L. Connors, C. Péan, S. Berger, N. Caud, Y. Chen, L. Goldfarb, M. I. Gomis, M. Huang, K. Leitzell, E. Lonnoy, J. B. R. Matthews, T. K. Maycock, T. Waterfield, O. Yelekçi, R. Yu and B. Zhou (Cambridge University Press) 3-32.

Li, M. J., Li, D. X., Feng, F. J., Zhang, S., Ma, F. W., and Cheng, L. L. (2016). Proteomic analysis reveals dynamic regulation of fruit development and sugar and acid accumulation in apple. *J. Exp. Bot.* 67, 5145–5157. doi: 10.1093/jxb/erw277

Li, W. X., Lu, X., and Li, J. M. (2022). The effect of organic nutrient solution on flavor in ripe cherry tomato fruit-transcriptome and metabolomic analyses. *Environ. Exp. Bot.* 194, 104721. doi: 10.1016/j.envexpbot.2021.104721

Li, Z. M., Palmer, W. M., Martin, A. P., Wang, R. Q., Rainsford, F., Jin, Y., et al. (2012). High invertase activity in tomato reproductive organs correlates with enhanced sucrose import into, and heat tolerance of, young fruit. *J. Exp. Bot.* 63, 1155–1166. doi: 10.1093/jxb/err329

Li, N., Wang, J., Wang, B. K., Huang, S. Y., Hu, J. H., Yang, T., et al. (2021). Identification of the carbohydrate and organic acid metabolism genes responsible for brix in tomato fruit by transcriptome and metabolome analysis. *Front. Genet.* 12. doi: 10.3389/fgene.2021.714942

Liao, L., Dong, T. T., Qiu, X., Rong, Y., Wang, Z. H., and Zhu, J. (2019). Nitrogen nutrition is a key modulator of the sugar and organic acid content in citrus fruit. *PloS One* 14, e0223356. doi: 10.1371/journal.pone.0223356

Liao, H. Z., Lin, X. K., Du, J. J., Peng, J. J., and Zhou, K. B. (2022). Transcriptomic analysis reveals key genes regulating organic acid synthesis and accumulation in the pulp of *Litchi chinensis sonn.* cv. feizixiao. *Sci. Hortic.* 303, 111220. doi: 10.1016/j.scienta.2022.111220

Lokesha, A. N., Shivashankara, K. S., Laxman, R. H., Geetha, G. A., and Shankar, A. G. (2019). Effect of high temperature on fruit quality parameters of contrasting tomato genotypes. *Int. J. Curr. Mic. Appli. Sci.* 8, 1019–1029. doi: 10.20546/ijcmas.2019.803.124

Ma, Y. P., Reddy, V. R., Devi, M. J., Song, L. H., and Cao, B. (2019). *De novo* characterization of the goji berry (*Lycium barbarium* l.) fruit transcriptome and analysis of candidate genes involved in sugar metabolism under different CO_2 concentrations. *Tree Physiol.* 39, 1032–1045. doi: 10.1093/treephys/tpz014

Mesa, T., Polo, J., Arabia, A., Caselles, V., and Munne-Bosch, S. (2022). Differential physiological response to heat and cold stress of tomato plants and its implication on fruit quality. *J. Plant Physiol.* 268, 153581. doi: 10.1016/j.jplph.2021.153581

Ordóñez, R. A., Savin, R., Cossani, C. M., and Slafer, G. A. (2015). Yield response to heat stress as affected by nitrogen availability in maize. *Field Crops Res.* 183, 184–203. doi: 10.1016/j.fcr.2015.07.010

Palmer, W. M., Ru, L., Jin, Y., Patrick, J. W., and Ruan, Y. L. (2015). Tomato ovary-to-Fruit transition is characterized by a spatial shift of mRNAs for cell wall invertase and its inhibitor with the encoded proteins localized to sieve elements. *Mol. Plant* 8, 315–328. doi: 10.1016/j.molp.2014.12.019

Parisi, M., Giordano, L., Pentangelo, A., D'Onofrio, B., and Villari, G. (2004). Effects of different levels of nitrogen fertilization on yield and fruit quality in processing tomato. *Acta Hortic.* 700, 129–132. doi: 10.17660/ActaHortic.2006.700.19

Powell, A. L. T., Nguyen, C. V., Hill, T., Cheng, K. L., Figueroa-Balderas, R., Aktas, H., et al. (2012). Uniform ripening encodes a golden 2-like transcription factor regulating tomato fruit chloroplast development. *Science* 336, 1711–1715. doi: 10.1126/science.1222218

Qin, G. Z., Zhu, Z., Wang, W. H., Cai, J. H., Chen, Y., Li, L., et al. (2016). A tomato vacuolar invertase inhibitor mediates sucrose metabolism and influences fruit ripening. *Plant Physiol.* 172, 1596–1611. doi: 10.1104/pp.16.01269

Quinet, M., Angosto, T., Yuste-Lisbona, F. J., Blanchard-Gros, R., Bigot, S., Martinez, J. P., et al. (2019). Tomato fruit development and metabolism. *Front. Plant Sci.* 10, 1554. doi: 10.3389/fpls.2019.01554

Renau-Morata, B., Molina, R. V., Minguet, E. G., Cebolla-Cornejo, J., Carrillo, L., Marti, R., et al. (2021). Integrative transcriptomic and metabolomic analysis at organ scale reveals gene modules involved in the responses to suboptimal nitrogen supply in tomato. *Agron. Basel* 11, 1320. doi: 10.3390/agronomy11071320

Ronga, D., Pentangelo, A., and Parisi, M. (2020). Optimizing n fertilization to improve yield, technological and nutritional quality of tomato grown in high fertility soil conditions. *Plants-Basel* 9, 575. doi: 10.3390/plants9050575

Ruan, Y. L., Jin, Y., Yang, Y. J., Li, G. J., and Boyer, J. S. (2010). Sugar input, metabolism, and signaling mediated by invertase: roles in development, yield potential, and response to drought and heat. *Mol. Plant* 3, 942–955. doi: 10.1093/mp/ssq044

Schroeder, J. I., Delhaize, E., Frommer, W. B., Guerinot, M. L., Harrison, M. J., Herrera-Estrella, L., et al. (2013). Using membrane transporters to improve crops for sustainable food production. *Nature* 497, 60–66. doi: 10.1038/nature11909

Shamshiri, R. (2017). Measuring optimality degrees of microclimate parameters in protected cultivation of tomato under tropical climate condition. *Measurement* 106, 236–244. doi: 10.1016/j.measurement.2017.02.028

Su, H. Z., Ma, S. Y., Ma, X. H., Song, Y., Wang, X. M., and Cheng, G. X. (2022). Transcriptome analyses show changes in heat-stress related gene expression in tomato cultivar 'Moneymaker' under high temperature. *J. Plant Biochem. Biotechnol.* 32, 328-337. doi: 10.1007/s13562-022-00808-y

Tang, S., Zhang, H. X., Liu, W. Z., Dou, Z., Zhou, Q. Y., Chen, W. Z., et al. (2019). Nitrogen fertilizer at heading stage effectively compensates for the deterioration of rice quality by affecting the starch-related properties under elevated temperatures. *Food Chem.* 277, 455–462. doi: 10.1016/j.foodchem.2018.10.137

Tao, X. Y., Wu, Q., Huang, S. Q., Zhu, B. W., Chen, F., Liu, B., et al. (2022). Exogenous abscisic acid regulates primary metabolism in postharvest cherry tomato fruit during ripening. *Sci. Hortic.* 299, 111008. doi: 10.1016/j.scienta.2022.111008

Tiwari, J. K., Challam, C., Chakrabarti, S. K., and Feingold, S. E. (2020). "Climate-smart potato: an integrated breeding, genomics, and phenomics approach," in *Genomic designing of climate-smart vegetable crops*. Ed. C. Kole (Cham: Springer International Publishing), 1–46.

Truffault, V., Ristorto, M., Brajeul, E., Vercambre, G., and Gautier, H. (2019). To stop nitrogen overdose in soilless tomato crop: a way to promote fruit quality without affecting fruit yield. *Agron. Basel* 9, 80. doi: 10.3390/agronomy9020080

Vijayakumar, A., Shaji, S., Beena, R., Sarada, S., Rani, T. S., Stephen, R., et al. (2021). High temperature induced changes in quality and yield parameters of tomato (*Solanum lycopersicum* l.) and similarity coefficients among genotypes using SSR markers. *Heliyon* 7, e05988. doi: 10.1016/j.heliyon.2021.e05988

Wang, F., Ge, S. F., Xu, X. X., Xing, Y., Du, X., Zhang, X., et al. (2021). Multiomics analysis reveals new insights into the apple fruit quality decline under high nitrogen conditions. *J. Agric. Food Chem.* 69, 5559–5572. doi: 10.1021/acs.jafc.1c01548

Wei, H. H., Meng, T. Y., Li, X. Y., Dai, Q. G., Zhang, H. C., and Yin, X. Y. (2018). Sink-source relationship during rice grain filling is associated with grain nitrogen concentration. *Field Crops Res.* 215, 23–38. doi: 10.1016/j.fcr.2017.09.029

Wu, K. J., Hu, C. X., Wang, J., Guo, J. D., Sun, X. C., Tan, Q. L., et al. (2023). Comparative effects of different potassium sources on soluble sugars and organic acids in tomato. *Sci. Hortic.* 308, 111601. doi: 10.1016/j.scienta.2022.111601

Wu, Z. F., Tu, M. M., Yang, X. P., Xu, J. H., and Yu, Z. F. (2020). Effect of cutting and storage temperature on sucrose and organic acids metabolism in postharvest melon fruit. *Postharvest Biol. Technol.* 161, 111081. doi: 10.1016/j.postharvbio.2019.111081

Xu, Y. Q., Guan, X. Y., Han, Z. Y., Zhou, L. J., Zhang, Y., Asad, M. A. U., et al. (2022). Combined effect of nitrogen fertilizer application and high temperature on grain quality properties of cooked rice. *Front. Plant Sci.* 13. doi: 10.3389/fpls.2022.874033

Yan, P., Chen, Y. Q., Dadouma, A., Tao, Z. Q., and Sui, P. (2017). Effect of nitrogen regimes on narrowing the magnitude of maize yield penalty caused by high temperature stress in north China plain. *Plant Soil Environ.* 63, 131–138. doi: 10.17221/6/2017-Pse

Yang, J., Chen, X., Zhu, C., Peng, X., He, X., Fu, J., et al. (2015). Using RNA-seq to profile gene expression of spikelet development in response to temperature and nitrogen during meiosis in rice (*Oryza sativa* l.). *PloS One* 10, e0145532. doi: 10.1371/journal.pone.0145532

Yue, C., Cao, H. L., Wang, L., Zhou, Y. H., Huang, Y. T., Hao, X. Y., et al. (2015). Effects of cold acclimation on sugar metabolism and sugar-related gene expression in tea plant during the winter season. *Plant Mol. Biol.* 88, 591–608. doi: 10.1007/s11103-015-0345-7

Zhang, L. H., Sun, S. M., Liang, Y. H., Li, B. Y., Ma, S. Y., Wang, Z. Y., et al. (2021). Nitrogen levels regulate sugar metabolism and transport in the shoot tips of crabapple plants. *Front. Plant Sci.* 12. doi: 10.3389/fpls.2021.626149

Zhang, M. F., Xu, R. W., Sun, G. C., Cheng, Y. J., and Wang, Z. H. (2022). The effect of short-term temperature pretreatments on sugars, organic acids, and amino acids metabolism in Valencia orange fruit. *J. Food Qual.* 2022, 1–9. doi: 10.1155/2022/8188000

Zheng, Y. J., Yang, Z. Q., Wei, T. T., and Zhao, H. L. (2022). Response of tomato sugar and acid metabolism and fruit quality under different high temperature and relative humidity conditions. *Phyton-Int. J. Exp. Bot.* 91, 2033–2054. doi: 10.32604/phyton.2022.019468

Zheng, Y. J., Yang, Z. Q., Xu, C., Wang, L., Huang, H. J., and Yang, S. Q. (2020). The interactive effects of daytime high temperature and humidity on growth and endogenous hormone concentration of tomato seedlings. *Hortic. Sci.* 55, 1575–1583. doi: 10.21273/Hortsci15145-20

Zhu, Z., Liu, R. L., Li, B. Q., and Tian, S. P. (2013). Characterisation of genes encoding key enzymes involved in sugar metabolism of apple fruit in controlled atmosphere storage. *Food Chem.* 141, 3323–3328. doi: 10.1016/j.foodchem.2013.06.025

frontiers | Frontiers in Plant Science

TYPE Original Research
PUBLISHED 27 July 2023
DOI 10.3389/fpls.2023.1197271

OPEN ACCESS

EDITED BY
Md Sazzad Hossain,
University of Kiel, Germany

REVIEWED BY
Rajib Roychowdhury,
Volcani Center, Israel
Divya Balakrishnan,
Indian Institute of Rice Research (ICAR), India
Yogesh Vikal,
Punjab Agricultural University, India

*CORRESPONDENCE
Nhung Thi Hong Phan
phannhung@vnua.edu.vn

RECEIVED 30 March 2023
ACCEPTED 04 July 2023
PUBLISHED 27 July 2023

CITATION
Phan NTH, Draye X, Pham CV and Bertin P (2023) Identification of quantitative trait loci controlling nitrogen use efficiency-related traits in rice at the seedling stage under salt condition by genome-wide association study.
Front. Plant Sci. 14:1197271.
doi: 10.3389/fpls.2023.1197271

Identification of quantitative trait loci controlling nitrogen use efficiency-related traits in rice at the seedling stage under salt condition by genome-wide association study

Nhung Thi Hong Phan[1,2]*, Xavier Draye[1], Cuong Van Pham[2] and Pierre Bertin[1]

[1]Earth and Life Institute, Université Catholique de Louvain, Louvain-la-Neuve, Belgium, [2]Agronomy Faculty, Vietnam National University of Agriculture, Hanoi, Vietnam

Rice cultivation is facing both salt intrusion and overuse of nitrogen fertilizers. Hence, breeding new varieties aiming to improve nitrogen use efficiency (NUE), especially under salt conditions, is indispensable. We selected 2,391 rice accessions from the 3K Rice Genomes Project to evaluate the dry weight under two N concentrations [2.86 mM – standard N (SN), and 0.36 mM – low N (LN)] crossed with two NaCl concentrations [0 (0Na) and 60 mM (60Na)] at the seedling stage. Genome-wide association studies for shoot, root, and plant dry weight (DW) were carried out. A total of 55 QTLs – 32, 16, and 7 in the whole, *indica*, and *japonica* panel – associated with one of the tested traits were identified. Among these, 27 QTLs co-localized with previously identified QTLs for DW-related traits while the other 28 were newly detected; 24, 8, 11, and 4 QTLs were detected in SN-0Na, LN-0Na, SN-60Na, and LN-60Na, respectively, and the remaining 8 QTLs were for the relative plant DW between treatments. Three of the 11 QTLs in SN-60Na were close to the regions containing three QTLs detected in SN-0Na. Eleven candidate genes for eight important QTLs were identified. Only one of them was detected in both SN-0Na and SN-60Na, while 5, 0, 3, and 2 candidate genes were identified only once under SN-0Na, LN-0Na, SN-60Na, and LN-60Na, respectively. The identified QTLs and genes provide useful materials and genetic information for future functional characterization and genetic improvement of NUE in rice, especially under salt conditions.

KEYWORDS

GWAS, 3K Rice Genomes Project, NUE, saline, dry weight

Abbreviations: SN-0Na, standard N and 0 mM NaCl treatment; LN-0Na, low N and 0 mM NaCl treatment; SN-60Na, standard N and 60 mM NaCl treatment; LN-60Na, low N and 60 mM NaCl treatment; SDW, shoot dry weight; RDW, root dry weight; PDW, whole plant dry weight; SRR, ratio of shoot dry weight on root dry weight; NUE, nitrogen use efficiency; PCA, principal component analysis; LD, linkage disequilibrium; QTL, quantitative trait locus; QTN, quantitative trait nucleotide; GWAS, genome-wide association study; SNP, single nucleotide polymorphism; EXP, experiment.

1 Introduction

Rice is a staple food for more than half of the world's population. Approximately 75% of the total area of harvested rice in the world is cultivated in South and South-East Asia countries (FAO, 2021). However, these regions are facing two severe environmental concerns: salt intrusion and overuse of nitrogen fertilizers (Heffer and Prud'homme, 2017; Smajgl et al., 2015; Eckstein et al., 2019; Wassmann et al., 2019). In the past five decades, N fertilizer consumption is an approximately 5-fold increase in the world, with a 2-fold and 15-fold increase in developed and developing countries, respectively (IFA, 2019). Among them, approximately 20% of the total N fertilizers are used for rice (Ladha et al., 2005). However, rice plants could absorb less than half of the N applied, and the rest is wasted in soil, water, and the atmosphere (Lea and Miflin, 2003; Ladha et al., 2005; Udvardi et al., 2021). Therefore, improving nitrogen use efficiency (NUE) for rice under saline conditions has become of primary importance.

NUE is defined as the yield (grain, starch, biomass, depending on the authors) per N applied unit. It can be partitioned into two processes within the plant: absorption NUE (that refers to the capacity of the plant to absorb the applied N) and physiological NUE (that refers to its efficiency to use the absorbed N for metabolic purposes) (Ladha et al., 2005; Murtaza et al., 2013; Nguyen et al., 2014; Beatty and Good, 2018). NUE is strongly correlated with plant growth and development affecting root morphology, tiller number, biomass, and yield, and is governed by multiple interacting genetic and environmental factors (Ladha et al., 2005; Nguyen et al., 2016; Sharma et al., 2021; Sandhu et al., 2021; Phan et al., 2023). Therefore, research on NUE has often been related to these traits, especially dry weights. Identification of the QTLs (quantitative trait loci) associated with NUE, or NUE-related traits is an important step to improve NUE in rice.

Salinity reduces NUE by affecting all processes of N metabolism in the plant, thus causing a severe decline in crop production. Salt inhibits NO_3^-, N content, glutamine synthetase, and nitrate reductase but enhances NH_4^+ content and glutamate synthase in rice (Hoai et al., 2003; Wang et al., 2012; Phan et al., 2023). Notably, NH_4^+ increase does not always bring advantages because high NH_4^+ uptake cannot always be assimilated, inducing ion toxicity and decrease in NUE (Ouyang et al., 2010). The subsequent decrease in N uptake and assimilation causes a decrease in photosynthesis, antioxidant enzymes activity, dry weight, and grain yield (Abdelgadir et al., 2005; Wang et al., 2012; Chen et al., 2022; Phan et al., 2023). The effects of salt on rice may alter the expression of some genes controlling N uptake and N assimilation: *OsNRT* family, *OsAMT* family, *OsNR1*, *OsGS1.2*, *OsNADH-GOGAT*, or *OsFd-GOGAT* (Wang et al., 2012; Rohilla and Yadav, 2019; Huang et al., 2020; Decui et al., 2022). Interestingly, some genes controlling N uptake were found to be associated with salt tolerance/susceptibility in rice. Shi et al. (2017) detected that *OsNRT2.2*, associated with nitrogen uptake in rice, was also related to salt susceptibility, whereas Batayeva et al. (2018) elucidated that *OsAMT1.3*, regulating ammonium transport, was also associated with salt tolerance under severe salinity stress. In previous studies, we demonstrated that applying high N rates under saline condition in rice did not result in a significant increase in grain yield but caused significant reduction in both NUE and dry weight; NUE was reduced by increasing either salinity or nitrogen levels, and the reduction was mainly linked to absorption NUE (Phan et al., 2017, 2023).

Previously, a large number of QTLs for NUE and its related traits have been detected under different N concentrations by using bi-parental linkage mapping populations (Fang and Wu, 2001; Lafitte et al., 2002; Price et al., 2002; Hittalmani et al., 2003; Lian et al., 2005; Li et al., 2005; Nguyen et al., 2016; Zhou et al., 2017). Indeed, eight QTLs for plant height were identified under low or high N levels (5 and 40 mg L^{-1}) in a double-haploid population consisting of 123 lines derived from a cross between IR64 and Azucena (Fang and Wu, 2001). Genomic regions for plant height, dry weight, and relative dry weight under two N treatments (1N - normal N and 1/6N - low N level) were identified by using 239 RILs from a cross between Zhenshan 97 and Minghui 63 (Lian et al., 2005). Also, 14 QTLs for NUE component traits and 63 QTLs for NUE-related traits were identified under three N levels (1N, 1/4N, and 1/8N) in hydroponics by using 174 RILs from the cross IR64/Azucena (Nguyen et al., 2016). Such bi-parental mapping method presents high statistical power due to using many individuals sharing an identical genotype at a given locus; however, it has a low resolution because of the limited number of recombination events in the development of the population.

In recent years, a lot of QTLs or candidate genes have been identified by genome-wide association study (GWAS) by using high-density genome-wide single nucleotide polymorphism (SNP) detected by next-generation sequencing of unrelated individuals in a population. The detected QTLs showed a high resolution due to the long recombination histories of natural populations (Shi et al., 2017; Batayeva et al., 2018; Naveed et al., 2018; Liu et al., 2019). A combination of GWAS, gene annotation based on high-quality reference genomes, and haplotype analysis is an effective way to identify candidate genes for the tested traits and elite materials that are useful for future breeding and molecular dissection for rice (Wang et al., 2017; Naveed et al., 2018; Norton et al., 2021). Regarding NUE traits, *OsNAC42, OsNPF6.1*, and *OsNLP4* have been detected by GWAS in rice recently (Tang et al., 2019; Yu et al., 2021). GWAS can be applied in a large amount of genotypes and save time compared to conventional methods. In the last decade, 29 million SNPs were discovered by sequencing 3,010 rice accessions from 89 countries in the 3,000 Rice Genomes Project (3K RGP), providing useful information for genetic research and breeding (3K RGP, 2014; Li et al., 2014). However, most QTLs and genes mentioned above have been detected under non-saline conditions. To date, no GWAS has been conducted yet to examine a large rice population for NUE-related traits under saline condition. Using the 3K RGP database, GWAS was used to detect a large number of QTLs related to agronomical traits: heading date, seedling length, 100-grain weight, grain width, grain length, culm diameter, culm length, culm number, leaf width, leaf length, leaf angle, panicle type, [https://snp-seek.irri.org/_gwas.zul]. We focused on finding genetic information related to the dry weight which is one of the most important NUE-related traits, under varying N and NaCl treatments.

2 Materials and methods

2.1 Plant growth

We selected 2,391 rice accessions from 75 countries from the 3,000 RGP (Supplementary Table S1; 3K RGP, 2014; Li et al., 2014) for the main experiment (main EXP). Then, a selection of 1,332 accessions from 68 countries was realized based on low relatedness criteria revealed by the phylogenetic tree, in order to realize a confirmatory experiment (confirmatory EXP). It was created by Archaeopteryx Tree image in TASSEL 5.2.57 by using the neighbor-joining cladogram function of 2,391 accessions with 5,902 SNPs (Bradbury et al., 2007) (Supplementary Figure S1). According to the 3K RGP, the accessions belonged to nine variety types, *viz. aromatic*, *aus*, *temperate japonica*, *tropical japonica*, *subtropical japonica*, *indica*-1A, *indica*-1B, *indica*-2, and *indica*-3, and the admixture (*japonica*-admixed, *indica*-admixed, and admixed). Confirmatory EXP was conducted with fewer accessions than the main EXP aiming to reduce the competition between the genotypes by increasing the space between the plants.

2.2 Main experiment

A hydroponic experiment was performed with 2,391 rice accessions in a phytotron at the Université Catholique de Louvain, Belgium, from March to April 2019. The seeds were sown directly in holes on extruded polystyrene plates floating in 40L tanks, 74.5cm length x 54.5 cm width x 10.0 cm height, at a density of eight seeds of the same genotype per hole, 630 holes per tank with each hole for each genotype. The tanks contained the Yoshida solution (Yoshida et al., 1976) which was renewed at 7, 10, 14, and 17 days after the treatment. The pH was adjusted daily between 5.0 and 5.5 with KOH 2M or HCl 1M. One week after sowing, five uniform plants per hole were maintained up to the end of the experiment. The climatic conditions in the phytotron were maintained at 30°C/25°C day/night, 85%-95% relative humidity, 12h photoperiod, and 210 µmol m^{-2} s^{-1} photon flux density at the top of the tanks.

At the sowing time, rice seeds were put in the Yoshida solution with two different N concentrations: standard N (SN, 2.86 mM N) and low N (LN, 0.38 mM N). At the same time, two salinity levels, viz. 0 mM NaCl (0Na) and 60 mM NaCl (60Na) were applied in the solutions. Thus, two N concentrations crossed with two NaCl levels led to a total of four treatments. Each treatment was carried out with 2,391 accessions; thus 4 tanks were used for each treatment. The experimental design was laid out as an augmented RCBD (Federer and Raghavarao, 1975) with four replications, comprising each of 4 tanks per treatment. Among the 2,391 accessions, 2,379 appeared only once (*i.e.* 8 seeds at sowing but remaining 5 plants in one hole) in each replicate, thus 594-595 accessions per tank. The 12 remaining accessions were replicated once in each of the four tanks. The 23-24 remaining holes in each tank were filled by three unsequenced genotypes to estimate the effect of the tanks. Hence, 4 treatments were conducted in 16 plates/tanks, and 50,400 plants. The tanks were moved in the phytotron twice a week. The plants were harvested after 21 days of treatment.

2.3 Confirmatory experiment

The confirmatory EXP was conducted to confirm the results of the main experiment, in an experimental design allowing lower the competition between plants. It was carried out in a greenhouse at UCLouvain, Belgium, from November to December 2019. The two N concentrations and NaCl levels were maintained as in the main EXP, whereas the number of accessions, plant density, duration of treatment, and climatic conditions were modified.

To reduce the competition between the accessions, we increased the space between the plants; thus, the number of accessions was reduced to 1,332 instead of 2,391 accessions in the main EXP, because of space constraints. Three seeds of each accession were sown in each hole of the plate, then two uniform seedlings were maintained after 5 days. Each plate – each tank – contained 360 holes with each genotype per hole. The space between the holes was 3 cm x 3.3 cm. Four tanks were used for each treatment. Among the 1,332 accessions from 3K RGP, 1,316 appeared only once, thus 329 accessions per tank. The 16 remaining accessions were replicated once in each of the four tanks. The other 15 remaining holes in each tank were filled by three unsequenced genotypes to calculate the effect of the tanks. In total, the experiment was conducted in 16 tanks, and 11,520 plants and was laid out as an augmented RCBD (Federer and Raghavarao, 1975). The tanks were moved inside the greenhouse twice a week.

The climatic conditions were the same as in the main EXP, except for the photoperiod which was set to 16h, in order to speed up growth. The solution treatments were applied and renewed as in the main EXP up to 14 days, then the plants were harvested after 17 days of treatment, which was adequate for screening.

2.4 Phenotyping

Shoot dry weight (SDW) and root dry weight (RDW) of each accession were determined after 21 days in the main EXP and 17 days in the confirmatory EXP. The shoot and root samples were collected individually, and oven-dried (48h at 70°C), and then dry weights were determined. Then, the data of SDW and RDW of each treatment were adjusted by augmentedRCBD package in R software (Aravind et al., 2020) based on the check-varieties in both EXPs.

Plant dry weight (PDW) is the sum of SDW and RDW of the same plant.

Shoot/root ratio (SRR) was calculated by SDW per RDW of each accession.

Relative plant dry weight (RePDW) was calculated by the following formulas:

$$RePDW_{LN-0N/SN-0Na} = PDW_{LN-0Na} / PDW_{SN-0Na} \quad (1)$$

$$RePDW_{SN-60Na/SN-0Na} = PDW_{SN-60Na} / PDW_{SN-0Na} \quad (2)$$

$$RePDW_{LN-60Na/LN-0Na} = PDW_{LN-60Na} / PDW_{LN-0Na} \quad (3)$$

$$RePDW_{LN-60Na/SN-60Na} = PDW_{LN-60Na} / PDW_{SN-60Na} \quad (4)$$

2.5 Genome-wide association study

A total of 1,011,601 GWAS SNPs were downloaded from the Rice SNP-Seek Database [https://snp-seek.irri.org, (Mansueto et al., 2016)]. We selected the SNPs with a minor allele frequency > 5% and missing rates< 5%, resulting in 588,792 SNPs. Subsequently, we randomly selected 40% of these SNPs and got 235,210 SNPs.

The GWAS was performed with a Factored Spectrally Transformed Linear Mixed Model (FaST-LMM) by FaST-LLM software (Lippert et al., 2011). We randomly selected 2.5% of these SNPs for measuring genetic similarities between the accessions. Principal components analysis of the 588,792 SNPs was done with the default setting by PLINK 1.9 (Purcell et al., 2007). Then, the eigenvalue of the top three components was selected as covariate data. The significant threshold was set at $p \leq 0.0001$ ($-\log_{10}$p-value ≥ 4).

2.6 Linkage disequilibrium decay

We analyzed LD decay in four populations, *viz.* whole panel 1 with 2,391 accessions, whole panel 2 with 1,332 accessions, *indica* panel 1 with 1,418 accessions, *japonica* panel 1 with 652 accessions, *aus* panel 1 with 182 accessions, and *aromatic* panel 1 with 66 accessions. Random selection of 20% of the 588,792 SNPs was used to calculate the LD decay rate. We calculated r^2 as an estimation of LD using PLINK software version 1.9 (Purcell et al., 2007). The syntax was "–r2 –ld-window-kb 1000 –ld-window 9999 –ld-window-r2 0". Marker pairs were grouped into bins of 1 kb and the average r^2 value of each bin was calculated. The LD decay rate was measured as a distance at which the average r^2 dropped to half of its maximum value (Huang et al., 2010; Shi et al., 2017).

2.7 Haplotype analysis and candidate gene identification

The process to identify candidate genes was described by Wang et al. (2017). Multiple significant SNPs that were in a range of linkage disequilibrium (LD) decay rates were considered as a single QTL. Among all detected QTLs, we focused on the most important QTLs to identify candidate genes by gene-based association analysis and focused on the QTLs detected in both whole panels instead of in either *indica* or *japonica* panels. The most important QTLs were selected when they met at least one of the two following criteria: either consistently identified in both EXPs or close to previously reported cloned genes or fine-mapped QTL. We identified candidate genes for each important QTL in the following steps. Firstly, we identified all genes located inside the important QTL region (± 100 kb from lead SNP) from the Rice Genome Annotation Project database [http://rice.uga.edu/cgi-bin/gbrowse/rice/ (Kawahara et al., 2013)]. Secondly, all available SNPs inside these QTLs were searched from the 32 M SNPs data generated from 3 K RGP in the Rice SNP-Seek Database [https://snp-seek.irri.org, (Mansueto et al., 2016)]. Thirdly, all SNPs with minor allele frequency less than 0.05 and missing rate over 5% were removed to maintain only high-quality SNPs which were used to analyze GWAS by the multi-locus GWAS analysis [mrMLM package in R software (Zhang, 2019)]. The threshold was defined as $-\log_{10}$p-value ≥ 3 (Naveed et al., 2018). Then, for each candidate gene, we assembled the different haplotypes based on all polymorphic SNPs contained in the gene region by using PLINK software version 1.9 (Purcell et al., 2007). Finally, we tested the significance of phenotypic differences among major haplotypes (containing more than 10 accessions per haplotype) through ANOVA with the *post-hoc* Tukey HSD test. The genes with a significance level p-value< 0.05 and significantly different between the major haplotypes in both EXPs were considered to be candidate genes of the target traits.

2.8 Statistical analysis

Pearson's correlation coefficients between pairs of tested traits, ANOVA, and Tukey's tests were conducted by using R software ver.3.4.2 (R Development Core Team, 2019).

3 Results

3.1 Phenotypic variation and traits correlations

There was a wide range of variation for SDW, RDW, and PDW traits among the tested accessions, and the variation differed depending on N and NaCl treatments (Table 1 and Figure 1). Among them, SN-60Na performed the largest variation in SDW, followed by SN-0Na (in the main EXP) and LN-60Na (in the confirmatory EXP), and finally the LN-0Na treatment. Among the accessions, Babaomi, Molok, Aomierte 168, Local::IRGC 53300-1, Nona Bokra, ARC 11867, Xitto, Moddai Karuppan, Dawk Put, Hansraj, and Parn A 191 produced much higher SDWs than the average value in the different treatments.

The correlations among the traits in different treatments of the whole panel 1 (2,391 accessions in the main EXP) and panel 2 (1,332 accessions in the confirmatory EXP) were calculated (Supplementary Table S2C). In both EXPs, there were strong correlations between SDW, PDW, and RDW. Among the four treatments, the correlation between SDW and RDW in LN-0Na (0.69 in the main EXP and 0.75 in the confirmatory EXP) was weaker than those in the three other treatments (0.90 and 0.87, 0.93 and 0.87, 0.76 and 0.86 in SN-0Na, SN-60Na, and LN-60Na in the main and confirmatory EXP, respectively).

N, NaCl and their interactions showed the significant effect on all the dry weights (Supplementary Tables S2A, B). SDW decreased with either N-deficiency or NaCl application. RDW, however, was

TABLE 1 SDW, RDW, and PDW of rice accessions under different N and NaCl treatments at the seedling stage in the two experiments.

Trait	Treatment	The main EXP			The confirmatory EXP		
		Mean ± SD (g)	Range (g)	CV (%)	Mean ± SD (g)	Range (g)	CV (%)
SDW	SN-0Na	0.052 ± 0.026	0.004–0.190	50.18	0.059 ± 0.022	0.011–0.160	37.63
	LN-0Na	0.028 ± 0.008	0.007–0.063	28.64	0.035 ± 0.011	0.009–0.076	30.04
	SN-60Na	0.043 ± 0.022	0.003–0.179	51.11	0.032 ± 0.013	0.004–0.097	41.78
	LN-60Na	0.027 ± 0.008	0.005–0.058	29.29	0.025 ± 0.010	0.003–0.071	41.16
RDW	SN-0Na	0.012 ± 0.007	0.002–0.056	58.11	0.013 ± 0.005	0.002–0.040	42.75
	LN-0Na	0.012 ± 0.004	0.002–0.042	35.27	0.016 ± 0.006	0.002–0.040	38.30
	SN-60Na	0.010 ± 0.006	0.002–0.047	63.08	0.008 ± 0.004	0.002–0.031	51.67
	LN-60Na	0.009 ± 0.003	0.002–0.031	35.15	0.010 ± 0.005	0.002–0.047	48.89
PDW	SN-0Na	0.063 ± 0.032	0.005–0.229	50.83	0.072 ± 0.027	0.013–0.198	37.71
	LN-0Na	0.040 ± 0.011	0.012–0.092	28.42	0.051 ± 0.016	0.014–0.107	30.69
	SN-60Na	0.053 ± 0.028	0.004–0.221	52.75	0.039 ± 0.017	0.004–0.128	42.74
	LN-60Na	0.036 ± 0.011	0.007–0.084	29.21	0.035 ± 0.015	0.003–0.118	42.00

SD, standard deviation; CV, coefficient of variation; SN-0Na, no NaCl added and standard N concentration; LN-0Na, no NaCl added and low N concentration; SN-60Na, 60 mM NaCl added and standard N concentration; LN-60Na, 60 mM NaCl added and low N concentration.
The main EXP: 2,391 accessions; the confirmatory EXP: 1332 accessions.

reduced by the presence of NaCl but increased under N-deficiency treatment. Compared with the results of the main EXP, DWs in LN-0Na in the confirmatory EXP were slightly higher, and DWs in SN-60Na slightly lower than in the main EXP. DWs in LN-60Na and SN-0Na in both EXPs were similar (Table 1).

The four genetic subgroups - *indica*, *japonica*, *aromatic*, and *aus* – showed similar trends in both EXPs. Comparing these subgroups with each other, SDW of *indicas* was the highest, followed by *japonicas*, and then by *aus* under SN-0Na – the standard Yoshida solution – in both EXPs. SDW of the *aromatic* accessions was much lower than that of the *indica* type in the main EXP, whereas there were similar in the confirmatory EXP (Supplementary Figure S3). Under both LN-0Na and SN-60Na, *indica* and *aromatic* showed the highest SDW, followed by *japonica*, and finally *aus*. Under LN-60Na, the highest SDW was found in *aromatic*, followed by both *indica* and *japonica*, and finally *aus*. Thus, the *aromatic* accessions appear to better resist the simultaneous decrease in N and rise in NaCl application than the other genetic subgroups, as far as PDW is concerned, whereas *aus* accessions always showed the lowest PDWs.

3.2 Principal component analysis and LD decay

The principal component analysis of 2,391 and 1,332 accessions classified them into four main subgroups: *indica*, *japonica*, *aromatic*, and *aus* (Figure 2). The admixed accessions spread out the whole plot. The top three principal components (PC) of the analysis of 2,391 accessions explained 43.1 (PC1), 17.2 (PC2), and 7.3% (PC3) of the total variation while those of the analysis of 1,332 accessions explained 43.0, 17.3 and 7.4% of the total variation. Hence, the population structure should be considered in the following GWAS analysis.

LD decay of both whole panels (2,391 and 1,332 accessions) and the four main subgroups (*indica* – 1,418 accessions and *japonica* – 652 accessions, *aus* – 182 accessions, and *aromatic* – 66 accessions from panel 1) were analyzed quickly with 1 kb bin. The results indicated that the LD decay in the *indica* panel occurred on shorter distances than in the *aus*, *japonica*, and *aromatic* panels (Figure 3). The LD decayed to its half-maximum within around 134 kb for *indica*, 186 kb for *aus*, 312 kb for *japonica*, 390 kb for *aromatic*, and 280 kb for two whole panels.

3.3 Detection of QTLs by GWAS

In this section, we present the results of GWAS of all accessions of both panels (2,391 accessions and 1,332 accessions in the main and confirmatory EXP, respectively) and their subpopulations (1,418 *indica* accessions and 652 *japonica* accessions in the main EXP, and 767 *indica* accessions and 375 *japonica* accessions in the confirmatory EXP). For each trait, we analyzed GWAS with phenotypic data three times: with 2,391 accessions in the main EXP, with 1,332 accessions in the confirmatory EXP, and with the same 1,332 accessions extracted from the 2,391 ones in the main EXP. The Manhattan and Q-Q plot of the GWAS runnings is shown in the Supplementary Figure S4. The Q-Q plots for the GWAS results indicated that the model was well-fitted to the data.

We selected the confirmed QTLs, *i.e.* those that were identified in both EXPs. Subsequently, a total of 55 confirmed QTLs for one of the measured traits were detected in each of the four treatments (Table 2 and Supplementary Table S4). These QTLs were named according to the report of McCouch and CGSNL (Committee on Gene Symbolization, Nomenclature and Linkage, Rice Genetics Cooperative) (2008): *qPDWNS, qRDWNS, qSDWNS, qRePDWNS,*

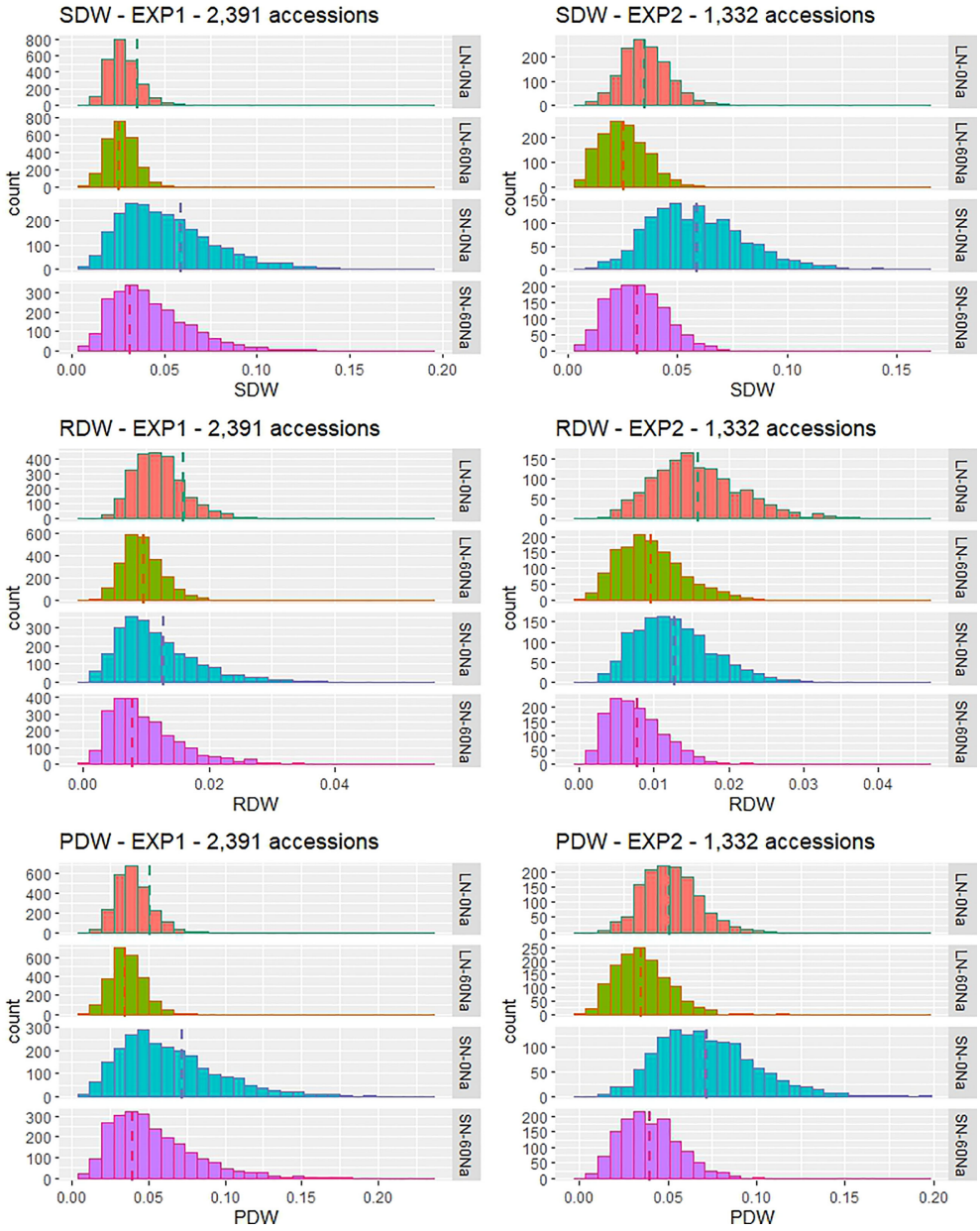

FIGURE 1
Frequency distribution of phenotypic values for SDW, RDW, and PDW in four treatments in two hydroponic experiments on the Yoshida et al. (1976) solution with 2,391 accessions (the main EXP) or 1,332 accessions (the confirmatory EXP) from the 3K Rice Genomes Project. LN: low N, 0.36 mM N, SN: standard N, 2.86 mM N, 0Na: no NaCl added, 60Na: 60 mM NaCl added, dashed line: mean value of the DWs in each treatment.

(PDWNS, RDWNS, SDWNS, RePDWNS, refers to plant dry weight, root dry weight, shoot dry weight, and the relative plant dry weight between treatments of nitrogen and salt concentrations, respectively) followed by the chromosome number and the detected QTL number in this chromosome. Among these 55 QTLs, 32, 16, and 7 were identified in the whole, the *indica*, and the *japonica* panel, respectively. QTLs were detected neither in all three panels together nor in both *japonica* or *indica* panels. There were some hotspots containing 5 pairs of QTLs detected in both the *indica* and the whole panel, *viz.*, *qPDWNS1.3* and *qPDWNS1.4, qSDWNS1.2* and *qSDWNS1.3, qPDWNS8.2* and *qPDWNS8.3, qRDWNS8.1* and *RDWNS8.2*, and *qSDWNS8.2* and *qSDWNS8.3*. Only one other hotspot contained a pair of QTLs detected in both the *japonica* and the whole panel: *qRePDWNS4.2* and *qRePDWNS4.3*.

More QTLs (24) were detected under standard conditions (SN-0Na) than in the three other treatments (8, 11, and 4 QTLs under LN-0Na, SN-60Na, and LN-60Na, respectively). Among the 32 QTLs detected in the whole panel, 12 were found in SN-0Na, 6 in LN-0Na, 6 in SN-60Na, 3 in LN-60Na, and 5 for the relative PDW between treatments. In the *indica* panel, the number of QTLs detected for these five treatments and relative PDW was 8, 1, 5, and 1, respectively, while in the *japonica* there were 4, 1, 0, and 0, respectively. One QTL for relative PDW between salinity and non-salinity under standard N was identified in the *indica* panel,

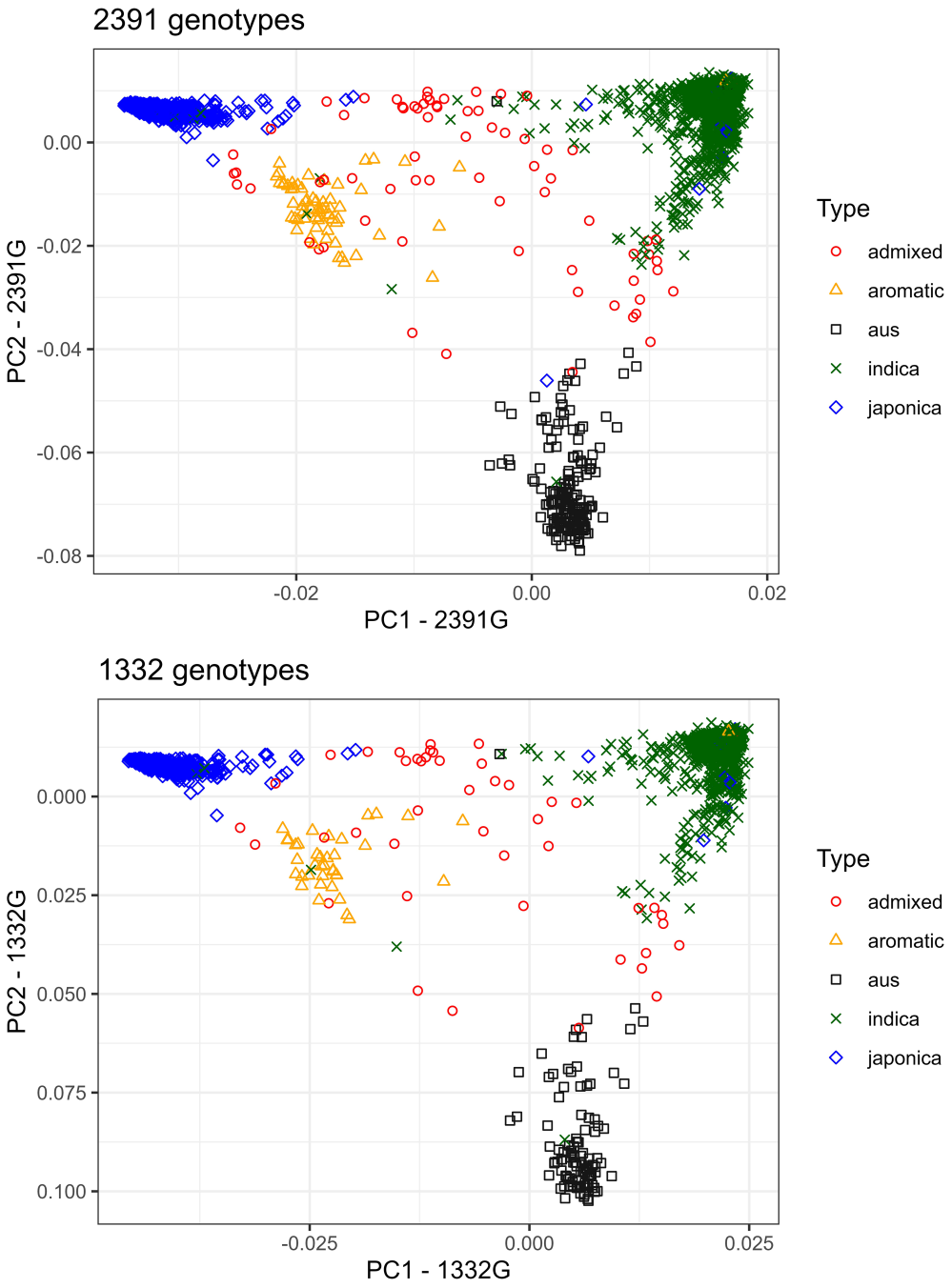

FIGURE 2
PCA plot (PC1 and PC2) of five genetic groups of rice accessions (the four *Oryza sativa* subspecies *indica*, *japonica*, *aus*, and *aromatic* and admixed accessions) using 588,792 SNPs from the 3K Rice Genomes Project. Left figure: PCA of 2,391 genotypes; right figure: PCA of the subset of 1,332 selected genotypes.

and 1 QTL for the relative PDW between low and standard N under saline treatment was detected in the *japonica* panel. None of the QTLs was detected in all four treatments simultaneously. Three QTLs were detected in SN-60Na overlapped with three QTLs detected in SN-0Na: *qPDWNS1.2*, *qSDWNS1.1*, *qPDWNS7.2* overlapped with *qPDWNS1.3*, *qSDWNS1.2*, and *qPDWNS7.1*, respectively. Another QTL *qPDWNS3.4* in SN-0Na was detected in an overlapping region containing *qPDWNS3.3* detected in LN-0Na.

3.4 Candidate genes for important QTLs

Among the 55 QTLs, we focused on some important QTLs in the whole panel – *i.e.* either with a lot of SNPs that passed the threshold or close to previously reported cloned genes or fine-mapped QTLs – to identify candidate genes. Thus, we detected 12 important QTLs, *viz. qRDWNS2.1*, *qPDWNS3.2*, *qSDWNS3.2*, *qPDWNS3.4*, *qPDWNS7.1*, *qSDWNS7.1*, *qPDWNS7.2*, *qPDWNS7.3*, *qPDWNS8.2*, *qRDWNS8.2*, *qSDWNS8.2*, and *qPDWNS9.1* that we retained for the further step of

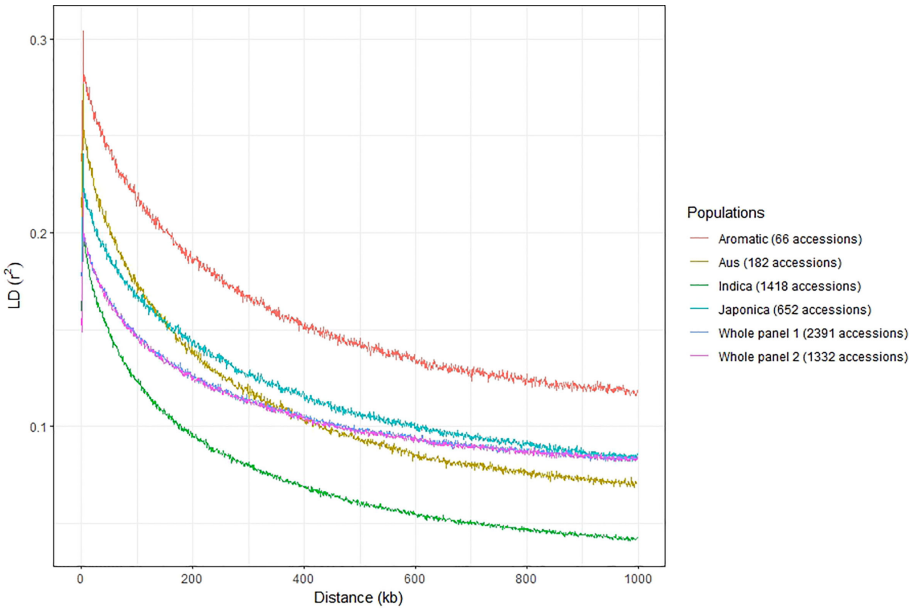

FIGURE 3
LD decay in whole panel 1 containing 2,391 accessions, whole panel 2 containing 1,332 accessions, and four subspecies *indica, japonica, aus*, and *aromatic* using 117,560 SNPs from the 3K Rice Genomes Project. Whole panels 1 and 2 share the same trend so that the curve for whole panel 1 is partially hidden by the curve of whole panel 2.

identifying candidate genes. Afterward, we were able to narrow down to a relatively small number of candidate genes, using a resolution of 200 kb for all identified important QTLs, resulting in 242 genes (Supplementary Table S6). Subsequently, we re-analyzed GWAS for the target traits by gene-based analysis of each QTL by multi-locus mrMLM (Zhang, 2019). Finally, matching SNPs passing the threshold in the gene-based analysis of the 242 genes above allowed us to select 12 genes harboring SNPs passing the threshold – $-\log_{10}$p-value ≥ 3 – to test significant phenotypic differences between haplotypes (Supplementary Table S7). Apart from the 12 genes above, we selected 3 additional genes based on their functional annotation in the database (Kawahara et al., 2013) for haplotype analysis (Supplementary Table S6). The values of the target traits for the different haplotypes in each of the 15 genes were analyzed through ANOVA. Significant differences were found among the major haplotypes in 11 of the 15 genes, which could be considered promising candidates associated with the target traits (Table 3; Figure 4; Supplementary Table S8). Meanwhile, 8 candidate genes were shortlisted from the 12 genes that passed the threshold ($-\log_{10}$p-value ≥ 3), and 3 other candidate genes that did not pass the threshold were identified from the selected genes in the annotation. Among them, six candidate genes of three important QTLs related to DW under SN-0Na were shortlisted, *viz. LOC_Os03g58350* and *LOC_Os03g58390* in *qPDWNS3.2* and *qSDWNS3.2; LOC_Os03g62480* and *LOC_Os03g62490* in *qPDWNS3.4; LOC_Os07g11290* and *LOC_Os07g11490* in *qPDWNS7.1*. Under SN-60Na, four candidate genes of three QTLs were detected, *viz. LOC_Os02g38230* and *LOC_Os02g38450* in *qRDWNS2.1, LOC_Os07g11420* and *LOC_Os07g11490* for *qSDWNS7.1* and *qPDWNS7.2*. Under LN-60Na, two candidate genes were detected in *qPDWNS9.1*: *LOC_Os09g20350* and *LOC_Os09g20480*. Finally, no candidate gene related to DW in LN-0Na was selected.

Based on the haplotype analysis and candidate genes identification, many useful accessions with high dry weight were shortlisted for future functional characterization related to NUE under saline condition. The accessions with haplotype 'CATTTACGACC' in *LOC_Os02g38230 (OsNAR2.1)* gene showed high RDW, e.g. Dawk Put, Nona Bokra, Ex Ebokozuru, Aus 78-125, Tsimatahopaosa, among other genotypes. The accessions with haplotype 'AGGTGATAGAGCACCAAGAG GAGGAGGCCAAATATAA' in *LOC_Os07g11420* and haplotype 'AAACTTAAC' in *LOC_Os07g11490* produced higher SDW and PDW than the accessions containing other haplotypes. These genotypes were – among others – Dawk Put, Do Khaw, Aus 278, Doc Phung D12, LG 9274, Khao Hae in *LOC_Os07g11420* and Khie Tom, Patnai 31-679, Kyauk Kyi, Suga Pankha, Quahng Luang, Toun, Pokkali, ARC 14737 in *LOC_Os07g11490*. The accessions with haplotype 'TCATCAC' in *OsDREB6 (LOC_Os09g20350)* gene showed higher PDW under LN-60Na conditions, e.g. Nona Bokra, Matali, Sachi, Mestre, RD 19, Babaomi, Sipot, San Bao Gu, Doc Phung D12 (Supplementary Table S9).

4 Discussion

This study investigated the dry weights of rice grown under different conditions of N and NaCl concentrations. The results showed that SDW decreased with either N-deficiency or NaCl application. It may be linked to a reduction in chlorophyll content, N uptake, N content, and photosynthetic capacity (Abdelgadir et al., 2005; Song et al., 2019; Phan et al., 2023). Moreover, under N-deficiency, rice plants do not have enough energy to maintain antioxidant activities to cope with oxidative damage, leading to over-accumulation of Na^+ and decrease in

TABLE 2A QTLs were detected for dry weight traits under different N and NaCl treatments in the whole panel in both EXPs.

No.	*QTL*	Trait	Treatment	Chr.	Peak position	Pvalue	Known genes/QTLs
1	*qPDWNS1.1*	PDW	SN-60Na	1	23013091	1.27E-06	_Na^+ uptake, K^+ uptake, ratio Na^+/K^+ (Koyama et al., 2001)
							_Root fresh weight (Li et al., 2005)
							_Drought tolerance (Hoang et al., 2019)
2	*qPDWNS1.4*	PDW	SN-0Na	1	29822571	2.73E-05	
3	*qPDWNS3.2*	PDW	SN-0Na	3	33327465	3.66E-06	_Fresh weight, dry weight, plant height, agNUE in low N (Nguyen et al., 2016)
4	*qPDWNS3.4*	PDW	SN-0Na	3	35608381	3.44E-06	_N uptake: *OsAMT3.2* (Suenaga et al., 2003)
							_Length of the third seedling leaf: *qLT3-1* (Cui et al., 2002)
							_1st internode length: *qIN1-3* (Yamamoto et al., 2001)
							_Plant height in low N (Nguyen et al., 2016)
5	*qPDWNS5.1*	PDW	SN-0Na	5	21591128	1.65E-06	_Fresh weight, shoot dry weight in standard N (Nguyen et al., 2016)
6	*qPDWNS7.1*	PDW	SN-0Na	7	6200245	1.13E-05	_Tillers/plant: *tp7b* (Li et al., 2000)
							_Fresh weight, dry weight (Nguyen et al., 2016)
7	*qPDWNS7.2*	PDW	SN-60Na	7	6226107	2.42E-06	_Tillers/plant: *tp7b* (Li et al., 2000)
							_Fresh weight, dry weight (Nguyen et al., 2016)
8	*qPDWNS7.3*	PDW	LN-0Na	7	26352042	6.57E-06	_Root length (Wan et al., 2003)
							_Shoot length: *qSL7* (Jahan et al., 2020)
							_N (Hsieh et al., 2018)
9	*qPDWNS8.2*	PDW	SN-0Na	8	27507063	1.27E-06	_ N (Hsieh et al., 2018)
							_aNUE, agNUE, fresh weight, dry weight (Nguyen et al., 2016)
10	*qPDWNS9.1*	PDW	LN-60Na	9	12272419	1.42E-05	_Salinity tolerance: *OsDREB6* (Ke et al., 2014)
							_Abiotic/biotic tolerance: *OsPAO7* (Liu et al., 2014)
							_Cl^- accumulation (Genc et al., 2014)
							_Shoot dry weight (Courtois et al., 2003)
							_Root dry weight: *rdw9* (Li et al., 2005)
							_NUE: *qPFP9.1* (Jewel et al., 2019)
							_Salt susceptible index (Tiwari et al., 2016)
11	*qRDWNS1.2*	RDW	SN-0Na	1	41096834	6.02E-06	_ Plant height in drought (Lafitte et al. 2002) _Biomass $plant^{-1}$: *qBMS1-2* (Hittalmani et al., 2003)
							_Plant height: *ph1* (Yu et al., 2002), *qPH1-1* (Cui et al., 2002)
12	*qRDWNS2.1*	RDW	SN-60Na	2	23177834	2.80E-07	_NUE: *OsNAR2.1* (Yan et al., 2011)
							_NUE: *qPFP1.2* (Jewel et al., 2019)
							_Plant height: *qPH-2* (Mao et al., 2004), *qCSH2* (Han et al., 2007)
							_Root thickness: *qRTT2-1* (Hemamalini et al., 2000)
13	*qRDWNS8.2*	RDW	SN-0Na	8	27640269	6.47E-06	_N (Hsieh et al., 2018)
							_aNUE, agNUE, fresh weight, dry weight (Nguyen et al., 2016)
14	*qRDWNS10.1*	RDW	LN-0Na	10	14391386	7.14E-06	
15	*qRePDWNS2.1*	RePDW	SN-60Na/SN-0Na	2	29744672	2.67E-05	
16	*qRePDWNS4.1*	RePDW	LN-60Na/LN-0Na	4	1740659	1.69E-06	

(Continued)

TABLE 2A Continued

No.	*QTL*	Trait	Treatment	Chr.	Peak position	Pvalue	Known genes/QTLs
17	*qRePDWNS4.2*	RePDW	LN-60Na/LN-0Na	4	4298186	1.46E-05	_Salt tolerance *qSKD_4.1* (Batayeva et al., 2018)
18	*qRePDWNS12.1*	RePDW	SN-60Na/SN-0Na	12	14854155	9.11E-06	
19	*qRePDWNS12.2*	RePDW	SN-60Na/SN-0Na	12	15112248	1.74E-05	_Drought tolerance (Bernier et al., 2007)
20	*qSDWNS1.3*	SDW	SN-0Na	1	29822571	2.08E-05	
21	*qSDWNS3.2*	SDW	SN-0Na	3	33327465	2.56E-06	_Fresh weight, dry weight, plant height, agNUE in low N (Nguyen et al., 2016)
22	*qSDWNS4.1*	SDW	LN-0Na	4	23135184	2.71E-05	_Nitrogen use efficiency *qNUE4.1* (Zhou et al., 2017) _Plant height: *qPH1-4-1* (Cui et al., 2004)
23	*qSDWNS5.1*	SDW	SN-0Na	5	21591128	1.58E-06	_Fresh weight, shoot dry weight in standard N (Nguyen et al., 2016)
24	*qSDWNS7.1*	SDW	SN-60Na	7	6307567	9.42E-07	_Tillers/plant: *tp7b* (Li et al., 2000) _Fresh weight, dry weight (Nguyen et al., 2016)
25	*qSDWNS7.2*	SDW	LN-0Na	7	20440198	1.83E-06	_Plant height: *Ph7a* (Zenbo et al., 1996) _Root dry weight (Wan et al., 2003)
26	*qSDWNS8.2*	SDW	SN-0Na	8	27507063	1.16E-06	_N (Hsieh et al., 2018) _aNUE, agNUE, fresh weight, dry weight (Nguyen et al., 2016)
27	*qSRRNS4.1*	SRR	LN-0Na	4	28212797	4.40E-08	
28	*qSRRNS5.1*	SRR	LN-60Na	5	18406533	3.52E-06	
29	*qSRRNS6.1*	SRR	SN-60Na	6	24725704	1.30E-06	_Root to shoot ratio (Ikeda et al., 2006)
30	*qSRRNS7.1*	SRR	SN-60Na	7	20705889	1.57E-05	
31	*qSRRNS7.1*	SRR	LN-60Na	9	1602896	7.57E-06	
32	*qSRRNS12.1*	SRR	LN-0Na	12	3395136	4.46E-07	

Chr, Chromosome.

TABLE 2B QTLs were detected for dry weight traits under different N and NaCl treatments in the *indica* panel in both EXPs.

No.	*QTL*	Trait	Treatment	Chr.	Peak position	Pvalue	Known genes/QTLs
1	*qPDWNS1.2*	PDW	SN-60Na	1	29517723	1.27E-06	
2	*qPDWNS1.3*	PDW	SN-0Na	1	29612773	1.16E-05	
3	*qPDWNS1.5*	PDW	SN-60Na	1	33808595	1.46E-05	
4	*qPDWNS2.1*	PDW	SN-0Na	2	29617039	1.60E-06	_Seedling dry weight: *qSDW2* (Han et al., 2007) _Plant height: *qPH-2* (Mao et al., 2004), in standard N (Nguyen et al., 2016)
5	*qPDWNS3.3*	PDW	LN-0Na	3	35495246	2.14E-05	_N uptake: *OsAMT3.2* (Suenaga et al., 2003) _Length of the third seedling leaf: *qLT3-1* (Cui et al., 2002) _1st internode length: *qIN1-3* (Yamamoto et al., 2001) _Plant height in low N (Nguyen et al., 2016)
6	*qPDWNS8.3*	PDW	SN-0Na	8	27602390	1.43E-05	_N (Hsieh et al., 2018) _aNUE, agNUE, fresh weight, dry weight (Nguyen et al., 2016)
7	*qRDWNS1.1*	RDW	SN-60Na	1	29517723	2.94E-05	

(Continued)

TABLE 2B Continued

No.	*QTL*	Trait	Treatment	Chr.	Peak position	Pvalue	Known genes/QTLs
8	*qRDWNS4.1*	RDW	LN-60Na	4	19933152	1.72E-07	
9	*qRDWNS8.1*	RDW	SN-0Na	8	27602390	5.92E-06	_N (Hsieh et al., 2018) _aNUE, agNUE, fresh weight, dry weight (Nguyen et al., 2016)
10	*qRePDWNS3.1*	RePDW	LN-60Na/SN-60Na	3	25687022	2.84E-10	
11	*qSDWNS1.1*	SDW	SN-60Na	1	29517723	8.08E-07	
12	*qSDWNS1.2*	SDW	SN-0Na	1	29612773	1.04E-05	
13	*qSDWNS1.4*	SDW	SN-0Na	1	30991676	7.13E-06	
14	*qSDWNS1.5*	SDW	SN-60Na	1	33808595	1.83E-05	
15	*qSDWNS1.6*	SDW	SN-0Na	1	37614990	1.34E-05	
16	*qSDWNS8.3*	SDW	SN-0Na	8	27602390	2.47E-05	_N (Hsieh et al., 2018) _aNUE, agNUE, fresh weight, dry weight (Nguyen et al., 2016)

Chr, Chromosome.

TABLE 2C QTLs were detected for dry weight traits under different N and NaCl treatments in the *japonica* panel in both EXPs.

No.	*QTL*	Trait	Treatment	Chr.	Peak position	Pvalue	Known genes/QTLs
1	*qPDWNS3.1*	PDW	SN-0Na	3	4974560	1.32E-06	
2	*qPDWNS8.1*	PDW	SN-0Na	8	573918	1.50E-06	
3	*qRePDWNS4.3*	RePDW	LN-60Na/LN-0Na	4	4403318	1.56E-06	_Salt tolerance *qSKD_4.1* (Batayeva et al., 2018)
4	*qRePDWNS8.1*	RePDW	LN-60Na/LN-0Na	8	26569164	7.25E-06	
5	*qSDWNS3.1*	SDW	SN-0Na	3	4974560	7.85E-06	
6	*qSDWNS8.1*	SDW	SN-0Na	8	573918	2.98E-06	
7	*qSDWNS10.1*	SDW	LN-0Na	10	18157987	8.57E-07	

Chr, Chromosome.

growth under saline conditions (Chen et al., 2022; Phan et al., 2023). RDW, however, was reduced by the presence of NaCl but increased under N-deficiency treatment. On the one hand, RDW may be reduced by salt by reducing root number, altering root morphological characteristics, as well as root oxidation capacity (Chen et al., 2022; Phan et al., 2023). On the other hand, RDW may be enhanced by decreasing N because N-deficiency promotes root length by enhancing cell division, cell elongation, amount of auxin, or by modifying the interaction between auxin and abscisic acid (Hsieh et al., 2018). The effect of N and NaCl also resulted in changes in phenotypic variation in SDW and RDW: with the largest variation in SN-0Na, following SN-60Na, LN-0Na, and the lowest in LN-60Na (Figure 3 and Table 1). The change in the phenotypic variation also might lead to a difference in the number of QTLs detected under different N and NaCl conditions. Indeed, SN-0Na treatment allowed to detect a very large number of QTLs (16), followed by SN-60Na (11), LN-0Na (8), and finally LN-60Na (4).

LD decay occurred more quickly in the *indica* panel, followed by *aus*, *japonica*, and finally in the *aromatic* panel. It was consistent with previous studies. Shi et al. (2017) also showed that LD decayed more quickly in the *indica* group than in non-*indica* groups. Mather et al. (2007) indicated that LD extends over a shorter distance in *indica* than *tropical japonica* and *temperate japonica*. The differences between the LDs among the groups were linked to differences in outcrossing and recombination rate. Higher recombination rates were associated with lower LD.

QTL identification can be influenced by both genotype-environment interactions and by the number of accessions in the population. Norton et al. (2021) and Talukdar et al. (2022) detected different QTLs in different years of research or different irrigated systems and none of the QTLs were detected under all the conditions. In our research, two EXPs were conducted with different numbers of accessions and light competition among the accessions. In the entire panel, we detected 157 loci for the tested traits from 2,391 accessions in the main EXP and 138 loci from 1,332 accessions in the confirmatory EXP (Supplementary Table S3A). Among them, 32 common QTLs were considered reliable because they were detected in both EXPs. Previously, Batayeva et al. (2018) detected two QTLs related to dry weight in non-saline condition but none of them under saline conditions by using a population containing 176 *temperate*

TABLE 3 List of 11 candidate genes for the important QTLs identified related to nitrogen use efficiency at the seedling stage under four N and NaCl treatments.

No	*Genes*	Chr.	Gene Product Name	Trait	Treatment	*QTL*
1	*LOC_Os02g38230*	2	high-affinity nitrate transporter, putative, expressed	RDW	SN-60Na	*qRDWNS2.1*
2	*LOC_Os02g38450*	2	expressed protein	RDW	SN-60Na	*qRDWNS2.1*
3	*LOC_Os03g58350*	3	*OsIAA14* - Auxin-responsive Aux/IAA gene family member, expressed	PDW, SDW	SN-0Na	*qPDWNS3.2, qSDWNS3.2*
4	*LOC_Os03g58390*	3	zinc finger, C3HC4 type domain containing protein, expressed	PDW, SDW	SN-0Na	*qPDWNS3.2, qSDWNS3.2*
5	*LOC_Os03g62480*	3	anthocyanidin 5,3-O-glucosyltransferase, putative, expressed	PDW	SN-0Na	*qPDWNS3.4*
6	*LOC_Os03g62490*	3	prohibitin-2, putative, expressed	PDW	SN-0Na	*qPDWNS3.4*
7	*LOC_Os07g11290*	7	expressed protein	PDW	SN-0Na	*qPDWNS7.1*
8	*LOC_Os07g11420*	7	transposon protein, putative, CACTA, En/Spm sub-class	PDW, SDW	SN-60Na	*qPDWNS7.2, qSDWNS7.1*
9	*LOC_Os07g11490*	7	expressed protein	PDW, SDW	SN-0Na, SN-60Na	*qPDWNS7.1, qSDWNS7.1, qPDWNS7.2*
10	*LOC_Os09g20350*	9	ethylene-responsive transcription factor, putative, expressed	PDW	LN-60Na	*qPDWNS9.1*
11	*LOC_Os09g20480*	9	transporter, putative, expressed	PDW	LN-60Na	*qPDWNS9.1*

Chr, chromosome.

japonica accessions. In the current study, we detected 3 of 32 QTLs under both saline and non-saline condition, with standard N supply. They co-localized with previously reported QTLs for tiller number per plant, fresh and dry weight of plants (Li et al., 2000; Nguyen et al., 2016). Other QTLs for DWs identified in our study under only saline but not under non-saline treatments were also found in the genomic regions containing QTLs for salt tolerance, *viz.* Na^+ uptake, K^+ uptake, and Na^+/K^+ concentration in the tissue (Koyama et al., 2001), drought tolerance (Hoang et al., 2019), salt susceptibility index (Tiwari et al., 2016), and Cl^- accumulation (Genc et al., 2014; Ke et al., 2014; Liu et al., 2014). Phan et al. (2023) reported that the salt-tolerant cultivars performed high NUE because they accumulated less Na^+ than the sensitive ones. Therefore, under saline conditions, the plants accumulating less toxic ions such as Na^+ and Cl^- could maintain water and nitrogen uptake. Consequently, the absorbed N can be better assimilated, resulting in higher tiller number, and finally, growth could be maintained. Among the 55 detected QTLs detected whether in the entire (32), or *indica* (16), or *japonica* panel (7) and confirmed in both EXPs in the present study, there were 28 QTLs for NUE-related traits which had never been reported before, *i.e* the QTLs located on chromosome 1, 2, 3, 5, 8, 10, and 12. The 27 other ones co-localized with previously reported QTLs for NUE-related traits (Table 2). Interestingly, a lot of QTLs co-localized with different traits in various studies. Indeed, *qPDWNS3.3* and *qPDWNS3.4* co-localized with the QTLs for the length of the first internode, length of the third leaf, plant height, and N uptake *OsAMT3.2* (Yamamoto et al., 2001; Cui et al., 2002; Li et al., 2012; Suenaga et al., 2003; Nguyen et al., 2016). *OsAMT3.2* is one of the ammonium transporter genes regulating ammonium uptake, expressed in old leaves, and was not influenced by salt stress (Wang et al., 2012). *qPDWNS7.3* in the region containing QTLs for root length, shoot length, and N metabolism (Wan et al., 2003; Hsieh et al., 2018; Jahan et al., 2020). *qRDWNS2.1* for RDW detected in SN-60Na was in an interval containing *OsNAR2.1* and *qPFP1.2* for NUE and in the region containing a QTL for root thickness (Hemamalini et al., 2000), and plant height (Mao et al., 2004; Han et al., 2007). *OsNAR2.1* regulates N uptake and is related to drought tolerance (Yan et al., 2011; Fan et al. 2017; Chen et al., 2019). *qPDWNS9.1* detected in the LN-60Na treatment has been related to dry weight and salinity tolerance in various studies (Courtois et al., 2003; Li et al., 2005; Genc et al., 2014; Ke et al., 2014; Liu et al., 2014; Tiwari et al., 2016; Jewel et al., 2019). This *qPDWNS9.1* region contained *OsDREB6* gene which was reported playing an important role in enhancing tolerance to osmotic, salinity, and cold stress (Ke et al., 2014).

Reanalyzing by multi-locus GWAS in mrMLM package plus searching genes with functional annotation and haplotype analysis allowed us to identify 11 candidate genes for SDW, RDW, and PDW in eight important QTLs under SN-0Na, SN-60Na, and LN-60Na (Table 3). Six, four, and two candidates were detected in SN-0Na, SN-60Na, and LN-60Na treatments, respectively. Among them, one gene was detected for PDW in both SN-0Na and SN-60Na treatments. In SN-0Na (normal condition), the six candidate genes detected in this study differed from the two QTLs identified previously (Batayeva et al., 2018). Among these six candidate genes, *LOC_Os03g58350* (*OsIAA14*) is a gene belonging to the auxin-responsive Aux/IAA gene family, that regulates lateral root development in rice *via* auxin signaling (Zhang et al., 2018). *LOC_Os03g58390 (OsSIRP2)* has been associated with salinity tolerance and osmotic tolerance (Chapagain et al., 2018). The other candidate genes were *LOC_Os03g62480*, *LOC_Os03g62490*, *LOC_Os07g11290*, and *LOC_Os07g11490*.

Under the SN-60Na condition, four candidate genes were identified: two candidate genes for RDW on chromosome 2 and two candidates for SDW and PDW together on chromosome 7. The two candidate genes for *qRDWNS2.1* controlling RDW in SN-60Na on chromosome 2:

10.3389/fpls.2023.1197271

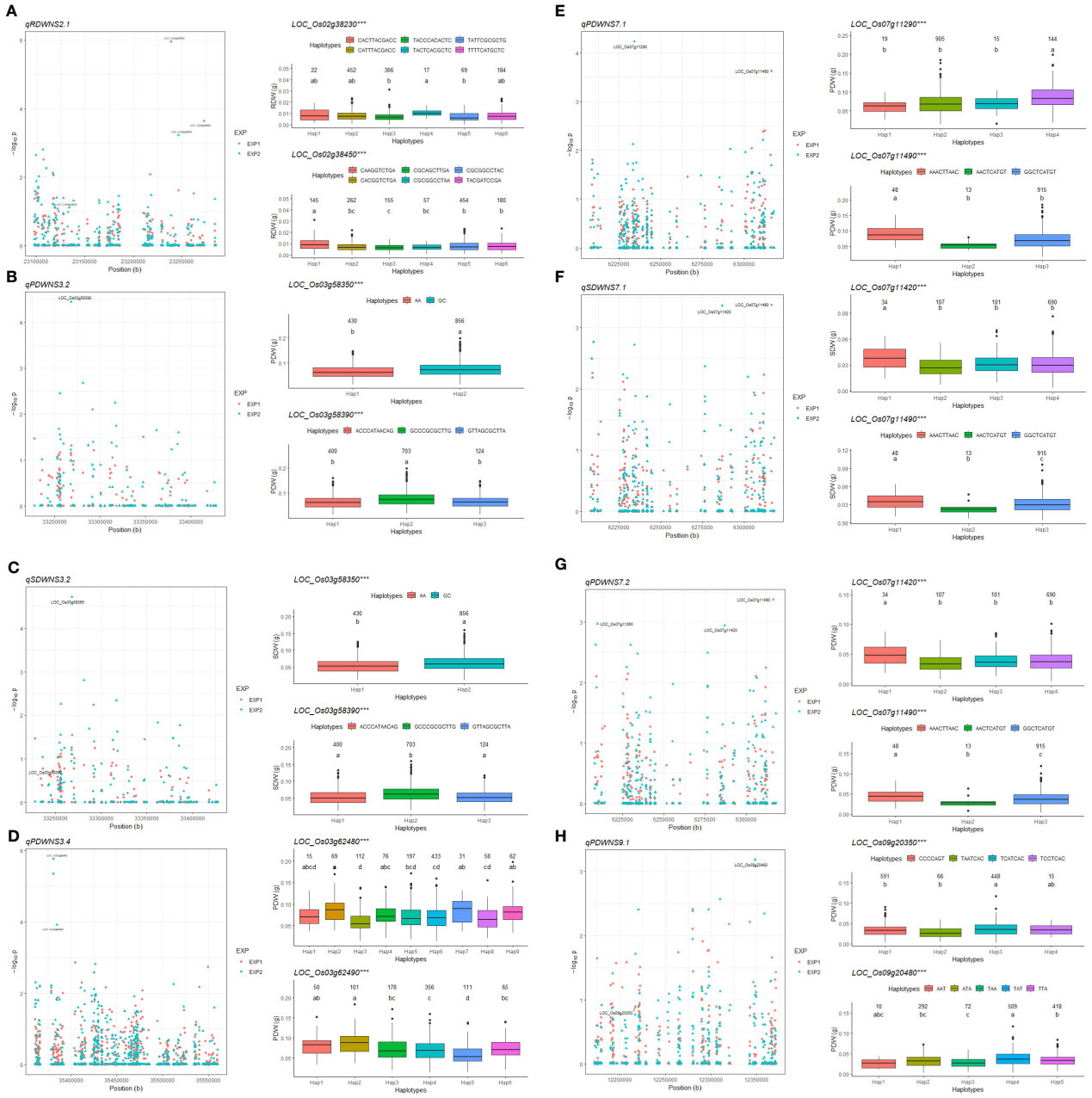

FIGURE 4
Gene-based association and haplotype analysis of targeted genes for *qRDWNS2.1* **(A)**, *qPDWNS3.2* **(B)**, *qSDW3.2* **(C)**, *qPDWNS3.4* **(D)**, *qPDWNS7.1* **(E)**, *qSDWNS7.1* **(F)**, *qPDWNS7.2* **(G)** and *qPDWNS9.1* **(H)**. Each point is one SNP in the association of the QTLs. The value and letter on the boxplot (a, b, c, and d) indicate the number of individuals in each haplotype in the confirmatory EXP and multiple comparison results at the significance level of 0.05, respectively. *** significance level of ANOVA for phenotypic value of the main haplotypes at $p < 0.001$.

LOC_Os02g38230 (OsNAR2.1) and *LOC_Os02g38450*. Overexpression of protein OsNAR2.1 improves N uptake as well as chlorophyll content, photosynthetic rate, water use efficiency, and grain yield under drought stress (Chen et al., 2019) but no information related to *OsNAR2.1* in rice has been reported under saline conditions. This gene interacts with *OsNRT2.1, OsNRT2.2*, and *OsNRT2.3a* and plays a key role in enabling plants to cope with a variable nitrate supply (Yan et al., 2011). Wang et al., (2012) reported that the expression level of the *OsNRT* gene family was influenced by salt stress, thereby reducing nitrate accumulation in salt conditions. Especially, Shi et al. (2017) also documented that the gene *OsNRT2.2*, which interacts with *OsNAR2.1*, was associated with the salt susceptibility index in rice at the germination stage. In our study, we found that *OsNAR2.1* is a candidate for controlling RDW under saline condition. Another candidate gene for *qRDWNS2.1* was *LOC_Os02g38450* for which no gene ontology classification has been published. Other candidate genes on chromosome 7, viz. *LOC_Os07g11420* and *LOC_Os07g11490* for *qPDWNS7.1*, *qSDWNS7.1*, and *qPDWNS7.2*. were poorly documented previously.

In LN-60Na treatment, *OsDREB6 (LOC_Os09g20350)* in *qPDWNS9.1* is an ethylene-responsive transcription factor that

controls tolerance to osmotic, drought, cold, and salinity stresses (Ke et al., 2014). Some varieties with 'TCATCAC' haplotype, such as Nona Bokra, Doc Phung D12 have been well-documented for their salt tolerance (Lutts et al., 1996; Ho et al., 2018). Another candidate gene for QTL *qPDWNS9.1*, *LOC_Os09g20480* (homolog to *Sb02g023340* in sorghum and *Traes_5AL_F8B48EC59* in wheat), encodes a transporter protein. This gene has been reported to be related to Cl^- accumulation in wheat (Genc et al., 2014).

5 Conclusion

By realizing a GWAS on 2,391 accessions with 235,210 SNPs and confirming the results on 1,332 accessions, we detected 55 QTLs for SDW, RDW, PDW, and relative PDW in different treatments. Among them, 28 QTLs were novel and the other 27 QTLs co-located with previously detected ones. Three of 11 QTLs that were identified under salt treatments were close to regions containing 3 QTLs detected in non-saline conditions. Some of the detected QTLs for DWs under saline conditions co-localized with known QTLs or genes for salt tolerance. Then further haplotype analysis allowed us to identify 11 candidate genes for eight important QTLs related to DW traits. Further study should be carried out to validate these genes in field environment. Moreover, salt and N concentrations in the tissue as well as NUE components should be determined and submitted to GWAS to find genetic information as well as candidate genes associated with these traits. Our results provide useful germplasm and genetic information for the future improvement of NUE in rice and rice production.

Data availability statement

The datasets presented in this study can be found in online repositories. The names of the repository or repositories and accession number(s) can be found in the article or Supplementary Material.

Author contributions

NP, CP, and PB designed the project. NP analyzed the GWAS and identified the candidate genes. NP, XD, and PB wrote and revised the manuscript. All authors read and approved the final manuscript.

Funding

This research received support from the Belgian Académie de Recherche et d'Enseignement Supérieur – Commission de la Coopération au Développement (ARES-CCD: www.ares-ac.be). The rice accessions were provided by IRRI to UCLouvain under SMTA2018-0139 and SMTA2018-0140 signed between these organizations.

Conflict of interest

The authors declare that the research was conducted in the absence of any commercial or financial relationships that could be construed as a potential conflict of interest.

Publisher's note

Supplementary material

The Supplementary Material for this article can be found online at: https://www.frontiersin.org/articles/10.3389/fpls.2023.1197271/full#supplementary-material

References

3K RGP (2014). The 3,000 Rice Genomes Project. *GigaScience* 3, 3–7. doi: 10.1186/2047-217X-3-7

Abdelgadir, E. M., Oka, M., and Fujiyama, H. (2005). Nitrogen nutrition of rice plants under salinity. *Biol. Plantarum* 49 (1), 99–104. doi: 10.1007/s10535-005-0104-8

Aravind, J., Mukesh Sankar, S., Wankhede, D., and Kaur, V. (2020). *augmentedRCBD: Analysis of Augmented Randomised Complete Block Designs* R package version 0.1.6.9000. Available at: https://aravind-j.github.io/augmentedRCBD/ https://cran.r-project.org/package=augmentedRCBD.

Batayeva, D., Labaco, B., Ye, C., Li, X., Usenbekov, B., Rysbekova, A., et al. (2018). Genome-wide association study of seedling stage salinity tolerance in *temperate japonica* rice germplasm. *BMC Genet.* 19, 2. doi: 10.1186/s12863-017-0590-7

Beatty, P. H., and Good, A. G. (2018). "Improving nitrogen use efficient in crop plants using biotechnology approaches," in *Engineering Nitrogen Utilization in Crop Plants*. Eds. A. Shrawat, A. Zayed and D. A. Lightfoot (Cham: Springer International Publishing), 15–35.

Bernier, J., Kumar, A., Ramaiah, V., Spaner, D., and Atlin, G. (2007). A large-Eeffect QTL for grain yield under reproductive-stage drought stress in upland rice. *Crop Sci.* 47, 507–516. doi: 10.2135/cropsci2006.07.0495

Bradbury, P. J., Zhang, Z., Kroon, D. E., Casstevens, T. M., Ramdoss, Y., and Buckler, E. S. (2007). TASSEL: Software for association mapping of complex traits in diverse samples. *Bioinformatics* 23, 2633–2635. doi: 10.1093/bioinformatics/btm308

Chapagain, S., Park, Y. C., Kim, J. H., and Jang, C. S. (2018). *Oryza sativa* salt-induced RING E3 ligase 2 (*OsSIRP2*) acts as a positive regulator of transketolase in plant response to salinity and osmotic stress. *Planta* 247, 925–939. doi: 10.1007/s00425-017-2838-x

Chen, J., Qi, T., Hu, Z., Fan, X., Zhu, L., Iqbal, M. F., et al. (2019). *OsNAR2.1* positively regulates drought tolerance and grain yield under drought stress conditions in rice. *Front. Plant Sci.* 10. doi: 10.3389/fpls.2019.00197

Chen, Y., Liu, Y., Ge, J., Li, R., Zhang, R., Zhang, Y., et al. (2022). Improved physiological and morphological traits of root synergistically enhanced salinity tolerance in rice under appropriate nitrogen application rate. *Front. Plant Sci.* 13. doi: 10.3389/fpls.2022.982637

Courtois, B., Shen, L., Petalcorin, W., Carandang, S., Mauleon, R., and Li, Z. (2003). Locating QTLs controlling constitutive root traits in the rice population IAC 165 × Co39. *Euphytica* 134, 335–345. doi: 10.1023/B:EUPH.0000004987.88718.d6

Cui, K., Peng, S., Xing, Y., Yu, S., and Xu, C. (2002). Molecular dissection of relationship between seedling characteristics and seed size in rice. *Acta Botanica Sin.* 44, 702–707.

Cui, K., Peng, S., Ying, Y., Yu, S., and Xu, C. (2004). Molecular dissection of the relationships among tiller number, plant height and heading date in rice. *Plant Production Sci.* 7, 309–318. doi: 10.1626/pps.7.309

Decui, Y., Qing, X., Fanggui, Z., Mian, L., and Xin, L. (2020). Effects of NaCl stress on nitrogen metabolism and related gene expression of rice with different resistance. *Acta Agriculturae Boreali-Sinica* 2, 187195.

Eckstein, D., Winges, M., Künzel, V., and Schäfer, L. (2019). *Global Climate Risk Index 2020: who suffers most from extreme weather events? wether-related loss events in 2018 and 1999 to 2018* (Bonn, Germany: Germanwatch Nord-Süd Initiative eV).

Fan, X., Naz, M., Fan, X., Xuan, W., Miller, A., and xu, G. (2017). Plant nitrate transporters: From gene function to application. *J. Exp. Bot.* 68, no. 10, 24632475. doi: 10.1093/jxb/erx011

Fang, P., and Wu, P. (2001). QTL × N-level interaction for plant height in rice (*Oriza Sativa* L.). *Plant Soil* 236, 237–242. doi: 10.1023/A:1012787510201

FAO (2021) *FAOSTAT Database*. Available at: http://www.fao.org/faostat/en/#data/QC (Accessed January 6, 2021).

Federer, W. T., and Raghavarao, D. (1975). On Augmented Designs. *Biometrics* 31, 29–35. doi: 10.2307/2529707

Genc, Y., Taylor, J., Rongala, J., and Oldach, K. (2014). A major locus for chloride accumulation on chromosome 5a in bread wheat. *PloS One* 9, e98845. doi: 10.1371/journal.pone.0098845

Han, L., Qiao, Y., Zhang, S., Zhang, Y., Cao, G., Kim, J., et al. (2007). Identification of quantitative trait loci for cold response of seedling vigor traits in rice. *J. Genet. Genomics* 34, 239–246. doi: 10.1016/S1673-8527(07)60025-3

Heffer, P., and Prud'homme, M. (2017). "Fertilizer Outlook 2017–2021," in *Proceedings of the 85th IFA Annual Conference*, Marrakech, Morocco. 2244 May.

Hemamalini, G. S., Shashidhar, H. E., and Hittalmani, S. (2000). Molecular marker assisted tagging of morphological and physiological traits under two contrasting moisture regimes at peak vegetative stage in rice (*Oryza sativa* L.). *Euphytica* 112, 69–78. doi: 10.1023/A:1003854224905

Hittalmani, S., Huang, N., Courtois, B., Venuprasad, R., Shashidhar, H. E., Zhuang, J.-Y., et al. (2003). Identification of QTL for growth- and grain yield-related traits in rice across nine locations of Asia. *Theor. Appl. Genet.* 107, 679–690. doi: 10.1007/s00122-003-1269-1

Ho, V. T., Quoc, N., and Cuong, B. (2018). Evaluating salt tolerance of twenty traditional rice varieties from Vietnam. *J. Sci. Technol. Food*, 3–11.

Hoai, N. T. T., Shim, I. S., Kobayashi, K., and Kenji, U.. (2003). Accumulation of some nitrogen compounds in response to salt stress and their relationships with salt tolerance in rice (*Oryza sativa* L.) seedlings. *Plant Growth Regul.* 41, 159–164. doi: 10.1023/A:1027305522741

Hoang, G. T., Van Dinh, L., Nguyen, T. T., Ta, N. K., Gathignol, F., Mai, C. D., et al. (2019). Genome-wide association study of a panel of Vietnamese rice landraces reveals new QTLs for tolerance to water deficit during the vegetative phase. *Rice* 12, 4. doi: 10.1186/s12284-018-0258-6

Hsieh, P.-H., Kan, C.-C., Wu, H.-Y., Yang, H.-C., and Hsieh, M.-H. (2018). Early molecular events associated with nitrogen deficiency in rice seedling roots. *Sci. Rep.* 8, 12207. doi: 10.1038/s41598-018-30632-1

Huang, J., Zhu, C., Hussain, S., Huang, J., Liang, Q., Zhu, L., et al. (2020). Effects of nitric oxide on nitrogen metabolism and the salt resistance of rice (Oryza sativa L.) seedlings with different salt tolerances. *Plant Physiol. Biochem.* 155, 374383. doi: 10.1016/j.plaphy.2020.06.013

Huang, X., Wei, X., Sang, T., Zhao, Q., Feng, Q., Zhao, Y., et al. (2010). Genome-wide association studies of 14 agronomic traits in rice landraces. *Nat. Genet.* 42, 961–967. doi: 10.1038/ng.695

IFA. (2019). *IFASTAT*. Available at: https://www.ifastat.org/databases/plant-nutrition (Accessed September 20, 2019).

Ikeda, H., Kamoshita, A., and Manabe, T. (2006). Genetic analysis of rooting ability of transplanted rice (*Oryza sativa* L.) under different water conditions. *J. Exp. Bot.* 58, 309–318. doi: 10.1093/jxb/erl162

Jahan, N., Zhang, Y., Lv, Y., Song, M., Zhao, C., Hu, H., et al. (2020). QTL analysis for rice salinity tolerance and fine mapping of a candidate locus *qSL7* for shoot length under salt stress. *Plant Growth Regul.* 90, 307–319. doi: 10.1007/s10725-019-00566-3

Jewel, Z. A., Ali, J., Mahender, A., Hernandez, J., Pang, Y., and Li, Z. (2019). Identification of quantitative trait loci associated with nutrient use efficiency traits, using SNP markers in an early backcross population of rice (*Oryza sativa* L.). *Int. J. Mol. Sci.* 20, 900. doi: 10.3390/ijms20040900

Kawahara, Y., Bastide, M., Hamilton, J., Kanamori, H., Mccombie, W., Ouyang, S., et al. (2013). Improvement of the *Oryza sativa* Nipponbare reference genome using next generation sequence and optical map data. *Rice* 6, 4. doi: 10.1186/1939-8433-6-4

Ke, Y.-G., Yang, Z.-J., Yu, S.-W., Li, T.-F., Wu, J.-H., Gao, H., et al. (2014). Characterization of *OsDREB6* responsive to osmotic and cold stresses in rice. *J. Plant Biol.* 57, 150–161. doi: 10.1007/s12374-013-0480-0

Koyama, M. L., Levesley, A., Koebner, R. M. D., Flowers, T. J., and Yeo, A. R. (2001). Quantitative trait loci for component physiological traits determining salt tolerance in rice. *Plant Physiol.* 125, 406 LP–422. doi: 10.1104/pp.125.1.406

Ladha, J. K., Pathak, H., J. Krupnik, T., Six, J., and van Kessel, C.B.T.-A. (2005). Efficiency of fertilizer nitrogen in cereal production: Retrospects and prospects. *Adv. Agron.* 87, 85-156. doi: 10.1016/S0065-2113(05)87003-8

Lafitte, H., Courtois, B., and Arraudeau, M. (2002). Genetic improvement of rice in aerobic systems: Progress from yield to genes. *Field Crops Res.* 75, 171–190. doi: 10.1016/S0378-4290(02)00025-4

Lea, P. J., and Miflin, B. J. (2003). Glutamate synthase and the synthesis of glutamate in plants. *Plant Physiol. Biochem.* 41, 555–564. doi: 10.1016/S0981-9428(03)00060-3

Li, S.-M., Li, B.-Z., and Shi, W.-M. (2012). Expression patterns of nine ammonium transporters in rice in response to N status. *Pedosphere* 22, 860–869. doi: 10.1016/S1002-0160(12)60072-1

Li, Z., Mu, P., Li, C., Zhang, H., Li, Z., Gao, Y., et al. (2005). QTL mapping of root traits in a doubled haploid population from a cross between upland and lowland japonica rice in three environments. *Theor. Appl. Genet.* 110, 1244–1252. doi: 10.1007/s00122-005-1958-z

Li, J.-Y., Wang, J., and Zeigler, R. S. (2014). The 3,000 rice genomes project: new opportunities and challenges for future rice research. *GigaScience* 3, 2047-217X-3–8. doi: 10.1186/2047-217X-3-8

Li, J. X., Yu, S. B., Xu, C. G., Tan, Y. F., Gao, Y. J., Li, X. H., et al. (2000). Analyzing quantitative trait loci for yield using a vegetatively replicated F2 population from a cross between the parents of an elite rice hybrid. *Theor. Appl. Genet.* 101, 248–254. doi: 10.1007/s001220051476

Lian, X., Xing, Y., Yan, H., Xu, C., Li, X., and Zhang, Q. (2005). QTLs for low nitrogen tolerance at seedling stage identified using a recombinant inbred line population derived from an elite rice hybrid. *Theor. Appl. Genet.* 112, 85–96. doi: 10.1007/s00122-005-0108-y

Lippert, C., Listgarten, J., Liu, Y., Kadie, C. M., Davidson, R. I., and Heckerman, D. (2011). FaST linear mixed models for genome-wide association studies. *Nat. Methods* 8, 833-835. doi: 10.1038/nmeth.1681

Liu, C., Chen, K., Zhao, X., Wang, X., Shen, C., Zhu, Y., et al. (2019). Identification of genes for salt tolerance and yield-related traits in rice plants grown hydroponically and under saline field conditions by genome-wide association study. *Rice* 12, 88. doi: 10.1186/s12284-019-0349-z

Liu, T., Kim, D. W., Niitsu, M., Maeda, S., Watanabe, M., Kamio, Y., et al. (2014). Polyamine Oxidase 7 is a terminal catabolism-type enzyme in *Oryza sativa* and is specifically expressed in anthers. *Plant Cell Physiol.* 55, 1110–1122. doi: 10.1093/pcp/pcu047

Lutts, S., Kinet, J. M., and Bouharmont, J. (1996). Effects of salt stress on growth, mineral nutrition and proline accumulation in relation to osmotic adjustment in rice (*Oryza sativa* L.) cultivars differing in salinity resistance. *Plant Growth Regul.* 19, 207–218. doi: 10.1007/BF00037793

Mansueto, L., Fuentes, R. R., Borja, F. N., Detras, J., Abriol-Santos, J. M., Chebotarov, D., et al. (2016). Rice SNP-seek database update: new SNPs, indels, and queries. *Nucleic Acids Res.* 45, D1075–D1081. doi: 10.1093/nar/gkw1135

Mao, B.-B., Cai, W.-J., Zhang, Z., Hu, Z.-L., Li, P., Zhu, L., et al. (2004). Characterization of QTLs for harvest index and source-sink characters in a DH population of rice (*Oryza sativa* L.). *Yi Chuan xue bao = Acta genetica Sin.* 30, 1118–1126.

Mather, K. A., Caicedo, A. L., Polato, N. R., Olsen, K. M., McCouch, S., and Purugganan, M. D. (2007). The extent of linkage disequilibrium in rice (*Oryza sativa* L.). *Genetics.* 177 (4), 2223–2232. doi: 10.1534/genetics.107.079616

McCouch, S. R. &CGSNL (Committee on Gene Symbolization, Nomenclature and Linkage, Rice Genetics Cooperative) (2008). Gene Nomenclature System for Rice. *Rice* 1, 72–84. doi: 10.1007/s12284-008-9004-9

Murtaza, G., Azooz, M. M., Murtaza, B., Usman, Y., and Saqib, M. (2013). "Nitrogen-use-efficiency (NUE) in plants under NaCl stress," in *Salt stress in plants*. Eds. P. Ahmad, M. M. Azooz and M. N. V. Prasad (New York, NY: Springer), 415–437. doi: 10.1007/978-1-4614-6108-1_16

Naveed, S. A., Zhang, F., Zhang, J., Zheng, T.-Q., Meng, L.-J., Pang, Y.-L., et al. (2018). Identification of QTN and candidate genes for salinity tolerance at the germination and seedling stages in rice by genome-wide association analyses. *Sci. Rep.* 8, 6505. doi: 10.1038/s41598-018-24946-3

Nguyen, H., Dang, T., Cuong, P., and Bertin, P. (2016). QTL mapping for nitrogen use efficiency and related physiological and agronomical traits during the vegetative phase in rice under hydroponics. *Euphytica* 212, 473500. doi: 10.1007/s10681-016-1778-z

Nguyen, H. T. T., Pham, C. V., and Bertin, P. (2014). The effect of nitrogen concentration on nitrogen use efficiency and related parameters in cultivated rices (*Oryza sativa* L. subsp. *indica* and *japonica* and *O. glaberrima* Steud.) in hydroponics. *Euphytica* 198, 137–151. doi: 10.1007/s10681-014-1101-9

Norton, G. J., Travis, A., Ruang-Areerate, P., Nicol, G. W., Adeosun, A. A., Hossain, M., et al. (2021). Genetic loci regulating cadmium content in rice grains. *Euphytica* 217, 35. doi: 10.1007/s10681-020-02752-1

Ouyang, J., Cai, Z., Xia, K., Wang, Y., Duan, J., and Zhang, M. (2010). Identification and analysis of eight peptide transporter homologs in rice. *Plant Sci.* 179, 374–382. doi: 10.1016/j.plantsci.2010.06.013

Phan, T. H. N., Tang, T. H., Bertin, P., and Pham, V. C. (2017). Effect of inorganic nitrogen forms and concentration on growth of rice genotypes under severe saline condition. *Vietnam J. Agri Sci.* 15, 189197.

Phan, N. T. H., Heymans, A., Bonnave, M., Lutts, S., Pham, C. V., and Bertin, P. (2023). Nitrogen use efficiency of rice cultivars (*Oryza sativa* l.) under salt stress and low nitrogen conditions. *J. Plant Growth Regul.* 42, 1789–1803. doi: 10.1007/s00344-022-10660-y

Price, A. H., Townend, J., Jones, M. P., Audebert, A., and Courtois, B. (2002). Mapping QTLs associated with drought avoidance in upland rice grown in the Philippines and West Africa. *Plant Mol. Biol.* 48, 683–695. doi: 10.1023/A:1014805625790

Purcell, S., Neale, B., Todd-Brown, K., Thomas, L., Ferreira, M. A. R., Bender, D., et al. (2007). PLINK: A tool set for whole-genome association and population-based linkage analyses. *Am. J. Hum. Genet.* 81, 559–575. doi: 10.1086/519795

R Development Core Team. (2019). *R: A language and environment for statistical computing* (Vienna, Austria: R Foundation for Statistical Computing). Available at: http://www.R-project.org.

Rohilla, P., and Yadav, J. P. (2019). Acute salt stress differentially modulates nitrate reductase expression in contrasting salt responsive rice cultivars. *Protoplasma* 256 (5), 1267–1278. doi: 10.1007/s00709-019-01378-y

Sandhu, N., Sethi, M., Kumar, A., Dang, D., Singh, J., and Chhuneja, P. (2021). Biochemical and genetic approaches improving nitrogen use efficiency in cereal crops: a review. *Front. Plant Sci.*

Sharma, N., Sinha, V. B., Prem Kumar, N. A., Subrahmanyam, D., Neeraja, C. N., Kuchi, S., et al. (2021). Nitrogen use efficiency phenotype and associated genes: roles of germination, flowering, root/shoot length and biomass. *Front. Plant Sci.* 11. doi: 10.3389/fpls.2020.587464

Shi, Y., Gao, L., Wu, Z., Zhang, X., Wang, M., Zhang, C., et al. (2017). Genome-wide association study of salt tolerance at the seed germination stage in rice. *BMC Plant Biol.* 17, 1–11. doi: 10.1186/s12870-017-1044-0

Smajgl, A., Toan, T. Q., Nhan, D. K., Ward, J., Trung, N. H., Tri, L. Q., et al. (2015). Responding to rising sea levels in the Mekong Delta. *Nat. Climate Change* 5, 167–174. doi: 10.1038/nclimate2469

Song, X., Zhou, G., Ma, B.-L., Wu, W., Ahmad, I., Zhu, G., et al. (2019). Nitrogen application improved photosynthetic productivity, chlorophyll fluorescence, yield and yield components of two oat genotypes under saline conditions. *Agronomy* 9, 115. doi: 10.3390/agronomy9030115

Suenaga, A., Moriya, K., Sonoda, Y., Ikeda, A., von Wirén, N., Hayakawa, T., et al. (2003). Constitutive expression of a novel-type ammonium transporter OsAMT2 in rice plants. *Plant Cell Physiol.* 44, 206–211. doi: 10.1093/pcp/pcg017

Talukdar, P., Travis, A. J., Hossain, M., Islam, M. R., Norton, G. J., and Price, A. H. (2022). Identification of genomic loci regulating grain iron content in aus rice under two irrigation management systems. *Food Energy Secur.* 11, e329. doi: 10.1002/fes3.329

Tang, W., Ye, J., Yao, X., Zhao, P., Xuan, W., Tian, Y., et al. (2019). Genome-wide associated study identifies NAC42-activated nitrate transporter conferring high nitrogen use efficiency in rice. *Nat. Commun.* 10, 5279. doi: 10.1038/s41467-019-13187-1

Tiwari, S., SL, K., Kumar, V., Singh, B., Rao, A., Mithra SV, A., et al. (2016). Mapping QTLs for salt tolerance in rice (*Oryza sativa* L.) by bulked segregant analysis of recombinant inbred lines using 50K SNP chip. *PloS One* 11, e0153610. doi: 10.1371/journal.pone.0153610

Udvardi, M., Below, F. E., Castellano, M. J., Eagle, A. J., Giller, K. E., Ladha, J. K., et al. (2021). A Research Road Map for Responsible Use of Agricultural Nitrogen. *Front. Sustain. Food Syst.* 5. doi: 10.3389/fsufs.2021.660155

Wan, J.-L., Zhai, H.-Q., Wan, J.-M., Yasui, H., and Yoshimura, A. (2003). Mapping QTL for traits associated with resistance to ferrous iron toxicity in rice (*Oryza sativa* L.), using *japonica* chromosome segment substitution lines. *Yi Chuan xue bao = Acta genetica Sin.* 30, 893–898.

Wang, H., Zhang, M., Guo, R., Shi, D., Liu, B., Lin, X., et al. (2012). Effects of salt stress on ion balance and nitrogen metabolism of old and young leaves in rice (Oryza sativa l.). *BMC Plant Biol.* 12, 194. doi: 10.1186/1471-2229-12-194

Wang, X., Pang, Y., Zhang, J., Wu, Z., Chen, K., Ali, J., et al. (2017). Genome-wide and gene-based association mapping for rice eating and cooking characteristics and protein content. *Sci. Rep.* 7, 17203. doi: 10.1038/s41598-017-17347-5

Wassmann, R., Phong, N. D., Tho, T. Q., Hoanh, C. T., Khoi, N. H., Hien, N. X., et al. (2019). High-resolution mapping of flood and salinity risks for rice production in the Vietnamese Mekong Delta. *Field Crops Res.* 236, 111–120. doi: 10.1016/j.fcr.2019.03.007

Yamamoto, T., Taguchi-Shiobara, F., Ukai, Y., Sasaki, T., and Yano, M. (2001). Mapping quantitative trait loci for days-to-heading, and culm, panicle and internode lengths in a BC1F3 population using an elite rice variety, Koshihikari, as the recurrent parent. *Breed. Sci.* 51, 63–71. doi: 10.1270/jsbbs.51.63

Yan, M., Fan, X., Feng, H., Miller, A. J., Shen, Q., and Xu, G. (2011). Rice OsNAR2.1 interacts with OsNRT2.1, OsNRT2.2 and OsNRT2.3a nitrate transporters to provide uptake over high and low concentration ranges. *Plant Cell Environ.* 34, 1360–1372. doi: 10.1111/j.1365-3040.2011.02335.x

Yoshida, S., Forno, D. A., Cock, J. H., and Gomez, K. A. (1976). "Routine procedure for growing rice plants in culture solution," in *Laboratory Manual for Physiological Studies of Rice* (The International Rice Research Institute), 61–66.

Yu, S., Li, J., Xu, C.-J., Tan, Y., Li, X., and Zhang, Q. (2002). Identification of quantitative trait loci and epistatic interactions for plant height and heading date in rice. *Theor. Appl. Genet.* 104, 619–625. doi: 10.1007/s00122-001-0772-5

Yu, J., Xuan, W., Tian, Y., Fan, L., Sun, J., Tang, W., et al. (2021). Enhanced OsNLP4-OsNiR cascade confers nitrogen use efficiency by promoting tiller number in rice. *Plant Biotechnol. J.* 19, 167–176. doi: 10.1111/pbi.13450

Zenbo, T., Lishuang, S., Haochi, K., Chaofu, L., Ying, C., Kaida, Z., et al. (1996). Identification of QTLs for lengthes of the top internodes and other traits in rice and analysis of their genetic effects. *Yi Chuan xue bao = Acta genetica Sin.* 23, 439–446.

Zhang, Y.-M. (2019). Editorial: The Applications of new multi-locus GWAS methodologies in the genetic dissection of complex traits. *Front. Plant Sci.* 9. doi: 10.3389/fpls.2019.00100

Zhang, G., Xu, N., Chen, H., Wang, G., and Huang, J. (2018). *OsMADS25* regulates root system development *via* auxin signaling in rice. *Plant J.* 95. doi: 10.1111/tpj.14007

Zhou, Y., Tao, Y., Tang, D., Wang, J., Zhong, J., Wang, Y., et al. (2017). Identification of QTL associated with nitrogen uptake and nitrogen use efficiency using high throughput genotyped CSSLs in rice (*Oryza sativa* L.). *Front. Plant Sci.* 8, 1166. doi: 10.3389/fpls.2017.01166

frontiers | Frontiers in Plant Science

TYPE Review
PUBLISHED 22 September 2023
DOI 10.3389/fpls.2023.1249202

OPEN ACCESS

EDITED BY
Karl H. Mühling,
University of Kiel, Germany

REVIEWED BY
Joska Gerendas,
University of Kiel, Germany
Wei-Wei Deng,
Anhui Agricultural University, China

*CORRESPONDENCE
Lizhi Long
longlizhi@tricaas.com
Jianyun Ruan
jruan@mail.tricaas.com

RECEIVED 28 June 2023
ACCEPTED 04 September 2023
PUBLISHED 22 September 2023

CITATION
Zhang W, Ni K, Long L and Ruan J (2023) Nitrogen transport and assimilation in tea plant (*Camellia sinensis*): a review. *Front. Plant Sci.* 14:1249202. doi: 10.3389/fpls.2023.1249202

Nitrogen transport and assimilation in tea plant (*Camellia sinensis*): a review

Wenjing Zhang[1,2], Kang Ni[1,3], Lizhi Long[1*] and Jianyun Ruan[1,3*]

[1]Key Laboratory of Tea Plant Biology and Resources Utilization, Ministry of Agriculture, Tea Research Institute, Chinese Academy of Agricultural Sciences, Hangzhou, China, [2]Graduate School of Chinese Academy of Agricultural Sciences, Beijing, China, [3]Xihu National Agricultural Experimental Station for Soil Quality, Hangzhou, China

Nitrogen is one of the most important nutrients for tea plants, as it contributes significantly to tea yield and serves as the component of amino acids, which in turn affects the quality of tea produced. To achieve higher yields, excessive amounts of N fertilizers mainly in the form of urea have been applied in tea plantations where N fertilizer is prone to convert to nitrate and be lost by leaching in the acid soils. This usually results in elevated costs and environmental pollution. A comprehensive understanding of N metabolism in tea plants and the underlying mechanisms is necessary to identify the key regulators, characterize the functional phenotypes, and finally improve nitrogen use efficiency (NUE). Tea plants absorb and utilize ammonium as the preferred N source, thus a large amount of nitrate remains activated in soils. The improvement of nitrate utilization by tea plants is going to be an alternative aspect for NUE with great potentiality. In the process of N assimilation, nitrate is reduced to ammonium and subsequently derived to the GS-GOGAT pathway, involving the participation of nitrate reductase (NR), nitrite reductase (NiR), glutamine synthetase (GS), glutamate synthase (GOGAT), and glutamate dehydrogenase (GDH). Additionally, theanine, a unique amino acid responsible for umami taste, is biosynthesized by the catalysis of theanine synthetase (TS). In this review, we summarize what is known about the regulation and functioning of the enzymes and transporters implicated in N acquisition and metabolism in tea plants and the current methods for assessing NUE in this species. The challenges and prospects to expand our knowledge on N metabolism and related molecular mechanisms in tea plants which could be a model for woody perennial plant used for vegetative harvest are also discussed to provide the theoretical basis for future research to assess NUE traits more precisely among the vast germplasm resources, thus achieving NUE improvement.

KEYWORDS

nitrogen transport, nitrate reduction, ammonia assimilation, NUE, camellia sinensis, challenges and prospects

1 Introduction

Nitrogen is an essential mineral nutrient for plant growth and reproduction. Apart from being a fundamental building block of proteins and nucleic acids, N also participates in carbon fixation through photosynthesis as a component of chlorophyll (Bernard and Habash, 2009). In agricultural production, applying N fertilizers generally leads to significant yield increases (Suárez et al., 2002; Liu et al., 2021c), for which N fertilizers' use is expected to increase up to 236 million metric tons to meet the global food demands by 2050 (Beatty and Good, 2018). However, less than 50% of the applied N as fertilizer is absorbed by plants and harvested in grains (Raun and Johnson, 1999; Camargo et al., 2005). Thus, a high amount of "unuse" N supplied as fertilizer is transferred to water and the atmosphere, resulting in energy waste, soil acidification, water eutrophication and greenhouse gas emissions (Godfray et al., 2010; Liu et al., 2010). This negative environmental consequence of nitrogen fertilization became a huge challenge for stable and sustainable agricultural production (Bodirsky et al., 2014). There is an urgent need for research advances on N metabolism in the ecosystem; in this context, we need to improve N use efficiency (NUE) by crops, for which the genetic potential for N uptake and assimilation must be further explored.

Tea is processed from the leaves of *Camellia sinensis* (L.) O. Kuntze and becoming one of the most widely non-alcoholic beverages consumed worldwide due to its unique taste and potential health benefits (Wei et al., 2018). Since 2011, the global planting area of tea have increased steadily and gradually, from 3.84 million hectares in 2011 to 5.09 million hectares in 2020 (Liu et al., 2023). This perennial evergreen woody plant is cultivated in over 30 countries, and China has the greatest cultivated area (Zhang et al., 2019b; Lei et al., 2022). In 2022, tea planting area of China reached 3.33 million hectares (Mei and Zhang, 2022). The geographic origin of the tea plant is assigned to Yunnan province and neighboring regions in southwestern China (Chen et al., 2005). China has traditionally been the largest tea producer worldwide with abundant germplasm resources, and China's tea have been exported to more than 140 countries or regions (Wei et al., 2012). Currently, many cultivated tea varieties are extensively grown in tropical and subtropical regions across the world, and tea cultivation may increase the local smallholder income, especially in mountainous areas, contributing to local economic development (Yao et al., 2012). The N concentration in young buds and leaves is about 60-70 $g{\cdot}kg^{-1}$ (Ma et al., 2013). Tea plants form new shoots every season, and multiple picking and pruning have been done. In agricultural production, tea plants have a high demand for N, which is generally fulfilled through fertilization, active N uptake, assimilation and translocation, as well as remobilization processes. In China, the average annual N inputs reach 300-450 $kg{\cdot}hm^{-2}$ to cover tea N demand; an excessive N application rate has been reported in over 30% of the tea plantation area (Ma et al., 2013; Ni et al., 2019). These numerical data reinforce the crucial and urgent need for optimizing the NUE of tea plant. A series of interconnected processes, including N transport, assimilation and remobilization, are involved in NUE, thus the understanding on N metabolism at molecular level will provide the basis for a more rational application of N fertilizers during tea production.

Nitrogen is involved in many important metabolic pathways closely related to the synthesis of amino acids (AAs), caffeine, polyphenols, and other substances responsible for tea quality (Tang et al., 2020). Inorganic N sources, including ammonium (NH_4^+) and nitrate (NO_3^-), and small organic N-containing compounds can be uptaken from the soil by the tea plant roots and subsequently transported to the leaves by ammonium transporters (AMTs), nitrate transporters (NRTs), and amino acid transporters (AATs). The absorbed NO_3^- is first reduced into nitrite (NO_2^-) in the cytoplasm by nitrate reductase (NR) and further reduced to NH_4^+ in plastids by nitrite reductase (NiR). Ammonium assimilation involves the conversion of inorganic N to organic N, mainly through the glutamine-glutamate (GS-GOGAT) cycle, catalyzed by glutamine synthetase (GS) and glutamine-2-oxoglutarate aminotransferase/ glutamate synthase (GOGAT) (Bernard and Habash, 2009; Liu et al., 2022). It is noteworthy that glutamate and ethylamine are catalyzed by theanine synthetase (TS) to biosynthesize theanine (γ-glutamyl-L-ethylamide), a unique non-proteinogenic amino acid responsible for umami taste and healthy beneficial component in tea. Thus, the content of Thea is an important indicator for cultivar breeding and evaluating NUE. These processes are schematically illustrated in Figure 1. Further details on substrates, transporters, enzyme isoforms, and cell compartments relevant to the N cycle in tea plants are given in the following sections.

Since the tea plant genome was sequenced (Xia et al., 2020), many enzymes involved in N metabolism and their encoding genes were identified. Nitrogen dynamic regulation and physiological function were widely investigated in tea plant, as these are all critical aspects to improve NUE. In this article, we outline the results of recent investigations about the mechanisms underlying: (1) N absorption and transport in the form of NH_4^+, NO_3^-, and AAs; (2) metabolic reduction of nitrate; (3) ammonia assimilation and theanine (γ-glutamyl-L-ethylamide) biosynthesis. We also discuss the use of genetic, genomic, and phenotyping technologies for improving NUE by tea plants and stress the relevance of understanding the genetic basis of tea plant adaptive responses to different N forms.

2 General nitrogen utilization traits by tea plants

2.1 Tea plants acquire N preferentially as NH_4^+

Tea plant shows a preferential uptake of N in the form of ammonium (NH_4^+-N). Using the scanning ion-selective electrode technique, Ruan et al. (2016) found that the NH_4^+ influx rate in the roots of tea plant was higher than that of NO_3^-, and the presence of NH_4^+ would promote NO_3^- influx rate. The yield of young shoots, total root length, N uptake rate, and the contents of caffeine,

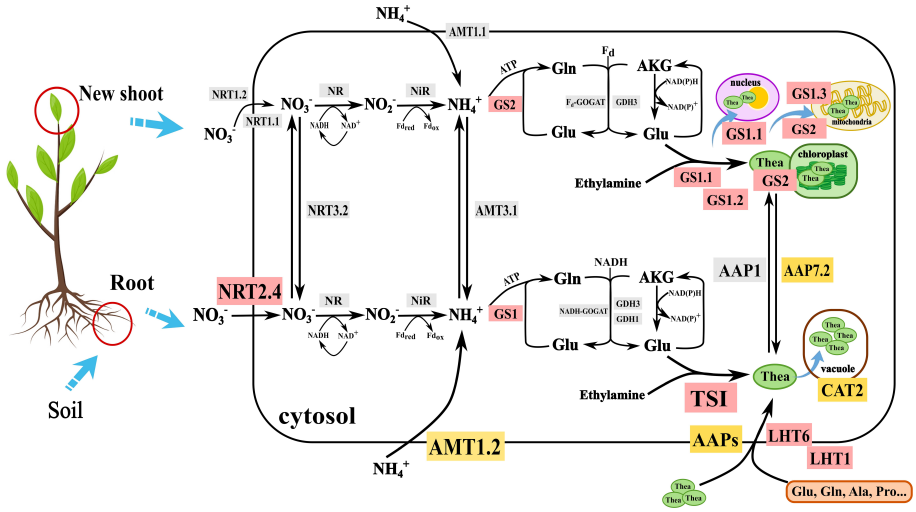

FIGURE 1
Molecular mechanism of nitrogen nutrient absorption and utilization in tea plant. NRT, nitrate transporter; NR, Nitrate reductase; NiR, Nitrite reductase; AMT, Ammonium transporter; GS, Glutamine synthetase; GOGAT, Glutamate synthase; GDH, Glutamate dehydrogenase; Gln, Glutamine; Glu, Glutamic acid; TS, Theanine synthetase; Thea, Theanine; LHT, Lysine and histidine transporter; CAT, Cationic amino acid transporter; Ala, Alanine; Pro: Proline; AKG, α-Ketoglutaric acid. Gray background represents the genes just were cloned in vitro; Yellow background represents functions of these proteins were validated in yeast; The red background represents functions of these proteins were validated in *Arabidopsis*, *Nicotiana tabacum* or *Camellia sinensis*.

theanine (Thea), glutamine (Gln), glutamate (Glu) and aspartate (Asp) in tea leaves were significantly higher when NH_4^+ was the main N source, compared with NO_3^- (Ruan et al., 2007; Ruan et al., 2010; Ruan et al., 2019; Wang et al., 2022a). NH_4^+-N can also promote phosphorus (P) uptake (Chen et al., 2019) and increase iron (Fe) and chloride (Cl) contents in mature leaves and sulfur (S) content in the roots (Tang et al., 2019). As a signaling molecule, NH_4^+ could induce Thea and catechin biosynthesis in a short period (Liu et al., 2017b; Huang et al., 2018). By sensing NH_4^+ levels, lysine-acetylated and crotonylated proteins profoundly influenced some primary metabolic processes involved in amino acid metabolism, photosynthesis, glycolysis, and carbon fixation (Jiang et al., 2018; Sun et al., 2019).

2.2 Nitrogen concentration influences tea plant growth and biochemical profile

To obtain an appropriate amount of harvestable product, i.e., young buds and leaves, multiple tender shoots are picked from the plants every year. Adequate N nutrition is necessary to increase the formation of young shoots, enhance the growth vigor and maintain the C/N balance (Ruan et al., 2010). A balanced C/N ratio is also important to promote chlorophyll biosynthesis (Yang, 2011) and to ensure adequate availability of free AAs (Liu et al., 2020; Wang et al., 2022a), thus providing N reserve for reproductive growth (Fan et al., 2019).

N metabolism of tea plant is dynamically regulated by environmental factors. Likewise, the growth of lateral roots was regulated by N levels: their length and numbers decreased with increasing N concentrations (Chen et al., 2023; Hu et al., 2023). Under N deficiency, the content of N, L-Thea, and chlorophyll decreased significantly. The activity of many antioxidant enzymes and leaf CO_2 assimilation capacity also diminished (Lin et al., 2016; Lin et al., 2019). However, low N levels positively regulated the expression of phosphate transporter genes and promoted flavonoids and polyphenols synthesis in tea leaves (Lin et al., 2023b). Appropriate N supply contributes to the aroma and flavor quality of tea infusion. The activity of the rate-limiting enzyme for N assimilation, GS, increased with N application level, and the content of total AAs, alcohols, and ketone compounds conferring aroma also increased, thus promoting tea products' integrated quality (Ruan et al., 2010; Deng et al., 2012; Liu et al., 2021b).The accumulation of caffeine, a component of the bitter taste and a central nervous system stimulant in tea, can be increased with the increasing N supply (Ruan et al., 2010). Sufficient N also promotes flavonol glycoside biosynthesis through the expression of relevant genes and the accumulation of the corresponding substrate carbohydrates (Dong et al., 2019). Lipidomic studies revealed that the content of precursors for the formation of aroma-related substances such as monogalactosyl diaclyglycerol (36:6 MGDG) and digalactosyl diacylglycerol (36:6 DGDG) increased when the N fertilizer was applied at adequate amounts, while an excessive N application led to overaccumulation of hexenol and hexenal, compounds which cause an unpleasant grassy smell in tea (Liu et al., 2017a). With the increase in N supply, more C was allocated to N-containing compounds in mature tea leaves and roots, leading to a decrease in flavonoid concentration in the young shoots (Liu et al., 2021a). Long-term N overfertilization reduced significantly benzyl alcohol and 2-phenylethanol contents in tea leaves, as well as those of (E)-nerolidol and indoles in withering leaves, becoming not conducive to the generation of floral and fruity fragrances (Chen et al., 2021).

3 Nitrogen transport in plants

In a wide range of organisms, N transport as NH_4^+, NO_3^-, and soluble organic compounds across membranes is mediated by transporter proteins (Wirén et al., 1997). These transporters can be divided into high-affinity transporter systems (HATS) and low-affinity transporter systems (LATS), depending on the specific substrate affinity. The external N level also regulates the affinities of transporters. For instance, there are inducible high-affinity transporter systems (iHATS) and constitutive high-affinity transporter systems (cHATS) to accomplish NO_3^- transport (Crawford and Glass, 1998; Forde, 2000). These transport proteins play a vital role in both short- and long-distance translocation of N inorganic ions and N-organic compounds.

3.1 NH_4^+ transport

The membrane-localized ammonium transporter/methylammonium permease (AMT/MEP) facilitates the import and export of NH_4^+ (Howitt and Udvardi, 2000). In higher plants, AMT proteins can be divided into two types: AMT1 and AMT2. Most AMT1 proteins belong to the HATS group and are synergically involved in NH_4^+ transport through the apoplastic and the symplastic routes (Yuan et al., 2007). AMT2 plays a role in the translocation of NH_4^+ from roots to shoots (Giehl et al., 2017). The transcription of the gene encoding this protein is tightly controlled through multiple factors, including external N level, circadian rhythm, hormone contents, and mycorrhizal symbiosis (Couturier et al., 2007; Kobae et al., 2010; Li et al., 2012; Li et al., 2016).

To cope with elevated NH_4^+ concentrations, the AMT activity may be post-translationally modified via the reversible phosphorylation of the cytosolic C-terminal region, thus allowing rapid adaptation to variable environmental conditions (Yuan et al., 2013; Wu et al., 2019). In tea plants, *CsAMTs* expression seems to be tissue-specific: *CsAMT1.2* reached the highest transcript abundance in roots, while *CsAMT1.4* was mainly expressed in flower buds. However, *CsAMT1.1* and *CsAMT3.1* were highly expressed in all tissues, suggesting that these genes might have diverse functions in NH_4^+ transport (Zhang et al., 2018; Wang et al., 2022c; Zhang et al., 2022a). Likewise, *AMTs* expression levels are responsive to changes in NH_4^+ availability. In roots, *CsAMT1.1* expression peaked at 12 h after the exogenous NH_4^+ resupply, while *CsAMT3.1* showed an upward trend after 24 h and *CsAMT1.2* expression level increased at 10 h, with a 2.5-fold change compared to 0 h, and then decreased again by 24 h. In NH_4^+-treated leaves, *CsAMT1.1* expression was up-regulated only after 4 h, exhibiting a 4.75-fold increase, whereas *CsAMT1.2* and *CsAMT3.1* expression levels did not change until 24 h later. These data indicate that NH_4^+ transport in tea roots is mainly regulated by *CsAMT1.2*, while in leaves, the NH_4^+ induction is mainly controlled by *CsAMT1.1* in the short term (Tang et al., 2020). Across different experimental NH_4^+ concentrations, most *CsAMTs* were expressed at higher levels in leaves than roots, except for *CsAMT1.2*, *CsAMT1.4*, and *CsAMT2.1a*. Remarkably, *CsAMT1.2* expression was significantly higher in roots than leaves under NH_4^+ deficiency (0 mM NH_4^+) or at 4 mM NH_4^+, demonstrating the major role of this transporter in NH_4^+ uptake. Other genes involved in NH_4^+ transport, such as *CsAMT2.1b*, *CsAMT3.3*, *CsAMT4.1a*, *CsAMT4.1b*, *CsAMT4.1c*, and *CsAMT4.1d*, exhibited similar expression profiles, with a decreasing trend under low N supply and a notorious induction under high N supply (Wang et al., 2022c). Furthermore, this report indicates that *CsAMTs* expression in tea leaves is differentially regulated over time by abiotic stresses, including drought and salinity, as well as after methyl jasmonate treatments. Under these treatments, specific *CsAMTs* genes were up-regulated or down-regulated in different ways, suggesting different functions to cope with various stresses (Wang et al., 2022c).

Transcriptome data revealed that *CsAMT1.2* expression could be highly induced by NH_4^+-resupply; weighted gene co-expression network analyses and the functional validation in an NH_4^+-uptake defective yeast line further corroborated that the high-affinity transporter *CsAMT1.2* was a "hub gene" in the N metabolic network of tea plants, controlling NH_4^+ uptake from the soil to the roots (Zhang et al., 2020). Also, Wang et al. (Wang et al., 2022c) found that 11 yeast transformant lines grew well on 0.3 mM NH_4^+ as the sole N source, indicating their high affinity for NH_4^+ permeation. The transcriptional regulation of *CsAMTs* differed even at the cultivar level (Li et al., 2017). *CsAMT1.1* and *CsAMT1.5* expression levels were significantly higher in the roots of the FuDingDaBaiCha cultivar than Longjin43 cultivar (Zhang et al., 2022a). After NH_4^+ resupply, *CsAMT1.2*, *CsAMT2.2*, and *CsAMT2.3* genes were differentially induced in tea cultivars with different NH_4^+-uptake efficiency, indicating the uneven NH_4^+ transport capacity among cultivars (Zhang et al., 2018; Zhang et al., 2022b).

3.2 NO_3^- transport

Membrane-bound nitrate transporters (NRTs) are required for NO_3^- uptake in plants. The members of the large NRT family can be divided into four subfamilies: nitrate transporter 1/peptide transporter (NRT1/PTR), collectively known as NPF, nitrate transporter 2 (NRT2), chloride channel (CLC), and slow anion channel associated/homologue (SLAC/ SLAH) (Krapp et al., 2014).

The NRT1 subfamily harbors many members, acting in NO_3^- transport from roots to shoots (Krapp et al., 2014). NRT transport activity is also regulated through phosphorylation. AtNRT1.1 is a dual-affinity protein: phosphorylation of the Thr101 residue by the CBL-interacting protein kinase 23 changes its substrate affinity (Sun et al., 2014). NRT2 are HATS proteins and belong to the nitrate/nitrite porter (NNP) family, mainly expressed in roots. These proteins have a role in both NO_3^- accumulation and NO_3^- transport (Chopin et al., 2007; Li et al., 2007; Kiba et al., 2012). To date, four *CsNRT1* and four *CsNRT2/3* genes have been isolated from tea plants. These genes show tissue-specific expression patterns and are differentially induced by exogenous NO_3^-. It was reported that *CsNRT1.1* and *CsNRT1.2* were mainly expressed in leaves. *CsNRT1.7*, *CsNRT2.5*, and *CsNRT3.2* had higher expression

levels in mature leaves than other tissues, while *CsNRT1.5*, *CsNRT2.4*, and *CsNRT3.1* transcripts mainly accumulated in tea roots (Feng et al., 2014; Wang, 2014; Wang et al., 2014; Yang et al., 2016; Zhang et al., 2021). Further research showed that *CsNRT2.4* expression was root-specific and strongly induced by N resupply. *Arabidopsis* seedlings overexpressing *CsNRT2.4* had a significantly higher fresh weight and lateral roots length than wild-type seedlings, especially under low N availability (0.1 mM NO_3^-), pointing out CsNRT2.4 as a high-affinity nitrate transporter that might improve NO_3^- uptake rate (Zhang et al., 2021). Additionally, Wang et al. (2022b) identified a total of 109 CsNPF members by analyzing the tea genome; these proteins could be divided into 8 groups according to their phylogenetic relationships, and the transcription of most of these genes responded to NO_3^- supply. Similarly, *CsNRTs* expression profiles varied in tea cultivars with different NUE (Wang et al., 2014). The expression of *CsNRT2.4* and *CsNRT3.2* in the cultivar LongJin43 was higher than that observed in ZhongCha108, indicating higher responsiveness to external NO_3^- supply in the former (Su et al., 2020).

Initially, CLC proteins were thought to be specifically involved in chloride (Cl^-) transport as channels or 2 Cl^-/1 H^+ antiporters (Jentsch, 2008). Further research showed that AtCLCa is a tonoplast-located 2 NO_3^-/1 H^+ antiporter that drives NO_3^- accumulation in the vacuoles (Jentsch, 2008; Monachello et al., 2009). As anion channels, SLAC/SLAH proteins showed a strong preference for NO_3^- and have been associated with CO_2 and abscisic acid-dependent stomatal closure (Negi et al., 2008; Vahisalu et al., 2008). In tea plants, Xing et al. (2020) identified eight *CLC* genes across the wide genome of this species and named them *CsCLC1-8*. Phylogenetic studies demonstrated that the proteins encoded by these genes belonged to two subclasses; further studies showed that CsCLC transporters might participate in the uptake and long-distance transport of Cl^- and F^-, as their expression levels varied in response to the addition of these two ions at different concentrations. However, the role of CsCLCs in NO_3^- transport has not been elucidated. Similarly, there are no published reports related to SLAC/SLAH proteins in tea plants.

To summarize the precedent information, Table 1 lists genes involved in NH_4^+ and NO_3^- sensing, uptake, and transport in tea plants reported to date. Further information about the subcellular localization, sequence data, and functional corroboration experiments is also provided.

3.3 Amino acid- N transport

Tea plants can directly absorb organic N and transport it to actively growing parts. The amino acid theanine (Thea) is synthesized and stored in root cells and then transported from the root to the flush shoot in spring. These movements, which include xylem loading/unloading, xylem-to-phloem transfer, and post-vascular movements into the sink cells, are driven by plasmatic membrane-localized amino acid transporters (AATs) (Fischer et al., 1995; Dong et al., 2020; Lin et al., 2023a). Studies on tea plants AAT proteins have mostly focused on amino acid permeases (AAP), lysine and histidine transporters (LHT), and cationic amino acid transporters (CAT), which play important roles in AAs acquisition and long-distance transport from source to sink (Guo et al., 2019; Guo et al., 2020; Li et al., 2020; Liu, 2020).

Six CsAAPs members, CsAAP1, CsAAP2, CsAAP4, CsAAP5, CsAAP6, and CsAAP8, were identified in tea plants through the screening of a *Saccharomyces cerevisiae* mutant library. The expression of genes encoding these transporters was tissue-specific and regulated by the season and N levels. Thus, *CsAAP1* expression in roots increased in March and decreased by mid-April and was highly correlated with root-to-bud Thea transport in seven tea cultivars (Dong et al., 2020; Li et al., 2020). Besides, shading promoted *CsAAP2*, *CsAAP4*, *CsAAP5*, and *CsAAP8* expression in young stems and suppressed *CsAAP1*, *CsAAP2*, *CsAAP4*, *CsAAP5*, and *CsAAP6* expression in the leaves, in accordance with Thea levels in these tissues. These findings indicate that CsAAP2, CsAAP4, CsAAP5, and CsAAP8 functions may be related to Thea movements in the xylem, leading to high Thea accumulation in the stem. The up-regulated genes might induce Thea transport into the companion cells in the sieve elements for phloem loading and Thea delivery to the terminal leaves (Yang et al., 2021).

LHT proteins were investigated more deeply. The CsLHTs family comprises multiple members, among which CsLHT1 and CsLHT6, highly expressed in roots, were identified as H^+-dependent high- and low-affinity amino acid transporters in yeast heterologous systems. The overexpression of *CsLHT1* and *CsLHT6* in *Arabidopsis* lines significantly increased the root ability to uptake exogenous nitrogen supplied as ^{15}N-Gln and ^{15}N-Glu, suggesting that these transporters may contribute to the use of organic N from the soil (Guo et al., 2019; Li et al., 2021). Likewise, the heterologous expression of *CsLHT4*, *CsLHT7*, and *CsLHT11* in *Arabidopsis* was associated with a decline in aerial parts biomass compared with WT plants, but *CsLHT11* overexpressing plants had increased biomass in the rosette leaves, regardless the N levels. Therefore, this protein might have a regulatory function relevant to the development of harvestable, young shoots in tea plants (Huang et al., 2023b).

Regarding the cationic acid transporters, it was reported that the *CsCAT* gene family includes six members, mainly expressed in roots and stems. It was also found that some *CsCATs* modify their expression levels in response to abiotic stress and the exogenous application of Thea, Gln, and ethylamine hydrochloride, a precursor of Thea biosynthesis (Feng et al., 2018). CsCAT2 from tea plant was homologous to glutamine permease 1 (GNP1) from yeast, and it was found to be localized in the tonoplast as an H^+-dependent amino acid transporter. *CsCAT2* was highly expressed in the roots in winter, and this was negatively correlated with Thea root-to-shoot translocation, providing evidence that this transporter may meditate Thea storage in tea cell vacuoles (Feng et al., 2021). These findings enrich our understanding of N homeostasis in the form of AAs. Table 2 lists the genes involved in AAs transport in tea plants. When available, data on subcellular localization, sequencing, tea cultivars analyzed, specific substrates, and functional corroboration experiments are supplied.

10.3389/fpls.2023.1249202

TABLE 1 Genes isolated from tea plants in NH_4^+ and NO_3^- transport.

Gene name	Sequence information		Functional verification			References
	Gene ID [a]	Cultivar [b]	Subcellular localization	System [c]	Function description	
CsAMT1.1	MV344632 KU361592	FD, LJ43	Predicted:plasma membrane	–	–	(Zhang et al., 2022a)
CsAMT1.2	MW344636 KU361593	FD,LJ43	Plasma membrane	Yeast *in planta* (*At.*)	A key gene for NH_4^+ uptake in roots	(Zhang et al., 2018; Zhang et al., 2022a; Zhang et al., 2022b)
CsAMT1.3	MW344633	FD	Predicted:plasma membrane	–	–	(Zhang et al., 2022a)
CsAMT1.4	MW344635	FD	Predicted:plasma membrane	–	–	(Zhang et al., 2022a)
CsAMT1.5	MW344634	FD	Predicted:plasma membrane	–	–	(Zhang et al., 2022a)
CsAMT3.1	KP338998	LJ43	Predicted:plasma membrane	–	–	(Zhang et al., 2018)
CsAMT2.1	MW751970	FD	Predicted:plasma membrane	Yeast	–	(Zhang et al., 2022b)
CsAMT2.2	MW751971	FD	Plasma membrane	Yeast	–	(Zhang et al., 2022b; Song et al., 2023)
CsAMT2.3	MW751972	FD	Plasma membrane	Yeast	–	(Zhang et al., 2022b; Song et al., 2023)
CsAMT2.4	MW751973	FD	Predicted:plasma membrane	Yeast	–	(Zhang et al., 2022b)
CsAMT2.5	MW751974	FD	Predicted:plasma membrane	Yeast	–	(Zhang et al., 2022b)
CsNRT1.1	–	ZC302	Predicted:plasma membrane	–	–	(Zhang et al., 2021)
CsNRT1.2	–	ZC302	Predicted:plasma membrane	–	–	(Zhang et al., 2021)
CsNRT1.5	–	ZC302	Predicted:plasma membrane	–	–	(Zhang et al., 2021)
CsNRT1.7	–	ZC302	Predicted:plasma membrane	–	–	(Zhang et al., 2021)
CsNRT2.4	–	ZC302	Plasma membrane	*in planta* (*Nt. At.*)	A key gene for NO_3^- uptake in roots	(Zhang et al., 2021)
CsNRT2.5	–	ZC302	Predicted:plasma membrane	–	–	(Zhang et al., 2021)
CsNRT3.1	–	ZC302	Predicted:plasma membrane	–	–	(Zhang et al., 2021)
CsNRT3.2	–	ZC302	Predicted:plasma membrane	–	–	(Zhang et al., 2021)
CsNPF2.3	CSS0041711	ZM#6	Plasma membrane	*in planta* (*Nt.*)		(Wang et al., 2022b)
CsNPF6.1	CSS0037113	ZM#6	Plasma membrane			(Wang et al., 2022b)
CsNRT	KJ160503	–	–	–	–	(Wang, 2014)
CsNRT1.2	KP453862	LJ43	Predicted:plasma membrane	–	–	(Feng, 2014)

[a]Gene ID, the beginning as "CSS" can be found in the tea plant genome database (http://tpia.teaplants.cn), others are GenBank accession numbers (https://www.ncbi.nlm.nih.gov/genbank/);
[b]Cultivar, FD, FudingDaBaiCha; LJ43, LongJin43; ZC302, ZhongCha302; ZM#6, ZhongMing#6.
[c]System, *At*, *Arabidopsis thaliana*; *Nt*, *Nicotiana tabacum*.
-, related information not presented or studied in corresponding literature.

10.3389/fpls.2023.1249202

TABLE 2 Genes isolated from tea plants in amino acids transport.

Gene name	Sequence information		Functional verification				Reference
	Gene ID [a]	Cultivar [b]	Subcellular localization	Substrate [c]	System [d]	Function description	
CsAAP1	TEA031577.1	SCZ	Plasma membrane and endoplasmic reticulum	Thea, Val, Asp, Glu, Gln, Ala, GABA	Yeast; *in planta* (*Nt. At.*)	Highly correlated to Thea root- to- shoot transport	(Dong et al., 2020; Li et al., 2020)
CsAAP2	TEA009392.1	SCZ	Plasma membrane and endoplasmic reticulum	Thea, Val, Asp, Glu, Gln, Ala, GABA	Yeast; *in planta* (*Nt. At.*)	–	(Dong et al., 2020; Li et al., 2020)
CsAAP3	TEA003112.1 MK532959	SCZ; LJ43	Predicted:plasma membrane	–	–	–	(Guo et al., 2020)
CsAAP4	TEA030129.1 MK532960	SCZ; LJ43	Predicted:plasma membrane	Thea, Val, Asp, Glu, Gln, Ala, GABA	Yeast	–	(Dong et al., 2020; Guo et al., 2020)
CsAAP5	TEA033139.1	SCZ	–	Thea, Val, Asp, Glu, Gln, Ala, GABA	Yeast	–	(Dong et al., 2020)
CsAAP6	TEA013446.1 MK532961	SCZ; LJ43	Plasma membrane and endoplasmic reticulum	Thea, Val, Asp, Glu, Gln, Ala, GABA	Yeast; *in planta* (*Nt. At.*)	–	(Dong et al., 2020; Guo et al., 2020; Li et al., 2020)
CsAAP7	TEA005296.1 MK532962	SCZ; LJ43	Predicted:plasma membrane	–	–	–	(Guo et al., 2020)
CsAAP7.1	XM_028244216.1	SCZ	–	–	–	–	(Li et al., 2022)
CsAAP7.2	MG523885	SCZ	Endoplasmic reticulum	Thea, Ala, GABA, Ser, Glu, Asn, Pro		Plays a role in AAs uptake from soil and Thea long- distance transport	(Li et al., 2022)
CsAAP8	TEA031424.1 MK532963	SCZ; LJ43	Predicted:plasma membrane	Thea, Val, Asp, Glu, Gln, Ala, GABA	Yeast	–	(Dong et al., 2020; Guo et al., 2020)
CsAAP9	TEA000756.1	SCZ	–			–	(Dong et al., 2020)
CsLHT1	TEA026462.1	SCZ; LJ43	Plasma membrane	Glu, Gln, Ala, Pro, Asn, Asp, GABA		H^+-dependent high affinity transporter in uptake AAs from soil	(Guo et al., 2019; Li et al., 2021)
CsLHT2	TEA021847.1	SCZ	Predicted:plasma membrane	–	–	–	(Li et al., 2021)
CsLHT3	TEA033469.1	SCZ	Predicted:plasma membrane	–	–	–	(Li et al., 2021)
CsLHT4	TEA029168.1 CSS0010852.1	SCZ; FD	Predicted:plasma membrane	–	in planta (*At.*)	–	(Li et al., 2021; Huang et al., 2023b)
CsLHT5	TEA016092.1	SCZ	Predicted:plasma membrane	–	–	–	(Li et al., 2021)
CsLHT6	TEA003706.1	SCZ; LJ43	Plasma membrane	Glu, Gln, Ala, Pro, Asn, Asp, GABA		H^+-dependent low affinity transporter in uptake AAs from soil	(Guo et al., 2019; Li et al., 2021)
CsLHT7	TEA021821.1 CSS0033052.1	SCZ; FD	Predicted:plasma membrane	–	in planta (*At.*)	–	(Feng et al., 2018; Li et al., 2021)
CsLHT11	CSS0019144.1	FD	–		in planta (*At.*)		(Huang et al. 2023b)
CsLHT8.1	–	LJ43	Predicted:plasma membrane	–	–	–	(Guo et al., 2019)
CsLHT8.2	–	LJ43	Predicted:plasma membrane	–	–	–	(Guo et al., 2019)

(Continued)

TABLE 2 Continued

Gene name	Sequence information		Functional verification				Reference
	Gene ID [a]	Cultivar [b]	Subcellular localization	Substrate [c]	System [d]	Function description	
CsCAT1	KY709681	SCZ	–	–	–	–	(Feng, 2017; Feng et al., 2018)
CsCAT2	KY709679	SCZ	Tonoplast	Thea, Asp, Glu, Ala, Gln, Val		Meditate Thea storage	(Feng, 2017; Feng et al., 2018; Feng et al., 2021)
CsCAT5	KY709680	SCZ	–	–	–	–	(Feng, 2017; Feng et al., 2018)
CsCAT6	KY709682	SCZ	–	–	–	–	(Feng, 2017; Feng et al., 2018)
CsCAT8	KY709684	SCZ	–	Thea, Glu, Gln,	–	–	(Feng, 2017; Feng et al., 2018)
CsCAT9	KY709683	SCZ	–	Thea, Glu, Gln	–	–	(Feng, 2017; Feng et al., 2018)

[a]Gene ID, the beginning as "TEA" and "CSS" can be found in the tea plant genome database (http://tpia.teaplants.cn), others are GenBank accession numbers (https://www.ncbi.nlm.nih.gov/genbank/);
[b]Cultivar, SCZ, ShuChaZao; LJ43, LongJing43; FD, FudingDaBaiCha.
[c]Substrate, Thea, theanine; Glu, glutamate; Gln, glutamine; Asp, aspartate; Asn, Asparagine; Ala, alanine; Val, valine; Pro, proline; Ser, serine; GABA, γ-aminobutyric acid.
[d]System, *At*, *Arabidopsis thaliana*; *Nt*, *Nicotiana tabacum*.
-, related information not presented or studied in corresponding literature.

4 N utilization

4.1 NO_3^- metabolic reduction

NO_3^- absorbed by plants is a nitrogen form in a highly oxidized state, which must be reduced to NH_4^+ through metabolic reduction to be further utilized. In this process, nitrate reductase (NR) is the rate-limiting enzyme (Jackson et al., 2008). Both NR and NiR are substrate-inducible enzymes; their function is to transfer electrons for NO_3^- reduction. NO_3^- taken up by roots was reduced into ammonium in mesophyll cells of shoots, and the metabolic reduction can also be catalyzed in roots (Miller and Cramer, 2005). In rice, the alleles of *OsNR2* present differences between the two most common subspecies, *indica* and *japonica*. Thus, OsNR2 in *indica* rice promotes NO_3^- uptake through OsNRT1.1B, conferring to this subspecies increased yield and greater NUE compared with *japonica* rice (Gao et al., 2019).

In tea plants, studies have mainly focused on the activity and expression of *CsNR* and *CsNiR*. The activity of NR was related to NO_3^- content. Besides, this activity was lower in the less vigorously growing organs, such as the larger roots, older leaves and stems. In the new shoots, the *in vitro* NR activity decreased with the degree of leaf development, being highest in the first leaf and lowest in the fifth one (Wang and Su, 1990; Wu and Wu, 1993). NR activity was also responsive to trace elements including copper (Cu) and zinc (Zn). Foliar spraying of Cu and Zn increased the content of N-containing compounds and the activity of NR (Han and Wu, 1992). Under the same conditions, *CsNR* and *CsNiR* expression levels in tea roots were more strongly influenced by NH_4^+ than NO_3^- (Tang et al., 2020). *CsNR* expression in tea roots was higher than in other tissues and was up-regulated by environmental stresses (Zhou, 2014). However, the expression level of this gene significantly differed across various cultivars (Zhou et al., 2013). On the other hand, the expression of *CsNiR* was higher in mature leaves than in new shoots and roots, and in roots, this gene expression was up-regulated after a short period of N resupply. The change in gene expression was slower in leaves, and this responsiveness also varied in different cultivars representing diverse genotypes (Zhang et al., 2016). Most of these findings correspond to earlier experiments; the experimental evidence for CsNR and CsNiR functions in tea plants is still scarce.

4.2 Ammonia assimilation

Both NH_4^+ absorbed directly by plant roots and NH_4^+/NH_3 formed through NO_3^- reduction can be derived to AAs synthesis using various keto acids generated through respiration; this process is known as ammonia assimilation. In higher plants, more than 95% of the NH_4^+/NH_3 pool is assimilated via the GS-GOGAT cycle. Glutamine synthetase (GS) is the key enzyme in this pathway, playing a major role in fixing NH_4^+ to the δ-carboxyl group of Glu to form Gln (Thomsen et al., 2014). Tea plants have a particular ammonia-assimilation route; their roots can biosynthesize a unique amino acid, Theanine (Thea), a homolog of Gln (Lin et al., 2023a). Glutamate synthase (GOGAT) catalyzes the conversion of Gln and 2-oxoglutarate to Glu, thus providing Glu for ammonia assimilation (Bernard and Habash, 2009; Valderrama-Martín et al., 2022). When plants germinate, senesce, and begin to form seeds, glutamate dehydrogenase (GDH) can catalyze the reversible amination/deamination so that the GS-GOGAT cycle allows NH_3 reuse, necessary for ammonia detoxification (Fontaine et al., 2012; Zhou et al., 2015). Through these pathways, N absorbed by roots is incorporated into proteins, nucleic acids, and other substances needed for plant growth.

4.2.1 Glutamine synthetase (GS) and theanine synthetase (TS)

Two isoforms of GS were first identified by ion exchange chromatography: cytosolic GS (GS1) and plastidic GS (GS2) (Bernard and Habash, 2009). GS1 is localized in the cytoplasm of non-photosynthetic tissues and is mainly involved in assimilating NH_4^+ absorbed from the soil and released from the plant N cycle. GS2 is localized in the chloroplast stroma and is the main isoform in chlorenchyma, having a major role in NH_4^+ assimilation within the photorespiratory pathway and NO_3^- reduction in plastids (Swarbreck et al., 2011; Thomsen et al., 2014).

GS has been studied in tea plants extensively. It may be noticed in the GenBank database that the Japanese researchers Tanaka and Taniguchi were the first to clone three CsGS1 genes from tea roots in 2011: *CsGS1.1* (AB115183), *CsGS1.2* (AB115184), and *CsGS1.3* (AB117934), but the functions of these genes had not been reported (Lin et al., 2023a). Tang et al. (2018) cloned three *CsGS1* genes from the leaf of the cultivar Longjing43; the information obtained from the sequence analysis showed that the 3'/5'-untranslated region differed from those obtained previously, and *CsGS1.1* and *CsGS1.3* were mainly expressed in roots, while *CsGS1.2* was mainly expressed in mature leaves. NH_4^+ or NO_3^- supply also influences the expression levels of these genes. The expression of *CsGS1.1* in leaves was up-regulated only by NO_3^- in a similar manner as *AtGLN1.2*, indicating that its role in ammonia assimilation originates from NO_3^- reduction (Lothier et al., 2011; Guan et al., 2014). However, under the NH_4^+ treatment, the expression of *CsGS1.2* was induced in both leaves and roots, and *CsGS1.3* expression was only significantly increased in leaves (Tang et al., 2018). Further research indicated that GS activity in tea plants was quickly inhibited upon methionine sulfoximine addition, leading to the reprogramming of AAs and nitrogenated lipids. This change involved a decrease in the biosynthesis of all other AAs and nitrogenated lipids, whereas the content of NH_4^+, Thea, and glycolysis and tricarboxylic acid cycle-related metabolites increased, indicating that the inhibition reduced N reutilization in the leaves (Liu et al., 2019).

L-theanine (γ-glutamyl-L-ethylamide), also known as L-Thea, is a distinctive non-proteinogenic amino acid that contributes an umami taste and exhibits anti-depression benefits (Liu et al., 2017d). Thea accumulation was dynamically regulated by developmental growth, and environmental factors, including N supply, temperature, light intensity, and salt stress (Ashihara, 2015). The synthesis of L-Thea is a unique and highly characteristic aspect of nitrogen assimilation in tea plants. Deciphering the underlying molecular mechanism of L-Thea synthesis will provide valuable guidance for fertilization and breeding strategies. Theanine synthetase (TS), an essential enzyme for Thea metabolism, catalyzes the biosynthesis of Thea from ethylamine and Glu, mainly in tea roots (Fu et al., 2021a). The structure and properties of L-Thea are similar to those of L-Gln, and some studies have confirmed that TS is highly homologous to GS (Cheng et al., 2017). As indicated before, *CsTS1* (DD410895) and *CsTS2* (DD410896) were firstly isolated through cDNA library screening. *CsTS1* is mainly expressed in the new shoots, roots, and mature leaves, while *CsTS2* reached higher expression levels in shoots (Deng et al., 2008). Both genes are involved in Thea biosynthesis; this was validated through a heterologous expression system (Lin et al., 2023a).

By performing genome studies, Wei et al. (Wei et al., 2018) found that the predicted *CsGS I* sequence shared high homology with that of *PtGS* (*Pseudomonas taetrolens*), and *PtGSI* has been engineered for Thea production at high levels, for which *CsGS I* was renamed as *CsTS I*. The function of CsTS and CsGS was investigated in depth through the transient overexpression in *Nicotiana benthamiana* leaves or the stable expression in *Arabidopsis* and knockdown in tea plants. The expression pattern and distribution of *CsTS I* correlated with Thea and Gln contents in different tissues. CsTS I mainly accumulated in root tip epidermal, pericycle, and procambium cells to form cytoplasmic proteins. When fed with 10 mM ethylamine, *CsTSI*-overexpressing *Arabidopsis* seedlings showed a significantly higher Thea content than wild-type seedlings. Further research allowed the construction of *CsTSI* RNAi and *CsTSI* overexpressing chimerical tea seedlings with transgenic hair roots; the results demonstrated that the content of Thea decreased and that of Gln increased, thus proving that CsTSI biosynthesized Gln and Thea used glutamate as an acceptor and ammonium or ethylamine as a donor, respectively (Wei et al., 2018; Fu et al., 2021b; She et al., 2022). Fu et al. (2021b) used a non-aqueous fractionation method and could determine that, in roots, L-Thea biosynthesis mainly occurred in the cytosol through the action of the key and cytosolic enzyme L-Thea synthetase CsTSI, whereas in shoots, both the cytosol and chloroplasts were the major sites for L-Thea biosynthesis, and CsGS1.1 and CsGS2 were, most likely, the fundamental L-theanine synthetase. CsGS2 was identified as a key enzyme regulating Thea biosynthesis in chloroplasts, L-Thea content and distribution in leaf tissues would be affected by light, as long-term shading treatment led to a decrease in the proportion of L-Thea in the plastids by reducing *CsGS2* expression levels. Thus, new shoots could accumulate more L-Thea. In contrast, *CsGS1.2* expression in albino new shoots was higher than that found in common cultivars as a way to compensate for the low CsGS2 expression in undeveloped chloroplasts. These findings indicate that the mechanism underlying Thea synthesis might differ across tea genotypes (Yu et al., 2021).

4.2.2 Glutamate synthase (GOGAT) and glutamate dehydrogenase (GDH)

There are two isoforms of GOGAT in plants, with different functions: ferredoxin-dependent GOGAT (Fd-GOGAT) and nicotinamide adenine dinucleotide-dependent GOGAT (NADH-GOGAT). Fd-GOGAT assimilates ammonia through photorespiration in leaves, while NADH-GOGAT accumulates in non-green tissues, playing a role in ammonia assimilation in root (Suzuki and Knaff, 2005; Konishi et al., 2014).

GDH is abundant in plant tissues; this enzyme catalyzes ammonia conversion to Glu and also deaminates Glu to α-ketoglutarate. GDH-mediated ammonia assimilation and as a stress-responsive enzyme, GDH detoxified the intracellular high ammonia and biosynthesize Glu (Lea and Miflin, 2003; Fontaine et al., 2012; Zhou et al., 2015). *CsGOGAT* was found to have significantly higher expression in the leaf than in the root (Chen

et al., 2015). Under N starvation, *CsGOGAT* expression increased, and *CsGDH* expression decreased significantly; these changes were correlated with leaf N content (Lin et al., 2014). CsGOGAT also have a regulatory role in AAs changes in postharvest tea plant leaves. The Thea content changed in spreading tea leaves under different treatments, and CsGOGAT was involved in Thea metabolic pathway, regardless of external light and temperature. Also, CsGOGAT would interact with CsTS I and CsNiR during N metabolism (Liu et al., 2017c). In tea plant, all CsGDHs identified to date belong to the NADH-GDH group. Accumulation of *CsGDH2* transcripts seemed to be flower-specific compared with the other five plant tissues analyzed; *CsGDH1* was mainly expressed in mature leaves and roots, and *CsGDH3* in new shoots and roots. Under high NH_4^+ supply, CsGS inhibition resulted in a significant up-regulation of *CsGDH3* and *CsGDH2* in roots and leaves, indicating the synergistic effect of CsGSs and CsGDHs in the process of ammonia assimilation (Tang et al., 2021). The expression of *CsGDH2.1* in shoots increased greatly in the late spring; further investigation revealed that Glu was a signal for Thea hydrolysis, and CsGDH2.1-mediated Glu catabolism negatively regulated Thea accumulation in the new shoots in the late spring, improving green quality by targeting to reduce *CsGDH2.1* expression (Chen et al., 2022).

Summing up, studies directed to analyze the genes related to N metabolism in tea plants mostly focused on their function in regulating AAs biosynthesis. Knowledge about the functioning and regulation of the enzymes involved in these processes is mostly based on transcript analyses. There are still many gaps in our understanding of their functions, especially for NR, NiR, and GOGAT, concerning NO_3^- reduction, N assimilation, remobilization, and reassimilation of photorespiratory NH_3. It is noteworthy that, apart from the transcriptional regulation, post-translational modifications (PTMs) can also be critical for the regulation of many proteins relevant to N metabolism in plants (Liu et al., 2022). Therefore, more detailed studies will deepen our understanding of NUE determinants and allow further optimization of NUE under actual tea garden production scenarios.

Genes involved in ammonia assimilation by tea plants and their most relevant data are shown in Table 3.

TABLE 3 Genes involved in ammonia assimilation in tea plant.

Gene name	Sequence information		Functional verification			References
	Gene ID [a]	Cultivar [b]	Subcellular localization	System [c]	Functional description	
CsNR	JX987133	LJ43	–	–	–	(Zhou et al., 2013)
CsNiR	–	LJ43	–	–	–	(Zhang et al., 2016)
CsGS1.1	AB115183 KY649469 TEA015580.1 MG778703	'Sayamakaori' posterity LJ43 JX	Cytosol and nucleus	*E. coli* *in planta* (*At.*)	Biosynthesizes Thea and Gln	(Cheng et al., 2017; Tang et al., 2018; Wei et al., 2018; Fu et al., 2021b; Yu et al., 2021)
CsGS1.2	AB115184 KY649470 TEA032123.1 MG778705	'Sayamakaori' posterity LJ43; JX	Cytosol	*E. coli* *in planta* (*At.*)		
CsGS1.3	AB117934 KY649471 TEA032217.1 MG778704	'Sayamakaori' posterity LJ43; JX	Mitochondria	*E. coli* *in planta* (*At.*)		
CsGS2	TEA028194.1 MG778706	JX	Chloroplast, mitochondria	*E. coli* *in planta* (*At.*)	Thea synthetase in chloroplasts	(Cheng et al., 2017; Wei et al., 2018; Fu et al., 2021b; Yu et al., 2021)
CsGS	EF055882	–	–	–	–	(Rana et al., 2008)
CsGS	JN602372	JLP	–	–	–	(Lin et al., 2014)
CsTS I	TEA015198.1	SCZ	Cytosol	*in planta* (*At.* Tea plant hairy roots)	Thea synthetase in cytosol.	(Wei et al., 2018; Fu et al., 2021b)
CsTS1	DD410896	–	–	*E. coli*	Biosynthesizes Thea after supply with ethylamine	(Cheng et al., 2017; Fu et al., 2021b)
CsTS2	DD410895	–	–	*E. coli*		(Cheng et al., 2017; Fu et al., 2021b)
CsTS3	JN226569	AJB	Predicted: cytoplasm peroxisome	–	–	(Li et al., 2011; Chen et al., 2015)
CsGOGAT	JN602373	JLP	–	–	–	(Lin et al., 2014)

(Continued)

TABLE 3 Continued

Gene name	Sequence information		Functional verification			References
	Gene ID [a]	Cultivar [b]	Subcellular localization	System [c]	Functional description	
CsGOGAT1	TEA003892.1	–	–	–	–	(Wei et al., 2018; Li et al., 2019)
CsGOGAT2	TEA026779.1	–	–	–	–	(Wei et al., 2018; Li et al., 2019)
CsGOGAT3	TEA030315.1	–	–	–	–	(Li et al., 2019)
CsFd–GOGAT	–	LJ43	–	–	–	(Liu et al., 2017c)
CsNADH–GOGAT	–	LJ43	–	–	–	(Liu et al., 2017c)
CsGDH	JN602371	JLP	–	–	–	(Lin et al., 2014)
CsGDH1	TEA034004.1	LJ43	–	–	–	(Tang et al., 2021)
CsGDH2	TEA009809.1	LJ43	–	–	–	(Tang et al., 2021)
CsGDH3	TEA034006.1 TEA006665.1	LJ43	–	–	–	(Tang et al., 2021)
CsGDH2.1	CSS0034454.1	SCZ	Mitochondria	Yeast *in planta (Nt.)* asODN in tea plant	Negatively regulates theanine accumulation in the late–spring	(Chen et al., 2022)
CsGDH2.2	CSS0007238.1	SCZ	Mitochondria	Yeast *in planta (Nt.)*	–	(Chen et al., 2022)

[a]Gene ID, the beginning as "TEA" and "CSS" can be found in the tea plant genome database (http://tpia.teaplants.cn), others are GenBank accession numbers (https://www.ncbi.nlm.nih.gov/genbank/);
[b]Cultivar, LJ43, LongJing43; JX, JinXuan; SCZ, ShuChaZao; JLP, JiuLongPao; AJB, AnJiBaicCha.
[c]System, *E. coli*, *Escherichia coli*; *At*, *Arabidopsis thaliana*; *Nt*, *Nicotiana tabacum*; asODN, antisense oligonucleotide.
-, related information not presented or studied in corresponding literature.

5 An overview of nitrogen use efficiency assessment by tea plants

Nitrogen use efficiency (NUE) is a complex trait influenced by the interaction between environmental factors and intrinsic plant factors; this variable can be approached at different levels and calculated in different ways (Santa-María et al., 2015). Initially, NUE was defined as the crop yield per unit of applied N, a parameter also termed partial fertilizer productivity (PFP) (Moll et al., 1982). Under specific N supply conditions, NUE can be divided into two components: nitrogen uptake efficiency (NUpE) and nitrogen utilization efficiency (NUtE) or nitrogen physiological efficiency (NPE). NUpE may be defined as the total amount N absorbed and NUtE as the dry weight or grain yield per unit of absorbed N, accounting for the results at this growth stage (Williams et al., 2021). Tea germplasm resources are abundant in China; the genetic diversity of this plant, resulting from a long time of artificial domestication and cultivar-breeding improvement, has determined quite different N requirements (Zhang et al., 2018). Additionally, because tea production does not target grain yield, dissimilar NUE assessment criteria were adopted. Here, we integrate the results of several studies and present four approaches to assess NUE by tea plants.

5.1 Biomass accumulation

By the end of the 20th century, it was reported that the rate of increase in tea ground stem diameter and height and dry matter production in different cultivars varied under sufficient N supply compared to no N application (Ruan et al., 1993). Under low N supply, tea plants' height, root and shoot dry weight, and leaf SPAD values were significantly decreased (Wang et al., 2015). Wang et al. (2004) measured the added-N content in the biomass and the growth of new shoots in six tea cultivars under four N levels (based on ^{15}N isotope labeling techniques), and redefined five interdependent traits—nitrogen use efficiency (NE), nitrogen uptake efficiency (NUE), nitrogen physiological utilization efficiency (NPE), nitrogen economic efficiency (NEE) and N responsiveness—according to growth characters and harvesting organs. They found that the biomass increase was significantly correlated with NEE, the weight of the new shoots was significantly (positively) correlated with NE, NUE, and NEE, while NUE was the main determinant of NE. These authors indicated that by comparing the NE values of different cultivars, it is possible to detect which cultivar can achieve the highest NUE for a given level of N supply.

5.2 Root-related traits

The root is the main organ for nutrient uptake and plays a direct role in N acquisition (Lynch, 2007; Zhu et al., 2011). Root development and activity are responsive to soil N levels (Ju et al., 2015). Studies on plant response to N concentration gradients using different tea cultivars suggested that N concentration has a significant effect on root/shoot ratio, and this ratio could be used as a screening index to detect low-N-tolerant cultivars (Wang et al., 2015). On the other hand, the differences among cultivars in root-related parameters such as root dry weight, root volume, or root active uptake area were greater than those of root activity. Likewise, root volume and active uptake area varied significantly across N levels. Further correlation studies provided evidence that these parameters may be considered as promising indices for selecting and breeding tea cultivars with high NUE (Wang et al., 2005).

5.3 NH_4^+ influx kinetics

In the early 1950s, Epstein and Hagen (1952) applied the Michaelis-Menten equation for the first time to describe the absorption process of ionic nutrients by plants. In this equation, V_{max} represents the maximum uptake rate; this value is directly proportional to the uptake rate for ions, and K_m is inversely proportional to the affinity of the cell membrane for nutrient ions (Zhang et al., 2018). Because tea roots show a preference for NH_4^+ uptake as the nitrogen source, the kinetic parameters of this cation are usually used to define tea adaptability to N availability. According to current studies on NH_4^+ dynamics, tea cultivars may be classified into three categories: (1) cultivars with high K_m and high V_{max} can produce high yields in soils with elevated N contents; TeiGuanYin, HuangDan, and Yubukita cultivars belong to this type; (2) cultivars with low K_m and low V_{max} may display a good performance in soils with low N concentrations; YingShuang and MaoXie belong to this type; (3) cultivars with high K_m and low V_{max} are the most flexible concerning N levels, being appropriate for both high and low N conditions; ZhongCha#302 and FuDingDaBaiCha belong to this type (Wang et al., 2005; Liu, 2016; Zhang et al., 2018; Zhang et al., 2022b). Notably, N flux was calculated as the N content in the roots based on ^{15}N labeling in most studies, and there are still many cultivars falling into different groups in different studies due to different number of tested cultivars and methodological approaches. Though NH_4^+ influx kinetics allowed a better understanding of N use by tea plants, more precise methods, such as non-invasive procedures based on micro-test technology, will be useful for future experiments (Ruan et al., 2016; Su et al., 2020).

5.4 Activity and gene expression of N-assimilation-related enzymes

The leaves are the main assimilation organs of inorganic N. The accumulation of N-assimilates and the enzymes and genes regulating these metabolic processes could indicate NUE-related sub-traits (Sun et al., 2019). Some studies showed that GS activity varied among cultivars and N levels and was positively correlated with N assimilation rate and NUpE (Wang et al., 2005; Du et al., 2015). Lin et al. (2017; 2018) examined the activity of some antioxidant enzymes and found increased activities in the low N-tolerant cultivar HuangDan in a nitrogen-deficient environment. This was linked to the maintenance of high photosynthetic rates and to the adequate output of N-assimilates in the leaves. Still, by combining genes, enzymes, and assimilates and exploring their affiliation links, it was possible to evaluate NUE traits comprehensively. Zhou (2012) measured soluble sugars, soluble proteins, total N content, N-related enzymatic activities, and the expression of AAs biosynthetic genes. Their results suggested that the differences in these indicators varied in the five cultivars tested as the N concentration increased and membership function could be used to evaluated the NUE of each cultivar synthetically. Also, *CsAMTs* expression profiles in response to NH_4^+ differed among cultivars (Zhang et al., 2018; Zhang et al., 2022b). Still, it was possible to detect that CsNRT2 participated in NO_3^- transport under low N conditions (Hu et al., 2023; Lin et al., 2023b). The AuTophaGy-related genes *CsATG8e* and *CsATG3a* were linked to an improved plant ability for N recycling and tolerance to low N levels (Huang et al., 2020; Huang et al., 2023a). These genes emerge as promising indicators and may contribute to identifying higher NUE among various germplasm resources.

Although multiple investigations have addressed NUE of tea plants, most NUE-related traits were identified based on individual morphology, physiological processes, relevant biochemical components, or gene expression patterns. Nevertheless, there are no universal standards for grading NUE in tea plants, and some cultivars have shown heterogeneous results. The measurement of biomass is time-consuming and susceptible to environmental changes. And only the processes of N uptake, transport or utilization not the comprehensive NUE have been measured in tea plants. The practicability of method also depends on the number of tested cultivars. Most importantly, NUE estimates are complicated and current evaluation methods are not comprehensive enough to cover and explain the meaning of NUE. The methodological limitations still resist our understanding of N metabolic mechanisms. Therefore, analyses combining omics data and molecular and genetic approaches will be useful to elucidate further heritability and inheritance in this species with a point of great value to improve NUE by tea plants.

6 Conclusions and perspectives

N is the driving factor for tea yield and quality. Facing the practical problem of the disproportionate amount of N fertilizers applied and the low N utilization rate by tea plantations, a comprehensive study on the process of N transport, absorption, and utilization is necessary to increase NUE, to improve quality features such as aroma and flavor, and, ultimately, to promote the sustainable development of the industry.

Currently, it is clear that tea plants show a preferential uptake and assimilation of NH_4^+ over NO_3^-, and more NH_4^+ availability allows tea plants to produce more AAs, which further act as signaling molecules involved in other metabolic pathways. In addition, great progress has been made in the elucidation of the N primary metabolism network. Genes contributing to N transport and assimilation have been cloned and sequenced, and the functions of many genes have been identified by transgenic experiments in yeast, *Arabidopsis*, and *Nicotiana tabacum*. However, the current methods to assess tea NUE under actual productive settings have limitations. For instance, some basic indices related to plant physiological performance and gene expression were proposed, but these approaches are time-consuming and inappropriate for large-scale field cultivar assessment. One drawback is that a stable transgenic system has not been established yet; hence, we cannot knock out or overexpress genes to provide functional evidence in homologous systems. Therefore, there is an urgent need to develop an efficient and stable gene transformation system for tea plants, even more considering that the N metabolism network is regulated by multiple genes. Future research should consider the following issues.

Firstly, most research on N uptake and utilization by tea plants has focused on ammonia assimilation and AAs biosynthesis. However, NH_4^+-based fertilizers and urea are widely applied in tea gardens, and these N forms are expected to be converted to NO_3^- by nitrification, entailing the risk of leaching. It has been reported that NO_3^- was the main chemical form of N loss by leaching: about 51%-63% of the added N is lost in this way (Zheng, 2022). Therefore, the biological significance of NRT, NR, and NiR in N utilization is not negligible. In rice, the nitrate sensor NRT1.1B could perceive NO_3^- signal at the plasma membrane and facilitated SPX4 degradation by recruiting NBIP1, resulting in the cytoplasm-to-nuclear shuttling of OsNLP3 to transduce NO_3^- response (Hu et al., 2019). Also, in *Arabidopsis*, the phosphorylation state of NRT1.1 regulates the nitrate signaling for lateral root growth, and the non-phosphorylable $NRT1.1^{T101A}$ would activate Ca^{2+}-CPKs-NLPs signaling pathway by inducing its endocytosis under high NO_3^- concentration (Zhang et al., 2019a).

Secondly, although significant progress has been made in recent years regarding our understanding of the transcriptional regulation of the GS-GOGAT cycle, there are few reports on how transcription factors (TFs) regulate the expression of these downstream genes. The latest research revealed that the lateral organ boundaries domain gene *CsLBD39* negatively regulated NO_3^- transduction (Teng et al., 2022). Functional studies on the regulation of N metabolism by TFs need to be further expanded in both scope and depth. Additionally, PTMs also influence NUE through their effects on relevant proteins in plants. Phosphorylation and dephosphorylation of NR are involved in regulating NR activity, and phosphorylation, oxidation, tyrosine nitration, and S-nitrosylation of GS protein are also key mechanisms for GS function in many crops, including wheat, rice, and maize (Liu et al., 2022). A recent study in tea plants found that CsALT, CsTSI, CsGS, and CsAlaDC, proteins involved in Thea synthesis, were modified through ubiquitination, implying that these enzymes' stabilities were regulated by this modification (Wang et al., 2021b). Consequently, to establish a comprehensive N mechanism network for tea plant, N transport, reduction and assimilation requires precise regulation at both the transcriptional and post translational levels, many efforts need to be made to explore the PTMs, particularly to identify the modification sites that may be relevant for N use regulation by tea plants.

Furthermore, plants can respond to changes in N uptake by adjusting leaf expansion and photosynthetic rates, as well as chlorophyll content. In senescent leaves, N assimilation decreased; this was associated with the degradation of proteins and nucleic acids; the released N was remobilized to developing tissues. The expression of genes related to GS/GOGAT cycle during leaf senescence was widely investigated; most of these genes were expressed in phloem companion and parenchyma cells in cereals, suggesting that GS/GOGAT cycle plays a vital role in N remobilization from senescent organs to developing organs (Havé et al., 2017; Liu et al., 2022). In addition, NH_4^+, NO_3^-, AAs, and peptide transporters also can be up- or down-regulated during leaf senescence. Thus, many aspects of N metabolic pathways would be influenced by N recycling and remobilization (Breeze et al., 2011). It is reasonable to hypothesize that there are some other undiscovered factors and pathways, for example, components of C metabolism that regulate N remobilization. Tea production involves the pruning and picking of the tender leaves every season; this leads to a more active N turnover between the senescent leaves and the new shoots. Hence, for tea plants, an overview of the mechanisms involved in N recycling and remobilization is important to improve N resorption efficiency and also to reduce the use of N chemical fertilizers, which are responsible for a large part of greenhouse gas emissions.

Finally, along with the deciphering of the tea genome in multiple cultivars (Wang et al., 2021a), whole genome resequencing could provide more efficient single nucleotide polymorphisms (SNPs) markers to construct a high-density linkage map of tea populations. Such maps will lay a foundation for further investigations of quantitative trait loci (QTL) mapping and genome-wide association studies (GWAS) in order to reveal the molecular basis for important agronomic traits. In rice, forward genetics approaches revealed that allelic variation at *OsNR2* and *OsNRT1.1B* resulted in the nitrate-use divergence between *indica* and *japonica* subspecies and were used to improve the NUE of rice (Hu et al., 2015; Gao et al., 2019). Multiple attempts have been made to detect relevant QTLs or variation sites and quality-related traits in tea plants, including biochemical components, leaf area (An et al., 2021), seed setting rate (Wei et al., 2021), bud flush timing (Tan et al., 2022), and AAs (Huang et al., 2022), caffeine (Ma et al., 2018), and flavonoid (Xu et al., 2018) contents. However, fewer attempts to unravel nutrient uptake and utilization traits in the context of genotype-to-phenotype mapping research have been reported. Nutrient-related traits are generally regulated by multiple genes and environmental factors, so it is difficult to quantify their phenotypes precisely. More attempts need to reveal the processes of N cycling, and to define the phenotypic indicators that reflect each step of N metabolism. For example, chlorate (ClO_3^-) is an analogic tracer for NO_3^- and the resistance ability to ClO_3^- is an efficient indicator for fast screening the process of NO_3^- transport and reduction divergency (Hu et al., 2015). How to apply this method in woody plants is a challenge

that needs to be considered in future research. Population genetics can help us to explore better the gene regulatory loci affecting NUE-related traits and to identify the TFs or promoters which are able to regulate or activate the transcription of downstream structural genes. Exploiting interpopulation genetic variation in different germplasms will be instrumental for cultivar improvement. Thus, the use of precise phenotyping methods on population is challenging but necessary for future studies of discovering genetic variation associated with NUE-related traits.

Therefore, future studies should focus on the regulation mechanisms of NO_3^- uptake and reduction in tea plants to increase the utilization of NO_3^- from the soils and reduce leaching losses, a point of great significance for the genetic improvement directed to high NUE cultivars as well as for developing a sustainable tea plantations.

Author contributions

WZ and LL contributed to the conceptualization. WZ prepared the first draft and figures. LL and KN contributed with inputs and made revisions in the text and figures. LL and JR supervised the overall process. All authors contributed to the article and approved the submitted version.

Funding

This work was supported by Agricultural Science and Technology Innovation Program of Chinese Academy of Agricultural Sciences (CAAS-ASTIP-TRICAAS) and Zhejiang Provincial Natural Science Foundation of China under Grant No. LY23C150008.

Conflict of interest

The authors declare that the research was conducted in the absence of any commercial or financial relationships that could be construed as a potential conflict of interest.

Publisher's note

References

An, Y., Chen, L., Tao, L., Liu, S., and Wei, C. (2021). QTL mapping for leaf area of tea plants (*Camellia sinensis*) based on a high-quality genetic map constructed by whole genome resequencing. *Front. Plant Sci.* 12. doi: 10.3389/fpls.2021.705285

Ashihara, H. (2015). Occurrence, biosynthesis and metabolism of theanine (γ-glutamyl-L-ethylamide) in plants: a comprehensive review. *Nat. Prod. Commun.* 10, 803–810. doi: 10.1177/1934578X15010005

Beatty, P. H., and Good, A. G. (2018). "Improving nitrogen use efficient in crop plants using biotechnology approaches," in *Engineering nitrogen utilization in crop plants*. Eds. A. Shrawat, A. Zayed and D. A. Lightfoot (Cham: Springer International Publishing), 15–35.

Bernard, S. M., and Habash, D. Z. (2009). The importance of cytosolic glutamine synthetase in nitrogen assimilation and recycling. *New. Phytol.* 182, 608–620. doi: 10.1111/j.1469-8137.2009.02823.x

Bodirsky, B. L., Popp, A., Lotze-Campen, H., Dietrich, J. P., Rolinski, S., Weindl, I., et al. (2014). Reactive nitrogen requirements to feed the world in 2050 and potential to mitigate nitrogen pollution. *Nat. Commun.* 5, 3858. doi: 10.1038/ncomms4858

Breeze, E., Harrison, E., McHattie, S., Hughes, L., Hickman, R., Hill, C., et al. (2011). High-resolution temporal profiling of transcripts during *Arabidopsis* leaf senescence reveals a distinct chronology of processes and regulation. *Plant Cell.* 23, 873–894. doi: 10.1105/tpc.111.083345

Camargo, J. A., Alonso, A., and Salamanca, A. (2005). Nitrate toxicity to aquatic animals: a review with new data for freshwater invertebrates. *Chemosphere* 58, 1255–1267. doi: 10.1016/j.chemosphere.2004.10.044

Chen, L., Chen, J., Wang, N., and Zhang, X. (2019). The role of plasma membrane H^+-ATPase on nitrogen-regulated phosphorus uptake in tea plants. *J. Tea Sci.* 39, 723–730. doi: 10.13305/j.cnki.jts.2019.06.011

Chen, T., Lin, S., Chen, Z., Yang, T., Zhang, S., Zhang, J., et al. (2023). Theanine, a tea-plant-specific non-proteinogenic amino acid, is involved in the regulation of lateral root development in response to nitrogen status. *Hortic. Res.* 10, uhac267. doi: 10.1093/hr/uhac267

Chen, T., Ma, J., Li, H., Lin, S., Dong, C., Xie, Y., et al. (2022). CsGDH2.1 negatively regulates theanine accumulation in the late-spring tea plants (*Camellia sinensis* var. sinensis). *Hortic. Res.* 10, uhac245. doi: 10.1093/hr/uhac245

Chen, Q., Meng, X., Jiang, X., Yu, S., and Wan, X. (2015). Tissue specificity expression analysis of theanine metabolism pathway related genes in *Camellia Sinensis*. *J. Nucl. Agric. Sci.* 29, 1285–1291.

Chen, Y., Wang, F., Wu, Z., Jiang, F., Yu, W., Yang, J., et al. (2021). Effects of long-term nitrogen fertilization on the formation of metabolites related to tea quality in subtropical China. *Metabolites* 11, 146. doi: 10.3390/metabo11030146

Chen, J., Wang, P., Xia, Y., Xu, M., and Pei, S. (2005). Genetic diversity and differentiation of *Camellia sinensis* L. (cultivated tea) and its wild relatives in Yunnan province of China, revealed by morphology, biochemistry and allozyme studies. *Genet. Resour. Crop Evol.* 52, 41–52. doi: 10.1007/s10722-005-0285-1

Cheng, S., Fu, X., Wang, X., Liao, Y., Zeng, L., Dong, F., et al. (2017). Studies on the biochemical formation pathway of the amino acid L-Theanine in tea (*Camellia sinensis*) and other plants. *J. Agric. Food Chem.* 65, 7210–7216. doi: 10.1021/acs.jafc.7b02437

Chopin, F., Orsel, M., Dorbe, M. F., Chardon, F., Truong, H.-N., Miller, A. J., et al. (2007). The *Arabidopsis* ATNRT2.7 nitrate transporter controls nitrate content in seeds. *Plant Cell* 19, 1590–1602. doi: 10.1105/tpc.107.050542

Couturier, J., Montanini, B., Martin, F., Brun, A., Blaudez, D., and Chalot, M. (2007). The expanded family of ammonium transporters in the perennial poplar plant. *New Phytol.* 174, 137–150. doi: 10.1111/j.1469-8137.2007.01992.x

Crawford, N. M., and Glass, A. D. M. (1998). Molecular and physiological aspects of nitrate uptake in plants. *Trends Plant Sci.* 3, 389–395. doi: 10.1016/S1360-1385(98)01311-9

Deng, W.-W., Ogita, S., and Ashihara, H. (2008). Biosynthesis of theanine (γ-ethylamino-l-glutamic acid) in seedlings of *Camellia sinensis*. *Phytochem. Lett.* 1, 115–119. doi: 10.1016/j.phytol.2008.06.002

Deng, M., Xu, Z., Hu, L., Yao, Y., Xu, M., and Pi, L. (2012). Effect of different levels of nitrogen application on yield and quality of FudingDabaicha. *Southwest Chin. J. Agric. Sci.* 25, 1330–1333. doi: 10.16213/j.cnki.scjas.2012.04.051

Dong, F., Hu, J., Shi, Y., Liu, M., Zhang, Q., and Ruan, J. (2019). Effects of nitrogen supply on flavonol glycoside biosynthesis and accumulation in tea leaves (*Camellia sinensis*). *Plant Physiol. Biochem.* 138, 48–57. doi: 10.1016/j.plaphy.2019.02.017

Dong, C., Li, F., Yang, T., Feng, L., Zhang, S., Li, F., et al. (2020). Theanine transporters identified in tea plants (*Camellia sinensis* L.). *Plant J.* 101, 57–70. doi: 10.1111/tpj.14517

Du, X., Peng, F., Jiang, J., Tan, P., Wu, Z. Z., Liang, Y. W., et al. (2015). Inorganic nitrogen fertilizers induce changes in ammonium assimilation and gas exchange in *Camellia sinensis* L. *Turk. J. Agric. For.* 39, 28–38. doi: 10.3906/TAR-1311-82

Epstein, E., and Hagen, C. E. (1952). A kinetic study of the absorption of alkali cations by barley roots. *Plant Physiol.* 27, 457–474. doi: 10.1104/pp.27.3.457

Fan, K., Zhang, Q., Liu, M., Ma, L., Shi, Y., and Ruan, J. (2019). Metabolomic and transcriptional analyses reveal the mechanism of C, N allocation from source leaf to flower in tea plant (*Camellia sinensis*. L). *J. Plant Physiol.* 232, 200–208. doi: 10.1016/j.jplph.2018.11.007

Feng, S. (2014). "Cloning an expressing of the nitrogen transporter Gene NRT1.2, NRT1.5 and NRT2.5 in tea plant," in *Dissertation* (Beijing: Chinese Academy of Agricultural Sciences). Chinese dissertation

Feng, L. (2017). "Cloning and functional analysis of CAT amino acid transporter genes in tea plant (*Camellia sinensis* L.)," in *Dissertation* (Hefei, Anhui Province: Anhui Agricultural University).

Feng, S., Wang, L., Chen, C., Lin, Z., Cheng, H., Wei, K., et al. (2014). Cloning and expressing analysis of a nitrogen transporter 2.5 gene from tea plant [*Camellia sinensis* (L.)]. *J. Tea Sci.* 34, 364–370.

Feng, L., Yang, T., Zhang, Z., Li, F., Chen, Q., Sun, J., et al. (2018). Identification and characterization of cationic amino acid transporters (CATs) in tea plant (*Camellia sinensis*). *Plant Growth Regul.* 84, 57–69. doi: 10.1007/s10725-017-0321-0

Feng, L., Yu, Y., Lin, S., Yang, T., Chen, Q., Liu, L., et al. (2021). Tonoplast-localized theanine transporter CsCAT2 may mediate theanine storage in the root of tea plants (*Camellia sinensis* L.). *Front. Plant Sci.* 12. doi: 10.3389/fpls.2021.797854

Fischer, W.-N., Kwart, M., Hummel, S., and Frommer, W. B. (1995). Substrate specificity and expression profile of amino acid transporters (AAPs) in *Arabidopsis**. *J. Biol. Chem.* 270, 16315–16320. doi: 10.1074/jbc.270.27.16315

Fontaine, J.-X., Tercé-Laforgue, T., Armengaud, P., Clément, G., Renou, J. P., Pelletier, S., et al. (2012). Characterization of a NADH-dependent glutamate dehydrogenase mutant of *Arabidopsis* demonstrates the key role of this enzyme in root carbon and nitrogen metabolism. *Plant Cell* 24, 4044–4065. doi: 10.1105/tpc.112.103689

Forde, B. G. (2000). Nitrate transporters in plants: structure, function and regulation. *BBA - Biomembranes* 1465, 219–235. doi: 10.1016/S0005-2736(00)00140-1

Fu, X., Liao, Y., Cheng, S., Deng, R., and Yang, Z. (2021a). Stable isotope-labeled precursor tracing reveals that L-alanine is converted to L-theanine via L-glutamate not ethylamine in tea plants *In Vivo*. *J. Agric. Food Chem.* 69, 15354–15361. doi: 10.1021/acs.jafc.1c06660

Fu, X., Liao, Y., Cheng, S., Xu, X., Grierson, D., and Yang, Z. (2021b). Nonaqueous fractionation and overexpression of fluorescent-tagged enzymes reveals the subcellular sites of L-theanine biosynthesis in tea. *Plant Biotechnol. J.* 19, 98–108. doi: 10.1111/pbi.13445

Gao, Z., Wang, Y., Chen, G., Zhang, A., Yang, S., Shang, L., et al. (2019). The indica nitrate reductase gene *OsNR2* allele enhances rice yield potential and nitrogen use efficiency. *Nat. Commun.* 10, 5207. doi: 10.1038/s41467-019-13110-8

Giehl, R. F. H., Laginha, A. M., Duan, F., Rentsch, D., Yuan, L., and von Wirén, N. (2017). A critical role of AMT2;1 in root-to-shoot translocation of ammonium in *Arabidopsis*. *Mol. Plant* 10, 1449–1460. doi: 10.1016/j.molp.2017.10.001

Godfray, H. C. J., Beddington, J. R., Crute, I. R., Haddad, L., Lawrence, D., Muir, J. F., et al. (2010). Food security: the challenge of feeding 9 billion people. *Science* 327, 812–818. doi: 10.1126/science.1185383

Guan, P., Wang, R., Nacry, P., Breton, G., Kay, S. A., Pruneda-Paz, J. L., et al. (2014). Nitrate foraging by *Arabidopsis* roots is mediated by the transcription factor TCP20 through the systemic signaling pathway. *Proc. Natl. Acad. Sci. U.S.A.* 111, 15267–15272. doi: 10.1073/pnas.1411375111

Guo, L., Zhang, F., Cheng, H., Wei, K., Ruan, L., Wu, L., et al. (2020). Molecular cloning and expression analysis of *CsAAPs* gene subfamily in *Camellia Sinensis*. *J. Tea Sci.* 40, 454–464. doi: 10.13305/j.cnki.jts.20200612.002

Guo, L., Zhang, F., Zhang, Y., Cheng, H., Wei, K., Ruan, L., et al. (2019). Molecular cloning and expression analysis of *CsLHTs* gene subfamily in tea plants (*Camellia sinensis*). *J. Tea Sci.* 39, 280–288. doi: 10.13305/j.cnki.jts.2019.03.005

Han, W., and Wu, X. (1992). Effect of copper and zinc on nitrate reductase activity in tea plant. *J. Tea Sci.* 12, 159–160. doi: 10.13305/j.cnki.jts.1992.02.010

Havé, M., Marmagne, A., Chardon, F., and Masclaux-Daubresse, C. (2017). Nitrogen remobilization during leaf senescence: lessons from Arabidopsis to crops. *J. Exp. Bot.* 68, 2513–2529. doi: 10.1093/jxb/erw365

Howitt, S. M., and Udvardi, M. K. (2000). Structure, function and regulation of ammonium transporters in plants. *BBA - Biomembranes* 1465, 152–170. doi: 10.1016/S0005-2736(00)00136-X

Hu, S., Hu, Y., Mei, H., Li, J., Xuan, W., Jeyaraj, A., et al. (2023). Genome-wide analysis of long non-coding RNAs (lncRNAs) in tea plants (*Camellia sinensis*) lateral roots in response to nitrogen application. *Front. Plant Sci.* 14. doi: 10.3389/fpls.2023.1080427

Hu, B., Jiang, Z., Wang, W., Qiu, Y., Zhang, Z., Liu, Y., et al. (2019). Nitrate–NRT1.1B–SPX4 cascade integrates nitrogen and phosphorus signalling networks in plants. *Nat. Plants* 5, 401–413. doi: 10.1038/s41477-019-0384-1

Hu, B., Wang, W., Ou, S., Tang, J., Li, H., Che, R., et al. (2015). Variation in *NRT1.1B* contributes to nitrate-use divergence between rice subspecies. *Nat. Genet.* 47, 834–838. doi: 10.1038/ng.3337

Huang, W., Ma, D. N., Liu, H. L., Luo, J., Wang, P., Wang, M. L., et al. (2020). Genome-wide identification of *CsATGs* in tea plant and the involvement of *CsATG8e* in nitrogen utilization. *Int. J. Mol. Sci.* 21, 7043. doi: 10.3390/ijms21197043

Huang, W., Ma, D., Xia, L., Zhang, E., Wang, P., Wang, M., et al. (2023a). Overexpression of *CsATG3a* improves tolerance to nitrogen deficiency and increases nitrogen use efficiency in arabidopsis. *Plant Physiol. Biochem.* 196, 328–338. doi: 10.1016/j.plaphy.2023.01.057

Huang, W., Ma, D., Zaman, F., Hao, X., Xia, L., Zhang, E., et al. (2023b). Identification of the lysine and histidine transporter family in *Camellia sinensis* and the characterizations in nitrogen utilization. *Hortic. Plant J.* doi: 10.1016/j.hpj.2023.01.009

Huang, R., Wang, J. Y., Yao, M. Z., Ma, C. L., and Chen, L. (2022). Quantitative trait loci mapping for free amino acid content using an albino population and SNP markers provides insight into the genetic improvement of tea plants. *Hortic. Res.* 9, uhab029. doi: 10.1093/hr/uhab029

Huang, H., Yao, Q., Xia, E., and Gao, L. (2018). Metabolomics and transcriptomics analyses reveal nitrogen influences on the accumulation of flavonoids and amino acids in young shoots of tea plant (*Camellia sinensis* L.) associated with tea flavor. *J. Agric. Food Chem.* 66, 9828–9838. doi: 10.1021/acs.jafc.8b01995

Jackson, L. E., Burger, M., and Cavagnaro, T. R. (2008). Roots, nitrogen transformations, and ecosystem services. *Annu. Rev. Plant Biol.* 59, 341–363. doi: 10.1146/annurev.arplant.59.032607.092932

Jentsch, T. (2008). CLC chloride channels and transporters: from genes to protein structure, pathology and physiology. *Crit. Rev. Biochem. Mol.* 43, 3–36. doi: 10.1080/10409230701829110

Jiang, J., Gai, Z., Wang, Y., Fan, K., Sun, L., Wang, H., et al. (2018). Comprehensive proteome analyses of lysine acetylation in tea leaves by sensing nitrogen nutrition. *BMC Genom.* 19, 840. doi: 10.1186/s12864-018-5250-4

Ju, C., Buresh, R. J., Wang, Z., Zhang, H., Liu, L., Yang, J., et al. (2015). Root and shoot traits for rice varieties with higher grain yield and higher nitrogen use efficiency at lower nitrogen rates application. *Field Crop Res.* 175, 47–55. doi: 10.1016/j.fcr.2015.02.007

Kiba, T., Feria-Bourrellier, A.-B., Lafouge, F., Lezhneva, L., Boutet-Mercey, S., Orsel, M., et al. (2012). The *Arabidopsis* nitrate transporter NRT2.4 plays a double role in roots and shoots of nitrogen-starved plants. *Plant Cell* 24, 245–258. doi: 10.1105/tpc.111.092221

Kobae, Y., Tamura, Y., Takai, S., Banba, M., and Hata, S. (2010). Localized expression of arbuscular mycorrhiza-inducible ammonium transporters in soybean. *Plant Cell Physiol.* 51, 1411–1415. doi: 10.1093/pcp/pcq099

Konishi, N., Ishiyama, K., Matsuoka, K., Maru, I., Hayakawa, T., Yamaya, T., et al. (2014). NADH-dependent glutamate synthase plays a crucial role in assimilating ammonium in the Arabidopsis root. *Physiol. Plant* 152, 138–151. doi: 10.1111/ppl.12177

Krapp, A., David, L. C., Chardin, C., Girin, T., Marmagne, A., Leprince, A.-S., et al. (2014). Nitrate transport and signalling in *Arabidopsis*. *J. Exp. Bot.* 65, 789–798. doi: 10.1093/jxb/eru001

Lea, P. J., and Miflin, B. J. (2003). Glutamate synthase and the synthesis of glutamate in plants. *Plant Physiol. Biochem.* 41, 555–564. doi: 10.1016/S0981-9428(03)00060-3

Lei, X., Wang, T., Yang, B., Duan, Y., Zhou, L., Zou, Z., et al. (2022). Progress and perspective on intercropping patterns in tea plantations. *Bev. Plant Res.* 2, 1–10. doi: 10.48130/BPR-2022-0018

Li, J., Deng, T., Wu, Y., Liu, S., Li, Q., Liu, Z., et al. (2011). Full-length cDNA cloning and sequence analysis of theanine synthease gene in *Camellia Sinensis*. *J. Tea Sci.* 31, 411–418. doi: 10.13305/j.cnki.jts.2011.05.012

Li, F., Dong, C., Yang, T., Bao, S., Fang, W., Lucas, W. J., et al. (2021). The tea plant CsLHT1 and CsLHT6 transporters take up amino acids, as a nitrogen source, from the soil of organic tea plantations. *Hortic. Res.* 8, 1–12. doi: 10.1038/s41438-021-00615-x

Li, F., Dong, C., Yang, T., Ma, J., Zhang, S., Wei, C., et al. (2019). Seasonal theanine accumulation and related gene expression in the roots and leaf buds of tea plants (*Camellia Sinensis* L.). *Front. Plant Sci.* 10. doi: 10.3389/fpls.2019.01397

Li, H., Han, J.-L., Chang, Y. H., Lin, J., and Yang, Q. S. (2016). Gene characterization and transcription analysis of two new ammonium transporters in pear rootstock (*Pyrus betulaefolia*). *J. Plant Res.* 129, 737–748. doi: 10.1007/s10265-016-0799-y

Li, F., Li, H., Dong, C., Yang, T., Zhang, S., Bao, S., et al. (2020). Theanine transporters are involved in nitrogen deficiency response in tea plant (*Camellia sinensis* L.). *Plant Signal. Behav.* 15, 1728109. doi: 10.1080/15592324.2020.1728109

Li, S. M., Li, B. Z., and Shi, W. M. (2012). Expression patterns of nine ammonium transporters in rice in response to N status. *Pedosphere* 22, 860–869. doi: 10.1016/S1002-0160(12)60072-1

Li, F., Lv, C., Zou, Z., Duan, Y., Zhou, J., Zhu, X., et al. (2022). *CsAAP7.2* is involved in the uptake of amino acids from soil and the long-distance transport of theanine in tea plants (*Camellia sinensis* L.). *Tree Physiol.* 42, 2369–2381. doi: 10.1093/treephys/tpac071

Li, W., Wang, Y., Okamoto, M., Crawford, N. M., Siddiqi, M. Y., and Glass, A. D. M. (2007). Dissection of the *AtNRT2.1*:*AtNRT2.2* inducible high-affinity nitrate transporter gene cluster. *Plant Physiol.* 143, 425–433. doi: 10.1104/pp.106.091223

Li, W., Xiang, F., Zhong, M., Zhou, L., Liu, H., Li, S., et al. (2017). Transcriptome and metabolite analysis identifies nitrogen utilization genes in tea plant (*Camellia sinensis*). *Sci. Rep.* 7, 1693. doi: 10.1038/s41598-017-01949-0

Lin, S., Chen, Z., Chen, T., Deng, W., Wan, X., and Zhang, Z. (2023a). Theanine metabolism and transport in tea plants (*Camellia sinensis* L.): advances and perspectives. *Crit. Rev. Biotechnol.* 43, 327–341. doi: 10.1080/07388551.2022.2036692

Lin, Z. H., Chen, C. S., Zhao, S. Q., Liu, Y., Zhong, Q. S., Ruan, Q. C., et al. (2023b). Molecular and physiological mechanisms of tea (*Camellia sinensis* (L.) O. Kuntze) leaf

and root in response to nitrogen deficiency. *BMC Genom.* 24, 27. doi: 10.1186/s12864-023-09112-y

Lin, Z., Zhong, Q., Chen, C., Chen, Z., and You, X. (2014). Expression analysis of key enzyme genes of nitrogen synthesis from tea tree leave under different nitrogen level. *J. Nucl. Agric. Sci.* 28, 985–989.

Lin, Z., Zhong, Q., Chen, C., Ruan, Q., Chen, Z., and You, X. (2016). Carbon dioxide assimilation and photosynthetic electron transport of tea leaves under nitrogen deficiency. *Bot. Stud.* 57, 37. doi: 10.1186/s40529-016-0152-8

Lin, Z., Zhong, Q., Hao, Z., You, X., Chen, Z., Chen, C., et al. (2017). Effects of chlorophyll fluorescence parameters of different tea cultivars in response to low nitrogen. *J. Tea Sci.* 37, 363–372. doi: 10.13305/j.cnki.jts.2017.04.008

Lin, Z., Zhong, Q., You, X., Chen, Z., Chen, C., Shan, R., et al. (2018). Antioxidant enzyme activity of tea plant (*Camellia sinensis*) in response to low temperature stress. *J. Tea Sci.* 38, 363–371. doi: 10.13305/j.cnki.jts.2018.04.004

Lin, Z., Zhong, Q., You, X., Chen, Z., Chen, C., Shan, R., et al. (2019). Antioxidant enzyme activity and growth of tea plants (*Camellia sinensis*) as affected by low-nitrogen stress. *Acta Tea Sin.* 60, 57–63.

Liu, Y. (2016). "The altered expression of genes related to nitrogen absorption and utilization of tea cultivars with different nitrogen use efficiency," in *Dissertation* (Beijing: Chinese Academy of Agricultural Sciences).

Liu, H. (2020). "Functional characterization of amino acid transporter genes *CsVAT1.3*, *CsLHT8L*, *CsCAT9.1*, *CsAAP3.1* in *Camellia sinensis*," in *Dissertation* (Wuhan, Hubei Province: HuangZhong Agricultural University).

Liu, M. Y., Burgos, A., Ma, L., Zhang, Q., Tang, D., and Ruan, J. (2017a). Lipidomics analysis unravels the effect of nitrogen fertilization on lipid metabolism in tea plant (*Camellia sinensis* L.). *BMC Plant Biol.* 17, 165. doi: 10.1186/s12870-017-1111-6

Liu, M.-Y., Burgos, A., Zhang, Q., Tang, D., Shi, Y., Ma, L., et al. (2017b). Analyses of transcriptome profiles and selected metabolites unravel the metabolic response to NH_4^+ and NO_3^- as signaling molecules in tea plant (*Camellia sinensis* L.). *Sci. Hortic.* 218, 293–303. doi: 10.1016/j.scienta.2017.02.036

Liu, X., Hu, B., and Chu, C. (2022). Nitrogen assimilation in plants: current status and future prospects. *J. Genet. Genomics* 49, 394–404. doi: 10.1016/j.jgg.2021.12.006

Liu, Z. W., Li, H., Liu, J. X., Wang, Y., and Zhuang, J. (2020). Integrative transcriptome, proteome, and microRNA analysis reveals the effects of nitrogen sufficiency and deficiency conditions on theanine metabolism in the tea plant (*Camellia sinensis*). *Hortic. Res.* 7, 1–13. doi: 10.1038/s41438-020-0290-8

Liu, Z. W., Li, H., Wang, W. L., Wu, Z. J., Cui, X., and Zhuang, J. (2017c). CsGOGAT is important in dynamic changes of theanine content in postharvest tea plant leaves under different temperature and shading spreadings. *J. Agric. Food Chem.* 65, 9693–9702. doi: 10.1021/acs.jafc.7b04552

Liu, J., Liu, M., Fang, H., Zhang, Q., and Ruan, J. (2021a). Accumulation of amino acids and flavonoids in young tea shoots is highly correlated with carbon and nitrogen metabolism in roots and mature leaves. *Front. Plant Sci.* 12. doi: 10.3389/fpls.2021.756433

Liu, M., Tang, D., Jiao, Z., Shi, Y., Ma, L., Zhang, Q., et al. (2021b). Suitable nitrogen fertilization rate effectively improve the quality of summer green tea. *J. Plant Nutr. Fer.* 27, 1407–1419. doi: 10.11674/zwyf.2021012

Liu, M. Y., Tang, D., Shi, Y., Ma, L., Li, Y., Zhang, Q., et al. (2019). Short-term inhibition of glutamine synthetase leads to reprogramming of amino acid and lipid metabolism in roots and leaves of tea plant (*Camellia sinensis* L.). *BMC Plant Biol.* 19, 425. doi: 10.1186/s12870-019-2027-0

Liu, Y., Wang, H., Jiang, Z., Wang, W., Xu, R., Wang, Q., et al. (2021c). Genomic basis of geographical adaptation to soil nitrogen in rice. *Nature* 590, 600–605. doi: 10.1038/s41586-020-03091-w

Liu, Z. W., Wu, Z. J., Li, H., Wang, Y. X., and Zhuang, J. (2017d). L-theanine content and related gene expression: novel insights into theanine biosynthesis and hydrolysis among different tea plant (*Camellia sinensis* L.) tissues and cultivars. *Front. Plant Sci.* 8. doi: 10.3389/fpls.2017.00498

Liu, J., You, L., Amini, M., Obersteiner, M., Herrero, M., Zehnder, A. J. B., et al. (2010). A high-resolution assessment on global nitrogen flows in cropland. *Proc. Natl. Acad. Sci. U.S.A.* 107, 8035–8040. doi: 10.1073/pnas.0913658107

Liu, S. X., Zhang, H. J., and Liu, X. Q. (2023). Comparative analysis and improvement of international competitiveness of Chinese tea industry. *Food Nutri China*. doi: 10.19870/j.cnki.11-3716/ts.20230609.002

Lothier, J., Gaufichon, L., Sormani, R., Lemaître, T., Azzopardi, M., Morin, H., et al. (2011). The cytosolic glutamine synthetase GLN1;2 plays a role in the control of plant growth and ammonium homeostasis in *Arabidopsis* rosettes when nitrate supply is not limiting. *J. Exp. Bot.* 62, 1375–1390. doi: 10.1093/jxb/erq299

Lynch, J. (2007). Roots of the second green revolution. *Aust. J. Bot.* 55, 493–512. doi: 10.1071/BT06118

Ma, L., Chen, H., Shan, Y., Jiang, M., Zhang, G., Geng, M., et al. (2013). Status and suggestions of tea garden fertilization on main green tea-producing counties in Zhejiang province. *J. Tea Sci.* 33, 74–84. doi: 10.13305/j.cnki.jts.2013.01.010

Ma, J. Q., Jin, J. Q., Yao, M. Z., Ma, C. L., Xu, Y. X., Hao, W. J., et al. (2018). Quantitative trait loci mapping for theobromine and caffeine contents in tea plant (*Camellia sinensis*). *J. Agric. Food Chem.* 66, 13321–13327. doi: 10.1021/acs.jafc.8b05355

Mei, Y., and Zhang, S. (2022). Analysis of China's tea production and domestic sales in 2022. *China Tea.* 45, 25–30.

Miller, A. J., and Cramer, M. D. (2005). Root nitrogen acquisition and assimilation. *Plant Soil* 274, 1–36. doi: 10.1007/s11104-004-0965-1

Moll, R. H., Kamprath, E. J., and Jackson, W. A. (1982). Analysis and interpretation of factors which contribute to efficiency of nitrogen utilization1. *Agron. J.* 74, 562–564. doi: 10.2134/agronj1982.00021962007400030037x

Monachello, D., Allot, M., Oliva, S., Krapp, A., Daniel-Vedele, F., Barbier-Brygoo, H., et al. (2009). Two anion transporters AtClCa and AtClCe fulfil interconnecting but not redundant roles in nitrate assimilation pathways. *New Phytol.* 183, 88–94. doi: 10.1111/j.1469-8137.2009.02837.x

Negi, J., Matsuda, O., Nagasawa, T., Oba, Y., Takahashi, H., Kawai-Yamada, M., et al. (2008). CO_2 regulator SLAC1 and its homologues are essential for anion homeostasis in plant cells. *Nature* 452, 483–486. doi: 10.1038/nature06720

Ni, K., Liao, W., Yi, X., Niu, S., Ma, L., Shi, Y., et al. (2019). Fertilization status and reduction potential in tea gardens of China. *J. Plant Nutr. Fer.* 25, 421–432. doi: 10.11674/zwyf.18078

Rana, N. K., Mohanpuria, P., and Yadav, S. K. (2008). Cloning and characterization of a cytosolic glutamine synthetase from *Camellia sinensis* (L.) O. Kuntze that is upregulated by ABA, SA, and H_2O_2. *Mol. Biotechnol.* 39, 49–56. doi: 10.1007/s12033-007-9027-2

Raun, W. R., and Johnson, G. V. (1999). Improving nitrogen use efficiency for cereal production. *Agron. J.* 91, 357–363. doi: 10.2134/agronj1999.00021962009100030001x

Ruan, J., Gerendás, J., Härdter, R., and Sattelmacher, B. (2007). Effect of root zone pH and form and concentration of nitrogen on accumulation of quality-related components in green tea. *J. Sci. Food Agr.* 87, 1505–1516. doi: 10.1002/jsfa.2875

Ruan, J., Haerdter, R., and Gerendás, J. (2010). Impact of nitrogen supply on carbon/nitrogen allocation: a case study on amino acids and catechins in green tea [*Camellia sinensis* (L.) O. Kuntze] plants*. *Plant Biol.* 12, 724–734. doi: 10.1111/j.1438-8677.2009.00288.x

Ruan, J., Wang, X., Cui, S., and Yao, G. (1993). Study on the mechanism in the difference of nitrogen nutrition among different cultivars. *China Tea*, 35–37.

Ruan, L., Wei, K., Wang, L., Cheng, H., Wu, L., and Li, H. (2019). Characteristics of free amino acids (the quality chemical components of tea) under spatial heterogeneity of different nitrogen forms in tea (*Camellia sinensis*) Plants. *Molecules* 24, 415. doi: 10.3390/molecules24030415

Ruan, L., Wei, K., Wang, L., Cheng, H., Zhang, F., Wu, L., et al. (2016). Characteristics of NH_4^+ and NO_3^- fluxes in tea (*Camellia sinensis*) roots measured by scanning ion-selective electrode technique. *Sci. Rep.* 6, 38370. doi: 10.1038/srep38370

Santa-María, G. E., Moriconi, J. I., and Oliferuk, S. (2015). Internal efficiency of nutrient utilization: what is it and how to measure it during vegetative plant growth? *J. Exp. Bot.* 66, 3011–3018. doi: 10.1093/jxb/erv162

She, G., Yu, S., Li, Z., Peng, A., Li, P., Li, Y., et al. (2022). Characterization of *CsTSI* in the biosynthesis of theanine in tea plants (*Camellia sinensis*). *J. Agric. Food Chem.* 70, 826–836. doi: 10.1021/acs.jafc.1c04816

Song, B., Zhang, L., Chen, Z., Liu, M., Zhang, W., Zhao, J., et al. (2023). Effects of different fertilization treatments on the physiological activities of roots and the expression of CsAMT2s of potted tea cuttings of the different varieties. *Chin. J. Appl. Environ. Biol.*, 1–11. doi: 10.19675/j.cnki.1006-687x.2022.09029

Su, J., Ruan, L., Wang, L., Wei, K., Wu, L., Bai, P., et al. (2020). Early identification of nitrogen absorption efficiency in tea plants. *J. Tea Sci.* 40, 576–587. doi: 10.13305/j.cnki.jts.2020.05.002

Suárez, M. F., Avila, C., Gallardo, F., Cantón, F. R., García-Gutiérrez, A., Claros, M. G., et al. (2002). Molecular and enzymatic analysis of ammonium assimilation in woody plants. *J. Exp. Bot.* 53, 891–904. doi: 10.1093/jexbot/53.370.891

Sun, J., Bankston, J. R., Payandeh, J., Hinds, T. R., Zagotta, W. N., and Zheng, N. (2014). Crystal structure of the plant dual-affinity nitrate transporter NRT1.1. *Nature* 507, 73–77. doi: 10.1038/nature13074

Sun, J., Qiu, C., Qian, W., Wang, Y., Sun, L., Li, Y., et al. (2019). Ammonium triggered the response mechanism of lysine crotonylome in tea plants. *BMC Genom.* 20, 340. doi: 10.1186/s12864-019-5716-z

Suzuki, A., and Knaff, D. B. (2005). Glutamate synthase: structural, mechanistic and regulatory properties, and role in the amino acid metabolism. *Photosynth. Res.* 83, 191–217. doi: 10.1007/s11120-004-3478-0

Swarbreck, S. M., Defoin-Platel, M., Hindle, M., Saqi, M., and Habash, D. Z. (2011). New perspectives on glutamine synthetase in grasses. *J. Exp. Bot.* 62, 1511–1522. doi: 10.1093/jxb/erq356

Tan, L., Cui, D., Wang, L., Liu, Q., Zhang, D., Hu, X., et al. (2022). Genetic analysis of the early bud flush trait of tea plants (*Camellia sinensis*) in the cultivar 'Emei Wenchun' and its open-pollinated offspring. *Hortic. Res.* 9, uhac086. doi: 10.1093/hr/uhac086

Tang, D., Jiao, Z., Zhang, Q., Liu, M.-Y., and Ruan, J. (2021). Glutamate dehydrogenase isogenes *CsGDHs* cooperate with glutamine synthetase isogenes *CsGSs* to assimilate ammonium in tea plant (*Camellia sinensis* L.). *Plant Sci.* 312, 111031. doi: 10.1016/j.plantsci.2021.111031

Tang, D., Liu, M., Zhang, Q., Fan, K., Shi, Y., Ma, L., et al. (2018). Isolation and expression profiles of cytosolic glutamine synthetase genes *CsGS1s* in tea plant (*Camellia sinensis*). *Plant Physiol. J.* 54, 71–80. doi: 10.13592/j.cnki.ppj.2017.0265

Tang, D., Liu, M.-Y., Zhang, Q., Ma, L., Shi, Y., and Ruan, J. (2020). Preferential assimilation of NH_4^+ over NO_3^- in tea plant associated with genes involved in nitrogen

transportation, utilization and catechins biosynthesis. *Plant Sci.* 291, 110369. doi: 10.1016/j.plantsci.2019.110369

Tang, D., Liu, M., Zhang, Q., Shi, Y., Ma, L., and Ruan, J. (2019). Effects of nitrogen form and root-zone pH on nutrient uptake and concentrations of organic anions in tea plants (*Camellia sinensis*). *J. Tea Sci.* 39, 159–170. doi: 10.13305/j.cnki.jts.2019.02.005

Teng, R. M., Yang, N., Li, J. W., Liu, C. F., Chen, Y., Li, T., et al. (2022). Isolation and characterization of an LBD transcription factor CsLBD39 from tea plant (*Camellia sinensis*) and its roles in modulating nitrate content by regulating nitrate-metabolism-related genes. *Int. J. Mol. Sci.* 23, 9294. doi: 10.3390/ijms23169294

Thomsen, H. C., Eriksson, D., Møller, I. S., and Schjoerring, J. K. (2014). Cytosolic glutamine synthetase: a target for improvement of crop nitrogen use efficiency? *Trends Plant Sci.* 19, 656–663. doi: 10.1016/j.tplants.2014.06.002

Vahisalu, T., Kollist, H., Wang, Y. F., Nishimura, N., Chan, W. Y., Valerio, G., et al. (2008). SLAC1 is required for plant guard cell S-type anion channel function in stomatal signalling. *Nature* 452, 487–491. doi: 10.1038/nature06608

Valderrama-Martín, J. M., Ortigosa, F., Ávila, C., Cánovas, F. M., Hirel, B., Cantón, F. R., et al. (2022). A revised view on the evolution of glutamine synthetase isoenzymes in plants. *Plant J.* 110, 946–960. doi: 10.1111/tpj.15712

Wang, J. (2014). "Cloning and expression analysis of genes related to nitrogen transporter in tea plants (*Camellia sinesis*)," in *Dissertation* (Hefei, Anhui Province: Anhui Agricultural University).

Wang, L., Chen, C., Lin, Z., Wei, K., Wu, L., Feng, S., et al. (2015). Growth characteristic of different cultivars of tea plant in response to nitrogen contents. *J. Tea Sci.* 35, 423–428. doi: 10.13305/j.cnki.jts.2015.05.003

Wang, Y., Cheng, X., Yang, T., Su, Y., Lin, S., Zhang, S., et al. (2021b). Nitrogen-regulated theanine and flavonoid biosynthesis in tea plant roots: protein-level regulation revealed by multiomics analyses. *J. Agric. Food. Chem.* 69, 10002–10016. doi: 10.1021/acs.jafc.1c02589

Wang, Y., Ouyang, J.-X., Fan, D.-M., Wang, S.-M., Xuan, Y.-M., Wang, X.-C., et al. (2022a). Transcriptome analysis of tea (*Camellia sinensis*) leaves in response to ammonium starvation and recovery. *Front. Plant Sci.* 13. doi: 10.3389/fpls.2022.963269

Wang, X., and Su, J. (1990). Relationship between nitrate reductase activity and yield traits and nitrogen nutrition in tea plants. *J. Tea Sci.* 64.

Wang, J., Tian, X., Jiang, C., and Li, Y. (2014). Cloning and expression analysis of nitrate transporter gene in *Camellia sinensis*. *Plant Physiol. J.* 50, 983–988. doi: 10.13592/j.cnki.ppj.2014.0049

Wang, Y., Wei, K., Ruan, L., Bai, P., Wu, L., Wang, L., et al. (2022b). Systematic investigation and expression profiles of the nitrate transporter 1/peptide transporter family (NPF) in tea plant (*Camellia sinensis*). *Int. J. Mol. Sci.* 23, 6663. doi: 10.3390/ijms23126663

Wang, Y., Xuan, Y.-M., Wang, S. M., Fan, D. M., Wang, X. C., and Zheng, X. Q. (2022c). Genome-wide identification, characterization, and expression analysis of the ammonium transporter gene family in tea plants (*Camellia sinensis* L.). *Physiol. Plant* 174, e13646. doi: 10.1111/ppl.13646

Wang, X., Yang, Y., Chen, L., and Ruan, J. (2004). Genotypic difference of nitrogen efficiency in tea plant [*Camellia sinensis* (L.) O. Kuntze]. *J. Tea Sci.* 24, 93–98. doi: 10.13305/j.cnki.jts.2004.02.004

Wang, X., Yang, Y., Chen, L., and Ruan, J. (2005). Preliminary study on physiological and biochemical indices related to nitrogen use efficiency in tea plant [*Camelliasinensis* (L.)O·Kuntze). *Acta Agronomica Sin.* 31, 926–931.

Wang, P., Yang, J., Zhang, X., and Ye, N. (2021a). Research advance of tea plant genome and sequencing technologies. *J. Tea Sci.* 41, 743–752. doi: 10.13305/j.cnki.jts.2021.06.002

Wei, G., Huang, J., and Yang, J. (2012). The impacts of food safety standards on China's tea exports. *China Econ. Rev.* 23, 253–264. doi: 10.1016/j.chieco.2011.11.002

Wei, K., Wang, X., Hao, X., Qian, Y., Li, X., Xu, L., et al. (2021). Development of a genome-wide 200K SNP array and its application for high-density genetic mapping and origin analysis of *Camellia sinensis*. *Plant Biotechnol. J.* 20, pbi.13761. doi: 10.1111/pbi.13761

Wei, C., Yang, H., Wang, S., Zhao, J., Liu, C., Gao, L., et al. (2018). Draft genome sequence of *Camellia sinensis* var. sinensis provides insights into the evolution of the tea genome and tea quality. *Proc. Natl. Acad. Sci. U.S.A.* 115, E4151–E4158. doi: 10.1073/pnas.1719622115

Williams, S., Arcand, M., and Congreves, K. (2021). Nitrogen use efficiency definitions of today and tomorrow. *Front. Plant Sci.* 12. doi: 10.3389/fpls.2021.637108

Wirén, N., Gazzarrini, S., and Frommer, W. (1997). Regulation of mineral nitrogen uptake in plants. *Plant Soil* 196, 191–199. doi: 10.1023/A:1004241722172

Wu, X., Liu, T., Zhang, Y., Duan, F., Neuhäuser, B., Ludewig, U., et al. (2019). Ammonium and nitrate regulate NH_4^+ uptake activity of Arabidopsis ammonium transporter AtAMT1;3 via phosphorylation at multiple C-terminal sites. *J. Exp. Bot.* 70, 4919–4930. doi: 10.1093/jxb/erz230

Wu, B., and Wu, X. (1993). Determination of nitrate reductase activity of tea pant leaves in *vitro* and in situ. *China Tea* 8–10.

Xia, E., Tong, W., Hou, Y., An, Y., Chen, L., Wu, Q., et al. (2020). The reference genome of tea plant and resequencing of 81 diverse accessions provide insights into its genome evolution and adaptation. *Mol. Plant* 13, 1013–1026. doi: 10.1016/j.molp.2020.04.010

Xing, A., Ma, Y., Wu, Z., Nong, S., Zhu, J., Sun, H., et al. (2020). Genome-wide identification and expression analysis of the CLC superfamily genes in tea plants (*Camellia sinensis*). *Funct. Integr. Genomics* 20, 497–508. doi: 10.1007/s10142-019-00725-9

Xu, L. Y., Wang, L. Y., Wei, K., Tan, L. Q., Su, J. J., and Cheng, H. (2018). High-density SNP linkage map construction and QTL mapping for flavonoid-related traits in a tea plant (*Camellia sinensis*) using 2b-RAD sequencing. *BMC Genom.* 19, 955. doi: 10.1186/s12864-018-5291-8

Yang, Y. (2011). "Quality-related constituents in tea (*Camellia sinensis* (L.) O. Kuntze) leaves as affected by nitrogen," in *Dissertation* (Nanjing, Jiangsu Province: Nanjing Agricultural University).

Yang, Y., Hu, Y., Wan, Q., Li, R., Wang, F., and Ruan, J. (2016). Cloning and expression analysis of nitrate transporter NRT1.1 gene in tea plant (*Camellia sinensis* (L.)). *J. Tea Sci.* 36, 505–512. doi: 10.13305/j.cnki.jts.2016.05.009

Yang, T., Xie, Y., Lu, X., Yan, X., Wang, Y., Ma, J., et al. (2021). Shading promoted theanine biosynthesis in the roots and allocation in the shoots of the tea plant (*Camellia sinensis* L.) cultivar Shuchazao. *J. Agric. Food Chem.* 69, 4795–4803. doi: 10.1021/acs.jafc.1c00641

Yao, M. Z., Ma, C. L., Qiao, T. T., Jin, J. Q., and Chen, L. (2012). Diversity distribution and population structure of tea germplasms in China revealed by EST-SSR markers. *Tree. Genet. Genomes.* 8, 205–220. doi: 10.1007/s11295-011-0433-z

Yu, Y., Kou, X., Gao, R., Chen, X., Zhao, Z., Mei, H., et al. (2021). Glutamine synthetases play a vital role in high accumulation of theanine in tender shoots of albino tea germplasm "Huabai 1." *J. Agric. Food Chem.* 69, 13904–13915. doi: 10.1021/acs.jafc.1c04567

Yuan, L., Gu, R., Xuan, Y., Smith-Valle, E., Loqué, D., Frommer, W. B., et al. (2013). Allosteric regulation of transport activity by heterotrimerization of *Arabidopsis* ammonium transporter complexes in *vivo*. *Plant Cell* 25, 974–984. doi: 10.1105/tpc.112.108027

Yuan, L., Loqué, D., Kojima, S., Rauch, S., Ishiyama, K., Inoue, E., et al. (2007). The organization of high-affinity ammonium uptake in *Arabidopsis* roots depends on the spatial arrangement and biochemical properties of AMT1-type transporters. *Plant Cell* 19, 2636–2652. doi: 10.1105/tpc.107.052134

Zhang, X., Cui, Y., Yu, M., Su, B., Gong, W., Baluška, F, et al. (2019a). Phosphorylation-mediated dynamics of nitrate transceptor NRT1.1 regulate auxin flux and nitrate signaling in lateral root growth. *Plant Physiol.* 181, 480–498. doi: 10.1104/pp.19.00346

Zhang, F., He, W., Yuan, Q., Wei, K., Ruan, L., Wang, L., et al. (2021). Transcriptome analysis identifies *CsNRT* genes involved in nitrogen uptake in tea plants, with a major role of *CsNRT2.4*. *Plant Physiol. Biochem.* 167, 970–979. doi: 10.1016/j.plaphy.2021.09.024

Zhang, X., Li, Y., Wang, Y., Cai, H., Zeng, H., and Wang, Z. (2019b). Influence of future climate change in suitable habitats of tea in different countries. *Biodivers. Sci.* 27, 595–606. doi: 10.17520/biods.2019085

Zhang, W., Lin, L., Chen, M., and Sun, W. (2022a). Molecular cloning and expression analysis of *CsAMT1s* gene subfamily in *Camellia sinensis*. *Chin. J. Appl. Environ. Biol.* 28, 57–66. doi: 10.19675/j.cnki.1006-687x.2020.10011

Zhang, W., Lin, L., Wang, T., Chen, M., Song, B., and Sun, W. (2022b). Genome-wide identification of AMT2-type ammonium transporters reveal that CsAMT2.2 and CsAMT2.3 potentially regulate NH_4^+ absorption among three different cultivars of *Camellia sinensis*. *Int. J. Mol. Sci.* 23, 15661. doi: 10.3390/ijms232415661

Zhang, F., Liu, Y., Wang, L., Bai, P., Ruan, L., Zhang, C., et al. (2018). Molecular cloning and expression analysis of ammonium transporters in tea plants (*Camellia sinensis* (L.) O. Kuntze) under different nitrogen treatments. *Gene* 658, 136–145. doi: 10.1016/j.gene.2018.03.024

Zhang, F., Wang, L., Bai, P., Wei, K., Zhang, Y., Ruan, L., et al. (2020). Identification of regulatory networks and hub genes controlling nitrogen uptake in tea plants [*Camellia sinensis* (L.) O. Kuntze]. *J. Agric. Food Chem.* 68, 2445–2456. doi: 10.1021/acs.jafc.9b06427

Zhang, F., Wang, L., Cheng, H., Wei, K., Hu, J., Zhang, C., et al. (2016). Molecular cloning and expression analysis of nitrite reductase gene *CsNiR* in tea plant. *Acta Hortica* 43, 1348–1356. doi: 10.16420/j.issn.0513-353x.2016-0324

Zheng, S. (2022). "Study on the monitoring of nitrate leaching and nitrogen balance in tea plantation," in *Dissertation* (Beijing: Chinese Academy of Agricultural Sciences).

Zhou, X. (2012). "Study on rapid diagnosis and physiology and biochemistry indexes of nitrogen nutrition in tea plants (*Camellia sinensis*)," in *Dissertation* (Hefei, Anhui Province: Anhui Agricultural University).

Zhou, Y. (2014). "Genotype difference study on nitrogen efficiency of tea plants (*Camellia sinensis*) and cloning, expression analysis of nitrate reductase," in *Dissertation* (Hefei, Anhui Province: Anhui Agricultural University).

Zhou, Y., Pang, L., Li, Y., and Jiang, C. (2013). Cloning and expression analysis nitrate reductase gene in *Camellia sinensis*. *Acta Bot. Boreal-Occident Sin.* 33, 1292–1297. Chinese dissertation

Zhou, Y., Zhang, C., Lin, J., Yang, Y., Peng, Y., Tang, D., et al. (2015). Over-expression of a glutamate dehydrogenase gene, *MgGDH*, from *Magnaporthe grisea* confers tolerance to dehydration stress in transgenic rice. *Planta* 241, 727–740. doi: 10.1007/s00425-014-2214-z

Zhu, J., Ingram, P. A., Benfey, P. N., and Elich, T. (2011). From lab to field, new approaches to phenotyping root system architecture. *Curr. Opin. Plant Biol.* 14, 310–317. doi: 10.1016/j.pbi.2011.03.020

frontiers | Frontiers in Plant Science

TYPE Original Research
PUBLISHED 27 October 2023
DOI 10.3389/fpls.2023.1268835

OPEN ACCESS

EDITED BY
Md Sazzad Hossain,
University of Kiel, Germany

REVIEWED BY
Catherine Rayon,
University of Picardie Jules Verne, France
Yan Lei,
Huazhong Agricultural University, China
Juan Camacho-Cristóbal,
Universidad Pablo de Olavide, Spain

*CORRESPONDENCE
Bing Hu
binghu@caf.ac.cn
Xiangyang Li
xiangylxiang@163.com

RECEIVED 28 July 2023
ACCEPTED 12 October 2023
PUBLISHED 27 October 2023

CITATION
Chen Z, Bai X, Zeng B, Fan C, Li X and Hu B (2023) Physiological and molecular mechanisms of *Acacia melanoxylon* stem in response to boron deficiency. *Front. Plant Sci.* 14:1268835. doi: 10.3389/fpls.2023.1268835

Physiological and molecular mechanisms of *Acacia melanoxylon* stem in response to boron deficiency

Zhaoli Chen[1], Xiaogang Bai[2], Bingshan Zeng[1], Chunjie Fan[1], Xiangyang Li[1]* and Bing Hu[1]*

[1]Key Laboratory of State Forestry and Grassland Administration on Tropical Forestry, Research Institute of Tropical Forestry, Chinese Academy of Forestry, Guangzhou, Guangdong, China, [2]College of Agriculture and Biology, Zhongkai University of Agriculture and Engineering, Guangzhou, Guangdong, China

Boron is an essential micronutrient for plant growth as it participates in cell wall integrity. The growth and development of *Acacia melanoxylon* stem can be adversely affected by a lack of boron. To explore the mechanism of boron deficiency in *A. melanoxylon* stem, the changes in morphological attributes, physiological, endogenous hormone levels, and the cell structure and component contents were examined. In addition, the molecular mechanism of shortened internodes resulting from boron deficiency was elucidated through transcriptome analysis. The results showed that boron deficiency resulted in decreased height, shortened internodes, and reduced root length and surface area, corresponding with decreased boron content in the roots, stems, and leaves of *A. melanoxylon*. In shortened internodes of stems, oxidative damage, and disordered hormone homeostasis were induced, the cell wall was thickened, hemicellulose and water-soluble pectin contents decreased, while the cellulose content increased under boron deficiency. Furthermore, plenty of genes associated with cell wall metabolism and structural components, including *GAUTs*, *CESAs*, *IRXs*, *EXPs*, *TBLs*, and *XTHs* were downregulated under boron deficiency. Alterations of gene expression in hormone signaling pathways comprising IAA, GA, CTK, ET, ABA, and JA were observed under boron deficiency. TFs, homologous to *HD1s*, *NAC10*, *NAC73*, *MYB46s*, *MYB58*, and *ERF92s* were found to interact with genes related to cell wall metabolism, and the structural components were identified. We established a regulatory mechanism network of boron deficiency-induced shortened internodes in *A. melanoxylon* based on the above results. This research provides a theoretical basis for understanding the response mechanism of woody plants to boron deficiency.

KEYWORDS

boron deficiency, transcriptome, cell wall, hormone, *Acacia melanoxylon*

1 Introduction

Boron is an essential trace mineral element for plants (Warington, 1923) and plays a critical role in plasma membrane integrity and function, cell wall structure and function, carbohydrate and nucleic acid metabolism, phenol, and hormone metabolism, as well as respiration and photosynthesis (García-Sánchez et al., 2020; Bolaños et al., 2023; Chen et al., 2023). Boron primarily exists in the form of boric acid (H_3BO_3) in soil, which is prone to leaching during heavy rainfall (Shorrocks, 1997; Brdar-Jokanović, 2020). In more than 80 countries globally, boron deficiency has become a widespread concern problem in both agriculture and forestry. Boron deficiency plants exhibit diverse visible symptoms in vegetative and reproductive organs, such as reduced root growth, suppressed plant height, decreased leaf area, lost apical shoot dominance, and reduced fertility (Shorrocks, 1997; Wang et al., 2015).

Boron is mainly involved in the formation and structural integrity of the primary cell wall by crosslinking pectin polysaccharide rhamnogalacturonan II (RG-II) (O'Neill et al., 2001; Camacho-Cristóbal et al., 2011). And nearly 90% of cellular boron is positioned on the cell wall (Kobayashi et al., 1997). When boron is lacking, the cell wall structure is disorganized, and the intercellular pectin polysaccharides are impacted, thereby preventing cell wall integrity (Martín-Rejano et al., 2011). When cell wall integrity is impaired, multiple signaling pathways are induced, such as hormone signaling, reactive oxygen species (ROS) accumulation, and the production of other cell wall components (Vaahtera et al., 2019). In *Arabidopsis* seedlings, the impaired cell wall integrity caused by boron deficiency triggers ethylene (ET), auxin (IAA), and ROS signals, consequently resulting in the reduction of root cell elongation (Camacho-Cristóbal et al., 2015). Unfavorable boron conditions also result in lipid peroxidation and imbalanced antioxidant enzyme activities through the excessive buildup of oxidative stress (Tewari et al., 2010). Specifically, boron deficiency increases the content of malondialdehyde (MDA) and proline (Pro), as well as upregulates the activity of lipoxygenase (LOX), and then regulates the activity of antioxidative enzymes, such as superoxide dismutase (SOD), catalase (CAT), and peroxidase (POD) (Molassiotis et al., 2006; Tewari et al., 2010; Yin et al., 2022).

Although the molecular mechanism of plant response to boron deficiency is not well studied, some results have been found at the transcriptional level. In the case of *Neolamarckia cadamba*, Yin et al. (2022) observed that the phenylalanine ammonia-lyase and phenylpropanoid biosynthesis pathways were induced under boron deficiency, resulting in increased shoot tip lignification. The expression levels of the genes related to the synthesis of pectin and cellulose in *N. cadamba* mature leaves were altered in response to boron deficiency stress. Moreover, numerous transcription factors (TFs) also serve as the switches of the regulatory signal cascade in response to the boron deficiency stress process. The earliest reported TFs involved in boron stress responses is *AtWRKY6* in *Arabidopsis* (Kasajima et al., 2010). A recent study further noted that *BnaWRKYs* participated in the response to low boron, and *BnaA9.WRKY47* contributed to the adaptation of *Brassica napus* to boron deficiency through upregulating *BnaA3.NIP5;1* (a boron transporter gene) expression to facilitate efficient boron uptake (Feng et al., 2020). The study conducted by Song et al. (2021) utilized transcriptome analysis to find numerous differentially expressed genes (DEGs) related to antioxidant enzymes, TFs, and boron transporters, which revealed the response mechanism of boron deficiency tolerance in leaves of *Beta vulgaris* seedlings.

Acacia melanoxylon is an evergreen and fast-growing tree belonging to the Leguminosae family and Mimosaceae subfamily (Bradbury et al., 2011). Due to its strong adaptability, good material properties, and short rotation period, it is an ideal species that integrates economic, ecological, and greening functions. *A. melanoxylon* is commonly distributed in areas with high rainfall and slightly acidic soil, such as Australia, South China, Brazil, and Ethiopia (Searle, 2000). This tree species is easily affected by a lack of boron which hinders its growth. Since the development of stem is a significant economic indicator for forest tree species, the present study explored the morphological and physiological effects of boron deficiency on *A. melanoxylon* stem and used RNA-seq technology to identify the DEGs related to the internode shortening caused by the deficiency. Furthermore, it revealed the interaction network among the cell wall organization or biogenesis, hormone signal transduction pathways, and TFs in response to boron deficiency stress, improving the understanding of the stem response mechanism to boron deficiency in tree species.

2 Materials and methods

2.1 Plant materials and culture conditions

The elite *A. melanoxylon* clone SR17 was selected as plant material. And two-month-old shoots were cultured into plastic containers (30 cm × 26 cm × 14 cm) with 1/2 MS (Murashige & Skoog) nutrient solution supplemented with the following concentrations of macro- and micro-nutrients; 10.31 mM NH_4NO_3, 9.39 mM KNO_3, 1.50 mM $CaCl_2$, 0.75 mM $MgSO_4$, 0.63 mM KH_2PO_4, 0.06 μM $CoCl_2$, 0.05 μM $CuSO_4{\cdot}5H_2O$, 50 μM FeNaEDTA, 50 μM $MnSO_4{\cdot}H_2O$, 0.52 μM $Na_2MoO_4{\cdot}2H_2O$, 2.5 μM KI, 14.96 μM $ZnSO_4{\cdot}7H_2O$. Then, the plants with consistent plant height and growth state were selected for further boron deficiency treatment (without H_3BO_3). The control was cultured with the nutrient solution with 50 μM of H_3BO_3. Each treatment was performed in three replications with 16 plants in each replication. The fresh nutrient solution was replaced every three days, and the pH was maintained at 5.5-6.0 to balance ion absorption and distribution. Experiments were conducted in a greenhouse facility under natural sunlight conditions, 75% atmospheric humidity, and a temperature range of 23-28 °C.

2.2 Growth parameters measurement and sample collection

After 60 days under boron deficiency, plant height, branch number, and internode length of the apical section (1st, 2nd, 3rd)

were measured. Meanwhile, the total root length, root diameter, and root surface area were calculated by using a scanner and root image analysis software WinRHIZO Pro (Regent Instruments, QC, Canada).

Roots, stems, and leaves were also harvested and immediately frozen in liquid nitrogen and then transferred to a -80 °C refrigerator for further physiology, hormones, and RNA-seq analysis. The 2.5 g fresh samples were dried in an oven at 75 °C for a constant weight and then determined for the boron content.

2.3 Boron content measurement

0.5 g dried samples were ground to a fine powder and underwent ashing at 500 °C. Then, the ash was digested in 0.1 M HCl for 30 min and filtered using quantitative filter paper. Finally, the boron content in plants was measured using the curcumin colorimetry method with a UA-spectrophotometer (UV-2450, Shimadzu, Kyoto, Japan) (Dible et al., 1954). The calculation formulae are as follows:

$$\textbf{Boron accumulation } (\mu g \cdot plant^{-1}) = \textbf{boron content } (\mu g \cdot g^{-1}) \times \textbf{corresponding dry weight } (g \cdot plant^{-1})$$

$$\textbf{Boron transport coefficient (BTC)} = \textbf{shoot boron content } (\mu g \cdot plant^{-1}) / \textbf{root boron content } (\mu g \cdot plant^{-1})$$

$$\textbf{Boron efficiency coefficient (BEC)} = \textbf{total dry weight of B0(g)} / \textbf{total dry weight of control(g)}$$

2.4 Physiological indicators measurement

The frozen stems (0.10 g) were selected for physiological analysis. MDA content was measured using the 20% (*w/v*) trichloroacetic (TCA) and 0.5% (*w/v*) thiobarbituric acid (TBA) method (Heath and Packer, 1968). LOX activity was determined by analyzing LOX-catalyzed linoleic acid oxidation at 234 nm (Pérez et al., 1999). Pro content was extracted from 3% (*w/v*) aqueous sulfosalicylic acid and estimated by ninhydrin reagent at 520 nm (Bates et al., 1973). SOD activity was evaluated using the nitrotetrazolium blue chloride (NBT) photochemical reduction method (Giannopolitis and Ries, 1977). POD activity was measured based on guaiacol oxidation at 470 nm using hydrogen peroxide (H_2O_2). CAT activity was determined by measuring the disappearance of H_2O_2 at 240 nm (Rao et al., 1996). Each assay had three independent replications.

2.5 Endogenous hormone contents measurement

An improved double antibody sandwich enzyme-linked immunosorbent assay (ELISA) was used to quantify IAA, CTK, GA, ABA, ET, and JA in stems according to the kit's instructions (Shanghai Enzyme-linked Biotechnology, Shanghai, China). Specifically, the frozen stems (0.20 g) were ground in liquid nitrogen and homogenized in 2 ml phosphate-buffered saline (PBS; 0.01 M, pH 7.5). After centrifugation at 10000 xg for 10 min, the supernatant (50.00 μL) and biotinylated plant corresponding antibodies were added to wells and incubated at 37°C for 30 min. The liquid was removed, and the plates were washed five times with washing buffer. Enzyme conjugate liquid (50 μL) was added to wells and incubated at 37 °C for 30 min, and the plates were washed five times with washing buffer. Next, color reagent A (50 μL) and B (50 μL) were added to wells and incubated at 37°C for 10 min. Finally, the reaction was terminated by adding color reagent C (50 μL). A standard curve was generated using five known contents of hormones, the absorbance (OD value) was measured at 450 nm, and the regression equation of the standard curve was used to determine the content of each hormone. Each assay had three independent replications.

2.6 Transmission electron microscope analysis

The TEM slices were performed using the method of Kong et al. (2013) with slight modifications. Specifically, stems from the same parts under different boron treatments were cut into small pieces (1 mm × 1 mm). The samples were fixed in glutaraldehyde in phosphate buffer solution (PBS, 0.1 M) for 12 h at 4°C. Then, the tissue blocks were rinsed four times using 0.1 M PBS (pH 7.4) and post-fixed for 2-3 h with 1% buffered osmium tetroxide, followed by rinsing in 0.1 M PBS (pH 7.4) for three times. Next, the samples were dehydrated using an increasing ethanol concentration series (30, 50, 70, 80, 95, 100, 100) and transferred into a mixture of ethanol and acetone (3:1, 1:1, 1:3, 0:1). Ultrathin sections were stained with 2% uranyl acetate and lead citrate, and were examined with a TEM (Hitachi, HT7800/HT7700, Japan). The cell wall thickness was measured (20 replicates for one treatment) with Image J's scale tool based on the TEM image scale.

2.7 Cellulose, hemicellulose, and water-soluble pectin content measurement

The contents of cellulose and hemicellulose of stems were determined as follows: 3.0 g dried samples were ground to a fine powder and digested in a mixture of acidic detergent and 1-octanol for 60 minutes. Then, the digestion liquor was filtered with a funnel. The residue was digested in H_2SO_4 for 3 hours, then filtered again and washed with hot water until neutral. Next, the residue was dried to constant weight at 105°C. Finally, the cellulose and hemicellulose content was determined using the gravimetric technique in a fully automated fiber analysis system (Fibertech TM 8000, FOSS, Denmark). Each assay had three independent replications.

0.3 g fresh stems were ground into powder and quickly homogenized in 1 mL 80% ethanol. The samples were incubated in a 95°C water bath for 20 min. After centrifugation at 4000 xg for 10 min, the precipitate was collected. The final residue was defined as a crude cell wall after being washed with 1.5 mL 80% ethanol and

acetone. 3 mg dried crude cell wall dissolved in 1 mL anhydrous sodium acetate (pH 6.5) was shaken for 15 hours. After centrifugation at 8000 xg for 10 min, the supernatant was collected. The content of WSP was measured by reading the absorbance at 530 nm with a tube photometer. Each assay had three independent replications.

2.8 Transcriptomics analysis

The RNA of stems was extracted using the RNAprep Pure Plant Kit (DP441, Tiangen, China). RNA quality and quantity were verified with an RNA integrity number (RIN) greater than 7.2, 260/280 ratio of 1.8 to 2.0, 260/230 ratio of 1.8 to 2.2, and a concentration greater than 300 ng·μL^{-1}, RNA samples were selected for further experiments. First-strand cDNA was synthesized using the SuperScriptTM II Reverse Transcriptase kit (18-064-022, Invitrogen, USA).

RNA-Seq of qualified libraries was performed using the Illumina HiSeq4000 platform, with a sequencing strategy of 150 bp paired-end. The clean reads were mapped to the *A. melanoxylon* reference genome sequence (unpublished) using HISAT2 (Kim et al., 2015). After alignment, mRNA expression levels were calculated by combining RNA-Seq by Expectation Maximization (RSEM) with Fragments Per Kilobase of exon model per Million mapped fragments (FPKM) values (Trapnell et al., 2010; Li and Dewey, 2011). DEGs were identified using DESeq2 with $|\text{Log}_2(\text{fold-change})| \geq 1$, FDR ≤ 0.05, and P-value< 0.05 (Love et al., 2014). All DEGs were mapped to GO terms in the GO database and pathways in the KEGG database. The TBtools software was used to delineate heatmaps based on the DEG results (Chen et al., 2020). The protein interaction networks were visualized with Cytoscape (Shannon et al., 2003). In addition, the RNA-seq data were submitted to NCBI with the submission number: PRJNA995919.

2.9 qRT-PCR validation and expression analysis

For quantitative real-time PCR (qRT-PCR), the same RNA and cDNA stem samples used for transcriptome sequencing were utilized. The qRT-PCR test was performed using the TB Green Premix Ex TaqTM kit (RR820, TaKaRa, China). The qRT-PCR reaction system and procedures were carried out according to the kit requirements. All qRT-PCR amplifications were repeated three times. All the genes were normalized against the level of protein phosphatase type 2A (*evm.TU.Chr3.536 PP2a*). The details of the gene-specific primers are listed in Supplementary File 1.

2.10 Statistical analysis

SPSS 26.0 (SPSS Inc., Chicago, USA) software was employed to conduct variance analysis. The minimum significant difference method (LSD) at P-value< 0.05 and 0.01. Principal component analysis (PCA), Pearson correlation analysis, and figures were prepared using Origin 2021 (OriginLab Co., Massachusetts, USA). Significant and extremely significant differences were expressed by * and **, respectively.

3 Results

3.1 Effect of boron deficiency on plant morphological attributes

Under the boron deficiency (B0) condition, the phenotype of decreased plant height, shortened internodes, increased branches, and brown roots were observed, compared to the control (50 μM boric acid) (Figures 1A, B). The results of growth parameters shown in Table 1 revealed that B0 treatment led to a 33.52% decrease in plant height, 27.76% decrease for the 1-st internode, 36.99% decrease for the 2-nd internode, and 42.59% decrease for the 3-rd internode, and a 118.33% increase in the branch number. Meanwhile, the primary root length and surface area were decreased by 32.08% and 24.89%, respectively. Interestingly, the root diameter increased by 41.37%. These results suggest that boron is essential for growth in *A. melanoxylon*.

3.2 Effect of boron deficiency on plant biomass and boron nutrient

Under the B0 condition, the fresh weights, dry weights, and root-shoot ratio were decreased (Figures 2A–C). Meanwhile, boron deficiency led to a 65.07% reduction of boron content in roots, 15.22% in stems, and 56.68% in leaves (Figure 2D). Under the control condition, boron accumulation in roots was higher than in stems, but under the B0 condition, it was lower than in the stems (Figure 2E). Moreover, the BTCs of plants were 0.63 and 1.02 under control and B0 conditions, respectively (Figure 2F). These results suggest that *A. melanoxylon* preferentially transports boron from roots to shoots during long-term boron deficiency. The BEC coefficient of *A. melanoxylon* under the B0 condition is 90%, indicating that the soluble boron content is low and the boron utilization of the *A. melanoxylon* cultivar (SR17) is efficient.

3.3 Effects of boron deficiency on physiological indicators and endogenous hormone contents in stem

The experiments showed that boron deficiency led to an increase in MDA content (15.04%, Figure 3A), LOX activity (47.79%, Figure 3C), and a decrease in Pro content (18.14%, Figure 3B). These changes induced increases in SOD (8.48%, Figure 3D) and POD (29.75%, Figure 3E) activities and a decrease in CAT activity (16.42%, Figure 3F).

Compared to the control condition, the endogenous IAA, GA, CTK, ET, and JA contents were significantly reduced by 33.55%, 21.36%, 29.78%, 21.27%, and 20.63%, respectively (Figures 3G–I, K, L), while ABA content increased significantly by 23.44% under B0 condition

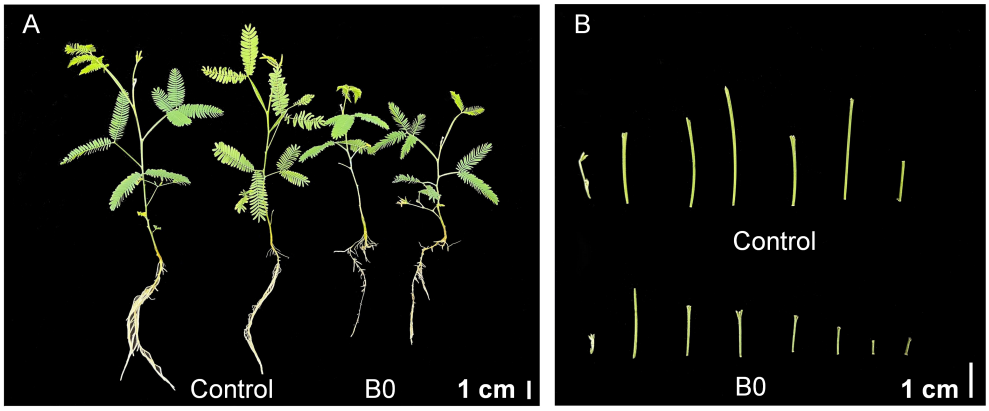

FIGURE 1
A. melanoxylon plants morphology under boron deficiency. **(A)** Phenotype; **(B)** Internodes morphology. Control (50 μM boric acid); B0 (0 μM boric acid). Scale bars of phenotype and internode morphology are 1 cm.

(Figure 3J). These results indicate that *A. melanoxylon* altered its stem's original endogenous hormone levels to adapt to boron deficiency.

3.4 Stem ultrastructure and cell wall components content

TEM micrograph analysis showed that the cell wall of the stem thickened under boron deficiency (Figure 4B), while it remained regular under the control condition (Figure 4A). Results of ImageJ software showed that the cell wall thickness under the boron deficiency condition significantly increased by 2.08 times compared to the control condition (Figure 4C). Moreover, the WSP and hemicellulose contents were significantly decreased by 27.52%, and 16.33%, respectively, in comparison to the control condition (Figures 4D, F), whereas the cellulose content increased significantly by 33.35% under B0 condition (Figure 4E).

3.5 Transcriptome profiling of stem under boron deficiency

After removing low-quality and short reads, the number of clean reads ranged from 7.2 to 8.7 Gb, and the percentage of Q30 was more than 88.9% (Supplementary File 2). The 77.51% to 80.76% of unique reads can match the reference genome sequence (Supplementary File 3). We assessed the similarities and differences among samples using Pearson correlation analysis and PCA. The Pearson correlation coefficient (R^2) between samples was higher than 0.87, and the clustering was obvious (Supplementary Figures 1A, B), indicating that the transcriptome data are reliable for subsequent analysis.

The gene expression levels were measured according to FPKM, with all samples restricted to the range $4 \geq \log_{10}(\text{FPKM}) \geq -2$ (Supplementary Figure 2A). Transcriptome analysis identified a total of 5012 DEGs, of which 2348 genes were upregulated and 2264 genes were down-regulated (Supplementary Figure 2B). A volcano plot was utilized to display the FC values in gene expression (Supplementary Figure 2C). Furthermore, to better understand the overall variation in DEG expression, a heatmap was built to visualize the expression patterns of all DEGs. The DEGs were classified into 3 clusters based on their expression patterns (Supplementary Figure 2D). These results indicate that there is a considerable change in the transcription levels of many genes in *A. melanoxylon* stem under boron deficiency.

3.6 Real-time qPCR validation

To verify the authenticity and reproducibility of the transcriptomic data, we selected 15 DEGs and designed specific

TABLE 1 Growth parameters of *A. melanoxylon* under boron deficiency.

Treatment	plant height	branch number	internode length-1st	internode length-2nd	internode length-3rd	main root length	root surface area	root diameter
Control	9.87 ± 2.33	1.20 ± 0.40	1.70 ± 0.64	2.31 ± 0.71	2.24 ± 0.87	7.16 ± 1.19	13.03 ± 5.29	0.53 ± 0.13
B0	6.46 ± 1.68**	2.62 ± 0.97	1.23 ± 0.47	1.46 ± 0.67**	1.29 ± 0.76**	4.85 ± 1.55**	9.79 ± 3.25	0.75 ± 0.19**

Control (50 μM boric acid); B0 (0 μM boric acid). All data are the mean of three replicates collected over 60 days of treatment. Values are the mean ± standard deviations. The ** indicates significant differences by the Duncan test (P-value< 0.01).

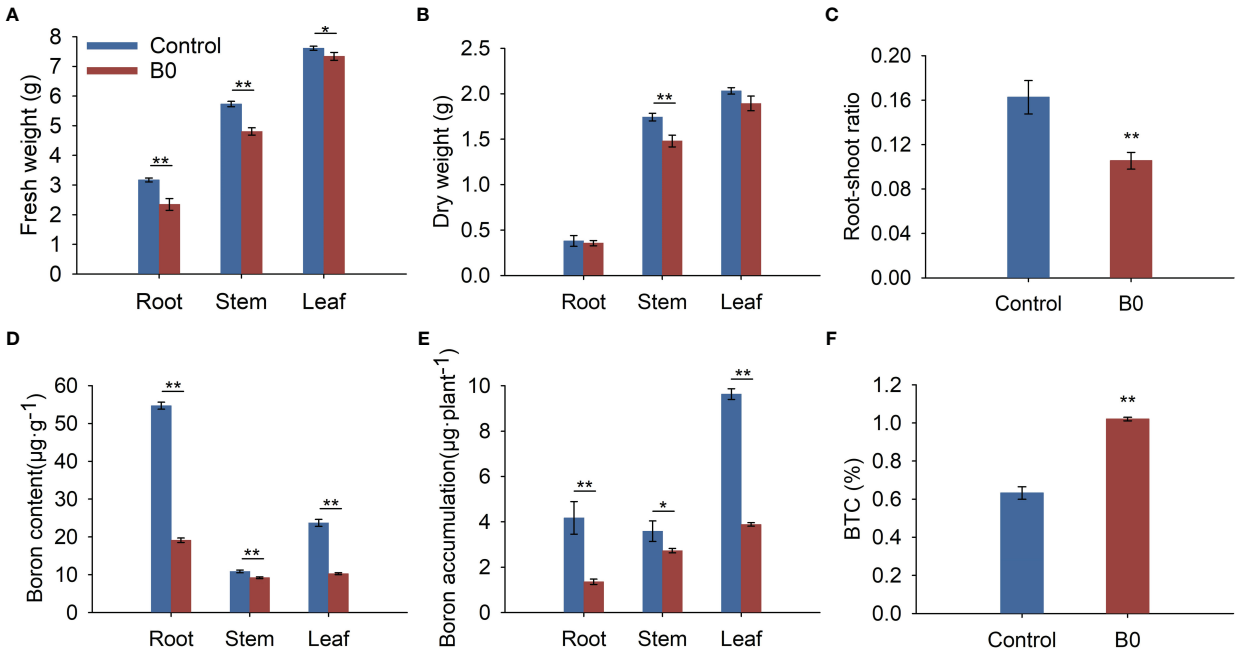

FIGURE 2
The biomass and boron nutrient of *A. melanoxylon* changes under boron deficiency. Control (50 μM boric acid); B0 (0 μM boric acid). **(A)** Fresh weight; **(B)** Dry weight; **(C)** Root-shoot ratio; **(D)** Boron content; **(E)** Boron accumulation; **(F)** BTC. All data are the mean of three replicates collected over 60 days of treatment. Data are the mean ± standard deviations. The * indicates significant differences at P-value< 0.05, and ** indicates significant differences at P-value< 0.01.

primers for qRT-PCR. The relative expression of the selected genes was compared with the results of RNA-seq analysis. The results showed that the 15 genes differed slightly from the sequencing data expression. Still, the overall expression trend was identical (Supplementary Figure 3), confirming the reliability of this study's transcriptome sequencing results.

3.7 GO and KEGG pathways analysis of DEGs

The 406 differentially expressed GO terms (P-value< 0.05) were identified through GO enrichment analysis. Specifically, the biological process (BP), molecular functions (MF), and cell component (CC) included 224, 125, and 57 terms, respectively (Supplementary File 4). The cell wall organization or biogenesis, oxidoreductase activity, and microtubule cytoskeleton were the most significantly enriched GO terms in BP, MF, and CC ontology, respectively. Besides these categories, DEGs were functionally related to lignin metabolism, secondary metabolism, and DNA replication processes (Figure 5A; Supplementary File 4).

To identify DEGs enriched in various metabolic pathways, the KEGG database was utilized, with a P-value< 0.05 as the screening threshold. The DEGs were categorized into 18 functional categories, including 2 environmental information processing, 2 genetic information processing, and 14 metabolism pathways (Supplementary File 5). The plant hormone signal transduction, biosynthesis of amino acids, and phenylpropanoid biosynthesis were identified as the most abundant KEGG pathways (Figure 5B).

3.8 Response of cell wall organization or biogenesis-related DEGs under boron deficiency

DEGs related to cell wall organization or biogenesis were examined to further investigate the effects of boron deficiency on cell wall structure and composition. 127 DEGs encoding proteins or enzymes were involved in cell wall metabolism, of which 106 were down-regulated and 21 were upregulated under boron deficiency (Figure 6; Supplementary File 6). 28 DEGs encoding pectinaceous components or pectin-modifying enzymes, such as *pectinesterase* (*PMEs*), *polygalacturonase* (*PGLs*), *pectin acetylesterase* (*PAEs*) and *galacturonosyltransferase* (*GAUT*) were identified, of which 5 were upregulated (*evm.TU.Chr11.2523 PME2*, *evm.TU.Chr6.186 PME29*, *evm.TU.Chr5.294 PME37*, *evm.TU.Chr10.3814 PGLR*, and *evm.TU.Chr7.278 PMTD*) and 23 down-regulated (Supplementary File 6). 44 DEGs encoded structural components of cell walls such as *cellulose*, *glucans*, *xylans*, and *galacturonans*. 44 DEGs encoded proteins such as *expansins* (*EXPs*), *trichome birefringence-like* (*TBLs*), and *xyloglucan endotransglucosylase/hydrolase* (*XTHs*), which are required for cell wall loosening during growth. In addition, 3 TFs (*evm.TU.Chr12.383 MYB46*, *evm.TU.Chr12.81 MYB58*, and *evm.TU.Chr11.734 HD1*) were downregulation under boron deficiency.

3.9 Transcription factors regulate cell wall-related genes under boron deficiency

A total of 314 DEGs encoding TFs (Supplementary File 7) were found in the transcriptome database, of which 171 were upregulated

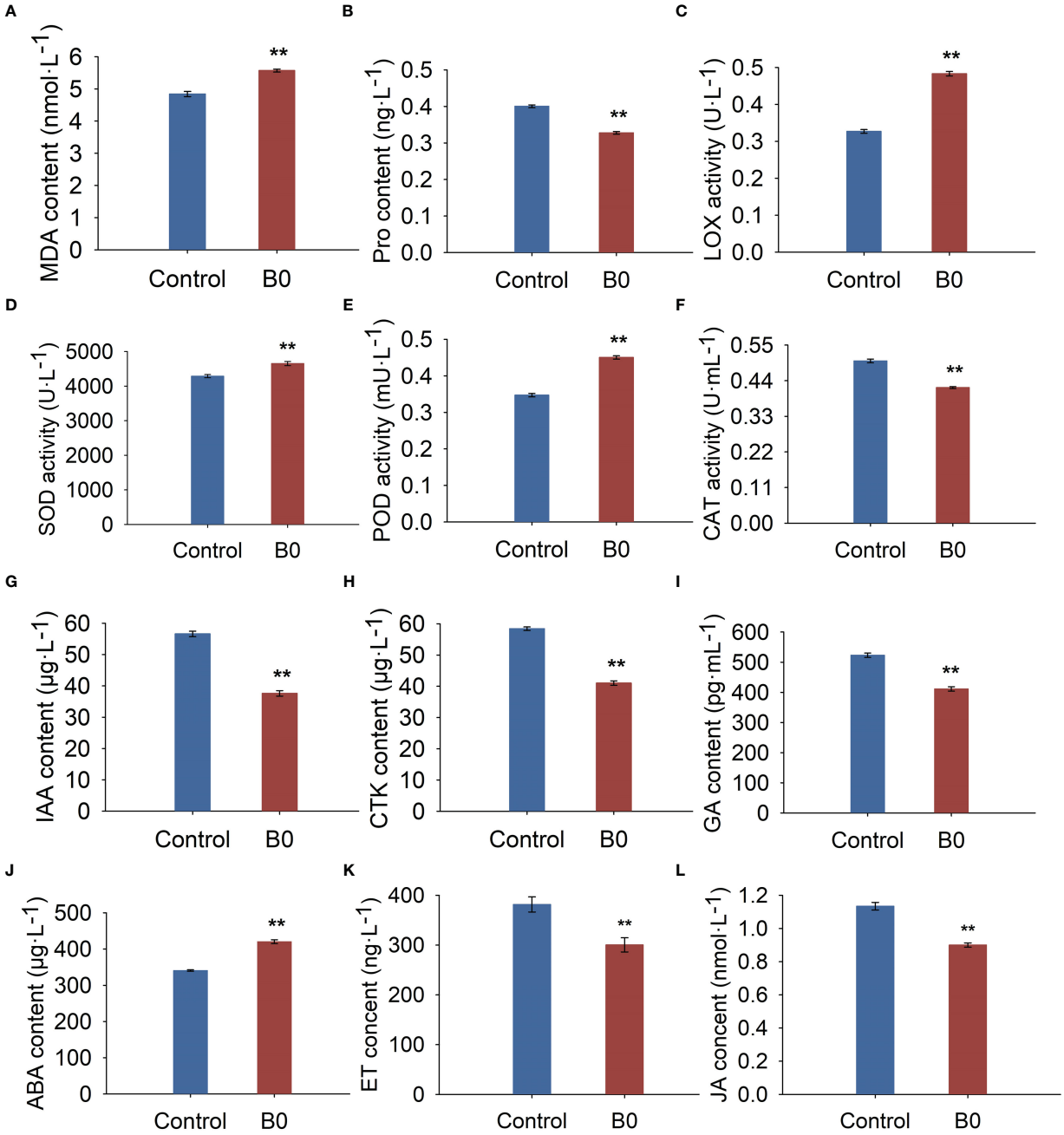

FIGURE 3
The physiology and hormone changes of *A. melanoxylon* stems under boron deficiency. Control (50 μM boric acid); B0 (0 μM boric acid). **(A)** MDA content; **(B)** Pro content; **(C)** LOX activity; **(D)** SOD activity; **(E)** POD activity; **(F)** CAT activity; **(G)** IAA content; **(H)** GA content; **(I)** CTK content; **(J)** ABA content; **(K)** ET content; **(L)** JA content. All data are the mean of three replicates collected over 60 days of treatment. Data are the mean ± standard deviations. The ** indicates significant differences at P-value< 0.01.

and 143 were downregulated. Among these, *MYBs* were the most abundant family (56), followed by *AP2-EREBPs* (43), *bHLHs* (26), *NACs* (25), and *WRKYs* (18) in turn.

The interaction network of TFs and cell wall organization or biogenesis-related genes was constructed to reveal the potential regulatory mechanisms in *A. melanoxylon* stem under boron deficiency. As shown in Figure 7, cell wall organization or biogenesis-related genes, such as *GAUTCs*, *CESAs*, and *IRXs*, were found to interact with TFs, containing 2 *HD1s*, 1 *NAC73*, and 3 *MYB46s*. Moreover, *NAC10* and *MYB58* served as master switches in charge of the transcriptional regulation of the cell wall network. It is noteworthy that 2 *HD1s* interacted not only with *MYBs* and *NACs* but also with several *CESAs* and *IRXs*. In addition, 3 *ERF92s*, which are part of the ET signaling pathway, interact with 4 *CHIs*.

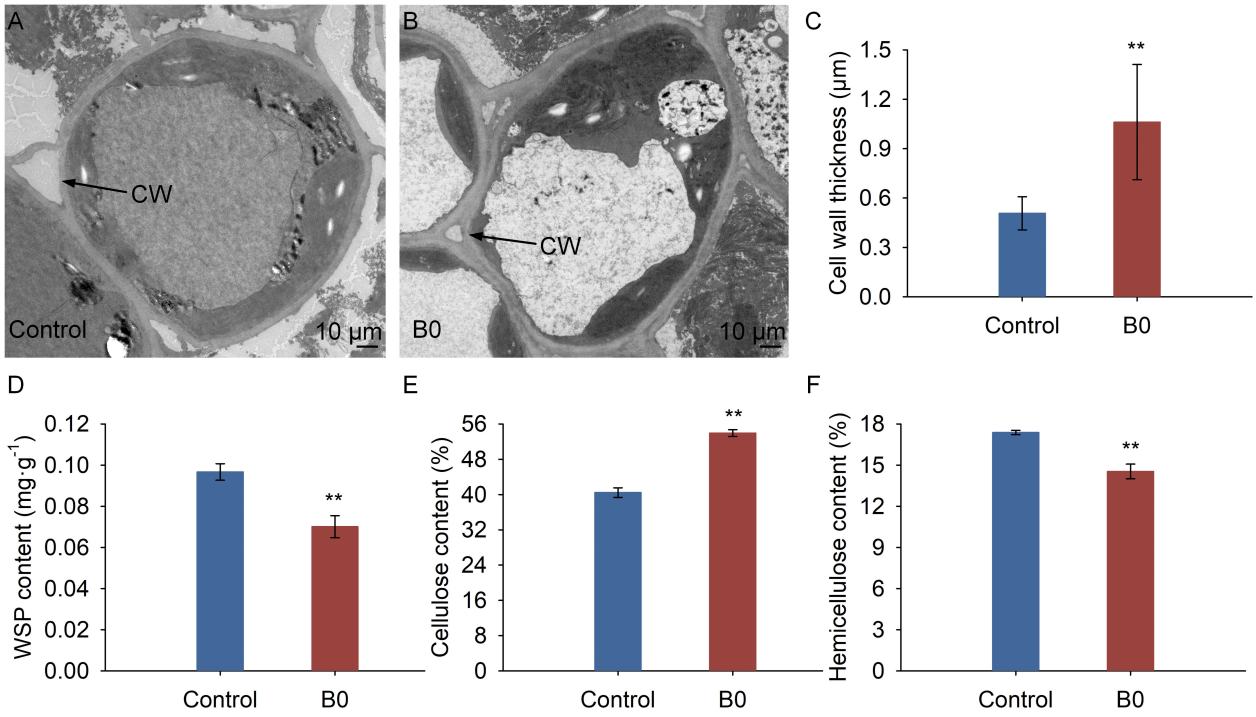

FIGURE 4
Structure and composition of cell wall under different boron conditions. Control (50 μM boric acid); B0 (0 μM boric acid). **(A)** Transmission electron microscope micrograph under control condition; **(B)** Transmission electron microscope micrograph under B0 condition; **(C)** Cell wall thickness; **(D)** WSP content means water soluble pectin content; **(E)** Cellulose content; **(F)** Hemicellulose content. All data are the mean of three replicates collected over 60 days of treatment. Data are the mean ± standard deviations. The ** indicates significant differences at P-value< 0.01.

3.10 Response of plant hormone-related DEGs under boron deficiency

Based on the DEGs' enrichment results, there were 81 DEGs involved in the plant hormone signal transduction pathways, of which 30 were upregulated and 51 were downregulated (Supplementary File 8). The number of DEGs involved in the IAA signaling pathway was the most, followed by ABA and ET signaling pathways. We further analyzed the expression pattern of DEGs in IAA, CTK, GA, ABA, ET, and JA pathways and visualized them with process maps. As shown in Figure 8, all 11 DEGs in the ET pathway were down-regulated. Hormone signal receptors (*GID1s*, *PYR/PYLs*, and *ETRs*) and response regulator (*AUX1s*, *AUX/IAAs*, *ARFs*, *A-ARRs*, *DELLAs*, and *ERFs*) genes were also all down-regulated. In the JA signal transduction pathway, boron deficiency upregulated *JAR1*, leading to the downregulation of

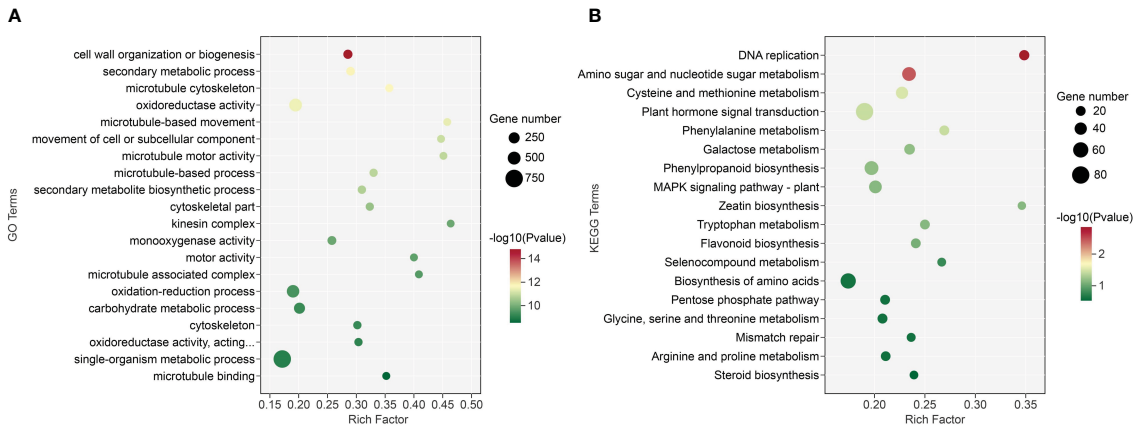

FIGURE 5
GO function and KEGG enrichment pathway analysis of *A. melanoxylon* stems under boron deficiency. **(A)** GO function analysis. "Oxidoreductase activity, acting..." means oxidoreductase activity, acting on paired donors, with incorporation or reduction of molecular oxygen, NAD(P)H as one donor, and incorporation of one atom of oxygen. **(B)** KEGG enrichment pathway analysis.

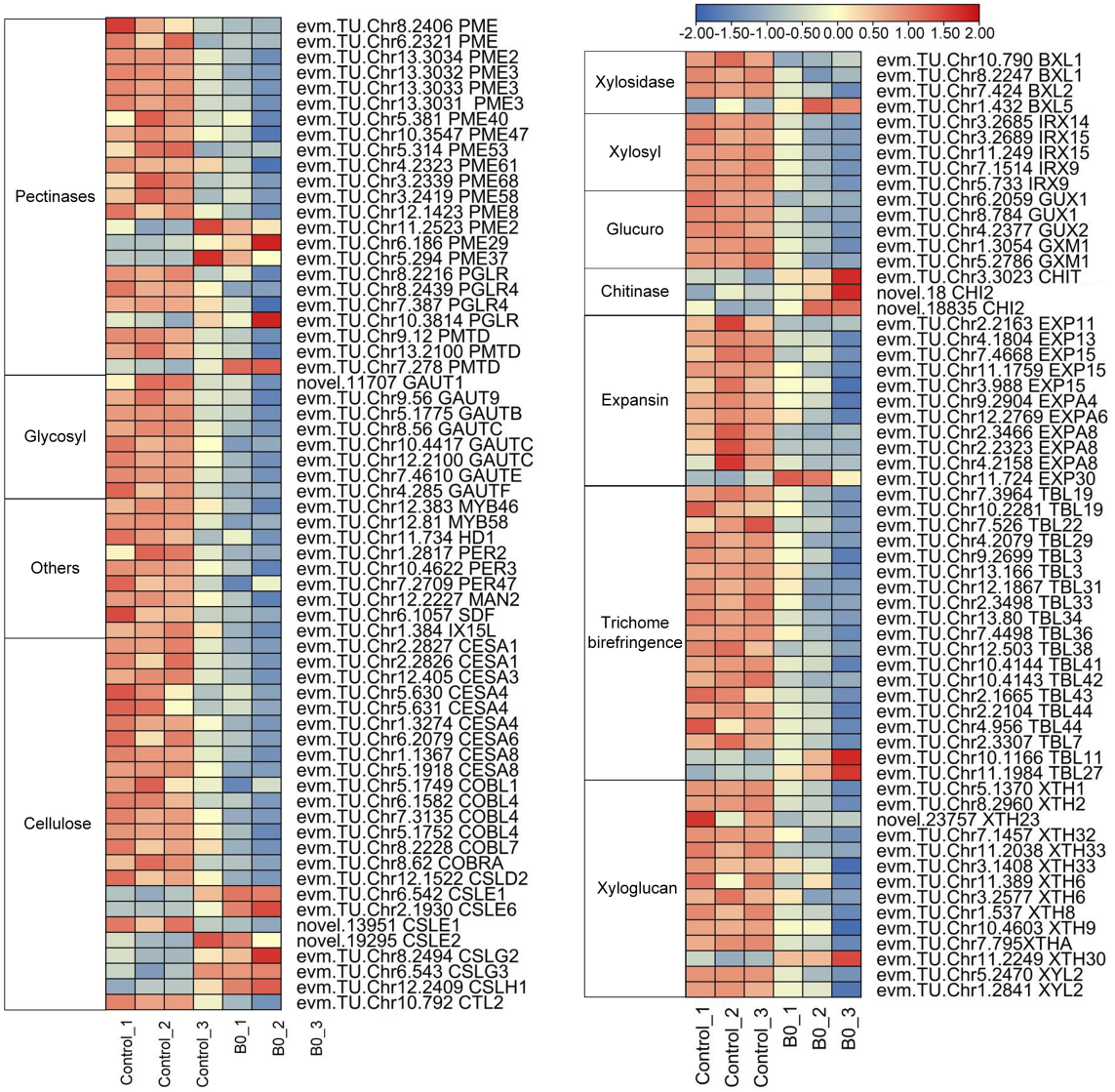

FIGURE 6
Expression of DEGs for cell wall organization or biogenesis under boron deficiency. The heatmaps show log_2FPKM values of the DEGs. Red indicates up-regulation and blue indicates down-regulation.

downstream protein *JAZs* and TF *MYC2s*. These results indicate that the gene expression changes associated with plant hormone signal transduction are likely to be implicated in the growth regulation of *A. melanoxylon* stem under boron deficiency.

To clarify the complex interaction network between hormones, we drew an interaction network diagram between DEGs (Supplementary Figure 4). *ABF* (*evm.TU.Chr.4.2387*) belonging to the ABA signal transduction pathway, interacted with the *AUX/IAA* genes (*evm.TU.Chr5.561* and *evm.TU.Chr9.973*) involved in the IAA signaling pathway. The *AHPs* (*evm.TU.Chr9.755*, *evm.TU.Chr8.2827*, and *evm.TU.Chr13.2653*) belonging to the CTK signal transduction pathway, interacted with *ETR92s* (*evm.TU.Chr6.540*, *evm.TU.Chr8.2490* and *evm.TU.Chr6.541*) involved in the ET signal transduction pathway.

4 Discussion

4.1 Boron deficiency inhibits the growth and development of *A. melanoxylon*

The present study showed that *A. melanoxylon* presented various symptoms under boron deficiency, such as dwarf plants, increased branches, shortened internodes, and notably shorter and thicker roots (Figure 1). The morphological changes observed in plants may be the end phenotypic results of altering cell wall integrity and hormone homeostasis-related pathways. For instance, Yin et al. (2022) found that severe morphological changes induced by boron deficiency may be caused by damaging the cell wall integrity in *N. Cadamba*. Chen et al. (2022) reported

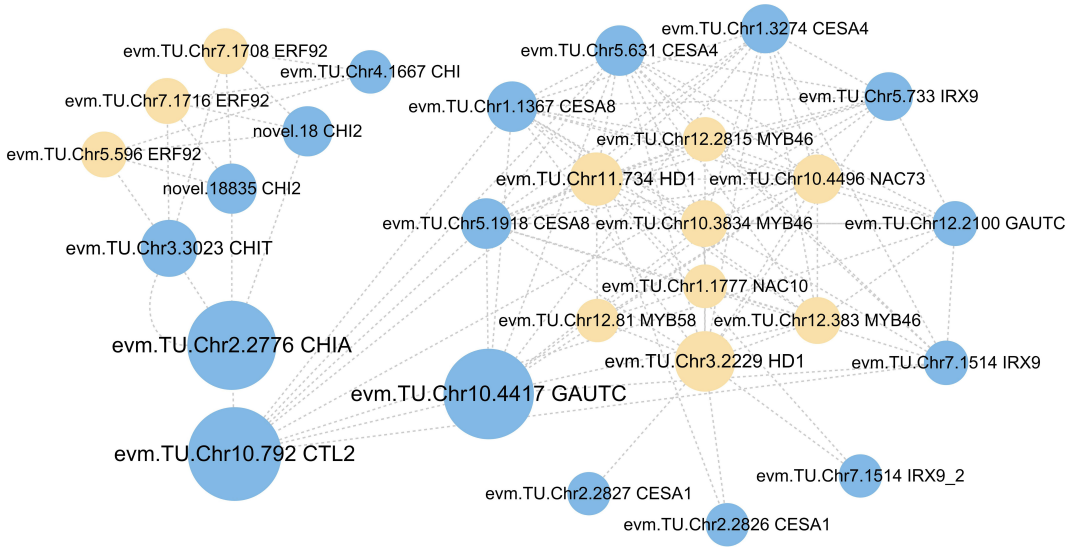

FIGURE 7
The network of transcription factors with cell wall organization or biogenesis-related genes. Cycle nodes represent genes, yellow nodes represent the transcription factors, while blue nodes represent cell wall organization or biogenesis-related genes. The size of node represents the power of the interrelation among the nodes by degree value.

that boron deficiency induced jasmonate signaling and remodeling of cell wall metabolism in pea (*Pisum sativum*) shoots, which was the reason for changes in shoot growth and architecture. In our study, long-term boron deficiency significantly altered the cell wall structure, composition, and endogenous hormone levels, resulting in morphological changes in *A. melanoxylon* stem. In addition, antioxidant enzyme (SOD, POD, CAT, and LOX) activities, antioxidant and oxidative stress indicators were also significantly changed in response to boron deficiency in *A. melanoxylon* stem (Figure 3). The reason may be that cells altered their osmotic potential and activated the antioxidant mechanism to protect cell membranes and maintain oxidative homeostasis under boron deficiency stress (Zhu, 2016; Zhu et al., 2020).

4.2 Boron deficiency affects cell wall organization or biogenesis in *A. melanoxylon* stem

The growth inhibition of apical meristems was one of the early responses to boron deficiency, which is attributable to the loss of cell wall plasticity (Dell and Huang, 1997; Chen et al., 2023). Boron deficiency disrupts the structural arrangement of the cell wall, which in turn affects cell function and cell wall components (Wang et al., 2015; Brdar-Jokanović, 2020). Boron crosslinked with RG-II in the cell wall and was closely associated with the biosynthesis of pectin, cellulose, and lignin (Hu and Brown, 1994; Wu et al., 2017; Yan et al., 2022). Boron deficiency caused the cell wall of *A. melanoxylon* stem to thicken, with a concomitant decrease in the hemicellulose and WSP contents (Figure 4). At the molecular level, boron deficiency caused a significant reduction in the expression of the great majority of genes involved in cell wall organization or biogenesis pathway in *A. melanoxylon* stem, as shown in Figure 5 and Supplementary File 3. A previous study has also reported that boron deficiency downregulates the expression of several cell wall-related genes in *Arabidopsis* roots (Camacho-Cristóbal et al., 2008). These results suggest that boron deficiency affects the structure and composition of the cell wall and is also involved in the expression of cell wall-related genes. Furthermore, the expression patterns of cell wall-related genes have been demonstrated to be connected with plant morphology. For example, overexpressing *PmCESA2* in poplar increased secondary cell wall thickness and xylem width, leading to higher cellulose and lignin content, and improved biomass production (Maleki et al., 2020). In *Arabidopsis*, overexpressing *AtEXPA4* enhanced primary root elongation, while knocking out *AtEXPA4* slowed down primary root growth (Liu et al., 2021). However, the functions of these genes in *A. melanoxylon* have rarely been reported. To gain a better understanding of the effects of boron deficiency on *A. melanoxylon* stem, further investigations are needed to identify the genes that are either activated or repressed by boron, and how they affect the cell wall structure and composition.

4.3 Boron deficiency induced interactions of cell wall and hormone-related genes in *A. melanoxylon* stem

Cell wall integrity is an essential foundation of plant growth and development. Previous studies have indicated that boron deficiency can lead to changes in cell wall integrity and endogenous phytohormone balance. For instance, in *Arabidopsis*, Camacho-Cristóbal et al. (2015) found that boron deficiency damages cell wall integrity and activates ethylene, auxin, and ROS signaling pathways, thus causing a rapid reduction in root elongation. Additionally, Chen et al. (2022) proposed that boron deficiency disorders cell wall structure, thereby triggering

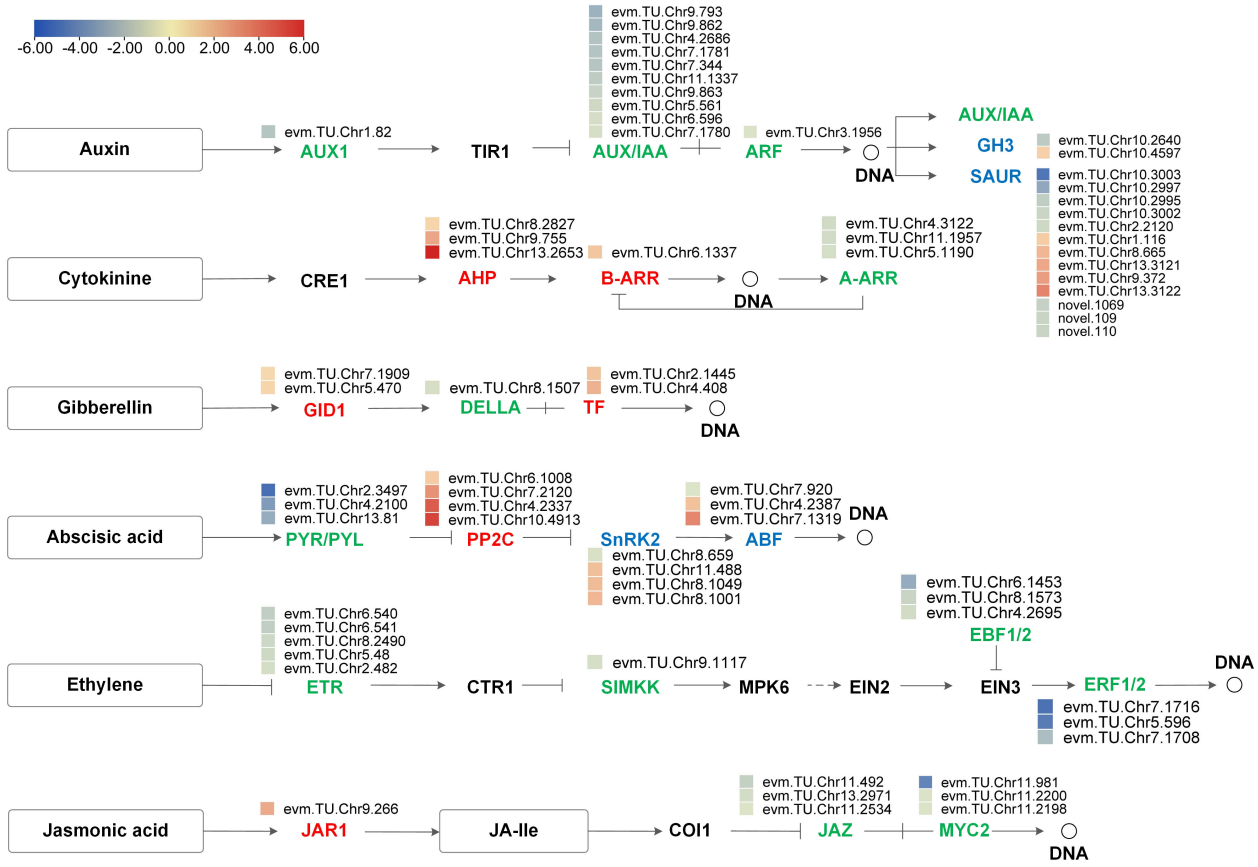

FIGURE 8
Process map of plant hormone signal transduction pathway for auxin, cytokinin, gibberellin, abscisic acid, ethylene and jasmonic acid. The heatmaps show log_2FC values of the DEGs. Red indicates up-regulation and blue indicates down-regulation.

the activation of JA signaling and subsequent compensatory changes in cell wall metabolism. Consequently, it can be inferred that there is an intricate interaction between cell walls and hormonal signaling mechanisms in response to boron deficiency. This hypothesis has also been validated by studies conducted on other plant species. Specifically, mutations in *AtCESAs* inhibit cellulose biosynthesis, leading to the redistribution of the auxin efflux carrier *AtPIN1* in the shoot apical meristem, thereby significantly affecting shoot apical meristem development (Sampathkumar et al., 2019). Our research found that 3 ET response factors (*ERF92s*) interact with the 4 class II chitinases (*CHIs*) (Figure 7). Previous research has shown that *CHI* participates in the catabolic process of cell wall macromolecules (De Andrade Silva et al., 2020). Under boron deficiency, *ERF92s* were downregulated, while *CHIs* were upregulated in *A. melanoxylon* stem (Supplementary Files 6, 8). This suggests that the upregulation of *CHIs* expression may enhance the disassembly of cell wall macromolecules, thereby impeding the transduction of ET signaling.

Previous studies have reported the existence of crosstalk among plant hormones under abiotic stress, forming complex signal transduction networks (Waadt et al., 2022). Additionally, it has been found that boron-related morphological and physiological disorders are associated with the production and signal transduction of plant hormones (Eggert and von Wirén, 2017; Chen et al., 2023). For example, in *Arabidopsis* seedlings, the crosstalk between CTKs, ETs, and IAAs functions acts as a signal in response to boron deficiency, regulating root cell elongation and boron transport (Herrera-Rodríguez et al., 2022). The interaction among IAAs, CTKs, and GAs also impacts plant stem elongation (Santner et al., 2009; Hedden and Thomas, 2012; Singh and Roychoudhury, 2022). In our study, we observed that the *ERF92s* belonging to the ET signaling pathway interacted with the *AHPs* belonging to the CTK signal transduction pathway (Figure S4). This indicates that CTK affects the cell wall of *A. melanoxylon* plants in a boron deficiency environment through its interaction with ET. Further research is needed to investigate the relationship between other hormonal signals and plant development and cell wall integrity under boron deficiency stress.

4.4 Boron deficiency induces TFs that regulate cell wall-related genes in *A. melanoxylon* stem

Previous studies have reported that *MYBs* and *NACs* are master transcriptional switches of the secondary cell wall. They regulate the expression of genes involved in the biosynthesis of cellulose, xylan, glucomannan, and lignin (Zhong and Ye, 2014). *AtMYB46* directly regulates the expression of secondary wall-associated *CESAs* in *Arabidopsis* (Kim et al., 2013). In *Thellungiella halophila*, the co-

overexpression of *TsHD1* and *TsNAC1* significantly inhibits plant growth by restraining cell expansion (Liu et al., 2019). In our study, network analysis reveals that *MYBs* (*evm.TU.Chr12.2815*, *evm.TU.Chr12.81*, *evm.TU.Chr10.3834*, and *evm.TU.Chr12.383*), *NACs* (*evm.TU.Chr1.1777* and *evm.TU.Chr10.4496*) and *HD1s* (*evm.TU.Chr11.734* and *evm.TU.Chr3.2229*) regulate numerous DEGs involved in cell wall organization or biogenesis (Figure 7). Our research also found that these *HD1s*, *NACs*, and *MYBs* exhibit significant down-regulation under boron deficiency (Supplementary File 7). This suggests that long-term boron deficiency inhibits TFs-mediated processes in cell wall organization or biosynthesis, ultimately retarding the development of *A. melanoxylon* stem.

Finally, we built a schematic model to visualize the process of *A. melanoxylon* in response to boron deficiency, as shown in Figure 9. Boron deficiency causes changes in boron nutrition, leading to oxidative stress and alterations in cell wall structure and composition. Hormone biosynthesis, transport, and signal transduction are also disturbed. In addition, TFs and plant hormone signal transduction-related genes impact cell wall organization or biosynthesis, suggesting that the response of plants to boron deficiency is a complex regulatory process. Taken together, the inhibitory effects of boron deficiency stress on the growth and development of *A. melanoxylon* stem are attributed to changes in cell wall structure and composition and transcriptional

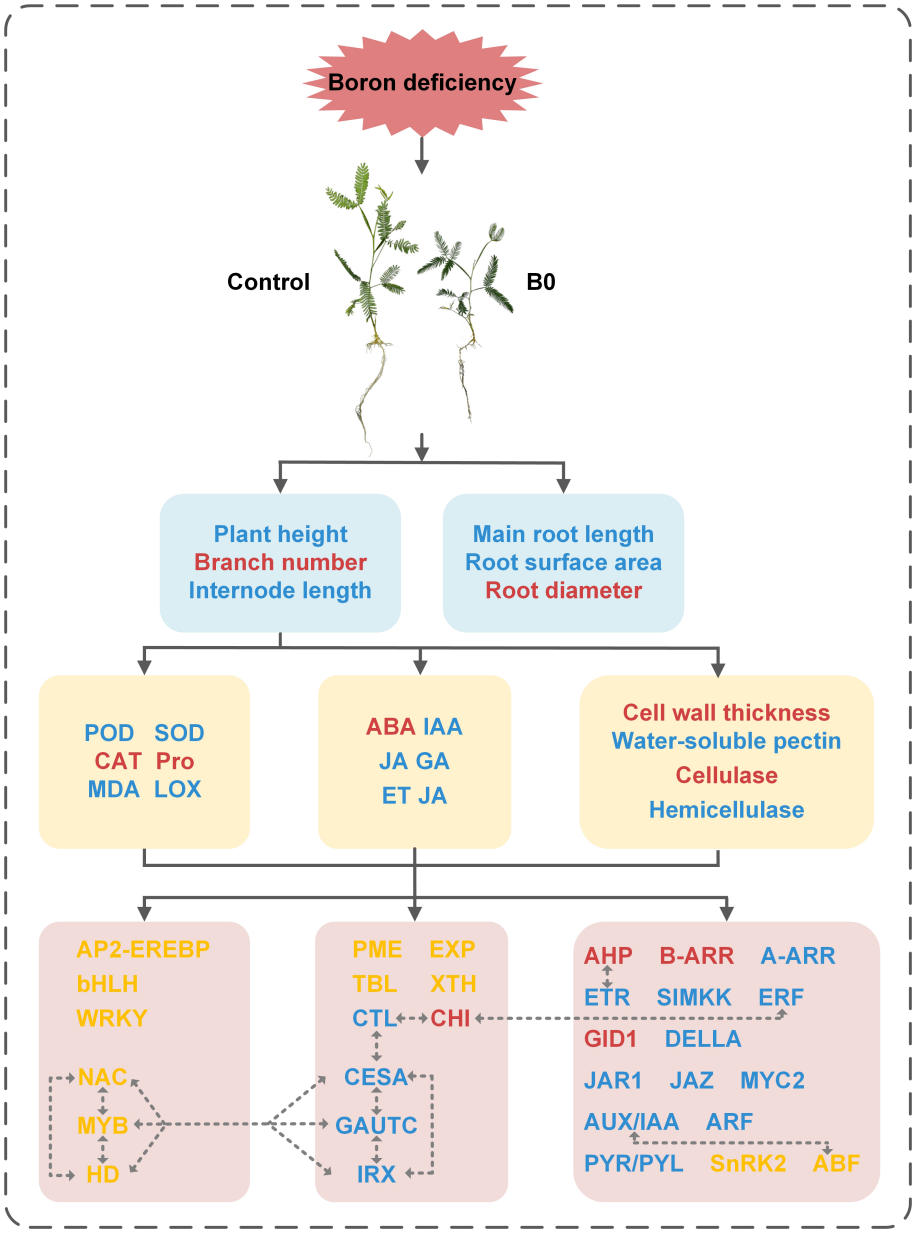

FIGURE 9
Schematic model of changes in the physiological and molecular mechanisms of *A. melanoxylon* stem under boron deficiency. The dashed line with arrows indicate speculative rules inferred by RNA-seq enrichment of DEGs. Red words represent the up-regulation of substances or genes, blue word represent down-regulation, and yellow words represent both up-regulation and down-regulation of genes.

regulation. This study provides a theoretical basis for further understanding the response mechanism of woody plants to boron deficiency stress.

Data availability statement

The datasets presented in this study can be found in online repositories. The names of the repository/repositories and accession number(s) can be found in the article/Supplementary Material.

Author contributions

ZC: Investigation, Data curation, Formal Analysis, Writing – original draft. XB: Data curation, Formal Analysis, Investigation, Writing – original draft. BZ: Data curation, Funding acquisition, Investigation, Methodology, Writing – review & editing. CF: Writing – review & editing. XL: Methodology, Writing – review & editing. BH: Conceptualization, Supervision, Methodology, Validation, Data curation, Writing – review & editing.

Funding

The author(s) declare financial support was received for the research, authorship, and/or publication of this article. This study was supported by the National Key Research and Development Program of China (2022YFD2200205) and Forestry Science and Technology Innovation Project of Guangdong Province (2020KJCX014).

Conflict of interest

The authors declare that the research was conducted in the absence of any commercial or financial relationships that could be construed as a potential conflict of interest.

Publisher's note

Supplementary material

The Supplementary Material for this article can be found online at: https://www.frontiersin.org/articles/10.3389/fpls.2023.1268835/full#supplementary-material

SUPPLEMENTARY FIGURE 1
Pearson correlation and principal component analysis between samples.

SUPPLEMENTARY FIGURE 2
The differentially expressed genes (DEGs) in *A. melanoxylon* stem.

SUPPLEMENTARY FIGURE 3
qRT-PCR validation of 15 DEGs. Data are the mean ± standard deviations (n=3).

SUPPLEMENTARY FIGURE 4
Correlation network diagram of plant hormone signal transduction pathway (KEGG: ko04075).

References

Bates, L. S., Waldren, R. A., and Teare, I. D. (1973). Rapid determination of free proline for water-stress studies. *Plant Soil* 39, 205–207. doi: 10.1007/BF00018060

Bolaños, L., Abreu, I., Bonilla, I., Camacho-Cristóbal, J. J., and Reguera, M. (2023). What can boron deficiency symptoms tell us about its function and regulation? *Plants* 12 (4), 777. doi: 10.3390/plants12040777

Bradbury, G. J., Potts, B. M., and Beadle, C. L. (2011). Genetic and environmental variation in wood properties of *Acacia melanoxylon*. *Ann. For. Sci.* 68 (8), 1363–1373. doi: 10.1007/s13595-011-0115-x

Brdar-Jokanović, M. (2020). Boron toxicity and deficiency in agricultural plants. *Int. J. Mol. Sci.* 21 (4), 1424. doi: 10.3390/ijms21041424

Camacho-Cristóbal, J. J., Herrera-Rodríguez, M. B., Beato, V. M., Rexach, J., Navarro-Gochicoa, M. T., Maldonado, J. M., et al. (2008). The expression of several cell wall-related genes in Arabidopsis roots is down-regulated under boron deficiency. *Environ. Exp. Bot.* 63 (1-3), 351–358. doi: 10.1016/j.envexpbot.2007.12.004

Camacho-Cristóbal, J. J., Martín-Rejano, E. M., Herrera-Rodríguez, M. B., Navarro-Gochicoa, M. T., Rexach, J., et al. (2015). Boron deficiency inhibits root cell elongation *via* an ethylene/auxin/ROS-dependent pathway in *Arabidopsis* seedlings. *J. Exp. Bot.* 66 (13), 3831–3840. doi: 10.1093/jxb/erv186

Camacho-Cristóbal, J. J., Rexach, J., Herrera-Rodríguez, M. B., Navarro-Gochicoa, M. T., and González-Fontes, A. (2011). Boron deficiency and transcript level changes. *Plant Sci.* 181 (2), 85–89. doi: 10.1016/j.plantsci.2011.05.001

Chen, C., Chen, H., Zhang, Y., Thomas, H. R., Frank, M. H., He, Y., et al. (2020). TBtools: an integrative toolkit developed for interactive analyses of big biological data. *Mol. Plant* 13 (8), 1194–1202. doi: 10.1016/j.molp.2020.06.009

Chen, X., Humphreys, J. L., Ru, Y., He, Y., Wu, F., Mai, J., et al. (2022). Jasmonate signaling and remodeling of cell wall metabolism induced by boron deficiency in pea shoots. *Environ. Exp. Bot.* 201, 104947. doi: 10.1016/j.envexpbot.2022.104947

Chen, X., Smith, S. M., Shabala, S., and Yu, M. (2023). Phytohormones in plant responses to boron deficiency and toxicity. *J. Exp. Bot.* 74 (3), 743–754. doi: 10.1093/jxb/erac443

De Andrade Silva, E. M., Reis, S. P. M., Argolo, C. S., Gomes, D. S., Barbosa, C. S., Gramacho, K. P., et al. (2020). *Moniliophthora perniciosa* development: key genes involved in stress-mediated cell wall organization and autophagy. *Int. J. Biol. Macromol.* 154, 1022–1035. doi: 10.1016/j.ijbiomac.2020.03.125

Dell, B., and Huang, L. (1997). Physiological response of plants to low boron. *Plant Soil* 193, 103–120. doi: 10.1023/A:1004264009230

Dible, W. T., Truog, E., and Berger, K. C. (1954). Boron determination in soils and plants. *Anal. Chem.* 26 (2), 418–421. doi: 10.1021/ac60086a047

Eggert, K., and von Wirén, N. (2017). Response of the plant hormone network to boron deficiency. *New Phytol.* 216 (3), 868–881. doi: 10.1111/nph.14731

Feng, Y., Cui, R., Wang, S., He, M., Hua, Y., Shi, L., et al. (2020). Transcription factor *BnaA9. WRKY47* contributes to the adaptation of *Brassica napus* to low boron stress by upregulating the boric acid channel gene *BnaA3. NIP5; 1. Plant Biotechnol. J.* 18 (5), 1241–1254. doi: 10.1111/pbi.13288

García-Sánchez, F., Simón-Grao, S., Martínez-Nicolás, J. J., Alfosea-Simón, M., Liu, C., Chatzissavvidis, C., et al. (2020). Multiple stresses occurring with boron toxicity and deficiency in plants. *J. Hazard. Mater.* 397, 122713. doi: 10.1016/j.jhazmat.2020.122713

Giannopolitis, C. N., and Ries, S. K. (1977). Superoxide dismutases: I. Occurrence in higher plants. *Plant Physiol.* 59 (2), 309–314. doi: 10.1104/pp.59.2.309

Heath, R. L., and Packer, L. (1968). Photoperoxidation in isolated chloroplasts: I. Kinetics and stoichiometry of fatty acid peroxidation. *Arch. Biochem. Biophys.* 125 (1), 189–198. doi: 10.1016/0003-9861(68)90654-1

Hedden, P., and Thomas, S. G. (2012). Gibberellin biosynthesis and its regulation. *Biochem. J.* 444 (1), 11–25. doi: 10.1042/BJ20120245

Herrera-Rodríguez, M. B., Camacho-Cristóbal, J. J., Barrero-Rodríguez, R., Rexach, J., Navarro-Gochicoa, M. T., and González-Fontes, A. (2022). Crosstalk of cytokinin with ethylene and auxin for cell elongation inhibition and boron transport in *Arabidopsis* primary root under boron deficiency. *Plants* 11 (18), 2344. doi: 10.3390/plants11182344

Hu, H., and Brown, P. H. (1994). Localization of boron in cell walls of squash and tobacco and its association with pectin (evidence for a structural role of boron in the cell wall). *Plant Physiol.* 105 (2), 681–689. doi: 10.1104/pp.105.2.681

Kasajima, I., Ide, Y., Yokota Hirai, M., and Fujiwara, T. (2010). WRKY6 is involved in the response to boron deficiency in *Arabidopsis thaliana*. *Physiol. Plant* 139 (1), 80–92. doi: 10.1111/j.1399-3054.2010.01349.x

Kim, D., Langmead, B., and Salzberg, S. L. (2015). HISAT: a fast spliced aligner with low memory requirements. *Nat. Methods* 12 (4), 357–360. doi: 10.1038/nmeth.3317

Kim, W. C., Ko, J. H., Kim, J. Y., Kim, J., Bae, H. J., and Han, K. H. (2013). MYB 46 directly regulates the gene expression of secondary wall-associated cellulose synthases in *A.rabidopsis*. *T. Plant J.* 73 (1), 26–36. doi: 10.1111/j.1365-313x.2012.05124.x

Kobayashi, M., Ohno, K., and Matoh, T (1997). Boron nutrition of cultured tobacco BY-2 cells. II. Characterization of the boron-polysaccharide complex. *Plant Cell Physiol* 38 (6), 676–683. doi: 10.1093/oxfordjournals.pcp.a029220

Kong, Y., Xu, X., and Zhu, L. (2013). Cyanobactericidal effect of Streptomyces sp. HJC-D1 on Microcystis auruginosa. *PloS One* 8 (2), e57654. doi: 10.1371/journal.pone.0057654

Li, B., and Dewey, C. N. (2011). RSEM: accurate transcript quantification from RNA-Seq data with or without a reference genome. *BMC Bioinform.* 12, 1–16. doi: 10.1186/1471-2105-12-323

Liu, C., Ma, H., Zhou, J., Li, Z., Peng, Z., and Guo, F. (2019). TsHD1 and TsNAC1 cooperatively play roles in plant growth and abiotic stress resistance of *Thellungiella halophile*. *Plant J.* 99 (1), 81–97. doi: 10.1111/tpj.14310

Liu, W., Xu, L., Lin, H., and Cao, J. (2021). Two expansin genes, *AtEXPA4* and *AtEXPB5*, are redundantly required for pollen tube growth and *AtEXPA4* is involved in primary root elongation in Arabidopsis thaliana. *Genes* 12 (2), 249. doi: 10.3390/genes12020249

Love, M. I., Huber, W., and Anders, S. (2014). Moderated estimation of fold change and dispersion for RNA-seq data with DESeq2. *Genome Biol.* 15 (12), 1–21. doi: 10.1186/s13059-014-0550-8

Maleki, S. S., Mohammadi, K., Movahedi, A., Wu, F., and Ji, K. S. (2020). Increase in cell wall thickening and biomass production by overexpression of *PmCesA2* in poplar. *Front. Plant Sci.* 11. doi: 10.3389/fpls.2020.00110

Martín-Rejano, E. M., Camacho-Cristóbal, J. J., Herrera-Rodríguez, M. B., Rexach, J., Navarro-Gochicoa, M. T., and González-Fontes, A. (2011). Auxin and ethylene are involved in the responses of root system architecture to low boron supply in *Arabidopsis* seedlings. *Physiol. Plant* 142 (2), 170–178. doi: 10.1111/j.1399-3054.2011.01459.x

Molassiotis, A., Sotiropoulos, T., Tanou, G., Diamantidis, G., and Therios, I. (2006). Boron-induced oxidative damage and antioxidant and nucleolytic responses in shoot tips culture of the apple rootstock EM 9 (*Malus domestica* Borkh). *Environ. Exp. Bot.* 56 (1), 54–62. doi: 10.1016/j.envexpbot.2005.01.002

O'Neill, M. A., Eberhard, S., Albersheim, P., and Darvill, A. G. (2001). Requirement of borate crosslinking of cell wall rhamnogalacturonan II for *Arabidopsis* growth. *Science* 294 (5543), 846–849. doi: 10.1126/science.1062319

Pérez, A. G., Sanz, C., Olías, R., and Olías, J. M. (1999). Lipoxygenase and hydroperoxide lyase activities in ripening strawberry fruits. *J. Agric. Food Chem.* 47 (1), 249–253. doi: 10.1021/jf9807519

Rao, M. V., Paliyath, G., and Ormrod, D. P. (1996). Ultraviolet-B-and ozone-induced biochemical changes in antioxidant enzymes of *Arabidopsis thaliana*. *Plant Physiol.* 110 (1), 125–136. doi: 10.1104/pp.110.1.125

Sampathkumar, A., Peaucelle, A., Fujita, M., Schuster, C., Persson, S., Wasteneys, G. O., et al. (2019). Primary wall cellulose synthase regulates shoot apical meristem mechanics and growth. *Development* 146 (10), dev179036. doi: 10.1242/dev.179036

Santner, A., Calderon-Villalobos, L. I. A., and Estelle, M. (2009). Plant hormones are versatile chemical regulators of plant growth. *Nat. Chem. Biol.* 5 (5), 301–307. doi: 10.1038/nchembio.165

Searle, S. D. (2000). Taylor & Francis online: acacia melanoxylon-A review of variation among planted trees. *Aust. For.* 63, 79–85. doi: 10.1080/00049158.2000.10674818

Shannon, P., Markiel, A., Ozier, O., Baliga, N. S., Wang, J. T., Ramage, D., et al. (2003). Cytoscape: a software environment for integrated models of biomolecular interaction networks. *Genome Res.* 13 (11), 2498–2504. doi: 10.1101/gr.1239303

Shorrocks, V. M. (1997). The occurrence and correction of boron deficiency. *Plant Soil* 193 (1-2), 121–148. doi: 10.1023/A:1004216126069

Singh, A., and Roychoudhury, A. (2022). "Mechanism of crosstalk between cytokinin and gibberellin," in *Auxins, Cytokinins and Gibberellins Signaling in Plants* (Germany: Springer International Publishing). doi: 10.1007/978-3-031-05427-3_4

Song, X., Wang, X., Song, B., Wu, Z., Zhao, X., Huang, W., et al. (2021). Transcriptome analysis reveals the molecular mechanism of boron deficiency tolerance in leaves of boron-efficient *Beta vulgaris* seedlings. *Plant Physiol. Biochem.* 168, 294–304. doi: 10.1016/j.plaphy.2021.10.017

Tewari, R. K., Kumar, P., and Sharma, P. N. (2010). Morphology and oxidative physiology of boron-deficient mulberry plants. *Tree Physiol.* 30 (1), 68–77. doi: 10.1093/treephys/tpp093

Trapnell, C., Williams, B. A., Pertea, G., Mortazavi, A., Kwan, G., Baren, M.J., et al. (2010). Transcript assembly and quantification by RNA-Seq reveals unannotated transcripts and isoform switching during cell differentiation. *Nat. Biotechnol.* 28 (5), 511–515. doi: 10.1038/nbt.1621

Vaahtera, L., Schulz, J., and Hamann, T. (2019). Cell wall integrity maintenance during plant development and interaction with the environment. *Nat. Plants* 5 (9), 924–932. doi: 10.1038/s41477-019-0502-0

Waadt, R., Seller, C. A., Hsu, P. K., Takahashi, Y., Munemasa, S., and Schroeder, J. I. (2022). Plant hormone regulation of abiotic stress responses. *Nat. Rev. Mol. Cell Bio.* 23 (10), 680–694. doi: 10.1038/s41580-022-00479-6

Wang, N., Yang, C., Pan, Z., Liu, Y., and Peng, S. A. (2015). Boron deficiency in woody plants: various responses and tolerance mechanisms. *Front. Plant Sci.* 6. doi: 10.3389/fpls.2015.00916

Warington, K. (1923). The effect of boric acid and borax on the broad bean and certain other plants. *Ann. Bot.* 37 (148), 629–672. doi: 10.1093/oxfordjournals.aob.a089871

Wu, X., Riaz, M., Yan, L., Du, C., Liu, Y., and Jiang, C. (2017). Boron deficiency in trifoliate orange induces changes in pectin composition and architecture of components in root cell walls. *Front. Plant Sci.* 8. doi: 10.3389/fpls.2017.01882

Yan, L., Li, S., Cheng, J., Zhang, Y., and Jiang, C. (2022). Boron-mediated lignin metabolism in response to aluminum toxicity in citrus (*Poncirus trifoliata* (L.) Raf.) root. *Plant Physiol. Biochem.* 185, 1–12. doi: 10.1016/j.plaphy.2022.05.018

Yin, Q., Kang, L., Liu, Y., Qaseem, M. F., Qin, W., Liu, T., et al. (2022). Boron deficiency disorders the cell wall in *Neolamarckia cadamba*. *Ind. Crops. Prod.* 176, 114332. doi: 10.1016/j.indcrop.2021.114332

Zhong, R., and Ye, Z. H. (2014). Complexity of the transcriptional network controlling secondary wall biosynthesis. *Plant Sci.* 229, 193–207. doi: 10.1016/j.plantsci.2014.09.009

Zhu, J. K. (2016). Abiotic stress signaling and responses in plants. *Cell* 167 (2), 313–324. doi: 10.1016/j.cell.2016.08.029

Zhu, Y., Jiang, X., Zhang, J., He, Y., Zhu, X., Zhou, X., et al. (2020). Silicon confers cucumber resistance to salinity stress through regulation of proline and cytokinins. *Plant Physiol. Biochem.* 156, 209–220. doi: 10.1016/j.plaphy.2020.09.014

frontiers | Frontiers in Plant Science

TYPE Original Research
PUBLISHED 31 October 2023
DOI 10.3389/fpls.2023.1287677

OPEN ACCESS

EDITED BY
Karl H. Mühling,
University of Kiel, Germany

REVIEWED BY
Shahbaz Khan,
Colorado State University, United States
Asif Naeem,
Nuclear Institute for Agriculture and Biology, Pakistan

*CORRESPONDENCE
Adel Siosemardeh
a33@uok.ac.ir

RECEIVED 02 September 2023
ACCEPTED 16 October 2023
PUBLISHED 31 October 2023

CITATION
Moradi L and Siosemardeh A (2023) Combination of seed priming and nutrient foliar application improved physiological attributes, grain yield, and biofortification of rainfed wheat.
Front. Plant Sci. 14:1287677.
doi: 10.3389/fpls.2023.1287677

Combination of seed priming and nutrient foliar application improved physiological attributes, grain yield, and biofortification of rainfed wheat

Layegh Moradi and Adel Siosemardeh*

Department of Agronomy and Plant Breeding, Faculty of Agriculture, University of Kurdistan, Sanandaj, Iran

Seed priming and foliar application are two crop management practices that can increase grain yield and quality. The research aimed to assess the influence of seed priming and foliar application on rainfed wheat. Two field experiments with two seed priming rates (control and priming) and five foliar applications [control, urea (4%), silicon (4 mM), $FeSO_4.7H_2O$ (0.6%), and $ZnSO_4.7H_2O$ (0.4%)] at the anthesis/Z61 stage were conducted. Seeds were primed for 12 h at 25 ± 2°C, by soaking in an aerating solution [urea (20 g L^{-1}) + $FeSO_4.7H_2O$ (50 ppm) + $ZnSO_4.7H_2O$ (50 ppm) + silicon (20 mg L^{-1})]. Seed weight-to-solution volume ratio was 1:5 (kg L^{-1}). A pot experiment was also conducted to examine the effect of priming on root growth. Overall, combined seed priming and foliar application induced a positive impact on physiological traits and attributes. Maximum chlorophyll a, chlorophyll b, total chlorophyll, and carotenoid concentrations (1.58, 0.669, 2.24, and 0.61 mg g^{-1} FW), membrane stability index (77.31%), superoxide dismutase and peroxidase activity (0.174 and 0.375 Unit mg^{-1} protein), 1,000-grain weight (35.30 g), biological yield, grain yield (8,061 and 2,456 kg ha^{-1}), and minimum malondialdehyde concentration (3.91 µg g^{-1} FW) were observed in seed priming combination with $ZnSO_4$ foliar application. The highest glycine betaine concentration (6.90 mg g^{-1} DW) and proline (972.8 µg g^{-1} FW) were recorded with the co-application of seed priming and foliar urea spraying. Foliar application of $ZnSO_4$, $FeSO_4$, and urea drastically enhanced grain Zn (29.17%), Fe (19.51%), and protein content (increased from 11.14% in control to 12.46% in urea foliar application), respectively. Compared to control, seed priming increased root length, root volume, and dry mass root by 8.95%, 4.31%, and 9.64%, respectively. It is concluded that adequate Zn, Fe, silicon, and N supply through seed priming and foliar applications of these compounds at the terminal stage of rainfed wheat alleviates drought stress and improves GY and biofortification.

KEYWORDS

antioxidant, biofortification, grain yield, malondialdehyde, micronutrients, silicon, terminal stage

1 Introduction

In general, approximately 20% of the calories needed by the global community are derived from wheat (*Triticum aestivum* L.), which is one of the main sources of food in the world (Liu et al., 2020). The demand for wheat production is rising in response to a growing global population and food consumption growth (Liu et al., 2015). Water scarcity has the greatest impact on agriculture, with yields in rainfed areas decreasing by 40% to 60% (Saha et al., 2022). During the wheat-growing season, uneven precipitation distribution leads to drought stress in the Mediterranean. As a result, rainfed wheat growth is negatively impacted by soil moisture shortages, especially during anthesis and grain filling (Moradi et al., 2022). Crop producers must maintain crops' ability to adapt to frequent stressors (Malko et al., 2022). Integrated agronomic crop management methods are needed to alleviate the deleterious impacts of drought and enhance quantitative and qualitative yields. The singleton approach will not achieve this (Melash et al., 2019). For this goal, we combined seed priming and foliar application of urea, $ZnSO_4$, $FeSO_4$, and silicon in an experiment. Research was conducted on the effects of these factors on physiological characteristics and wheat yield quantitatively and qualitatively.

Seed priming practice has been utilized in plants to boost the quality of seed, thereby benefiting stand establishment and mitigating drought stress in farmers' fields (Liu et al., 2015). The technique involves partially hydrating seeds in a specified environment until the germination process begins without exhibiting any signs of radical emergence. It is followed by dehydrating to attend to the original seed's dry weight. In addition, priming can activate metabolic systems normally activated during germination ("pre-germinative metabolism") and therefore accelerate germination and emergence, and therefore allows seedlings to adapt to various environmental stresses. Typical priming approaches include water (Hydro) priming, osmopriming, hormonal priming, and nutritional priming (Liu et al., 2015; Rai-Kalal and Jajoo, 2021). Seeds are soaked in a solution containing nutrients during nutritional priming. Soil, leaf, and seed nutrients may be applied to fulfill plant nutrient demands (Farooq et al., 2012; Rehman et al., 2018; Farooq et al., 2021). Fertilizer applied to soil takes effect slowly (5–6 days) if environmental variables are favorable. It is difficult to apply fertilizers uniformly to the surface of the soil in a soil application (Johnson et al., 2005). It is advantageous to prime seeds so that nutrients can easily be accessed by germinating seeds, and it is also considered a cost-efficient method because very few nutrients are required to prime seeds (Farooq et al., 2021). Seed priming contributes to enhance drought resistance via increased photosynthesis pigments, antioxidant defense, osmotic adjustments, and membrane integrity (Saha et al., 2022). Research has documented that in wheat plants, seed priming boosts nutrient uptake, antioxidant enzymes, osmolyte concentrations like glycine betaine (GB) and proline, chlorophyll content, membrane integrity, yield characteristics and yield, and grain nutrient and protein concentrations (Farooq et al., 2012; Rehman et al., 2018; Reis et al., 2018; Malko et al., 2022).

Drought stress becomes more intensified under mineral nutrient deficiencies (Farooq et al., 2021). Rainfed wheat development is typically impacted by drought stress in Mediterranean regions due to unbalanced rainfall distribution (Moradi et al., 2022). In such regions, foliage application nutrients are a suitable technique to mitigate adverse drought stress effects and improve rainfed wheat physiological characteristics, grain yield (GY), and quality. Foliar nutrition is a method proposed to reduce chemical fertilizers and environmental risks (Aziz et al., 2019; Melash et al., 2019). In rainfed wheat farming, where the plant has difficulty absorbing nutrients from the soil in the final stages of its growth due to low soil moisture and reduced root activity, this method can be very effective in supplying nutrients (Melash et al., 2019).

Nitrogen (N) optimal utilization is vital for enhanced wheat grain and protein production (Nehe et al., 2020). Because of the utilization of N during the flowering and grain-filling stages, nutrients tend to be transported efficiently to higher metabolic demand points (grain) (Blandino et al., 2020). During the terminal stages of growth, N intake has less effect on yield but a significant influence on grain quality (Wang et al., 2021). Silicon enhances crop yield, quality, and productivity by improving photosynthetic activity and N assimilation. The International Plant Nutrition Institute identifies silicon as a beneficial mineral based on its useful role in plants. Owing to the potential for accumulation, plants collect silicon between 0.1% and 10% of their dry matter. It is, however, not recognized as a necessary nutrient for proper plant development and growth (Bukhari et al., 2021; Sattar et al., 2021). Research has found silicon to have a positive impact on various plant species, notably when exposed to environmental stress, by elevating antioxidant enzyme activity and osmolytes, which help plants resist abiotic and non-abiotic stresses (Bukhari et al., 2021). Zn and Fe are indispensable micronutrients for crop growth. Many scientists have documented that foliage application of these minerals is able to amplify drought tolerance of plants due to their participation in the construction of many antioxidant enzymes as cofactors, raising GY, and enriching wheat grains (Karim et al., 2012; Zain et al., 2015; Sultana et al., 2018; Melash et al., 2019; Sattar et al., 2021). Optimal fertilizer usage and the value of micronutrients for soil and human wellbeing have been carefully discussed in recent years, and with the change of approach toward nutrient management, rather than focusing exclusively on boosting yields, it also addresses its impact on society. In addition to increasing yields per hectare, it also emphasizes its impact on people, aiming to diminish malnutrition in countries and societies, and most noteworthy, it emphasizes the role of Zn and Fe (Das et al., 2022; Szerement et al., 2022). Thus, the utilization of such micronutrients in crop production increases GY and product quality, which will result in better health for humans.

Several studies have examined wheat priming and foliar applications of nutrients (Amanullah et al., 2010; Farooq et al., 2012; Zain et al., 2015; Rehman et al., 2018; Melash et al., 2019; Farooq et al., 2021). Nevertheless, there is limited information regarding the effects of simultaneous seed priming and continued foliar fertilization on physiological characteristics, yield attributes, and grain quality; such knowledge would be extremely useful for

managing nutrients with the aim of reducing drought stress in rainfed wheat crops and improving yields and quality. Here, we evaluate the influence of priming and foliar spray of N, Zn, Fe, and silicon on rainfed wheat. The hypothesis was that seed priming and foliar application of nutrients could improve root growth, morpho-physiological traits, productivity, and grain quality in rainfed wheat crops. Therefore, the objectives of our experiment are to (a) assess the effect of priming on root attributes; (b) assess the effect of priming, foliar application of nutrients, and their interaction under rainfed conditions on the photosynthetic pigments, compatible osmolytes, malondialdehyde (MDA), superoxide dismutase (SOD), and peroxidase (POD) activity; (c) investigate the effect of foliar application nutrients and priming on the rainfed wheat yield components and yield; (d) compare grain Fe, Zn, and protein content (grain quality) of wheat grain under the influence of priming and foliar minerals spraying; and (e) examine relationships between physiological traits, yield, and yield attributes.

2 Materials and methods

2.1 Field experiment

2.1.1 Site descriptions

The field experiment was conducted at the University of Kurdistan's research farm, which is situated on the Dehgolan plain (35 −19′ 1′′ N, 47 −18′ 54′′ E, 1,862 m above mean sea level) during the wheat-growing seasons of 2021–2023. Table 1 shows organic C, available phosphorus, total N, and available potassium, Zn, and Fe in the 0–0.3 m soil layer of the field. The research field soil texture was loam. During the growing seasons of 2021–2022 and 2022–2023, 262.4 and 368.6 mm of precipitation were recorded. In Table 2, the monthly precipitation, temperature, and average relative humidity at the wheat-growing site are presented.

2.1.2 Experimental design

In the two growing seasons, this study was conducted in factorial with four replications utilizing a randomized complete block design (RCBD) to assess the effect of seed priming and foliar application on rainfed wheat (Cv. Baran). The experimental factors included two priming levels (control and priming with) and five foliar applications [control, urea (4%), silicon (4 mM), $FeSO_4.7H_2O$ (0.6%), and $ZnSO_4.7H_2O$ (0.4%)]. Each plot was 2.9×8 m^2, and the distance between plots and blocks was 1 m and 2 m, respectively.

Seeds were primed for 12 h at 25 ± 2°C, by soaking in an aerating solution [urea (20 g L^{-1}) + $FeSO_4.7H_2O$ (50 ppm) + $ZnSO_4.7H_2O$ (50 ppm) + silicon (20 mg L^{-1})]. The ratio of seed weight to solution volume was 1:5 (kg L^{-1}). During the soak, an aquarium pump supplied aeration. To ensure clump-free sowing of the seeds, the seeds were dried in the shade after being removed from the solution. Two foliar applications were performed, first at the anthesis/Z61 (Zadoks et al., 1974) stage and again 10 days later, using a manual high-pressure sprayer at a rate of 500 L ha^{-1}. The control plots were sprayed with water. A water spray was applied to the control plots.

2.1.3 Crop management

During seeding, plots were fertilized with 150 kg ha^{-1} of urea and 200 kg ha^{-1} of triple superphosphate. Wheat seeds were sown at a density of 350 plants per m^2. Tilling, planting, pest control, and weed control are similar to those used in typical wheat production.

2.1.4 Measurements

Physiological characteristics were measured 8 days after the last foliar application. To determine parameters such as chlorophyll pigment, proline, GB, MDA concentration, SOD and POD activity, flag leaf samples were randomly collected in each plot. Liquid nitrogen was used to freeze samples and they were stored at −40° C until analysis. We measured the membrane stability index (MSI) after separating flag leaves from plots to study this parameter.

2.1.4.1 Carotenoids and chlorophyll content

A method based on Arnon's (1949) method was used to determine chlorophyll in flag leaves. We homogenized the leaf samples in 10 mL of 80% acetone and centrifuged them at 5,000 rpm for 5 min. The extract absorbance was recorded at 645-nm (A645), 663-nm (A663), and 470-nm (A470) wavelengths using a spectrophotometer (UV-2100 Model).

2.1.4.2 Proline concentration

Based on Bates et al. (1973), proline concentration was measured. In 10 mL of 3% (w/v) sulfosalicylic acid solution, samples (0.5 g) were homogenized. For 1 h at 100°C, 2 mL of the extract reacted with 2 mL of glacial acetic acid and 2 mL of fresh acid ninhydrin solution in a test tube, and the reaction was finished in an ice bath. A spectrophotometer (UV-2100 Model) was used to measure the supernatant absorbance at 520 nm after adding 4 mL of toluene.

TABLE 1 Pre-sow nutrient condition of experimental plots at 0–0.30 m depth.

Growing season	Organic C (%)	Total N (g kg^{-1})	Available P (mg kg^{-1})	Available K (mg kg^{-1})	Zn (mg kg^{-1})	Fe (mg kg^{-1})
2021–2022	0.78	0.40	12.00	336.1	0.44	2.10
2022–2023	0.81	0.45	12.80	351.0	0.42	2.03
Pot experiment						
2022–2023	0.73	0.37	13.10	330.0	0.38	2.30

TABLE 2 Wheat-growing season rainfall, minimum and maximum temperatures (T_{min}; T_{max}), and mean relative humidity (RH_{avg}).

Month	2021–2022				2022–2023			
	Precipitation (mm)	T_{min} (°C)	T_{max} (°C)	RH_{avg} (%)	Precipitation (mm)	T_{min} (°C)	T_{max} (°C)	RH_{avg} (%)
Oct.	21.4	1.77	21.16	44.20	5.60	3.70	23.57	41.63
Nov.	32.4	−1.11	10.63	72.79	36.4	−2.03	12.85	63.36
Dec.	24.2	−4.32	9.00	65.39	22.00	−3.80	4.80	80.03
Jan.	32.4	−9.76	4.6	68.61	50.40	−11.06	0.18	83.50
Feb.	74.6	−6.30	6.79	74.16	15.20	−10.33	3.68	72.90
Mar.	34.6	−2.03	10.86	52.39	106.00	0.80	13.42	56.94
Apr.	33.8	2.68	19.77	45.89	81.20	1.75	17.36	54.06
May.	8.6	4.09	21.29	49.75	76.60	5.38	21.15	51.25
Jun.	0.4	8.25	30.79	35.24	5.2	7.14	28.49	39.87
Total	262.4	–	–	–	398.60	–	–	–

2.1.4.3 GB concentration

The GB was extracted from dry flag leaves using hot distilled water (70°C). Dry flag leaves were soaked in distilled water for 48 h and then shaken vigorously to measure GB. 2N HCl and potassium tri-iodide solution were added to the extract (0.25 ml). A 90-min ice bath was used to cool the contents after shaking. Following this, 20 mL of 1,2-dichloromethane (cooled at −10°C) and 2 mL of ice-cold distilled water were added. There were two layers formed from the mixture; 365-nm optical density measurements were performed after discarding the upper aqueous layer (Grieve and Grattan, 1983).

2.1.4.4 MDA concentration

The Heath and Packer (1968) method was used to determine MDA content in leaf. Five milliliters of 0.1% trichloroacetic acid (TCA) was homogenized with leaf samples (0.5 g), followed by centrifugation at 10,000 *g* for 5 min at 4°C.

2.1.4.5 SOD activity

Superoxide dismutase activity was determined based on Beauchamp and Fridovich (1971). Each sample was prepared using 970 µL of mixed buffer, 20 µL of riboflavin, and 20 µL of extract. For 10 min, the samples were shaken under the light. Using a spectrophotometer, the absorbance at 562 nm was measured at the end.

2.1.4.6 POD activity

Peroxidase activity was determined based on Hemeda and Klein (1990). In an overall volume of 1.0 mL, the reaction mixture contained 780 µL of 50 mmol potassium phosphate buffer (pH 6.6), 90 µL of 0.3% hydrogen peroxide, 40 µL of crude extract, and 90 µL of 1% guaiacol. The activity was detected by the rise in absorption at 470 nm in response to guaiacol oxidation (E026.6 mM^{-1} cm^{-1}).

2.1.4.7 MSI

To determine the MSI, leaf discs were cut with scissors and inserted into glass vials. The samples were washed twice with double-distilled water for 5 min each. Following draining the water from each vial, 10 mL of double-distilled water was added. The vials were then shaken (150 rpm, 25°C, 30 min). The electrical conductivity was measured using a conductivity electrode. The conductivity was measured after 60 min of hot water bathing all vials. According to Bajji et al. (2002), the MSI was calculated.

2.1.4.8 Yield components and yields

Grain yield at maturity was determined by cutting 3 m^2 of each plot in the center and expressing it at 12% moisture content. Divide GY by biological yield (BY) at maturity to calculate the harvest index (HI). We also measured the kernels per spike at maturity and the 1,000-grain weight.

2.1.4.9 Fe and Zn content

The dried wheat grain samples were ashed at 550°C in a furnace for 6 h, then dissolved in a 1:1 (v:v) HNO_3 solution to determine Fe and Zn content. Atomic absorption spectrometry was used to detect Fe and Zn in grains (Jones and Case, 1990).

2.1.4.10 Grain protein content

To measure grain protein content, the N concentration was initially measured with the Kjeldahl method. By multiplying the grain N content by the N-to-protein conversion factor (5.7), the grain protein content was calculated (Moradi et al., 2022).

2.1.5 Statistical analysis

In order to analyze the combined variance of the data, after Bartlett's test and ensuring homogeneity of variance, the factorial combined analysis model based on the RCBD was used. Years were considered random, and seed priming and foliar application were

used as fixed effects. Using SAS 9.4 software, we conducted an analysis of variance. To compare the means, Duncan's multiple range test was used at a $p \leq 0.05$ (Duncan, 1966). To assess the relationship between the variables, Pearson correlation coefficients were employed.

2.2 Pot experiment

2.2.1 Plant materials and experiment setup

The pot experiment was carried out during the 2022–2023 growing season at the University of Kurdistan, Kurdistan, Iran. The purpose of this experiment was to evaluate the effect of seed priming on root growth in rainfed wheat (Cv. Baran). The pot experiment was conducted with soil obtained from the field. Table 1 shows some of the physical and chemical characteristics of the medium soil. The experiment was designed as a 4-replicate completely randomized design with seed priming treatment [non-primed and primed seeds with urea (20 g L^{-1}) + $FeSO_4.7H_2O$ (50 ppm) + $ZnSO_4.7H_2O$ (50 ppm) + silicon (20 mg L^{-1})]. As described in *section 2.1.2*, the priming of seeds was done the same way in the field experiment. First, plastic pots (12 in diameter and 100 cm in height) were filled with 15 kg of soil (Table 1). A pot was placed in the excavated ground and the surrounding area was filled with soil so that it had the same surface as a field. Three seedlings remained per pot after seedling establishment, and they were grown to physiological maturity. Plants did not show any signs of disease or pest activity.

2.2.2 Plant growth attributes

At maturity, plant dry mass (DM) and grain weight were measured in grams for each pot in this experiment. The pots were removed from the ground after harvesting the aboveground part at maturity in order to measure root length, root volume, and root dry weight. For 12 h, the pots were placed in water-filled barrels. Roots were stirred and poured into a sieve (0.25 mm^2 mesh). As the sieve was suspended over a water bath, it was repeatedly shaken until soil was removed from the roots. The remaining soil materials were manually removed from the sieve. The measured root length, root volume, and root DM were then averaged. Root length was calculated using a ruler from the base to the tip, and total measurements were taken. Root masses were placed in a water-filled measuring cylinder to determine root volume. Water level increase was measured as cm^3 pot^{-1}. For each pot, roots were oven dried for 48 h at 72°C, and root DM was calculated as g pot^{-1}.

2.2.3 Statistical analysis

Statistical Analysis Software (SAS Version 9.4) was used to analyze the data using a completely randomized design (ANOVA). To compare the means, Duncan's multiple range test was used at a $p \leq 0.05$ (Duncan, 1966).

3 Results

3.1 Variance analysis of studied characteristics

A combined ANOVA for traits revealed that there was a significant year, seed priming, and foliar application effect for almost all traits (Table 3). Moreover, the interactions between seed priming × foliar application for Chl a, Chl b, Chl T, and carotenoid content, proline, GB, and MDA concentration, POD and SOD activity, 1,000-grain weight, BY, and GY were also significant (Table 3).

3.2 Chlorophyll and carotenoid content

In the 2022–2023 growing season, Chl a, Chl b, Chl T, and carotenoid concentrations were 13.85%, 18%, 15.08%, and 14.58% higher than in the 2021–2022 growing season, respectively (Table 3). Leaf chlorophyll content for both primed and unprimed seeds decreased in order to $ZnSO_4$ > silicon > $FeSO_4$ > urea > control foliar application. Foliar application of $ZnSO_4$, silicon, $FeSO_4$, and urea at seed-primed treatment increased total chlorophyll content by 26.97%, 21.25%, 12.07%, and 7.99%, respectively, compared to the control. Furthermore, silicon, $ZnSO_4$, $FeSO_4$, and urea applied as foliar treatments at non-primed seed treatment increased Chl T by 17.48%, 16.83%, 12.08%, and 8.23% in comparison with the control (Figures 1A–C). Maximum carotenoid content (0.610 mg g^{-1} FW) was recorded with seed priming and $ZnSO_4$ foliar application, which was significantly higher compared to other treatments (Figure 1D).

3.3 Proline concentration

Proline concentration was 6.65% higher in the first growing season than in the second growing season (Table 3). For all foliar applications, the highest proline concentration was obtained during primed seed treatment. Proline concentration ranged from 604.1 μg g^{-1} FW in non-primed seed and control foliar application to 942.7 μg g^{-1} FW in combination primed seed and urea foliar application. Seed priming recorded greater proline concentrations (972.8, 942.7, 873.4, 814.1, and 725.5 μg g^{-1} FW) at foliar application of urea, $ZnSO_4$, silicon, and $FeSO_4$ and no foliar application (Figure 2A).

3.4 GB concentration

A higher concentration of GB was observed in the 2021–2022 growing season (6.08 mg g^{-1} DW) than in the 2022–2023 growing season (5.86 mg g^{-1} DW). The highest GB concentration (6.71 mg g^{-1} DW) was observed at the co-application of seed priming and

TABLE 3 Analysis of variance (ANOVA) of factorial design for wheat studied wheat traits at two priming rates and foliar applications.

		Year (Y)	Priming (P)	Foliar application (FA)	Y×P	Y×FA	P × FA	Y × P × FA
Degrees of freedom (df)		1	1	4	4	4	4	4
Physiological and biochemical	Chlorophyll a	**	**	**	ns	ns	*	ns
	Chlorophyll b	**	**	**	ns	ns	*	ns
	Total chlorophyll	**	**	**	ns	ns	**	ns
	Carotenoid	**	**	**	ns	ns	**	ns
	Membrane stability index	**	*	**	ns	ns	**	ns
	proline	*	**	**	ns	ns	**	ns
	Glycine betaine	*	**	**	ns	ns	*	ns
	Malondialdehyde	**	**	**	ns	ns	**	ns
	Peroxidase activity	**	**	**	ns	ns	*	ns
	Superoxide dismutase	ns	**	**	ns	ns	**	ns
	Spike per m^2	**	**	ns	ns	ns	ns	ns
Yield components and yield	Kernels per spike	**	**	**	ns	ns	ns	ns
	1,000-grain weight	**	**	**	ns	ns	**	ns
	Biological yield	**	**	**	ns	ns	*	ns
	Grain yield	**	**	**	ns	ns	*	ns
	Harvest index	ns	**	**	ns	ns	ns	ns
Grain quality	Protein	ns	*	**	ns	ns	ns	ns
	Zn	ns	**	**	ns	ns	ns	ns
	Fe	ns	**	**	ns	ns	ns	ns

Mean comparisons	Chl a	Chl b	Chl T	Carotenoid	Proline (ug g^{-1} FW)	GB (mg g^{-1} DW)	MSI (%)	MDA (μg g^{-1} FW)	POD (Unit mg^{-1} protein)
	(mg g FW^{-1})								
Year									
2021–2022	1.30^{b} ± 0.02	0.50^{b} ± 0.010	1.79^{b} ± 0.027	0.48^{b} ± 0.018	818^{a} ± 14.3	6.08^{a} ± 0.10	68.5^{b} ± 0.68	5.17^{a} ± 0.11	0.318^{a} ± 0.006
2022–2023	1.48^{a} ± 0.02	0.59^{a} ± 0.012	2.06^{a} ± 0.031	0.55^{a} ± 0.010	767^{b} ± 21.1	5.86^{b} ± 0.13	72.7^{a} ± 0.93	4.80^{b} ± 0.10	0.307^{b} ± 0.007

ns, non-significant error within-group variance. *: $p \leq 0.05$; **: $p \leq 0.01$. Mean comparisons for chlorophyll a, chlorophyll b, total chlorophyll, and carotenoid concentration, membrane stability index, proline, glycine betaine, malondialdehyde, and peroxidase activity. As determined by Duncan's test, no significant difference at $p \leq 0.05$ exists between values in a column containing the same letter within a group. Data are the mean ± SE [n = 40 for year].

foliar spraying of urea. Foliar application of urea, $ZnSO_4$, silicon, and $FeSO_4$ compared to control at seed priming treatment elevated GB concentrations by 19.22%, 15.86%, 14.31%, and 10.06%, respectively (Figure 2B).

3.5 MDA concentration

The concentration of MDA decreased by 7.15% in the second growing season compared to the first growing season (Table 3). The results of the study confirm that, as a result of foliar applications, the MDA concentration in wheat leaf was significantly smaller at primed and non-primed treatments. However, the outcomes of foliar application of $ZnSO_4$ and silicon resulted in a greater reduction in MDA concentrations than other foliar applications. The highest MDA concentration (6.19 μg g^{-1} FW) was detected in the control foliar application and non-primed seed. Foliar application of $ZnSO_4$, silicon, $FeSO_4$, and urea compared to control at seed priming treatment reduced MDA concentrations by 30.61%, 28.80%, 17.40%, and 11.17%, respectively (Figure 3A).

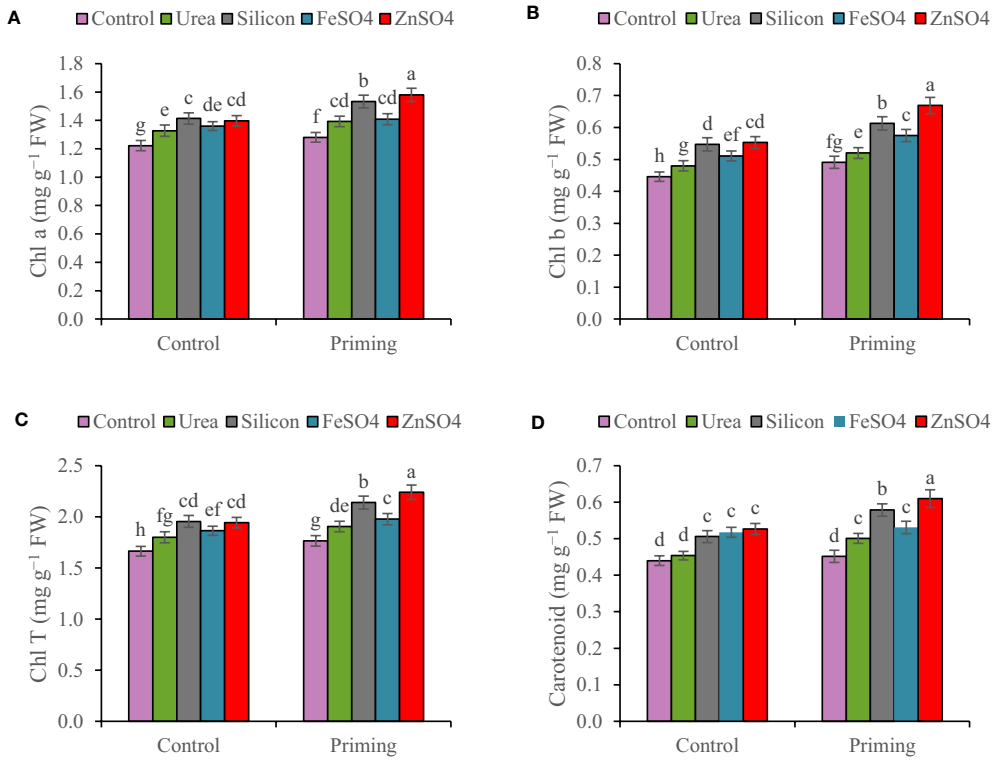

FIGURE 1
Mean comparison for interactions of seed priming × foliar application on **(A)** chlorophyll a (Chl a), **(B)** chlorophyll b (Chl b), **(C)** total chlorophyll (Chl T), and **(D)** carotenoid of wheat. The Duncan's test indicates that columns labeled by the same letter are not significantly different at the $p \leq 0.05$ level. Each mean is accompanied by a standard error ($n = 8$).

3.6 MSI

The MSI increased from 68.5% in the 2021–2022 growing season to 72.7% in the 2022–2023 growing season (Table 3). MSI values ranged from 64.71% in non-primed seed and no foliar application to 77.321% in primed seed and silicon foliar application. Seed priming recorded significantly elevated MSI (77.32%, 77.07%, 74.55%, and 68.68%) at foliar application of $ZnSO_4$, silicon, $FeSO_4$, and urea, respectively (Figure 3B).

3.7 SOD activity

In both non-primed seed and seed primed treatments, $ZnSO_4$, urea, silicon, and $FeSO_4$ foliar applications significantly improved SOD activity. SOD activity values ranged from 0.13 Unit mg^{-1} protein in non-primed seed and no foliar application to 0.174 Unit mg^{-1} protein in primed seed and $ZnSO_4$ foliar application. $ZnSO_4$, $FeSO_4$, silicon, and urea applications significantly increased SOD activity compared to no application in the seed priming treatment by 20.83%, 19.44%,

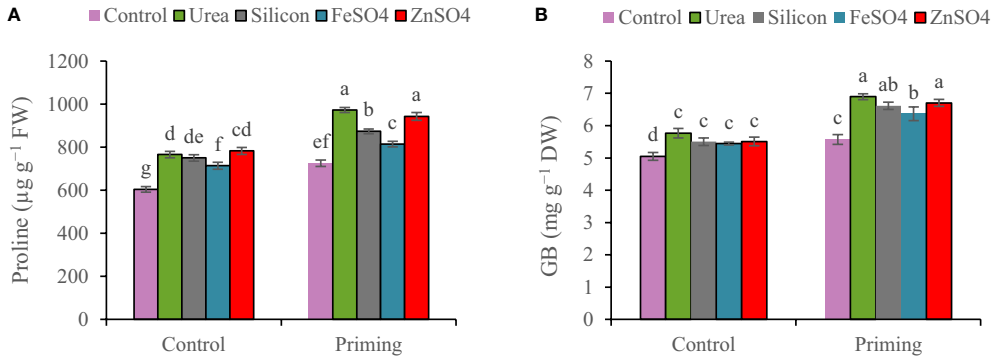

FIGURE 2
Mean comparison for interactions of seed priming × foliar application on concentrations of **(A)** proline and **(B)** glycine betaine (GB) in wheat. The Duncan's test indicates that columns labeled by the same letter are not significantly different at the $p \leq 0.05$ level. Each mean is accompanied by a standard error ($n = 8$).

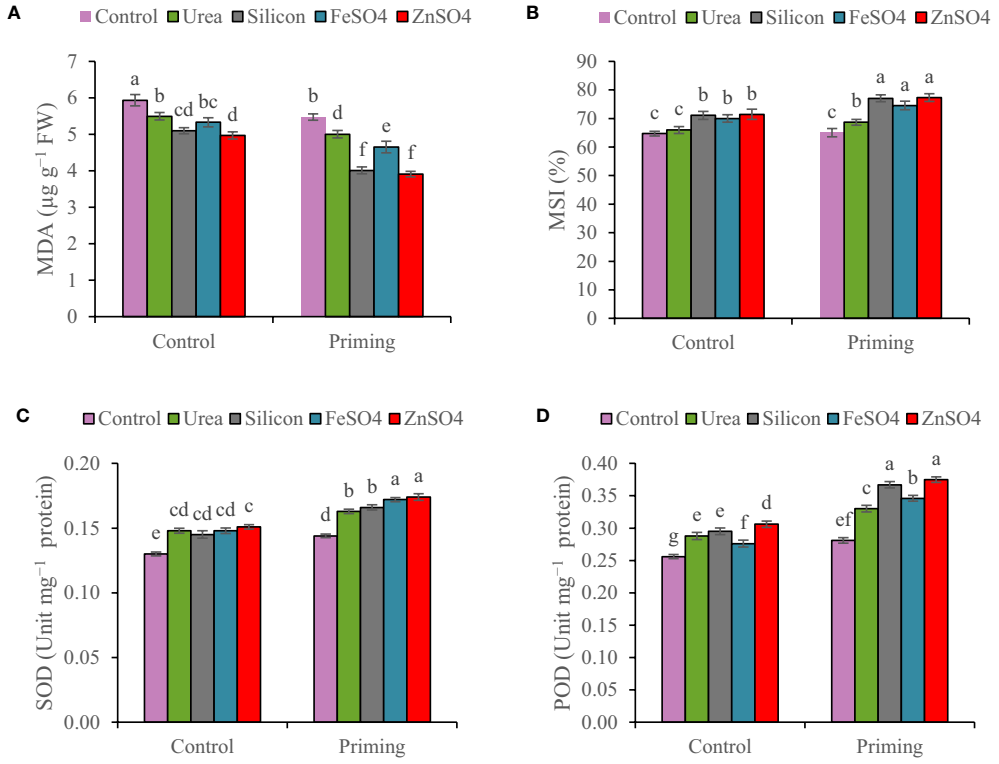

FIGURE 3
Mean comparison for interactions of seed priming × foliar application on **(A)** malondialdehyde concentration (MDA), **(B)** membrane stability index (MSI), **(C)** superoxide dismutase (SOD), and **(D)** peroxidase activity (POD) of wheat. The Duncan's test indicates that columns labeled by the same letter are not significantly different at the $p \leq 0.05$ level. Each mean is accompanied by a standard error ($n = 8$).

15.28%, and 13.19%. For non-primed seeds, there is no statistically significant difference in SOD activity between $ZnSO_4$, silicon, $FeSO_4$, and urea foliar applications (Figure 3C).

3.8 POD activity

Peroxidase activity in 2021–2022 was higher than the 2022–2023 growing season (Table 3). At both non-primed seed and seed primed treatments, $ZnSO_4$, urea, silicon, and $FeSO_4$ foliar applications significantly boosted POD activity. The highest POD activity (0.375 Unit mg^{-1} protein) was observed in seed priming in combination with $ZnSO_4$ foliar application. This was statistically similar to the foliar application of silicon (0.367 Unit mg^{-1} protein) at seed priming treatment. In seed priming treatment, foliar application of $ZnSO_4$, silicon, $FeSO_4$, and urea significantly increased POD activity compared to no foliar application by 33.45%, 30.60%, 23.13%, and 17.44%, respectively (Figure 3D).

3.9 Yield and yield components

In the 2022–2023 growing season, spike per m^2, kernels per spike, 1000-grain weight, BY, and GY were 22.63%, 7.84%, 7.64%, 46.52%, and 45.50% higher than in the 2021–2022 growing season, respectively (Table 4). A seed priming treatment resulted in an overall improvement in yield components and yield. In comparison to the control, seed priming increased spikes per m^2 and kernels per spike by 8.60% and 13.42%, respectively. A higher HI was found in the seed priming (29.2%) treatment compared to the control treatment (28.9%) (Table 4). Data in Table 4 indicated that kernels per spike increased in the order control < $ZnSO_4$ < silicon < $FeSO_4$ < urea foliar applications. Foliar application of $ZnSO_4$, silicon, and $FeSO_4$ had a positive effect on 1,000-grain weight at both seed priming and control treatments, in contrast to foliar application of urea, which slightly decreased 1,000-grain weight. The maximal 1,000-grain weight on the whole foliar application was observed in $ZnSO_4$ foliar application at both priming (35.30 g) and control (30.96 g) treatments (Figure 4A). For all foliar applications, the highest BY and GY were obtained at primed seed treatment. Biological yield ranged from 6,466 kg ha^{-1} in non-primed seed and control foliar application to 8,062 kg ha^{-1} in combination primed seed and $ZnSO_4$ foliar application (Figure 4B). The highest GY (2,456 kg ha^{-1}) was observed in seed priming in combination with $ZnSO_4$ foliar application. This was statistically similar to the foliar application of silicon (2,353 kg ha^{-1}) at seed priming treatment. Foliar application of $ZnSO_4$ at seed primed and non-primed seed treatments increased GY by 18.51% and 9.60%, respectively. In addition, silicon foliar application at seed primed and non-primed seed treatments improved GY by 13.52% and 12.15%, respectively (Figure 4C). According to the results of the pot experiments, seed primed attained enlarged aboveground DM, grain weight, root DM, root volume, and root length by 9.56%, 10.56%, 9.64%, 8.95%, and 4.37%, respectively (Table 4).

TABLE 4 The mean comparisons of spike per m^2, kernels per spike, biological yield (BY), grain yield (GY), harvest index (HI), and grain Zn, Fe, and protein content of wheat are influenced by seed priming (SP) and foliar applications (FA).

Mean comparisons	Spike per m^2	Kernels per spike	HI (%)	Zn	Fe	Protein (%)
				(mg kg^{-1} DW)		
Year						
2021–2022	402^{b} ± 5.35	15.3^{b} ± 0.20	28.9^{a} ± 0.24	40.2^{a} ± 0.76	53.3^{a} ± 0.73	11.1^{a} ± 0.08
2022–2023	493^{a} ± 6.84	16.5^{a} ± 0.23	28.6^{a} ± 0.23	41.2^{a} ± 0.87	53.8^{a} ± 0.89	11.6^{a} ± 0.10
Priming						
Control	430^{a} ± 6.87	14.9^{b} ± 0.18	28.3^{b} ± 0.20	39.4^{b} ± 0.68	52.1^{b} ± 0.69	11.5^{b} ± 0.09
Priming	467^{a} ± 7.25	16.9^{a} ± 0.18	29.2^{a} ± 0.24	42.0^{a} ± 0.88	55.0^{a} ± 0.86	11.8^{a} ± 0.10
Foliar application						
Control	448^{a} ± 12.39	15.0^{d} ± 0.34	28.3^{b} ± 0.29	38.2^{b} ± 0.64	51.1^{b} ± 0.82	11.1^{c} ± 0.15
Urea	460^{a} ± 13.89	15.5^{cd} ± 0.28	27.1^{c} ± 0.27	38.0^{b} ± 0.46	51.6^{b} ± 0.55	12.5^{a} ± 0.14
Silicon	456^{a} ± 12.28	16.3^{ab} ± 0.37	29.4^{a} ± 0.26	38.7^{b} ± 0.60	51.7^{b} ± 0.95	11.4^{bc} ± 0.08
$FeSO_4$	437^{a} ± 10.96	16.0^{bc} ± 0.32	29.2^{a} ± 0.30	39.2^{b} ± 0.90	61.1^{a} ± 0.83	11.6^{b} ± 0.09
$ZnSO_4$	442^{a} ± 11.81	16.7^{a} ± 0.38	29.8^{a} ± 0.36	49.4^{a} ± 0.95	52.1^{b} ± 0.92	11.6^{b} ± 0.13

Year	1,000-grain weight (g)	BY	GY
		(kg ha^{-1})	
2021–2022	30.1^{b} ± 0.32	$5,808^{b}$ ± 63.0	$1,677^{b}$ ± 30.09
2022–2023	32.4^{a} ± 0.40	$8,510^{a}$ ± 95.4	$2,440^{a}$ ± 41.50

The mean comparisons of aboveground dry mass, grain weight, root dry mass, root length, and root volume wheat in the pot experiment.

	Dry mass weight	Grain weight	Root dry mass	Root length (cm)	Root volume (cm3 pot^{-1})
	(g pot^{-1})				
Control	13.6^{b} ± 0.33	5.49^{b} ± 0.21	1.66^{b} ± 0.04	5.03^{b} ± 0.11	84.7^{b} ± 1.1
Priming	14.9^{a} ± 0.48	6.07^{a} ± 0.12	1.82^{a} ± 0.06	5.48^{a} ± 0.16	88.4^{a} ± 0.92

As determined by Duncan's test, no significant difference at $p \leq 0.05$ exists between values in a column containing the same letter within a group. Data are the mean ± SE [n = 40 for year; n = 40 for seed priming; n = 16 for foliar application; n = 4 for seed priming in the pot experiment].

3.10 Grain Fe and Zn content

Grain Fe (55.0 mg kg^{-1} DW) and Zn (42.0 mg kg^{-1} DW) content in seed priming treatment was significantly higher than control. Maximum grain zinc content (49.4 mg kg^{-1} DW) was achieved in $ZnSO_4$ foliar spray. In comparison to the control, foliar applications of $ZnSO_4$ enhanced grain Zn content by 29.32%. Only $FeSO_4$ foliar application significantly increased grain Fe content compared to no foliar application. Grain Fe content ranged from 51.1 mg kg^{-1} DW for no foliar application to 61.1 mg kg^{-1} DW for $FeSO_4$ foliar application (Table 4).

3.11 Grain protein content

Because of seed priming, grain protein content increased from 11.5% to 11.8% in comparison with control. Overall, urea, $ZnSO_4$, $FeSO_4$, and silicon applied foliarly improved grain protein content as compared with control. However, silicon foliar applications are statistically similar to no foliar application in grain protein content. The protein content of grains ranged from 11.1% for no foliar application to 12.5% for urea foliar application (Table 4).

3.12 Correlation among traits

According to Table 5, there is a significant positive association between GY and all physiological traits except MDA concentration ($r = -0.62$, $p \leq 0.01$). Furthermore, there was a positive association among GY with BY ($r = 0.97$, $p \leq 0.01$), spike per m^2 ($r = 0.75$, $p \leq 0.01$), kernels per spike ($r = 0.69$, $p \leq 0.01$), 1,000-grain weight ($r = 0.61$, $p \leq 0.01$), and Zn content in grains ($r = 0.35$, $p \leq 0.01$). A positive correlation was found between BY, spike per m^2, kernels per spike, 1,000-grain weight, MSI, SOD and POD activity, Chl T, carotenoid, proline concentration, and grain Zn content. MSI was positively associated with Chl T ($r = 0.75$, $p \leq 0.01$), carotenoid ($r = 0.76$, $p \leq 0.01$), proline ($r = 0.44$, $p \leq 0.01$), GB ($r = 0.49$, $p \leq 0.01$), SOD activity ($r = 0.63$, $p \leq 0.01$), POD activity ($r = 0.64$, $p \leq 0.01$), grain Zn content ($r = 0.47$, $p \leq 0.01$), and grain Fe content ($r = 0.35$, $p \leq 0.05$), while MSI showed a strong negative relation with MDA

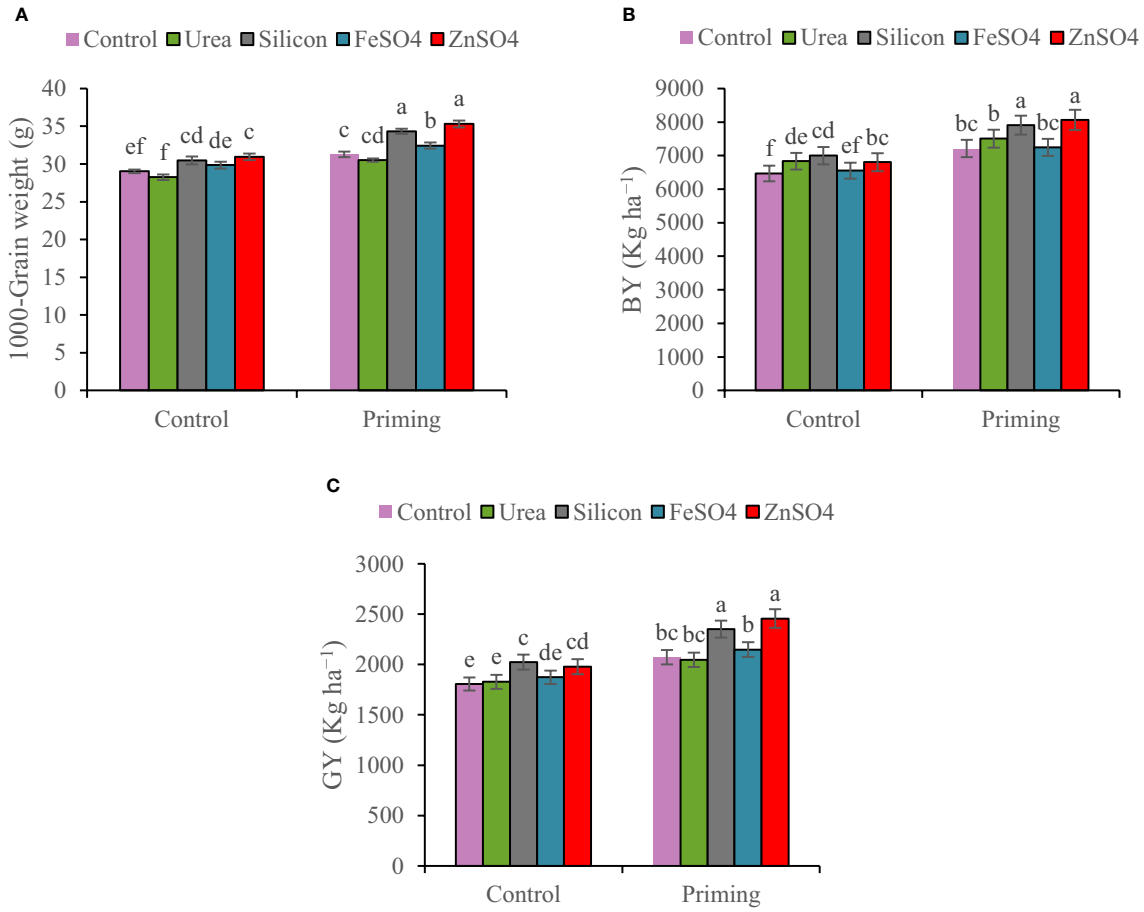

FIGURE 4
Mean comparison for interactions of seed priming × foliar application on **(A)** 1,000-grain weight, **(B)** biological yield (BY), and **(C)** grain yield (GY) of wheat. The Duncan's test indicates that columns labeled by the same letter are not significantly different at the $p \leq 0.05$ level. Each mean is accompanied by a standard error ($n = 8$).

content ($r = -0.75$, $p \leq 0.01$). The MSI is positively related to all traits except grain protein content while there is a significant negative relation between MDA and all traits investigated excluding grain protein content (no significant correlation between MDA with grain protein content). There was no significant relationship between Zn, Fe, and protein content of grains. Grain protein content exclusively had a significant association with proline and GB concentrations, and SOD and POD activity (Table 5).

4 Discussion

Uneven precipitation patterns in Mediterranean areas during rainfed wheat growing lead to soil moisture shortages (Moradi et al., 2022). In such situations, integrated agronomic crop management practices are required to alleviate drought stress's negative impacts (Melash et al., 2019). Seed priming (Liu et al., 2015; Rai-Kalal and Jajoo, 2021) and foliar application of nutrients and different compounds (Bukhari et al., 2021; Malik et al., 2021; Ghani et al., 2022) are two drought amelioration techniques. The combination of these practices can perform a key role in elevating plant tolerance to drought stress and improving GY and quality.

N, Fe, and Zn are essential nutrients needed for growth of plant and are essential components of a variety of critical physiological processes (Zain et al., 2015; Nehe et al., 2020; Sattar et al., 2021). Silicon is a nutrient that is currently receiving heightened interest from the scientific community, most notably in its application to drought resistance (Ayed et al., 2021; Bukhari et al., 2021; Sattar et al., 2021). Utilization of these elements through nutritional seed priming is considered a cost-efficient approach since only a small amount of nutrients are utilized to prime and ensure nutrient availability for germinating seeds (Farooq et al., 2021). In the late growth stages of rainfed wheat, insufficient soil moisture and limited root activity result in a reduction in nutrient uptake (Moradi et al., 2022). In the present study, the crop was exposed to a continuous increase in ambient temperature with a lack of atmospheric moisture and a decrease in soil moisture storage, especially during grain filling due to lack of rainfall. As a consequence, foliar application of nutrients during the final stages of growth, when soil nutrient application is impossible due to moisture limitations, leads to rapid absorption by the leaves (Aziz

TABLE 5 Correlation coefficients of grain yield (GY), biological yield (BY), harvest index (HI), spike per m2 (SP), kernels per spike (KS), 1,000-grain weight (GW), total chlorophyll (Chl T) and carotenoid (Car) content, membrane stability index (MSI), proline, glycine betaine (GB), and malondialdehyde (MDA) concentration, superoxide dismutase (SOD), peroxidase activity (POD), grain Zn content (Zn), grain Fe content (Fe), and grain protein content (GPC) of wheat are affected by priming levels and foliar applications.

	GY	BY	HI	SP	KS	GW	Chl T	Car	MSI	Proline	GB	MDA	SOD	POD	Zn	Fe	GPC
GY	1																
BY	0.97**	1															
HI	0.30**	0.06^{ns}	1														
SP	0.75**	0.80**	0.05^{ns}	1													
KS	0.69**	0.62**	0.39**	0.49**	1												
GW	0.61**	0.49**	0.57**	0.30**	0.75**	1											
Chl T	0.85**	0.78**	0.43**	0.53**	0.75**	0.75**	1										
CAR	0.77**	0.69**	0.44**	0.47**	0.70**	0.73**	0.92**	1									
MSI	0.61**	0.55**	0.32**	0.37**	0.67**	0.63**	0.75**	0.76**	1								
Proline	0.26*	0.23*	0.22*	0.17^{ns}	0.58**	0.54**	0.51**	0.46**	0.44**	1							
GB	0.23*	0.21^{ns}	0.28*	0.18^{ns}	0.52**	0.52**	0.44**	0.44**	0.49**	0.83**	1						
MDA	−0.62**	−0.52**	−0.50**	−0.35**	−0.75**	−0.83**	−0.82**	−0.81**	−0.75**	−0.61**	−0.63**	1					
SOD	0.30**	0.22*	0.41**	0.17*	0.63**	0.61**	0.55**	0.54**	0.63**	0.74**	0.80**	−0.73**	1				
POD	0.30**	0.24*	0.44**	0.10^{ns}	0.64**	0.71**	0.59**	0.59**	0.64**	0.77**	0.80**	−0.79**	0.87**	1			
Zn	0.35**	0.25*	0.40**	0.08^{ns}	0.46*	0.54**	0.6**	0.57**	0.47**	0.45**	0.38**	−0.48**	0.46**	0.52**	1		
Fe	0.10^{ns}	0.05^{ns}	0.25*	0.11^{ns}	0.23	0.18^{ns}	0.14^{ns}	0.27*	0.35**	0.10^{ns}	0.33**	−0.24*	0.46**	0.25*	0.04^{ns}		
GPC	−0.10^{ns}	−0.03^{ns}	−0.19^{ns}	0.02^{ns}	0.07^{ns}	−0.07^{ns}	0.03^{ns}	−0.01^{ns}	−0.01^{ns}	0.52**	0.49**	−0.10^{ns}	0.40**	0.29**	0.04^{ns}	0.16^{ns}	1

ns, non-significant; *p ≤ 0.05; **p ≤ 0.01.

10.3389/fpls.2023.1287677

et al., 2019; Melash et al., 2019). In this study, it was observed that seed priming and foliar spraying of $ZnSO_4$, silicon, $FeSO_4$, and urea alleviated adverse drought effects and improved plant physiological properties (Figures 1A–D, 2A, B, 3A–D).

Chlorophyll and carotenoids, which are pigments essential for photosynthesis, also play a crucial role (Kiran et al., 2021; Zhang et al., 2023). Water shortages exacerbate nutrients such as N, Zn, and Fe deficiency that reduce leaf pigment content due to a decrease in pigment synthesis, a reduction in the enzyme activity engaged in photosynthetic pigment synthesis, and a rise in photosynthetic pigment degradation (Kiran et al., 2021; Moradi et al., 2022; Zhang et al., 2023). Chlorophyll and carotenoid content are indicators of plant resistance to environmental stresses because it is directly linked with photosynthesis (Ayed et al., 2021). Nevertheless, our results indicated that overall chlorophyll and carotenoid content in primed seed was greater than in non-primed seed; foliar application (especially $ZnSO_4$ and silicon) increased photosynthetic pigments in both primed and unprimed seed treatments; however, foliage spraying had the greatest effect in primed seeds (Figures 1A–D). The increase in photosynthetic pigment contents due to priming and foliar application treatments enhances nutrient availability and water conservation (Hussain et al., 2019; Farooq et al., 2021). Numerous studies indicated that seed priming and foliar spraying of N, Fe, Zn, and silicon mitigated the injurious impacts of drought stress and enhanced leaf carotenoid and chlorophyll content (Hussain et al., 2019; Melash et al., 2019; Ayed et al., 2021; Farooq et al., 2021; Sattar et al., 2021). In the same way, our observations are also supported by Khan et al. (2022) and Anwar et al. (2021), who reported that seed priming and foliar application improved photosynthetic pigments. The higher content of photosynthetic pigments as a result of foliar spray and priming of nutrients can be associated with the presence of these elements in the structure of pigments (such as N in chlorophyll structure) and their effect on reducing negative effects of drought stress and ultimately preserving pigments. Increased leaf chlorophyll and carotenoid concentrations were detected under seed priming and foliar application, which not only improved photosynthesis but likewise enhanced crop growth, GY, and grain quality.

Under drought stress, plants maintain potential water balance and cellular metabolism by synthesizing and collecting compatible osmolytes such as GB and proline. Owing to osmolytes' functions of regulating osmotic pressure, maintaining turgor pressure, and regulating cell volume, metabolic activity is preserved under low water potential. Plants can also utilize GB and proline as nitrogen and carbon sources under extreme conditions (Tian et al., 2017; Bukhari et al., 2021). In the current research, seed priming and foliar application improved proline and GB concentrations. Foliar spraying of nutrients (mainly N and Zn) enhanced these compatible osmolytes in primed and non-primed seed treatment; however, proline and GB concentration improvement in primed seed was highest (Figures 2A, B). Foliar application of nutrients and seed priming preserve the plant and enhance growth by stimulating the synthesis of osmolytes and maintaining osmotic potential when water is scarce (Malik et al., 2021; Sattar et al., 2021; Saha et al., 2022). Various enzymatic antioxidants, such as SOD and POD, as well as non-enzymatic antioxidants, participate in ROS detoxification (Khan et al., 2023). Proline and GB are non-enzymatic antioxidants that protect the plant from negative effects by stabilizing reactive oxygen species (ROS; Malik et al., 2021; Malko et al., 2022). Several factors may have contributed to this elevation in GB and proline accumulation, including those attributed to the presence of these components in the structure of these osmolytes, as their participation in the structure of many enzymes engaged in the synthesis of these osmolytes as cofactors and the expression of genes encoding key enzymes involved in the synthesis of proline and GB have increased (Umair Hassan et al., 2020; Saha et al., 2022). Previous research demonstrated that foliar nutrients and seed priming raised proline and GB accumulation under drought stress (Bukhari et al., 2021; Malik et al., 2021; Singhal et al., 2021; Ghani et al., 2022).

Mineral nutrition acts as a key function in alleviating stress caused by drought in plants. Plants have several processes for dealing with drought damage, including enzymatic (for example POD) and antioxidants that are not enzyme-based (for example, proline and GB as free amino acids) (Malik et al., 2021; Malko et al., 2022). Seed priming and foliar application of nutrients reduce ROS damage via elevating enzymatic and non-enzymatic antioxidant contents and strengthening drought resistance in plants (Farooq et al., 2021; Malik et al., 2021; Sattar et al., 2021). In plants, antioxidants play an essential role in enhancing plant tolerance to stress in response to abiotic stresses (Khan et al., 2023). According to our results, seed priming and foliar application positively affected antioxidant enzymes (POD and SOD) activity. Seed priming together with foliar application of silicon, $ZnSO_4$, $FeSO_4$, and urea compared to foliar application of these compounds in unprimed seed increased POD activity by 24.40%, 22.55%, 25.36%, and 14.58%, respectively. Likewise, POD activity in no foliar application and primed seed treatment was 9.77% higher than in no foliar application and non-primed seed (Figure 3D). This study demonstrated that seed priming and foliar application of nutrients and elevated nutrient availability have a positive effect on POD and SOD activity, because it is due to the presence of these nutrients in the enzyme structure as well as many antioxidants contain this compound as cofactors (Karim et al., 2012; Rehman et al., 2018; Umair Hassan et al., 2020; Kiran et al., 2021; Saha et al., 2022). In previous research, it has been displayed that seed priming and foliar application of these components enhance the enzyme-based antioxidant defenses of plants (Kiran et al., 2021; Lv et al., 2021; Malik et al., 2021; Sattar et al., 2021; Singhal et al., 2021; Khan et al., 2022; Raza et al., 2023).

Stress induced by water and nutrient deficiency results in oxidative stress in plants, causing membrane lipid peroxidation. Tissue MDA amounts represent membrane lipid peroxidation, which eventually damages integrity of membranes (Chavoushi et al., 2020; Farooq et al., 2021). The MSI is widely recognized as a physiological marker and stress tolerance evaluation tool. Abiotic tolerance in plants relies heavily on maintaining membrane integrity and stability since membranes are the main targets of environmental stresses (Malik et al., 2021). The contents of the cell leak out when the membrane of cell is disrupted, reducing cell membrane development and elevating electrolyte leakage (Malik

et al., 2021; Singhal et al., 2021). In this study, seed priming and foliar spray of nutrients, and a co-application of these techniques, reduced MDA concentration and improved MSI (Figures 3A, B). The results of this experiment suggest that seed priming enhances root growth (Table 4) and increases access to water and nutrients. Nutrient supply via foliar spray and seed priming modulated ROS adversity by reducing the rate of lipid peroxidation (Figure 3A). As a result of regulating antioxidant mechanisms (Figures 3C, D) and maintaining lipid biological membranes (Figure 3B), it was evident that enzymatic activity (SOD and POD activity) had a strong positive correlation with non-enzymatic (carotenoid, proline, and GB concentration) antioxidants and MSI, and there was a significant negative correlation between MDA concentration with SOD and POD activity and carotenoid, proline, and GB concentration (Table 5). Our result is supported by previous studies that indicated that nutrient supply by foliar spray and seed priming stabilizes the membranes and reduces MDA concentration, which consequently mitigates oxidative stress and lowers membrane injury (Hussain et al., 2019; Chavoushi et al., 2020; Ayed et al., 2021; Farooq et al., 2021; Malik et al., 2021; Raza et al., 2023).

The growth, yield components, and GY are strongly related and the efficiency of one influences the other. Furthermore, a significant boost in growth and yield components improves the GY (Malko et al., 2022). According to this study, the seed priming had a positive influence on the kernels per spike, 1,000-grain weight, BY, GY, HI, and root growth (Table 4; Figure 4). Recently, numerous researchers (Rehman et al., 2018; Hussain et al., 2019; Ayed et al., 2021; Raza et al., 2023) reported that seed priming increased yield components and yield that supported our results. Enhanced tolerance in plants grown from a primed seed resulted in improved root development and, consequently, assisted in improved water and nutrition uptake under water scarcity conditions (Farooq et al., 2021). During the reproductive stage, water shortage, reduction in root activity, and nutrient deficiency in rainfed wheat affect grain development, kernels per spike, and grain weight, eventually reducing the yield and quality of final products (Saha et al., 2022). The present research found that foliar spray of $ZnSO_4$, silicon, and $FeSO_4$ during the terminal stage significantly increased kernels per spike, 1000-grain weight, BY, and GY in comparison with the control (Table 4 and Figure 4). Furthermore, urea foliar application significantly enhanced BY compared with the control (Figure 4). In this study, it seems that urea foliar spray, despite staying green (maintaining photosynthetic capacity and improving current photosynthesis) and increasing BY, has delayed leaf senescence and remobilization of dry matter to grain; ultimately, it had no significant effect on GY (the lowest HI obtained in urea foliar spray treatment). In the past, researchers have consistently published that foliar application of nutrients significantly improved yield components and GY (Karim et al., 2012; Zain et al., 2015; Sultana et al., 2018; Kiran et al., 2021). Analyses of correlation clearly confirmed that GY was closely associated with physiological characteristics (Table 5). This study describes that seed priming and foliar application of nutrients improved drought resistance through the increase in compatible osmolytes (GB and proline) and carotenoid concentrations (Figure 1D; Figure 2) and antioxidant enzyme (POD and SOD) activity (Figure 3B), decrease in MDA concentration (Figure 3A), and maintenance of cell membrane integrity (Figure 3B); prevented chlorophyll degradation (Figures 1A–C); and eventually enhanced GY (Figure 4C). Our results indicated that chlorophyll content, MSI (Table 3), spike per m^2, kernels per spike, 1,000-grain weight, and BY (Table 4) in plants during 2022–2023 were higher than those during the 2021–2022 growing season (Table 5; Figure 2), which might be associated with more precipitation in the second growing season (Table 2).

In this study, seed priming and nutrient foliar application influenced grain quality. We found that seed priming significantly increased grain Fe, Zn, and protein content (Table 4). An adequate nutrient source is extremely vital in seed germination and the initial stages of development; nutritional seed priming improves root growth, nutrient uptake, and plant growth (Farooq et al., 2021; Malko et al., 2022; Saha et al., 2022). Results of our pot experiment indicate that root growth is significantly improved by seed priming (Table 4). These findings suggest that the mechanism of improved grain quality by seed priming practice is based on the improvement in boosted root growth and development, enhanced nutrient absorption, and translocation of nutritional elements from root to shoot and grain, and ultimately led to improved grain quality (grain Zn, Fe, and protein content). This finding was in line with previous investigations suggesting that seed priming improves grain quality (Rehman et al., 2018; Anwar et al., 2021; Singhal et al., 2021). The application of nutrients in the terminal stage of rainfed wheat due to the high efficiency of foliar spraying is rapidly absorbed by plants. This permits nutrients to be transported directly to points with high metabolic demand (grains). Earlier studies showed that foliar nutrient application could boost grain quality (Melash et al., 2019; Sultana et al., 2018; Kiran et al., 2021; Kiran et al., 2021). In the current study, foliar nutrient application also improved grain quality. Foliar application of $ZnSO_4$, $FeSO_4$, and urea drastically boosted grain Zn, Fe, and protein content, respectively (Table 4). Thus, foliar nutrient delivery at the terminal stage is a high-efficiency method for biofortification in rainfed wheat cultivation. The farmer community can use seed priming and nutrient foliar application at the terminal stage to mitigate the adverse effects of drought stress and improve growth attributes, grain yield, and quality of rainfed wheat.

5 Conclusion

Results from this study have clearly demonstrated that the combination of seed priming [by urea (20 g L^{-1}) + $FeSO_4.7H_2O$ (50 ppm) + $ZnSO_4.7H_2O$ (50 ppm) + silicon (20 mg L^{-1}) solution] and foliar application of these compounds [urea (4%), silicon (4 mM), $FeSO_4.7H_2O$ (0.6%), and $ZnSO_4.7H_2O$ (0.4%)] improved physiological and yield characteristics. Foliar application of $ZnSO_4$, $FeSO_4$, and urea drastically affected grain Zn, Fe, and protein content, respectively. To improve drought resistance, GY, and quality of rainfed wheat, seed priming and foliar spraying are recommended as crop management practices. Future investigations are necessary to assess the influence of seed priming and foliar spray of these compounds at various growth stages on rainfed wheat in various cultivars and soils.

Data availability statement

The original contributions presented in the study are included in the article/supplementary material. Further inquiries can be directed to the corresponding author.

Author contributions

LM: Formal Analysis, Project administration, Software, Validation, Writing – original draft. AS: Funding acquisition, Investigation, Methodology, Project administration, Resources, Writing – review & editing.

Funding

The author(s) declare financial support was received for the research, authorship, and/or publication of this article. The authors are indebted to University of Kurdistan (UOK) for the financial support given to carry out this study.

Conflict of interest

The authors declare that the research was conducted in the absence of any commercial or financial relationships that could be construed as a potential conflict of interest.

Publisher's note

All claims expressed in this article are solely those of the authors and do not necessarily represent those of their affiliated organizations, or those of the publisher, the editors and the reviewers. Any product that may be evaluated in this article, or claim that may be made by its manufacturer, is not guaranteed or endorsed by the publisher.

References

Amanullah, K. A., Hussain, Z., and Jan, D. (2010). Performance of wheat cultivars sown at different seeding rates under drought-stress conditions. *Arch. Agron. Soil Sci.* 56, 99–105. doi: 10.1080/03650340902897641

Anwar, Z., Basharat, Z., Bilal Hafeez, M., Zahra, N., Rafique, Z., and Maqsood, M. (2021). Biofortification of maize with zinc and iron not only enhances crop growth but also improves grain quality. *Asian J. Agric. Biol.*. doi: 10.35495/ajab.2021.02.079

Arnon, D. I. (1949). Copper enzymes in isolated chloroplasts. Polyphenoloxidase in *Beta vulgaris*. *Plant Physiol.* 24 (1), 1. doi: 10.1104/pp.24.1.1

Ayed, S., Othmani, A., Bouhaouel, I., Rasâa, N., Othmani, S., and Amara, H. S. (2021). Effect of silicon (Si) seed priming on germination and effectiveness of its foliar supplies on durum wheat (*Triticum turgidum* L. ssp. durum) genotypes under semi-arid environment. *Silicon* 14, 1731–1741. doi: 10.1007/s12633-021-00963-2

Aziz, M. Z., Yaseen, M., Abbas, T., Naveed, M., Mustafa, A., Hamid, Y., et al. (2019). Foliar application of micronutrients enhances crop stand, yield and the biofortification essential for human health of different wheat cultivars. *J. Integr. Agric.* 18, 1369–1378. doi: 10.1016/S2095-3119(18)62095-7

Bajji, M., Kinet, J. M., and Lutts, S. (2002). The use of the electrolyte leakage method for assessing cell membrane stability as a water stress tolerance test in durum wheat. *Plant Growth Regul.* 36, 61–70. doi: 10.1023/A:1014732714549

Bates, L. S., Waldren, R. A., and Teare, I. D. (1973). Rapid determination of free proline for water-stress studies. *Plant soil.* 39, 205–207. doi: 10.1007/BF00018060

Beauchamp, C., and Fridovich, I. (1971). Superoxide dismutases: improved assays and an assay applicable to acrylamide gels. *Anal. Biochem.* 44, 276–287. doi: 10.1016/0003-2697(71)90370-8

Blandino, M., Visioli, G., Marando, S., Marti, A., and Reyneri, A. (2020). Impact of late-season N fertilisation strategies on the gluten content and composition of high protein wheat grown under humid Mediterranean conditions. *J. Cereal Sci.* 94, 102995. doi: 10.1016/j.jcs.2020.102995

Bukhari, M. A., Ahmad, Z., Ashraf, M. Y., Afzal, M., Nawaz, F., Nafees, M., et al. (2021). Silicon mitigates drought stress in wheat (*Triticum aestivum* L.) through improving photosynthetic pigments, biochemical and yield characters. *Silicon* 13, 4757–4772. doi: 10.1007/s12633-020-00797-4

Chavoushi, M., Najafi, F., Salimi, A., and Angaj, A.. (2020). Effect of salicylic acid and sodium nitroprusside on growth parameters, photosynthetic pigments and secondary metabolites of safflower under drought stress. *Sci. Hortic.* 259, 108–121. doi: 10.1016/j.scienta.2019.108823

Das, B. S., Wani, S. P., Benbi, D. K., Muddu, S., Bhattacharyya, T., Mandal, B., et al. (2022). Soil health and its relationship with food security and human health to meet the sustainable development goals in India. *Soil Secur.* 8, 100071. doi: 10.1016/j.soisec.2022.100071

Duncan, O. D. (1966). Path analysis: sociological examples. *Am. J. Sociol.* 72, 116. doi: 10.1086/224256

Farooq, M., Almamari, S. A. D., Rehman, A., Al-Busaidi, W. M., Wahid, A., and Al-Ghamdi, S. S. (2021). Morphological, physiological and biochemical aspects of zinc seed priming-induced drought tolerance in faba bean. Sci. *Hortic* 281, 109894. doi: 10.1016/j.scienta.2021.109894

Farooq, M., Wahid, A., and Siddique, K. H. (2012). Micronutrient application through seed treatments: a review. *J. Soil Sci. Plant Nutr.* 12 (1), 125–142. doi: 10.4067/S0718-95162012000100011

Ghani, M. I., Saleem, S., Rather, S. A., Rehmani, M. S., Alamri, S., Rajput, V. D., et al. (2022). Foliar application of zinc oxide nanoparticles: An effective strategy to mitigate drought stress in cucumber seedling by modulating antioxidant defense system and osmolytes accumulation. *Chemosphere* 289, 133202. doi: 10.1016/j.chemosphere.2021.133202

Grieve, C. M., and Grattan, S. R. (1983). Rapid assay for determination of water soluble quaternary ammonium compounds. *Plant Soil.* 70, 303–307. doi: 10.1007/BF02374789

Heath, R. L., and Packer, L. (1968). Photo peroxidation in isolated chloroplasts: I. Kinetics and stoichiometry of fatty acid peroxidation. *Arch. Biochem. Biophys.* 125 (1), 189–198. doi: 10.1016/0003-9861(68)90654-1

Hemeda, H. M., and Klein, B. P. (1990). Effects of naturally occurring antioxidants on peroxidase activity of vegetable extracts. *J. Food. Sci.* 55 (1), 184–185. doi: 10.1111/j.1365-2621.1990.tb06048.x

Hussain, A., Rizwan, M., Ali, Q., and Ali, S. (2019). Seed priming with silicon nanoparticles improved the biomass and yield while reduced the oxidative stress and cadmium concentration in wheat grains. *Environ. Sci. pollut. Res.* 26, 7579–7588. doi: 10.1007/s11356-019-04210-5

Johnson, S. E., Lauren, J. G., Welch, R. M., and Duxbury, J. M. (2005). A comparison of the effects of micronutrient seed priming and soil fertilization on the mineral nutrition of chickpea (*Cicer arietinum*), lentil (*Lens culinaris*), rice (*Oryza sativa*) and wheat (*Triticum aestivum*) in Nepal. *Exp. Agric.* 41, 427–448. doi: 10.1017/S0014479705002851

Jones, J. B., and Case, V. W. (1990). Sampling, handling, and analyzing plant tissue samples. *Soil Test Plant Anal.* 3, 389–427. doi: 10.2136/sssabookser3.3ed.c15

Karim, M. R., Zhang, Y. Q., Zhao, R. R., Chen, X. P., Zhang, F. S., and Zou, C. Q. (2012). Alleviation of drought stress in winter wheat by late foliar application of zinc, boron, and manganese. *J. Plant Nutr. Soil Sci.* 175 (1), 142–151. doi: 10.1002/jpln.201100141

Khan, S., Ibrar, D., Bashir, S., Rashid, N., Hasnain, Z., Nawaz, M., et al. (2022). Application of moringa leaf extract as a seed priming agent enhances growth and physiological attributes of rice seedlings cultivated under water deficit regime. *Plants* 11 (3), 261. doi: 10.3390/plants11030261

Khan, S., Ibrar, D., Hasnain, Z., Nawaz, M., Rais, A., Ullah, S., et al. (2023). Moringa leaf extract mitigates the adverse impacts of drought and improves the yield and grain quality of rice through enhanced physiological, biochemical, and antioxidant activities. *Plants* 12 (13)2511. doi: 10.3390/plants12132511

Kiran, A., Wakeel, A., Sultana, R., Khalid, A., Mubaraka, R., Shahzad, A. N., et al. (2021). Concentration and localization of Fe and Zn in wheat grain as affected by its application to soil and foliage. *Bull. Environ. Contam. Toxicol.* 106, 852–858. doi: 10.1007/s00128-021-03183-x

Liu, C., Yang, Z., and Hu, Y. G. (2015). Drought resistance of wheat alien chromosome addition lines evaluated by membership function value based on multiple traits and drought resistance index of grain yield. *Field Crops Res.* 179, 103–112. doi: 10.1016/j.fcr.2015.04.016

Liu, Y., Zhang, P., Li, M., Chang, L., Cheng, H., Chai, S., et al. (2020). Dynamic responses of accumulation and remobilization of water soluble carbohydrates in wheat stem to drought stress. *Plant Physiol. Biochem.* 155, 262–270. doi: 10.1016/j.plaphy.2020.07.024

Lv, X., Ding, Y., Long, M., Liang, W., Gu, X., Liu, Y., et al. (2021). Effect of foliar application of various nitrogen forms on starch accumulation and grain filling of wheat (*Triticum aestivum* L.) under drought stress. *Front. Plant Sci.* 12. doi: 10.3389/fpls.2021.645379

Malik, M. A., Wani, A. H., Mir, S. H., Rehman, I. U., Tahir, I., Ahmad, P., et al. (2021). Elucidating the role of silicon in drought stress tolerance in plants. *Plant Physiol. Biochem.* 165, 187–195. doi: 10.1016/j.plaphy.2021.04.021

Malko, M. M., Khanzada, A., Xiao, W. A. N. G., Samo, A., Li, Q., Dong, J. I. A. N. G., et al. (2022). Chemical treatment refines drought tolerance in wheat and its implications in changing climate: A review. *Plant Stress* 100118. doi: 10.1016/j.stress.2022.100118

Melash, A. A., Mengistu, D. K., Aberra, D. A., and Tsegay, A. (2019). The influence of seeding rate and micronutrients foliar application on grain yield and quality traits and micronutrients of durum wheat. *J. Cereal Sci.* 85, v221–v227. doi: 10.1016/j.jcs.2018.08.005

Moradi, L., Siosemardeh, A., Sohrabi, Y., Bahramnejad, B., and Hosseinpanahi, F. (2022). Dry matter remobilization and associated traits, grain yield stability, N utilization, and grain protein concentration in wheat cultivars under supplemental irrigation. *Agric. Water Manage.* 263, 107449. doi: 10.1016/j.agwat.2021.107449

Nehe, A. S., Misra, S., Murchie, E. H., Chinnathambi, K., Tyagi, B. S., and Foulkes, M. J. (2020). Nitrogen partitioning and remobilization in relation to leaf senescence, grain yield, and protein concentration in Indian wheat cultivars. *Field Crops Res.* 251, 107778. doi: 10.1016/j.fcr.2020.107778

Rai-Kalal, P., and Jajoo, A. (2021). Priming with zinc oxide nanoparticles improve germination and photosynthetic performance in wheat. *Plant Physiol. Biochem.* 160, 341–351. doi: 10.1016/j.plaphy.2021.01.032

Raza, M. A. S., Zulfiqar, B., Iqbal, R., Muzamil, M. N., Aslam, M. U., Muhammad, F., et al. (2023). Morpho-physiological and biochemical response of wheat to various treatments of silicon nano-particles under drought stress conditions. *Sci. Rep.* 13, 2700. doi: 10.1038/s41598-023-29784-6

Rehman, A., Farooq, M., Naveed, M., Nawaz, A., and Shahzad, B. (2018). Seed priming of Zn with endophytic bacteria improves the productivity and grain biofortification of bread wheat. *Eur. J. Agron.* 94, 98–107. doi: 10.1016/j.eja.2018.01.017

Reis, S., Pavia, I., Carvalho, A., Moutinho-Pereira, J., Correia, C., and Lima-Brito, J. (2018). Seed priming with iron and zinc in bread wheat: effects in germination, mitosis and grain yield. *Protoplasma* 255, 1179–1194. doi: 10.1007/s00709-018-1222-4

Saha, D., Choyal, P., Mishra, U. N., Dey, P., Bose, B., Prathibha, M. D., et al. (2022). Drought stress responses and inducing tolerance by seed priming approach in plants. *Plant Stress* 4, 100066. doi: 10.1016/j.stress.2022.100066

Sattar, A., Wang, X., Abbas, T., Sher, A., Ijaz, M., Ul-Allah, S., et al. (2021). Combined application of zinc and silicon alleviates terminal drought stress in wheat by triggering morpho-physiological and antioxidants defense mechanisms. *PloS One* 16 (10), e0256984. doi: 10.1371/journal.,pone.0256984

Singhal, R. K., Pandey, S., and Bose, B. (2021). Seed priming with Mg (NO3) 2 and $ZnSO_4$ salts triggers physio-biochemical and antioxidant defense to induce water stress adaptation in wheat (*Triticum aestivum* L.). *Plant Stress* 2, 100037. doi: 10.1016/j.stress.2021.100037

Sultana, S., Naser, H. M., Quddus, M. A., Shill, N. C., and Hossain, M. A. (2018). Effect of foliar application of iron and zinc on nutrient uptake and grain yield of wheat under different irrigation regimes. *Bangladesh J. Agric. Res.* 43 (3), 395–406. doi: 10.3329/bjar.v43i3.38388

Szerement, J., Szatanik-Kloc, A., Mokrzycki, J., and Mierzwa-Hersztek, M. (2022). Agronomic biofortification with Se, Zn, and Fe: An effective strategy to enhance crop nutritional quality and stress defense—A Review. *J. Soil Sci. Plant Nutr.* 22, 1129–1159. doi: 10.1007/s42729-021-00719-2

Tian, F., Wang, W., Liang, C., Wang, X., Wang, G., and Wang, W. (2017). Over accumulation of glycine betaine makes the function of the thylakoid membrane better in wheat under salt stress. *Crop J.* 5, 73–82. doi: 10.1016/j.cj.2016.05.008

Umair Hassan, M., Aamer, M., Umer Chattha, M., Haiying, T., Shahzad, B., Barbanti, L., et al. (2020). The critical role of zinc in plants facing the drought stress. *Agriculture* 10, 396. doi: 10.3390/agriculture10090396

Wang, S., Sun, N., Yang, S., Tian, X., and Liu, Q. (2021). The effectiveness of foliar applications of different zinc source and urea to increase grain zinc of wheat grown under reduced soil nitrogen supply. *J. Plant Nutr.* 44, 644–659. doi: 10.1080/01904167.2020.1849286

Zadoks, J. C., Chang, T. T., and Konzak, C. F. (1974). A decimal code for the growth stages of cereals. *Weed Res.* 14, 415–421. doi: 10.1111/j.1365-3180.1974.tb01084.x

Zain, M., Khan, I., Qadri, R. W. K., Ashraf, U., Hussain, S., Minhas, S., et al. (2015). Foliar application of micronutrients enhances wheat growth, yield and related attributes. *Am. J. Plant Sci.* 6, 864. doi: 10.4236/ajps.2015.67094

Zhang, J., Mu, J., Hu, Y., Ren, A., Lei, B., Ding, B., and Gao, Z. (2023). Effect of Planting Patterns and Seeding Rate on Dryland Wheat Yield Formation and Water Use Efficiency on the Loess Plateau, China. *Agronomy* 13, 851. doi: 10.4236/ajps.2015.67094

frontiers | Frontiers in Plant Science

TYPE Review
PUBLISHED 03 April 2024
DOI 10.3389/fpls.2024.1377964

OPEN ACCESS

EDITED BY
Md Sazzad Hossain,
University of Kiel, Germany

REVIEWED BY
Liu Haitao,
Henan Agricultural University, China
Ewa Joanna Hanus-Fajerska,
University of Agriculture in Krakow, Poland

*CORRESPONDENCE
Mohammad Mukarram
mdmukarram007@gmail.com

RECEIVED 28 January 2024
ACCEPTED 18 March 2024
PUBLISHED 03 April 2024

CITATION
Mukarram M, Ahmad B, Choudhary S, Konôpková AS, Kurjak D, Khan MMA and Lux A (2024) Silicon nanoparticles *vs* trace elements toxicity: *Modus operandi* and its omics bases.
Front. Plant Sci. 15:1377964.
doi: 10.3389/fpls.2024.1377964

Silicon nanoparticles *vs* trace elements toxicity: *Modus operandi* and its omics bases

Mohammad Mukarram [1,2*], Bilal Ahmad [3], Sadaf Choudhary [4], Alena Sliacka Konôpková [5,6], Daniel Kurjak [5,6], M. Masroor A. Khan [4] and Alexander Lux [7,8]

[1]Food and Plant Biology Group, Department of Plant Biology, School of Agriculture, Universidad de la Republica, Montevideo, Uruguay, [2]Department of Phytology, Faculty of Forestry, Technical University in Zvolen, Zvolen, Slovakia, [3]Plant Physiology Section, Department of Botany, Government Degree College for Women, Pulwama, Jammu and Kashmir, India, [4]Advance Plant Physiology Section, Department of Botany, Aligarh Muslim University, Aligarh, India, [5]Department of Integrated Forest and Landscape Protection, Faculty of Forestry, Technical University in Zvolen, Zvolen, Slovakia, [6]Institute of Forest Ecology, Slovak Academy of Sciences, Zvolen, Slovakia, [7]Department of Plant Physiology, Faculty of Natural Sciences, Comenius University in Bratislava, Bratislava, Slovakia, [8]Institute of Chemistry, Slovak Academy of Sciences, Bratislava, Slovakia

Phytotoxicity of trace elements (commonly misunderstood as 'heavy metals') includes impairment of functional groups of enzymes, photo-assembly, redox homeostasis, and nutrient status in higher plants. Silicon nanoparticles (SiNPs) can ameliorate trace element toxicity. We discuss SiNPs response against several essential (such as Cu, Ni, Mn, Mo, and Zn) and non-essential (including Cd, Pb, Hg, Al, Cr, Sb, Se, and As) trace elements. SiNPs hinder root uptake and transport of trace elements as the first line of defence. SiNPs charge plant antioxidant defence against trace elements-induced oxidative stress. The enrolment of SiNPs in gene expressions was also noticed on many occasions. These genes are associated with several anatomical and physiological phenomena, such as cell wall composition, photosynthesis, and metal uptake and transport. On this note, we dedicate the later sections of this review to support an enhanced understanding of SiNPs influence on the metabolomic, proteomic, and genomic profile of plants under trace elements toxicity.

KEYWORDS

silica, trace elements, metal stress, nanoparticles, heavy metal, oxidative stress, metalloid stress, sequestration

1 Prologue: 'heavy metals' or 'trace elements': a terminological dilemma?

The term 'heavy metal' loosely signifies metals with a density higher than 7 g/cm^3 (Bjerrum, 1936). The group supposedly enlist metals considered contaminants and can cause phytotoxicity or ecotoxicity *sensu lato*. However, there are several inconsistencies. Firstly, no authoritative list exists till now that notes all the heavy metals. Secondly, the 'heaviness' is somehow perceived as 'toxicity', which gave rise to anomalies such as including arsenic and antimony in this group even when they are not metals. Thirdly, density is neither a promising predictive factor when studying metal interaction with living organisms nor explains significant details about the element itself (Nieboer and Richardson, 1980). Thus, categorising them according to density is crude and non-scientific. Understandably, this classification has been refuted several times by plant scientists and others alike (Hodson, 2004; Appenroth, 2010). While Chapman (2007) amusingly suggests that the term would be better off with the 'music' industry rather than science, Duffus (2002) considers the word 'meaningless' and 'misleading'. The IUPAC (International Union of Pure and Applied Chemistry) has neither recommended this term. It is unfortunate to witness the ever-increasing use of 'heavy metals' in the title and topic of refereed publications from several highly cited journals of plant and environmental science (see Pourret and Bollinger, 2017). It poses a moral dilemma for young researchers whether to use this term since the keyword 'heavy metals' still has massive indexing and visibility on scientific databases e.g., Web of Science and Scopus. Maybe it is what encourages the established research from the field to still use this misnomer (Cobbett and Goldsbrough, 2002; Rascio and Navari-Izzo, 2011; Ali et al., 2013; Pollard et al., 2014; Adrees et al., 2015).

Contrary to 'heavy' metals, other more appropriate and scientifically sound terms should be used to signify the characteristics and properties of the studied element. This could include 'trace metals', 'toxic trace elements', or 'potentially toxic trace elements' in perspective research. 'Trace elements' are those elements 'found in low concentration, in mass fractions of ppm or less, in some specified source, e.g., soil, plant, tissue, groundwater, etc.' (Duffus, 2002). However, referring to these elements or metals as toxic is imprecise again or redundant at best. Paracelsus (1493-1541) laid the fundamental rule of toxicology: all elements and their derivatives are toxic in high enough doses (see Duffus, 2002). Therefore, we recommend the usage of 'trace elements' in the title and as a topic for future studies related to toxic trace elements. We also urge the responsible authorities, particularly editorial board members, to discourage the usage of the 'heavy metals' keyword in future submissions.

2 Introduction

A plant's health chiefly depends on soil composition. Soils have frequently been exposed to excessive amounts of essential and non-essential nutrients through industrial wastes, municipal composts, agricultural effluents, sewage sludge and surface mining wastes, and their toxic levels damage plant species differently (DalCorso, 2012). Trace elements (TEs) are a group of elements present in low concentration (mass fraction of ppm or less) in the specified medium (soil, plant, etc.) and includes Cd, Pb, Mn, As, Fe, Cr, Cu, Ni, Co, Ag, Zn, Sb, Ti, and Hg. TEs contamination has become a severe environmental threat worldwide. Besides naturally deriving from parent rocks, most of the TEs in the soils result from anthropogenic activities such as mining and processing of metal ores, energy and fuel production, intensive agriculture, and sewage processing, including several other industrial processes (Tóth et al., 2000; Khan et al., 2008; Brunetti et al., 2009; Yadav et al., 2019). TEs are not bio- or thermo-degradable so that they may persist in the soil for thousands of years, given their relative non-mobility and their technically and financially demanding remediation from the soil (Rahimi et al., 2017; Masindi and Muedi, 2018). Natural soils are the primary source of TEs in plants. Despite the selective membrane of root cells, much of the elements present in the soil translocate into plant tissues. In contrast, their availability depends mainly on the solubility in the soil solution or the root exudates (Blaylock and Huang, 2000). Therefore, the plants may efficiently uptake hazardous TE levels, affecting their functioning and animal and human health through the food chain (Adriano, 2001).

Some trace elements such as Zn, Cu, Ni, Fe, Mo, and Mn are essential for plant metabolism. Zn has been shown to play a crucial role in enzyme systems involved in carbohydrate and protein metabolism, auxin formation, and stabilises cell membrane integrity (Hafeez, 2013). There is also evidence that Zn may contribute to the plant defence system by regulating stress protein expression and stimulating the antioxidant enzymes (Cabot et al., 2019; Hassan et al., 2020). Ni has been reported as an integral component of various enzymes essential for ureolysis, nitrogen fixation, hydrogen metabolism, and antioxidant system (Fabiano et al., 2015; Lavres et al., 2016; Siqueira Freitas et al., 2018). Similarly, Fe forms cofactors of many vital enzymes and is a central component of the electron transport chain and a crucial element for chlorophyll biosynthesis (Schmidt et al., 2020). Cu plays a pivotal role in regulating the photosynthetic and respiratory electron transport chain, besides affecting cell wall formation, antioxidant activities, and hormone perception (Yamasaki et al., 2008; Printz et al., 2016). Furthermore, Mn is crucial for photosynthetic machinery as the primary cofactor for the oxygen-evolving complex in photosystem II (PSII) and may participate in plant antioxidative system (Millaleo et al., 2010; Alejandro et al., 2020). Besides the earlier mentioned TEs, several studies proved the beneficial role of Co and Cr for plant growth and yield, although they are not classified as essential nutrients (Samantaray et al., 1998; Gad, 2012; Akeel and Jahan, 2020). On the contrary, TEs such as Pb, Cd, Hg, and As have no documented beneficial role in the metabolism of higher plants. They are considered the "main threats" even in trace amounts (Chibuike and Obiora, 2014). The effect of TEs toxicity depends, of course, on a particular element involved in the process and its concentration in the soil. However, it may vary significantly among plant species and varieties. Such variations result from the different (i) pathways and mechanics through which TEs are absorbed by roots (Williams et al., 2000), (ii)

mechanisms of their releasing and redistribution into the shoot, and (iii) abilities to exclude, chelate or accumulate TEs in particular structures, which plants have adopted (Salt et al., 1998). These mechanisms are involved in the maintenance of essential TEs homeostasis. Furthermore, the plant species can be divided into (hyper)accumulating and non-accumulating plants, whereas most of the plant kingdom is considered non-accumulators (Viehweger, 2014). However, in general, TEs toxicity leads to the blocking of functional groups of many enzymes (Tang et al., 2020), malfunctions in photosynthetic machinery (Giannakoula et al., 2021), production of reactive oxygen species (ROS) and associated oxidative damage (Ma et al., 2022; Sardar et al., 2022), and impairment of plant mineral nutrition through the replacement of essential nutrients at cation exchange sites of plants (Arif et al., 2016). Such alterations in overall biochemistry and physiology affect plant development and growth and may lead to plant death in severe cases (Chibuike and Obiora, 2014).

To date, only a handful of published articles target the interaction of TEs with silicon nanoparticles (SiNPs). The existing reviews on this nexus deal mostly with heavy metals, the term which is in itself confusing (*vide supra* section Prologue), and therefore, several toxic elements were purposefully left behind. Also, the existing literature reviews often need to restrict their significant discussion to SiNPs over bulk silicon or address the omics aspect sufficiently. In our earlier review article, we demonstrated SiNPs potential in mitigating the abiotic stress in general, where heavy metal stress was also discussed (Mukarram et al., 2022). Nonetheless, one of this article's limitations was the absence of an elaborated mechanism on SiNPs dialogue with TEs toxicity.

To overcome these concerns, we included a wide range of toxic elements in the present review that were studied with SiNPs, irrespective of their 'heavy metals' stigma. We also addressed how SiNPs could interact with plant metabolomics, proteomics, and genomics during TEs toxicity. So, the novelty of this review article over the existing ones lies in its understanding of the SiNPs-TEs interaction and its omics perspective. Through this article, we hope to instigate a discussion among the silicon community regarding its active correspondence with plant physiology, especially when there are still several ambiguities around this nexus.

3 Trace elements phytotoxicity

Although several TEs are essential to plants, their overaccumulation in agricultural soils endangers plant growth and development while compromising crop marketability and global food security (Asati et al., 2016; Figure 1). Variations in responses of different plant species to TEs toxicity have been observed. Plant behaviour can change with soil pH and composition and specific TEs. TEs toxicity potentially alters root and shoot morphology and anatomy (Martinka et al., 2014). It adversely affects photosynthesis and respiration by changing the leaf's structural integrity and physiology, damaging energy (photon) allocation, and regulating critical metabolic processes (Küpper et al., 2002; Ying et al., 2010; Chandra and Kang, 2016). Hampered growth, chlorosis, necrosis, changes in stomatal functions, leaf rolling, lowered water potential, altered membrane function, efflux of cations, and changes in the activities of critical metabolic enzymes are the widely reported symptoms of TEs toxicity in plants (Van Assche and Clijsters, 1990; Marschner, 2012; Hasan et al., 2017; Aponte et al., 2020). TEs toxicity severely affects PSI and PSII, restricting photosynthetic output. TEs accumulation targets two crucial photosynthetic enzymes, i.e., ribulose 1,5-bisphosphate carboxylase (RuBisCO) and phosphoenol pyruvate carboxylase. Cd has been reported to alter the structure and activity of RuBisCO by substituting Mg^{++} ions, which are needed as a cofactor of carboxylation reactions (Ashfaque et al., 2016). At the cellular level, these TEs cause configurational changes in the

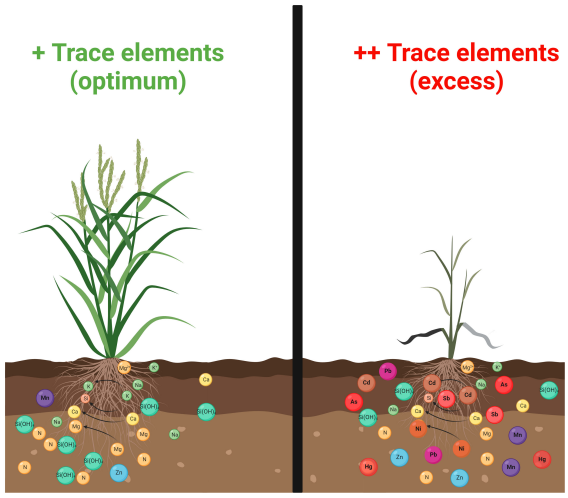

FIGURE 1
Trace elements (TEs) phytotoxicity in higher plants. The optimum concentration of several TEs promotes plant growth and development (such as Zn, Cu, Ni, Fe, Mo, Mn, Cu, and Cr) (panel on the left). Nonetheless, their overaccumulation, in addition to other toxic elements (such as Hg, As, Cd, and Pb), jeopardises cellular homeostasis and retard plant physiology and productivity (panel on the right).

endoplasmic reticulum, Golgi apparatus, chloroplast, and mitochondria and increase nucleus size and cellular vacuolisation (Małkowski et al., 2019; Sperdouli et al., 2022; Liu et al., 2023). A rise in oxidative stress linked with excessive accumulation of TE ions is strongly considered the first symptom of TE-induced toxicity (Rodríguez-Serrano et al., 2009; Sharma and Dietz, 2009; Ghori et al., 2019; Gupta et al., 2019; Ma et al., 2022). To cope with the oxidative stress caused by TEs toxicity and protect cellular and subcellular compartments, plants have developed several mechanisms to sustain the essential TEs ion concentrations and lessen exposure to non-essential TEs. Among these tolerance mechanisms, some are required for metal homeostasis that lowers the damage via exclusion, detoxification, the restriction of metal ions into the apoplast, and the extracellular chelation of metal ions (Ovečka and Takáč, 2014). However, other mechanisms involve extruding individual TE ions from the intracellular environment or their sequestration into the compartments to separate them from other important cellular components (Manara, 2012). Hyper-tolerance and the hyperaccumulation of TEs in the plant body without having any harmful effect on viability are the best-known strategies employed by plants under a TEs-induced toxic environment (Baker and Brooks, 1989; Assunção et al., 2001, Assunção et al., 2003; Vaculík et al., 2009, Vaculík et al., 2012; Van der Ent et al., 2013; Baker et al., 2020; Pinto Irish et al., 2023).

4 SiNPs and plants: uptake and action during the optimal environment

Although biogenic silicon (bulk-Si) is classified as a non-essential element for plant growth and development, its stress-mitigating potential has been widely reported (Korndörfer and Lepsch, 2001; Ma, 2004; Liang et al., 2015; Luyckx et al., 2017; Vaculík et al., 2020). Silicon is the most abundant metalloid on the earth's surface. However, most Si is present in the soil as insoluble oxides or silicates, which is unavailable for plant uptake. The chemical weathering of silicate minerals liberates dissolved Si as plant-available monosilicic acid, whereas its concentration in soil solution commonly varies between 0.1 and 0.6 mM (Epstein, 1994; Hodson et al., 2005). In this context, recent advances in nanotechnology could alleviate the scarfed amount of monosilicic acid in most cultivated soil and the limits of silicate fertilisation via the connection of Si-derived benefits with benefits associated with the properties of nanoparticles (Bhat et al., 2021). The smaller size and broader absorption surface area of SiNPs over bulk-Si should enable their easier absorption, distribution, and accumulation in plants (Galbraith, 2007). However, Etxeberria et al. (2009) consider nanoparticle uptake an active transport requiring various other cellular mechanisms such as recycling, signalling, and regulating the plasma membrane.

Despite a scarcity of available reports, Mukarram et al. (2022) discussed the SiNPs could follow a similar transport route as their bulk counterpart – the plant root absorbs Si from the soil solution in the form of monosilicic acid ($Si(OH)_4$) (Mitani-Ueno and Ma, 2021). The absorption and distribution of Si in the plant are ensured by two different types of Si transporters: channel-type transporters (referred to as Low Silicon 1, Lsi1) and efflux transporters (referred to as Low Silicon 2, Lsi2), which were first described in rice (Ma et al., 2006, Ma et al., 2007). The Lsi1 from the nodulin-26 major intrinsic protein (NIP) III subgroup of aquaporins drives the passive influx of Si from the apoplast into the root cells. At the same time, Lsi2, belonging to an uncharacterised anion transporter family, is responsible for the active efflux of Si from the root cells towards the xylem, i.e., xylem loading (Ma and Yamaji, 2015). Following monosilicic acid absorption in the root stele, Si is transported to the shoot through the xylem by transpirational flow, with subsequent Si unloading to the leaf epidermal cells. As the content of monosilicic acid in the cells increases, monosilicic acid becomes highly polymerised and changes to form an amorphous silica gel ($SiO_2{\cdot}nH_2O$) (Mitani et al., 2005; Schaller et al., 2021; de Tombeur et al., 2022). The silica can accumulate under the epidermal cell wall, forming cuticle-silica double layers which provide additional protection against mechanical injury and fungal, bacterial, nematode, and insect attacks (Debona et al., 2017; Rastogi et al., 2019; Zellner et al., 2021). The transporter ensuring the xylem loading is not yet fully known undoubtedly. However, Yamaji et al. (2008) described the Lsi6 transporter in rice, which is responsible for the Si unloading from the xylem and subsequently regulating its deposition in the shoots (Figure 2).

All abovementioned transporters are localised in the plasma membrane; however, they show different tissue and/or cellular specificity of their localisation, indicating that they are involved in different steps of absorption, xylem loading, and distribution of Si (Ma et al., 2011; Ma and Yamaji, 2015). Besides, interspecific differences in the presence, tissue, cellular localisation, and polarity of transporters, as well as their expression patterns, exist, determining the different abilities to accumulate Si in various plant species (Ma et al., 2011; Ma and Yamaji, 2015; Mitani-Ueno and Ma, 2021). Accordingly, the plant species are divided into accumulators, intermediate accumulators, and non-accumulators (Takahashi et al., 1990). The Poaceae, Equisetaceae and Cyperaceae families are known accumulators (>4% Si), the Cucurbitales, Urticales and Commelinaceae intermediate Si accumulators (2–4% Si), while most of the other species have little or no ability to accumulate Si (Hodson et al., 2005; Currie and Perry, 2007).

SiNPs involvement with several metabolic and physiological activities has been described under optimal and stress conditions (El-Shetehy et al., 2021; Fan et al., 2022; Naaz et al., 2023). SiNPs can improve photosynthesis by PSII reaction centres opening and promoting the absorption, transmission, and transformation of light energy, the electron transport rate of PSII, chlorophyll and carotenoid biosynthesis, and other related enzymes (Sharifi-Rad et al., 2016; Fatemi et al., 2020; Mukarram et al., 2021). Moreover, SiNPs can upregulate the expression of many genes encoding proteins directly involved in photosynthetic machinery (Song et al., 2014; Hassan et al., 2021). The smaller sized-SiNPs can penetrate seed coat promptly and improve seed germination and growth and later overall growth, development, and crop yield (Epstein, 1994; Haghighi et al., 2012; Azimi et al., 2014; Janmohammadi et al., 2016; Karunakaran et al., 2016; Sun et al., 2016; Kheyri et al., 2019). In addition, SiNPs can trigger the

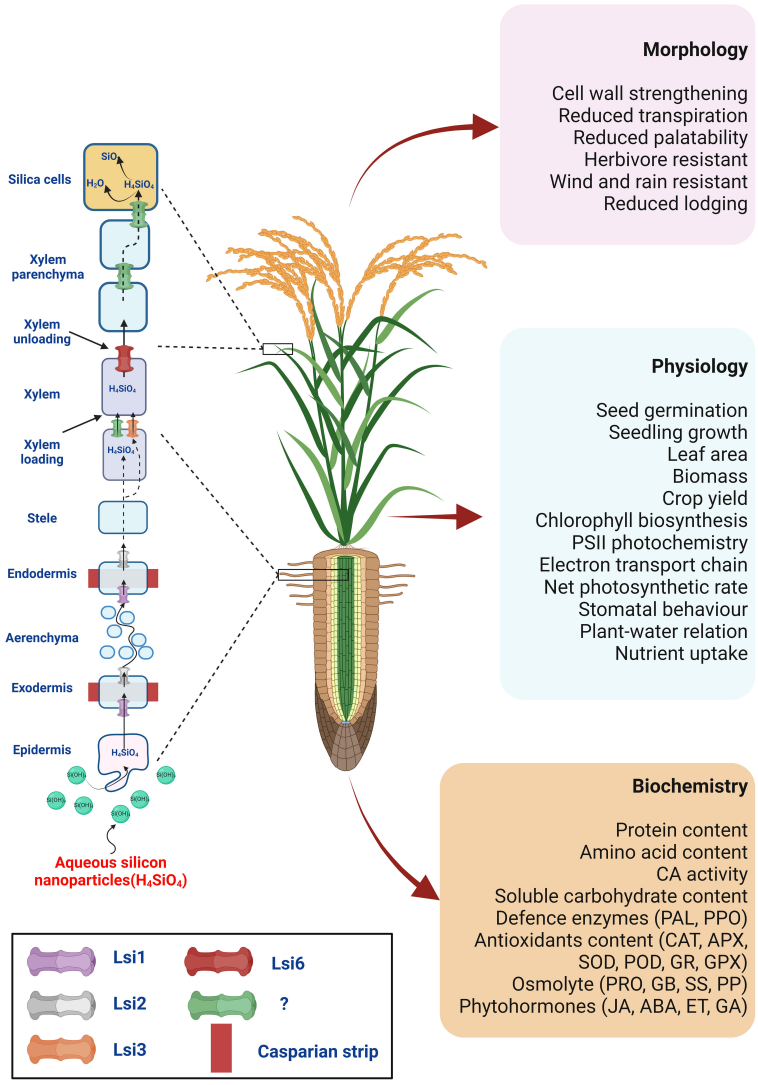

FIGURE 2
The hypothetical model for SiNPs uptake, transport, and action in higher plants under physiological settings. It is possible that SiNPs, like bulk silicates, could be absorbed by plant roots in the form of silicic acid ($Si(OH)_4$) and transported to endodermis by aquaporin channel Lsi1. Lsi2 might facilitate xylem loading at the endodermis-stellar apoplast junction. From there, it could join the transpiration stream to move to aerial parts. Lsi6 could assist xylem unloading at the shoot for distribution to shoot tissues or deposition in the cell walls or as specified silica cells (phytoliths). Silica deposition at the cell wall, silica cells or phytoliths are crucial to cell wall strengthening, reduced palatability for herbivores, and resisting wind, rain, and lodging. This action can be understood as the 'direct' effects of SiNPs. Additionally, SiNPs supplementation shows a strong correlation with superior plant physiology. This includes improved seed germination and seedling development, photosynthesis, gas-exchange, plant-water relation, nutrient uptake, and redox homeostasis. The direct involvement of SiNPs in these upgrades still lacks unequivocal proof. Nonetheless, several research findings support the possible 'indirect' interaction of SiNPs with plant biochemistry and physiology. These mechanical and physiological enhancements mediate SiNPs-induced growth and productivity in higher plants.

multiplication of growth-promoting rhizobacteria responsible for nutrient recycling and soil health maintenance, promoting plant maturation (Karunakaran et al., 2013). All these functions contribute to plant resistance against various physical, chemical, and biological stressors (Figure 2).

5 SiNPs-mediated TEs sequestration

The TEs sequestration from plant environs, such as soil, air, and water, is a constant challenge. Several experiments have recently targeted sustainable approaches to remedy TEs excess. Among various methods, the application of SiNPs in the form of a foliar spray, seed priming, and soil incorporation has emerged as a novel and eco-friendly approach to combat TEs stress (Asgari et al., 2018; Hussain et al., 2019; Rizwan et al., 2019). SiNPs treatment effectively enhanced the photosynthesis and growth in plants exposed to TEs-stressed conditions (Cui et al., 2017; Khan et al., 2020a). At the latest, the magnetic properties of SiNPs are curative towards contaminated water (Mahboub et al., 2022). SiNPs might operate in several ways to sequestrate different TEs, such as forming complexes with toxic TE ions, arresting their uptake, TEs

compartmentalisation within plants, stimulating the antioxidant defence system, and other omics aspects (Kopittke et al., 2012; Lukačová et al., 2013; Tripathi et al., 2016; Zhou et al., 2021). We will explore these possibilities in the later sections.

5.1 Cadmium

Being a non-essential trace element, the accumulation of Cd in agricultural soils is an onerous threat to plants (Haider et al., 2021). Thus, eliminating Cd from the soil is crucial to sustaining food security and environmental safety. SiNPs-mediated amelioration of Cd has been reported in several plant species, including *Phyllostachys edulis* (Emamverdian et al., 2021), *Satureja hortensis* (Memari-Tabrizi et al., 2021), *Oryza sativa* (Cui et al., 2017; Hussain et al., 2020), and *Triticum aestivum* (Hussain et al., 2019). Applying SiNPs against Cd stress has been considered more efficient than regular fertilisers (Chen et al., 2018). The experiment on *Phyllostachys edulis* suggested that SiNPs make a complex with Cd ions via adsorption and reduce the accumulation of Cd in roots and leaves (Emamverdian et al., 2021). It subsequently enhances the germination and growth parameters. Soil-applied SiNPs can alleviate Cd stress in *Triticum aestivum* plants with improved growth and chlorophyll content (Ali et al., 2019; Khan et al., 2020a). Further, SiNPs minimise Cd accumulation and oxidative stress while improving nutrient uptake and antioxidant defence system in *Triticum aestivum* (Thind et al., 2021). Roots treated with SiNPs have increased the xylem cell wall lignification in *Trigonella foenum-graceum* (Nazaralian et al., 2017). The increased cell wall lignification was coupled with an improved xylem cell wall thickness. Such cell wall adjustments improve nutrient transport and silicon for faster growth (Asgari et al., 2018). SiNPs engage the Cd ions on the root surface to terminate their translocation in the aerial parts or immobilise them in the soil (Silva et al., 2017). Cui et al. (2017) also reported the downregulation of *OsLCT1* and *OsNramp5*, genes with SiNPs application involved in Cd uptake and transport, respectively, in *Oryza sativa*. At the same time, SiNPs upregulated genes involved in Cd transport into the vacuole (*OsHMA3*) and Si uptake (*OsLsi1*). Higher silicon uptake can further restrict Cd uptake and transport and, thus, Cd toxicity.

5.2 Lead

Pb is a non-essential element and a detrimental contaminant for agricultural soils. It hampers plant metabolism, cell adhesion, and signalling by accumulating ROS in the cell wall (Küpper, 2017; Aslam et al., 2021). Foliar application of SiNPs boosted photosynthetic machinery and antioxidant enzymes in *Coriandrum sativum* and restricted Pb toxicity (Fatemi et al., 2020). A tissue culture experiment on Pb stress mitigation via silicon dioxide nanoparticles in *Pleioblastus pygmaeus* showed a reduction in the soluble protein content assimilated in the cell membrane while maintaining the cell membrane vitality (Emamverdian et al., 2019).

5.3 Arsenic

Arsenic contaminates groundwater globally, and irrigation with As-rich water amplifies its bioaccumulation and toxicity in several crops (Finnegan and Chen, 2012; Farooq et al., 2016; Vaculík and Vaculíková, 2017; Abbas et al., 2018; Abedi and Mojiri, 2020). Nonetheless, SiNPs application arrests As uptake and translocation to aerial parts of tissues and alleviates phytotoxicity in *Solanum lycopersicum* (González-Moscoso et al., 2019, González-Moscoso et al., 2022). SiNPs were reported to lower oxidative stress via improving antioxidative defence (SOD, APX, GR, and DHAR) in *Zea mays* seedlings (Tripathi et al., 2016). Further, SiNPs increase the mechanical strength of the cell wall in rice suspension cells under As toxicity via increasing pectin content, cation exchange capacity, and pectin methyl-esterase activity, reducing pectin methyl-esterification. SiNPs also blocked the uptake of As by inhibiting the expression of genes encoding As uptake (*OsLSi* 1, low silicon 1; *OsLSi* 2, low silicon 2) (Cui et al., 2020) since As and Si share a common transport system. Thus, adding SiNPs into the As medium causes a direct competition for the transport proteins (Cui et al., 2020). Moreover, SiNPs treatment enhances the expression levels of plasma-membrane localised NIP aquaporin family proteins, *OsNIP1;1* and *OsNIP3;3*, which are permeable to arsenite (Mitani-Ueno et al., 2011; Sun et al., 2018). The overexpressed *OsNIP1;1* and *OsNIP3;3* are reported to reduce the As accumulation in *Oryza sativa* plants (Sun et al., 2018).

5.4 Mercury

Mercury (Hg) is a highly toxic pollutant that contaminates cropland to different extents worldwide (Liu et al., 2020a). Li et al. (2020) demonstrated that exogenously applied SiNPs ameliorate the adverse effects of Hg in *Glycine max* seedlings. SiNPs significantly reduced Hg uptake, accumulation, and translocation in these seedlings. Further analysis with synchrotron radiation X-ray fluorescence showed lower Hg accumulation in the epidermis and pericycle of roots and stems of *Glycine max* plants treated with SiNPs.

5.5 Chromium

SiNPs-mediated alleviation of Cr toxicity has been reported in *Pisum sativum* via reduced Cr uptake and accumulation in plant tissues (Tripathi et al., 2015). It was proposed that SiNPs facilitated mineral nutrient uptake and downplayed ROS synthesis by triggering antioxidant enzymes. SiNPs protected leaf ultrastructure under Cr toxicity in *Triticum aestivum* (Manzoor et al., 2022). While Cr deteriorated cellular organelles, SiNPs protected the cell walls, cell membranes, mitochondria, granal lamellae, thylakoids, nucleoli, and nuclear membrane. In a hydroponic study with *Brassica napus*, Huang et al., 2024 witnessed 100 um SiNPs (20 nm) boosted Si content in leaves increased by 169%, mostly restricted to intercellular spaces,

chloroplasts, guard cells, and stomata. This can upgrade PSII biochemistry (NPQ, ETR, and quantum yield of PSII) and photosynthetic productivity. In the same study, SiNPs hampered the expression of Cr (and related TEs) transporter genes such as *ST1*, *ST8*, *ABCG37*, *HMA*, and *MT*, resulting in decreased Cr uptake (by 92% in roots and 76% in leaves). In *Oryza sativa* seedlings, SiNPs reversed the Cr-induced cell cycle arrest at the G2/M phase along with IAA application (Sharma et al., 2022). Similarly, endogenous NO levels in root tips were improved which could assist in ROS scavenging and upregulated antioxidant activity as was reported in the study.

5.6 Copper

Emamverdian et al. (2020) demonstrated the mitigative effect of SiNPs on three different TEs stresses: Mn, Cu, and Cd on *Arudinaria pygmaea*. Enhanced localisation of Cu and Mn by SiNPs was observed in the root surface, which could minimise TEs accumulation in the stem and leaves. Also, SiNPs treatment enhanced the photosynthetic capacity, biomass, and overall growth, which authors correlated with the reduced TEs uptake and accumulation in the plant shoot. Similarly, Riaz et al. (2022) suggested that SiNPs can relieve Cu^{2+} toxicity in wheat seedlings. SiNPs treated plants showed increased root length and plant height and enhanced antioxidant defence system. It was manifested by decreased malondialdehyde (MDA) and H_2O_2 contents and Cu^{2+} concentrations in shoots.

5.7 Manganese

Si-induced alleviation of Mn toxicity has been reported in several studies, suggesting Si could contribute to the depression of Mn uptake and transport (Li et al., 2015). It could restrict lipid peroxidation by upregulating non-enzymatic and enzymatic antioxidants (Shi et al., 2005; Li et al., 2015). The reduced ·OH accumulation was also detected in the leaf apoplast (Dragišić Maksimović et al., 2007, Dragišić Maksimović et al., 2012). Moreover, Doncheva et al. (2009) observed a substantial thickening of epidermal layers after the Si treatment in the Mn-sensitive maize variety over a tolerant one. It suggests that Si could induce Mn storage in non-photosynthetic tissue to prevent Mn-toxicity effects on chloroplast functions. Similarly, Iwasaki and Matsumura (1999) assume that Si could assist in displacing and storing Mn in a metabolically inactive form around the base of the trichomes on the leaf surface. The mitigative effect of Si in the form of nanoparticles on Mn-toxicity was also described in the aforementioned study (Emamverdian et al., 2020; see Chapter 5.6).

5.8 Zinc

Generally, Zn is a vital element for plant growth, as it is imperative in numerous metabolic pathways. Its deficiency is one of the plant's most widespread micronutrient deficiencies (Anwaar et al., 2015; Kaur and Garg, 2021). However, as was reported by Long et al. (2003), a concentration above 3000 mg kg^{-1} Zn in dry soil can have a noxious effect on plant yield and growth as it alters the ionome of plants through the inhibition of nutrients' uptake and translocation (Bokor et al., 2015). The potential utilisation of Si in alleviating Zn toxicity has been studied, for example, in cotton or bamboo species (Anwaar et al., 2015; Emamverdian et al., 2018a). Both studies suggested that Si can limit Zn bioavailability and instigate the plant defence system by increasing antioxidant capacity and non-enzymatic activity, thus alleviating cellular oxidative damage. Similarly, Song et al. (2014) described that Si activated and regulated some photosynthesis-related genes in *Oryza sativa* with high-Zn exposure, improving photosynthesis over Zn-stressed plants that lacked Si treatments. These studies operated with bulk-Si, whereas using the SiNPs could potentially support its beneficial effects. However, in highly Zn-polluted soils, Zn can coexist with silica in the form of a Zn-silicate complex (Goswami et al., 2022), and Bokor et al. (2015) revealed such a complex can have a comparable negative effect on Lsi gene expression and mineral nutrition homeostasis as high concentration of Zn alone.

5.9 Antimony

Sb is a non-essential metalloid with noxious effects for plants. However, studies to manage Sb-toxicity with SiNPs are rare. Still, there are several reports of Si-induced mitigation of Sb-toxicity in higher plants that could point in the right direction. Vaculíková et al. (2014, 2016) described Si-induced alleviation of Sb-toxicity on root growth and architecture in maize seedlings. Si supported the antioxidant defence system and thus reduced oxidative stress symptoms, and although Si did not reduce Sb content in roots, it considerably restricted Sb translocation to shoot. Shetty et al. (2021) attributed the blocked Sb translocation to root lignification, which was observed to a greater extent in Si-treated plants of *Arundo donax*. Moreover, enhanced photosynthetic pigments and overall photosynthetic yield were described. In poplar callus exposed to Sb-stress, Si declined the content of Sb in the calli and supported overall callus growth and nutrient uptake as well as the content of photosynthetic pigments. The improved Sb tolerance was secured via the Si-induced modification of antioxidant enzyme activity (Labancová et al., 2023). These findings also correspond to results obtained from the wild-type and the low-silica rice mutant cultivated with 10 or 30 µmol L^{-1} Sb (Huang et al., 2012). Si treatment promoted growth and decreased Sb content in the shoots of both mutants by regulating the Sb distribution between the roots and shoots.

5.10 Nickel

Although Ni is an essential component of several metalloenzymes of plants, it could be very toxic at supraoptimal concentrations. Like Sb, Ni-toxicity management is something least discussed in the literature with SiNPs. Exogenous Si was investigated in rice as a possible mitigative driver for Ni stress. Si protected the seedlings by upregulating the antioxidant defence components and glyoxalase

systems, helping the ROS scavenge and detoxify cytotoxic methylglyoxal (Hasanuzzaman et al., 2013). The Si-induced recovery of growth, gas exchange, and pigment contents in cotton seedlings under the Ni stress was observed. It was secured by decreasing the Ni uptake and accumulation in the leaf, stem, and roots. It also increased antioxidant enzyme activities to restrict MDA, H_2O_2, and electrolyte leakage in leaves and roots (Khaliq et al., 2016). The enhanced antioxidant system, improved integrity of cell membranes and averted Ni-induced root anatomy alteration were also denoted as the mechanisms of Si-induced mitigation of Ni toxicity in maize plants (Vaculík et al., 2021). Improved leaf water status, enzymatic and non-enzymatic defence systems, and increased content of assimilatory pigments and leaf area were also described by Fiala et al. (2021).

6 Mechanisms underlying SiNPs-mediated defence responses

There are several mechanisms and pathways that SiNPs can adopt to mitigate TEs phytotoxicity. For instance, silicon can limit TEs uptake and translocation by lowering the ion activities in the medium. At a cellular level, it can regulate the co-precipitation of elements, antioxidant machinery, gene expression concerning TE transport and chelation, and morphological adjustments (Adrees et al., 2015; Emamverdian et al., 2018b). Here, we discussed the active processes of SiNPs against TEs toxicity (Figure 3).

6.1 TEs immobilisation in soil

Exogenous SiNPs ameliorate toxic TEs effects and improve overall plant growth (Tripathi et al., 2016; de Sousa et al., 2019; El-Saadony et al., 2021). These overcome responses have been correlated with soil physical properties, including TEs speciation, changes in soil pH, or deprivation of TEs due to co-precipitation with silicon (Bhat et al., 2019). Pretreatment of bulk-Si enhances phenolic root exudation (Chen et al., 2016) and organic acid exudation (Fan et al., 2016), which might be critical in TEs mitigation. Silicon immobilises TEs on the root's outer surface by increasing the soil's pH or altering TEs speciation by forming silicate complexes in soil solution. He et al. (2013) observed the complexification of most Cd with wall-bound silicon in rice root cells, leading to reduced Cd uptake and translocation. Kopittke et al. (2017) performed synchrotron studies and confined most of the Al complexed with Si in the *Sorghum bicolor* root cap. They evinced that this Si-Al complex formation in the root periphery could minimise the metal accumulation in the cell wall. Thus, the Si-mediated extrinsic defence mechanism through organic acid or phenolic exudation could be crucial in TEs toxicity mitigation.

6.2 Barrier to uptake and transport

Non-controlled silica deposition can harm a plant; hence, plants evolved effective mechanisms of cell walls' silicification (Kumar et al., 2017). Silicon binds to lignin in the cell wall to form a Si-TE ion complex that subsequently arrests ion translocation from the root to the other plant organs (He et al., 2013; Sheng and Chen, 2020; Soukup et al., 2020). Most Si-mediated fruitful effects are reported to be linked with the accumulation of Si in roots, stems, leaves, and hulls, which acts as a physical barrier by enhancing the mechanical strength of plant tissues (Ma et al., 2006; Emamverdian et al., 2018b). Si, along with lignin, can deposit in dermal regions of the cell walls, thickening the Casparian strips and blocking the TE transport in plants (Kim et al., 2014). Si-induced changes in the cell wall binding properties might be essential in mitigating TEs toxicity. Si reduced Cd accumulation in roots and grains of rice (Chen et al., 2019) and maize (Liu et al., 2020b) which could result from Si deposition in root cells apoplast hindering Cd uptake (Song et al., 2009; Wang et al., 2015). It is stipulated that Si enhances Lsi expression while suppressing Nramp 5 (Cd transporter gene) in rice roots, suggesting that upregulated Si transporters resist Cd toxicity under ample silicon supply (da Cunha and do Nascimento, 2009; Ma et al., 2015). Considerable amounts of covalent-bound Si are also complexed with hydroxyl groups of pectin contained in the cell wall (Schwarz, 1973; Sheng and Chen, 2020). He et al. (2015) suggests that hemicellulose, rather than pectin and cellulose, is the primary ligand bound to Si complexes in rice. Si accumulated in the cell walls in hemicellulose-bound organosilicon compounds can improve cell wall mechanical properties and regeneration and inhibit the Cd uptake by a mechanism of Cd complexation and subsequent co-deposition (He et al., 2015; Ma et al., 2015).

6.3 Active participation in the antioxidant defence system

TEs overaccumulation stages the ROS-induced oxidative emergency, threatening many vital processes. Thus, the plant's top priority for survival under such scenarios is scavenging ROS. This goal is facilitated by an antioxidant system comprising several enzymatic (SOD, CAT, APX, POD, and GR) and non-enzymatic (ascorbic acid, α-tocopherol, proline, carotenoids, flavonoids, and reduced glutathione) antioxidants. In this context, pretreatment of SiNPs was reported to stimulate the enzymatic antioxidants against TEs toxicity in *Solanum lycopersicum* under As stress (González-Moscoso et al., 2019, González-Moscoso et al., 2022), *Glycine max* under Hg stress (Li et al., 2020), and *Satureja hortensis* (Memari-Tabrizi et al., 2021) and *Triticum aestivum* under Cd toxicity (Ali et al., 2019). The formation of free radicals under TEs toxicity directly damages the cell membrane permeability and stability that, in time, would cause the homeostasis collapse of cells and tissues. However, silicon counteracts it by enhancing the stability of the plasma membrane under TEs stress (Vaculík et al., 2020). Another TEs detoxifying mechanism is the synthesis of various chelating agents, i.e., flavonoids, phenolics, and organic acids (Bhat et al., 2019). Silicon reportedly influences the synthesis of several chelating compounds, including cysteine, glutathione, and phytochelatins, under TEs toxicity (Rahman et al., 2017).

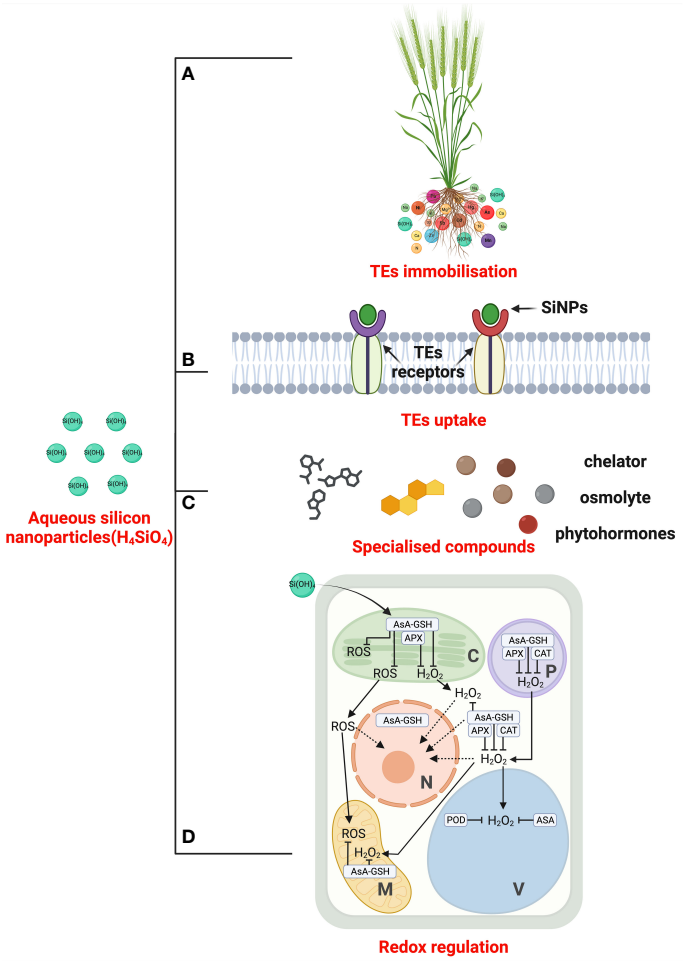

FIGURE 3
The mechanistic overview of silicon nanoparticles (SiNPs)-mediated TEs tolerance. SiNPs can increase the pH of the growing medium (soil and hydroponics) or alter elemental speciation by forming silicate complexes. It leads to TEs adsorption and immobilisation **(A)**. Further, the remaining TEs translocation is discouraged by blocking TEs receptors **(B)**. At inter- and intracellular spaces, SiNPs boost the biosynthesis of chelators compound, organic acid, and phenolic root exudation to minimise TEs toxicity **(C)**. SiNPs optimise redox status under TEs excess through supporting enzymatic and non-enzymatic antioxidant defence systems **(D)** and contribute to overall TEs tolerance in higher plants. TEs: trace elements; SiNPs: silicon nanoparticles; AsA: Ascorbic acid; GSH: glutathione; APX: ascorbate peroxidase; ROS: reactive oxygen species; H_2O_2: hydrogen peroxide; CAT: catalase; POD: peroxidase; alphabetic abbreviations inside panel **(D)** – C: chloroplast; P: Peroxisomes; N: Nucleus; V: Vacuole; M: mitochondria.

7 'Omics' bases of SiNPs-induced TEs sequestration

7.1 Metabolomics

Plants evolved several responsive manoeuvers against TEs toxicity, such as minimising TEs bioavailability and uptake, enriching plants with nutrients, and stimulating the antioxidant system and the biosynthesis of protective agents (osmolytes, organic acids, metallothioneins, and phytochelatins) (Tripathi et al., 2015; Moharem et al., 2019; Cao et al., 2020; Lian et al., 2020; Wang et al., 2020a, Wang et al., 2020b). Among the different NPs applied, SiNPs have proven to be quite promising (Tripathi et al., 2015; Wang et al., 2015; Tripathi et al., 2017; Khan et al., 2020a). Though not an exclusively effective metal/metalloid barricade, the apoplasmic barrier also fulfils essential defensive functions in plant roots by regulating the flow of ions, oxygen and water (Lux et al., 2004; Chao et al., 2013). The efficiency of apoplasmic barriers as contaminant barricades can be enhanced by NPs application (Rossi et al., 2017). NPs attach to the TEs in the root cell walls, making stable complexes and rendering them unavailable. NPs-TEs complexes, once adsorbed, become immobile, obstructing the mobility of the TEs inside the plants and reducing their biological activity (Cui et al., 2017; Wang et al., 2021; Zhou et al., 2021). Accumulating organic acids (behaving as metal chelators) and chelating TE contaminants are necessary adaptations to TEs tolerance. The biosynthesis of such protective organic acids is improved by SiNPs, reducing the damage caused by TEs like Cd and As (Cui et al., 2017; Tripathi et al., 2017; Zhou et al., 2021). The interaction of SiNPs with the TEs is crucial while studying the different characteristics of TEs stress alleviation. SiNPs can also reduce the mobility and bioavailability of TE contaminants in the soil (Tripathi et al., 2015; Wang et al., 2015; Tripathi et al., 2017; Khan et al., 2020a). The application of

mercapto SiNPs increased the stability of Cd and, thus, decreased its mobility (Wang et al., 2020b). Alternatively, Si may co-precipitate with metals/metalloids as silicates in the roots and leaves of different plants. Co-precipitation of Zn as Zn silicates or Si–Zn complexes in the cell walls of leaf epidermal cells was seen in *Minuartia verna* and *Cardaminopsis halleri* (Neumann et al., 1997; Neumann and Zur Nieden, 2001). Gu et al. (2011, 2012) suggested the sequestration of Zn–Si and Zn-Cd precipitates in rice to the cell walls of less bioactive tissues. Similarly, Mn, Cu, and Cd might co-precipitate with Si to restrict their accumulation in shoot phytoliths, but it is not fully confirmed yet (Iwasaki et al., 2002; Zhang et al., 2008; Oliva et al., 2011; Emamverdian et al., 2020).

SiNPs regulate a variety of physiological phenomena in plants, notably nutrient assimilation, CO_2 fixation, accretion of secondary metabolism products and activities of different enzymes under normal as well as perturbed environmental conditions (Tripathi et al., 2015, Tripathi et al., 2017; Ahmad et al., 2019; Khan et al., 2020a; Mukarram et al., 2021). Al-toxicity alleviation in barley and maize after Si supplementation has been endorsed to accumulate phenolic compounds (Adrees et al., 2015; Vega-Mas et al., 2019). SiNPs have also been observed to modulate the regulatory enzymes of the shikimic acid pathway, leading to increased accretion of phenols in the leaves, as has been reported in *Mentha piperita* (Ahmad et al., 2019). Because of their metal-chelation capacity with flavonoid-phenolics, phenols play a critical role in TE toxicity mitigation by reducing the uptake and translocation of toxic TEs, as has been reported for Al and Mn (Kidd et al., 2001; Dragišić Maksimović et al., 2007; Shahnaz et al., 2011). Bulk-Si facilitates phenol overaccumulation by triggering phenylalanine ammonia-lyase (PAL), a critical regulatory enzyme of the phenylpropanoid pathway (Rahman et al., 2015; Ahanger et al., 2020). It also upregulated PAL, cinnamyl alcohol dehydrogenase, and chalcone synthase in *Rosa hybrida* (Shetty et al., 2011). Likewise, Si-induced PAL activity also assisted in managing Cu stress in *Arabidopsis thaliana* roots (Li et al., 2008).

Bulk-Si can influence the biosynthesis of H_2O_2, nitric oxide (NO), and hydrogen sulphide (H_2S) to govern Ag and Cd toxicity in mustard and pepper (Soundararajan et al., 2018; Vishwakarma et al., 2020; Kaya et al., 2020a). Si decreases electrolyte leakage and H_2O_2 and MDA content by boosting the antioxidant system, possibly with NO involvement, and regulates plant growth and development under TE toxicity (Tripathi et al., 2021). SiNPs-induced NR biosynthesis in *Mentha piperita* and restricted H_2O_2 production in *Cymbopogon flexuosus* suggests SiNPs crosstalk with H_2O_2 and NO (Ahmad et al., 2019; Mukarram et al., 2023). Thus, it does not seem hasty speculation that SiNPs could interact with gaseous signalling molecules in a similar fashion to bulk-Si. It will hold relevance during TEs stress alleviation as well. The nitrate reductase (NR) pathway is the best-characterised NO biosynthetic pathway (Planchet and Kaiser, 2006). In addition to the general function of nitrate-to-nitrite reduction, NR also performs a crucial part in plants by transferring an electron to nitrite using NAD(P)H as a source of electrons, ultimately resulting in NO biosynthesis (Planchet and Kaiser, 2006). The synergistic interaction of NO and Si can discourage As uptake and increase phytochelatin biosynthesis, reducing As translocation in mustard (Ahmad et al., 2021). In a similar study, Liu et al. (2020b) established the collegial effect of Si and NO in mitigating Cd toxicity in *Triticum aestivum* seedlings. Si stimulates endogenous H_2S accretion that upregulates antioxidants' activity in *Capsicum annuum* raised on Cd- and B-spiked soils (Kaya et al., 2020a, 2020b).

7.2 Proteomics

Given the scanty literature concerning the SiNPs-mediated TEs tolerance in plants, the proteomic approach is comparatively novel to gaining insights into the expression of various stress-related enzymes and proteins. TEs-stimulated oxidative stress leads to altered protein expression and structure, leading to loss of protein activity or its content. Nevertheless, silicon and SiNPs supplementation regulates the expression of several proteins and enzymes of signal transduction cascades of the antioxidant defence system (Tripathi et al., 2015; Muneer and Jeong, 2015a; Mukarram et al., 2022). Once inside the cells, silicon plays an imperative role in stress alleviation by maintaining ion homeostasis and structural rigidity, upregulating antioxidant metabolism, and increasing the expression of genes and proteins involved in stress alleviation (Ma, 2004). SiNPs-induced upregulation of the different primary and secondary metabolic enzymes is well-reported. Mukarram et al. (2021) reported that the expression of terpene (neral, geranial) and NR enzyme activity was upregulated in SiNPs-treated *Cymbopogon flexuosus*. Si application improves PSII polyprotein expression under Zn toxicity (Song et al., 2014). Further, the bulk-silicon enhanced the protein content related to stress (17%), hormones (11%), and other cellular biosynthesis (11%), and many others associated with gene expression and secondary metabolism in 25 mM salt-stressed *Lycopersicon esculentum* plants (Muneer and Jeong, 2015b). The stress-related proteins included zinc finger A20, COPINE 1 family protein, caffeoyl-CoA O-methyltransferase, and others. Down-regulation of Zn transporter (*OsZIP1*) protein after Si supplementation decreases Zn uptake in *Oryza sativa* (Huang and Ma, 2020). Si accumulation involves both influx and efflux transporters. The SiNPs application has been endorsed for upregulating the menthol-reductase enzyme to proliferate menthol in mint oil (Ahmad et al., 2019). Similarly, geraniol dehydrogenase enzyme activity was positively influenced by SiNPs foliar application in *Cymbopogon flexuosus* under 160 mM and 240 mM salt stress (Mukarram et al., 2023). SiNPs-induced antioxidants can improve isoenzyme patterns and genomic alterations to restrict TE toxicity in *Pisum sativum* and UV-B stress in *Triticum aestivum* (Tripathi et al., 2015, Tripathi et al., 2017). Further, Si can delay chlorophyll-protein complex degradation such as supercomplexes, PSI core binding LHCI, PSI core, F1-ATPase binding Cytb6/f complex, PSII core, and trimeric and monomeric LHCII (Wang et al., 2019). Si can also improve photosynthetic performance, given its observed benefits on absorption, transformation, and transfer of light energy through optimising thylakoid membrane proteins in water-deprived *Oryza sativa* seedlings (Wang et al., 2019).

7.3 Genomics

Studies on TEs-stressed plants have indicated that ROS-induced DNA damage was more pronounced in the Cd and Pb-exposed

plants, as indicated by the disappearance of several normal bands in the RAPD pattern of the DNA. In contrast, new DNA amplicons could be located in TE-exposed plants treated with different NPs. Moreover, oxidation of proteins is a common TEs toxicity symptom as TEs ions directly interact with protein molecules due to their strong affinity with carboxyl- thionyl- and histidyl groups (Hossain et al., 2015). Studies have revealed that the NPs within the plant cell systems may interact with these sulfhydryl and carboxyl groups, eventually altering the protein activity by acting and reacting similarly to the metal ions (Hossain et al., 2015). As discussed, different NPs upregulate the expression of various genes in plants, speeding up the biosynthesis of several primary and secondary metabolism products (Večeřová et al., 2016; Marslin et al., 2017).

The role of SiNPs exemplifies regulating an array of transcription factors (TFs) implicated in abiotic mitigation, notably DREB2, NAC, NAM, and CUC. These TFs overexpress genes associated with scavenging free radicals and maintaining osmotic potential and ionic homeostasis (Manivannan and Ahn, 2017). Moreover, silicon can induce regulatory proteins coupled to gene expression under stress, particularly TFs for transcription elongation (SPT4), ribosomal protein L16, RNA polymerase mediator, tRNA-lysidine synthase, MADS-box, ribosome-recycling factor and reverse transcriptase (Muneer and Jeong, 2015b; Al Murad et al., 2020).

Exogenous application of SiNPs modifies plant's nutrient status, facilitating N, Fe, Mg, Zn, and Si absorption (Wang et al., 2015; Ahmad et al., 2019; Mukarram et al., 2021). SiNPs-mediated increase in Si uptake leads to a decrease in the Cd uptake, facilitating the growth of *Oryza sativa* seedlings raised on Cd-rich soils. Cui et al. (2017), in their study on rice, observed that SiNPs upregulate the expression of Si transporter (*OsLsi1*) while the expression of Cd-transporters (*OsLCT1, OsNramp5*) is down-regulated. Down-regulation of essential abiotic stress tolerance genes, notably *ERF5* (ethylene response factor 5, *RBOH1* (respiratory burst oxidase), *MAPK2, and MAPK3* (mitogen-activated protein kinases), by the application of SiNPs, is well-reported (Almutairi, 2016). SiNPs-mediated regulation of primary metabolism, biosynthesis and modifications of secondary metabolism products, particularly phenols, possibly enhances the tolerance against stress (Rahman et al., 2015; Tripathi et al., 2015, Tripathi et al., 2017; Ahmad et al., 2019; Ahanger et al., 2020). Furthermore, SiNPs were suggested to induce different transcripts (*CfADH2a*-b, *CfADH1, CfAKR2b, CfAAT3*, and *CfALDH*) to regulate the constitutional makeup of plant essential oil (Mukarram et al., 2021).

Despite growing studies on SiNPs, most publications need more genomic insights. Here we introduce significant recent findings dealing with the influence of Si on gene activity, generally to indicate a possible role with SiNPs. Different studies have suggested the positive regulation of gene transcripts of various metabolic processes by Si application (Brunings et al., 2009; Chain et al., 2009; Debona et al., 2017). The role of Si in upregulating photosynthetic genes has been studied in detail. For example, Zn-induced damage in *PsbY* expression was overcome by Si supplementation (Song et al., 2014). Moreover, increased PSII activity and electron transfer rate by upregulating *PsbY* mRNA transcripts are endorsed for Si supplementation in rice under Zn stress. The other Si-upregulated genes under Zn-toxicity include *PetC, PsaH, PetH* encoding chloroplast, cytochrome proteins, and ferredoxin $NADP^+$ reductases, respectively (Song et al., 2014). Moreover, Si upregulates several genes encoding for electron transport chain proteins and light-harvesting complex viz., *PetE*, *PetF*, *PsbQ, PsbP*, *PsbW, and Psb28*. Furthermore, increased expression of gene transcripts (*PsbW, Psb28, PsbQ, and PsbP*) involved in the photolysis of water has been attributed to Si application (Zhang et al., 2018). *PetH*, *Os03g57120* and *Os09g26810* genes involved in stress mitigation, NAD(P)H and glutathione biosynthesis are also upregulated by Si (Manivannan and Ahn, 2017). Kaushik and Saini (2019) have reported the upregulation of *LeGR* (glutathione reductase gene) in *Solanum lycopersicum* after Si supplementation. In *Triticum aestivum*, Si attenuates TEs toxicity by upregulating metallothionein and phytochelatin synthase gene expression (*TaMT1*, *TaPCS1*) (Hossain et al., 2018). Genes coding for enzymatic oxidants (*SlCAT*, *SlGR*, *SlGST*, *SlSOD*, *SlPOD*, *SlGPX*) have been observed to be upregulated by exogenous sourcing of Si attenuating stress response in *Solanum lycopersicum* (Khan et al., 2020b).

8 Conclusion and future trends

Only a few published articles have focused on the interaction between SiNPs and TEs toxicity, with existing reviews mainly discussing heavy metals and neglecting other toxic elements. These reviews also fail to emphasise SiNPs over bulk silicon or adequately address the omics aspect. In our previous review (Mukarram et al., 2022), we explored SiNPs potential in alleviating abiotic stress, including metals stress, but needed TEs and a detailed *modus operandi*. To address these concerns, our present review includes a wide range of toxic elements studied with SiNPs, regardless of the 'heavy metals' label, and explores how SiNPs interact with plant metabolomics, proteomics, and genomics during TEs toxicity. The novelty of our review lies in its understanding of the SiNPs-TEs interaction and its omics perspective, aiming to stimulate a discussion within the silicon community about its active involvement (if any) in plant physiology, particularly given the existing uncertainties in this field.

In the present review, we focused mainly on the action of SiNPs during TEs presence. It could be understood from several studies that SiNPs have superior benefits against TEs excess over bulk-Si. The *modus operandi* relies upon SiNPs-induced chelation and immobilisation of TEs at the first contact site, i.e., soil. Once toxic elements are inside the plant, SiNPs might compartmentalise TEs or restrict them in vacuoles and cell walls. SiNPs further attenuate TEs stress by inducing biochemical defence such as antioxidants, osmolytes, and other specialised compounds. Several proteins and genes have been identified to support SiNPs action in TEs-stressed plants. Nonetheless, future studies could address the following concerns:

1. Much prospective research is encouraged on SiNPs interaction with TEs toxicity.

2. It is high time to produce empirical proof of whether SiNPs provide more anatomical and structural support or physiological participation during TEs toxicity.
3. More research is required for SiNPs action on certain (less-discussed) trace elements such as Mo and Se.
4. A lack of omics approaches in contemporary studies is still prevalent.
5. The aquaporins for TEs uptake and distribution need to be identified and sequenced.
6. Silicon channels are needed for other model plant species, especially C4 plants, such as sorghum and sugarcane where silica can be stored at higher concentrations.

Author contributions

MM: Conceptualization, Project administration, Resources, Supervision, Visualization, Writing – original draft. BA: Writing – original draft. SC: Writing – original draft. AK: Writing – original draft. DK: Funding acquisition, Project administration, Writing – original draft, Writing – review & editing. MK: Project administration, Supervision, Validation, Visualization, Writing – review & editing. AL: Project administration, Supervision, Validation, Visualization, Writing – review & editing.

Funding

The author(s) declare financial support was received for the research, authorship, and/or publication of this article. This publication is the result of the project implementation: Comprehensive research of mitigation and adaptation measures to diminish the negative impacts of climate changes on forest ecosystems in Slovakia (FORRES), ITMS: 313011T678 supported by the Operational Programme Integrated Infrastructure (OPII) funded by the ERDF".

Acknowledgments

We apologise to several colleagues whose important work on SiNPs and TEs nexus could not be referred to due to word limitation. Figures were created with Biorender.com. MM was supported by the COST association (CA19116 "Trace Metal Metabolism in Plants - PLANTMETALS"). AL was supported by the Operation Program of Integrated Infrastructure – co-financed by the European Regional Development Fund (ITMS2014+) (313021BUZ3).

Conflict of interest

The authors declare that the research was conducted in the absence of any commercial or financial relationships that could be construed as a potential conflict of interest.

Publisher's note

References

Abbas, G., Murtaza, B., Bibi, I., Shahid, M., Niazi, N. K., Khan, M. I., et al. (2018). Arsenic uptake, toxicity, detoxification, and speciation in plants: physiological, biochemical, and molecular aspects. *Int. J. Environ. Res. Public Health* 15, 59. doi: 10.3390/ijerph15010059

Abedi, T., and Mojiri, A. (2020). Arsenic uptake and accumulation mechanisms in rice species. *Plants* 9, 129. doi: 10.3390/plants9020129

Adrees, M., Ali, S., Rizwan, M., Zia-ur-Rehman, M., Ibrahim, M., Abbas, F., et al. (2015). Mechanisms of silicon-mediated alleviation of heavy metal toxicity in plants: a review. *Ecotoxicol. Environ. Saf.* 119, 186–197. doi: 10.1016/j.ecoenv.2015.05.011

Adriano, D. C. (2001). *Trace elements in terrestrial environments* (New York, NY: Springer New York). doi: 10.1007/978-0-387-21510-5

Ahanger, M. A., Bhat, J. A., Siddiqui, M. H., Rinklebe, J., and Ahmad, P. (2020). Integration of silicon and secondary metabolites in plants: a significant association in stress tolerance. *J. Exp. Bot.* 71, 6758–6774. doi: 10.1093/jxb/eraa291

Ahmad, B., Khan, M., Jaleel, H., Shabbir, A., Sadiq, Y., and Uddin, M. (2019). Silicon nanoparticles mediated increase in glandular trichomes and regulation of photosynthetic and quality attributes in *Mentha piperita* L. *J. Plant Growth Regul.* 39, 346–357. doi: 10.1007/s00344-019-09986-x

Ahmad, A., Khan, W. U., Shah, A. A., Yasin, N. A., Naz, S., Ali, A., et al. (2021). Synergistic effects of nitric oxide and silicon on promoting plant growth, oxidative stress tolerance and reduction of arsenic uptake in *Brassica juncea*. *Chemosphere* 262, 128384. doi: 10.1016/j.chemosphere.2020.128384

Akeel, A., and Jahan, A. (2020). "Role of cobalt in plants: Its stress and alleviation," in *Contaminants in agriculture: Sources, impacts and management*. Eds. M. Naeem, A. A. Ansari and S. S. Gill (Springer International Publishing, Cham), 339–357. doi: 10.1007/978-3-030-41552-5_17

Alejandro, S., Höller, S., Meier, B., and Peiter, E. (2020). Manganese in plants: from acquisition to subcellular allocation. *Front. Plant Sci.* 11. doi: 10.3389/fpls.2020.00300

Ali, H., Khan, E., and Sajad, M. A. (2013). Phytoremediation of heavy metals—concepts and applications. *Chemosphere* 91, 869–881. doi: 10.1016/j.chemosphere.2013.01.075

Ali, S., Rizwan, M., Hussain, A., ur Rehman, M. Z., Ali, B., Yousaf, B., et al. (2019). Silicon nanoparticles enhanced the growth and reduced the cadmium accumulation in grains of wheat (*Triticum aestivum* L.). *Plant Physiol. Biochem.* 140, 1–8. doi: 10.1016/j.plaphy.2019.04.041

Al Murad, M., Khan, A. L., and Muneer, S. (2020). Silicon in horticultural crops: cross-talk, signaling, and tolerance mechanism under salinity stress. *Plants* 9, 460. doi: 10.3390/plants9040460

Almutairi, Z. (2016). Effect of nano-silicon application on the expression of salt tolerance genes in germinating tomato (*Solanum lycopersicum* L.) seedlings under salt stress. *Plant Omics J.* 9, 106–114.

Anwaar, S. A., Ali, S., Ali, S., Ishaque, W., Farid, M., Farooq, M. A., et al. (2015). Silicon (Si) alleviates cotton (*Gossypium hirsutum* L.) from zinc (Zn) toxicity stress by limiting Zn uptake and oxidative damage. *Environ. Sci. pollut. Res.* 22, 3441–3450. doi: 10.1007/s11356-014-3938-9

Aponte, H., Meli, P., Butler, B., Paolini, J., Matus, F., Merino, C., et al. (2020). Meta-analysis of heavy metal effects on soil enzyme activities. *Sci. Total Environ.* 737, 139744. doi: 10.1016/j.scitotenv.2020.139744

Appenroth, K. J. (2010). What are "heavy metals" in plant sciences? *Acta Physiol. Plant* 32, 615–619. doi: 10.1007/s11738-009-0455-4

Arif, N., Yadav, V., Singh, S., Singh, S., Ahmad, P., Mishra, R. K., et al. (2016). Influence of high and low levels of plant-beneficial heavy metal ions on plant growth and development. *Front. Environ. Sci.* 4. doi: 10.3389/fenvs.2016.00069

Asati, A., Pichhode, M., and Nikhil, K. (2016). Effect of heavy metals on plants: an overview. *Int. J. Appl. Innov. Eng. Manage.* 5, 56–66. doi: 10.1016/j.matpr.2021.06.278

Asgari, F., Majd, A., Jonoubi, P., and Najafi, F. (2018). Effects of silicon nanoparticles on molecular, chemical, structural and ultrastructural characteristics of oat (*Avena sativa* L.). *Plant Physiol. Biochem.* 127, 152–160. doi: 10.1016/j.plaphy.2018.03.021

Ashfaque, F., Inam, A., Sahay, S., and Iqbal, S. (2016). Influence of heavy metal toxicity on plant growth, metabolism and its alleviation by phytoremediation – a promising technology. *J. Agric. Ecol.* 6, 1–19. doi: 10.9734/JAERI/2016/23543

Aslam, M., Aslam, A., Sheraz, M., Ali, B., Ulhassan, Z., Najeeb, U., et al. (2021). Lead toxicity in cereals: Mechanistic insight into toxicity, mode of action, and management. *Front. Plant Sci.* 11. doi: 10.3389/fpls.2020.587785

Assunção, A. G. L., Martins, P. D. C., De Folter, S., Vooijs, R., Schat, H., and Aarts, M. G. M. (2001). Elevated expression of metal transporter genes in three accessions of the metal hyperaccumulator Thlaspi caerulescens. *Plant Cell Environ.* 24, 217–226. doi: 10.1111/j.1365-3040.2001.00666.x

Assunção, A. G., Schat, H., and Aarts, M. G. (2003). Thlaspi caerulescens, an attractive model species to study heavy metal hyperaccumulation in plants. *New Phytol.* 159, 351–360. doi: 10.1046/j.1469-8137.2003.00820.x

Azimi, R., Borzelabad, M. J., Feizi, H., and Azimi, A. (2014). Interaction of SiO_2 nanoparticles with seed prechilling on germination and early seedling growth of tall wheatgrass (*Agropyron elongatum* L.). *Pol. J. Chem. Technol.* 16, 25-29. doi: 10.2478/pjct-2014-0045

Baker, A. J., and Brooks, R. (1989). Terrestrial higher plants which hyperaccumulate metallic elements. A review of their distribution, ecology and phytochemistry. *Biorecovery* 1, 81–126.

Baker, A. J., McGrath, S. P., Reeves, R. D., and Smith, J. A. C. (2020). "Metal hyperaccumulator plants: a review of the ecology and physiology of a biological resource for phytoremediation of metal-polluted soils," in *Phytoremediation of contaminated soil and water* (Boca Raton, FL, USA: CRC Press, Taylor & Francis), 85–107.

Bhat, J. A., Rajora, N., Raturi, G., Sharma, S., Dhiman, P., Sanand, S., et al. (2021). Silicon nanoparticles (SiNPs) in sustainable agriculture: Major emphasis on the practicality, efficacy and concerns. *Nanoscale Adv.* 3, 4019–4028. doi: 10.1039/D1NA00233C

Bhat, J. A., Shivaraj, S. M., Singh, P., Navadagi, D. B., Tripathi, D. K., Dash, P. K., et al. (2019). Role of silicon in mitigation of heavy metal stresses in crop plants. *Plants* 8, 71. doi: 10.3390/plants8030071

Bjerrum, N. (1936). *Bjerrum's Inorganic Chemistry. 3rd Danish ed* (London: Heinemann).

Blaylock, M. J., and Huang, J. W. (2000). "Phytoextraction of metals," in *Phytoremediation of toxic metals: Using plants to clean up the environment*. Eds. I. Raskin and B. D. Ensley (New York, USA: Wiley New York, USA), 53–70.

Bokor, B., Bokorová, S., Ondoš, S., Švubová, R., Lukačová, Z., Hýblová, M., et al. (2015). Ionome and expression level of Si transporter genes (Lsi1, Lsi2, and Lsi6) affected by Zn and Si interaction in maize. *Environ. Sci. pollut. Res.* 22, 6800–6811. doi: 10.1007/s11356-014-3876-6

Brunetti, G., Soler-Rovira, P., Farrag, K., and Senesi, N. (2009). Tolerance and accumulation of heavy metals by wild plant species grown in contaminated soils in Apulia region, Southern Italy. *Plant Soil.* 318, 285–298. doi: 10.1007/s11104-008-9838-3

Brunings, A. M., Datnoff, L. E., Ma, J. F., Mitani, N., Nagamura, Y., Rathinasabapathi, B., et al. (2009). Differential gene expression of rice in response to silicon and rice blast fungus *Magnaporthe oryzae*. Annu. *Appl. Biol.* 155, 161–170. doi: 10.1111/j.1744-7348.2009.00347.x

Cabot, C., Martos, S., Llugany, M., Gallego, B., Tolrà, R., and Poschenrieder, C. (2019). A role for zinc in plant defense against pathogens and herbivores. *Front. Plant Sci.* 10. doi: 10.3389/fpls.2019.01171

Cao, F., Dai, H., Hao, P. F., and Wu, F. (2020). Silicon regulates the expression of vacuolar H^+-pyrophosphatase 1 and decreases cadmium accumulation in rice (*Oryza sativa* L.). *Chemosphere* 240, 124907. doi: 10.1016/j.chemosphere.2019.124907

Chain, F., Côté-Beaulieu, C., Belzile, F., Menzies, J. G., and Bélanger, R. R. (2009). A comprehensive transcriptomic analysis of the effect of silicon on wheat plants under control and pathogen stress conditions. *Mol. Plant Microbe Interact.* 22, 1323–1330. doi: 10.1094/MPMI-22-11-1323

Chandra, R., and Kang, H. (2016). Mixed heavy metal stress on photosynthesis, transpiration rate, and chlorophyll content in poplar hybrids. *For. Sci. Technol.* 12, 55–61. doi: 10.1080/21580103.2015.1044024

Chao, D. Y., Xia, Z., Guo-Feng, L., Jun-Wei, Z., Man-Zhu, B., and Zhi-Xiang, Z. (2013). Progress on the structure and physiological functions of apoplastic barriers in root. *Bull. Bot. Res.* 33, 114–119. doi: 10.7525/j.issn.1673-5102.2013.01.019

Chapman, P. M. (2007). Heavy metal—music, not science. *Environ. Sci. Technol.* 41, 6. doi: 10.1021/es072552o

Chen, D., Chen, D., Xue, R., Long, J., Lin, X., Lin, Y., et al. (2019). Effects of boron, silicon and their interactions on cadmium accumulation and toxicity in rice plants. *J. Hazard. Mat.* 367, 447–455. doi: 10.1016/j.jhazmat.2018.12.111

Chen, H., Huang, Y., Zhao, W., Cao, S., Yang, H., Liu, Q., et al. (2016). Effect of silicon-mediated alleviation of cadmium toxicity with a cypress variety: *Juniperus formosana* Hayata. *Bangladesh J. Bot.* 45, 845–853.

Chen, R., Zhang, C., Zhao, Y., Huang, Y., and Liu, Z. (2018). Foliar application with nano-silicon reduced cadmium accumulation in grains by inhibiting cadmium translocation in rice plants. *Environ. Sci. pollut. Res.* 25, 2361–2368. doi: 10.1007/s11356-017-0681-z

Chibuike, G. U., and Obiora, S. C. (2014). Heavy Metal polluted soils: Effect on plants and bioremediation methods. *Appl. Environ. Soil Sci.* 2014, e752708. doi: 10.1155/2014/752708

Cobbett, C., and Goldsbrough, P. (2002). Phytochelatins and metallothioneins: roles in heavy metal detoxification and homeostasis. *Annu. Rev. Plant Biol.* 53, 159–182. doi: 10.1146/annurev.arplant.53.100301.135154

Cui, J., Li, Y., Jin, Q., and Li, F. (2020). Silica nanoparticles inhibit arsenic uptake into rice suspension cells via improving pectin synthesis and the mechanical force of the cell wall. *Environ. Sci. Nano.* 7, 162–171. doi: 10.1039/C9EN01035A

Cui, J., Liu, T., Li, F., Yi, J., Liu, C., and Yu, H. (2017). Silica nanoparticles alleviate cadmium toxicity in rice cells: mechanisms and size effects. *Environ. pollut.* 228, 363–369. doi: 10.1016/j.envpol.2017.05.014

Currie, H. A., and Perry, C. C. (2007). Silica in plants: biological, biochemical and chemical studies. *Ann. Bot.* 100, 1383–1389. doi: 10.1093/aob/mcm247

da Cunha, K. P. V., and do Nascimento, C. W. A. (2009). Silicon effects on metal tolerance and structural changes in maize (*Zea mays* L.) grown on a cadmium and zinc enriched soil. *Wat. Air And Soil Poll* 197, 323–330. doi: 10.1007/s11270-008-9814-9

DalCorso, G. (2012). "Heavy metal toxicity in plants," in *Plants and Heavy Metals*. Ed. A. Furini (Springer, Dordrecht), 1–25. doi: 10.1007/978-94-007-4441-7_1

Debona, D., Rodrigues, F. A., and Datnoff, L. E. (2017). Silicon's role in abiotic and biotic plant stresses. *Ann. Rev. Phytopathol.* 55, 85–107. doi: 10.1146/annurev-phyto-080516-035312

de Sousa, A., Saleh, A. M., Habeeb, T. H., Hassan, Y. M., Zrieq, R., Wadaan, M. A., et al. (2019). Silicon dioxide nanoparticles ameliorate the phytotoxic hazards of aluminum in maize grown on acidic soil. *Sci. Total Environ.* 693, 133636. doi: 10.1016/j.scitotenv.2019.133636

de Tombeur, F., Raven, J. A., Toussaint, A., Lambers, H., Cooke, J., Hartley, S. E., et al. (2022). Why do plants silicify? *Trends Ecol. Evol.* 38, 275–288. doi: 10.1016/j.tree.2022.11.002

Doncheva, Sn., Poschenrieder, C., Stoyanova, Zl., Georgieva, K., Velichkova, M., and Barceló, J. (2009). Silicon amelioration of manganese toxicity in Mn-sensitive and Mn-tolerant maize varieties. *Environ. Exp. Bot.* 65, 189–197. doi: 10.1016/j.envexpbot.2008.11.006

Dragišić Maksimović, J., Bogdanović, J., Maksimović, V., and Nikolic, M. (2007). Silicon modulates the metabolism and utilization of phenolic compounds in cucumber (*Cucumis sativus* L.) grown at excess manganese. *J. Plant Nutr. Soil Sci.* 170, 739–744. doi: 10.1002/jpln.200700101

Dragišić Maksimović, J., Mojović, M., Maksimović, V., Römheld, V., and Nikolic, M. (2012). Silicon ameliorates manganese toxicity in cucumber by decreasing hydroxyl radical accumulation in the leaf apoplast. *J. Exp. Bot.* 63, 2411–2420. doi: 10.1093/jxb/err359

Duffus, J. H. (2002). " Heavy metals" a meaningless term? (IUPAC Technical Report). *Pure Appl. Chem.* 74, 793–807. doi: 10.1351/pac200274050793

El-Saadony, M. T., Desoky, E. S. M., Saad, A. M., Eid, R., Selem, E., and Elrys, A. S. (2021). Biological silicon nanoparticles improve *Phaseolus vulgaris* L. yield and minimize its contaminant contents on a heavy metals-contaminated saline soil. *Environ. Sci.* 106, 1–14. doi: 10.1016/j.jes.2021.01.012

El-Shetehy, M., Moradi, A., Maceroni, M., Reinhardt, D., Petri-Fink, A., Rothen-Rutishauser, B., et al. (2021). Silica nanoparticles enhance disease resistance in *Arabidopsis* plants. *Nat. Nanotechnol.* 16, 344–353. doi: 10.1038/s41565-020-00812-0

Emamverdian, A., Ding, Y., Mokhberdoran, F., Ahmad, Z., and Xie, Y. (2020). Determination of heavy metal tolerance threshold in a bamboo species (*Arundinaria pygmaea*) as treated with silicon dioxide nanoparticles. *Glob. Ecol. Conserv.* 24, e01306. doi: 10.1016/j.gecco.2020.e01306

Emamverdian, A., Ding, Y., Mokhberdoran, F., Ahmad, Z., and Xie, Y. (2021). The effect of silicon nanoparticles on the seed germination and seedling growth of moso bamboo (*Phyllostachys edulis*) under cadmium stress. *Pol. J. Environ. Stud.* 30, 6. doi: 10.15244/pjoes/129683

Emamverdian, A., Ding, Y., Mokhberdoran, F., Xie, Y., Zheng, X., and Wang, Y. (2019). Silicon dioxide nanoparticles improve plant growth by enhancing antioxidant enzyme capacity in bamboo (*Pleioblastus pygmaeus*) under lead toxicity. *Trees* 34, 469–481. doi: 10.1007/s00468-019-01929-z

Emamverdian, A., Ding, Y., and Xie, Y. (2018a). Effects of silicon in the amelioration of Zn toxicity on antioxidant enzyme activities. *Toxicol. Environ. Health Sci.* 10, 90–96. doi: 10.1007/s13530-018-0351-7

Emamverdian, A., Ding, Y., Xie, Y., and Sangari, S. (2018b). Silicon mechanisms to ameliorate heavy metal stress in plants. *BioMed. Res. Int.* 2018, 8492898. doi: 10.1155/2018/8492898

Epstein, E. (1994). The anomaly of silicon in plant biology. *Proc. Natl. Acad. Sci. U.S.A.* 91, 11–17. doi: 10.1073/pnas.91.1.11

Etxeberria, E., Gonzalez, P., and Pozueta, J. (2009). Evidence for two endocytic transport pathways in plant cells. *Plant Sci.* 177, 341–348. doi: 10.1016/j.plantsci.2009.06.014

Fabiano, C. C., Tezotto, T., Favarin, J. L., Polacco, J. C., and Mazzafera, P. (2015). Essentiality of nickel in plants: a role in plant stresses. *Front. Plant Sci.* 6. doi: 10.3389/fpls.2015.00754

Fan, X., Wen, X., Huang, F., Cai, Y., and Cai, K. (2016). Effects of silicon on morphology, ultrastructure and exudates of rice root under heavy metal stress. *Acta Physiol. Plant* 38, 1–9. doi: 10.1007/s11738-016-2221-8

Fan, N., Zhao, C., Yue, L., Ji, H., Wang, X., Xiao, Z., et al. (2022). Nanosilicon alters oxidative stress and defence reactions in plants: a meta-analysis, mechanism and perspective. *Environ. Sci. Nano* 9, 3742–3755. doi: 10.1039/D2EN00478J

Farooq, M. A., Islam, F., Ali, B., Najeeb, U., Mao, B., Gill, R. A., et al. (2016). Arsenic toxicity in plants: cellular and molecular mechanisms of its transport and metabolism. *Environ. Exp. Bot.* 132, 42–52. doi: 10.1016/j.envexpbot.2016.08.004

Fatemi, H., Pour, B. E., and Rizwan, M. (2020). Isolation and characterization of lead (Pb) resistant microbes and their combined use with silicon nanoparticles improved the growth, photosynthesis and antioxidant capacity of coriander (*Coriandrum sativum* L.) under Pb stress. *Environ. pollut.* 266, 114982. doi: 10.1016/j.envpol.2020.114982

Fiala, R., Fialová, I., Vaculík, M., and Luxová, M. (2021). Effect of silicon on the young maize plants exposed to nickel stress. *Plant Physiol. Biochem.* 166, 645–656. doi: 10.1016/j.plaphy.2021.06.026

Finnegan, P. M., and Chen, W. (2012). Arsenic toxicity: the effects on plant metabolism. *Front. Physiol.* 3, 182. doi: 10.3389/fphys.2012.00182

Gad, N. (2012). Physiological and chemical response of groundnut (*Arachis hypogaea*) to cobalt nutrition. *World Appl. Sci. J.* 2, 327–335.

Galbraith, D. W. (2007). Silica breaks through in plants. *Nat. Nanotechnol.* 2, 272–273. doi: 10.1038/nnano.2007.118

Ghori, N. H., Ghori, T., Hayat, M. Q., Imadi, S. R., Gul, A., Altay, V., et al. (2019). Heavy metal stress and responses in plants. *Int. J. Sci. Environ. Technol.* 16, 1807–1828. doi: 10.1007/s13762-019-02215-8

Giannakoula, A., Therios, I., and Chatzissavvidis, C. (2021). Effect of lead and copper on photosynthetic apparatus in citrus (*Citrus aurantium* L.) plants. The role of antioxidants in oxidative damage as a response to heavy metal stress. *Plants* 10, 155. doi: 10.3390/plants10010155

González-Moscoso, M., Juárez-Maldonado, A., Cadenas-Pliego, G., Meza-Figueroa, D., SenGupta, B., and Martínez-Villegas, N. (2022). Silicon nanoparticles decrease arsenic translocation and mitigate phytotoxicity in tomato plants. *Environ. Sci. pollut. Res.* 29, 34147–34163. doi: 10.1007/s11356-021-17665-2

González-Moscoso, M., Martínez-Villegas, N. V., Cadenas-Pliego, G., Benavides-Mendoza, A., Rivera-Cruz, M. D. C., González-Morales, S., et al. (2019). Impact of silicon nanoparticles on the antioxidant compounds of tomato fruits stressed by arsenic. *Foods* 8, 612. doi: 10.3390/foods8120612

Goswami, P., Mathur, J., and Srivastava, N. (2022). Silica nanoparticles as novel sustainable approach for plant growth and crop protection. *Heliyon* 8, e09908. doi: 10.1016/j.heliyon.2022.e09908

Gu, H. H., Qiu, H., Tian, T., Zhan, S. S., Deng, T. H. B., Chaney, R. L., et al. (2011). Mitigation effects of silicon rich amendments on heavy metal accumulation in rice (*Oryza sativa* L.) planted on multi-metal contaminated acidic soil. *Chemosphere* 83, 1234–1240. doi: 10.1016/j.chemosphere.2011.03.014

Gu, H. H., Zhan, S., Wang, S. Z., Tang, Y. T., Chaney, R. L., Fang, X. H., et al. (2012). Silicon-mediated amelioration of zinc toxicity in rice (*Oryza sativa* L.) seedlings. *Plant Soil.* 350, 193–204. doi: 10.1007/s11104-011-0894-8

Gupta, N., Yadav, K. K., Kumar, V., Kumar, S., Chadd, R. P., and Kumar, A. (2019). Trace elements in soil-vegetables interface: translocation, bioaccumulation, toxicity and amelioration – a review. *Sci. Total Environ.* 651, 2927–2942. doi: 10.1016/j.scitotenv.2018.10.047

Hafeez, B. (2013). Role of zinc in plant nutrition – A review. *Am. J. Exp. Agric.* 3, 374–391. doi: 10.9734/AJEA/2013/2746

Haghighi, M., Afifipour, Z., and Mozafarian, M. (2012). The effect of N-Si on tomato seed germination under salinity levels. *J. Biol. Environ. Sci.* 6, 87–90.

Haider, F. U., Liqun, C., Coulter, J. A., Cheema, S. A., Wu, J., Zhang, R., et al. (2021). Cadmium toxicity in plants: Impacts and remediation strategies. *Ecotoxicol. Environ. Saf.* 211, 111887. doi: 10.1016/j.ecoenv.2020.111887

Hasan, M. K., Cheng, Y., Kanwar, M. K., Chu, X. Y., Ahammed, G. J., and Qi, Z. Y. (2017). Responses of plant proteins to heavy metal stress – a review. *Front. Plant Sci.* 8. doi: 10.3389/fpls.2017.01492

Hasanuzzaman, M., Nahar, K., Alam, M., Roychowdhury, R., and Fujita, M. (2013). Physiological, biochemical, and molecular mechanisms of heat stress tolerance in plants. *Int. J. Mol. Sci.* 14, 9643–9684. doi: 10.3390/ijms14059643

Hassan, M. U., Aamer, M., Chattha, M. U., Haiying, T., Shahzad, B., Barbanti, L., et al. (2020). The critical role of zinc in plants facing the drought stress. *Agri* 10, 396. doi: 10.3390/agriculture10090396

Hassan, H., Alatawi, A., Abdulmajeed, A., Emam, M., and Khattab, H. (2021). Roles of Si and SiNPs in improving thermotolerance of wheat photosynthetic machinery via upregulation of PsbH, PsbB and PsbD genes encoding PSII core proteins. *Horticulturae* 7, 16. doi: 10.3390/horticulturae7020016

He, C., Ma, J., and Wang, L. (2015). A hemicellulose-bound form of silicon with potential to improve the mechanical properties and regeneration of the cell wall of rice. *New Phytol.* 206, 1051–1062. doi: 10.1111/nph.13282

He, C., Wang, L., Liu, J., Liu, X., Li, X., Ma, J., et al. (2013). Evidence for 'silicon' within the cell walls of suspension-cultured rice cells. *New Phytol.* 200. doi: 10.1111/nph.12401

Hodson, M. E. (2004). Heavy metals—geochemical bogey men? *Environ. pollut.* 129, 341–343. doi: 10.1016/j.envpol.2003.11.003

Hodson, M. J., White, P. J., Mead, A., and Broadley, M. R. (2005). Phylogenetic variation in the silicon composition of plants. *Annal. Bot.* 96, 1027–1046. doi: 10.1093/aob/mci255

Hossain, M. M., Khatun, M. A., Haque, M. N., Bari, M. A., Alam, M. F., Mandal, A., et al. (2018). Silicon alleviates arsenic-induced toxicity in wheat through vacuolar sequestration and ROS scavenging. *Int. J. Phytoremediation* 20, 796–804. doi: 10.1080/15226514.2018.1425669

Hossain, Z., Mustafa, G., and Komatsu, S. (2015). Plant responses to nanoparticle stress. *Int. J. Mol. Sci.* 16, 26644–26653. doi: 10.3390/ijms161125980

Huang, Q., Ayyaz, A., Farooq, M. A., Zhang, K., Chen, W., Hannan, F., et al. (2024). Silicon dioxide nanoparticles enhance plant growth, photosynthetic performance, and antioxidants defence machinery through suppressing chromium uptake in *Brassica napus* L. *Environ. pollut.* 342, 123013. doi: 10.1016/j.envpol.2023.123013

Huang, S., and Ma, J. F. (2020). Silicon suppresses zinc uptake through down-regulating zinc transporter gene in rice. *Physiol. Plant* 170, 580–591. doi: 10.1111/ppl.13196

Huang, Y. Z., Zhang, W. Q., and Zhao, L. J. (2012). Silicon enhances resistance to antimony toxicity in the low-silica rice mutant, lsi1. *Chem. Ecol.* 28, 341–354. doi: 10.1080/02757540.2012.656609

Hussain, B., Lin, Q., Hamid, Y., Sanaullah, M., Di, L., Khan, M. B., et al. (2020). Foliage application of selenium and silicon nanoparticles alleviates Cd and Pb toxicity in rice (*Oryza sativa* L.). *Sci. Total Environ.* 712, 136497. doi: 10.1016/j.scitotenv.2020.136497

Hussain, A., Rizwan, M., Ali, Q., and Ali, S. (2019). Seed priming with silicon nanoparticles improved the biomass and yield while reduced the oxidative stress and cadmium concentration in wheat grains. *Environ. Sci. pollut. Res.* 26, 7579–7588. doi: 10.1007/s11356-019-04210-5

Iwasaki, K., Maier, P., Fecht, M., and Horst, W. J. (2002). Leaf apoplastic silicon enhances manganese tolerance of cowpea (*Vigna unguiculata*). *J. Plant Physiol.* 159, 167–173. doi: 10.1078/0176-1617-00691

Iwasaki, K., and Matsumura, A. (1999). Effect of silicon on alleviation of manganese toxicity in pumpkin *(Cucurbita moschata* Duch cv. Shintosa). *Soil Sci. Plant Nutr.* 45, 909–920. doi: 10.1080/00380768.1999.10414340

Janmohammadi, M., Amanzadeh, T., Sabaghnia, N., and Ion, V. (2016). Effect of nano-silicon foliar application on safflower growth under organic and inorganic fertilizer regimes. *Bot. Lith.* 22, 53–64. doi: 10.1515/botlit-2016-0005

Karunakaran, G., Suriyaprabha, R., Manivasakan, P., Yuvakkumar, R., Rajendran, V., Prabu, P., et al. (2013). Effect of nanosilica and silicon sources on plant growth promoting rhizobacteria, soil nutrients and maize seed germination. *IET Nanobiotechnol.* 7, 70–77. doi: 10.1049/iet-nbt.2012.0048

Karunakaran, G., Suriyaprabha, R., Rajendran, V., and Kannan, N. (2016). Influence of ZrO_2, SiO_2, Al_2O_3 and TiO_2 nanoparticles on maize seed germination under different growth conditions. *IET Nanobiotechnol.* 10, 171–177. doi: 10.1049/iet-nbt.2015.0007

Kaur, H., and Garg, N. (2021). Zinc toxicity in plants: a review. *Planta* 253, 129. doi: 10.1007/s00425-021-03642-z

Kaushik, P., and Saini, D. K. (2019). Silicon as a vegetable crops modulator – a review. *Plants* 8, 148. doi: 10.3390/plants8060148

Kaya, C., Akram, N. A., Ashraf, M., AlYemeni, M. N., and Ahmad, P. (2020a). Exogenously supplied silicon (Si) improves cadmium tolerance in pepper (*Capsicum annuum* L.) by up-regulating the synthesis of nitric oxide and hydrogen sulfide. *J. Biotechnol.* 316, 35–45. doi: 10.1016/j.jbiotec.2020.04.008

Kaya, C., Ashraf, M., Al-Huqail, A. A., Alqahtani, M. A., and Ahmad, P. (2020b). Silicon is dependent on hydrogen sulphide to improve boron toxicity tolerance in pepper plants by regulating the AsA-GSH cycle and glyoxalase system. *Chemosphere* 257, 127241. doi: 10.1016/j.chemosphere.2020.127241

Khaliq, A., Ali, S., Hameed, A., Farooq, M. A., Farid, M., Shakoor, M. B., et al. (2016). Silicon alleviates nickel toxicity in cotton seedlings through enhancing growth, photosynthesis, and suppressing Ni uptake and oxidative stress. *Arch. Agron. Soil Sci.* 62, 633–647. doi: 10.1080/03650340.2015.1073263

Khan, S., Cao, Q., Zheng, Y. M., Huang, Y. Z., and Zhu, Y. G. (2008). Health risks of heavy metals in contaminated soils and food crops irrigated with wastewater in Beijing, China. *Environ. pollut.* 152, 686–692. doi: 10.1016/j.envpol.2007.06.056

Khan, A., Khan, A. L., Imran, M., Asaf, S., Kim, Y. H., Bilal, S., et al. (2020b). Silicon-induced thermotolerance in *Solanum lycopersicum* L. via activation of antioxidant system, heat shock proteins, and endogenous phytohormones. *BMC Plant Biol.* 20, 248. doi: 10.1186/s12870-020-02456-7

Khan, Z. S., Rizwan, M., Hafeez, M., Ali, S., Adrees, M., Qayyum, M. F., et al. (2020a). Effects of silicon nanoparticles on growth and physiology of wheat in cadmium contaminated soil under different soil moisture levels. *Environ. Sci. pollut. Res.* 27, 4958–4968. doi: 10.1007/s11356-019-06673-y

Kheyri, N., Norouzi, H. A., Mobasser, H. R., and Torabi, B. (2019). Effects of silicon and zinc nanoparticles on growth, yield, and biochemical characteristics of rice. *Agron. J.* 111, 3084–3090. doi: 10.2134/agronj2019.04.0304

Kidd, P. S., Llugany, M., Poschenrieder, C. H., Gunse, B., and Barcelo, J. (2001). The role of root exudates in aluminium resistance and silicon-induced amelioration of aluminium toxicity in three varieties of maize (*Zea mays* L.). *J. Exp. Bot.* 52, 1339–1352. doi: 10.1093/jexbot/52.359.1339

Kim, Y. H., Khan, A. L., Kim, D. H., Lee, S. Y., Kim, K. M., Waqas, M., et al. (2014). Silicon mitigates heavy metal stress by regulating P-type heavy metal ATPases, *Oryza sativa* low silicon genes, and endogenous phytohormones. *BMC Plant Biol.* 14, 1–13. doi: 10.1186/1471-2229-14-13

Kopittke, P. M., de Jonge, M. D., Menzies, N. W., Wang, P., Donner, E., McKenna, B. A., et al. (2012). Examination of the distribution of arsenic in hydrated and fresh cowpea roots using two-and three-dimensional techniques. *Plant Physiol.* 159, 1149–1158. doi: 10.1104/pp.112.197277

Kopittke, P. M., Gianoncelli, A., Kourousias, G., Green, K., and McKenna, B. A. (2017). Alleviation of Al toxicity by Si is associated with the formation of Al–Si complexes in root tissues of sorghum. *Front. Plant Sci.* 8. doi: 10.3389/fpls.2017.02189

Korndörfer, G. H., and Lepsch, I. (2001). "Effect of silicon on plant growth and crop yield," in *Studies in plant science*, vol. 8 . Eds. L. E. Datnoff, G. H. Snyder and G. H. Korndörfer (Amsterdam, The Netherlands: Elsevier), 133–147.

Kumar, S., Soukup, M., and Elbaum, R. (2017). Silicification in grasses: variation between different cell types. *Front. Plant Sci.* 8. doi: 10.3389/fpls.2017.00438

Küpper, H. (2017). "Lead toxicity in plants," in *Lead: Its Effects on Environment and Health*. Eds. A. Sigel, H. Sigel and R. K. O. Sigel (De Gruyter, Berlin, Boston), 491–500. doi: 10.1515/9783110434330-015

Küpper, H., Šetlík, I., Spiller, M., Küpper, F. C., and Prášil, O. (2002). Heavy metal-induced inhibition of photosynthesis: targets of in *vivo* heavy metal chlorophyll formation. *J. Phycol.* 38, 429–441. doi: 10.1046/j.1529-8817.2002.01148.x

Labancová, E., Vivodová, Z., Šípošová, K., and Kollárová, K. (2023). silicon actuates Poplar calli tolerance after longer exposure to antimony. *Plants* 12, 689. doi: 10.3390/plants12030689

Lavres, J., Castro Franco, G., and de Sousa Câmara, G. M. (2016). Soybean seed treatment with nickel improves biological nitrogen fixation and urease activity. *Front. Environ. Sci.* 4. doi: 10.3389/fenvs.2016.00037

Li, J., Leisner, S. M., and Frantz, J. (2008). Alleviation of copper toxicity in *Arabidopsis thaliana* by silicon addition to hydroponic solutions. *J. Am. Soc Hortic. Sci.* 133, 670. doi: 10.21273/JASHS.133.5.670

Li, P., Song, A., Li, Z., Fan, F., and Liang, Y. (2015). Silicon ameliorates manganese toxicity by regulating both physiological processes and expression of genes associated with photosynthesis in rice (*Oryza sativa* L.). *Plant Soil.* 397, 289–301. doi: 10.1007/s11104-015-2626-y

Li, Y., Zhu, N., Liang, X., Bai, X., Zheng, L., Zhao, J., et al. (2020). Silica nanoparticles alleviate mercury toxicity via immobilization and inactivation of Hg (II) in soybean (*Glycine max*). *Environ. Sci. Nano.* 7, 1807–1817. doi: 10.1039/D0EN00091D

Lian, J., Zhao, L., Wu, J., Xiong, H., Bao, Y., Zeb, A., et al. (2020). Foliar spray of TiO_2 nanoparticles prevails over root application in reducing Cd accumulation and mitigating Cd-induced phytotoxicity in maize (*Zea mays* L.). *Chemosphere* 239, 124794. doi: 10.1016/j.chemosphere.2019.124794

Liang, Y., Nikolic, M., Bélanger, R., Gong, H., and Song, A. (2015). *Silicon in agriculture: from theory to practice* (Dordrecht, the Netherlands: Springer). doi: 10.1007/978-94-017-9978-2

Liu, D., Gao, Z., Li, J., Yao, Q., Tan, W., Xing, W., et al. (2023). Effects of cadmium stress on the morphology, physiology, cellular ultrastructure, and BvHIPP24 gene expression of sugar beet (*Beta vulgaris* L.). *Int. J. Phytoremediation* 25, 455–465. doi: 10.1080/15226514.2022.2090496

Liu, Y., Liangliang, Z., Shaoqi, Z., and Xie, F. (2020a). Effects of mercury binding by humic acid and humic acid resistance on mercury stress in rice plants under high Hg/humic acid concentration ratios. *Environ. Sci. pollut. Res. Int.* 27, 18650–18660. doi: 10.1007/s11356-020-08328-9

Liu, X., Yin, L., Deng, X., Gong, D., Du, S., Wang, S., et al. (2020b). Combined application of silicon and nitric oxide jointly alleviated cadmium accumulation and toxicity in maize. *J. Hazard Mater.* 395, 122679. doi: 10.1016/j.jhazmat.2020.122679

Long, X. X., Yang, X. E., Ni, W. Z., Ye, Z. Q., He, Z. L., Calvert, D. V., et al. (2003). Assessing zinc thresholds for phytotoxicity and potential dietary toxicity in selected vegetable crops. *Commun. Soil Sci. Plant Anal.* 34, 1421–1434. doi: 10.1081/CSS-120020454

Lukačová, Z., Švubová, R., Kohanová, J., and Lux, A. (2013). Silicon mitigates the Cd toxicity in maize in relation to cadmium translocation, cell distribution, antioxidant enzymes stimulation and enhanced endodermal apoplasmic barrier development. *Plant Growth Regul.* 70, 89–103. doi: 10.1007/s10725-012-9781-4

Lux, A., Šottníková, A., Opatrná, J., and Greger, M. (2004). Differences in structure of adventitious roots in Salix clones with contrasting characteristics of cadmium accumulation and sensitivity. *Physiol. Plant* 120, 537–545. doi: 10.1111/j.0031-9317.2004.0275.x

Luyckx, M., Hausman, J. F., Lutts, S., and Guerriero, G. (2017). Silicon and plants: Current knowledge and technological perspectives. *Front. Plant Sci.* 8. doi: 10.3389/fpls.2017.00411

Ma, J. F. (2004). Role of silicon in enhancing the resistance of plants to biotic and abiotic stresses. *Soil Sci. Plant Nutr.* 50, 11–18. doi: 10.1080/00380768.2004.10408447

Ma, J., Cai, H., He, C., Zhang, W., and Wang, L. (2015). A hemicellulose-bound form of silicon inhibits cadmium ion uptake in rice (*Oryza sativa*) cells. *New Phytol.* 206, 1063–1074. doi: 10.1111/nph.13276

Ma, J., Saleem, M. H., Ali, B., Rasheed, R., Ashraf, M. A., Aziz, H., et al. (2022). Impact of foliar application of syringic acid on tomato (*Solanum lycopersicum* L.) under heavy metal stress-insights into nutrient uptake, redox homeostasis, oxidative stress, and antioxidant defense. *Front. Plant Sci.* 13. doi: 10.3389/fpls.2022.950120

Ma, J. F., Tamai, K., Yamaji, N., Mitani, N., Konishi, S., Katsuhara, M., et al. (2006). A silicon transporter in rice. *Nature* 440, 688–691. doi: 10.1038/nature04590

Ma, J. F., and Yamaji, N. (2015). A cooperative system of silicon transport in plants. *Trends Plant Sci.* 20, 435–442. doi: 10.1016/j.tplants.2015.04.007

Ma, J. F., Yamaji, N., Mitani, N., Tamai, K., Konishi, S., Fujiwara, T., et al. (2007). An efflux transporter of silicon in rice. *Nature* 448, 209–212. doi: 10.1038/nature05964

Ma, J. F., Yamaji, N., and Mitani-Ueno, N. (2011). Transport of silicon from roots to panicles in plants. *Proc. Jpn. Acad. Ser. B* 87, 377–385. doi: 10.2183/pjab.87.377

Mahboub, H. H., Shahin, K., Mahmoud, S. M., Altohamy, D. E., Husseiny, W. A., Mansour, D. A., et al. (2022). Silica nanoparticles are novel aqueous additive mitigating heavy metals toxicity and improving the health of African catfish, *Clarias gariepinus*. *Aquat. Toxicol.* 249, 106238. doi: 10.1016/j.aquatox.2022.106238

Małkowski, E., Sitko, K., Zieleźnik-Rusinowska, P., Gieroń, Ż., and Szopiński, M. (2019). "Heavy metal toxicity: Physiological implications of metal toxicity in plants," in *Plant Metallomics and Functional Omics*. Ed. G. Sablok (Switzerland: Springer Cham), 253–301. doi: 10.1007/978-3-030-

Manara, A. (2012). "Plant responses to heavy metal toxicity," in *Plants and Heavy Metals*. Ed. A. Furini (New York, USA: Springer Dordrecht), 27–53. doi: 10.1007/978-94-007-4441-7_2

Manivannan, A., and Ahn, Y. K. (2017). Silicon regulates potential genes involved in major physiological processes in plants to combat stress. *Front. Plant Sci.* 8. doi: 10.3389/fpls.2017.01346

Manzoor, N., Ali, L., Ahmed, T., Rizwan, M., Ali, S., Shahid, M. S., et al. (2022). Silicon oxide nanoparticles alleviate chromium toxicity in wheat (*Triticum aestivum* L.). *Environ. pollut.* 315, 120391. doi: 10.1016/j.envpol.2022.120391

Marschner, H. (2012). *Marschner's mineral nutrition of higher plants* (London, UK: Academic press).

Marslin, G., Sheeba, C. J., and Franklin, G. (2017). Nanoparticles alter secondary metabolism in plants via ROS burst. *Front. Plant Sci.* 8. doi: 10.3389/fpls.2017.00832

Martinka, M., Vaculík, M., and Lux, A. (2014). "Plant cell responses to cadmium and zinc," in *Applied Plant Cell Biology*. Eds. P. Nick and Z. Opatrny (Springer Berlin, Heidelberg), 209–246. doi: 10.1007/978-3-642-41787-0_7

Masindi, V., and Muedi, K. L. (2018). "Environmental contamination by heavy metals," in *Heavy Metals*. Eds. H. E. D. M. Saleh and R. F. Aglan (London, UK: Tech). doi: 10.5772/intechopen.76082

Memari-Tabrizi, E. F., Yousefpour-Dokhanieh, A., and Babashpour-Asl, M. (2021). Foliar-applied silicon nanoparticles mitigate cadmium stress through physio-chemical changes to improve growth, antioxidant capacity, and essential oil profile of summer savory (*Satureja hortensis* L.). *Plant Physiol. Biochem.* 165, 71–79. doi: 10.1016/j.plaphy.2021.04.040

Millaleo, R., Reyes- Diaz, M., Ivanov, A. G., Mora, M. L., and Alberdi, M. (2010). Manganese as essential and toxic element for plants: Transport, accumulation and resistance mechanisms. *J. Soil Sci. Plant Nutr.* 10, 470–481. doi: 10.4067/S0718-95162010000200008

Mitani, N., Ma, J. F., and Iwashita, T. (2005). Identification of the silicon form in xylem sap of rice (*Oryza sativa* L.). *Plant Cell Physiol.* 46, 279–283. doi: 10.1093/pcp/pci018

Mitani-Ueno, N., and Ma, J. F. (2021). Linking transport system of silicon with its accumulation in different plant species. *Soil Sci. Plant Nutr.* 67, 10–17. doi: 10.1080/00380768.2020.1845972

Mitani-Ueno, N., Yamaji, N., Zhao, F. J., and Ma, J. F. (2011). The aromatic/arginine selectivity filter of NIP aquaporins plays a critical role in substrate selectivity for silicon, boron, and arsenic. *J. Exp. Bot.* 62, 4391–4398. doi: 10.1093/jxb/err158

Moharem, M., Elkhatib, E., and Mesalem, M. (2019). Remediation of chromium and mercury polluted calcareous soils using nanoparticles: Sorption-desorption kinetics, speciation and fractionation. *Environ. Res.* 170, 366–373. doi: 10.1016/j.envres.2018.12.054

Mukarram, M., Khan, M. M. A., and Corpas, F. J. (2021). Silicon nanoparticles elicit an increase in lemongrass (*Cymbopogon flexuosus* (Steud.) Wats) agronomic parameters with a higher essential oil yield. *J. Hazard. Mater.* 412, 125254. doi: 10.1016/j.jhazmat.2021.125254

Mukarram, M., Khan, M. M. A., Kurjak, D., Lux, A., and Corpas, F. J. (2023). Silicon nanoparticles (SiNPs) restore photosynthesis and essential oil content by upgrading enzymatic antioxidant metabolism in lemongrass (*Cymbopogon flexuosus*) under salt stress. *Front. Plant Sci.* 17. doi: 10.3389/fpls.2023.1116769

Mukarram, M., Petrik, P., Mushtaq, Z., Khan, M. M. A., Gulfishan, M., and Lux, A. (2022). Silicon nanoparticles in higher plants: Uptake, action, stress tolerance, and crosstalk with phytohormones, antioxidants, and other signalling molecules. *Environ. Pol.* 310, 119855. doi: 10.1016/j.envpol.2022.119855

Muneer, S., and Jeong, B. R. (2015a). Genotypic variation under Fe deficiency results in rapid changes in protein expressions and genes involved in Fe metabolism and antioxidant mechanisms in tomato seedlings (*Solanum lycopersicum* L.). *Int. J. Mol. Sci.* 16, 28022–28037. doi: 10.3390/ijms161226086

Muneer, S., and Jeong, B. R. (2015b). Proteomic analysis of salt-stress responsive proteins in roots of tomato (*Lycopersicon esculentum* L.) plants towards silicon efficiency. *Plant Growth Regul.* 77, 133–146. doi: 10.1007/s10725-015-0045-y

Naaz, H., Rawat, K., Saffeullah, P., and Umar, S. (2023). Silica nanoparticles synthesis and applications in agriculture for plant fertilization and protection: A review. *Environ. Chem. Lett.* 21, 539–559. doi: 10.1007/s10311-022-01515-9

Nazaralian, S., Majd, A., Irian, S., Najafi, F., Ghahremaninejad, F., Landberg, T., et al. (2017). Comparison of silicon nanoparticles and silicate treatments in fenugreek. *Plant Physiol. Biochem.* 115, 25–23. doi: 10.1016/j.plaphy.2017.03.009

Neumann, D., and Zur Nieden, U. (2001). Silicon and heavy metal tolerance of higher plants. *Phytochemistry* 56, 685–692. doi: 10.1016/S0031-9422(00)00472-6

Neumann, D., zur Nieden, U., Schwieger, W., Leopold, I., and Lichtenberger, O. (1997). Heavy metal tolerance of *Minuartia verna*. *J. Plant Physiol.* 151, 101–108. doi: 10.1016/S0176-1617(97)80044-2

Nieboer, E., and Richardson, D. H. (1980). The replacement of the nondescript term 'heavy metals' by a biologically and chemically significant classification of metal ions. *Environ. pollut. Ser. B Chem. Phys.* 1, 3–26. doi: 10.1016/0143-148X(80)90017-8

Oliva, S. R., Mingorance, M. D., and Leidi, E. O. (2011). Effects of silicon on copper toxicity in *Erica andevalensis* Cabezudo and Rivera: a potential species to remediate contaminated soils. *J. Environ. Monit.* 13, 591–596. doi: 10.1039/c0em00549e

Ovečka, M., and Takáč, T. (2014). Managing heavy metal toxicity stress in plants: Biological and biotechnological tools. *Biotechnol. Adv.* 32, 73–86. doi: 10.1016/j.biotechadv.2013.11.011

Pinto Irish, K., Harvey, M. A., Harris, H. H., Aarts, M. G., Chan, C. X., Erskine, P. D., et al. (2023). Micro-analytical and molecular approaches for understanding the distribution, biochemistry, and molecular biology of selenium in (hyperaccumulator) plants. *Planta* 257, 2. doi: 10.1007/s00425-022-04017-8

Planchet, E., and Kaiser, W. M. (2006). Nitric oxide (NO) detection by DAF fluorescence and chemiluminescence: a comparison using abiotic and biotic NO sources. *J. Exp. Bot.* 57, 3043–3055. doi: 10.1093/jxb/erl070

Pollard, A. J., Reeves, R. D., and Baker, A. J. (2014). Facultative hyperaccumulation of heavy metals and metalloids. *Plant Sci.* 217, 8–17. doi: 10.1016/j.plantsci.2013.11.011

Pourret, O., and Bollinger, J. C. (2017). 'Heavy metals'-what to do now: to use or not to use? *Sci. Total Environ.* 610, 419–420. doi: 10.1016/j.scitotenv.2017.08.043

Printz, B., Lutts, S., Hausman, J. F., and Sergeant, K. (2016). Copper trafficking in plants and its implication on cell wall dynamics. *Front. Plant Sci.* 7. doi: 10.3389/fpls.2016.00601

Rahimi, G., Kolahchi, Z., and Charkhabi, A. (2017). Uptake and translocation of some heavy metals by rice crop (*Oryza sativa*) in paddy soils. *Agric. Polnohospodárstvo* 63, 163–175. doi: 10.1515/agri-2017-0016

Rahman, M. F., Ghosal, A., Alam, M. F., and Kabir, A. H. (2017). Remediation of cadmium toxicity in field peas (*Pisum sativum* L.) through exogenous silicon. *Ecotoxicol. Environ. Saf.* 135, 165–172. doi: 10.1016/j.ecoenv.2016.09.019

Rahman, A., Wallis, C. M., and Uddin, W. (2015). Silicon-induced systemic defense responses in perennial ryegrass against infection by *Magnaporthe oryzae*. *Phytopathol* 105, 748–757. doi: 10.1094/PHYTO-12-14-0378-R

Rascio, N., and Navari-Izzo, F. (2011). Heavy metal hyperaccumulating plants: how and why do they do it? And what makes them so interesting? *Plant Sci.* 180, 169–181. doi: 10.1016/j.plantsci.2010.08.016

Rastogi, A., Tripathi, D. K., Yadav, S., Chauhan, D. K., Živčák, M., Ghorbanpour, M., et al. (2019). Application of silicon nanoparticles in agriculture. *3 Biotech.* 9, 1–11. doi: 10.1007/s13205-019-1626-7

Riaz, M., Zhao, S., Kamran, M., Ur Rehman, N., Mora-Poblete, F., Maldonado, C., et al. (2022). Effect of nano-silicon on the regulation of ascorbate-glutathione contents, antioxidant defense system and growth of copper stressed wheat (*Triticum aestivum* L.) seedlings. *Front. Plant Sci.* 13. doi: 10.3389/fpls.2022.986991

Rizwan, M., Ali, S., Malik, S., Adrees, M., Qayyum, M. F., Alamri, S. A., et al. (2019). Effect of foliar applications of silicon and titanium dioxide nanoparticles on growth, oxidative stress, and cadmium accumulation by rice (*Oryza sativa*). *Acta Physiol. Plant* 41, 1–12. doi: 10.1007/s11738-019-2828-7

Rodríguez-Serrano, M., Romero-Puertas, M. C., Pazmino, D. M., Testillano, P. S., Risueño, M. C., Del Río, L. A., et al. (2009). Cellular response of pea plants to cadmium toxicity: cross talk between reactive oxygen species, nitric oxide, and calcium. *Plant Physiol.* 150, 229–243. doi: 10.1104/pp.108.131524

Rossi, L., Zhang, W., Schwab, A. P., and Ma, X. (2017). Uptake, accumulation, and in planta distribution of coexisting cerium oxide nanoparticles and cadmium in *Glycine max* (L.) Merr. *Environ. Sci. Technol.* 51, 12815–12824. doi: 10.1021/acs.est.7b03363

Salt, D. E., Smith, R. D., and Raskin, I. (1998). Phytoremediation. *Annu. Rev. Plant Physiol. Plant Mol. Biol.* 49, 643–668. doi: 10.1146/annurev.arplant.49.1.643

Samantaray, S., Rout, G. R., and Das, P. (1998). Role of chromium on plant growth and metabolism. *Acta Physiol. Plant* 20, 201–212. doi: 10.1007/s11738-998-0015-3

Sardar, R., Ahmed, S., Shah, A. A., and Yasin, N. A. (2022). Selenium nanoparticles reduced cadmium uptake, regulated nutritional homeostasis and antioxidative system in *Coriandrum sativum* grown in cadmium toxic conditions. *Chemosphere* 287, 132332. doi: 10.1016/j.chemosphere.2021.132332

Schaller, J., Puppe, D., Kaczorek, D., Ellerbrock, R., and Sommer, M. (2021). Silicon cycling in soils revisited. *Plants* 10, 295. doi: 10.3390/plants10020295

Schmidt, W., Thomine, S., and Buckhout, T. J. (2020). Iron nutrition and interactions in plants. *Front. Plant Sci.* 10. doi: 10.3389/fpls.2019.01670

Schwarz, K. (1973). A bound form of silicon in glycosaminoglycans and polyuronides. *Proc. Natl. Acad. Sci. U.S.A.* 70, 1608–1612. doi: 10.1073/pnas.70.5.1608

Shahnaz, G., Shekoofeh, E., Kourosh, D., and Moohamadbagher, B. (2011). Interactive effects of silicon and aluminum on the malondialdehyde (MDA), proline, protein and phenolic compounds in *Borago officinalis* L. *J. Med. Plant Res.* 5, 5818–5827.

Sharifi-Rad, J., Sharifi-Rad, M., and Teixeira da Silva, J. A. (2016). Morphological, physiological and biochemical responses of crops (*Zea mays* L., *Phaseolus vulgaris* L.), medicinal plants (*Hyssopus officinalis* L., *Nigella sativa* L.), and weeds (*Amaranthus retroflexus* L., *Taraxacum officinale* FH Wigg) exposed to SiO_2 nanoparticles. *J. Agr. Sci. Tech.* 18, 1027–1040.

Sharma, S. S., and Dietz, K. J. (2009). The relationship between metal toxicity and cellular redox imbalance. *Trends Plant Sci.* 14, 43–50. doi: 10.1016/j.tplants.2008.10.007

Sharma, A., Vishwakarma, K., Singh, N. K., Prakash, V., Ramawat, N., Prasad, R., et al. (2022). Synergistic action of silicon nanoparticles and indole acetic acid in alleviation of chromium (CrVI) toxicity in *Oryza sativa* seedlings. *J. Biotechnol.* 343, 71–82. doi: 10.1016/j.jbiotec.2021.09.005

Sheng, H., and Chen, S. (2020). Plant silicon-cell wall complexes: Identification, model of covalent bond formation and biofunction. *Plant Physiol. Biochem.* 155, 13–19. doi: 10.1016/j.plaphy.2020.07.020

Shetty, R., Frett´e, X., Jensen, B., Shetty, N. P., Jensen, J. D., Jørgensen, H. J., et al. (2011). Silicon-induced changes in antifungal phenolic acids, flavonoids, and key phenylpropanoid pathway genes during the interaction between miniature roses and the biotrophic pathogen *Podosphaera pannosa*. *Plant Physiol.* 157, 2194–2205. doi: 10.1104/pp.111.185215

Shetty, R., Vidya, C. S. N., Weidinger, M., and Vaculík, M. (2021). Silicon alleviates antimony phytotoxicity in giant reed (*Arundo donax* L.). *Planta* 254, 100. doi: 10.1007/s00425-021-03756-4

Shi, Q., Bao, Z., Zhu, Z., He, Y., Qian, Q., and Yu, J. (2005). Silicon-mediated alleviation of Mn toxicity in *Cucumis sativus* in relation to activities of superoxide dismutase and ascorbate peroxidase. *Phytochem* 66, 1551–1559. doi: 10.1016/j.phytochem.2005.05.006

Silva, A. J., Nascimento, C. W. A., and Gouveia-Neto, A. S. (2017). Assessment of cadmium toxicities in potted garlic plants. *Acta Physiol. Plant* 38, 211. doi: 10.3390/biology11060850

Siqueira Freitas, D., Wurr Rodak, B., Rodrigues dos Reis, A., de Barros Reis, F., Soares de Carvalho, T., Schulze, J., et al. (2018). Hidden nickel deficiency? nickel fertilization via soil improves nitrogen metabolism and grain yield in soybean genotypes. *Front. Plant Sci.* 9. doi: 10.3389/fpls.2018.00614

Song, A., Li, P., Fan, F., Li, Z., and Liang, Y. (2014). The effect of silicon on photosynthesis and expression of its relevant genes in rice (*Oryza sativa* L.) under high-zinc stress. *PloS One* 9, e113782. doi: 10.1371/journal.pone.0113782

Song, A., Li, Z., Zhang, J., Xue, G., Fan, F., and Liang, Y. (2009). Silicon-enhanced resistance to cadmium toxicity in *Brassica chinensis* L. @ is attributed to Si-suppressed cadmium uptake and transport and Si-enhanced antioxidant defense capacity. *J. Hazard. Mat.* 172, 74–83. doi: 10.1016/j.jhazmat.2009.06.143

Soukup, M., Rodriguez Zancajo, V. M., Kneipp, J., and Elbaum, R. (2020). Formation of root silica aggregates in sorghum is an active process of the endodermis. *J. Exp. Bot.* 71, 6807–6817. doi: 10.1093/jxb/erz387

Soundararajan, P., Manivannan, A., Ko, C. H., and Jeong, B. R. (2018). Silicon enhanced redox homeostasis and protein expression to mitigate the salinity stress in Rosa hybrid 'Rock fire. *J. Plant Growth Regul.* 37, 16–34. doi: 10.1007/s00344-017-9705-7

Sperdouli, I., Adamakis, I. D. S., Dobrikova, A., Apostolova, E., Hanć, A., and Moustakas, M. (2022). Excess zinc supply reduces cadmium uptake and mitigates cadmium toxicity effects on chloroplast structure, oxidative stress, and photosystem II photochemical efficiency in *Salvia sclarea* plants. *Toxics* 10, 36. doi: 10.3390/toxics10010036

Sun, S. K., Chen, Y., Che, J., Konishi, N., Tang, Z., Miller, A. J., et al. (2018). Decreasing arsenic accumulation in rice by overexpressing *OsNIP1;1* and *OsNIP3;3* through disrupting arsenite radial transport in roots. *New Phytol.* 219, 641–653. doi: 10.1111/nph.15190

Sun, D., Hussain, H. I., Yi, Z., Rookes, J. E., Kong, L., and Cahill, D. M. (2016). Mesoporous silica nanoparticles enhance seedling growth and photosynthesis in wheat and lupin. *Chemosphere* 152, 81–91. doi: 10.1016/j.chemosphere.2016.02.096

Takahashi, E., Ma, J. F., and Miyake, Y. (1990). The possibility of silicon as an essential element for higher plants. *J. Agric. Food Chem.* 2, 99–122.

Tang, J., Zhang, L., Zhang, J., Ren, L., Zhou, Y., Zheng, Y., et al. (2020). Physicochemical features, metal availability and enzyme activity in heavy metal-polluted soil remediated by biochar and compost. *Sci. Total Environ.* 701, 134751. doi: 10.1016/j.scitotenv.2019.134751

Thind, S., Hussain, I., Rasheed, R., Ashraf, M. A., Perveen, A., Ditta, A., et al. (2021). Alleviation of cadmium stress by silicon nanoparticles during different phenological stages of Ujala wheat variety. *Arab. J. Geosci.* 14, 1028. doi: 10.1007/s12517-021-07384-w

Tóth, É.C., Vissi, E., Kovács, I., Szöke, A., Ariño, J., Gergely, P., et al. (2000). Protein phosphatase 2A holoenzyme and its subunits from *Medicago sativa*. Plant Mol. *Biol* 43, 527–536. doi: 10.1023/A:1006436925253

Tripathi, D. K., Singh, V. P., Prasad, S. M., Chauhan, D. K., and Dubey, N. K. (2015). Silicon nanoparticles (SiNp) alleviate chromium (VI) phytotoxicity in *Pisum sativum* (L.) seedlings. *Plant Physiol. Biochem.* 96, 189–198. doi: 10.1016/j.plaphy.2015.07.026

Tripathi, D. K., Singh, S., Singh, V. P., Prasad, S. M., Chauhan, D. K., and Dubey, N. K. (2016). Silicon nanoparticles more efficiently alleviate arsenate toxicity than silicon in maize cultiver and hybrid differing in arsenate tolerance. *Front.Environ. Sci.* 4. doi: 10.3389/fenvs.2016.00046

Tripathi, D. K., Singh, S., Singh, V. P., Prasad, S. M., Dubey, N. K., and Chauhan, D. K. (2017). Silicon nanoparticles more effectively alleviated UV-B stress than silicon in wheat (*Triticum aestivum*) seedlings. *Plant Physiol. Biochem.* 110, 70–81. doi: 10.1016/j.plaphy.2016.06.026

Tripathi, D. K., Vishwakarma, K., Singh, V. P., Prakash, V., Sharma, S., Muneer, S., et al. (2021). Silicon crosstalk with reactive oxygen species, phytohormones and other signaling molecules. *J. Hazard. Mat.* 408, 124820. doi: 10.1016/j.jhazmat.2020.124820

Vaculík, M., Kováč, J., Fialová, I., Fiala, R., Jašková, K., and Luxová, M. (2021). Multiple effects of silicon on alleviation of nickel toxicity in young maize roots. *J. Hazard. Mater.* 415, 125570. doi: 10.1016/j.jhazmat.2021.125570

Vaculík, M., Landberg, T., Greger, M., Luxová, M., Stoláriková, M., and Lux, A. (2012). Silicon modifies root anatomy, and uptake and subcellular distribution of cadmium in young maize plants. *Ann. Bot.* 110, 433–443. doi: 10.1093/aob/mcs039

Vaculík, M., Lukačová, Z., Bokor, B., Martinka, M., Tripathi, D. K., and Lux, A. (2020). Alleviation mechanisms of metal (loid) stress in plants by silicon: a review. *J. Exp. Bot.* 71, 6744–6757. doi: 10.1093/jxb/eraa288

Vaculík, M., Lux, A., Luxová, M., Tanimoto, E., and Lichtscheidl, I. (2009). Silicon mitigates cadmium inhibitory effects in young maize plants. *Environ. Exp. Bot.* 67, 52–58. doi: 10.1016/j.envexpbot.2009.06.012

Vaculík, M., and Vaculíková, M. (2017). "Role of silicon under heavy metal and toxic element stress: An emphasis on root biology," in *Silicon in Plants: Advances and Future Prospects*. Eds. D. K. Tripathi, V. P. Singh, P. Ahmad, D. K. Chauhan and S. M. Prasad (Boca Raton, FL, USA: CRC Press, Taylor & Francis), 175–194.

Vaculíková, M., Vaculík, M., Šimková, L., Fialová, I., Kochanová, Z., Sedláková, B., et al. (2014). Influence of silicon on maize roots exposed to antimony – Growth and antioxidative response. *Plant Physiol. Biochem.* 83, 279–284. doi: 10.1016/j.plaphy.2014.08.014

Vaculíková, M., Vaculík, M., Tandy, S., Luxová, M., and Schulin, R. (2016). Alleviation of antimonate (SbV) toxicity in maize by silicon (Si). *Environ. Exp. Bot.* 128, 11–17. doi: 10.1016/j.envexpbot.2016.04.001

Van Assche, F., and Clijsters, H. (1990). Effects of metals on enzyme activity in plants. *Plant Cell Environ.* 13, 195–206. doi: 10.1111/j.1365-3040.1990.tb01304.x

Van der Ent, A., Baker, A. J., Reeves, R. D., Pollard, A. J., and Schat, H. (2013). Hyperaccumulators of metal and metalloid trace elements: facts and fiction. *Plant Soil.* 362, 319–334. doi: 10.1007/s11104-012-1287-3

Večeřová, K., Večeřa, Z., Dočekal, B., Oravec, M., Pompeiano, A., Tříska, J., et al. (2016). Changes of primary and secondary metabolites in barley plants exposed to CdO nanoparticles. *Environ. pollut.* 218, 207–218. doi: 10.1016/j.envpol.2016.05.013

Vega-Mas, I., Rossi, M. T., Gupta, K. J., González-Murua, C., Ratcliffe, R. G., Estavillo, J. M., et al. (2019). Tomato roots exhibit in *vivo* glutamate dehydrogenase aminating capacity in response to excess ammonium supply. *J. Plant Physiol.* 239, 83–91. doi: 10.1016/j.jplph.2019.03.009

Viehweger, K. (2014). How plants cope with heavy metals. *Bot. Stud.* 55, 35. doi: 10.1186/1999-3110-55-35

Vishwakarma, K., Singh, V. P., Prasad, S. M., Chauhan, D. K., Tripathi, D. K., and Sharma, S. (2020). Silicon and plant growth promoting rhizobacteria differentially regulate AgNP-induced toxicity in *Brassica juncea*: implication of nitric oxide. *J. Hazard. Mater.* 390, 121806. doi: 10.1016/j.jhazmat.2019.121806

Wang, Y., Liu, Y., Zhan, W., Zheng, K., Lian, M., Zhang, C., et al. (2020b). Long-term stabilization of Cd in agricultural soil using mercapto-functionalized nano-silica (MPTS/nano-silica): A three-year field study. *Ecotoxicol. Environ. Saf.* 197, 110600. doi: 10.1016/j.ecoenv.2020.110600

Wang, S., Wang, F., and Gao, S. (2015). Foliar application with nano-silicon alleviates Cd toxicity in rice seedlings. *Environ. Sci. pollut. Res.* 22, 2837–2845. doi: 10.1007/s11356-014-3525-0

Wang, K., Wang, Y., Wan, Y., Mi, Z., Wang, Q., Wang, Q., et al. (2021). The fate of arsenic in rice plants (*Oryza sativa* L.): Influence of different forms of selenium. *Chemosphere* 264, 128417. doi: 10.1016/j.chemosphere.2020.128417

Wang, Z., Yue, L., Dhankher, O. P., and Xing, B. (2020a). Nano-enabled improvements of growth and nutritional quality in food plants driven by rhizosphere processes. *Environ. Int.* 142, 105831. doi: 10.1016/j.envint.2020.105831

Wang, Y., Zhang, B., Jiang, D., and Chen, G. (2019). Silicon improves photosynthetic performance by optimizing thylakoid membrane protein components in rice under drought stress. *Environ. Exp. Bot.* 158, 117–124. doi: 10.1016/j.envexpbot.2018.11.022

Williams, L. E., Pittman, J. K., and Hall, J. L. (2000). Emerging mechanisms for heavy metal transport in plants. *Biochim. Biophys. Acta BBA - Biomembr.* 1465, 104–126. doi: 10.1016/S0005-2736(00)00133-4

Yadav, M., Gupta, R., and Sharma, R. K. (2019). "Green and sustainable pathways for wastewater purification," in *Advances in water purification techniques*. Ed. S. Ahuja (Amsterdam, The Netherlands: Elsevier), 355–383.

Yamaji, N., Mitatni, N., and Ma, J. F. (2008). A transporter regulating silicon distribution in rice shoots. *Plant Cell* 20, 1381–1389. doi: 10.1105/tpc.108.059311

Yamasaki, H., Pilon, M., and Shikanai, T. (2008). How do plants respond to copper deficiency? *Plant Signal. Behav.* 3, 231–232. doi: 10.4161/psb.3.4.5094

Ying, R. R., Qiu, R. L., Tang, Y. T., Hu, P. J., Qiu, H., Chen, H. R., et al. (2010). Cadmium tolerance of carbon assimilation enzymes and chloroplast in Zn/Cd hyperaccumulator *Picris divaricata*. J. *Plant Physiol.* 167, 81–87. doi: 10.1016/j.jplph.2009.07.005

Zellner, W., Tubaña, B., Rodrigues, F. A., and Datnoff, L. E. (2021). Silicon's role in plant stress reduction and why this element is not used routinely for managing plant health. *Plant Dis.* 105, 2033–2049. doi: 10.1094/PDIS-08-20-1797-FE

Zhang, Y., Shi, Y., Gong, H., Zhao, H., Li, H., Hu, Y., et al. (2018). Beneficial effects of silicon on photosynthesis of tomato seedlings under water stress. *J. Integr. Agric.* 17, 2151–2159. doi: 10.1016/S2095-3119(18)62038-6

Zhang, C., Wang, L., Nie, Q., Zhang, W., and Zhang, F. (2008). Long-term effects of exogenous silicon on cadmium translocation and toxicity in rice (*Oryza sativa* L.). *Environ. Exp. Bot.* 62, 300–307. doi: 10.1016/j.envexpbot.2007.10.024

Zhou, P., Adeel, M., Shakoor, N., Guo, M., Hao, Y., Azeem, I., et al. (2021). Application of nanoparticles alleviates heavy metals stress and promotes plant growth: An overview. *Nanomater* 11, 26. doi: 10.3390/nano11010026

frontiers | Frontiers in Plant Science

TYPE Original Research
PUBLISHED 24 April 2024
DOI 10.3389/fpls.2024.1371123

OPEN ACCESS

EDITED BY
Md Sazzad Hossain,
University of Kiel, Germany

REVIEWED BY
Patrick Enrico Hayes,
University of Western Australia, Australia
Darko Jevremović,
Fruit Research Institute, Serbia

*CORRESPONDENCE
P. J. Barra
patricio.barra@ufrontera.cl
M. Delgado
mabel.delgado@ufrontera.cl

RECEIVED 15 January 2024
ACCEPTED 08 April 2024
PUBLISHED 24 April 2024

CITATION
Delgado M, Barra PJ, Berrios G, Mora ML, Durán P, Valentine A and Reyes-Díaz M (2024) Do aluminum (Al)-hyperaccumulator and phosphorus (P)-solubilising species assist neighbouring plants sensitive to Al toxicity and P deficiency?
Front. Plant Sci. 15:1371123.
doi: 10.3389/fpls.2024.1371123

Do aluminum (Al)-hyperaccumulator and phosphorus (P)-solubilising species assist neighbouring plants sensitive to Al toxicity and P deficiency?

M. Delgado[1]*, P. J. Barra[1,2]*, G. Berrios[3], M. L. Mora[1], P. Durán[1,2,4], A. Valentine[5] and M. Reyes-Díaz[1,3]

[1]Center of Plant, Soil Interaction and Natural Resources Biotechnology, Scientific and Technological Bioresource Nucleus (BIOREN), Universidad de La Frontera, Temuco, Chile, [2]Biocontrol Research Laboratory, Universidad de La Frontera, Temuco, Chile, [3]Departamento de Ciencias Químicas y Recursos Naturales, Facultad de Ingeniería y Ciencias, Universidad de La Frontera, Temuco, Chile, [4]Facultad de Ciencias Agropecuarias y Medioambiente, Departamento de Producción Agropecuaria, Universidad de La Frontera, Temuco, Chile, [5]Department of Horticultural Sciences, Faculty of AgriSciences, University of Stellenbosch, Stellenbosch, South Africa

We aimed to evaluate the facilitation effects of an aluminum (Al) hyperaccumulator species bearing cluster roots, *Gevuina avellana*, on the seedling growth and performance of an Al-intolerant and phosphorus (P)-deficient-sensitive plant, *Vaccinium corymbosum*. For this, seedlings of *G. avellana* and *V. corymbosum* were grown alone or together as follows: i) two *G. avellana* seedlings, ii) one *G. avellana* + one *V. corymbosum* and iii) two *V. corymbosum*, in soil supplemented with Al (as $Al_2(SO_4)_3$) and in the control (without Al supplementation). We determined relative growth rate (RGR), photosynthetic rate, chlorophyll concentration, lipid peroxidation and Al and nutrient concentration [Nitrogen (N), P, potassium (K), calcium (Ca), magnesium (Mg), sodium (Na), manganese (Mn), iron (Fe), copper (Cu), zinc (Zn), and sulfur (S)] in leaves and roots of both species. The results showed that, in general, *G. avellana* did not assist *V. corymbosum* to enhance its RGR nor reduce its Al uptake. However, *G. avellana* assisted *V. corymbosum* in enhanced N acquisition and, consequently, to increase its chlorophyll concentration and photosynthetic rate. Besides, *V. corymbosum* had lower lipid peroxidation in leaves when grown in the soil with high Al supplementation in association with *G. avellana*. Our results suggest a facilitating effect of *G. avellana* to *V. corymbosum* when grown in soils with high Al concentration, by enhancing chlorophyll concentrations and photosynthetic rate, and decreasing the oxidative damage to lipids.

KEYWORDS

cluster roots, facilitation, nutrients, Proteaceae, *Gevuina avellana*, highbush blueberry

Introduction

Acidic soils (pH ≤ 5.5) are widely distributed, representing about 30% of the total world's land area and, approximately 50% of the world's potential arable lands. However, soil acidity is an important limitation for crop productivity. This is because, various restrictive factors for agricultural production usually coincide in these soils, such as toxic levels of aluminum (Al) and deficiencies in essential minerals for robust plant nutrition, such as phosphorus (P). Although Al is the third most abundant element in the earth's crust, it lacks any discernible role in known biological processes (Tolrà et al., 2011). Under acidic conditions, the Al is released from soil particles into the soil solution as the trivalent ionic form (Al^{3+}), which is particularly toxic for plants (Kochian et al., 2015). Aluminum rapidly hinders root growth, limiting both root expansion, and consequently constraining the absorption of water and essential nutrients vital for the plant's fitness. Aluminum exists not only in the Al^{3+} ionic form but also is found as several insoluble forms including aluminosilicates, Al-humus complexes and other precipitated forms. Both the soluble and insoluble forms of Al can react and strongly retain minerals with negative charge, such as phosphate ($H_2PO_4^-$, HPO_4^{2-}), decreasing its availability for plant nutrition (Kochian et al., 2004). Thus, both Al toxicity and P deficiency converge to exert a deep impact on plant growth and crop yields on acidic soils (Kochian et al., 2004; Chen and Liao, 2016).

In Southern Chile, soils from volcanic origin represent about 50-60% of arable land and support most of the agricultural production and forestry activities of the country (Borie and Rubio, 2003). The two main soil orders found in the southern-central Chile are Andisols and Ultisols, which inherently predisposed to natural acidity, harbor substantial amounts of active Al^{3+} and strong phosphate retention (Mora et al., 2006, 2017). Therefore, these soils are characterized by having high amounts of total P although with a very low P availability (Borie and Rubio, 2003). Consequently, traditional agricultural practices on acidic soils requires continuous application of agrochemicals, such as P fertilizers (a non-renewable resource) to increase P availability, and lime application (calcium carbonate) to increase soil pH and reduce Al phytotoxicity (Mora et al., 1999). However, these agricultural practices continued over time are unsustainable, since often they present negative environmental and socio-economic impact, and are not economically viable or physically manageable for many farmers worldwide (Samac and Tesfaye, 2003). Consequently, there is an increasing interest to develop environmentally friendly strategies to diminish our agrochemical dependency, and contribute to more sustainable agriculture.

Intercropping systems have proven to be an effective and sustainable alternative to counteract nutrient deficiency, along with increasing the use efficiency of fertilizers in the soil. This achievement can be attributed to the phenomenon of interspecific facilitation, encompassing both above- and belowground interactions (Michel et al., 2019; Schoebitz et al., 2020; Xu et al., 2020). Within belowground interactions, there are several studies evidencing that nutrient mobilization by the roots of some species plays an important role in the facilitation process, enhancing the nutrient uptake and growth of neighboring non-mobilizing species (Li et al., 2014; Lambers et al., 2018; Shen et al., 2023). In general, the nutrient mobilization is via root exudation of organic compounds, including phosphatases, organic acids, phenolic compounds, which increases the mineralization and solubilization of nutrients in the soil. The interspecific facilitation of nutrient acquisition by association of two or more plant species having different abilities to mobilize nutrient, have involved numerous species, including species bearing specialized root structures, such as cluster roots (Muler et al., 2013; Teste et al., 2014; Shen et al., 2023).

Cluster roots are described as ephemeral rootlets and root hairs around the central root forming structures type "brush" or "raceme" that actively exude organic compounds which play a pivotal role in efficiently mobilizing essential nutrients (Lambers et al., 2006; Lambers et al., 2015a). Many species have this type of root adaptation, including species that belong to Proteaceae family, which have been widely described as plants with remarkable ability to both acquire and utilize P efficiently (Lambers et al., 2015a). The nutrient-acquisition strategy of Proteaceae involves chemical modification of its rhizosphere through the exudates from their cluster roots, which release nutrients from the soil (Delgado et al., 2015; Lambers et al., 2015a). The primary exudates consist of organic acids which carry negative charges, enabling them to displace phosphate bound in the soil through interactions with cations such as Al^{3+}, Fe^{3+} and Ca^{2+} (Ryan et al., 2001), making the previously bound phosphate readily available for plant uptake. Additionally, the organic acids chelate Al^{3+} to form stable and non-toxic complexes and, therefore, it is also involved in the detoxification of this metal (Kochian et al., 2015; Chen and Liao, 2016).

Certain cluster root-bearing species, such as several members of Proteaceae family have been classified as Al hyperaccumulator species. This means that they are able to accumulate high concentrations of Al within their leaves (≥ 1000 mg kg^{-1} dry weight) without manifesting any signs of stress or toxicity (Jansen et al., 2002). This intriguing trait suggests that the roots of these Al hyperaccumulator plants might absorb Al from their rhizosphere, potentially leading to a reduction of soil Al levels through continuous Al accumulation in leaves, bark and wood, as was early proposed by Webb (1954). Conversely, there are studies indicating that Al-hyperaccumulator species might acidify the rhizosphere, thereby increasing Al availability, as observed in *Camellia sinensis* L (Ruan et al., 2004; Chen et al., 2006). Despite these insights, our current understanding remains lacking in providing a comprehensive clarification regarding the influence of Al-hyperaccumulator species on soil Al availability, particularly within the context of species possessing cluster roots. Furthermore, the potential facilitative effect of an Al hyperaccumulator species, coupled with its ability to solubilize P, on a plant species sensitive to both Al toxicity and P deficiency, remains largely unexplored. In light of this, our study aimed to evaluate the effects of an Al hyperaccumulator species bearing cluster roots, *Gevuina avellana* Mol (Delgado et al., 2019), on the growth and performance of a neighboring species. For this investigation, we used *Vaccinium corymbosum* L., an economically important crop species, as a

model species sensitive to both Al toxicity (Cárcamo-Fincheira et al., 2023) and P deficiency (Pinochet et al., 2014). Consequently, we posit that species with the dual ability to accumulate Al and solubilize P, may be suitable for the establishment and growth of neighboring plants in soils with high Al content and low P availability, such as volcanic soils in Southern Chile.

Material and methods

Study species

Gevuina avellana is a native species from temperate rain forest of southern South America. This species belongs to the Proteaceae family, that typically produce cluster roots (Supplementary Figure S1), which exude large amounts of organic acids (Delgado et al., 2021). In their natural habitat, *G. avellana* grows in a wide range of soil conditions, whose P (Olsen) availability are in a range of 2.0 to 12.4 mg kg^{-1} (Delgado et al., 2018). In nursery conditions, this species can grow under nursery substrate having high P availability (22 mg kg^{-1}) and it continues to forming cluster roots (Fajardo and Piper, 2019). Delgado et al. (2019) reported that *G. avellana* has the ability to accumulate large amounts of Al in its leaves (> 3,500 mg Al kg^{-1} dry weight) when growing under natural conditions. Thus, according to the criteria established by Jansen et al. (2002) *G. avellana* is considered an Al hyperaccumulating species (≥ 1,000 mg Al kg^{-1} in leaves).

Vaccinium corymbosum L. is an economically important crop cultivated in southern-central Chile for its world-famous and high-demand fruits (Montalba et al., 2019). Despite the fact that this species is adapted to acid soils, it is sensitive to Al^{3+} toxicity. The presence of Al^{3+} triggers a cascade of molecular, physiological and morphological changes in *V. corymbosum*, culminating in reduced productivity and yield (Reyes-Díaz et al., 2010, 2011; Inostroza-Blancheteau et al., 2011a, b; Inostroza-Blancheteau et al., 2013; Ulloa-Inostroza et al., 2016). Indeed, gypsum amendments are frequently used to ameliorate Al^{3+} toxicity in *V. corymbosum* (Alarcón-Poblete et al., 2019, 2020). According to the manual of fertilization for *V. corymbosum* cultivated in southern Chile (Pinochet et al., 2014), the maximum availability of exchangeable Al is 0.2 $cmol^{+}$ kg^{-1}, above which the *V. corymbosum* presents Al-toxicity. Likewise, according to Alarcón-Poblete et al. (2019), different cultivars of *V. corymbosum* presented leaf morphology alterations as well as photochemical and biochemical damages when grown in soil containing 22% of Al saturation. On the other hand, mineral fertilizers (including phosphate fertilizers) are required to ensure a better growth and yield of *V. corymbosum*. The optimal mineral content in soils for maximum performance of *V. corymbosum* depends on the mineralogical characteristics of the soil. Thus, in some regions of the world, the optimal available P content in the soil lies in a range between 30-60 mg kg^{-1} (Komosa et al., 2017; Ochmian et al., 2018). In contrast, the critical level for cultivating this species is 16 mg kg^{-1}; below this value, *V. corymbosum* yield decline due to P deficiency (Pinochet et al., 2014). Therefore, we propose that the *V. corymbosum* is a good model species to study the facilitating effects of *G. avellana* under Al toxicity and P deficiency.

Plant material

Plants of *G. avellana* and *V. corymbosum* were obtained from commercial nurseries. *Gevuina avellana* plants were cultivated from seeds, and were two years old when the experiment commenced, whereas *V. corymbosum* plants were produced *in vitro* and were one-year-old. At the beginning of the experiment, mean initial biomass (± s.e.) for *G. avellana* and *V. corymbosum* were 1.2 ± 0.8 and 2.6 ± 0.3 g, respectively. In this study, we used *V. corymbosum* cultivar Star because according to recent studies that evaluated the resistance to Al toxicity in different cultivars established in Chile, this cultivar emerged as the most Al-sensitive among the ones evaluated (Cárcamo et al., 2019; Cárcamo-Fincheira et al., 2023).

Experimental design

In order to determine the facilitating effect of *G. avellana* on a sensitive species to Al toxicity and P deficiency, a greenhouse assay was carried out in the Universidad de La Frontera, Temuco, Chile. For this, soil from the series Freire, collected in Experimental Station Maquehue (38° 50′ 27″ S, 72° 41′ 39.03″ W) of the Universidad de La Frontera was used. To increase the Al in soil, we added Al sulfate ($Al_2(SO_4)_3$), following the methodology reported by González-Villagra et al. (2021). We added 25 g of $Al_2(SO_4)_3$ per 1.5 kg of soil, and after a month of soil incubation at room temperature (25° C approximately), we achieve values of exchangeable Al and percentage of Al saturation of 4.7 cmol+ kg^{-1} and 26.5%, respectively. Another part of the soil was not added with $Al_2(SO_4)_3$ to be used as a control. The supplementation with $Al_2(SO_4)_3$ to the soil shift the pH from ~5.7-6.2 down to 4.4-4.7, increasing significantly the availability of other elements such as Mn and S at the end of the experiment (Table 1).

In this study, we conducted a greenhouse experiment in which both *G. avellana* (n = 60) and *V. corymbosum* (n = 60) individuals were subjected to two different conditions: i) the 'Al supplemented soil', where the soil was supplemented with $Al_2(SO_4)_3$ and ii) the control, where no additional Al was added to the soil. The experiment utilized 4 L pots to accommodate the plants in the Al supplemented soil and the control, and they were allowed to grow either alone or together in the following combinations: i) 2 seedlings of *G. avellana* (conspecific species, n=10 pots), ii) 1 seedling of *G. avellana* + 1 seedling of *V. corymbosum* (interspecific species, n=10 pots), and iii) 2 seedlings of *V. corymbosum* (conspecific species, n =10 pots). The experiment was carried out under greenhouse conditions for 16 months (see the plants at the end of the experiment in Supplementary Figure S2). During the experiment, plants were watered regularly with tap water according to their requirements. Temperatures inside the greenhouse fluctuated between -1.6 and 31° C for the autumn-winter season (mean temperature: 11°C), and between 6.3 – 36.6°C for the spring-summer season (mean temperature: 18°C). The maximum light intensity recorded at noon varied between 129 and 485 μmol m^{-2} s^{-1} for the autumn-winter

TABLE 1 Soil chemical analysis of the experiment at the start and at the end of the experiment where *Gevuina avellana* and *Vaccinium corymbosum* were grown alone or in combination with or without aluminum sulfate supplementation in the following combinations: i) 2 seedlings of *G. avellana* (2Ga), 1 seedling of *G. avellana* + 1 seedling of *V. corymbosum* (1Ga + 1Vc), and iii) 2 seedlings of *V. corymbosum* (2Vc).

	Start	- $(Al_2(SO_4)_3)$			Start	+ $(Al_2(SO_4)_3)$		
		End of experiment				End of experiment		
		2Ga	1Ga+1Vc	2Vc		2Ga	1Ga+1Vc	2Vc
N (mg kg^{-1})	16.5 (1.4)	11.0 (0.4) a	12.5 (1.0) a	11.7 (1.8) a	14 (1.00)	11.3 (1.0) a	9.8 (1.2) a	8.8 (0.5) a
P-Olsen (mg kg^{-1})	18 (0.00)	16 (0.7) a	16 (0.0) a	11.7 (0.3) a	15 (0.00)	13.8 (0.3) a	13.3 (0.3) a	13.8 (0.3) a
K (mg kg^{-1})	174 (14.6)	102.6 (5.1) b	163.2 (4.3) a	180.8 (19.5) a	195.5 (2.3)	110.5 (8.0) b	114.4 (6.3) b	145.6 (10.0) a
pH (H_2O)	5.7 (0.12)	6.2 (0.0) a	6.1 (0.0) a	6.0 (0.1) a	4.4 (0.02)	4.7 (0.0) b	4.7 (0.0) b	4.7 (0.0) b
Organic Matter (%)	15.5 (0.3)	14.3 (0.3) a	14.8 (0.3) a	14.5 (0.3) a	14.7 (0.33)	14.3 (0.3) a	14.3 (0.3) a	14.5 (0.3) a
K ($cmol_+$ kg^{-1})	0.4 (0.04)	0.3 (0.0) b	0.4 (0.0) a	0.5 (0.0) a	0.5 (0.01)	0.3 (0.0) b	0.3 (0.0) b	0.4 (0.0) a
Na ($cmol_+$ kg^{-1})	0.1 (0.03)	0.7 (0.0) ab	0.7 (0.0) b	0.7 (0.1) ab	0.2 (0.00)	0.7 (0.0) ab	0.8 (0.0) ab	0.9 (0.0) a
Ca ($cmol_+$ kg^{-1})	9.3 (0.31)	9.2 (0.3) b	8.3 (0.2) b	8.4 (0.5) b	11 (0.07)	11.8 (0.3) a	11.1 (0.2) a	11.5 (0.4) a
Mg ($cmol_+$ kg^{-1})	1.4 (0.02)	1.5 (0.0) a	1.4 (0.0) ab	1.4 (0.1) ab	1.5 (0.01)	1.4 (0.0) ab	1.3 (0.0) b	1.5 (0.0) a
Al ($cmol_+$ kg^{-1})	0.1 (0.01)	0.1 (0.0) b	0.1 (0.0) b	0.1 (0.0) b	4.7 (0.07)*	1.6 (0.0) a	1.8 (0.0) a	1.9 (0.0) a
Al saturation (%)	0.5 (0.4)	0.5 (0.0) b	0.6 (0.0) b	0.7 (0.1) b	26.5 (0.39)*	10.0 (0.3) a	11.7 (0.3) a	11.7 (0.4) a
Mn (mg kg^{-1})	n.d.	7.2 (0.3) b	7.6 (0.5) b	6.1 (0.4) b	8.7 (0.3)	18.9 (0.6) a	18.0 (1.0) a	14.9 (1.7) a
S (mg kg^{-1})	n.d.	28 (1.3) b	27 (0.3) b	25 (2.6) b	n.d.	625 (10) a	600 (0.0) a	619 (6.3) a
*ECEC ($cmol^+$ kg^{-1})	11.4 (0.3)	11.7 (0.0) b	10.9 (0.3) b	11.1 (0.6) b	17.8 (0.01)	15.7 (0.3) a	15.2 (0.2) a	16.0 (0.4) a
Sum of cations ($cmol^+$ kg^{-1})	11.3 (0.3)	11.7 (0.3) b	10.9 (0.3) b	11.0 (0.6) b	13.1 (0.08)	14.2 (0.3) a	13.5 (0.2) a	14.3 (0.4) a

[1]ECEC, effective cation-exchange capacity.
Each value corresponds to a mean of 3 samples ± standard error in brackets. Different letters indicate significant differences among treatments at the end of the experiment ($P \leq 0.05$). * Indicate significant differences between treatments at the start the experiment ($P< 0.01$).

season, and between 283 and 712 µmol m^{-2} s^{-1} spring-summer season. At the end of the experiment, the morphological, chemical and physiological responses of these species were analyzed.

Morphological measurements

Relative growth rate in height (RGRh) and biomass (RGRb) were determined in all surviving plants (Plant survival was 80 to 100% per treatment). For RGRh, seedling height (H) was recorded for all seedlings at the beginning ($H_{Initial}$) and at the end (H_{Final}) of the experiment. The RGRh was calculated according to Barrow (1977), where RGR (cm cm^{-1} day^{-1})= (ln H_{Final} – ln $H_{Initial}$)/(t), t being the time (days) between the initial and final height measurements. The same calculations were made for RGRb, where the initial biomass was the average biomass of 8 initial plants. For biomass determinations, the leaves, stem and roots (non-cluster roots and cluster roots) of the seedlings were separated and weighed fresh using an analytical balance (Radwag AS 220.R2 Plus, Poland). Subsequently, leaves samples were divided into two subsamples: one for lipid peroxidation analyses; and the other for biomass and chemical analyses. For biomass analyses, the fresh samples (subsamples in the case of leaves) were dried in an oven at 60°C for 48 h to obtain dry weight. The dry biomass of total leaves of each seedling were calculated as the total fresh weight corrected for the moisture content of the leaves biomass subsample. The biomass distribution was calculated according to the percentage of each organ with respect to the total dry biomass of the plant. The total biomass of each individual corresponds to the sum of the dry weights of the different organs of the plant.

Photosynthetic performance

Two days before the plants were harvested, photosynthetic rate, transpiration rate and stomatal conductance were measured between 9 and 12 a.m. in mature leaves formed during the experiment of both species, *G. avellana* and *V. corymbosum*. Two photosynthetic measurements were made per plant and six biological replicates per treatment were determined. For this, we used a portable infra-red gas analyzer photosynthesis system (LI-6400, LI-COR Bioscience, Inc., Lincoln, Nebraska, US) using a broad-leaf cuvette (area 2.5 cm^2) and controlled light source (500 µmol photons m^{-2} s^{-1}), temperature (20° C) and external CO_2 (360 ppm). We decided to use 500 µmol photons m^{-2} s^{-1} because, in the case of *V. corymbosum*, previous studies reported that this species reach their maximum photosynthetic response at this photosynthetic photon flux density (PPFD) (Reyes-Díaz et al., 2016; Petridis et al., 2018). In the case of *G. avellana*, prior to determining the photosynthesis rate, we performed photosynthesis curves in response to PPFD, and we found that at 500 µmol photons m^{-2} s^{-1} this species had already reached its maximum

photosynthesis rate, not being photoinhibited at this light intensity (Supplementary Figure S4). Additionally, at the end of the experiment, photosynthetic pigments such as Chlorophyll a, Chlorophyll b and carotenoids were determined in mature leaves. For this, 0.1 g of fresh leaf sample was homogenized with 1 mL of ethanol 96%. Homogenized sample mixture was centrifuged for 13,000 rpm for 5 min at 4°C. The supernatant was separated and the same step is repeated with the precipitate and then the two supernatants are combined. The solution mixture was spectrophotometrically measured at 665 nm, 649 nm and 470 nm. The quantification of Chlorophyll a, Chlorophyll b, and carotenoids were determined according to Lichtenthaler and Wellburn (1983).

Lipid peroxidation

At the end of the experiment, lipid peroxidation was evaluated by thiobarbituric acid reacting substance (TBARS) quantification in fresh leaves of *G. avellana* and *V. corymbosum* following the modified protocol by Du and Bramlage (1992) using a Multimodal Microplate Reader Synergy HTX (BIOTEK). For this, we used 8-10 biological replicates per treatment.

Chemical measurements in leaves and roots

At the end of the experiment, leaves and roots of all surviving plants of *G. avellana* and *V. corymbosum* were washed with tap water and later dried at 60°C for 48 h (n = 8 -10 replicates per species and treatment). The dried samples were ground to a powder using a grinding machine made of stainless steel (Bioscientific instruments, MRC, UK), and ground samples were used to analyze macro- and micronutrients including P, nitrogen (N), sulfur (S), manganese (Mn), iron (Fe), copper (Cu), zinc (Zn), calcium (Ca), sodium (Na), potassium (K), magnesium (Mg) and Al. For concentrations of micronutrients (Na, Mn, Cu, Fe, and Zn) and some macronutrients (Ca, K and Mg) as well as Al, 0.5 g of sample were ashed at 500°C for 8 h. The resulting ash was digested using hydrochloric acid (2 M) as described in Sadzawka et al. (2004b) and the different elements were quantified using an atomic absorption spectrophotometer (GBC Scientific Equipment Pty Ltd., SavantAA, Sigma, Dandenong, Victoria, Australia). Phosphorus concentrations were determined spectrophotometrically using the vanado-phosphomolybdate method, while N concentrations were determined by Kjeldahl distillation after acidic digestion (Sadzawka et al., 2004b). For S concentration, leaves and roots were dried as mentioned above, treated with 95% magnesium nitrate ($MgNO_3 \times 6H_2O$), and ashed at 500°C for 4 h. Ashed samples were digested in 10 mL of HCl (2 M) at 150°C for 60 min, filtered and graduated with deionized water to 50 mL. Subsequently, filtered samples were mixed with barium chloride ($BaCl_2$) and Tween-80. The resulting solution was measured spectrophotometrically (Spectronic GenesysTM, NY) at 440 nm, as described by Sadzawka et al. (2004b).

Chemical measurements in soil

Three soil samples per treatment were analyzed at the beginning and end of the experiment (Sadzawka et al., 2004a). Mineral N were determined using the Kjeldahl method according to Bremner (1960) using a Kjeldahl UDK129 distiller equipment (VELP Scientific, Italy). Soil P (Olsen) was determined colorimetrically by applying the phosphoantimonylmolybdenum blue complex method (Drummond and Maher, 1995). Organic matter was measured following the wet digestion method by Walkley and Black (1934). Exchangeable cations [potassium (K), sodium (Na), calcium (Ca), and magnesium (Mg)] and exchangeable Al were extracted according to Sadzawka et al. (2004a) and determined using an atomic absorption spectrophotometer (GBC Scientific Equipment Pty Ltd.). Percentage of Al saturation was calculated with respect to the total sum of the exchangeable cations (Ca^+, K^+, Na^+, Mg^+, Al^+). Soil pH was determined in soil suspended in water (ratio 1:2.5; w/v H_2O). Soil Mn concentration was determined using the diethylenetriamine pentaacetic acid (DTPA) method described by Lindsay and Norvell (1978) and measured by atomic absorption spectrophotometry (GBC Scientific Equipment Pty Ltd.).

Sulfur in soil was measured according the methodology by Sadzawka et al. (2004b). Briefly, sulfur was extracted using a Ca $(H_2PO_4)_2$ 0.01 M solution, followed by a turbidimetric measurement of sulphate as $BaSO_4$ and measured spectrophotometrically (Spectronic GenesysTM, NY) at 372 nm.

Statistics

Statistical analyses were carried out separately for each species using a one-way ANOVA with Tukey's posteriori test ($P \leq 0.05$) for parameters related to growth (n = 8-10 replicates), physiological [photosynthetic rate, chlorophyll concentration, (n = 6 replicates)], biochemical [lipid peroxidation, (n = 8-10 replicates)] and chemical [nutrients and Al concentrations, (n = 8-10 replicates)] responses of *G. avellana* and *V. corymbosum* when grown alone or in combination with or without Al supplementation. All data passed the normality and equal variance tests. Statistical analyses were performed using the Sigma Plot v.12.

Results

Relative growth rate and biomass distribution

The findings of this study revealed significant increases in the total biomass (Supplementary Table S1) and RGR in biomass for *G. avellana* when it grew together with *V. corymbosum* in both soil conditions, regardless of the presence or absence of Al (Figure 1). In contrast, similar RGR in biomass were recorded for *V. corymbosum* across all treatments, irrespective of soil condition and neighboring species (Figure 1). Upon analyzing the biomass allocation patterns, it was observed that *G. avellana* allocated approximately 48% of its

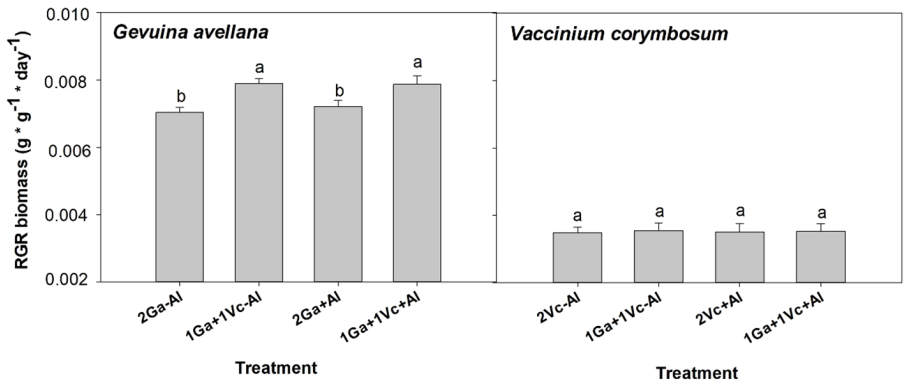

FIGURE 1
Relative growth rate (RGR) in biomass of *Gevuina avellana* and *Vaccinium corymbosum* growing alone or in combination with or without aluminum sulfate supplementation in the following combinations: i) 2 seedlings of *G. avellana* (2Ga), 1 seedling of *G. avellana* + 1 seedling of *V. corymbosum* (1Ga + 1Vc), and iii) 2 seedlings of *V. corymbosum* (2Vc). Each bar corresponds to mean of eight to ten samples ± standard error (SE). Different letters indicate significant differences among treatments ($P \leq 0.05$).

biomass to leaves, 15% to the stem, 25% to non-cluster roots, and 12% to the formation of cluster roots. In contrast, *V. corymbosum* allocated its biomass differently, with approximately 16% directed to leaves, 23% to the stem, and the majority, 61%, to non-cluster roots (Supplementary Figure S3). These biomass allocations remained unaffected by the experimental treatments.

Photosynthetic performance

Although no significant differences were observed in the leaf chlorophyll (a + b) concentration of *G. avellana* plants (Figure 2A), this species showed a significantly higher photosynthetic rate when grown in Al-supplemented soil compared to control plants (Table 2). On the contrary, *V. corymbosum* presented a higher leaf chlorophyll concentration and photosynthetic rate in control soil conditions (Table 2, Figure 2B). Interestingly, *V. corymbosum* plants grown in Al-supplemented soil, significantly increased its photosynthesis rate and leaf chlorophyll concentration when grown together with *G. avellana* than when grown accompanied by a conspecific species (Table 2, Figure 2B). The ratio of chlorophyll a:b showed that *G. avellana* leaves presented significatively higher chlorophyll-a when grown in Al supplemented soil (Figure 2C). In leaves of *V. corymbosum* plants it was observed that the ratio of chlorophyll a:b was significantly lower in plants grown in the control soil but only when was accompanied by *G. avellana* (Figure 2D). The carotenoids concentration in *G. avellana* leaves decreased significantly when plants were grown in Al supplemented soil (Figure 2E), whereas in leaves of *V. corymbosum* the carotenoid concentration increased significantly in plants grown in the control soil but only when was accompanied by *G. avellana* (Figure 2F).

Leaf N:P ratio

The leaf N:P ratio served as a reliable indicator to assess whether N or P limitation influenced the plants, with values < 10 suggesting N limitation, values > 16 indicating P limitation, and values between 10 and 16 implying that plant growth was equally constrained by N and P (Koerselman and Meuleman, 1996). The results showed that *G. avellana* was co-limited by N and P in all treatments, whereas *V. corymbosum* was P limited in the control soil and co-limited by N and P when plants grown in Al supplemented soil (Figure 3).

Lipid peroxidation

The lipid peroxidation of *G. avellana* leaves was higher in plants that grew in the control soil. On the contrary, higher lipid peroxidation was observed in the leaves of *V. corymbosum* plants that grew in the Al-supplemented soil and accompanied by another *V. corymbosum* plant (Figure 4).

Leaves and roots nutrient concentration

The Al-supplemented soil significantly affected the nutrients uptake from the plants, depending on the species (Tables 3, 4). For example, *G. avellana* maintains its levels of foliar and roots N concentration independent of the soil from which it grew and the neighboring species (conspecific or interspecific). In contrast, *V. corymbosum* presented lower N values in the Al supplemented soil, these being significantly lower when this species grows accompanied by a conspecific species than when it grows accompanied by *G. avellana*.

The leaf and roots P concentration was significantly lower in *G. avellana* plants that grew in the Al supplemented soil and when grown with a conspecific species (Table 3). In contrast, *V. corymbosum* did not show significant differences in foliar P concentration in the different treatments evaluated, although it did show a significantly higher P concentration in roots when it grew in control soil and accompanied by a conspecific species (Table 4).

In general, mineral nutrients such as K, Mg and Mn significantly increased their concentration in the leaves and roots of both species when they were grown in the Al supplemented,

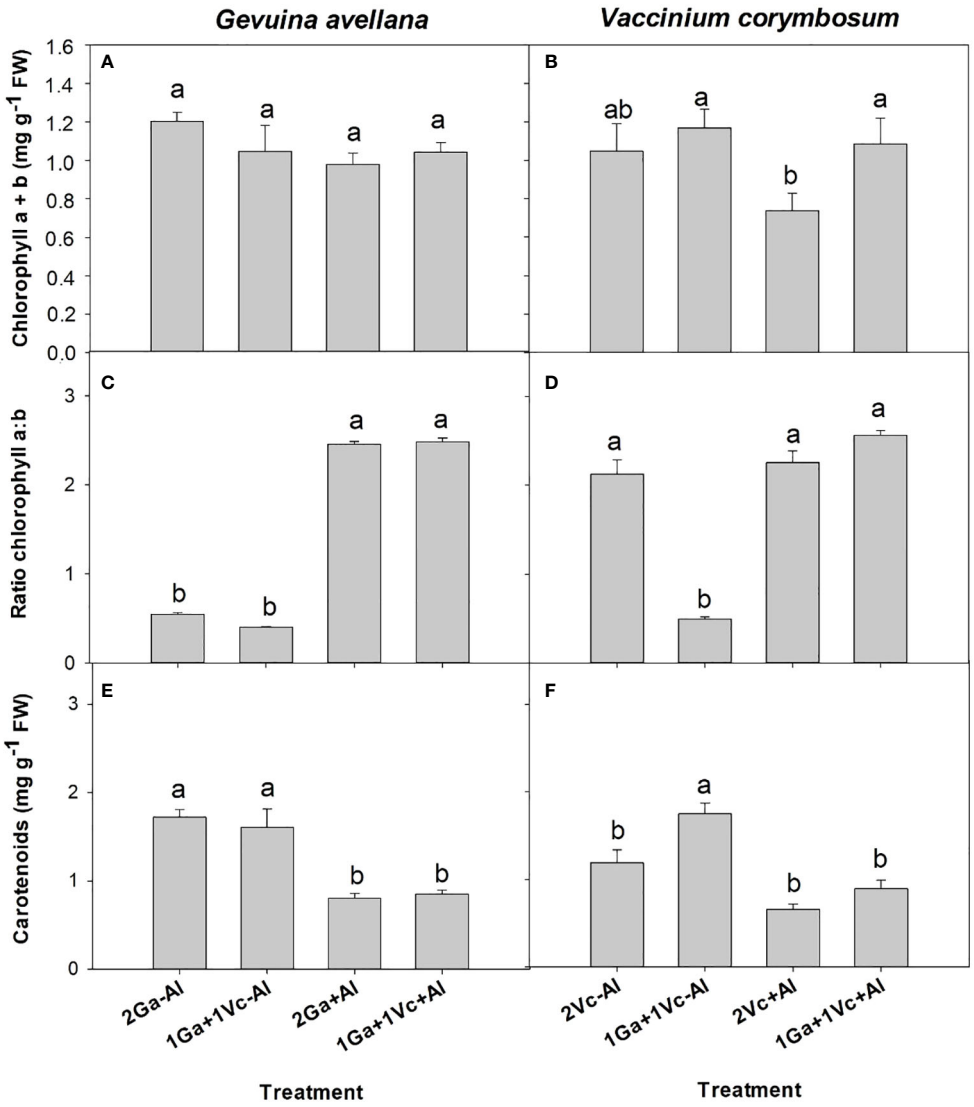

FIGURE 2
Chlorophyll a + b concentration, ratio chlorophyll a:b and total carotenoids of *Gevuina avellana* **(A, C, E)** and *Vaccinium corymbosum* **(B, D, F)** growing alone or in combination with or without aluminum sulfate supplementation in the following combinations: i) 2 seedlings of *G. avellana* (2Ga), 1 seedling of *G. avellana* + 1 seedling of *V. corymbosum* (1Ga + 1Vc), and iii) 2 seedlings of *V. corymbosum* (2Vc). Each bar corresponds to mean of six samples ± standard error (SE). Different letters indicate significant differences among treatments ($P \leq 0.05$).

regardless of whether the neighboring species was interspecific or conspecific. Similar trend was found in Na concentration in leaves and roots of *G. avellana* (Table 3). However, Na concentration in leaves and roots of *V. corymbosum* tends to decrease with Al supplementation, being significantly lower in the leaves of *V. corymbosum* plants that grew together with an interspecific species and in the roots of plants that grew together with a conspecific species (Table 4).

The concentration of Ca and Cu in the leaves of *G. avellana* and *V. corymbosum* also increased with Al supplementation, however, this was only significantly higher when both species were accompanied by an interspecific species. No significant differences were found in roots Ca concentration of both species in the different treatments evaluated (Tables 3, 4).

The Zn concentration in leaves and roots varied depending on the species and the treatment. First, *G. avellana* did not present significant differences in leaf Zn concentration, but root Zn concentration increased when the plants grew with Al supplementation and when they were accompanied by a conspecific species (Table 3). On the contrary, in *V. corymbosum* plants a decrease in the leaf Zn

10.3389/fpls.2024.1371123

TABLE 2 Photosynthesis rate, transpiration rate and stomatal conductance of *Gevuina avellana* and *Vaccinium corymbosum* growing alone or in combination with or without aluminum sulfate supplementation in the following combinations: i) 2 seedlings of *G. avellana* (2Ga), 1 seedling of *G. avellana* + 1 seedling of *V. corymbosum* (1Ga + 1Vc), and iii) 2 seedlings of *V. corymbosum* (2Vc).

Treatment	Photosynthesis rate (μmol CO_2 m^{-2} s^{-1})	Transpiration rate (mmol H_2O m^{-2} s^{-1})	Stomatal conductance (mol H_2O m^{-2} s^{-1})
Gevuina avellana			
2Ga-Al	4.4 (0.2) b	1.3 (0.03) n.s.	0.4 (0.01) b
1Ga+1Vc-Al	4.7 (0.1) b	1.4 (0.05) n.s.	0.4 (0.02) ab
2Ga+Al	5.3 (0.0) a	1.3 (0.05) n.s.	0.5 (0.01) a
1Ga+1Vc+Al	5.3 (0.1) a	1.5 (0.04) n.s.	0.5 (0.01) a
Vaccinium corymbosum			
2Vc-Al	5.4 (0.1) a	1.3 (0.03) b	0.4 (0.01) b
1Ga+1Vc-Al	5.4 (0.1) a	1.5 (0.05) a	0.5 (0.02) a
2Vc+Al	3.4 (0.2) c	1.1 (0.02) b	0.3 (0.02) c
1Ga+1Vc+Al	4.8 (0.1) b	1.5 (0.04) a	0.5 (0.02) a

Each value corresponds to mean of six samples ± standard error (SE). Different letters in each column indicate significant differences among treatments ($P \leq 0.05$). n.s., There are no significant differences among treatments.

concentration was observed in the soil supplemented with Al, being significantly lower when the plants grew accompanied by a conspecific species (Table 4).

No significant differences were observed in Fe concentration in leaves and roots of *V. corymbosum* plants among the evaluated treatments (Table 4). On the contrary, *G. avellana* presented a decrease in leaf Fe concentration when the plants grew in the Al supplemented soil and accompanied by a conspecific species compared to the control plants. On the other hand, an increase in roots Fe concentration was observed in *G. avellana* plants in all the treatments compared to the plants that grew in the control soil and accompanied by a conspecific species (Table 3).

In both species, leaf Al concentration was similar among treatments, independent of soil conditions and neighboring species. In the control soil, the roots Al concentration of *G. avellana* plants was significantly lower when this species grows together with a conspecific species than when it grows together with *V. corymbosum*. The Al supplemented soil increased significantly S levels in leaves and roots of both species (Tables 3, 4).

Discussion

Contrary to initial expectations, there was no evidence of the facilitating effect of *G. avellana* on the *V. corymbosum* seedlings growth (Figure 1). Rather surprisingly, *G. avellana* exhibited an enhancement in its own growth when grown alongside with *V. corymbosum* (Figure 1; Supplementary Table S1). These findings align with the observations made by Fajardo and Piper (2019), who reported that *Nothofagus* species did not experience an improvement in their survival

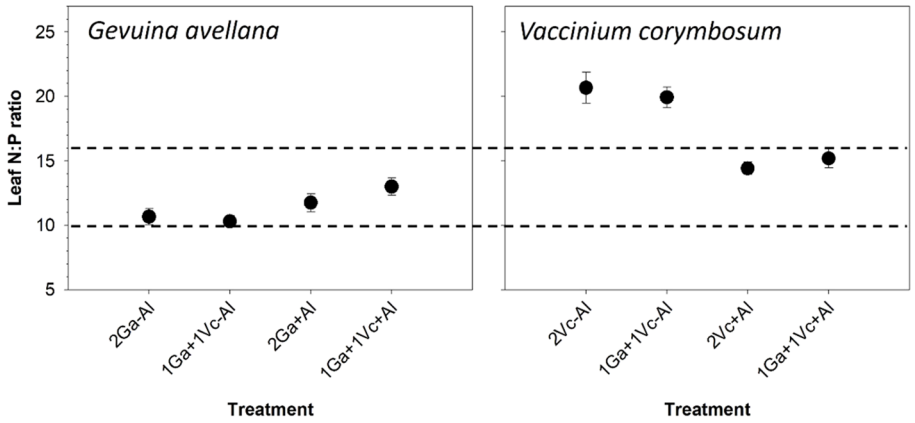

FIGURE 3
Leaf N:P ratio of *Gevuina avellana* and *Vaccinium corymbosum* growing alone or in combination with or without aluminum sulfate supplementation in the following combinations: i) 2 seedlings of *G. avellana* (2Ga), 1 seedling of *G. avellana* + 1 seedling of *V. corymbosum* (1Ga + 1Vc), and iii) 2 seedlings of *V. corymbosum* (2Vc). Each bar corresponds to mean of eight to ten samples ± standard error (SE). Different letters indicate significant differences among treatments ($P \leq 0.05$).

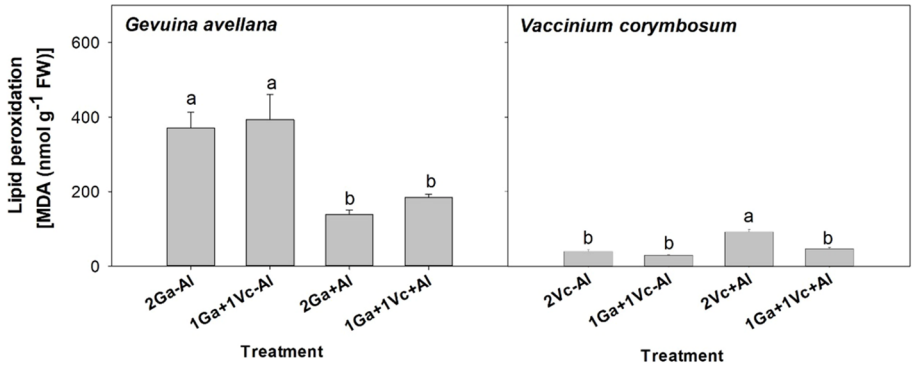

FIGURE 4
Lipid peroxidation of leaves of *Gevuina avellana* and *Vaccinium corymbosum* growing alone or in combination with or without aluminum sulfate supplementation in the following combinations: i) 2 seedlings of *G. avellana* (2Ga), 1 seedling of *G. avellana* + 1 seedling of *V. corymbosum* (1Ga + 1Vc), and iii) 2 seedlings of *V. corymbosum* (2Vc). Each bar corresponds to mean of eight to ten samples ± standard error (SE). Different letters indicate significant differences among treatments ($P \leq 0.05$).

and growth when they were planted next to *G. avellana*. Notably, however, *G. avellana* did exhibit growth enhancement when co-cultivated with *Nothofagus* or some conspecifics species. These authors concluded that Proteaceae species have a competitive advantage over non-cluster root-bearing species at the seedling stage, especially on nutrient-rich substrates. In our study, it was observed that *V. corymbosum* showed lower roots P concentration when it grows in association with *G. avellana* (Table 3). This suggests that the competitive advantage of *G. avellana* may be attributed to the significant exudation of carboxylates such as oxalate and succinate from its large cluster roots (Delgado et al., 2021; Zúñiga-Feest et al., 2021). These exudates likely contributed to the higher leaf P concentration compared with *V. corymbosum* (Tables 3 and 4). While there are currently no studies specifically addressing P mobilization around the cluster roots of *G. avellana*, research conducted on other Proteaceae species, such as *Embothrium coccineum* (Delgado et al., 2015; Renderos et al., 2022), have shown similar levels in the labile P fraction in the rhizosphere of mature cluster roots compared to non-cluster roots and bulk soil, hinting at the possibility of localized P mobilization and accelerated P uptake by plants with cluster roots.

Based on the N:P ratio thresholds established by Koerselman and Meuleman (1996), our findings indicate that *G. avellana* consistently experiences co-limitation of both N and P across all treatments. In contrast, the growth of *V. corymbosum* appeared to be predominantly constrained by P, when plants were grown under control soil conditions (Figure 3). This observation reaffirms the high P demands of the *V. corymbosum* species, as previously described Pinochet et al. (2014) (≥ 16 mg P kg^{-1} soil). Interestingly, in the Al-supplemented soil, *V. corymbosum* plants were co-limited by N and P. This was attributed to a decrease in foliar N concentration, particularly evident in conspecific plant pairs. The decrease in foliar N concentration due to Al toxicity has been previously reported in *V. corymbosum* (cv. Brigitta) (Qilong et al., 2020). This phenomenon is primarily associated with reduced root growth, resulting in a diminished nutrient uptake ability. In our study, a reduction in roots growth of *V. corymbosum* (Supplementary Figure S3) was not observed. It can be speculated that a nutrient imbalance, rather than direct Al toxicity, was most likely the underlying reason for the negative effects of soil $Al_2(SO_4)$ supplementation on the foliar N concentration.

Although it was expected to observe a facilitating effect on P acquisition, as in the case of other Proteaceae species inhabiting in extremely P-poor environments (Teste et al., 2020; Shen et al., 2023), a facilitating effect was found for *G. avellana* on *V. corymbosum* in foliar chlorophyll concentration and photosynthesis rate (Figure 2, Table 2), when both species growth together in Al supplemented soil. Since N is a fundamental element for photosynthetic pigments and consequently for the photosynthesis process (Lambers and Oliveira, 2019), the facilitating effect of *G. avellana* can be attributed to the fact that this species induced a higher N uptake rate in *V. corymbosum* when it grew in Al supplemented soil, presenting values similar to those when it grew in the control soil (Table 4). In this context, it is relevant to mention that there is some evidence showing that, unlike other species of Proteaceae species inhabiting in extremely P-impoverished soil (e.g. South Africa and Australia), the southern South American Proteaceae *Embothrium coccineum* induced cluster roots formation mainly under poor N soils, suggesting that this roots structures could promote N–acquisition (Piper et al., 2013). In *Hakea actites* (Proteaceae), the cluster roots formation and expression of peptide transporter were up-regulated in response to N starvation, probably to increase N uptake under conditions of low N availability (Paungfoo-Lonhienne et al., 2009). From these insights, it is proposed that cluster roots of *G. avellana* could indeed possess mechanisms which can facilitate N availability to neighboring plant species. In this regard, one plausible mechanism could involve organic acid release, which stimulate microbial activity in the rhizosphere. Microbial degradation of organic matter can release N, which may subsequently contribute to higher levels of available N for plants. While this hypothesis provides a compelling direction, additional studies are required to reveal the actual role of cluster roots of *G. avellana* in N acquisition and its possible mechanisms underlying this process.

A significantly higher photosynthetic rate was observed in *G. avellana* plants when they were grown in Al supplemented soil, regardless of the plant combinations involved. This intriguing

10.3389/fpls.2024.1371123

TABLE 3 Nitrogen (N), phosphorus (P), potassium (K), calcium (Ca), magnesium (Mg), sodium (Na), manganese (Mn), iron (Fe), copper (Cu), zinc (Zn), aluminum (Al) and sulfur (S) concentrations in leaves and roots of *Gevuina avellana* grown alone or in combination with or without aluminum sulfate supplementation in the following combinations: i) 2 seedlings of *G. avellana* (2Ga), 1 seedling of *G. avellana* + 1 seedling of *V. corymbosum* (1Ga + 1Vc), and iii) 2 seedlings of *V. corymbosum* (2Vc).

	Gevuina avellana (Leaves)			
	- $(Al_2 (SO_4)_3)$		+ $(Al_2 (SO_4)_3)$	
	2Ga	1Ga+1Vc	2Ga	1Ga+1Vc
N (mg g^{-1})	10.1 (0.21) a	10.6 (0.45) a	9.6 (0.37) a	10.3 (0.64) a
P (mg g^{-1})	0.99 (0.06) a	1.06 (0.07) a	0.75 (0.06) b	0.89 (0.06) ab
K (mg g^{-1})	2.9 (0.1) c	3.7 (0.2) b	7.1 (0.6) a	8.54 (0.9) a
Ca (mg g^{-1})	7.03 (0.21) b	6.4 (0.3) b	7.5 (0.4) ab	9.3 (1.0) a
Mg (mg g^{-1})	0.96 (0.03) b	1.0 (0.1) b	3.2 (0.3) a	2.8 (0.2) a
Na (mg g^{-1})	1.13 (0.6) b	1.0 (0.1) b	2.5 (0.2) a	2.7 (0.4) a
Mn (mg kg^{-1})	552 (31.3) b	532 (38.6) b	1161 (95) a	1286 (170) a
Fe (mg kg^{-1})	95.0 (6.8) a	74.8 (4.1) ab	65.9 (2.2) b	88.4 (14.09) ab
Cu (mg kg^{-1})	2.74 (0.14) b	2.6 (0.2) b	3.2 (0.18) ab	3.9 (0.2) a
Zn (mg kg^{-1})	12.3 (0.8) a	12.2 (1.0) a	15.2 (1.1) a	13.0 (0.8) a
Al (mg kg^{-1})	1501 (80.7) a	1599 (142) a	1325 (82) a	1594 (149) a
S (mg g^{-1})	0.9 (0.0) b	1.00 (0.1) b	11.9 (1.0) a	10.5 (0.7) a
	Gevuina avellana (Roots)			
	- $(Al_2 (SO_4)_3)$		+ $(Al_2 (SO_4)_3)$	
	2Ga	1Ga+1Vc	2Ga	1Ga+1Vc
N (mg g^{-1})	9.8 (0.2) a	10.6 (0.3) a	10.7 (0.6) a	9.2 (0.4) a
P (mg g^{-1})	0.20 (0.00) ab	0.23 (0.01) a	0.19 (0.01) b	0.22 (0.01) a
K (mg g^{-1})	2.48 (0.12) b	2.81 (0.33) b	4.10 (0.36) ab	5.94 (0.39) a
Ca (mg g^{-1})	4.19 (0.10) a	4.22 (0.10) a	3.72 (0.14) a	3.63 (0.28) a
Mg (mg g^{-1})	1.25 (0.04) b	1.32 (0.06) b	1.37 (0.06) ab	1.62 (0.13) a
Na (mg g^{-1})	1.80 (0.10) b	1.89 (0.21) b	2.11 (0.10) b	2.79 (0.19) a
Mn (mg kg^{-1})	92.9 (6.0) b	152.3 (14.6) b	334.8 (20.7) a	364.7 (39.34) a
Fe (mg kg^{-1})	1768 (130) b	3859 (444) a	3334 (404) a	2738 (347) ab
Cu (mg kg^{-1})	17.55 (1.6) b	22.43 (2.3) ab	29.5 (2.2) a	23.1 (1.3) ab
Zn (mg kg^{-1})	12.7 (0.9) b	16.8 (1.2) ab	31.2 (6.8) a	16.8 (0.7) ab
Al (mg k^{1})	3775 (205) b	7026 (692) a	8277 (639) a	7882 (541) a
S (mg g^{-1})	0.99 (0.06) b	1.17 (0.04) b	5.7 (0.4) a	5.0 (0.2) a

Each value corresponds to a mean of eight to ten samples ± standard error in brackets. Different letters indicate significant differences among treatments ($P \leq 0.05$).

finding is congruent with the growing body of evidence which underscores the benefits associated with the presence of Al in the soil. This is especially pertinent for plant species that are naturally adapted to acidic environments and particularly pronounced in Al hyperaccumulator species (Watanabe and Osaki, 2002; Bojórquez-Quintal et al., 2017; Muhammad et al., 2018; Sun et al., 2020). Similarly, studies have reported higher photosynthetic rates in Al hyperaccumulator plants, such as *Camelia sinensis* and *C. japonica* when were supplied with Al compared to control conditions (Mukhopadyay et al., 2012; Hajiboland et al., 2013; Liu et al., 2020). In *Qualea grandiflora*, another Al hyperaccumulator plant species, a significant increase in photosynthetic pigment concentrations, encompassing chlorophyll a, b, and carotenes, was observed in plants supplied with Al (Cury et al., 2019). Our findings support the contention that Al may exert a positive impact on the photosynthetic rate in the Al-hyperaccumulator plant. In our study, the increase in the photosynthetic rate in *G. avellana* is probably due to the increased stomatal conductance (Table 2) and increased proportion of chlorophyll a (Figure 2C), the primary chlorophyll pigment for photochemisty (Björn et al., 2009). Furthermore, the

10.3389/fpls.2024.1371123

TABLE 4 Nitrogen (N), phosphorus (P), potassium (K), calcium (Ca), magnesium (Mg), sodium (Na), manganese (Mn), iron (Fe), copper (Cu), zinc (Zn), aluminum (Al) and sulfur (S) concentrations in leaves and roots of *Vaccinium corymbosum* grown alone or in combination with or without aluminum sulfate supplementation in the following combinations: i) 2 seedlings of *G. avellana* (2Ga), 1 seedling of *G. avellana* + 1 seedling of *V. corymbosum* (1Ga + 1Vc), and iii) 2 seedlings of *V. corymbosum* (2Vc).

	Vaccinium corymbosum (Leaves)			
	- $(Al_2 (SO_4)_3)$		+ $(Al_2 (SO_4)_3)$	
	2Vc	1Ga+1Vc	2Vc	1Ga+1Vc
N (mg g^{-1})	11.1 (0.4) a	10.7 (0.2) a	8.5 (0.2) b	10.5 (0.4) a
P (mg g^{-1})	0.56 (0.02) a	0.54 (0.02) a	0.63 (0.02) a	0.66 (0.03) a
K (mg g^{-1})	7.0 (0.2) b	7.7 (0.3) b	13.2 (0.4) a	13.7 (0.8) a
Ca (mg g^{-1})	6.6 (0.3) b	7.6 (0.5) ab	7.9 (0.3) a	8.7 (0.6) a
Mg (mg g^{-1})	1.8 (0.1) b	2.1 (0.1) b	3.2 (0.1) a	3.4 (0.4) a
Na (mg g^{-1})	1.0 (0.1) a	1.2 (0.1) a	0.9 (0.1) ab	0.7 (0.1) b
Mn (mg kg^{-1})	78 (5.9) c	123 (14.8) b	717 (37) a	718 (86) a
Fe (mg kg^{-1})	114 (9.6) a	139 (12.8) a	107 (13.3) a	81 (5.3) a
Cu (mg kg^{-1})	3.2 (0.2) b	4.0 (0.3) ab	3.3 (0.12) ab	4.3 (0.3) a
Zn (mg kg^{-1})	23.8 (1.1) a	21.8 (1.3) ab	16.3 (0.7) c	18.0 (1.2) bc
Al (mg kg^{-1})	157 (18.2) a	196 (26.6) a	142 (21.1) a	121 (9.3) a
S (mg g^{-1})	0.48 (0.03) c	0.62 (0.04) b	8.2 (0.4) a	8.5 (0.9) a
	Vaccinium corymbosum (Roots)			
	- $(Al_2 (SO_4)_3)$		+ $(Al_2 (SO_4)_3)$	
	2Vc-Al	1Ga+1Vc-Al	2Vc+Al	1Ga+1Vc+Al
N (mg g^{-1})	9.9 (0.3) a	9.6 (0.21) a	8.67 (0.26) b	8.7 (0.2) ab
P (mg g^{-1})	0.87 (0.04) a	0.25 (0.02) b	0.26 (0.01) b	0.28 (0.03) b
K (mg g^{-1})	2.78 (0.11) b	2.60 (0.22) b	2.59 (0.11) b	3.16 (0.14) a
Ca (mg g^{-1})	3.51 (0.15) a	3.21 (0.42) a	3.69 (0.27) a	2.93 (0.27) a
Mg (mg g^{-1})	1.24 (0.03) b	1.23 (0.17) b	1.63 (0.04) a	1.84 (0.07) a
Na (mg g^{-1})	0.50 (0.02) a	0.56 (0.08) a	0.43 (0.02) b	0.51 (0.05) a
Mn (mg kg^{-1})	172 (14.6) c	225 (26.4) c	580 (30.2) b	743 (45.3) a
Fe (mg kg^{-1})	3543 (425) a	4008 (862) a	3703 (399) a	4723 (731.8) a
Cu (mg kg^{-1})	25.8 (2.2) b	28.7 (5.6) ab	28.8 (1.9) ab	37.5 (3.4) a
Zn (mg kg^{-1})	17.3 (0.9) a	20.2 (4.3) a	20.0 (0.8) a	23.4 (2.3) a
Al (mg kg^{-1})	5723 (556) a	6411 (820) a	8022 (605) a	8395 (958) a
S (mg g^{-1})	1.13 (0.05) b	1.12 (0.04) b	3.93 (0.26) a	3.78 (0.3) a

Each value corresponds to a mean of eight to ten samples ± standard error in brackets. Different letters indicate significant differences among treatments ($P \leq 0.05$).

increase in leaf Mg concentration (Table 3), a central element within the chlorophyll molecule, may also contribute to this effect (Farhat et al., 2016).

In addition to Mg, the concentration of other essential mineral nutrients such as K and Mn significantly increased in both leaves and roots of both species when grown in the Al supplemented soil. This effect held true regardless of whether the neighboring species is interspecific or conspecific. Furthermore, in the Al hyperaccumulator species, *G. avellana*, there was a significant rise in Na levels in leaves; and a concurrent increase in Fe, Cu and Zn in the roots was observed. The beneficial effects of Al on plant nutrient uptake have been observed in other species. For instance, Osaki et al. (1997) reported increased content of N, P, Mg and K in different organs of several plant species upon Al treatment. Similarly, the stimulation of growth by Al in the Al hyperaccumulator *C. sinensis* was attributed to the increased absorption of vital plant nutrients, such as Ca, Mg, K and Mn (Fung et al., 2008), as well as N and P (Konishi et al., 1985). Bojórquez-Quintal et al. (2017) proposed that Al could induce the expression or

activity of transport proteins (channels and transporters) and an alteration in the membrane potential and proton (H+) flux. This, in turn, could facilitate nutrients uptake by plant roots.

Carotenoids are known to play important roles in plants as antioxidants, and during environmental stress, plants usually respond by increasing their carotenoid concentrations (Havaux, 2014). Intriguingly, our observations revealed significantly lower concentrations in leaf carotenoids of *G. avellana* plants cultivated in Al-supplemented soil compared to control (Figure 2E), suggesting that this species may not have been experiencing stress during Al exposure. Indeed, the lipid peroxidation of *G. avellana* leaves was lower in plants that were cultivated in the Al supplemented soil. Similar results were found in the roots of *C. sinensis*, where it was observed that Al reduced the lipid peroxidation in root tips, which was related to the fact that Al-induced an increase in the activities of antioxidant enzymes (e.g. superoxide dismutase, catalase, and ascorbate peroxidase (Ghanati et al., 2005). Thus, the results suggest a positive effects of Al on the membrane integrity of *G. avellana* plants. On the contrary, higher lipid peroxidation was observed in the leaves of *V. corymbosum* plants that were cultivated in the Al supplemented soil, supporting previous reports indicating membrane damage induced by Al in this species (Ulloa-Inostroza et al., 2016; González-Villagra et al., 2021). Interestingly, *V. corymbosum* accompanied by *G. avellana* reduced significantly the lipid peroxidation in leaves when grew in the Al supplemented soil, clearly showing a facilitating effect of *G. avellana* towards *V. corymbosum*. It is proposed that, by increasing the N concentration of *V. corymbosum* when it grew with *G. avellana* (Table 4), *V. corymbosum* could have increased the activities of antioxidant enzymes, thus decreasing lipid oxidation.

In both species, leaf Al concentration was similar among treatments, suggesting a high self-regulation in Al uptake. This adaptive mechanism is highlighted by Delgado et al. (2019), who found that *G. avellana* growing in natural conditions showed similar leaf Al concentrations, independent of Al saturation percentage and soil pH. These authors reported ranges from 3,959 to 6,256 mg Al kg^{-1} for mature leaves and 7,150 to 11,040 mg Al kg^{-1} for senescent leaves of adult plants. In contrast, the current study used of 2-year-old plants, with an average of 1,505 mg Al kg^{-1}. It is most probable that the capacity for Al hyperaccumulation in this species, increases with the age of the plant. With respect to roots Al concentration, *G. avellana* plants exhibit significantly higher values when grown alongside *V. corymbosum*, compared to cultivation alongside conspecific species in soil without Al supplementation (Table 3). It was found that in this soil condition, leaves of *V. corymbosum* were limited by P (Figure 3) and therefore, it is likely that *V. corymbosum* activated mechanisms such as roots carboxylate exudation to mobilize P from the soil. Such responses are common among plants facing P deficiency (Chen and Liao, 2016). Beyond liberating P from the soil, it also serves as a formidable defense against Al toxicity, particularly in plants that possess the inherent ability to exclude the entry of Al into their tissues. This is achieved through the formation of harmless Al-organic complexes within the rhizosphere, reducing the potential harm posed by Al (Kochian et al., 2004; Chen and Liao, 2016). Thus, it is proposed that the greater Al uptake of *G. avellana* was due to the fact that it took up the Al excluded by *V. corymbosum*. Interestingly, *V. corymbosum* presented higher Al concentrations in the roots than in leaves (36 to 69 times more), a pattern observed in Al-sensitive plants (Kochian et al., 2004; Alarcón-Poblete et al., 2020; Cárcamo-Fincheira et al., 2023). This trend underscores a limited translocation of Al, thus, confirming the low Al tolerance in the aerial part of the *V. corymbosum* (Star cultivar) plant.

When plants were grown in Al supplemented soil, both species increased their Mn uptake. This could be due to Al supplementation decreasing the soil pH from 6.1 to 4.7 (Table 1) thereby increasing the solubility of Mn with decreasing soil pH (Lambers and Oliveira, 2019). On the other hand, several authors have reported that leaf Mn concentration is a good proxy for rhizosphere carboxylate concentrations (Shane and Lambers, 2005; Lambers et al., 2015b; Pang et al., 2018; Lambers et al., 2021). This is because carboxylates exuded by roots simultaneously mobilize P and other nutrients from the rhizosphere, especially Mn, which enters roots via transporters with limited substrate specificity (Lambers et al., 2021). Indeed, the leaf Mn concentration in 100 chickpea genotypes has been positively correlated with carboxylate amount in rhizosheath (Pang et al., 2018). In the current study, there was a 2-fold increase in foliar Mn concentration in *G. avellana* when grown in Al supplemented soil, while in *V. corymbosum* this increase was 7-fold, which was independent of the neighboring species. These results suggest that *V. corymbosum* presented high stress in the Al-supplemented soil and it is likely that this species may have exuded large amounts of carboxylates under these conditions.

The S values were exceptionally high in the soil supplemented with $Al_2(SO_4)_3$ compared with those values found in the soil of control treatment (Table 1). Consequently, leaf S concentrations of *G. avellana* and *V. corymbosum* plants supplemented with $Al_2(SO_4)_3$ were up to 12 and 15 times more than control plants (Tables 3, 4), with these values being considered in the high ranges for plants (~ 10 mg kg^{-1} DW) (Lambers and Oliveira, 2019). Sulfur is integral to numerous physiological processes in plants, including protein synthesis, enzyme activation, chlorophyll formation, defense mechanisms, and secondary metabolite production (Kopriva et al., 2019). It has been reported that S can alleviate the toxicity of metals such as cadmium (Ferri et al., 2017; Lyčka et al., 2023) and Al (Guo et al., 2017), because some S-containing compounds, such as glutathione and phytochelatins, play vital roles in the complexation of metals and their subsequent sequestration into vacuoles. Additionally, these S-containing compounds contribute to the alleviation of oxidative stress by functioning as antioxidant molecules. Our results showed that the addition of $Al_2(SO_4)_3$ seems to benefit *G. avellana*, due to increased proportion of chlorophyll a (Figure 2C), photosynthetic rate (Table 2), leaf Mg concentration (Table 3) and decreased lipid peroxidation (Figure 4). On the contrary, *V. corymbosum* plants worsens their condition under the soil supplemented with $Al_2(SO_4)_3$, raising the possibility that S supplementation may not have been sufficient to alleviate Al toxicity or that the S could have generated a toxic effect on the plant. Most studies have focused on the interactions occurring between S and other macro and micro-nutrients when plants are subjected to S deficiency (Courbet et al., 2019), however, the excess of S and its effect on the plant has been scarcely explored. We recognize that future studies are necessary to elucidate the effect of Al and S separately on these plants. In any case, it is important to highlight and report that *G. avellana* facilitate to *V. corymbosum* when both species

grown in the $Al_2(SO_4)_3$ supplemented soil. Additionally, it is interesting to mention that unlike *G. avellana*, another Proteaceae species, *Hakea prostrata*, tightly controls its S acquisition (Prodhan et al., 2017). The ability to modulate S and N uptake in some species, has been linked to match its low protein concentration and low demand for rRNA, and its consequently low P requirements (Prodhan et al., 2017), as an adaptation of plants that have evolved in extremely P-impoverished habitats [values of total soil P ranging from 6.6 to 20.3 mg P kg^{-1} (Hayes et al., 2014)]. Thus, it is probable that *G. avellana*, which has evolved on relatively nutrient-rich soils (values of total soil P ranging from 63.1 to 951.6 mg P kg^{-1} (Delgado et al., 2018)), has not evolved the ability to regulate S uptake.

Conclusions

Contrary to expectations, it was rather surprisingly found that *G. avellana* did not contribute to higher growth rates either P acquisition in *V. corymbosum*. On the contrary, *G. avellana* shows better growth rates when grown associated with *V. corymbosum*. In addition, *V. corymbosum* had a decrease in root P concentrations, when grown in association with *G. avellana*, indicating a highly competitive capacity of this latter species for P acquisition. On the other hand, *G. avellana* did not assist in the decrease of Al uptake of *V. corymbosum*, although it contributed to an increase in N acquisition, and consequently higher chlorophyll concentrations and photosynthesis rates. Besides, *V. corymbosum* decreased the lipid peroxidation in leaves when grown in soil with Al supplementation and accompanied by *G. avellana*. Overall, our results suggest a facilitating effect of *G. avellana* to *V. corymbosum* and *vice versa*. The benefit of facilitation of *G. avellana* to *V. corymbosum* is only observed when both species grown in the Al supplemented soil. The information provided in this manuscript is relevant to know some nutritional and physiological aspects of these species. Future research is required to reveal the possible role of cluster roots of *G. avellana* in the N acquisition. Finally, this study has opened avenues for future research, suggesting the need for additional facilitation tests employing soil with more pronounced contrasts of the studied element (e.g. N, P or Al, and maintaining other soil properties constant) in order to find a greater impact of the nutrient under study on growth of the plant.

Data availability statement

The raw data supporting the conclusions of this article will be made available by the authors, without undue reservation.

Author contributions

MD: Conceptualization, Data curation, Formal analysis, Funding acquisition, Investigation, Methodology, Project administration, Resources, Software, Supervision, Validation, Visualization, Writing – original draft, Writing – review & editing. PB: Conceptualization, Funding acquisition, Investigation, Methodology, Supervision, Writing – review & editing. GB: Funding acquisition, Methodology, Writing – review & editing, Formal analysis. ML: Investigation, Methodology, Resources, Writing – review & editing. PD: Investigation, Methodology, Resources, Writing – review & editing. AV: Conceptualization, Supervision, Visualization, Writing – review & editing. MR-D: Investigation, Methodology, Resources, Writing – review & editing.

Funding

The author(s) declare financial support was received for the research, authorship, and/or publication of this article. This study was financed by the Agencia Nacional de Investigación y Desarrollo (ANID) of Chilean government through FONDECYT initiation project N° 11170368 (MD), 11220462 (GB), 11200377 (PB), FONDECYT Regular projects N° 1210684 (MD), 1211856 (MR-D), 1241293 (PB), ANID/FONDAP/15130015 (MR-D), Proyecto Anillo de Investigación en Áreas Temáticas Específicas ATE220038 (MD, PD and PB), ATE230007 (MD and MR-D). We also thank Dirección de Investigación of Universidad de La Frontera (DiUFRO) for their support through the Proyecto de Investigación Vinculados a la Red Nexer No. DNX22-0009 (MD and PB).

Acknowledgments

We thank the Soil and Plant Laboratory of the Agroindustry Institute, Universidad de la Frontera, especially Maria Brígida Sobarzo and Pamela Morales, for their assistance in chemical determinations. The authors acknowledge Scientific and Technological Bioresource Nucleus of Universidad de La Frontera (BIOREN–UFRO) and Service Management Analytical Research and Training Center (SmartC-BIOREN).

Conflict of interest

The authors declare that the research was conducted in the absence of any commercial or financial relationships that could be construed as a potential conflict of interest.

Publisher's note

Supplementary material

The Supplementary Material for this article can be found online at: https://www.frontiersin.org/articles/10.3389/fpls.2024.1371123/full#supplementary-material

References

Alarcón-Poblete, E., González-Villagra, J., de Oliveira Silva, F. M., Nunes-Nesi, A., Inostroza-Blancheteau, C., Alberdi, M., et al. (2020). Metabolic responses of *Vaccinium corymbosum* L. cultivars to Al^{3+} toxicity and gypsum amendment. *Environ. Exp. Bot.* 176, 104119. doi: 10.1016/j.envexpbot.2020.104119

Alarcón-Poblete, E., Inostroza-Blancheteau, C., Latsague, M., Alberdi, M., de Oliveira Silva, F. M., Nunes-Nesi, A., et al. (2019). Gypsum application ameliorates morphological and photochemical damages provoked by Al toxicity in *Vaccinium corymbosum* L. cultivars. *J. Berry. Res.* 9, 665–685. doi: 10.3233/JBR-190420

Barrow, N. (1977). Phosphorus uptake and utilization by tree seedlings. *Aust. J. Bot.* 25, 571–584. doi: 10.1071/BT9770571

Björn, L. O., Papageorgiou, G. C., Blankenship, R. E., and Govindjee, (2009). A viewpoint: why chlorophyll a? *Photosynthesis. Res.* 99, 85–98. doi: 10.1007/s11120-008-9395-x

Bojórquez-Quintal, E., Escalante-Magaña, C., Echevarría-MaChado, I., and Martínez-Estévez, M. (2017). Aluminum, a friend or foe of higher plants in acid soils. *Front. Plant Sci.* 8. doi: 10.3389/fpls.2017.01767

Borie, F., and Rubio, R. (2003). Total and organic phosphorus in Chilean volcanic soils. *Gayana. Bot.* 60, 69–78. doi: 10.4067/S0717-66432003000100011

Bremner, J. (1960). Determination of nitrogen in soil by the Kjeldahl method. *J. Agric. Sci.* 55, 11–33. doi: 10.1017/S0021859600021572

Cárcamo, M. P., Reyes-Díaz, M., Rengel, Z., Alberdi, M., Omena-Garcia, R. P., Nunes-Nesi, A., et al. (2019). Aluminum stress differentially affects physiological performance and metabolic compounds in cultivars of highbush blueberry. *Sci. Rep.* 9, 1–13. doi: 10.1038/s41598-019-47569-8

Cárcamo-Fincheira, P., Reyes-Díaz, M., Omena-Garcia, R. P., Nunes-Nesi, A., and Inostroza-Blancheteau, C. (2023). Physiological and metabolic responses to aluminum toxicity reveal differing resistance mechanisms to long-term exposure in highbush blueberry cultivars. *Sci. Hortic.* 309, 111665. doi: 10.1016/j.scienta.2022.111665

Chen, Z. C., and Liao, H. (2016). Organic acid anions: An effective defensive weapon for plants against aluminum toxicity and phosphorus deficiency in acidic soils. *J. Genet. Genomics* 43, 631–638. doi: 10.1016/j.jgg.2016.11.003

Chen, Y. M., Wang, M. K., Zhuang, S. Y., and Chiang, P. N. (2006). Chemical and physical properties of rhizosphere and bulk soils of three tea plants cultivated in Ultisols. *Geoderma* 136, 378–387. doi: 10.1016/j.geoderma.2006.04.003

Courbet, G., Gallardo, K., Vigani, G., Brunel-Muguet, S., Trouverie, J., Salon, C., et al. (2019). Disentangling the complexity and diversity of crosstalk between sulfur and other mineral nutrients in cultivated plants. *J. Exp. Bot.* 70, 4183–4196. doi: 10.1093/jxb/erz214

Cury, N. F., Silva, R. C., Andre, M. S., Fontes, W., Ricart, C. A., Castro, M. S., et al. (2019). Root proteome and metabolome reveal a high nutritional dependency of aluminium in *Qualea grandiflora* Mart. (Vochysiaceae). *Plant Soil.* 446, 125–143. doi: 10.1007/s11104-019-04323-3

Delgado, M., Valle, S., Barra, P. J., Reyes-Díaz, M., and Zúñiga-Feest, A. (2019). New aluminum hyperaccumulator species of the Proteaceae family from southern South America. *Plant Soil* 444, 475–487. doi: 10.1007/s11104-019-04289-2

Delgado, M. F., Valle, S., Reyes-Díaz, M., Barra, P. J., and Zúñiga-Feest, A. (2018). Nutrient use efficiency of southern South America Proteaceae species. Are there general patterns in the Proteaceae family? *Front. Plant Sci.* 9. doi: 10.3389/fpls.2018.00883

Delgado, M., Zúñiga-Feest, A., Almonacid, L., Lambers, H., and Borie, F. (2015). Cluster roots of *Embothrium coccineum* (Proteaceae) affect enzyme activities and phosphorus lability in rhizosphere soil. *Plant Soil* 395, 189–200. doi: 10.1007/s11104-015-2547-9

Delgado, M., Zúñiga-Feest, A., Reyes-Díaz, M., Barra, P., Ruiz, S., Bertin-Benavides, A., et al. (2021). Ecophysiological performance of proteaceae species from southern south america growing on substrates derived from young volcanic materials. *Front. Plant Sci.* 12. doi: 10.3389/fpls.2021.636056

Drummond, L., and Maher, W. (1995). Determination of phosphorus in aqueous solution via formation of the phosphoantimonylmolybdenum blue complex. Re-examination of optimum conditions for the analysis of phosphate. *Anal. Chim. Acta* 302, 69–74. doi: 10.1016/0003-2670(94)00429-P

Du, Z., and Bramlage, W. J. (1992). Modified thiobarbituric acid assay for measuring lipid oxidation in sugar-rich plant tissue extracts. *J. Agric. Food Chem.* 40, 1566–1570. doi: 10.1021/jf00021a018

Fajardo, A., and Piper, F. I. (2019). Cluster root-bearing Proteaceae species show a competitive advantage over non-cluster root-bearing species. *Ann. Bot.* 124, 1121–1131. doi: 10.1093/aob/mcz128

Farhat, N., Elkhouni, A., Zorrig, W., Smaoui, A., Abdelly, C., and Rabhi, M. (2016). Effects of magnesium deficiency on photosynthesis and carbohydrate partitioning. *Acta Physiol. Plant* 38, 145. doi: 10.1007/s11738-016-2165-z

Ferri, A., Lancilli, C., Maghrebi, M., Lucchini, G., Sacchi, G. A., and Nocito, F. F. (2017). The sulfate supply maximizing *Arabidopsis* shoot growth is higher under long-than short-term exposure to cadmium. *Front. Plant Sci.* 8. doi: 10.3389/fpls.2017.00854

Fung, K. F., Carr, H. P., Zhang, J., and Wong, M. H. (2008). Growth and nutrient uptake of tea under different aluminium concentrations. *J. Sci. Food Agric.* 88, 1582–1591. doi: 10.1002/jsfa.3254

Ghanati, F., Morita, A., and Yokota, H. (2005). Effects of aluminum on the growth of tea plant and activation of antioxidant system. *Plant Soil* 276, 133–141. doi: 10.1007/s11104-005-3697-y

González-Villagra, J., Pino, R., Inostroza-Blancheteau, C., Cartes, P., Ribera-Fonseca, A., and Reyes-Díaz, M. J. P. (2021). Pre-harvest MeJA application counteracts the deleterious impact of Al and Mn toxicity in Highbush Blueberry grown in acid soils. *Plants* 10, 2730. doi: 10.3390/plants10122730

Guo, P., Li, Q., Qi, Y.-P., Yang, L.-T., Ye, X., Chen, H.-H., et al. (2017). Sulfur-mediated-alleviation of aluminum-toxicity in *Citrus grandis* seedlings. *Int. J. Mol. Sci.* 18, 2570. doi: 10.3390/ijms18122570

Hajiboland, R., Bahrami Rad, S., Barceló, J., and Poschenrieder, C. (2013). Mechanisms of aluminum-induced growth stimulation in tea (*Camellia sinensis*). *J. Plant Nutr. Soil Sci.* 176, 616–625. doi: 10.1002/jpln.201200311

Havaux, M. (2014). Carotenoid oxidation products as stress signals in plants. *Plant J.* 79, 597–606. doi: 10.1111/tpj.12386

Hayes, P., Turner, B. L., Lambers, H., and Laliberté, E. (2014). Foliar nutrient concentrations and resorption efficiency in plants of contrasting nutrient-acquisition strategies along a 2-million-year dune chronosequence. *J. Ecol.* 102, 396–410. doi: 10.1111/1365-2745.12196

Inostroza-Blancheteau, C., Aquea, F., Loyola, R., Slovin, J., Josway, S., Rengel, Z., et al. (2013). Molecular characterisation of a calmodulin gene, VcCaM1, that is differentially expressed under aluminium stress in highbush blueberry. *Plant Biol.* 15, 1013–1018. doi: 10.1111/j.1438-8677.2012.00722.x

Inostroza-Blancheteau, C., Aquea, F., Reyes-Díaz, M., Alberdi, M., and Arce-Johnson, P. (2011a). Identification of aluminum-regulated genes by cDNA-AFLP analysis of roots in two contrasting genotypes of highbush blueberry (*Vaccinium corymbosum* L.). *Mol. Biotechnol.* 49, 32–41. doi: 10.1007/s12033-010-9373-3

Inostroza-Blancheteau, C., Reyes-Diaz, M., Aquea, F., Nunes-Nesi, A., Alberdi, M., and Arce-Johnson, P. (2011b). Biochemical and molecular changes in response to aluminium-stress in highbush blueberry (*Vaccinium corymbosum* L.). *Plant Physiol. Biochem.* 49, 1005–1012. doi: 10.1016/j.plaphy.2011.04.009

Jansen, S., Broadley, M. R., Robbrecht, E., and Smets, E. (2002). Aluminum hyperaccumulation in Angiosperms: A review of its phylogenetic significance. *Bot. Rev.* 68, 235–269. doi: 10.1663/0006-8101

Kochian, L. V., Hoekenga, O. A., and Piñeros, M. A. (2004). How do crop plants tolerate acid soils? Mechanisms of aluminum tolerance and phosphorous efficiency. *Annu. Rev. Plant Biol.* 55, 459–493. doi: 10.1146/annurev.arplant.55.031903.141655

Kochian, L. V., Piñeros, M. A., Liu, J., and Magalhaes, J. V. (2015). Plant adaptation to acid soils: the molecular basis for crop aluminum resistance. *Annu. Rev. Plant Biol.* 66, 571–598. doi: 10.1146/annurev-arplant-043014-114822

Koerselman, W., and Meuleman, A. F. (1996). The vegetation N:P ratio: a new tool to detect the nature of nutrient limitation. *J. Appl. Ecol.* 33, 1441–1450. doi: 10.2307/2404783

Komosa, A., Roszyk, J., and Mieloch, M. (2017). Content of nutrients in soils of highbush blueberry (*Vaccinium corymbosum* L.) plantations in Poland in a long-term study. *J. Elem.* 22, 1193–1207. doi: 10.5601/jelem.2016.21.4.1329

Konishi, S., Miyamoto, S., and Taki, T. (1985). Stimulatory effects of aluminum on tea plants grown under low and high phosphorus supply. *Soil Sci. Plant Nutr.* 31, 361–368. doi: 10.1080/00380768.1985.10557443

Kopriva, S., Malagoli, M., and Takahashi, H. (2019). Sulfur nutrition: impacts on plant development, metabolism, and stress responses. *J. Exp. Bot.* 70, 4069–4073. doi: 10.1093/jxb/erz319

Lambers, H., Albornoz, F., Kotula, L., Laliberté, E., Ranathunge, K., Teste, F. P., et al. (2018). How belowground interactions contribute to the coexistence of mycorrhizal and non-mycorrhizal species in severely phosphorus-impoverished hyperdiverse ecosystems. *Plant Soil* 424, 11–33. doi: 10.1007/s11104-017-3427-2

Lambers, H., Finnegan, P. M., Jost, R., Plaxton, W. C., Shane, M. W., and Stitt, M. (2015a). Phosphorus nutrition in Proteaceae and beyond. *Nat. Plants* 1, 15109. doi: 10.1038/nplants.2015.109

Lambers, H., Hayes, P. E., Laliberté, E., Oliveira, R. S., and Turner, B. L. (2015b). Leaf manganese accumulation and phosphorus-acquisition efficiency. *Trends Plant Sci.* 20, 83–90. doi: 10.1016/j.tplants.2014.10.007

Lambers, H., and Oliveira, R. S. (2019). "Mineral nutrition," in *Plant physiological ecology* (Switzerland: Springer).

Lambers, H., Shane, M. W., Cramer, M. D., Pearse, S. J., and Veneklaas, E. J. (2006). Root structure and functioning for efficient acquisition of phosphorus: Matching morphological and physiological traits. *Ann. Bot.* 98, 693–713. doi: 10.1093/aob/mcl114

Lambers, H., Wright, I. J., Pereira, C. G., Bellingham, P. J., Bentley, L. P., Boonman, A., et al. (2021). Leaf manganese concentrations as a tool to assess belowground plant

functioning in phosphorus-impoverished environments. *Plant Soil* 461, 43–61. doi: 10.1007/s11104-020-04690-2

Li, L., Tilman, D., Lambers, H., and Zhang, F.-S. (2014). Plant diversity and overyielding: insights from belowground facilitation of intercropping in agriculture. *New Phytol.* 203, 63–69. doi: 10.1111/nph.12778

Lichtenthaler, H. K., and Wellburn, A. R. (1983). Determinations of total carotenoids and chlorophylls a and b of leaf extracts in different solvents. *Biochem. Soc. Trans.* 603, 591–592. doi: 10.1042/bst0110591

Lindsay, W. L., and Norvell, W. A. (1978). Development of a DTPA soil test for zinc, iron, manganese, and copper 1. *Soil Sci. Soc. Am. J.* 42, 421–428. doi: 10.2136/sssaj1978.03615995004200030009x

Liu, Y., Tao, J., Cao, J., Zeng, Y., Li, X., Ma, J., et al. (2020). The beneficial effects of aluminum on the plant growth in *Camellia japonica*. *J. Soil Sci. Plant Nutr.* 20, 1799–1809. doi: 10.1007/s42729-020-00251-9

Lyčka, M., Barták, M., Helia, O., Kopriva, S., Moravcová, D., Hájek, J., et al. (2023). Sulfate supplementation affects nutrient and photosynthetic status of *Arabidopsis thaliana* and *Nicotiana tabacum* differently under prolonged exposure to cadmium. *J. Hazard. Mater.* 445, 130527. doi: 10.1016/j.jhazmat.2022.130527

Michel, L., Beyá-Marshall, V., Rombolà, A. D., Pastenes, C., and Covarrubias, J. I. (2019). Evaluation of Fe-heme applications or intercropping for preventing iron deficiency in blueberry. *J. Soil Sci. Plant Nutr.* 19, 117–126. doi: 10.1007/s42729-019-0017-9

Montalba, R., Vieli, L., Spirito, F., and Muñoz, E. (2019). Environmental and productive performance of different blueberry (*Vaccinium corymbosum* L.) production regimes: Conventional, organic, and agroecological. *Sci. Hortic.* 256, 108592. doi: 10.1016/j.scienta.2019.108592

Mora, M., Alfaro, M., Jarvis, S., Demanet, R., and Cartes, P. (2006). Soil aluminium availability in Andisols of southern Chile and its effect on forage production and animal metabolism. *Soil Use Manag.* 22, 95–101. doi: 10.1111/j.1475-2743.2006.00011.x

Mora, M. L., Demanet, R., Acuña, J. J., Viscardi, S., Jorquera, M., Rengel, Z., et al. (2017). Aluminum-tolerant bacteria improve the plant growth and phosphorus content in ryegrass grown in a volcanic soil amended with cattle dung manure. *Appl. Soil Ecol.* 115, 19–26. doi: 10.1016/j.apsoil.2017.03.013

Mora, M., Schnettler, B., and Demanet, R. (1999). Effect of liming and gypsum on soil chemistry, yield, and mineral composition of ryegrass grown in an acidic Andisol. *Commun. Soil Sci. Plant Anal.* 30, 1251–1266. doi: 10.1080/00103629909370282

Muhammad, N., Zvobgo, G., and Guo-ping, Z. (2018). A review: the beneficial effect of aluminum on plant growth in acid soil and the possible mechanisms. *J. Integr. Agric.* 17, 60345–60347. doi: 10.1016/S2095-3119(18)61991-4

Mukhopadyay, M., Bantawa, P., Das, A., Sarkar, B., Bera, B., Ghosh, P., et al. (2012). Changes of growth, photosynthesis and alteration of leaf antioxidative defence system of tea [*Camellia sinensis* (L.) O. Kuntze] seedlings under aluminum stress. *BioMetals* 25, 1141–1154. doi: 10.1007/s10534-012-9576-0

Muler, A. L., Oliveira, R. S., Lambers, H., and Veneklaas, E. J. (2013). Does cluster-root activity benefit nutrient uptake and growth of co-existing species? *Oecologia* 174, 23–31. doi: 10.1007/s00442-013-2747-z

Ochmian, I., Oszmiański, J., Jaśkiewicz, B., and Szczepanek, M. (2018). Soil and highbush blueberry responses to fertilization with urea phosphate. *Folia Hort.* 30, 295–305. doi: 10.2478/fhort-2018-0025

Osaki, M., Watanabe, T., and Tadano, T. (1997). Beneficial effect of aluminum on growth of plants adapted to low pH soils. *Soil Sci. Plant Nutr.* 43, 551–563. doi: 10.1080/00380768.1997.10414782

Pang, J., Bansal, R., Zhao, H., Bohuon, E., Lambers, H., Ryan, M. H., et al. (2018). The carboxylate-releasing phosphorus-mobilizing strategy can be proxied by foliar manganese concentration in a large set of chickpea germplasm under low phosphorus supply. *New Phytol.* 219, 518–529. doi: 10.1111/nph.15200

Paungfoo-Lonhienne, C., Schenk, P. M., Lonhienne, T. G., Brackin, R., Meier, S., Rentsch, D., et al. (2009). Nitrogen affects cluster root formation and expression of putative peptide transporters. *J. Exp. Bot.* 60, 2665–2676. doi: 10.1093/jxb/erp111

Petridis, A., van der Kaay, J., Chrysanthou, E., McCallum, S., Graham, J., and Hancock, R. D. (2018). Photosynthetic limitation as a factor influencing yield in highbush blueberries (*Vaccinium corymbosum*) grown in a northern European environment. *J. Exp. Bot.* 69, 3069–3080. doi: 10.1093/jxb/ery118

Pinochet, D., Artacho, P., and Maraboli, A. (2014). *Manual de fertilización de arándanos cultivados en el sur de Chile* (Valdivia, Chile: Imprenta América).

Piper, F. I., Baeza, G., Zuniga-Feest, A., and Fajardo, A. (2013). Soil nitrogen, and not phosphorus, promotes cluster-root formation in a South American Proteaceae, *Embothrium coccineum*. *Am. J. Bot.* 100, 2328–2338. doi: 10.3732/ajb.1300163

Prodhan, M. A., Jost, R., Watanabe, M., Hoefgen, R., Lambers, H., and Finnegan, PMJNP (2017). Tight control of sulfur assimilation: an adaptive mechanism for a plant from a severely phosphorus-impoverished habitat. *New Phytol.* 215, 1068–1079. doi: 10.1111/nph.14640

Qilong, Z., Jiang, Y., Gangqiang, D., Jiguang, W., Jiang, J., Liangliang, T., et al. (2020). Effect of Al on the growth and nutrients uptake of blueberries (*Vaccinium* spp.). *Notulae. Botanicae. Horti. Agrobotanici. Cluj-Napoca.* 48, 656–665. doi: 10.15835/nbha48211643

Renderos, L., Zúñiga-Feest, A., Delgado, M., Muñoz, G., Carú, M., and Orlando, J. (2022). Cluster roots of *Embothrium coccineum* growing under field conditions differentially shape microbial diversity according to their developmental stage. *J. Soil Sci. Plant Nutr.* 22, 2418–2433. doi: 10.1007/s42729-022-00818-8

Reyes-Díaz, M., Inostroza-Blancheteau, C., Millaleo, R., Cruces, E., Wulff-Zottele, C., Alberdi, M., et al. (2010). Long-term aluminum exposure effects on physiological and biochemical features of highbush blueberry cultivars. *J. Am. Soc. Hortic. Sci.* 135, 212–222. doi: 10.21273/JASHS.135.3.212

Reyes-Díaz, M., Meriño-Gergichevich, C., Alarcón, E., Alberdi, M., and Horst, W. J. (2011). Calcium sulfate ameliorates the effect of aluminum toxicity differentially in genotypes of highbush blueberry (*Vaccinium corymbosum* L.). *J. Soil Sci. Plant Nutr.* 11, 59–78. doi: 10.4067/S0718-95162011000400005

Reyes-Díaz, M., Meriño-Gergichevich, C., Inostroza-Blancheteau, C., Latsague, M., Acevedo, P., and Alberdi, M. (2016). Anatomical, physiological, and biochemical traits involved in the UV-B radiation response in highbush blueberry. *J. Biol. Plantarum.* 60, 355–366. doi: 10.1007/s10535-015-0580-4

Ruan, J., Ma, L., Shi, Y., and Zhang, F. (2004). Effects of litter incorporation and nitrogen fertilization on the contents of extractable aluminium in the rhizosphere soil of tea plant (*Camellia sinensis* (L.) O. Kuntze). *Plant Soil* 263, 283–296. doi: 1023/B:PLSO.0000047744.44940.96

Ryan, P. R., Delhaize, E., and Jones, D. L. (2001). Function and mechanism of organic anion exudation from plant roots. *Annu. Rev. Plant Physiol. Plant Mol. Biol.* 52, 527–560. doi: 10.1146/annurev.arplant.52.1.527

Sadzawka, A., Carrasco, M., and Grez, R, ML M (2004a). *Métodos de análisis recomendados para los suelos Chilenos* (Chile: Sociedad Chilena de la Ciencia del Suelo).

Sadzawka, A., Grez, R., Carrasco, M., and Mora, M. (2004b). *Métodos de análisis de tejidos vegetales* (Chile: Comisión de normalización y acreditación sociedad Chilena de la ciencia del suelo).

Samac, D. A., and Tesfaye, M. (2003). Plant improvement for tolerance to aluminum in acid soils–a review. *Plant Cell Tissue Organ Cult.* 75, 189–207. doi: 10.1023/A:1025843829545

Schoebitz, M., Castillo, D., Jorquera, M., and Roldan, A. (2020). Responses of microbiological soil properties to intercropping at different planting densities in an acidic Andisol. *Agronomy* 10, 781. doi: 10.3390/agronomy10060781

Shane, M. W., and Lambers, H. (2005). Manganese accumulation in leaves of *Hakea prostrata* (Proteaceae) and the significance of cluster roots for micronutrient uptake as dependent on phosphorus supply. *Physiol. Plant* 124, 441–450. doi: 10.1111/j.1399-3054.2005.00527.x

Shen, Q., Ranathunge, K., Zhong, H., Finnegan, P. M., and Lambers, H. (2023). Facilitation of phosphorus acquisition by *Banksia attenuata* allows *Adenanthos cygnorum* (Proteaceae) to extend its range into severely phosphorus-impoverished habitats. *Plant Soil* 496, 51–70. doi: 10.1007/s11104-023-05935-6

Sun, L., Zhang, M., Liu, X., Mao, Q., Shi, C., Kochian, L. V., et al. (2020). Aluminium is essential for root growth and development of tea plants (*Camellia sinensis*). *J. Integr. Plant Biol.* 62, 984–997. doi: 10.1111/jipb.12942

Teste, F. P., Dixon, K. W., Lambers, H., Zhou, J., and Veneklaas, E. J. J. O. (2020). The potential for phosphorus benefits through root placement in the rhizosphere of phosphorus-mobilising neighbours. *Oecologia* 193, 843–855. doi: 10.1007/s00442-020-04733-6

Teste, F. P., Veneklaas, E. J., Dixon, K. W., Lambers, H., and Watling, J. (2014). Complementary plant nutrient-acquisition strategies promote growth of neighbour species. *Funct. Ecol.* 28, 819–828. doi: 10.1111/1365-2435.12270

Tolrà, R., Vogel-Mikuš, K., Hajiboland, R., Kump, P., Pongrac, P., Kaulich, B., et al. (2011). Localization of aluminium in tea (*Camellia sinensis*) leaves using low energy X-ray fluorescence spectro-microscopy. *J. Plant Res.* 124, 165–172. doi: 10.1007/s10265-010-0344-3

Ulloa-Inostroza, E. M., Alberdi, M., Meriño-Gergichevich, C., and Reyes-Díaz, M. (2016). Low doses of exogenous methyl jasmonate applied simultaneously with toxic aluminum improve the antioxidant performance of *Vaccinium corymbosum*. *Plant Soil* 412, 81–96. doi: 10.1007/s11104-016-2985-z

Walkley, A., and Black, I. A. (1934). An examination of the Degtjareff method for determining soil organic matter, and a proposed modification of the chromic acid titration method. *Soil Sci.* 37, 29–38.

Watanabe, T., and Osaki, M. (2002). Mechanisms of adaptation to high aluminum condition in native plant species growing in acid soils: a review. *Commun. Soil Sci. Plant Anal.* 33, 1247–1260. doi: 10.1081/CSS-120003885

Webb, L. (1954). Aluminium accumulation in the Australian–New Guinea flora. *Aust. J. Bot.* 2, 176–196. doi: 10.1071/BT9540176

Xu, Z., Li, C., Zhang, C., Yu, Y., van der Werf, W., and Zhang, F. (2020). Intercropping maize and soybean increases efficiency of land and fertilizer nitrogen use; A meta-analysis. *Field Crops Res.* 246, 107661. doi: 10.1016/j.fcr.2019.107661

Zúñiga-Feest, A., Sepúlveda, F., Delgado, M., Valle, S., Muñoz, G., Pereira, M., et al. (2021). *Gevuina avellana* and Lomatia dentata, two Proteaceae species from evergreen temperate forests of South America exhibit contrasting physiological responses under nutrient deprivation. *Plant Soil* 464, 29–44. doi: 10.1007/s11104-020-04640-y

frontiers | Frontiers in Plant Science

TYPE Original Research
PUBLISHED 11 June 2024
DOI 10.3389/fpls.2024.1386039

OPEN ACCESS

EDITED BY
Marta Wilton Vasconcelos,
Catholic University of Portugal, Portugal

REVIEWED BY
Asif Naeem,
Nuclear Institute for Agriculture and Biology, Pakistan
Adriana Fernanda Spara,
National University of the Center of the Province of Buenos Aires, Argentina

*CORRESPONDENCE
Karl H. Mühling
khmuehling@plantnutrition.uni-kiel.de
Britta Pitann
bpitann@plantnutrition.uni-kiel.de

RECEIVED 14 February 2024
ACCEPTED 28 May 2024
PUBLISHED 11 June 2024

CITATION
Pitann B and Mühling KH (2024) Oat—an alternative crop under waterlogging stress? *Front. Plant Sci.* 15:1386039. doi: 10.3389/fpls.2024.1386039

Oat—an alternative crop under waterlogging stress?

Britta Pitann* and Karl H. Mühling*

Institute of Plant Nutrition and Soil Science, Kiel University, Kiel, Germany

Introduction: Waterlogging is one vast environmental constraint that limits crop growth and yield worldwide. Most major crop species are very sensitive to waterlogging, leading to enormous yield losses every year. Much is already known about wheat, barley or maize; however, hardly any data exist on oat and its tolerance against waterlogging. Thus, this study aimed to investigate if oats can be an adequate alternative in crop rotation under conditions of temporal submergence and if cultivar differences exist. Furthermore, this study was to test (1) whether yield was differently affected when stress is applied at different developmental stages (BBCH 31 and 51), and (2) nutrient imbalances are the reason for growth restrictions.

Methods: In a large-scale container experiment, three different oat varieties were cultivated and exposed to 14 consecutive days of waterlogging stress at two developmental stages.

Results: Even though vegetative growth was impaired after early waterlogging and which persists till maturity, mainly due to transient nutrient deficiencies, growth performance after late waterlogging and grain yield of all three oat varieties at maturity was not affected. A high tolerance was also confirmed after late waterlogging in the beginning generative stage: grain yield was even increased.

Discussion: Overall, all oat varieties performed well under both stress treatments, even though transient nutrient imbalances occurred, but which were ineffective on grain yield. Based on these results, we conclude that oats, independently of the cultivar, should be considered a good alternative in crop production, especially when waterlogging is to be expected during the cultivation phase.

KEYWORDS

nitrogen, oat, phosphorus, waterlogging, yield

1 Introduction

Climate change has been and is a serious topical global issue. While in the past the focus was mostly laid on the increase of climate-relevant gases, today, it is also important to understand the impact of hydrological changes. For example, in the course of climate change, an increase in the frequency and intensity of extreme weather events is to be

expected, which threatens not only the security of the water supply but also food production as such. According to the Intergovernmental Panel on Climate Change (IPCC, 2022), almost half of the world's population is already particularly affected by water scarcity. However, also the opposite is to be expected with more phases of heavy rainfall events, resulting in an increased risk of flooding associated with temporary waterlogging. Climate models already show that the global amount of precipitation increases by approximately 2% for every one-degree increase in temperature (Kreienkamp et al., 2016).

According to actual estimates, approximately 12% of the world's arable land is currently at risk of waterlogging, and this is being exacerbated by unfavorable soil conditions (e.g., high clay content) and/or poor management systems (e.g., soil compaction and poor drainage) (Najeeb et al., 2015; Ploschuk et al., 2018; Alifu et al., 2022). Also, in Europe, the problem of waterlogging has long since arrived, with prolonged phases of heavy rainfall in winter and early spring, being more the rule than the exception (Deumlich and Gericke, 2020).

For Germany, it is undisputed that so-called heavy rainfall events have occurred more frequently over the past 15 years, at least regionally (Winterrath et al., 2017). This, in turn, has a vast effect on the agricultural sector, causing high yield losses of the major crops (e.g., Ploschuk et al., 2018).

Waterlogging induces several physiological changes in crops and thus affects various aspects of plant metabolism and growth (Horchani et al., 2009). These changes are primarily a response to a reduced availability of oxygen in the soil. Waterlogging as such is defined as the saturation of soil with water beyond its holding capacity (Striker, 2012). As a result, gaseous exchange with the atmosphere is inhibited, and gas diffusion in the soil is impeded (Jackson and Ricard, 2003), further driven as remaining oxygen is consumed by microbial activity. This lack of oxygen together with an increase in CO_2 leads to anoxic soils (Ponnamperuma, 1972) and, consequently, results in severe hypoxia/anoxia within plant roots (Armstrong, 1980). This leads to root damage and decay, and also oxygen-depleted roots immediately shift from aerobic respiration to low ATP-yielding fermentation (Gibbs and Greenway, 2003). As a consequence, plants subsequently respond with stomata closure, which in turn reduces transpiration, a driver for water uptake and translocation. As an inevitable result, also nutrient uptake and translocation are restricted (Jackson and Drew, 1984; Colmer and Voesenek, 2009; McDonald, 2021), which may be further exacerbated by a shift of redox potential toward more reducing conditions. Together with the hampered gas exchange at the stomata and thus CO_2 uptake, also photosynthesis is reduced, which in combination with restricted nutrient uptake leads to a marked decrease in plant biomass production and yield (Ashraf, 2012; Shao et al., 2013; Voesenek and Sasidharan, 2013; Arguello et al., 2016).

Depending on plant species, physiological tolerance, timing, and duration of the waterlogging event, yield losses can largely vary (Setter and Waters, 2003; de San Celedonio et al., 2014; Arduini et al., 2016; Ploschuk et al., 2018). Notably, high-yielding crops such as wheat or rapeseed are more susceptible to waterlogging in later developmental stages (Araki et al., 2012; Wollmer et al., 2018a, b; Hussain et al., 2022, 2023). According to Pampana et al. (2016), the yield of durum wheat was not affected when waterlogging occurs at the three- to four-leaf stage, which is also in line with de San Celedonio et al. (2014), who reported that wheat and barley are more sensitive at anthesis compared to tillering. This contradicts the results of Wu et al. (2015) and Ghobadi and Ghobadi (2010), who found that wheat was more prone to waterlogging when stressed at the seedling stage compared to later growth stages. However, there is a great consensus that the longer the waterlogging event persists, the greater the yield loss (Ghobadi and Ghobadi, 2010; Zhang et al., 2016; Tian et al., 2020).

Oats (*Avena sativa* L.) are among the food crops that rank sixth regarding cereal production right after wheat, maize, rice, barley, and sorghum (Ruja et al., 2021). Although being displaced by higher-yielding energy and protein crops in the past (Hoffman, 1995), today, oats are experiencing a revival as "super food" owing to their nutritional composition, and their production is gaining popularity again. Oats are well known for their versatility, thus tolerating a wide range of climatic conditions (Welsh, 1995; Ruja et al., 2021). However, while yield performance under waterlogging of the major crops has been well documented, studies on the response of oats to waterlogging are still scarce. However, there are indications that oats show a higher agronomic tolerance; i.e., they have the capability to maintain yields despite facing waterlogging during their growth cycle (Arduini et al., 2019). Watson et al. (1976) and Cannell et al. (1985) suggested that the better recovery potential of oats may be due to their capability to stay green during waterlogging and higher tiller fertility at maturity (Setter and Waters, 2003).

Based on these early findings and a lack of information, this study aims to investigate whether oats can be used as an alternative crop, especially under the changing climatic conditions present in Northern Germany. To gain further knowledge about possible cultivar variations, three oat varieties, namely, black oats, white oats, and yellow oats, were compared to facilitate cultivar choice on waterlogging-affected sites. Thus, it is hypothesized that 1) oats growth performance is less affected by waterlogging at later compared to earlier growth stages, 2) different oat varieties show no differences in growth performance and yield formation upon waterlogging, and 3) waterlogging-induced nutrient deficiencies are not yield-effective in oats.

2 Materials and methods

2.1 Plant cultivation and SPAD measurements

The experiment was conducted in the outdoor area of the Experimental Station of the Institute of Plant Nutrition and Soil Science, Kiel University, Germany (54°20′50″N, 10°6′55″E) starting in March 2021. Three oat (*A. sativa* L.) varieties (obtained from Saaten Union, Niedersachsen, Germany), Zorro (black oat; *A. sativa* var. *nigra*), Symphony (white oat; *A. sativa* var. *alba*), and Apollon (yellow oat; *A. sativa* var. *aurea*), were grown to maturity in large-scale containers (height, 0.9 m; area, 0.16 m^2; volume, 120 L; see also Hohmann et al., 2016) with a seeding density of 300 seeds per

container, which were later thinned to 90 plants after emergence. As a substrate, a subsoil (Cambisol; IUSS Working Group WRB, 2015) from the experimental station "Hohenschulen" of Kiel University, Germany, and arable topsoil from the district of Ost-Holstein (Schleswig-Holstein, Germany) were selected (see details in Table 1).

The containers were filled with air-dried and homogenized soil as follows (from bottom to top): 1) 20 kg gravel as a drainage layer, 2) 100 kg subsoil + sand (1:1, w/w), 3) 30 kg subsoil + topsoil (1:1, w/w), 4) 10 kg topsoil plus fertilizer according to standard application for oats [in kg/ha: 100 N (split into N1 prior to seeding and N2 at shooting stage), 55 P, 80 K]. Weed and pathogen control were applied as required.

Soil plant analysis development (SPAD) values were measured on the fifth leaf after waterlogging at BBCH 31 and on the flag leaf after stress treatment at BBCH 51 (Meier, 2001). An average of 10 readings per container was taken using a chlorophyll meter (SPAD-502, Konica Minolta Sensing Europe B.V., Wrocław, Poland).

2.2 Stress treatments

Soil moisture was maintained at 60% water-holding capacity (WHC) until treatments started. While the respective controls (W0) were watered at 60% WHC throughout the entire crop cycle, waterlogging (100% WHC) was imposed for a total of two consecutive weeks: 1) W1 = early waterlogging at BBCH 31 and 2) W2 = late waterlogging at BBCH 51. Water treatment was checked every 2 days, and re-irrigation was performed based on weight loss if necessary. After terminating waterlogging, water was drained to achieve a target WHC of 60%, which was then retained until harvest. The experiment was set up with four replicates per treatment and oat variety in a completely randomized design (CRD). Randomization of the position of containers was performed twice a week together with the check of WHC.

2.3 Plant sampling and analysis

Two weeks after terminating waterlogging (W1 and W2), 30 plants (including side shoots) were randomly selected and harvested, and fresh weights were recorded. At maturity, the 30 remaining plants (including side shoots) per container were harvested and separated into straw and panicles. Subsequently, the biomass of straw and panicles, grain yield, and yield parameters were quantified. Panicles per container were counted and hand-threshed to determine total grain and thousand kernel weight. The number of grains per panicle was calculated as follows (Equation 1):

$$Grains\ per\ panicle = \frac{Total\ grain\ weight \div thousand\ kernel\ weight \times 1,000}{Panicles\ per\ container} \quad (1)$$

To record dry weights, samples of each treatment were oven-dried at 60°C to constant weight and subsequently milled (Cyclotec 1093, Foss Tecator, Höganäs, Sweden) to fine powder for further analysis.

For mineral nutrient analysis, 200 mg of finely ground plant material of each plant part per replicate was digested with 10 mL 69% HNO_3 in a microwave oven (1800 W, MARS 6, Xpress, CEM, Matthews, MC, USA) at 190°C for 45 min and subsequently analyzed by inductively coupled plasma–mass spectrometry (ICP-MS; Agilent Technologies 7700 Series, Böblingen, Germany) according to the method described by Jezek et al. (2015).

Determination of total N was conducted using a CNS elemental analyzer (Flash EA 1112 NCS, Thermo Fisher Scientific, Waltham, MA, USA), for which 5–10 mg of finely ground plant material was weighed into tin capsules. Results were validated using a certified wheat flour standard (Isotopenstandard Weizenmehl, IVA Analysentechnik, Meerbusch, Germany) as a reference.

TABLE 1 Physico-chemical properties of the soils.

	Subsoil[a]	Topsoil[b]
Soil type	sL	lS
pH ($CaCl_2$)	5.5	6.1
Total N (g/kg soil)	<0.3	n.a.
Phosphorus (mg/100 g soil)	5.0	5.0
Potassium (mg/100 g soil)	4.0	7.9
Magnesium (mg/100 g soil)	8.1	5.1

[a]According to analysis by Institut Koldingen GmbH, Germany.
[b]According to analysis by AGROLAB Agrar und Umwelt GmbH, Germany.
n.a., not applicable.

2.4 Statistical analysis

Data were statistically analyzed using SPSS software (version 25.0). The analysis was based on four replicate containers per treatment set up as CRD. The effects of treatments per cultivar were tested using one-way ANOVA according to Duncan's (homogeneity of variance) or Games–Howell (heterogeneity of variance) multiple-range tests at $p \leq 0.05$. Significant differences are indicated by different letters. The significance of the correlations was tested using two-tailed Pearson's correlation coefficient at $p \leq 1\%$.

3 Results

3.1 Fresh weights and SPAD values

After 14 days of waterlogging at BBCH 31 (W1), all oat varieties clearly showed stunted growth and beginning chlorosis at older leaves (see Supplementary Figure 1). All oat varieties were similarly affected and showed a significant reduction in fresh weight of 58%, 57%, and 53% for black, white, and yellow oats, respectively (Figure 1A). Except in white oats, dry weight was not significantly reduced compared to the corresponding non-stressed control (data not shown).

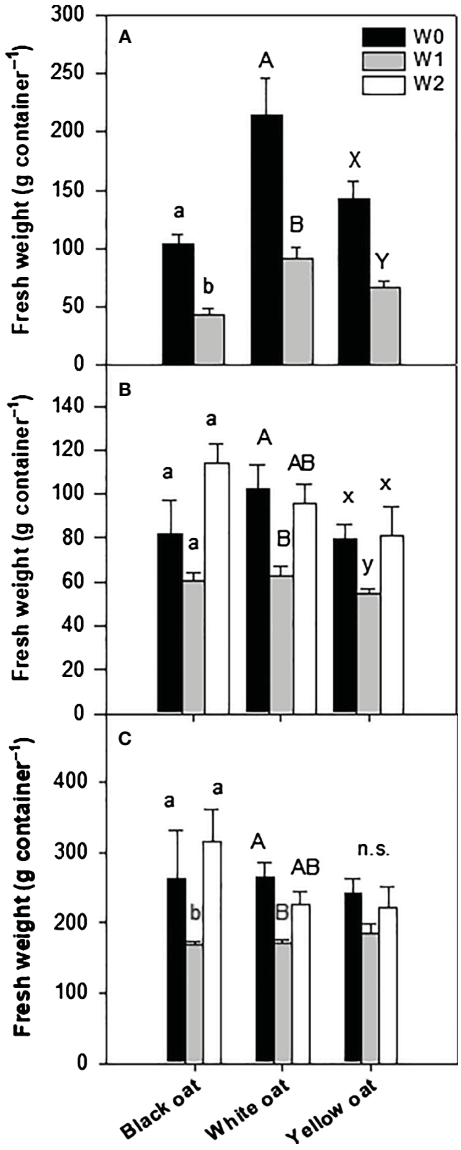

FIGURE 1
Fresh weight of the whole aboveground plant material after 14 days of waterlogging **(A)** at BBCH 31 and **(B)** at BBCH 51, as well as **(C)** at harvest after maturity. Bars represent means + standard errors (n = 4). Different letters refer to significant differences (p = 0.05; n.s., non-significant) between waterlogging treatments always within one oat variety. W0, control; W1, waterlogging at BBCH 31; W2, waterlogging at BBCH 51.

At the second sampling date, 1 week after the late waterlogging event (W2), differences in the recovery potential between varieties became obvious (Figure 1B). While black oats were able to recover from early waterlogging, white and yellow oats still showed significantly impaired growth 6 weeks after water drainage. Interestingly, late waterlogging at BBCH 51 had no negative effect on the total fresh weight of all oat varieties and could maintain weights similar to the corresponding control (Figure 1B).

These results were largely confirmed at the final harvest (Figure 1C). While the recovery of white oats after the early waterlogging was not confirmed till maturity, fresh weight increased to the level of control for black and yellow oats (Figure 1C). However, the fresh weight of all oat varieties remained unaffected by late waterlogging.

SPAD values were measured always right after the termination of the waterlogging treatment. Significant differences were monitored between control plants and plants waterlogged at BBCH 31 for all three oat varieties (Figure 2A; Supplementary Figure 2). This waterlogging-induced decline in SPAD values was even more pronounced after stress treatment at BBCH 51 for white and yellow oats when compared to early waterlogging and control, while SPAD values in black oats remained unaffected by late waterlogging (Figure 2B; Supplementary Figure 3).

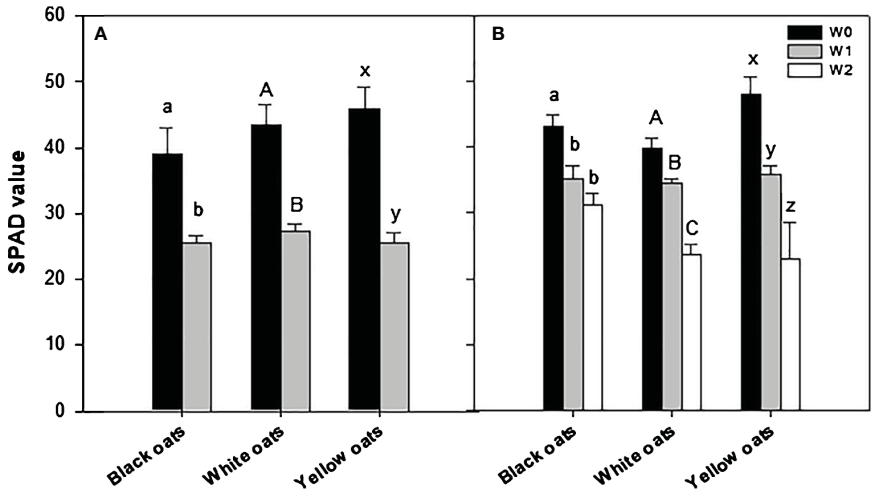

FIGURE 2
SPAD values after waterlogging **(A)** at BBCH 31 and **(B)** at BBCH 51. Bars represent means + standard errors (n = 4). Different letters refer to significant differences (p = 0.05) between waterlogging treatments always within one oat variety. W0, control; W1, waterlogging at BBCH 31; W2, waterlogging at BBCH 51; SPAD, soil plant analysis development.

3.2 Yield and yield parameters

Whether the fresh weight was now broken down into the individual main major yield components, differences between oat varieties became obvious. While the number of panicles of black oats showed a slight but non-significant reduction at W1 and W2, white and yellow oats showed a significant reduction (Figure 3A). Concerning the number of grains per panicle, in black and white oats, W1 had a negative effect, leading to a reduced number of grains, while yellow oats were not influenced (Figure 3B). However, after W2, white oats compensated for the reduced number of panicles with the number of grains per panicle on the level of the control. Similarly, also, black and yellow oats significantly increased the number of grains after late waterlogging compared to W1 and remained on the level of their respective control (Figure 3B). Contrary to this, thousand kernel weight was not responsive at all to W1 and W2 in either black or white oats, while it was on a relatively high level in yellow oats compared to the other two varieties, but with a reduction after W2 (Figure 3C). This in turn led to an unchanged grain yield under W1 for both black and white oats, while under W2, there was even an increase in grain yield for both varieties (Figure 3D). However, yellow oats were the only variety that reacted sensitively to early waterlogging but could regain grain yield at least on the level of the control after late waterlogging (Figure 3D). Although differences in the major yield parameters were recognizable, the harvest index and the grain:straw ratio were unresponsive to both timings of waterlogging (data not shown).

Correlating yield with the single yield parameters showed that there was no correlation between yield and the number of panicles per container and thousand kernel weight for all three oat varieties, with all coefficients of determination being non-significant (Supplementary Figures 3A–C, G–I). However, yield significantly correlated to the number of grains per panicle at least for black oats (R^2 = 0.735; Supplementary Figure 3D) and white oats (R^2 = 0.779; Supplementary Figure 3E). Only yellow oats lacked such a correlation between yield and number of grains (R^2 = 0.118, Supplementary Figure 3F).

3.3 Nutrient concentration in plant tissues

Early waterlogging (W1) resulted in a reduction of nitrogen (N) concentration in all three oat varieties. Hereby, the decrease was the highest in white oats (55%) followed by yellow oats (44%), and the lowest was in black oats (36%) (Figure 4A). Similarly to N, all oat varieties showed a strong decline in phosphorus (P) concentration, with white oats being most responsive compared to yellow oats and black oats (Figure 4B). Additionally, also S showed a marked decrease after early waterlogging (data not shown).

After late waterlogging, all oat varieties were able to recover, showing a N concentration similar to their respective control (Figure 5A). Furthermore, no effect of W2 on shoot N concentration could be determined. Similarly, the P status could be restored to the control level (black oats) or even increased (white oats and yellow oats) till BBCH 51 (Figure 5B). However, similar to early waterlogging, W2 led to a significant decrease in P in all three oat varieties (Figure 5B).

At the timepoint of maturity, all plants were harvested, and nutrient concentrations in straw and grains were determined. With respect to straw N, it was observed that both black oats and white oats showed no changes in N concentration (Figure 6A). Only in yellow oats was a significant difference between W1 and W2 measurable, whereas no significant difference between W2 and the respective control was obvious. Likewise, also in grains of black and white oats, no effect of either W1 or W2 could be detected on N concentration (Figure 6B). However, yellow oats showed an increase in N at maturity when waterlogged at BBCH 51.

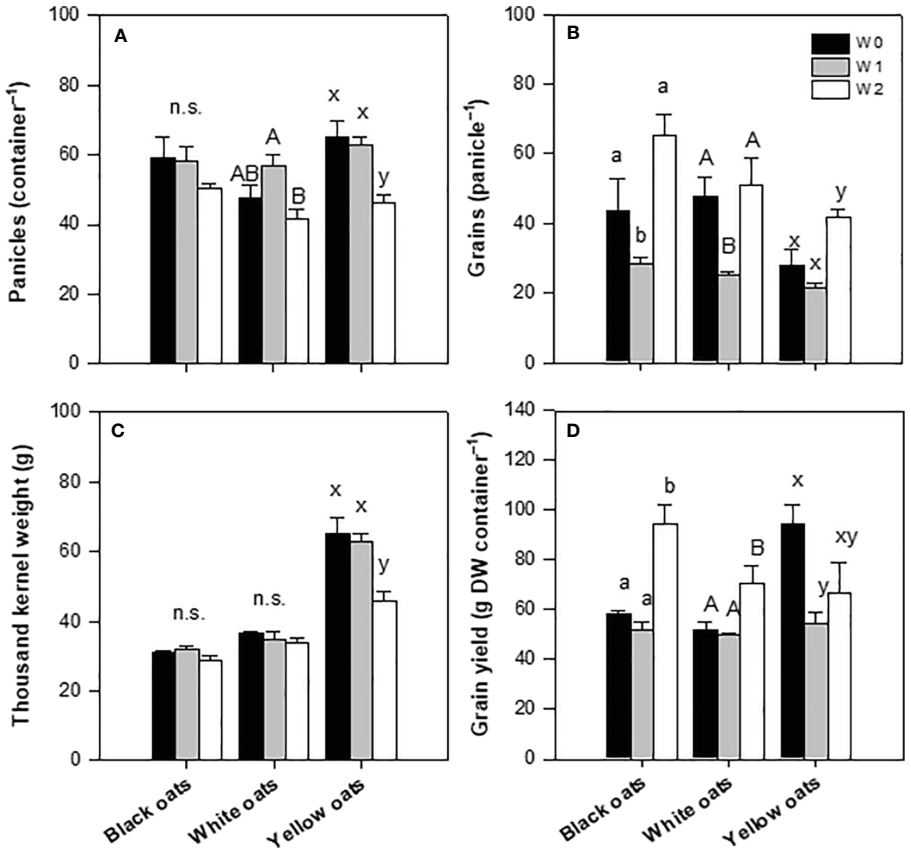

FIGURE 3
Yield components after harvest at maturity. **(A)** Number of panicles. **(B)** Grains per panicle. **(C)** Thousand kernel weight. **(D)** Grain yield. Bars represent means + standard errors (n = 4). Different letters refer to significant differences (p = 0.05; n.s. = non-significant) between waterlogging treatments within one oat variety. W0, control; W1, waterlogging at BBCH 31; W2, waterlogging at BBCH 51.

A similar pattern was measured for P concentration. Black oats were unable to regenerate the straw P level at W2, while in white and yellow oats, P concentration increased to the level of the well-drained control (Figure 6C). However, in grains of black and yellow oats, no waterlogging effect was measured (Figure 6D), but a significant increase in P in white oats at W1 and W2.

Furthermore, N and P concentrations in total shoot biomass as well as in grain at harvest were not effective on grain yield, with all coefficients of the determination being non-significant (Supplementary Figure 4).

4 Discussion

Globally, anthropogenic climate change intensified the risk of waterlogging, having multifaceted and severe impacts on economic and political pathways (IPCC, 2022), but also on crop production as such (Yang et al., 2017; Kaur et al., 2020b). Excess soil water has reduced rice, maize, soybean, and wheat yields by up to 50% annually (Hossain and Uddin, 2011; Ploschuk et al., 2018; Borgomeo et al., 2020; Ding et al., 2020; Tian et al., 2021). In Europe, according to actual estimates, flood-related risks and thus waterlogging will increase with a mean increment in annual output losses of approximately 11 million € per 1.5°C increase in global warming level (GWL) (Koks et al., 2019). However, are there any options to counteract such losses?

Identifying and breeding crop species being tolerant to waterlogging, in addition to other agronomical tools, can help mitigate the negative impact on crop physiology and improve overall agricultural resilience, especially in the long term (Kaur et al., 2020b). To date, many studies have focused on the major high-yielding energy and protein crops, such as wheat, oilseed rape, or maize. However, less is known about whether there are alternative crops that can be included in crop rotations and thus increase crop diversity when there is a risk of temporal waterlogging, which otherwise will delay farm operations (e.g., planting, fertilization, and harvest). Oats may represent one such alternative; that is why this study was conducted to evaluate the response of three different oat varieties to temporal waterlogging at two important developmental stages: shooting and panicle emergence. In order to simulate field-like conditions and to overcome limitations such as root growth restriction, which ultimately will affect nutrient uptake, large containers were chosen.

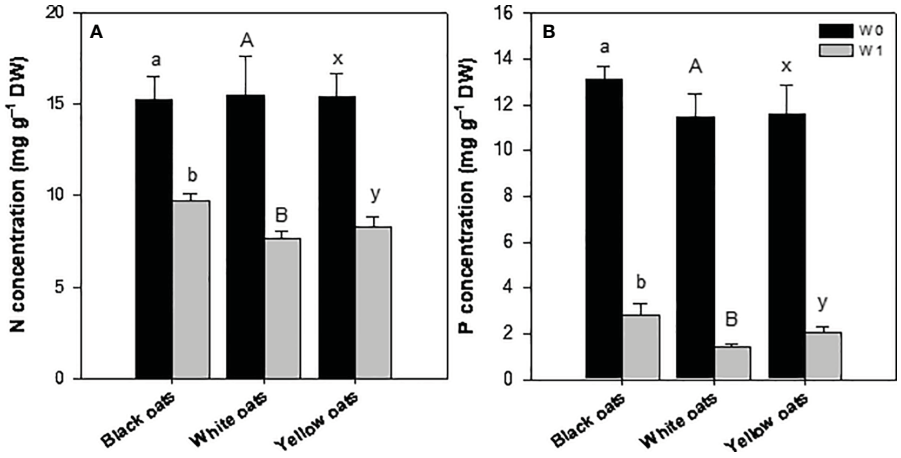

FIGURE 4
(A) Nitrogen and **(B)** phosphorus concentration of the whole aboveground plant material after 14 days of waterlogging at BBCH 31. Bars represent means + standard errors (n = 4). Different letters refer to significant differences (p = 0.05; n.s., non-significant) between waterlogging treatments within one oat variety. W0, control; W1, waterlogging at BBCH 31.

4.1 Growth performance and nutrient status of oats under temporal waterlogging

Waterlogged plants usually show wilting and development of chlorosis especially of the older basal leaves (Arbona et al., 2008). Also, Wollmer et al. (2018a) reported chlorosis formation on older leaves and even spot necrosis in winter wheat, which they explain as the oxidation of cell membranes by reactive oxygen species (ROS) formation and their reduced detoxification under waterlogging (Tan et al., 2008). Generally, chlorophyll reduction can be accredited to oxygen deficiency-induced changes in plant metabolism, promoting overproduction of ROS, mainly H_2O_2, and thus photooxidative damage of chloroplast (Yordanova et al., 2004; Zhang et al., 2015; Ren et al., 2016; Hasanuzzaman et al., 2017). As a consequence, photosynthesis will be decreased and thus biomass production (Zeng et al., 2020; Pais et al., 2023). However, even though SPAD measurements confirmed a decrease in chlorophyll in this study after early waterlogging (Figure 2), all tested oat varieties showed no distinct chlorosis but slightly brighter color compared to non-stressed plants (see Supplementary Figure 1). This is in contrast to wheat or barley, as oats have the capability to become less chlorotic and stay green even under waterlogged conditions, which gives an advantage to tolerate transient water stress (Setter and Waters, 2003). However, even though reduced biomass production under waterlogging is associated with lower photosynthetic activity (Ashraf, 2012), it is more likely a consequence of disturbed water and mineral uptake, rather than a photosynthesis effect (Colmer and Greenway, 2010; de San Celedonio et al., 2017).

As other crops (e.g., de San Celedonio et al., 2014; Ploschuk et al., 2018; Arduini et al., 2019; Hussain et al., 2022), oats also

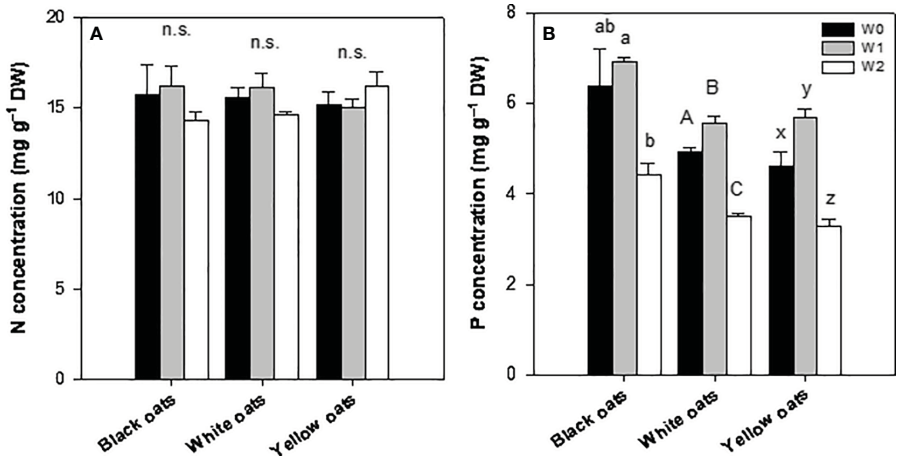

FIGURE 5
(A) Nitrogen and **(B)** phosphorus concentration of the whole aboveground plant material after 14 days of waterlogging at BBCH 51. Bars represent means + standard errors (n = 4). Different letters refer to significant differences (p = 0.05; n.s., non-significant) between waterlogging treatments within one oat variety. W0, control; W1, waterlogging at BBCH 31; W2, waterlogging at BBCH 51.

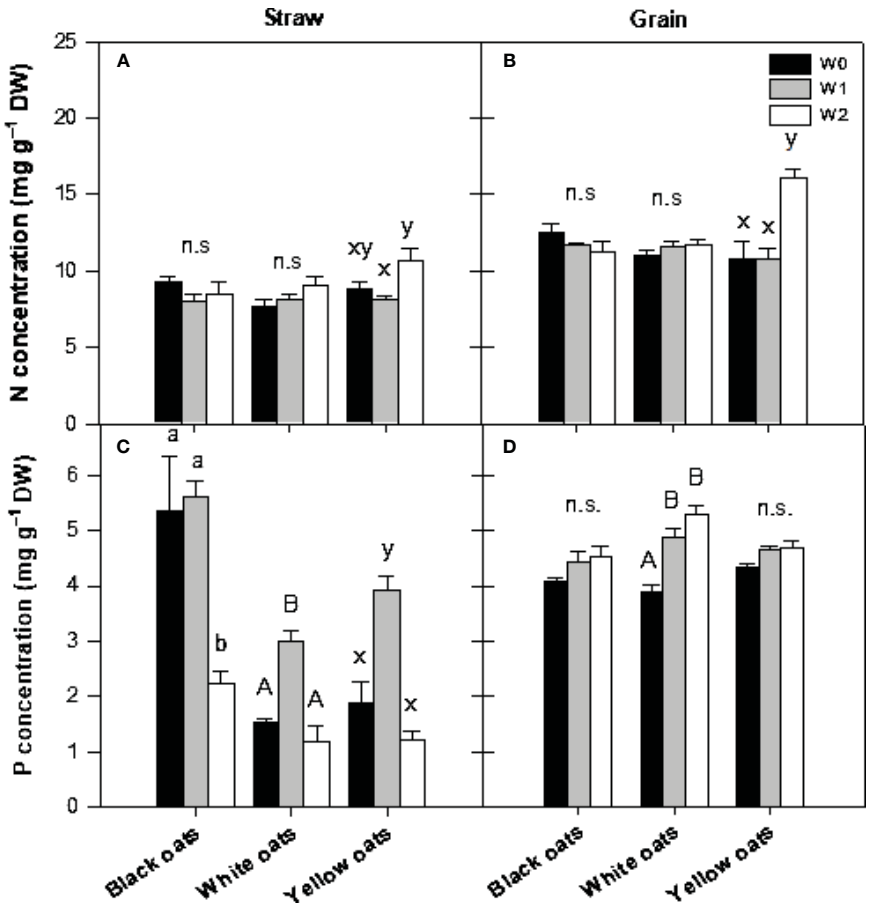

FIGURE 6
(A, B) Nitrogen and **(C, D)** phosphorus concentration in straw **(A, C)** and grains **(B, D)** after harvest at maturity. Bars represent means + standard errors (n = 4). Different letters refer to significant differences (p = 0.05; n.s., non-significant) between waterlogging treatments within one oat variety. W0, control; W1, waterlogging at BBCH 31; W2, waterlogging at BBCH 51.

respond with an initial reduction in shoot growth especially when waterlogged in an early developmental phase (Figure 1A; Supplementary Figure 1). In agreement with Watson et al. (1976), growth reduction in oats under waterlogging was more pronounced when applied in an early growth stage and must be ascribed to a reduced or damaged root system. Notably, a loss in seminal roots and death of seminal root apical meristem were described, e.g., wheat (see Herzog et al., 2016). Ploschuk et al. (2023) also showed that root mass density was significantly reduced after early waterlogging in wheat, barley, oilseed rape, and pea, triggered by a lack of oxygen and the formation of ethylene. Likewise, also in oats, an initial decrease in shoot dry weight of 40% was explained by a decline in root dry weight of 50% (Watson et al., 1976; Cannell et al., 1985).

Hampered root growth is always accompanied by a decline in nutrient uptake, subsequently contributing to growth reduction. This effect is further triggered by a drop of redox potential and changes in pH in soil, also affecting nutrient transformation and availability, i.e., N and P (Patrick and Mahapatra, 1968; Hasanuzzaman et al., 2017, and literature within; Kaur et al., 2020b, and literature within). Such an effect is also shown in this study: nitrogen concentration dropped in W1 plants in all oat varieties (Figure 4A), corresponding to SPAD data (Figure 2), indicating a transient undersupply in the shooting stage. These results are in agreement with Arduini et al. (2019) for oats, Ren et al. (2017) for maize, Zhou et al. (1997) for oilseed rape, and Wollmer et al. (2018a) for wheat. In soil, nitrogen concentration, i.e., nitrate, will be decreased by several processes under waterlogging, such as runoff, denitrification, or nitrate leaching (see Kaur et al., 2020b, and literature within). However, decreasing nutrient concentrations in the vegetative shoot tissues can be explained not only by reduced root growth but also by inhibited uptake mechanisms. As plants switch to anaerobic respiration, they lack ATP, a necessity to drive ion uptake and xylem loading mediated by H^+-ATPases (Colmer and Greenway, 2010; Elzenga and van Veen, 2010). Such decline in N concentration was not prominent in W2 plants (Figure 5A), which is attributed to the N fertilization (see Section 2.1) performed right after drainage of W1. This N dose served as a "post-waterlogging rescue N fertilizer" (Watson et al., 1976; Rasaei et al., 2012; Kaur et al., 2020a), leading to a regeneration of N status, which could be maintained until maturity in both straw and grain (Figure 6A). However, among all temperate cereals, oats must be considered as the crop with the greatest ability to regenerate from waterlogging (Watson et al., 1976; Cannell et al., 1985; Solaiman

et al., 2007). Setter and Waters (2003) suggested that this is due to an extensive formation of aerenchyma, which coincides with increased root porosity (Herzog et al., 2016). Also, Solaiman et al. (2007) described an increase in root porosity from 6% (well drained) to approximately 20% (waterlogged) in adventitious roots of oats compared to 2% in seminal roots. By this, O_2 in roots is kept high, allowing the roots to maintain aerobic respiration and high ATP levels and thus improve nutrient uptake characteristics (Colmer and Greenway, 2010; Takahashi et al., 2014).

As the redox potential drops, the solubility of P increases due to a loss of sorption sites. This in turn leads to a higher pore water concentration (Patrick and Mahapatra, 1968) and thus plant availability and uptake. However, like N concentration, P concentration also declined at W1 (Figure 4B), indicating a period of deficiency. As this was not expected, it must be reasoned that 1) P either leached down (Smith, 2020; Rupngam et al., 2023), 2) P retention in soil was increased due to sorption and/or precipitation with free Fe (Patrick and Mahapatra, 1968; Smith, 2020; Rupngam et al., 2023), or 3) uptake is inhibited, as the limited internal energy under waterlogging is directed to internal pH regulations and transport of solutes involved in anaerobic respiration (Greenway and Gibbs, 2003). This effect was reversed at W2 for all oat varieties (Figure 5B), indicating a full regeneration of the P status in W1 plants, which can be ascribed to an increased uptake due to higher available P and uptake in submerged soils. However, submergence at W2 again led to an undersupply of P in all three oat varieties. However, these were only of a transient nature in white and yellow oats (Figure 6C). Even though it seems that the time span till maturity was not enough for full recovery in black oats, a dilution effect must be assumed, as P content was on the level of control for all waterlogging treatments in all oat varieties (data not shown), though grains were not affected at all by all waterlogging events (Figure 6D). This is in line with Cannell et al. (1985), who also found no differences in N and P concentrations at harvest between treatments.

4.2 Yield response of oats under early and late waterlogging

Although much research was conducted on various crops, such as wheat (e.g., de San Celedonio et al., 2017; Ploschuk et al., 2018; Wollmer et al., 2018a; Pais et al., 2023), oilseed rape (e.g., Wollmer et al., 2019; Hussain et al., 2023; Zhu et al., 2023), barley (e.g., Masoni et al., 2016; de San Celedonio et al., 2017), or maize (e.g., Tian et al., 2019; Liang et al., 2020), there are hardly any data available on oats' response to waterlogging, especially regarding cultivar differences, the existence of flooding-related quantitative trait loci (QTLs), or -omics data on waterlogging and associated O_2 deprivation (Mustroph, 2018).

While yield decreases in a range of a few percent up to an almost total loss are reported, a meta-study by Tian et al. (2021) revealed that approximately 3% of all database samples showed contrasting behavior, thus increasing yield. One explanation for this phenomenon is the capability of such crop varieties to tolerate time periods of waterlogging. Thereby, it plays a crucial role in which developmental stage waterlogging occurs and for how long crops are submerged. In this study, it was found that oats, for the most part, are characterized by a high tolerance to both early and late waterlogging. While the grain yield of black and white oats was unaffected by early waterlogging and even increased after late waterlogging (Figure 3D), only yellow oats were sensitive to early waterlogging. However, the grain yield reduction of yellow oats after late waterlogging was only slightly but non-significantly reduced (Figure 3D). Such high recovery rates, at least as shown for black and white oats, are also consistent with the few published data for oats. For example, Watson et al. (1976) showed that when waterlogging ceased, oats recovered better than, e.g., wheat or barley. They reported that especially ear emergence was more delayed in these crops, which was even more pronounced at very early waterlogging (2 weeks after seeding) or when seeding was already delayed, shortening the recovery phase and leading to less grain per ear. In contrast, similarly to waterlogging at BBCH 51 in this study, waterlogging 6 weeks after seeding or at ear emergence was of minor effect, which was also confirmed for winter wheat (Watson et al., 1976; Cannell et al., 1985). Also, other studies, e.g., on wheat, report that early reproductive states are more adversely affected than tillering stages (Setter and Waters, 2003). However, this contradicts the results of Wollmer et al. (2018a), who showed the highest yield reduction of wheat after waterlogging in the generative phase.

In oats, the by far largest reduction in grain yield was observed when plants were waterlogged at the tillering stage, caused by the formation of smaller grains. This effect was almost completely eliminated, when N was applied (Watson et al., 1976). This is in agreement with this study, in which the grain yield of W1 and W2 plants was similar or even increased in the case of black and white oats (Figure 3). Only in yellow oats was the speed of grain yield recovery somewhat slower but could reach a value comparable to the control after W2. Similar results were found for winter oats (Cannell et al., 1985), where tillering was reduced but could be reversed by N application. Reductions in tillers though were not found in this study at W1, rather than an increase for white oats (data not shown), probably compensation grain yield reductions. Only white and yellow oats at W2 showed a reduced number of panicle-bearing tillers, but this was also reversed and did not affect grain yield due to compensation by a distinct increase in grain number per panicle in yellow oats (Figure 3). A reduction in kernel weight of 9% in oats, as reported by Cannell et al. (1985), could thereby only be confirmed in yellow oats (Figure 3), while the other two varieties did not show any change compared to the well-drained treatment. In comparison, under similar conditions, for wheat, a reduction of 10%–30% was reported (Cannell et al., 1985; Ploschuk et al., 2018), indicating the high recovery potential of the tested oat varieties in this study. However, the observed reduction is not caused by a reduced number of grains per panicle rather than the reduced number of panicles in total.

In complete contradiction to the already discussed studies are data by Arduini et al. (2019). Similar to this study, oats were waterlogged at tillering after seeding in spring, differently from Watson et al. (1976), who used winter oats. This difference has of

large effect on the regeneration period; while winter oats had a prolonged phase of 118 days after draining, the recovery phase in spring oats is much shorter. Therefore, Arduini et al. (2019) argued that higher temperatures of 20°C during waterlogging could in part be responsible for the higher sensitivity observed in their study. Although after 14 days of waterlogging a not yet significant decrease in harvest index became obvious, *A. sativa* compared to *Avena byzantina* showed a 79% and 83% reduction in grain yield, respectively, resulting in a decrease in harvest index of 8% and 10%, respectively, after 35 days of submergence (Arduini et al., 2019). Similarly, in the present study, the harvest index remained on the level of the respective controls for all three oat varieties (data not shown) at W1 and W2 after only 14 days of waterlogging, which may go back to an increased tiller fertility (Watson et al., 1976; Cannell et al., 1985).

5 Conclusions

Even though there are only limited data on oats' response to waterlogging, it is obvious from the literature that a high diversity exists among different varieties. Thus, this study contributes to the understanding of the stress tolerance of oats and offers a solution to rethink established crop rotations, especially in the context of climate change and the associated risk of flooding/waterlogging in the future.

The oat varieties tested in this study, i.e., black, white, and yellow oats, are standard cultivars recommended in Germany due to their stable yield potential. All varieties differed slightly in their response to waterlogging, but all showed an initial decrease in fresh weights when waterlogged in the vegetative phase. This growth reduction was most probably caused by a transient deficiency in nitrogen and phosphorus; however, N deficiency was counteracted by a second N-fertilizer dose right after ceasing the stress, guaranteeing a proper N supply till maturity. Further, also, the P status recovered, although the oat varieties differed in the regeneration time, which may be attributed to the restoration capacity of the root system. Although all varieties were differently affected regarding yield components, i.e., number of panicles, grains per panicle, or thousand kernel weight, all oat varieties showed grain yields comparable to well-drained soil conditions or even higher in case of black and white oats, independent from the timing of the waterlogging stress. However, early waterlogging in the vegetative phase (BBCH 31) was more harmful in contrast to late waterlogging in the generative phase (BBCH 51), but all varieties were able to compensate till maturity. Thus, it is reasoned that oats, or at least the varieties used in this study, showed a high tolerance level to temporal submergence, which was not affected by waterlogging-induced nutrient deficiency.

Therefore, we conclude that oats represent a suitable alternative and can compete with high-yielding but more sensitive crops, such as wheat, especially on marginal sites with lower yield potential and sites that are prone to waterlogging in Northern Germany.

Data availability statement

The original contributions presented in the study are included in the article/Supplementary Material. Further inquiries can be directed to the corresponding authors.

Author contributions

BP: Writing – original draft, Writing – review & editing, Conceptualization, Investigation. KM: Conceptualization, Writing – review & editing.

Funding

The author(s) declare that no financial support was received for the research, authorship, and/or publication of this article.

Acknowledgments

We acknowledge the kind provision of the three oat varieties by Saaten Union. We also thank M. Bach, B. Biegler, T. Heimbeck, and S. thor Straten for excellent technical assistance.

Conflict of interest

The authors declare that the research was conducted in the absence of any commercial or financial relationships that could be construed as a potential conflict of interest.

The author(s) declared that they were an editorial board member of Frontiers, at the time of submission. This had no impact on the peer review process and the final decision.

The reviewer AN declared a past co-authorship with the authors to the handling editor.

Publisher's note

Supplementary material

The Supplementary Material for this article can be found online at: https://www.frontiersin.org/articles/10.3389/fpls.2024.1386039/full#supplementary-material

References

Alifu, H., Hirabayashi, Y., Imada, Y., and Shiogama, H. (2022). Enhancement of river flooding due to global warming. *Sci. Rep.* 12, 20687. doi: 10.1038/s41598–022-25182–6

Araki, H., Hamada, A., Hossain, M. A., and Takahashi, T. (2012). Waterlogging at jointing and/or after anthesis in wheat induces early leaf senescence and impairs grain filling. *Field Crop Res.* 137, 27–36. doi: 10.1016/j.fcr.2012.09.006

Arbona, V., Hossain, Z., López-Climent, M. F., Pérez-Clemente, R. M., and Gómez-Cadenas, A. (2008). Antioxidant enzymatic activity is linked to waterlogging stress tolerance in citrus. *Physiol. Plant* 132, 452–466. doi: 10.1111/j.1399-3054.2007.01029.x

Arduini, I., Baldanzi, M., and Pampana, S. (2019). Reduced growth and nitrogen uptake during waterlogging at tillering permanently affect yield components in late sown oats. *Front. Plant Sci.* 10. doi: 10.3389/fpls.2019.01087

Arduini, I., Orlandi, C., Pampana, S., and Masoni, A. (2016). Waterlogging at tillering affects spike and spikelet formation in wheat. *J. Crop Past. Sci.* 67, 703–711. doi: 10.1071/CP15417

Arguello, M. N., Mason, R. E., Roberts, T. L., Subramanian, N., Acuña, A., Addison, C. K., et al. (2016). Performance of soft red winter wheat subjected to field soil waterlogging: Grain yield and yield components. *Field Crop Res.* 194, 57–64. doi: 10.1016/j.fcr.2016.04.040

Armstrong, W. (1980). "Aeration in higher plants," in *Advances in botanical research*. Ed. H. W. Woolhouse (Academic Press, New York, NY), 225–332.

Ashraf, M. A. (2012). Waterlogging stress in plants: A review. *Afr. J. Agric. Res.* 7, 1976–1981. doi: 10.5897/AJARX11.084

Borgomeo, E., Khan, H. F., Heino, M., Zaveri, E., Kummu, M., Brown, C., et al. (2020). Impact of green water anomalies on global rainfed crop yields. *Environ. Res. Lett.* 15, 124030. doi: 10.1088/1748-9326/abc587

Cannell, R. Q., Belford, R. K., Blackwell, P. S., Govi, G., and Thomson, R. J. (1985). Effects of waterlogging on soil aeration and on root and shoot growth and yield of winter oats (*Avena sativa* L.). *Plant Soil* 85, 361–373. doi: 10.1007/BF02220191

Colmer, T. D., and Greenway, H. (2010). Ion transport in seminal and adventitious roots of cereals during O_2 deficiency. *J. Exp. Bot.* 62, 39–57. doi: 10.1093/jxb/erq271

Colmer, T. D., and Voesenek, L. A. C. J. (2009). Flooding tolerance: suites of plant traits in variable environments. *J. Funct. Biol.* 36, 665–681. doi: 10.1071/FP09144

de San Celedonio, R. P., Abeledo, L. G., Mantese, A. I., and Miralles, D. J. (2017). Differential root and shoot biomass recovery in wheat and barley with transient waterlogging during preflowering. *Plant Soil* 417, 481–498. doi: 10.1007/s11104-017-3274-1

de San Celedonio, R. P., Abeledo, L. G., and Miralles, D. J. (2014). Identifying the critical period for waterlogging on yield and its components in wheat and barley. *Plant Soil* 378, 265–277. doi: 10.1007/s11104-014-2028-6

Deumlich, D., and Gericke, A. (2020). Frequency trend analysis of heavy rainfall days for Germany. *Water* 12, 1950. doi: 10.3390/w12071950

Ding, J., Liang, P., Wu, P., Zhu, M., Li, C., Zhu, X., et al. (2020). Effects of waterlogging on grain yield and associated traits of historic wheat cultivars in the middle and lower reaches of the Yangtze River, China. *Field Crop Res.* 246, 107695. doi: 10.1016/j.fcr.2019.107695

Elzenga, J. T. M., and van Veen, H. (2010). "Waterlogging and plant nutrient uptake," in *Waterlogging signalling and tolerance in plants*. Eds. S. Mancuso and S. Shabala (Springer Berlin Heidelberg, Berlin, Heidelberg), 23–35.

Ghobadi, M. E., and Ghobadi, M. (2010). Effect of anoxia on root growth and grain yield of wheat cultivars. *Int. J. Agric. Eng.* 46, 729–732. doi: 10.5281/zenodo.1081583

Gibbs, J., and Greenway, H. (2003). Mechanisms of anoxia tolerance in plants. I. Growth, survival and anaerobic catabolism. *Funct. Plant Biol.* 30, 1–47. doi: 10.1071/PP98095

Greenway, H., and Gibbs, J. (2003). Mechanisms of anoxia tolerance in plants. II. Energy requirements for maintenance and energy distribution to essential processes. *Funct. Plant Biol.* 30, 999–1036. doi: 10.1071/PP98096

Hasanuzzaman, M., Al Mahmud, J., Nahar, K., Anee, T. I., Inafuku, M., Oku, H., et al. (2017). "Responses, adaptation, and ROS metabolism in plants exposed to waterlogging stress," in *Reactive oxygen species and antioxidant systems in plants: role and regulation under abiotic stress*. Eds. M. I. R. Khan and N. A. Khan (Springer Singapore, Singapore), 257–281.

Herzog, M., Striker, G. G., Colmer, T. D., and Pedersen, O. (2016). Mechanisms of waterlogging tolerance in wheat–A review of root and shoot physiology. *Plant Cell Environ.* 39, 1068–1086. doi: 10.1111/pce.12676

Hoffman, L. A. (1995). "World production and use of oats," in *The oat crop: production and utilization*. Ed. R. W. Welch (Springer Netherlands, Dordrecht), 34–61.

Hohmann, M., Stahl, A., Rudloff, J., Wittkop, B., and Snowdon,, R. J. (2016). Not a load of rubbish: Simulated field trials in large-scale containers. *Plant Cell Environ.* 39, 2064–73. doi: 10.1111/pce.12737

Horchani, F., Khayati, H., Raymond, P., Brouquisse, R., and Aschi-Smiti, S. (2009). Contrasted effects of prolonged root hypoxia on tomato root and fruit (*Solanum lycopersicum*) metabolism. *J. Agron. Crop Sci.* 195, 313–318. doi: 10.1111/j.1439-037X.2009.00363.x

Hossain, M. A., and Uddin, S. N. (2011). Mechanisms of waterlogging tolerance in wheat: Morphological and metabolic adaptations under hypoxia or anoxia. *Aust. J. Crop Sci.* 5, 1094–1101.

Hussain, M. A., Naeem, A., Pitann, B., and Mühling, K. H. (2023). High sulfur (S) supplementation imparts waterlogging tolerance to oilseed rape (*Brassica napus* L.) through upregulating s metabolism and antioxidant pathways. *J. Plant Growth Regul.* 42, 7591–7605. doi: 10.1007/s00344-023-11034-8

Hussain, M. A., Naeem, A., Sulieman, S., Pitann, B., and Mühling, K. H. (2022). Sulfur uptake and distribution, grain yield, and quality of hybrid and inbred winter wheat (*Triticum aestivum* L.) varieties under early and late waterlogging. *J. Plant Nutr. Soil Sci.* 185, 622–631. doi: 10.1002/jpln.202200149

IPCC. (2022). Climate Change 2022: Impacts, adaptation and vulnerability. Available online at: https://www.ipcc.ch/report/sixth-assessment-report-working-group-ii/.

IUSS Working Group WRB. (2015). World Reference Base for Soil Resources 2014, Update 2015. International Soil Classification System for Naming Soils and Creating Legends for Soil Maps. (Rome, Italy: FAO).

Jackson, M. B., and Drew, M. C. (1984). Effects of flooding on growth and metabolism of herbaceous plants. *Flooding Plant Growth* 47–128. doi: 10.1016/B978-0-12-424120-6.50008-0

Jackson, M. B., and Ricard, B. (2003). "Physiology, biochemistry and molecular biology of plant root systems subjected to flooding of the soil," in *Root ecology*. Eds. H. de Kroon and E. J. W. Visser (Springer Berlin Heidelberg, Berlin, Heidelberg), 193–213.

Jezek, M., Geilfus, C.-M., Bayer, A., and Mühling, K.-H. (2015). Photosynthetic capacity, nutrient status, and growth of maize (*Zea mays* L.) upon $MgSO_4$ leaf-application. *Front. Plant Sci.* 5. doi: 10.3389/fpls.2014.00781

Kaur, G., Nelson, K. A., Motavalli, P. P., and Singh, G. (2020a). Adaptation to early-season soil waterlogging using different nitrogen fertilizer practices and corn hybrids. *Agronomy* 10, 378. doi: 10.3390/agronomy10030378

Kaur, G., Singh, G., Motavalli, P. P., Nelson, K. A., Orlowski, J. M., and Golden, B. R. (2020b). Impacts and management strategies for crop production in waterlogged or flooded soils: A review. *Agron. J.* 112, 1475–1501. doi: 10.1002/agj2.20093

Koks, E. E., Thissen, M., Alfieri, L., De Moel, H., Feyen, L., Jongman, B., et al. (2019). The macroeconomic impacts of future river flooding in Europe. *Environ. Res. Lett.* 14, 084042. doi: 10.1088/1748-9326/ab3306

Kreienkamp, F., Deutschländer, T., Malitz, G., Rauthe, M., Becker, A., Früh, B., et al. (2016). *Starkniederschläge in deutschland* (Offenbach am Main, Germany: Deutscher Wetterdienst). Available at: https://www.dwd.de/DE/leistungen/klimareports/download_einleger_report_2016.pdf?:blob=publicationFile&v=1.

Liang, K., Tang, K., Fang, T., and Qiu, F. (2020). Waterlogging tolerance in maize: genetic and molecular basis. *Mol. Breed.* 40, 111. doi: 10.1007/s11032-020-01190-0

Masoni, A., Pampana, S., and Arduini, I. (2016). Barley response to waterlogging duration at tillering. *Crop Sci.* 56, 2722–2730. doi: 10.2135/cropsci2016.02.0106

McDonald, G. (2021). Waterlogging. Available online at: https://www.agric.wa.gov.au/waterlogging/waterlogging-%E2%80%93-science.

Meier, U. (2001). *Growth stages of mono-and dicotyledonous plants. BBCH Monograph* (Bonn, Germany: Federal Biological Research Centre for Agriculture and Forestry).

Mustroph, A. (2018). Improving flooding tolerance of crop plants. *Agronomy* 8, 160. doi: 10.3390/agronomy8090160

Najeeb, U., Bange, M. P., Tan, D. K. Y., and Atwell, B. J. (2015). Consequences of waterlogging in cotton and opportunities for mitigation of yield losses. *AoB Plants* 7, 80. doi: 10.1093/aobpla/plv080

Pais, I. P., Moreira, R., Semedo, J. N., Ramalho, J. C., Lidon, F. C., Coutinho, J., et al. (2023). Wheat crop under waterlogging: Potential soil and plant effects. *Plants* 12, 149. doi: 10.3390/plants12010149

Pampana, S., Masoni, A., and Arduini, I. (2016). Grain yield of durum wheat as affected by waterlogging at tillering. *Cereal Res. Commun.* 44, 706–716. doi: 10.1556/0806.44.2016.026

Patrick, W. H., and Mahapatra, I. C. (1968). Transformation and availability to rice of nitrogen and phosphorus in waterlogged soils. *Adv. Agron.* 20, 323–359. doi: 10.1016/S0065-2113(08)60860-3

Ploschuk, R. A., Miralles, D. J., Colmer, T. D., Ploschuk, E. L., and Striker, G. G. (2018). Waterlogging of winter crops at early and late stages: Impacts on leaf physiology, growth and yield. *Front. Plant Sci.* 9. doi: 10.3389/fpls.2018.01863

Ploschuk, R. A., Miralles, D. J., and Striker, G. G. (2023). Waterlogging tolerance of winter crops: Root mass density and canopy dynamics. *Agron. J.* 115, 2506–2520. doi: 10.1002/agj2.21403

Ponnamperuma, F. N. (1972). The chemistry of submerged soils. *Adv. Agron.* 24, 29–96. doi: 10.1016/S0065-2113(08)60633-1

Rasaei, A., Ghobadi, M.-E., Jalali-Honarmand, S., Ghobadi, M., and Saeidi, M. (2012). Waterlogging and its effects on nitrogen of soil and plant. *Ann. Biol. Res.* 3, 119–124.

Ren, B., Dong, S., Zhao, B., Liu, P., and Zhang, J. (2017). Responses of nitrogen metabolism, uptake and translocation of maize to waterlogging at different growth stages. *Front. Plant Sci.* 8. doi: 10.3389/fpls.2017.01216

Ren, B., Zhang, J., Dong, S., Liu, P., and Zhao, B. (2016). Effects of waterlogging on leaf mesophyll cell ultrastructure and photosynthetic characteristics of summer maize. *PloS One* 11, e0161424. doi: 10.1371/journal.pone.0161424

Ruja, A., Toma, I., Bulai, A., Agapie, A. L., Negrut, G., Suhai, K., et al. (2021). The impact of climate changes on production in the autumn and spring oats. *Life Sci. Sustain. Dev.* 2, 73–81. doi: 10.58509/lssd.v2i2.131

Rupngam, T., Messiga, A. J., and Karam, A. (2023). Phosphorus mobility in heavily manured and waterlogged soil cultivated with ryegrass (*Lolium multiflorum*). *Agronomy* 13, 2168. doi: 10.3390/agronomy13082168

Setter, T. L., and Waters, I. (2003). Review of prospects for germplasm improvement for waterlogging tolerance in wheat, barley and oats. *Plant Soil* 253, 1–34. doi: 10.1023/A:1024573305997

Shao, G. C., Lan, J. J., Yu, S. E., Liu, N., Guo, R. Q., and She, D. L. (2013). Photosynthesis and growth of winter wheat in response to waterlogging at different growth stages. *Photosynthetica* 51, 429–437. doi: 10.1007/s11099-013-0039-9

Smith, G. J. (2020). *The influence of anaerobic conditions and redox on phosphorus loss from waterlogged soils.* [Dissertation]. Lincoln University, Christchurch.

Solaiman, Z., Colmer, T., Loss, S., Thomson, B., and Siddique, K. (2007). Growth responses of cool-season grain legumes to transient waterlogging. *Aust. J. Agric. Res.* 58, 406–412. doi: 10.1071/AR06330

Striker, G. G. (2012). "Flooding stress on plants: Anatomical, morphological and physiological responses," in *Botany*. Ed. J. K. Mworia (London, UK: InTech), 3–28.

Takahashi, H., Yamauchi, T., Colmer, T. D., and Nakazono, M. (2014). "Aerenchyma formation in plants," in *Low-oxygen stress in plants: oxygen sensing and adaptive responses to hypoxia*. Eds. J. T. van Dongen and F. Licausi (Springer Vienna, Vienna), 247–265.

Tan, W., Liu, J., Dai, T., Jing, Q., Cao, W., and Jiang, D. (2008). Alterations in photosynthesis and antioxidant enzyme activity in winter wheat subjected to post-anthesis water-logging. *Photosynthetica* 46, 21–27. doi: 10.1007/s11099-008-0005-0

Tian, L., Bi, W., Liu, X., Sun, L., and Li, J. (2019). Effects of waterlogging stress on the physiological response and grain-filling characteristics of spring maize (*Zea mays* L.) under field conditions. *Acta Physiol. Plant* 41, 63. doi: 10.1007/s11738–019-2859–0

Tian, L.-X., Bi, W.-S., Ren, X.-S., Li, W.-L., Sun, L., and Li, J. (2020). Flooding has more adverse effects on the stem structure and yield of spring maize (*Zea mays* L.) than waterlogging in Northeast China. *Eur. J. Agron.* 117, 126054. doi: 10.1016/j.eja.2020.126054

Tian, L.-X., Zhang, Y.-C., Chen, P.-L., Zhang, F.-F., Li, J., Yan, F., et al. (2021). How does the waterlogging regime affect crop yield? A global meta-analysis. *Front. Plant Sci.* 12. doi: 10.3389/fpls.2021.634898

Voesenek, L. A. C. J., and Sasidharan, R. (2013). Ethylene – and oxygen signalling – drive plant survival during flooding. *Plant Biol.* 15, 426–435. doi: 10.1111/plb.12014

Watson, E., Lapins, P., and Barron, R. (1976). Effect of waterlogging on the growth, grain and straw yield of wheat, barley and oats. *Aust. J. Exp. Agric.* 16, 114–122. doi: 10.1071/EA9760114

Welsh, R. W. (1995). *The oat crop: production and utilization* (Berlin/Heidelberg, Germany: Springer Science). doi: 10.1007/978-94-011-0015-1

Winterrath, T., Brendel, C., Hafer, M., Junghänel, T., Klameth, A., Walawender, E., et al. (2017). *Erstellung einer radargestützten Niederschlagsklimatologie* (Offenbach am Main, Germany: DWD).

Wollmer, A.-C., Pitann, B., and Mühling, K.-H. (2018a). Nutrient deficiencies do not contribute to yield loss after waterlogging events in winter wheat (*Triticum aestivum*). *Ann. Apl. Bot.* 173, 141–153. doi: 10.1111/aab.12449

Wollmer, A.-C., Pitann, B., and Mühling, K. H. (2018b). Grain storage protein concentration and composition of winter wheat (*Triticum aestivum* L.) as affected by waterlogging events during stem elongation or ear emergence. *J. Cereal Sci.* 83, 9–15. doi: 10.1016/j.jcs.2018.07.007

Wollmer, A.-C., Pitann, B., and Mühling, K.-H. (2019). Timing of waterlogging is crucial for the development of micronutrient deficiencies or toxicities in winter wheat and rapeseed. *J. Plant Growth Regul.* 38, 824–830. doi: 10.1007/s00344-018-9893-9

Wu, X., Tang, Y., Li, C., Wu, C., and Huang, G. (2015). Chlorophyll fluorescence and Yield responses of winter wheat to waterlogging at different growth stages. *Plant Prod. Sci.* 18, 284–294. doi: 10.1626/pps.18.284

Yang, H., Zhai, S., Li, Y., Zhou, J., He, R., Liu, J., et al. (2017). Waterlogging reduction and wheat yield increase through long-term ditch-buried straw return in a rice—wheat rotation system. *Field Crop Res.* 209, 189–197. doi: 10.1016/j.fcr.2017.05.012

Yordanova, R. Y., Christov, K. N., and Popova, L. P. (2004). Antioxidative enzymes in barley plants subjected to soil flooding. *Environ. Exp. Bot.* 51, 93–101. doi: 10.1016/S0098-8472(03)00063-7

Zeng, R., Chen, L., Wang, X., Cao, J., Li, X., Xu, X., et al. (2020). Effect of waterlogging stress on dry matter accumulation, photosynthesis characteristics, yield, and yield components in three different ecotypes of peanut (*Arachis hypogaea* L.). *Agronomy* 10, 1244. doi: 10.3390/agronomy10091244

Zhang, Y., Chen, Y., Lu, H., Kong, X., Dai, J., Li, Z., et al. (2016). Growth, lint yield and changes in physiological attributes of cotton under temporal waterlogging. *Field Crop Res.* 194, 83–93. doi: 10.1016/j.fcr.2016.05.006

Zhang, Y., Song, X., Yang, G., Li, Z., Lu, H., Kong, X., et al. (2015). Physiological and molecular adjustment of cotton to waterlogging at peak-flowering in relation to growth and yield. *Field Crop Res.* 179, 164–172. doi: 10.1016/j.fcr.2015.05.001

Zhou, W., Zhao, D., and Lin, X. (1997). Effects of waterlogging on nitrogen accumulation and alleviation of waterlogging damage by application of nitrogen fertilizer and mixtalol in winter rape (*Brassica napus* L.). *J. Plant Growth Regul.* 16, 47–53. doi: 10.1007/PL00006974

Zhu, B., Yu, J., Shi, H., Yue, K., Lu, J., and Zhang, T. (2023). Effects of waterlogging stress on rapeseed yield, oil content, fatty acid composition, and transcriptome differences. *Plant Growth Regul.* 101, 769–779. doi: 10.1007/s10725-023-01055-4

frontiers | Frontiers in Plant Science

TYPE Original Research
PUBLISHED 08 July 2024
DOI 10.3389/fpls.2024.1385977

OPEN ACCESS

EDITED BY
Md Sazzad Hossain,
University of Kiel, Germany

REVIEWED BY
Hongmei Cai,
Huazhong Agricultural University, China
Guillaume Pilot,
Virginia Tech, United States

*CORRESPONDENCE
Shibin Gao
shibingao@163.com

†These authors have contributed equally to this work and share first authorship

RECEIVED 14 February 2024
ACCEPTED 17 June 2024
PUBLISHED 08 July 2024

CITATION
Luo B, Sahito JH, Zhang H, Zhao J, Yang G, Wang W, Guo J, Zhang S, Ma P, Nie Z, Zhang X, Liu D, Wu L, Gao D, Gao S, Su S, Gishkori ZGN and Gao S (2024) SPX family response to low phosphorus stress and the involvement of *ZmSPX1* in phosphorus homeostasis in maize. *Front. Plant Sci.* 15:1385977. doi: 10.3389/fpls.2024.1385977

SPX family response to low phosphorus stress and the involvement of *ZmSPX1* in phosphorus homeostasis in maize

Bowen Luo[1,2,3†], Javed Hussain Sahito[2,4†], Haiying Zhang[2,3†], Jin Zhao[2,3], Guohui Yang[2,3], Wei Wang[2,3], Jianyong Guo[2,3], Shuhao Zhang[2,3], Peng Ma[5], Zhi Nie[6], Xiao Zhang[2,3], Dan Liu[2,3], Ling Wu[2,3], Duojiang Gao[2,3], Shiqiang Gao[2,3], Shunzong Su[7], Zeeshan Ghulam Nabi Gishkori[8] and Shibin Gao[1,2,3*]

[1]State Key Laboratory of Crop Gene Exploration and Utilization in Southwest China, Chengdu, Sichuan, China, [2]Maize Research Institute, Sichuan Agricultural University, Chengdu, Sichuan, China, [3]Key Laboratory of Biology and Genetic Improvement of Maize in Southwest Region, Ministry of Agriculture, Chengdu, Sichuan, China, [4]National Key Laboratory of Wheat and Maize Crop Science, College of Agronomy, Henen Agricultural University, Zhengzhou, China, [5]Maize Research Institute, Mianyang Academy of Agricultural Sciences, Mianyang, Sichuan, China, [6]Sichuan Academy of Agricultural Sciences, Biotechnology and Nuclear Technology Research Institute, Chengdu, Sichuan, China, [7]College of Resources, Sichuan Agricultural University, Chengdu, Sichuan, China, [8]Institute of Biotechnology, College of Agriculture and Biotechnology, Zhejiang University, Hangzhou, China

Phosphorus (P) is a crucial macronutrient for plant growth and development, and low-Pi stress poses a significant limitation to maize production. While the role of the SPX domain in encoding proteins involved in phosphate (Pi) homeostasis and signaling transduction has been extensively studied in other model plants, the molecular and functional characteristics of the *SPX* gene family members in maize remain largely unexplored. In this study, we identified six *SPX* members, and the phylogenetic analysis of *ZmSPX*s revealed a close relationship with *SPX* genes in rice. The promoter regions of *ZmSPX*s were abundant in biotic and abiotic stress-related elements, particularly associated with various hormone signaling pathways, indicating potential intersections between Pi signaling and hormone signaling pathways. Additionally, *ZmSPX*s displayed tissue-specific expression patterns, with significant and differential induction in anthers and roots, and were localized to the nucleus and cytoplasm. The interaction between *ZmSPX*s and *ZmPHR*s was established via yeast two-hybrid assays. Furthermore, overexpression of *ZmSPX1* enhanced root sensitivity to Pi deficiency and high-Pi conditions in *Arabidopsis thaliana*. Phenotypic identification of the maize transgenic lines demonstrated the negative regulatory effect on the P concentration of stems and leaves as well as yield. Notably, polymorphic sites including 34 single-nucleotide polymorphisms (SNPs) and seven insertions/deletions (InDels) in *ZmSPX1* were significantly associated with 16 traits of low-Pi tolerance index. Furthermore, significant sites were classified into five haplotypes, and haplotype5 can enhance biomass production by promoting root development. Taken together, our results suggested that *ZmSPX* family members possibly play a pivotal role in Pi stress signaling in plants by interacting

with *ZmPHR*s. Significantly, *ZmSPX1* was involved in the Pi-deficiency response verified in transgenic *Arabidopsis* and can affect the Pi concentration of maize tissues and yield. This work lays the groundwork for deeper exploration of the maize *SPX* family and could inform the development of maize varieties with improved Pi efficiency.

KEYWORDS

maize, low-Pi stress, *SPX* gene family, *PHRS*, candidate gene association analysis

1 Introduction

Maize (*Zea mays* L.) stands as a pivotal crop globally, not only as a source of food and high-quality feed but also for industrial applications (Feng et al., 2022; Jiao et al., 2023). P is an essential macronutrient for plant growth and development and plays a vital role either directly or indirectly in many physiological and biochemical processes, such as photosynthesis, respiration, signal transduction, and metabolic processes (Luo et al., 2019). Plants primarily acquire P in the inorganic form of Pi from the soil to support their growth and yield (Kumar et al., 2019). The low availability of Pi in soils is a significant limiting factor for plant growth and yield, posing a significant challenge (Balyan et al., 2016). Consequently, the growing need for increased food production and higher crop yields is expected to lead to a rise in the demand for Pi inputs in cropland. The global application of Pi fertilizer on croplands has increased several times from 1961 to 2013 and already surpassed the estimated planetary boundary (Zou et al., 2022). Excessive fertilizer application has led to a myriad of environmental and ecological issues, including water eutrophication.

In response to low-Pi stress, plants have developed a series of adaptive mechanisms, primarily manifested through changes in root morphological structure, physiological and biochemical regulation, and the expression of Pi starvation-inducible genes. Specifically, under low-Pi stress, alterations in root morphology and configuration were characterized by the inhibition of primary roots, accompanied by an increase in the length and quantity of lateral roots and root hairs (Raghothama, 1999; Lynch, 2011). Additionally, the root radius decreases, resulting in a higher root–shoot ratio and a shallower root system. These morphological changes facilitate plants in expanding the contact area between roots and the superficial soil (Raghothama, 1999; Lynch, 2011; Luo et al., 2023). Furthermore, low-Pi stress triggers modifications in plant enzyme system activity, further contributing to the plant's adaptation to Pi scarcity. For example, Pi deficiency inhibits the activity of ATP synthase, which subsequently impacts ATP and NADPH production, thereby reducing the photosynthetic rate, carbon fixation, and overall plant growth (Carstensen et al., 2018; Garcia et al., 2023; Iqbal et al., 2023; Saengwilai et al., 2023). Enhancing the activities of sulfur lipid and glycolipid synthases, as well as phospholipid hydrolases, contributes to altering the composition of the lipid membrane. Moreover, low-Pi stress can elevate the activity of defense-related enzymes, enabling plants to better adapt to the low-Pi environment (Shimojima, 2011; Liang et al., 2014; Chen et al., 2015). Additionally, the increase in root exudates represents another strategy for plants to cope with low-Pi stress. This includes the secretion of protons, organic acids, and acid phosphatase, which serve to acidify the soil surrounding the roots and release inorganic Pi for plant uptake (Lynch et al., 2005; Shen et al., 2005; Zhang et al., 2010). When encountering Pi deficiency, plants also maintain Pi homeostasis through a series of molecular reactions. For instance, the phosphate starvation response (PSR) pathway involves a MYB transcription factor known as *PHR1*, which serves as a key regulator in PSR. It governs transcription and takes part in physiological and biochemical adaptations (Zhang et al., 2014). PHR1 is capable of directly binding to the *cis*-elements P1BS (PHR binding sequence, GNATATNC), which were found in the promoter regions of several PSR genes, including Phosphate 1 (*PHO1*), phosphate transporter traffic facilitator 1 (*PHF1*), phosphate transporters (PTs), induced by phosphate starvation (*IPS1*), miRNA399, and miRNA827 (Rubio et al., 2001; Puga et al., 2017). As Pi sensors, SPX proteins can interact with AtPHR1 or OsPHR2, and under normal conditions, they inhibit their transcriptional activity. This interaction between SPX proteins and PHR transcription factors serves to prevent the toxicity resulting from excessive Pi accumulation (Wang et al., 2014). Notably, the SPX proteins themselves do not directly sense Pi but instead sense soluble inositol polyphosphates (InsPs) with a high affinity (Wild et al., 2016). Recently, the crystal structure of the SPX domain revealed the basic surface for InsP6, and biochemical studies have shown that InsP7 stimulated the interaction between *OsSPX4* and *OsPHR2* with higher binding affinity than InsP6 (Jung et al., 2018). Among these, InsP8 acts as an intracellular Pi signaling substance, regulating Pi balance by modulating the interaction between *AtSPX1* and *AtPHR1* (Dong et al., 2019). Consequently, *SPX* genes play a crucial role in Pi signaling pathways and homeostasis in plants (Li et al., 2021).

The SPX proteins, namely, SYG1 (suppressor of yeast gpa1), Pho81 (CDK inhibitor in the yeast PHO pathway), and XPR1 (xenotropic and polytropic retrovirus receptor), can be classified

into four subfamilies based on the presence of structural characteristics: class 1 only contained SPX domain, and the other three have (SPX-MFS, SPX-EXS, and SPX-RING) domains (Chiou and Lin, 2011; Yang et al., 2017; Yue et al., 2017). Recently, two additional classes of SPX proteins, namely, SPX-SLC and SPX-VTC, had been characterized in algae, and they were involved in Pi synthesis and transportation in vacuoles. However, these classes appear to have been lost throughout the evolution of plants, with the type of Pi storage changing from polyphosphates in algae to Pi in the later-diverging *streptophytes* (Wang et al., 2021a). It seems that the SPX domain has some extra domains that may have been lost during the evolution of SPX proteins and have not been comprehensively identified yet (Kopriva and Chu, 2018; Nezamivand-Chegini et al., 2021). *SPX* gene family members have been studied for their significant roles in Pi signaling and homeostasis in various plant species, including four *SPX*s in *Arabidopsis thaliana* and six *SPX*s in rice (Secco et al., 2012). In *A. thaliana*, *AtSPX1* and *AtSPX3* played a positive role in plant adaptation to Pi starvation. Additionally, *AtSPX1* and *AtSPX3* demonstrated redundancy, and *AtSPX3* may negatively regulate the expression of *AtSPX1* (Duan et al., 2008). Moreover, under normal-Pi conditions, *AtSPX4* acted as a negative regulator of PSR gene expression in shoots, influencing both PHR1-dependent and PHR1-independent Pi starvation responses. Disruption of the *AtSPX4* function led to excessive Pi accumulation in the shoots (Osorio et al., 2019). In rice, *OsSPX3/5* negatively regulated the transport of Pi from roots to shoots. *OsSPX4* interacted with *OsPHR2* in the cytoplasm, inhibiting Pi signaling. Meanwhile, *OsSPX6* was upregulated under low-Pi stress, leading to the activation of *OsPHR2* (Lv et al., 2014; Zhong et al., 2018). Furthermore, OsSPX4 was involved in the regulation pathway of nitrogen and Pi signals, and ubiquitinated OsSPX4 facilitated the activation of Pi signaling by nitrate, coordinating the utilization of nitrogen and Pi (Hu et al., 2019). Moreover, *SPX* genes have been reported via bioinformatics analysis in diverse species (Yao et al., 2014b; Du et al., 2017; Kumar et al., 2019; Xiao et al., 2021) because of their possible involvement in a number of physiological and molecular processes. However, despite these advancements, the specific functions of these *SPX* gene family members have remained unknown in maize. In our previous study, SPX proteins carrying only the SPX domain were predicted under low-Pi conditions in maize (Nie et al., 2021). Therefore, in the present study, we conducted a bioinformatics analysis to investigate the relationship of SPX proteins containing only the SPX domain across various species. Additionally, we explored the expression patterns of these *SPX* genes in maize, examined their interaction with PHRs, and elucidated the function of *ZmSPX1* through transgenic experiments and candidate gene association analysis in maize.

Taken together, our findings suggested the involvement of *ZmSPX*s in transcription regulations during Pi starvation and found that *ZmSPX1* was involved in response to low-Pi conditions and provide a solid foundation for a deeper understanding of the molecular mechanism of genes and improving P use efficiency (PUE) in maize and will promote future studies on this important gene family in plants.

2 Materials and methods

2.1 Plant material and growth conditions

Using the CRISPR/Cas9 (Clustered regularly interspaced short palindromic repeats/CRISPR-associated protein 9) system, the *ZmSPX1* gene was knocked out in the maize inbred line KN5585 by the *Agrobacterium tumefaciens*-mediated transformation method. The mutation site was detected using ZmSPX1-KO-F and R primers (Supplementary Figure S1; Supplementary Table S1). The construction method for maize overexpressing lines utilizes the homologous recombination method to introduce the coding sequence (CDS) of the *ZmSPX1* gene into the vector pCAMBIA3301. Subsequently, *A. tumefaciens*-mediated transformation of the maize recipient line KN5585 was employed to generate transgenic plants. The results for the detection of overexpression and the specific primers used for detection are provided in Supplementary Figure S2 and Supplementary Table S1, respectively. Seeds of 178 (low-Pi tolerant maize inbred line), *A. thaliana* (Columbia), and tobacco (*Nicotiana benthamiana*) were provided by the Maize Research Institute of Sichuan Agricultural University. A relatively low-Pi field site in Wenjiang farm (WJ, Chengdu, Sichuan Province, plain region, available Pi 22.8 mg/kg) of Sichuan Agricultural University was selected for the experiments on low-Pi treatment of maize inbred line 178. Each plot received two levels of Pi treatments (low- and normal-Pi conditions), with each treatment replicated thrice. The plots measured 3 m in length with 0.8 m between rows. Prior to reaching the five-leaf stage, plant thinning reduced the number to 14 plants per plot (58,000 plants/ha). In the normal-Pi treatment plots, the following fertilizers (Stanley Agriculture Group Co., Ltd.) were applied: 150 kg of urea, 900 kg of calcium superphosphate, and 350 kg of potassium chloride per hectare before planting; 130 kg of urea per hectare at the six-leaf stage; and 210 kg of urea per hectare as a side dressing prior to tasseling. The low-Pi treatment plots received the same fertilizer combination as the normal-Pi plots, with the exception of the calcium superphosphate. The seeds of *A. thaliana* were planted in nutrient soil and soil sterilized at 121°C for 20 min and cooled for 30 min. Then, seeds were cultured in nutrient soil at 23°C for 12 h of light and darkness until the *A. thaliana* mature.

2.2 Bioinformatics identification of *ZmSPX*s in maize

Based on our previous research (Nie et al., 2021), *ZmSPX* homologous genes were identified with high similarity sequence: *ZmSPX1* (GRMZM2G035579), *ZmSPX2* (GRMZM2G171423), *ZmSPX3* (GRMZM2G024705), *ZmSPX4* (GRMZ2G122108), *ZmSPX5* (GRMZM5G828488), *ZmSPX6* (GRMZM2G065989), and *ZmSPX7* (GRMZM2G083655). The *ZmSPX* family members were identified in maize, and the reliability of the *ZmSPX* CDS was predicted using BioXM 2.6 software. The conserved domain of *ZmSPX*s was verified using the National Center for Biotechnology Information (NCBI) search database (Marchler-Bauer et al., 2015).

Amino acid sequences query homologous amino acid sequences of *SPX*s in maize, wheat, soybean, rape, rice, and *Arabidopsis* using the BLASTP program from the NCBI (http://www.ncbi.nlm.nih.gov); phylogenetic relationships were aligned using Mega (version 11.0.13) (Kumar et al., 1994). The gene IDs of the *SPX* gene family in other species were acquired from previous research studies (Secco et al., 2012; Yao et al., 2014b; Du et al., 2017; Kumar et al., 2019). Finally, *ZmSPX*s were studied for cloning and functional analyses based on protein comparison and transcriptome sequencing, respectively. The promoter region (2,000 bp) of *ZmSPX*s was utilized to predict the functional region of these genes using the BDGP online database (http://www.fruitfly.org/seq_tools/promoter.html) (Supplementary Table S2), and the *cis*-acting elements within the promoter were predicted using the plantCARE web server (http://bioinformatics.psb.ugent.be/webtools/plantcare/html).

2.3 Cloning of *ZmSPX* family members in maize

Total RNA was extracted from the leaves and roots of 178 inbred lines following the manufacturer's protocol of Thermo Fisher Scientific, Life Technologies (TRIzol Reagent®; the protocol can be found at https://www.thermofisher.com). The cDNA reverse transcription was performed using the PrimeScript™ II 1st Strand cDNA Synthesis Kit (Takara Bio Inc., Otsu, Japan). The CDS of *ZmSPX*s was then amplified using the cDNA as a template. The polymerase chain reaction (PCR) primers were designed based on the CDS of the B73 reference, targeting the specific sequences of the *ZmSPX* family members using Primer Premier 5 software. The forward and reverse primers are listed in Supplementary Table S3. The PCR was performed in a 25-μL volume containing phanta max buffer 12.5 μL (Phanta Max Super-Fidelity DNA Polymerase, Nanjing Vazyme Biotech Co., Ltd., Nanjing, China), phanta max super fidelity 0.5 μL, dNTP 4 μL, cDNA 1 μL, 1 μL of each forward and reverse primer, and 7 μL ddH_2O. PCR was programmed for 3 min at 95°C followed by 30 cycles of 95°C for 15 s, annealing for 15 s, 72°C for 45 s, extension for 5 min at 72°C, and final 12°C for preservation. Then, PCR products were separated using 1% agarose gel, purified using a DNA purification kit, and cloned into pEASY®-Blunt zero Cloning Vector (TransGen Biotech Co., Ltd., Beijing, China) according to the manufacturer's protocol. Finally, positive clones were selected for sequencing by TsingKe Biological Technology Co., Ltd. (Beijing, China). The coding sequence of *ZmSPX*s was compared with that of the B73 reference inbred line using DNAMAN v6.0 software.

2.4 Expression pattern of *ZmSPX* family members under Pi deficiency in different tissues

Different maize tissues were harvested in the silking stage from normal-Pi and low-Pi treatments. Total RNA was extracted from different maize tissues of 178 inbred lines including leaf, stem, anther, cornsilk, root, ear, and ear bract according to the TRIzol Reagent® (Invitrogen, Carlsbad, CA, USA) manufacturer's instructions, and reverse transcription was performed using PrimeScript™ II 1st Strand cDNA synthesis kit (Takara Bio Inc., Otsu, Japan). Relative quantitative results were calculated by normalization to the reference gene (GAPDH). At least three independent experiments were performed, and each experiment was performed in technical triplicate. All primers used in the qRT-PCR assay were designed in BEACON DESIGNER 7 and are listed in Supplementary Table S4. qRT-PCR data were analyzed using the $2^{-\Delta\Delta CT}$ method.

2.5 Subcellular localization of ZmSPX protein

The full-length CDS region was cloned into plant expression vector pCAMBIA2300 for the *ZmSPX*s. The homologous recombination primers with enzyme cutting sites (*Sma*I and *Xba*I) were designed by CEDesignV1.04 software and are shown in Supplementary Table S5. The subcellular localization was assayed in tobacco leaves according to the previously reported transit transformation method (Zhou et al., 2018; Sahito et al., 2020a, b). The transformed tobacco epidermal cells were observed using the A1R-si laser confocal microscope (LSCM, Nikon, Tokyo, Japan) to visualize the green fluorescent protein (GFP) fluorescent signals. The experiment was repeated at least three times to ensure consistency of results.

2.6 Yeast two-hybrid assays of ZmSPXs and ZmPHRs

The full-length CDSs of *ZmSPX* family members *ZmPHR1* (GRMZM2G006477) and *ZmPHR2* (GRMZM2G162409) were amplified using gene-specific primers from the cDNA samples. The primers were designed using CE design v1.04 and Primer 5.0 to incorporate (*Eco*R I, *Bam*H I, and *Nde* I) restriction sites, as specified in Supplementary Table S6. Phanta Max high-fidelity DNA polymerase (Nanjing Vazyme Biotech Co., Ltd.) was used to amplify the targeted fragments, and then the amplified fragments were inserted into bait (pGBKT7) and prey (pGADT7) vectors. All possible combinations were co-transferred into the Y2HGold yeast-competent cell. pGBKT7-53 and pGBKT7-lam were used as positive and negative controls, respectively. To exclude the possible autoactivation of *ZmSPX* members, a control experiment was carried out by transformation of loaded bait and prey plasmids with empty prey and bait plasmids, respectively. After screening on solid DDO (–Leu/–Trp) medium for 2–4 days at 28°C, selected monoclonals were inoculated in liquid DDO (–Leu/–Trp) medium until OD600 = 0.3–0.5. These cultures were inoculated on QDO (SD/–Ade/–His/–Trp/–Leu/X-α-Gal) medium after 10-fold dilution. Results were observed after 3–5 days of incubation at 30°C.

2.7 Overexpression of *ZmSPX1* in *A. thaliana*

Cloning of the full open reading frame (ORF) of *ZmSPX1* into the vector pCAMBIA3300-35s-PROII MCS-bar and subsequent transformation into wild-type (WT) *Arabidopsis* produced several transformants through the floral dip method previously described (Clough and Bent, 1998). The seeds of the T0 generation were harvested and sown in the soil to select positive transgenic seedlings. Two-week-old seedlings of T1 plants were screened by spraying with Basta (1/1,000) solution. After the transgenic plants were harvested, DNA was extracted, and PCR was performed to confirm the positive *ZmSPX1* transgenic lines.

2.8 Phenotypic characterization of *ZmSPX1* transgenic lines under low-Pi stress

The seeds of both WT and *ZmSPX1* transgenic lines were sterilized with 75% (v/v) ethanol for 60–90 s and 2% sodium hypochlorite for 8–15 min, followed by several rinses with distilled water. Fifty seeds of both WT and transgenic lines were cultured on 1/2 normal MS agar medium, initially kept at 4°C for 2 days, and subsequently transferred to a greenhouse with a light cycle of 16 hours at 22°C and a dark cycle of 8 hours at 18°C for 7 days. After 7 days, seedlings were transferred to 1/8 normal MS agar medium and subjected to different Pi concentrations: 0 mmol/L (control), low Pi (0.1 mmol/L), normal Pi (1 mmol/L), and high Pi (10 mmol/L). The seedlings were kept in a controlled environment for 2 weeks. Phenotypic observations under different Pi concentrations were recorded after 2 weeks, and their roots were scanned using a WinRHIZO root-scanning method. All *Arabidopsis* seedlings were dried and digested for the detection of P and nitrogen concentration through a chemical continuous flow analyzer.

2.9 Sequencing and association analysis of *ZmSPX1* in maize association population

A total of 211 out of 360 inbred lines were screened from the current Southwest China breeding program (Zhang et al., 2016). These lines were used for association analysis of *ZmSPX1* in maize. The genomic DNA was extracted from leaves at the seedling stage according to the cetyltrimethylammonium bromide (CTAB) method (Porebski et al., 1997). The genomic sequence of *ZmSPX1* from the B73 inbred line was utilized as the reference sequence and obtained from the Maize Genomic Database (http://www.maizegdb.org). The targeted fragment was amplified using high-fidelity phanta max enzyme polymerase (Vazyme Biotech Co., Ltd.). Amplified fragments were sequenced by TsingKe Biological Technology Co., Ltd. Then, the targeted sequence of *ZmSPX1* was compared with the reference genomic sequence of the B73 using DNAMAN v6.0 software, and the sequences of 211 maize inbred lines were trimmed neatly using Bio-Edit 7.1 software (Strable and Scanlon, 2009). Single-nucleotide polymorphisms (SNPs) and insertions/deletions (InDels) were identified in all tested inbred lines with a <0.05 minor allele frequency (MAF), and linkage disequilibrium (LD) between two polymorphic sites was generated using Tassel software v2.1 (Bradbury et al., 2007). Association analysis was carried out between SNPs and InDels and 22 phenotypic traits using Tassel software (Bradbury et al., 2007; Luo et al., 2019). The standard mixed linear model (MLM) including a population structure (Q) and kinship matrix (K) was chosen to detect the significant association of SNPs and InDels as described previously (Zhang et al., 2016; Luo et al., 2019). The association of sites was considered significant at $p < 0.05$, and the calculated p-values were converted into $-\log_{10}{}^{(p\ \text{value})}$.

3 Results

3.1 Evolutionary tree analysis of *SPX*s in plants

The *SPX* homologous genes *ZmSPX1* (GRMZM2G03557), *ZmSPX2* (GRMZM2G171423), *ZmSPX3* (GRMZM2G024705), *ZmSPX4* (GRMZM2G122108), *ZmSPX5* (GRMZM5G828488), *ZmSPX6* (GRMZM2G065989), and *ZmSPX7* (GRMZM2G0836555) were predicted in our previous study, and genes were located on different chromosomes (Supplementary Table S7). However, in the fourth edition of the maize genome, *ZmSPX1* and *ZmSPX7* were merged into a single gene. Additionally, preliminary transcriptome results indicated that *ZmSPX7* (GRMZM2G0836555) did not respond to low-Pi stress (Supplementary Table S7). Hence, in subsequent experiments, the ZmSPX1–6 in the third version of the maize genome were exclusively analyzed. Furthermore, *ZmSPX1*, *ZmSPX2*, *ZmSPX3*, *ZmSPX4*, *ZmSPX5*, and *ZmSPX6* were amplified in maize according to the targeted CDS by PCR. Specifically, the CDS length of *ZmSPX1* was 354 bp, encoding a protein comprising 117 amino acids. Correspondingly, *ZmSPX2*, *ZmSPX3*, *ZmSPX4*, *ZmSPX5*, and *ZmSPX6* have CDS lengths of 846 bp, 687 bp, 996 bp, 765 bp, and 759 bp, encoding proteins of 281, 228, 331, 254, and 252 amino acids, respectively. Simultaneously, *SPX* genes of wheat, soybean, rape, rice, and *Arabidopsis* were also searched for in the database (Secco et al., 2012; Yao et al., 2014b; Du et al., 2017; Kumar et al., 2019). Among them, *Arabidopsis* has four *SPX* genes (*AtSPX1–4*), rice has six *SPX* genes (*OsSPX1–6*), soybean has nine *SPX* genes (*GmSPX1–9*), and rape and wheat have 11 and 15 *SPX* genes, respectively (Supplementary Table S8). To deepen our understanding of the evolutionary relationships between these SPX proteins, a phylogenetic tree based on the SPX proteins in these plants was constructed (Figure 1). The six *SPX* genes of maize were distributed across different clades. Notably, *ZmSPX5* and *ZmSPX6* displayed the closest evolutionary relationship, clustering within the same clade but occupying distinct branch points (Figure 1). Interestingly, the closest evolutionary relationship existed between the *SPX* genes in maize and rice. Specifically, *ZmSPX5* and *OsSPX5*, *ZmSPX3* and *OsSPX3*, and *ZmSPX1* and *OsSPX1* were all located at the same branch point (Figure 1). Furthermore, while *ZmSPX4* and *OsSPX4* were positioned at different branch points on the evolutionary tree, they belonged to the same clade and were situated at adjacent branch points (Figure 1).

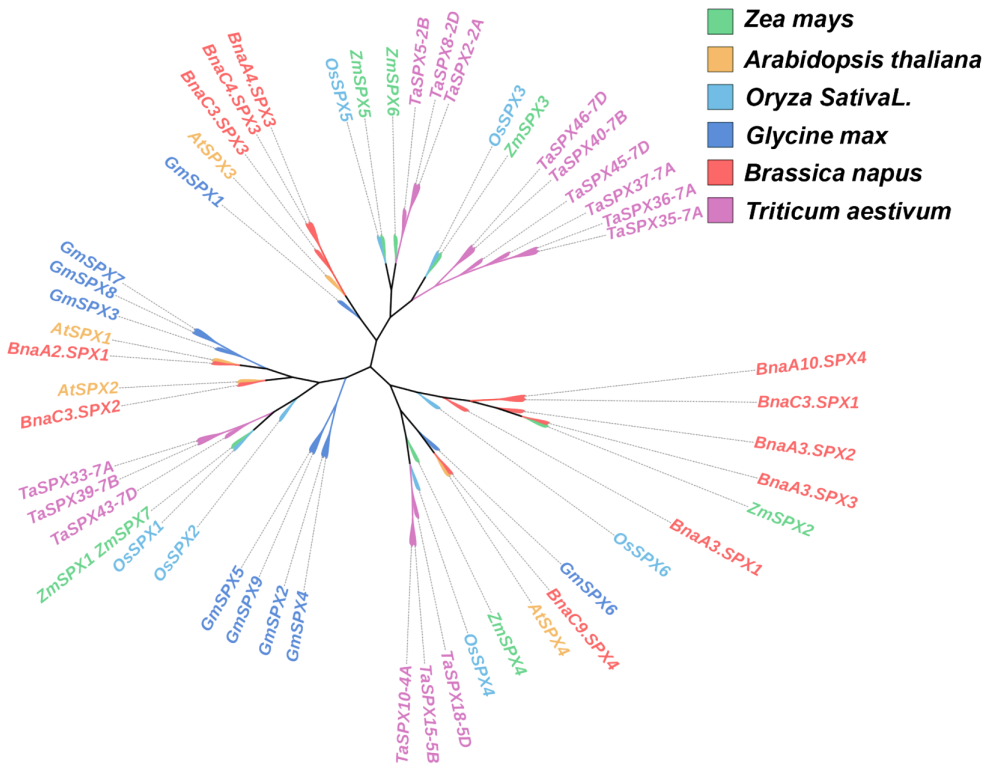

FIGURE 1
Phylogenetic tree of *SPX*s in plants. The phylogenetic tree was created in the Mega 11 program. In plants, proteins harboring the SPX domain are classified into four families based on the presence of additional domains in their structure, namely, the SPX, SPX-EXS, SPX-MFS, and SPX-RING families. The SPX proteins of this phylogenetic tree carry only the SPX domain.

Remarkably, *ZmSPX2* showed a close evolutionary relationship with *BnaA3SPX3* (Figure 1).

3.2 *cis*-Acting element analysis of promoter region of *ZmSPX*s

Generally, the results showed that *ZmSPX* gene family members were associated with abscisic acid response, light reaction, methyl jasmonate (MeJA) reaction, low-temperature response, auxin response, and regulation of zein metabolism *cis*-acting elements (Supplementary Table S9). Specifically, *ZmSPX* gene family members also possess unique *cis*-acting regulatory elements. For instance, *ZmSPX1* contains response elements for gibberellin and salicylic acid. The *ZmSPX2* gene responds to light and is also involved in defense and stress responses. *ZmSPX3* is involved in the light responsiveness. *ZmSPX4* contains a conserved DNA module (ATCT-motif) involved in photoreaction. *ZmSPX5* is involved in anaerobic induction. *ZmSPX6* contains DNA-binding protein binding sites and responds to light. It also contains MYB binding sites involved in the regulation of flavonoid biosynthesis genes. Previous studies have demonstrated that *SPX*s can interact with the MYB domain and the CC domain of PHRs (Jia et al., 2023). Additionally, our results also indicated that *ZmSPX* gene family members also contain MYB binding sites or MYB recognition sites (Supplementary Table S9). All of these findings suggested that *ZmSPX*s may play a role in the regulation of *ZmPHR*s in association with certain hormones.

3.3 Expression pattern of *ZmSPX*s under low- and normal-Pi conditions

Expression patterns of *ZmSPX*s were analyzed under low- and normal-Pi treatments in different tissues of 178 maize inbred lines, including ear leaf, stem, anther, cornsilk, root, ear, and ear bract (Figure 2). Notably, the *ZmSPX*s exhibited higher expression levels in anthers compared to other tissues but were significantly inhibited under low-Pi conditions. Meanwhile, *ZmSPX1–5* were induced by low-Pi stress in roots (Figure 2). Collectively, these results showed that the *ZmSPX* family members were involved in response to the low-Pi stress and play a specific function in different tissues of maize.

3.4 Subcellular localization of ZmSPX proteins

ZmSPX1, ZmSPX3, ZmSPX4, ZmSPX5, and ZmSPX6 were found to be localized in the nucleus and cytoplasm (Supplementary Figure S3). ZmSPX2 was mainly localized in the

10.3389/fpls.2024.1385977

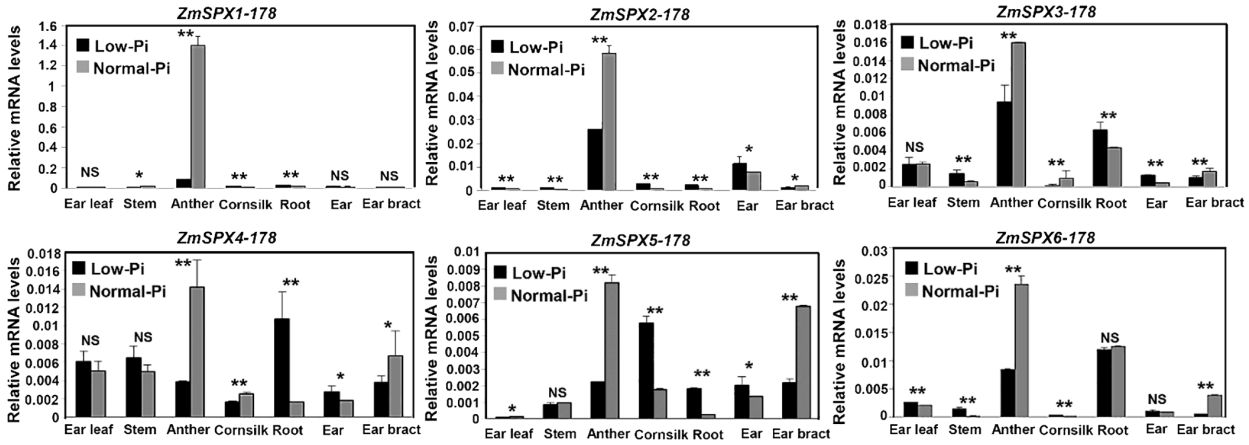

FIGURE 2
Expression pattern of ZmSPX family members in different tissues of 178 inbred lines under low- and normal-Pi conditions. Significant differences are indicated by Student's *t*-test: *$p < 0.05$, **$p < 0.01$. NS, No significance.

nucleus (Supplementary Figure S3). In a previous study (Xiao et al., 2021), subcellular localization studies of ZmSPXs in maize protoplasts revealed that ZmSPX1 (equivalent to ZmSPX5 in this study) and ZmSPX3 (equivalent to ZmSPX4 in this study) were localized in both the nucleus and cytoplasm. ZmSPX5 (equivalent to ZmSPX2 in this study) was exclusively localized in the nucleus. Moreover, ZmSPX4 (equivalent to ZmSPX6 in this study) and ZmSPX5 (equivalent to ZmSPX2 in this study) were detected in both the nucleus and cytoplasm, while ZmSPX6 (equivalent to ZmSPX1 in this study) was found in the chloroplast. The results showed partial consistency in the subcellular localization between tobacco tissue and maize protoplasts. However, some discrepancies were observed, presumably attributed to variations in cell types across different species.

3.5 Interaction between ZmSPXs and ZmPHRs in maize

In this study, a yeast two-hybrid assay was conducted to identify the interaction between ZmSPX and ZmPHR proteins. Initially, the self-activation of *ZmSPX* and *ZmPHR* genes was assessed. Our findings showed that *ZmPHR1* and *ZmPHR2* demonstrated normal growth on SD/−Ade/−His/−Trp-deficient medium, while the *ZmSPX*s transformed with yeast cells did not grow on the selective medium (Figure 3A), indicating that the *ZmSPX*s had no self-activation effect. Therefore, SPX protein was chosen as bait and PHR protein as prey to verify the interaction. Furthermore, protein interaction was examined in various combinations of ZmSPXs, ZmPHR1, and ZmPHR2. Results revealed that combinations such

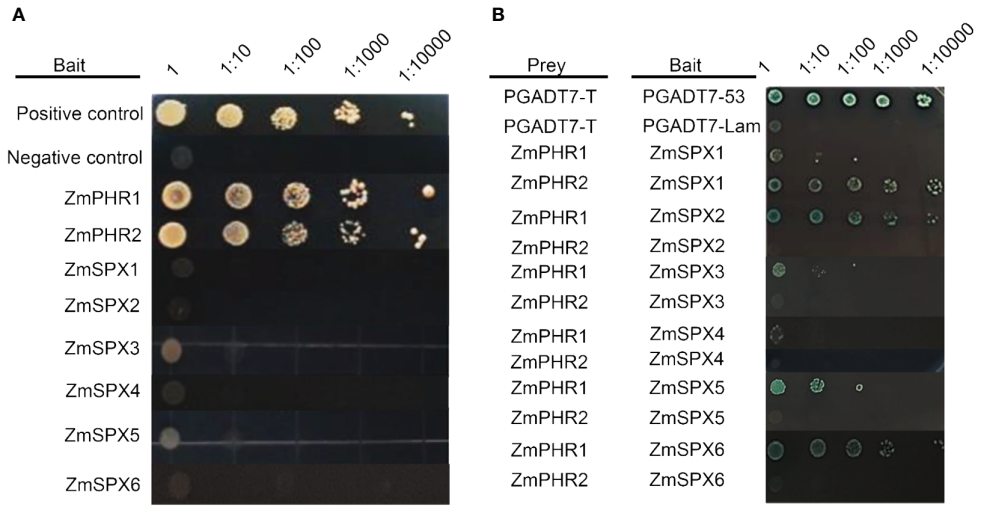

FIGURE 3
Yeast two-hybrid (Y2H) assay of ZmSPXs and ZmPHRs. **(A)** Self-activation analysis of ZmSPXs, ZmPHR1, and ZmPHR2. The medium is SD/−Leu-Trp-His-Ade (the medium lacking leucine, tryptophan, histidine, and adenine). **(B)** Y2H assay of ZmSPXs and ZmPHRs. PGADT7 and PGBKT7 vectors were used for positive and negative control, respectively. Yeast dilution ratio was 1, 1:10, 1:100, 1:1,000, and 1:10,000. The medium is SD/−Ade/−His/−Leu/−Trp/+X-α-Gal.

as ZmSPX1 and ZmPHR2, ZmSPX2 and ZmPHR1, ZmSPX3 and ZmPHR1, ZmSPX5 and ZmPHR1, and ZmSPX6 and ZmPHR1 all exhibited robust growth on SD/−Ade/−His/−Leu/−Trp/+X-α-gal medium, indicating their protein interactions (Figure 3B). It is suggested that *ZmSPX*s and *ZmPHR*s may modulate the maize response to low-Pi stress at the post-transcriptional level.

3.6 Overexpressing and knocking out *ZmSPX1* in maize revealed its correlation with Pi absorption and its effect on yield and yield-related traits

To investigate the function of *ZmSPX*s in response to low-Pi stress, overexpression lines of *ZmSPX*s were created in *Arabidopsis*. However, only the overexpression of *ZmSPX1* served to enhance root sensitivity to Pi deficiency and high-Pi conditions in *A. thaliana* (Supplementary Figures S4, S5). In order to further explore the function and role of *ZmSPX1*, we generated knockout and overexpressing maize transgenic lines for this gene. Our experimental results demonstrated a significant reduction in the hundred-grain weight and grain weight per year in the overexpressing lines compared to the wild type, while the knockout lines exhibited a marked increase (Figures 4A, B, D, E). Moreover, analysis of the P concentration in the grains of the knockout and overexpressing lines revealed no significant difference compared to the wild type (Figures 4C, F). We also assessed the P concentration in the internode, sheath, and leaf of the transgenic plants in the field trials. The findings indicated a higher P concentration in the knockout lines in these tissues than in the wild-type lines, whereas the overexpressing lines showed lower P concentrations compared to the wild-type lines (Figures 4G–I). These results suggested that *ZmSPX1* affected the P concentration in maize stems and leaves and exerted a certain impact on the yield of maize, but not on the grains.

3.7 Sequence variation and association analysis of *ZmSPX1*

To identify significant variations associated with phenotypic traits, we performed genome sequence amplification on 211 inbred lines and conducted multiple sequence alignments. We obtained a total of 1,390 bp of sequences, comprising 780 bp upstream of the initiation codon, 354 bp of the coding region, and 256 bp downstream of the initiation codon (Supplementary Table S10). We identified a total of 41 variants, which included 34 SNPs and seven InDels. The average distances between SNPs and InDels were 40.89 bp and 198.57 bp, respectively. The sequence variation frequencies varied across regions, with the highest frequency observed in the upstream sequence of the initiation codon (0.038) and the lowest in the coding region (0.006) (Supplementary Table S10). By utilizing a 200-bp sliding window with a 50-bp step size, we analyzed the nucleotide

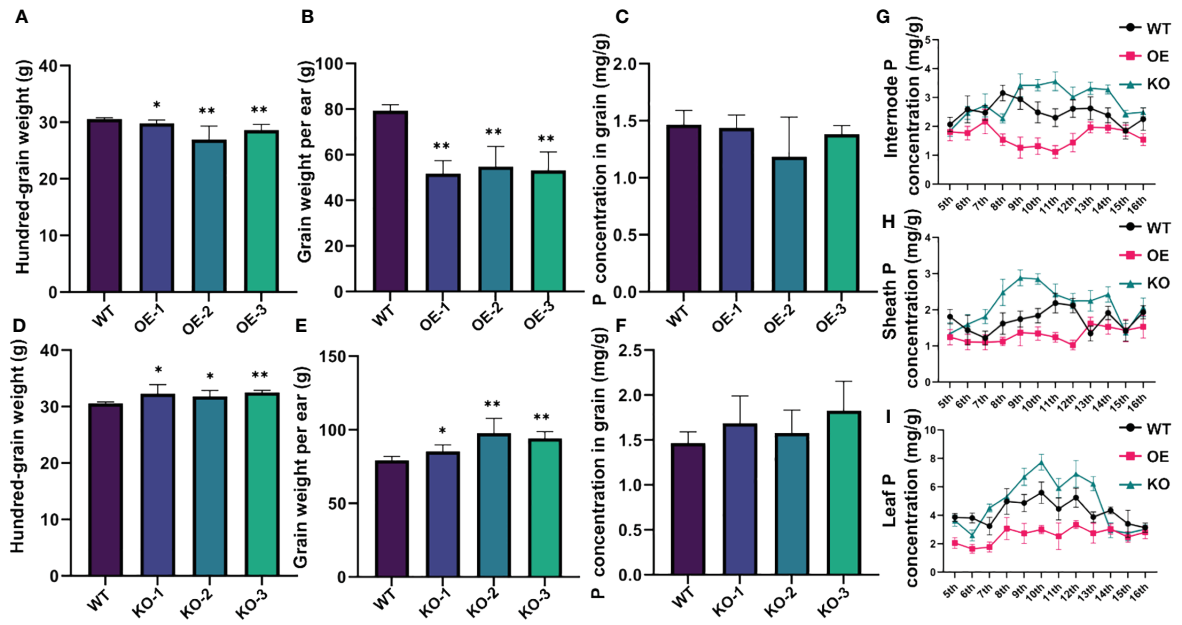

FIGURE 4
Phenotypic identification of *ZmSPX1* transgenic maize materials. **(A–C)** Statistical analysis of differences in hundred-grain weight, grain weight per ear, and P concentration in grain between *ZmSPX1* overexpressing lines and wild-type lines. **(D–F)** Statistical analysis of differences in hundred-grain weight, grain weight per ear, and P concentration in grain between *ZmSPX1* knockout lines and wild-type lines. **(G–I)** The internode P concentration, sheath P concentration, and leaf P concentration in *ZmSPX1* overexpressing lines, knockout lines, and wild-type lines. Significant differences are indicated by Student's *t*-test: **p* < 0.05, ***p* < 0.01.

10.3389/fpls.2024.1385977

diversity ($\pi \times 1{,}000$) of the *ZmSPX1*. We observed the overall nucleotide diversity to be 0.009, with the upstream sequence of the initiation codon exhibiting the highest diversity (0.013) among all regions and the coding region displaying the lowest diversity (0.002). Additionally, we investigated the selection pressure of *ZmSPX1* using Tajima's D, Fu and Li's D*, and F* tests (Supplementary Table S10). The results showed that the upstream sequences displayed positive values, indicating a mode of balanced selection in their sequence evolution, with both Tajima's D and Fu and Li's F* tests being significant (Supplementary Table S10). Conversely, the coding region and downstream showed negative values, suggesting that these regions have experienced either negative selection or population expansion (Supplementary Table S10).

Additionally, to further investigate the relationship between sequence variations of *ZmSPX1* and the phenotype in the maize seedling stage, we employed an MLM for candidate gene association analysis. We identified, under normal-Pi treatment, 37 markers (30 SNPs and seven InDels) as significantly associated with 17 traits, explaining 2.6% to 8.6% of the phenotypic variation (Supplementary Table S11). We found, under low-Pi treatment, a total of 10 markers to be significantly correlated with 13 traits, with R^2 ranging from 2.8% to 5.4% (Supplementary Table S12). Moreover, 37 markers were significantly correlated with 16 traits of low-Pi tolerance index, explaining 2.8% to 20.2% of the phenotypic variation (Figures 5A, B; Supplementary Table S13). As the low-Pi tolerance index integrated traits under low- and normal-Pi conditions, we utilized all sequence variant sites significantly associated with the low-Pi tolerance index for haplotype division. First, LD analysis revealed the presence of multiple LD blocks with high linkage relationships (Figure 5C). Then, we categorized all variant sites into five haplotypes (MAF > 0.05) and conducted comparisons among the different haplotypes (Figure 5D; Supplementary Table S14). The findings indicated that in the low-Pi tolerance index of root traits, the fresh weight of the crown root index of Hap5 was significantly higher than that of Hap1, Hap2, and Hap4, while the fresh weight of the seminal root index was higher than that of Hap3 and Hap1. Additionally, the root volume of Hap5 was significantly higher than that of Hap1. Furthermore, we observed that the dry weight of the whole plant index of Hap5 was significantly higher than that of other

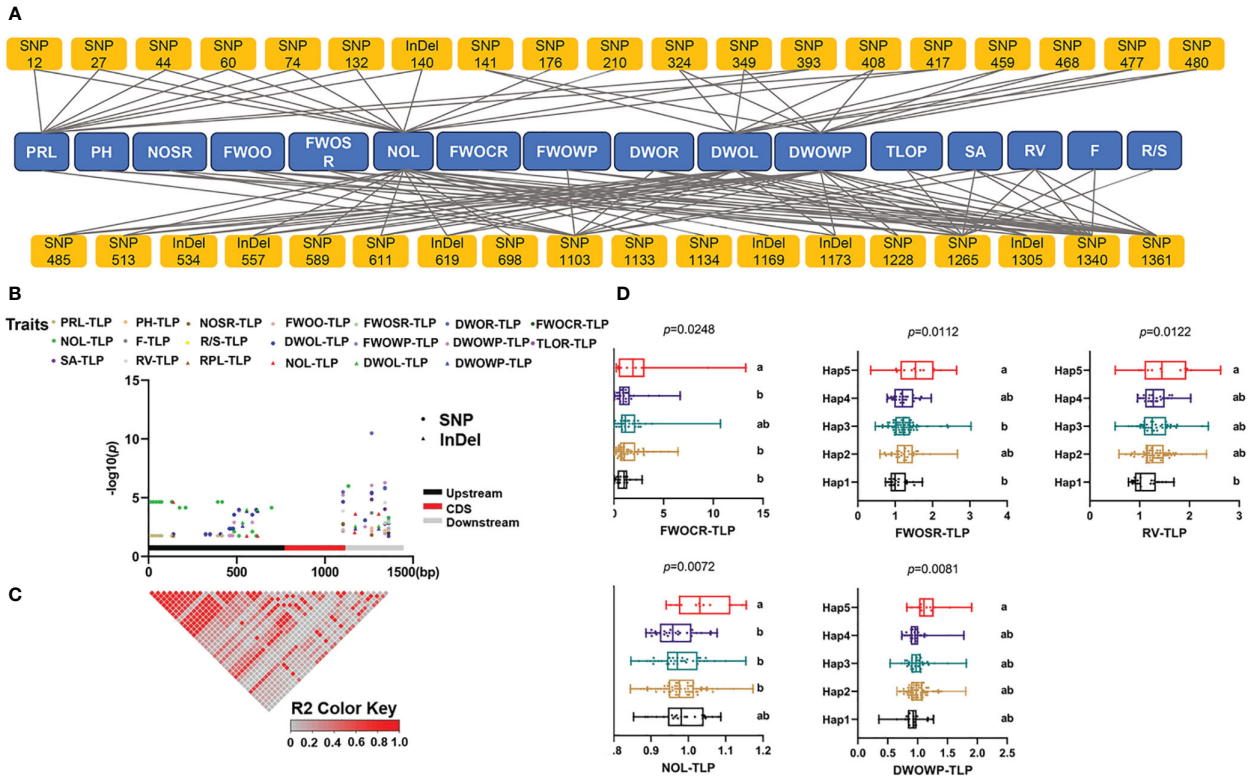

FIGURE 5
Candidate gene association analysis of *ZmSPX1* with traits of low-Pi tolerance index. **(A, B)** The results of the candidate gene association analysis. **(C)** Linkage disequilibrium (LD) heatmap of *ZmSPX1*. **(D)** Phenotypic difference between different haplotypes. The abbreviation for each trait: primary root length (PRL), plant height (PH), number of seminal roots (NOSR), fresh weight of overground (FWOO), fresh weight of seminal root (FWOSR), dry weight of root (DWOR), fresh weight of crown root (FWOCR), number of leaves (NOL), number of root forks **(F)**, root/shoot ratio (R/S), dry weight of leaves (DWOL), fresh weight of whole plant (FWOWP), dry weight of whole plant (DWOWP), total length of root (TLOR), root surface area (SA), and root volume (RV). TLP means the low-Pi tolerance index (Low-Pi/Normal-Pi). Means with the same letter in **(D)** are not significantly different at $p < 0.05$ according to one-way ANOVA followed by Tukey's multiple comparison test.

haplotypes. Based on these results, it can be inferred that Hap5 enhances biomass production by promoting root development.

4 Discussion

4.1 The maize transgenic lines of *ZmSPX1* exhibited significant impacts on P concentration and yield

Pi homeostasis is crucial for plant growth and development, with *ZmSPX1* playing a pivotal role in Pi uptake by plants from both the source and reservoir. Consequently, we first analyzed the phenotypes in *ZmSPX1* overexpression transgenic *A. thaliana* and WT under different Pi concentration treatments. Under both Pi deficiency and high-Pi conditions, we observed a more robust root system development in the WT plants, whereas the growth of the root system was inhibited in the overexpressing (OE) lines. These results indicated that overexpression of the *ZmSPX1* gene in *A. thaliana* enhanced the sensitivity of roots to both Pi deficiency and high-Pi conditions. Therefore, we proceeded to construct transgenetic lines for *ZmSPX1* in maize. The knockout *ZmSPX1* in maize led to an increase in P content in the stems and leaves. Additionally, a significant rise in hundred-grain weight and grain yield per ear was also observed in the knockout maize lines. Conversely, overexpression of *ZmSPX1* in maize demonstrated contrasting phenotypes. Studies in dicotyledonous model plants have demonstrated that *SPX*s, functioning as negative regulators, can impede the central regulator *PHR1* from acting on downstream low-Pi response genes (Jia et al., 2023). Conversely, research reports in monocotyledonous model plants such as *A. thaliana* and soybean suggest that *SPX*s serve as positive regulators. Overexpression of *SPX1* induced the expression of low-Pi response genes and thus increased plant P concentration (Duan et al., 2008; Yao et al., 2014a). These results indicated that the expression patterns and functions of the *SPX1* gene in maize and *A. thaliana* are different, which may also explain why the P concentration in *A. thaliana* overexpressing lines of *SPX* was higher than that in wild-type plants under normal-Pi conditions.

Additionally, a previous study demonstrated that *OsPHO1;2* and *ZmPHO1;2* play a crucial role in Pi allocation during grain filling. The activity of ADP-glucose pyrophosphorylase (AGPase) was inhibited in the knockout mutants of *OsPHO1;2* and *ZmPHO1;2*, resulting in a defect in grain filling and a reduction in hundred-grain weight (Ma et al., 2021). Regarding the plant Pi signaling pathway (Wang et al., 2021b), the E2 ubiquitin-binding enzyme PHO2 can degrade PHO1 through its N-terminal SPX domain. The mRNA level of *PHO2* was regulated by the cleavage of miR399. PHR1 can bind to the promoter region of miRNA399 to modulate its expression. Therefore, the relationship between SPX proteins and PHO1 was established through this network. However, further research is needed to investigate whether the impact of *ZmSPX1* on maize grain yield, as observed in this study, is related to *ZmPHO1*.

4.2 Association analysis of the *ZmSPX1* gene: implications for low-Pi signaling pathway and marker development for efficient Pi utilization in maize

To further investigate the relationship between the *ZmSPX1* gene and low-Pi stress response-related traits, we conducted an association analysis utilizing sequence variations of the gene in the population and integrated the corresponding phenotypes. The results revealed that variant sites in *ZmSPX1* are significantly associated with numerous low-Pi-related traits. This finding complements the findings from the phenotypic identification experiments in *Arabidopsis* involving the overexpression of the *ZmSPX1* gene, providing strong evidence for the pivotal role of the *ZmSPX1* gene in the low-Pi stress response pathway in maize. Additionally, we identified beneficial haplotypes based on 37 markers significantly associated with low-Pi tolerance indexes. Among these, Hap5 manifested a notable low-Pi tolerance phenotype, presenting an opportunity for the development of low-Pi-tolerant maize materials based on this outcome, and the identification of novel markers for screening purposes.

5 Conclusion

In conclusion, our study delineated the evolutionary relationship of maize *SPX*s with counterparts in other plants, particularly revealing a close relationship and collinearity with rice *SPX* genes. The presence of hormone-responsive elements in *ZmSPX*s promoters suggests their involvement at the nexus of hormone and Pi signaling. Expression pattern analyses indicated that *ZmSPX*s genes were upregulated under low-Pi stress, with pronounced expression in anthers and roots, and were localized to the nucleus and cytoplasm. The interaction of ZmSPXs with PHR proteins underscored the significance of *SPX*s in maize's low-Pi stress signaling pathways. Specifically, overexpression of *ZmSPX1* can enhance root sensitivity to Pi deficiency and high-Pi conditions in *A. thaliana*, emphasizing the pivotal role of the *SPX* gene family in the Pi stress response in maize. Finally, *ZmSPX1* transgenic maize lines exhibited changes in P concentration in different tissues and yield, demonstrating that *ZmSPX1* plays an important role in regulating the transport and distribution of P in maize and ultimately influencing yield. These findings will provide valuable information for further investigations into the mechanisms of the *SPX*-mediated Pi signaling pathway.

Data availability statement

The datasets presented in this study can be found in online repositories. The names of the repository/repositories and accession number(s) can be found in the article/Supplementary Material.

Author contributions

BL: Conceptualization, Formal analysis, Funding acquisition, Methodology, Visualization, Writing – original draft, Writing – review & editing. JS: Conceptualization, Formal analysis, Methodology, Validation, Visualization, Writing – original draft, Writing – review & editing. HZ: Formal analysis, Visualization, Writing – original draft. JZ: Writing – review & editing. GY: Writing – review & editing. WW: Writing – review & editing. JG: Writing – review & editing. SZ: Writing – review & editing. PM: Writing – review & editing. ZN: Writing – review & editing. XZ: Writing – review & editing. DL: Project administration, Resources, Writing – review & editing. LW: Project administration, Resources, Writing – review & editing. DG: Project administration, Resources, Writing – review & editing. SQG: Project administration, Resources, Writing – review & editing. SS: Project administration, Resources, Writing – review & editing. ZG: Investigation, Writing – review & editing. SBG: Writing – review & editing, Conceptualization, Funding acquisition, Methodology, Project administration.

Funding

The author(s) declare financial support was received for the research, authorship, and/or publication of this article. This study was supported by the National Natural Science Foundation of China (grant no. 32101655), the China Postdoctoral Science Foundation (grant no. 2022M712292), Sichuan Science and Technology Support Project (grant nos. 2023YFH0038, 2021YFYZ0027, 2021YFYZ0020, and 2021YFFZ0017), and the earmarked fund for China Agriculture Research System (grant no. CARS-02).

Acknowledgments

The bioinformatics analyses in this study were supported by the High-Performance Computing Platform of Sichuan Agricultural University.

Conflict of interest

The authors declare that the research was conducted in the absence of any commercial or financial relationships that could be construed as a potential conflict of interest.

Publisher's note

Supplementary material

The Supplementary Material for this article can be found online at: https://www.frontiersin.org/articles/10.3389/fpls.2024.1385977/full#supplementary-material

SUPPLEMENTARY FIGURE 1
CRISPR/Cas9-induced mutation in the *ZmSPX1* gene.

SUPPLEMENTARY FIGURE 2
Detection of expression level of *ZmSPX1* gene in overexpressing plants. Significant differences are indicated by Student's *t*-test: **P* < 0.05, ***P* < 0.01.

SUPPLEMENTARY FIGURE 3
Subcellular localization of ZmSPXs in tobacco epidermal. GFP, green fluorescence protein.

SUPPLEMENTARY FIGURE 4
Detection of overexpression of the *ZmSPX1* in *Arabidopsis thaliana*. M: DNA marker BM2000.

SUPPLEMENTARY FIGURE 5
Characterization of Arabidopsis thaliana ZmSPX1-overexpression plants in response to low-Pi conditions. **(A)** The WT and OE seedlings were subjected to treatments with P concentrations of 0 mM, 0.1 mM, 1 mM, and 10 mM for 14 days. **(B-C)** The expression of AtPHR1 and ZmSPX1 in WT and OE. The numbers 1 and 2 on the abscissa represent different independent replicates. **(D-F)** Measurement of root traits. Significant differences are indicated by Student's t-test: *P < 0.05, **P < 0.01. Under Pi-free and high-Pi conditions, only the *ZmSPX1* overexpression lines exhibited negative regulation of root growth when compared with the WT. Phenotypic of OE and WT was analyzed under Pi deficiency (0 mmol/L), low-Pi (0.1 mmol/L), normal-Pi (1 mmol/L) and high-Pi (10 mmol/L) treatments. The results indicated that, except under low-Pi conditions, the total root length, total root projected area, and total root surface area of the OE were significantly lower than those of the WT. Furthermore, the expression patterns of the *AtPHR1* and *ZmSPX1* genes were analyzed in the WT and OE plants. The results demonstrated significant downregulation of the *AtPHR1* in the OE plants and substantial upregulation in the WT plants. In contrast, *ZmSPX1* was upregulated in the OE plants and downregulated in the WT plants. Concurrently, we also examined the nitrogen and P concentration of the OE and WT (Supplementary Figure S6). Under low-Pi conditions, the nitrogen concentration in the OE was notably lower than that in the WT. However, under 1mM Pi concentration treatment, the nitrogen concentration in the OE was significantly higher than in the WT, while at 10mM Pi concentration conditions, the difference in nitrogen concentration between OE and WT was not statistically significant. Under Pi deficiency and low-Pi conditions, there was no significant difference in P concentration between the OE and WT. Nevertheless, at Pi concentrations of 1mM and 10mM, the P concentration in the OE was markedly elevated compared to that in the WT. Owing to the exceptionally low biomass of Arabidopsis tissues, there was a potential for deviations in the measurement of nutrient concentrations, and no consistent results were observed with regard to root traits. As a result, this study advanced to develop overexpression and knockout lines for *ZmSPX1* in maize to investigate the gene's impact on P concentration in maize tissues.

SUPPLEMENTARY FIGURE 6
The nitrogen and P concentrations of ZmSPX1 overexpression Arabidopsis lines under varying Pi levels. **(A)** Nitrogen concentrations. **(B)** P concentrations.

References

Balyan, H. S., Gahlaut, V., Kumar, A., Jaiswal, V., Dhariwal, R., Tyagi, S., et al. (2016). Nitrogen and phosphorus use efficiencies in wheat: physiology, phenotyping, genetics, and breeding. *Plant Breed. Rev.* 40, 167–234. doi: 10.1002/9781119279723.ch4

Bradbury, P. J., Zhang, Z., Kroon, D. E., Casstevens, T. M., Ramdoss, Y., and Buckler, E. S. (2007). TASSEL: software for association mapping of complex traits in diverse samples. *Bioinformatics* 23, 2633–2635. doi: 10.1093/bioinformatics/btm308

Carstensen, A., Herdean, A., Schmidt, S. B., Sharma, A., Spetea, C., Pribil, M., et al. (2018). The impacts of phosphorus deficiency on the photosynthetic electron transport chain. *Plant Physiol.* 177, 271–284. doi: 10.1104/pp.17.01624

Chen, S., Ding, G., Wang, Z., Cai, H., and Xu, F. (2015). Proteomic and comparative genomic analysis reveals adaptability of Brassica napus to phosphorus-deficient stress. *J. Proteomics* 117, 106–119. doi: 10.1016/j.jprot.2015.01.012

Chiou, T.-J., and Lin, S.-I. (2011). Signaling network in sensing phosphate availability in plants. *Annu. Rev. Plant Biol.* 62, 185–206. doi: 10.1146/annurev-arplant-042110-103849

Clough, S. J., and Bent, A. F. (1998). Floral dip: a simplified method for Agrobacterium-mediated transformation of Arabidopsis thaliana. *Plant J.* 16, 735–743. doi: 10.1046/j.1365-313x.1998.00343.x

Dong, J., Ma, G., Sui, L., Wei, M., Satheesh, V., Zhang, R., et al. (2019). Inositol pyrophosphate InsP8 acts as an intracellular phosphate signal in Arabidopsis. *Mol. Plant* 12, 1463–1473. doi: 10.1016/j.molp.2019.08.002

Du, H., Yang, C., Ding, G., Shi, L., and Xu, F. (2017). Genome-wide identification and characterization of SPX domain-containing members and their responses to phosphate deficiency in Brassica napus. *Front. Plant Sci.* 8, 35. doi: 10.3389/fpls.2017.00035

Duan, K., Yi, K., Dang, L., Huang, H., Wu, W., and Wu, P. (2008). Characterization of a sub-family of Arabidopsis genes with the SPX domain reveals their diverse functions in plant tolerance to phosphorus starvation. *Plant J.* 54, 965–975. doi: 10.1111/j.1365-313X.2008.03460.x

Feng, X., Jia, L., Cai, Y., Guan, H., Zheng, D., Zhang, W., et al. (2022). ABA-inducible DEEPER ROOTING 1 improves adaptation of maize to water deficiency. *Plant Biotechnol. J.* 20, 2077–2088. doi: 10.1111/pbi.13889

Garcia, A., Gaju, O., Bowerman, A. F., Buck, S. A., Evans, J. R., Furbank, R. T., et al. (2023). Enhancing crop yields through improvements in the efficiency of photosynthesis and respiration. *New Phytol.* 237, 60–77. doi: 10.1111/nph.18545

Hu, B., Jiang, Z., Wang, W., Qiu, Y., Zhang, Z., Liu, Y., et al. (2019). Nitrate–NRT1. 1B–SPX4 cascade integrates nitrogen and phosphorus signalling networks in plants. *Nat. Plants* 5, 401–413. doi: 10.1038/s41477-019-0384-1

Iqbal, A., Qiang, D., Xiangru, W., Huiping, G., Hengheng, Z., Xiling, Z., et al. (2023). Genotypic variation in cotton genotypes for low phosphorus tolerance and efficiency under different growth conditions. *Gesunde Pflanzen* 75, 1975–1993. doi: 10.1007/s10343-022-00823-y

Jia, X., Wang, L., Nussaume, L., and Yi, K. (2023). Cracking the code of plant central phosphate signaling. *Trends Plant Science* 28, 267–270. doi: 10.1016/j.tplants.2022.12.008

Jiao, P., Liu, T., Zhao, C., Fei, J., Guan, S., and Ma, Y. (2023). ZmTCP14, a TCP transcription factor, modulates drought stress response in Zea mays L. *Environ. Exp. Bot.* 208, 105232. doi: 10.1016/j.envexpbot.2023.105232

Jung, J.-Y., Ried, M. K., Hothorn, M., and Poirier, Y. (2018). Control of plant phosphate homeostasis by inositol pyrophosphates and the SPX domain. *Curr. Opin. Biotechnol.* 49, 156–162. doi: 10.1016/j.copbio.2017.08.012

Kopriva, S., and Chu, C. (2018). Are we ready to improve phosphorus homeostasis in rice? *J. Exp. Bot.* 69, 3515–3522. doi: 10.1093/jxb/ery163

Kumar, A., Sharma, M., Gahlaut, V., Nagaraju, M., Chaudhary, S., Kumar, A., et al. (2019). Genome-wide identification, characterization, and expression profiling of SPX gene family in wheat. *Int. J. Biol. macromolecules* 140, 17–32. doi: 10.1016/j.ijbiomac.2019.08.105

Kumar, S., Tamura, K., and Nei, M. (1994). MEGA: molecular evolutionary genetics analysis software for microcomputers. *Bioinformatics* 10, 189–191. doi: 10.1093/bioinformatics/10.2.189

Li, C., You, Q., and Zhao, P. (2021). Genome-wide identification and characterization of SPX-domain-containing protein gene family in Solanum lycopersicum. *PeerJ* 9, e12689. doi: 10.7717/peerj.12689

Liang, C., Wang, J., Zhao, J., Tian, J., and Liao, H. (2014). Control of phosphate homeostasis through gene regulation in crops. *Curr. Opin. Plant Biol.* 21, 59–66. doi: 10.1016/j.pbi.2014.06.009

Luo, B., Ma, P., Nie, Z., Zhang, X., He, X., Ding, X., et al. (2019). Metabolite profiling and genome-wide association studies reveal response mechanisms of phosphorus deficiency in maize seedling. *Plant J.* 97, 947–969. doi: 10.1111/tpj.14160

Luo, B., Zhang, Z., Li, B., Zhang, H., Ma, J., Li, J., et al. (2023). Chromatin remodeling analysis reveals the RdDM pathway responds to low-phosphorus stress in maize. *Plant J.* 117, 33–52. doi: 10.1111/tpj.16468

Lv, Q., Zhong, Y., Wang, Y., Wang, Z., Zhang, L., Shi, J., et al. (2014). SPX4 negatively regulates phosphate signaling and homeostasis through its interaction with PHR2 in rice. *Plant Cell* 26, 1586–1597. doi: 10.1105/tpc.114.123208

Lynch, J. P. (2011). Root phenes for enhanced soil exploration and phosphorus acquisition: tools for future crops. *Plant Physiol.* 156, 1041–1049. doi: 10.1104/pp.111.175414

Lynch, J. P., Ho, M. D., and Phosphorus, L. (2005). Rhizoeconomics: Carbon costs of phosphorus acquisition. *Plant Soil* 269, 45–56. doi: 10.1007/s11104-004-1096-4

Ma, B., Zhang, L., Gao, Q., Wang, J., Li, X., Wang, H., et al. (2021). A plasma membrane transporter coordinates phosphate reallocation and grain filling in cereals. *Nat. Genet.* 53, 906–915. doi: 10.1038/s41588-021-00855-6

Marchler-Bauer, A., Derbyshire, M. K., Gonzales, N. R., Lu, S., Chitsaz, F., Geer, L. Y., et al. (2015). CDD: NCBI's conserved domain database. *Nucleic Acids Res.* 43, D222–D226. doi: 10.1093/nar/gku1221

Nezamivand-Chegini, M., Ebrahimie, E., Tahmasebi, A., Moghadam, A., Eshghi, S., Mohammadi-Dehchesmeh, M., et al. (2021). New insights into the evolution of SPX gene family from algae to legumes; a focus on soybean. *BMC Genomics* 22, 915. doi: 10.1186/s12864-021-08242-5

Nie, Z., Luo, B., Zhang, X., Wu, L., Liu, D., Guo, J., et al. (2021). Combined transcriptome and proteome analysis of maize (Zea mays l.) reveals a complementary profile in response to phosphate deficiency. *Curr. Issues Mol. Biol.* 43, 1142–1155. doi: 10.3390/cimb43020081

Osorio, M. B., Ng, S., Berkowitz, O., De Clercq, I., Mao, C., Shou, H., et al. (2019). SPX4 acts on PHR1-dependent and -independent regulation of shoot phosphorus status in Arabidopsis. *Plant Physiol.* 181, 332–352. doi: 10.1104/pp.18.00594

Porebski, S., Bailey, L. G., and Baum, B. R. (1997). Modification of a CTAB DNA extraction protocol for plants containing high polysaccharide and polyphenol components. *Plant Mol. Biol. Rep.* 15, 8–15. doi: 10.1007/BF02772108

Puga, M. I., Rojas-Triana, M., De Lorenzo, L., Leyva, A., Rubio, V., and Paz-Ares, J. (2017). Novel signals in the regulation of Pi starvation responses in plants: facts and promises. *Curr. Opin. Plant Biol.* 39, 40–49. doi: 10.1016/j.pbi.2017.05.007

Raghothama, K. G. (1999). PHOSPHATE ACQUISITION. *Annu. Rev. Plant Physiol. Plant Mol. Biol.* 50, 665–693. doi: 10.1146/annurev.arplant.50.1.665

Rubio, V., Linhares, F., Solano, R., Martín, A. C., Iglesias, J., Leyva, A., et al. (2001). A conserved MYB transcription factor involved in phosphate starvation signaling both in vascular plants and in unicellular algae. *Genes Dev.* 15, 2122–2133. doi: 10.1101/gad.204401

Saengwilai, P. J., Bootti, P., and Klinnawee, L. (2023). Responses of rubber tree seedlings (Hevea brasiliensis) to phosphorus deficient soils. *Soil Sci. Plant Nutr.* 69, 78–87. doi: 10.1080/00380768.2022.2164675

Sahito, J. H., Zhang, X., Zhong, H., He, X., Zhen, C., Ma, P., et al. (2020a). Identification, association of natural variation and expression analysis of ZmNAC9 gene response to low phosphorus in maize seedling stage. *Plants* 9, 1447. doi: 10.3390/plants9111447

Sahito, J. H., Zheng, F., Tang, H., He, X., Luo, B., Zhang, X., et al. (2020b). Identification, association, and expression analysis of ZmNAC134 gene response to phosphorus deficiency tolerance traits in maize at seedling stage. *Euphytica* 216, 1–19. doi: 10.1007/s10681-020-02634-6

Secco, D., Wang, C., Arpat, B. A., Wang, Z., Poirier, Y., Tyerman, S. D., et al. (2012). The emerging importance of the SPX domain-containing proteins in phosphate homeostasis. *New Phytol.* 193, 842–851. doi: 10.1111/j.1469-8137.2011.04002.x

Shen, J., Li, H., Neumann, G., and Zhang, F. (2005). Nutrient uptake, cluster root formation and exudation of protons and citrate in Lupinus albus as affected by localized supply of phosphorus in a split-root system. *Plant Sci.* 168, 837–845. doi: 10.1016/j.plantsci.2004.10.017

Shimojima, M. (2011). Biosynthesis and functions of the plant sulfolipid. *Prog. Lipid Res.* 50, 234–239. doi: 10.1016/j.plipres.2011.02.003

Strable, J., and Scanlon, M. J. (2009). Maize (Zea mays): a model organism for basic and applied research in plant biology. *Cold Spring Harbor Protoc.* 2009, pdb. emo132. doi: 10.1101/pdb.emo132

Wang, Z., Ruan, W., Shi, J., Zhang, L., Xiang, D., Yang, C., et al. (2014). Rice SPX1 and SPX2 inhibit phosphate starvation responses through interacting with PHR2 in a phosphate-dependent manner. *Proc. Natl. Acad. Sci.* 111, 14953–14958. doi: 10.1073/pnas.1404680111

Wang, L., Jia, X., Zhang, Y., Xu, L., Menand, B., Zhao, H., et al. (2021a). Loss of two families of SPX domain-containing proteins required for vacuolar polyphosphate accumulation coincides with the transition to phosphate storage in green plants. *Mol. Plant* 14, 838–846. doi: 10.1016/j.molp.2021.01.015

Wang, Y., Chen, Y. F., and Wu, W. H. (2021b). Potassium and phosphorus transport and signaling in plants. *J. Integr. Plant Biol.* 63, 34–52. doi: 10.1111/jipb.13053

Wild, R., Gerasimaite, R., Jung, J.-Y., Truffault, V., Pavlovic, I., Schmidt, A., et al. (2016). Control of eukaryotic phosphate homeostasis by inositol polyphosphate sensor domains. *Science* 352, 986–990. doi: 10.1126/science.aad9858

Xiao, J., Xie, X., Li, C., Xing, G., Cheng, K., Li, H., et al. (2021). Identification of SPX family genes in the maize genome and their expression under different phosphate regimes. *Plant Physiol. Biochem.* 168, 211–220. doi: 10.1016/j.plaphy.2021.09.045

Yang, J., Wang, L., Mao, C., and Lin, H. (2017). Characterization of the rice NLA family reveals a key role for OsNLA1 in phosphate homeostasis. *Rice* 10, 1–6. doi: 10.1186/s12284-017-0193-y

Yao, Z., Liang, C., Zhang, Q., Chen, Z., Xiao, B., Tian, J., et al. (2014a). SPX1 is an important component in the phosphorus signalling network of common bean regulating root growth and phosphorus homeostasis. *J. Exp. Bot.* 65, 3299–3310. doi: 10.1093/jxb/eru183

Yao, Z., Tian, J., and Liao, H. (2014b). Comparative characterization of GmSPX members reveals that GmSPX3 is involved in phosphate homeostasis in soybean. *Ann. Bot.* 114, 477–488. doi: 10.1093/aob/mcu147

Yue, W., Ying, Y., Wang, C., Zhao, Y., Dong, C., Whelan, J., et al. (2017). Os NLA 1, a RING-type ubiquitin ligase, maintains phosphate homeostasis in Oryza sativa via degradation of phosphate transporters. *Plant J.* 90, 1040–1051. doi: 10.1111/tpj.13516

Zhang, H., Huang, Y., Ye, X., and Xu, F. (2010). Analysis of the contribution of acid phosphatase to P efficiency in Brassica napus under low phosphorus conditions. *Sci. China Life Sci.* 53, 709–717. doi: 10.1007/s11427-010-4008-2

Zhang, Z., Liao, H., and Lucas, W. J. (2014). Molecular mechanisms underlying phosphate sensing, signaling, and adaptation in plants. *J. Integr. Plant Biol.* 56, 192–220. doi: 10.1111/jipb.12163

Zhang, X., Zhang, H., Li, L., Lan, H., Ren, Z., Liu, D., et al. (2016). Characterizing the population structure and genetic diversity of maize breeding germplasm in Southwest China using genome-wide SNP markers. *BMC Genomics* 17, 697. doi: 10.1186/s12864-016-3041-3

Zhong, Y., Wang, Y., Guo, J., Zhu, X., Shi, J., He, Q., et al. (2018). Rice SPX6 negatively regulates the phosphate starvation response through suppression of the transcription factor PHR2. *New Phytol.* 219, 135–148. doi: 10.1111/nph.15155

Zhou, L., Zhou, J., Xiong, Y., Liu, C., Wang, J., Wang, G., et al. (2018). Overexpression of a maize plasma membrane intrinsic protein ZmPIP1; 1 confers drought and salt tolerance in Arabidopsis. *PLoS One* 13, e0198639. doi: 10.1371/journal.pone.0198639

Zou, T., Zhang, X., and Davidson, E. (2022). Global trends of cropland phosphorus use and sustainability challenges. *Nature* 611, 81–87. doi: 10.1038/s41586-022-05220-z

Frontiers in Plant Science

Cultivates the science of plant biology and its applications

The most cited plant science journal, which advances our understanding of plant biology for sustainable food security, functional ecosystems and human health.

Discover the latest Research Topics

See more →

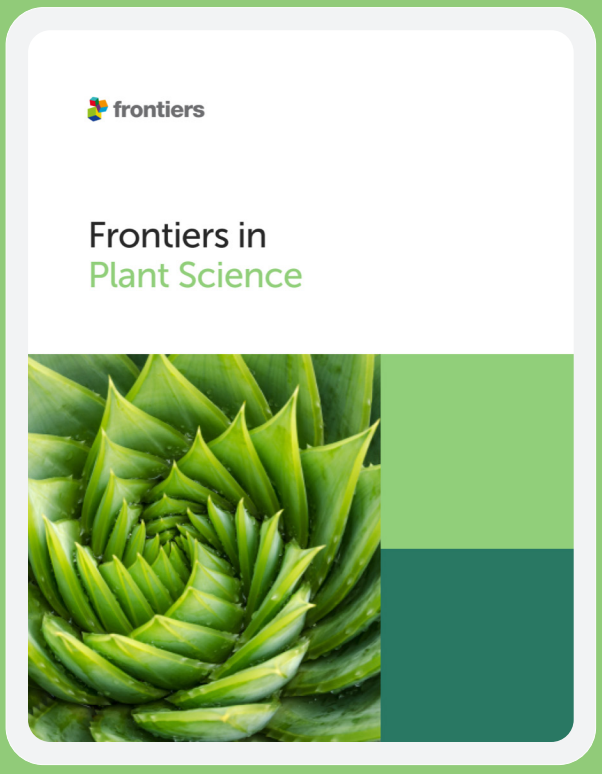

Frontiers

Avenue du Tribunal-Fédéral 34
1005 Lausanne, Switzerland
frontiersin.org

Contact us

+41 (0)21 510 17 00
frontiersin.org/about/contact